UNIVERSITY OF BELGRADE
TECHNICAL FACULTY IN BOR
CHAMBER OF COMMERCE AND
INDUSTRY OF SERBIA

PROCEEDINGS

XIII International MINERAL PROCESSING and RECYCLING CONFERENCE

Editors:
Grozdanka Bogdanović
Milan Trumić

Belgrade, Serbia, 8 – 10 May 2019

UNIVERSITY OF BELGRADE
TECHNICAL FACULTY IN BOR

PRIVREDNA KOMORA SRBIJE 1857

CHAMBER OF COMMERCE AND INDUSTRY OF SERBIA

PROCEEDINGS

XIII INTERNATIONAL MINERAL PROCESSING and RECYCLING CONFERENCE

Editors:
Grozdanka Bogdanović
Milan Trumić

Belgrade, Serbia, 8 – 10 May 2019

XIII INTERNATIONAL
MINERAL PROCESSING and RECYCLING CONFERENCE

PUBLISHER
University of Belgrade, Technical Faculty in Bor

FOR THE PUBLISHER
DEAN: Prof. Dr Nada Štrbac

EDITORS
Prof. Dr Grozdanka Bogdanović
Prof. Dr Milan Trumić

PROCEEDINGS COVER DESIGN
Predrag Stolić

PRINTED BY
Grafomed Trade doo, Bor, Serbia

Printed: 200 copies

CIP – Каталогизација у публикацији
Народна библиотека Србије, Београд

ISBN 978-86-6305-091-4

Conference is financially supported by Republic of Serbia, Ministry of Education, Science and Technological Development

INTERNATIONAL SCIENTIFIC COMMITTEE

Prof. Dr Ljubiša Andrić (Serbia)
Prof. Dr Dušan Stanojević (Serbia)
Prof. Dr Marina Stamenović (Serbia)
Prof. Dr Mile Dimitrijević (Serbia)
Prof. Dr Dejan Ubavin (Serbia)
Doc. Dr Zoran Štirbanović (Serbia)
Doc. Dr Maja Trumić (Serbia)
Doc. Dr Vladimir Pavićević (Serbia)
Doc. Dr Vladimir Despotović (Serbia)
Dr Miroslav Ignjatović (Serbia)
Dr Zoran Stevanović (Serbia)
Dr Dragan Milanović (Serbia)
Dr Dragan Radulović (Serbia)
Dr Sonja Milićević (Serbia)
Dr Radmila Marković (Serbia)

ORGANIZING COMMITTEE

Prof. Dr Grozdanka Bogdanović (Serbia), President
Prof. Dr Milan Trumić (Serbia)
Dr Miroslav Ignjatović (Serbia)
Prof. Dr Jovica Sokolović (Serbia)
Doc. Dr Zoran Štirbanović (Serbia)
Doc. Dr Maja Trumić (Serbia)
M.Sc. Aleksandra Stojanović (Serbia)
M.Sc. Vladimir Nikolić (Serbia)
M.Sc. Dragana Marilović (Serbia)
M.Sc. Predrag Stolić (Serbia)
B.Sc. Katarina Balanović (Serbia)
Sandra Vasković, English language teacher (Serbia)
Dobrinka Trujić (Serbia)

TABLE OF CONTENTS

PLENARY LECTURES

XIII International Mineral Processing and Recycling Conference
Belgrade, Serbia, 8-10 May 2019

University of Belgrade, Technical Faculty in Bor
Vojske Jugoslavije 12, 19210 Bor, Serbia
Tel. +381 30 424 555 Fax +381 30 421 078

MINERAL BIOFLOTATION: A SHORT REVIEW OF MY RESEARCH GROUP EXPERIENCE

Antonio Gutierrez Merma, Maurício Leonardo Torem #, Ronald Rojas Hacha
Pontifical Catholic University, Department of Chemical Engineering and Materials, Gávea, Rio de Janeiro, Brazil

ABSTRACT – The purpose of this paper is to succinctly present key achievements of the Mineral and Environmental Technology Research Group (METG) – Materials Engineering Department of the Pontifical Catholic University of Rio de Janeiro (PUC-Rio) – regarding to mineral processing. The behavior of several microorganisms (*Rhodococcus opacus*, *rhodococcus erythropolis* and *candida stellata*) and their byproducts (biosurfactants) is presented. It was emphasized the use of these biorreagents in the flotation of hematite and quartz. The adsorption of the biorreagents on the mineral surface could be due to specific and/or non-specific interactions, which will depend on several factors, as their surface charge and hydrophobic character. The zeta potential evaluation of the mineral particles before and after interaction with the biorreagents showed a modification of the minerals zeta potential profiles, which confirm their adsorption. The adsorption was higher for hematite and due to their hydrophobic character flotation was successful. The mineral floatability was found to be dependent on pH and biorreagent concentration.

Key words: bioprocessing, bioflotation, bacteria, yeast, biosurfactant.

INTRODUCTION

Biotechnology applied to mineral processing has been studied by many researchers [1 - 8] around the world, where emerging and promising technologies as bioflotation and bioflocculation remark. It is believed that these biotechnologies could be capable to resolve the current and future challenges in mineral processing (Depletion of minerals deposits, treatment of complex ore and tailings). Mineral bioprocessing is defined as a process that uses bioreagents (microorganism´s cells and their byproducts) with hydrophobic character during mineral concentration operations, as flotation and flocculation. These bioreagents present several polar and non-polar functional groups, as amines, amides, micolic acids, phosphates, etc, which make possible their use as collectors and/or modifiers agents on mineral processing and biosorption-bioflotation processes as suggested in the literature [2, 3, 9 - 13].

Thus, the main objective of this work is to briefly review the key-achievements

corresponding author: torem@puc.br

related to Mineral Processing developed by the METG of the Materials Engineering Department of the Pontifical Catholic University of Rio de Janeiro (PUC-Rio).

MINERAL BIOFLOTATION

Bioprocessing studies are normally conducted at laboratory scale using pure minerals; these studies include microorganism development, bioreagents production, equilibrium adsorption and flotation and/or flocculation studies; some of them are more specific and may embrace the interaction of the bioreagent onto the mineral surface [10, 14, 15]. Some others deal with the use of microorganism's by-products, extracellular polymeric substances (EPS) [1, 16 - 19] and the so-called biosurfactants [20]. According to Natarajan [2], the production rate of these by-products can be modified, rendering the bioreagent more hydrophobic or ever more selective. This modification can be done through substrate adaptation or by genetic modifications [1, 16, 18, 19, 21, 22] and could bring about changes in the cellular morphology, besides quantitative and qualitative modifications in the secretion of proteins and polysaccharides. Finally, the literature depicts some relevant works on bioflotation of ores [20, 23, 24] and coal [25, 26] using specific bioreagents.

Considering the previous the METG have been developing different works in mineral bioprocessing, specifically in mineral bioflotation, using several bacteria strains, as *Rhodococcus opacus*, *Rhodococcus Ruber*, *Rhodococcus erythropolis*. However, the *R. opacus* strain presented the most relevant results [4, 9, 10, 11]. This microorganism is an unicellular gram positive bacterium with different types of compounds on their cell-wall; mainly, polysaccharides, carboxylic acids, lipid groups and micolic acids, which give an amphoteric behavior (hydrophobic and/or hydrophilic properties) to the bacteria [2, 9, 12], due to the functional groups presented. However, according to literature the application of the microorganisms is difficult because the complexity of their surface structure, which could affect the selectivity of the process. This fact was observed during our studies, where large concentrations of the microorganism and flotation times are needed to achieve a relevant floatability value. Thus, a hot-ethanol extraction technique was used to obtain the biosurfactant presented on the microorganisms, more information of the extraction can be found in Puelles [27]. These by-products were used in the flotation of several minerals; the results are in fact promising. Low biosurfactant concentrations and flotation times are required to achieved high floatability values. All these works show the possible use of these bioreagents (microorganisms and their by-products) as collectors and/or frothers in mineral processing. Their application requires several fundamental aspects, e.g. composition, surface charge and hydrophobic character, which are considered as the most relevant factors.

RESULTS AND DISCUSSION

Microorganisms characterization

FTIR-spectroscopy of biorreagents

FTIR spectra of bacteria and their biosurfactant can be seen in Fig. 1a and Fig.1b, respectively. According to Schmitt and Flemming [28] bacteria produced similar FTIR-spectra, since most of them are composed of similar functional groups, on the

other hand Puzey et al. [29] affirmed that each bacterial species produces a unique fingerprint-like FTIR spectra, however, Naumann [30] referred to the spectral domain between 900 and 600 cm^{-1} as the "true fingerprint region". The bacteria used are from the *Rhodococci* family, which would be the reason for the similarity presented in their FTIR-spectra. The only difference between bacteria is the presence of the band 1,750 cm^{-1} for the *R. opacus,* which correspond to the C=O stretching mode of esters, from fatty acids or glycerol. The FTIR-spectra of both biosurfactants is also very similar, presenting peaks at bands 3400, cm^{-1}, between 2,930 cm^{-1} and 2,850 cm^{-1}, ~ 1,620 cm^{-1} and 1,400 cm^{-1}, corresponding to stretching mode of NH and OH; stretching mode of C-H; stretching mode of C=O or stretching mode of C=C (alkene); stretching mode of C=C (aromatic) [31, 32], respectively. The main difference can be seen in the region between 1,200 and 600 cm^{-1}.

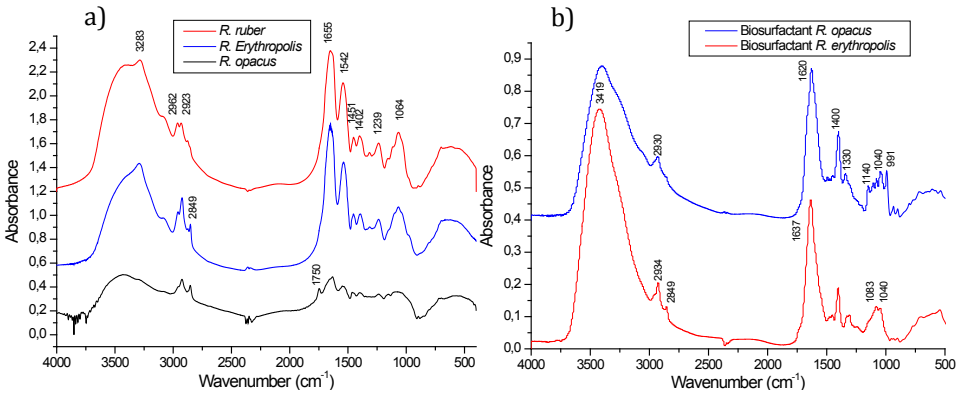

Figure 1. FTIR spectra of the bacteria **(a)** and biosurfactant **(b)** used for the METG

Table 1 presents the main possible functional groups found in bacteria and biosurfactant from their components as lipoproteins, peptidoglycan, teichoic and tichuronic acid and glycerol-containing macromolecules, built up by a phosphate-carrying backbone with side chains of variable composition [30].

Zeta Potential of biorreagents

The charge of the cell wall of any microorganism is determined by the dissociation, protonation or ionization of acidic and basic groups present on their surface, which implies that the net charge is strongly pH dependent [2, 3, 12, 37]. Moreover, the surface charge of any particle in aqueous solution is related to its zeta potential value.

The surface of the these cells is negatively charged over a wide range of pH, which could be associated to the presence of anionic groups that dominate over the cationic groups, thus, an acidic IEP (isoelectric point) value between 2.5 and 3.2, is generally observed [4, 9, 27, 34]. This range of values is related to different factors, as grown conditions, source of the strain, technical used and experimental conditions used during zeta potential measurements.

Table 1. Possible functional groups identified by FTIR

Rhodococcus bacteria			
Wavenumber(cm^{-1})	Intensity	Possible functional group	Structures
~ 3,500	High	Alcohols	
~ 3,200	Medium	Amide A of proteins	
2,960	Medium	Alkanes	
1,746.00	Medium	Aromatic, aldehydes, ketones, esters	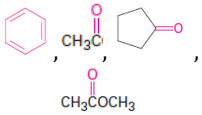
1,632.00	High	Alkenes	
1,548.59	Medium	Aromatic	
1,400.78	Medium	carboxil	C=O of COO^-
1,237.15	Medium	P=O str (sym) of > PO_2^-	
1,079.02	Medium	P=O str (asym) of > PO_2^-	
Crude Biosurfactants			
3,400	High	Alcohols	
2,930	Medium	Alkanes	
1,620-1,640	High	Alkenes, ketones	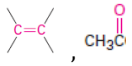
1,400.41	Medium	carboxil	C=O of COO^-
1,047.35	Medium	Alkanes	

Zeta Potential of the minerals before and after interactions with the bioreagents

The IEP of different mineral samples, before and after interacting with bioreagent can be observed in Table 1. All the measurements were done using KCl as indifferent electrolyte in an electrophoretic Malvern equipment. Hematite samples presented an IEP value between 5.1 and 7, which is in agreement with the values reported in the literature [27, 34, 35]. It is well known that quartz presents a high negative surface charge and present IEP between 1.8 and 3.0 [4, 9, 35]. According to Botero et al. [10] the IEP of calcite and magnesite are in accordance with equivalent studies by Pokrovsky et al. (1999) and Vdovic & Bigdan (1998) where the IEP values were around 8.4 and 10 for magnesite and calcite, respectively. Finally, the apatite IEP was not observed under the present conditions; however, IEP values of apatite between 2.0 and 8.0 were reported in literature [36, 37]. This apatite behavior could be explained due to its tolerance to isomorphic substitutions, regardless of its origin and composition, factors which alter the IEP value.

Zeta potential profile of the minerals after interaction with microorganisms cells as a function of pH can help to elucidate the interaction mechanisms involved in their onto mineral surface. It is also possible to observe a window in the pH range that could be a potential region for electrostatic interaction, between pH higher than the IEP of the microorganism and pH lower than the IEP of the mineral. For example, for hematite this region is presented in the pH range between 3.2 and ~ 5.5. Table 2 shows the point of charge reversal (PCR) for each mineral after interacting with microorganism. According to the results the higher shift of the IEP is for hematite, this modification could be attributed to the adhesion of bacterial cells onto mineral surface, and higher the difference between IEP and PCR the bigger the adhesion of the bacteria, it means that the bacteria would preferentially adhered onto that mineral.

Table 2. IEP of the mineral samples before and after interaction with bioreagents

Mineral	IEP	PCR	Bacteria	|I|EP	PCR	Biosurfactant
	5.1	2.6	*R. opacus*	6.2	3.9	From *R. opacus*
Hematite	5.3	2.1	*R. erythropolis*	5.2	4.4	From *R. Erythropolis*
	5.5	2.8	*R. ruber*			
Quartz	2.0	3.7	*R. opacus*	2.5	2.2	From R. *opacus*
Calcite	10	9.8	*R. opacus*	NI	NI	From R. *opacus*
Magnesite	8.4	7.9	*R. opacus*	NI	NI	From R. *opacus*
Apatite	NI	NI	*R. opacus*	NI	NI	From R. *opacus*

After interacting with biosurfactant the zeta potential profile suffered a modification, this also could be related to adsorption of the biosurfactant. According to literature the main functional groups, under acidic conditions, is the carboxylic, which has a pKa at pH 2. So, we suggest that between pH higher than 2 until the IEP of the mineral the adsorption mechanism is controlled by electrostatic interactions, however, the contribution of other mechanisms is not discarded. The main results are simplified in the Table 2, the different extent of the PCR indicates that the nature and type of surface-chemical changes brought about by bioreagent interaction could be different for each mineral. The most interesting result was observed for the system hematite-quartz, thus several bioreagents were tested.

Finally, both bioreagents present a similar behavior, present a PCR at a pH value lower than the IEP, this value was even lower for the microorganism-mineral interaction. This could be related to a higher modification in the surface properties of the mineral, due to bacterial cells adhesion.

Mineral Flotation studies

Mineral flotation studies using microorganisms as collectors

The hydrophobic character of a bioreagent (microorganisms and their by-products) is associated with the source of the microorganism, its specie and so, and may change depending on their composition (functional groups), especially the presence of lipidic and proteic groups associated [1, 10]. If a hydrophobic bioreagent adsorbed onto a hydrophilic mineral surface, then the hydrophilic mineral surface could be turned into hydrophobic. The hydrophobic character of the mineral surface can be related to its flotability, and a bioreagent can be evaluated by the floatability

of the mineral before and after interacting with the bioreagent (microorganism and/or metabolic product).

In this section we present the flotation results of six pure minerals using the *Rhodococcus opacus* and *Rhodococcus erythropolis* bacteria as collectors. All experiments were done under same conditions, as particle size (- 106 + 75 μm), cell volume (160 mL), temperature (23 °C), air flow (20 mL min^{-1}), magnetic stirring, and using a modified-*Hallimond* tube. Table 3 presents a summary of the results.

Table 3. Mineral flotability using the microorganisms as the collector (Particle size range: -106+75 μm)

Mineral	pH	Concentration (g L^{-1})	Time (min.)	Floatability (%)	Bacteria
Magnesite	5	0.1	10	93	*R. opacus*
	7	0.1	10	83	
	9	0.1	10	86	
Calcite	5	0.22	10	40	*R. opacus*
	7	0.22	10	55	
	9	0.22	10	37	
	5	0.15	2	10	
Quartz	3	0.6	5	42	*R opacus*
	5	0.15	2	20	
	5	0.15	2	18	*R. erythropolis*
Apatite	3	0.15	2	46	*R. opacus*
	5	0.15	2	60	
	5	0.15	5	90	
	7	0.15	2	40	
	5	0.125	2	60	*R. erythropolis*
Dolomite	7	0.30	2	25	*R. opacus*
	7	0.30	7	55	
	7	0.125	2	33	*R. erythropolis*
	9	0.150	2	28	
Hematite	4	600	5	90	*R. opacus*
	6	600	5	72	
	7	75	2	45	
	7	150	2	36	*R. Erythropolis*
	3	150	5	30	*R. ruber*

During the flotation of magnesite it was observed that the *R. opacus* bacteria improved the magnesite flotability in the entire studied pH. The highest floatability of magnesite achieved a value of 92 % using 0.1 g L^{-1} of *R. opacus* at pH 5. Beyond this concentration value, the flotability decreased. The last effect suggested that there exist a *R. opacus* critical concentration, with higher bacterial concentration the microorganism would reduce their collector character [10]. This effect was observed for some minerals and was not observed for calcite and hematite. For calcite, hematite and quartz the floatability increased with increasing the bacterial concentration. The highest floatability of calcite (55 %) was achieved with a *R. opacus* concentration of 0.22 g L^{-1} at pH 7.0 [10]; the *R. erythropolis* bacteria couldn´t

increase the floatability of calcite, values lower than 10 % were achieved in all pH range studied. The floatability of a cleaned quartz (washed with KOH 0.1 mol L^{-1}) was increased after adhesion of the *R. opacus* bacteria from 0.5 to 14 % after two min. of flotation, at pH 5, and using 0.15 g L^{-1} of the biomass, which was noticed as the critical bacterial concentration; a similar result was found with the *R. erythropolis* bacteria. Moreover, insignificant quartz floatability was observed at different pH, also higher flotation time caused any significant floatability improvement. At pH 3 a higher concentration of *R. opacus* could increase the quartz floatability (~ 40 %), using 600 mg/L, and with a higher flotation time (5 min.).

The use of the *R. opacus* bacteria was able to increase the floatability of a highly hydrophilic apatite sample from 2% to around 60 % using 0.15 g L^{-1} of bacteria (critical concentration). This floatability value was attained at pH 5, whilst at pH 3 and pH 7, the floatability achieved values of 46 % and 40 %, respectively. Smaller floatability values were observed in alkaline medium. The flotation time also affected the apatite floatability, after five minutes a maximum floatability was achieved (around of 90 %). Very similar results were observed when *R. erythropolis* bacteria was used.

Flotation of dolomite was possible at neutral conditions, however it is necessary a high concentration of the microorganism (300 mg L^{-1}) and a larger flotation time (more than 7 minutes) to achieve a considerable floatability value.

It was observed a similar behavior of the microorganisms during the flotation of quartz, dolomite, calcite and apatite. However, for hematite each microorganism has a different response. It is possible to float hematite with *R. opacus* between pH 4 and 7, achieving 90 % of floatability when large bacterial concentration (600 mg L^{-1}) and large flotation time (5 min.) are used. Lower floatability values (33 %) were attained with *R. erythropolis*, at pH 7, higher flotation time didn´t significantly affect the result. Finally, the best result for *R. ruber* (30 %) was attained at pH 3, but in this case it was necessary the use of a frother (flotanol) in order to stabilize the froth. Moreover, the floatability of hematite increased considerably (~ 60 %) when a finer particle size was used (- 53 + 38 μm) [38].

Mineral flotation studies using by-products of the microorganisms

In this section we present flotation results of five minerals using the biosurfactants extracted from *Rhodococcus opacus* (BS-*R.opacus*) and *Rhodococcus erythropolis* (BS-*R.erythropolis*) bacteria. All experiments were done under same conditions, as particle size (- 106 +75 μm), cell volume (160 mL), temperature (23 °C), air flow (20 mL min^{-1}), flotation time of 2 min., magnetic stirring, and using a modified-*Hallimond* tube. Table 4 presents a summary of the more relevant results. The performance of the biosurfactant was better than expected; low BS-bacteria concentration and short flotation time were required to achieve relevant results.
The flotation of quartz using both biosurfactants presented similar results, achieving floatability values of around 30 %, with a BS-bacteria concentration equal and higher than 100 mg L^{-1} and at a pH 3, at higher pH the floatability was negligible.

Similar results were found for dolomite, both biosurfactants can be used at very acid conditions (pH 3), but the BS-*R.opacus* can also be used at pH 5. High floatability values (85 %) can be achieved using 25 mg L^{-1} of the biosurfactants, larger concentrations increased the floatability until a value of around 95 %.

The higher performance of the biosurfactants in comparison with the bacteria can be seen during the flotation of calcite, when bacteria was used the floatability of calcite was negligible, while with biosurfactants the floatability achieve values higher than 85 %. These results were observed at pH range between 5 and 7 to BS-*R. opacus* and between 5 and 9 to BS-*R.erythropolis* and using concentrations equal and higher than 100 mg L^{-1}.

Table 4. Mineral floatability using crude biosurfactant as collector (Particle size range: -106+75 μm)

Mineral	pH	Concentration (g L^{-1})	Time (min.)	Floatability (%)	Bioreagent
Quartz	3	150	2	33	BS - *R. opacus*
	3	100	2	30	BS - *R. erythropolis*
Dolomite	3 - 5	25 - 150	2	85 - 95	BS - *R. opacus*
	3	25 - 150	2	> 90	BS - *R. erythropolis*
Calcite	5 - 7	100 - 150	2	> 85	BS - *R. opacus*
	5 - 9	100-150	2	> 85	BS - *R. erythropolis*
Hematite	3	50 - 150	< 1	> 95	BS - *R. opacus*
	5 - 7	50-150	< 1	70 to 90	BS - *R. opacus*
	3	50 - 150	< 1	> 95	BS - R. *erythropolis*
	5	50 - 150	1	70 to 85	BS - *R. erythropolis*
Apatite	3	25 - 150	< 1	> 90	BS - *R. opacus*
	5	25 - 150	< 1	> 85	BS - *R. opacus*
	7 - 11	50 - 150	< 1	85 to 95	BS - *R. opacus*
	3	100 - 150	2	70 to 80	BS - *R. erythropolis*
	5	75 - 150	2	70 to 80	BS - *R. erythropolis*

The floatability of hematite presented a similar behavior with both biosurfactants. This was exceptionally fast (good results at only 30 seconds) and very low concentrations were required (about 85 % with 25 mg L^{-1}) to achieve excellent results. The best results were achieved at pH 3 (~ 99 %, using 50 mg L^{-1}). Moreover, for BS-*R.opacus* good results (70 to 90 %) are also found at the pH range between 5 and 7. Whilst, the performance of BS-*R.erythropolis* decreased with higher pH values, at pH 5 (70 to 85 %), lower than 40 % at pH 7 and negligible at alkaline medium.

Different behavior of both biosurfactants was observed during the flotation of apatite. The performance of BS-*R.opacus* was excellent at the entire studied pH, the maximum floatability (~ 99 %) was achieved at pH 3, using at least 50 mg L^{-1} and within 40 seconds. Whilst, when the BS-*R.erythropolis* was used the floatability of apatite achieved a maximum value of 80 %; these values were obtained at the pH range between 3 and 5. Moreover, it was necessary a higher biosurfactant concentration and larger flotation time than when the BS-*R.opacus* was used.

According to the previous results it is possible to stablish pH-concentrations regions for a selective mineral separation, e.g., for the calcite-dolomite system, these minerals are the most abundant carbonate mineral in the Earth [39] and their flotation understanding is still a relevant subject [40]. The flotation of dolomite will be possible using the BS-*R.opacus* (25 mg L^{-1}) at pH between 3 and 7, under these conditions it will be possible to obtain an average floatability of about 70 %. Using

higher BS concentrations (more than 100 mg L^{-1}) the dolomite floatability could achieve values of around 90 %, at pH 3. Floatability of calcite at this pH was no possible due to its high solubility degree. Between pH 5 and 7 the calcite floatability was around 15 %. It is possible to obtain lower floatability values of calcite (less than 10 %) at pH between 9 and 11, but the floatability of dolomite would also decrease (around 60 %). It was not observed a calcite-dolomite separation region for the BS-*R.erythropolis*.

The separation of apatite from hematite is important because an iron ore concentrate with high content of phosphorous can cause cold brittleness of steel produced [41]. The separation of apatite and hematite using the BS-*R.opacus* would be possible at low levels concentrations (25 mg L^{-1}) and at pH 9, under these conditions it is possible to achieve 80 % of apatite and less than 5 % of hematite. Higher concentration will increase the floatability of both minerals. The separation it is also possible at pH 11, using 50 - 75 mg L^{-1}, obtaining 85-90 % of apatite and around 10 % of quartz. The region for this separation, using the BS-*R.erythropolis*, was observed at pH 3, using 25 mg L^{-1}, but the content of hematite would be higher, achieving around 25 %.

Other important mineral system is the dolomite-apatite, according to literature the separation of apatite from dolomite is still unsatisfactory [42, 43]. In our studies it was observed that a separation would be promote using the BS-*R.erythropolis* at very low concentrations (25 mg L^{-1}) and at pH 3, however, the selectivity wouldn´t be satisfactory, dolomite floatability would be around 80 % and apatite´s around 25 %. Higher concentration values would increase the floatability of both minerals. At the pH range between 5 and 11 the floatability values of both minerals is very similar.

The most studied mineral system is the hematite-quartz [9, 27, 34, 44, 45], the separation of these minerals using BS-*R.opacus* would be possible at acidic conditions and using more than 50 mg L^{-1}. At pH 3 the floatability of hematite would be 80% and quartz around 10 %, increasing the BS concentration the flotability of both minerals would increase. The floatability of quartz would be lower (> 10 %) from pH 5 to 7, however the floatability of hematite also would be lower (around 70 %), the last could increase with higher BS concentration, achieving around 85 %. This higher concentration would not affect the quartz floatability. The use of the BS-*R.erythropolis* would promote the separation of quartz and hematite at pH 3 and 5. Low BS concentration (25 - 50 mg L^{-1}) promoted hematite and quartz floatability values around 90 % and 10 %, respectively. The maximum hematite floatability (~ 99 %) can be attained using 75 mg L^{-1}, but the floatability of quartz would also increase to values > 25 %. At pH 5 the separation is possible with BS concentrations higher than 100 mg L^{-1}, achieving floatability values around 80 %, while quartz would achieve around 10 %.

Iron ore flotation using biosurfactants

The previous results were applied in the flotation of iron ore using the BS-*R.opacus* as collector. All experiments were done under same conditions, as cell volume (300 mL). temperature (23 °C), air flow (30 mL min^{-1}), magnetic stirring and using a *Patridge-smith* cell, conditioning time (2 min.), flotation time (2 min.), mass of the sample (5 - 10 g.). The chemical analysis of the sample can be seen in Table 5, it was an itabiritic ore. Table 6 presents summary results of the iron ore flotation.

Table 5. Chemical composition of iron ore samples

Sample	Fe	SiO_2
Iron ore	47.05	31.82

As previously found flotation of hematite using the BS-*R.opacus* was possible at pH 3, with higher pH values the recovery was negligible. The last results are very different from *Hallimond-tube* results, this could be related to the higher volume cell and higher mass sample. Recovery of hematite achieved values up to 73 % and Fe grade up to 64 %, both are functions of the biosurfactant concentration, higher BS concentration the higher the recovery, but the lower the Fe grade. This effect is also found with conventional reagents. It was not possible to test higher masses due to the low suspension of the particles at this condition, which is a limiting condition of this flotation cell. These results confirm the founding in *Hallimond*-tube, and show the potential of these biosurfactants types for the flotation of iron ore.

Table 6. Flotation of iron ore - Patridge-smith cell

Experiment	1	2	3	4	5
Mass (g)	5	5	5	5	10
pH	3	3	5	7	3
BS Concentration (mg L^{-1})	50	100	100	100	25
Recovery (%)	59.17 ± 0.5	73.4 ± 1.2	6.77 ± 1.5	5.81 ± 2.3	31.0 ± 0.55
% Fe grade	61.38 ± 1.38	57.96 ± 0.8	55.4 ± 1.4	48.2 ± 1.1	63.89 ± 2.1

FINAL CONSIDERATIONS

These results showed that the interaction between highly hydrophilic minerals and bioreagents (microorganism cells and crude biosurfactants) promote a modification of the mineral surface becoming partially hydrophobic and as a consequence able to be floated. The adsorption mechanisms depend on the bioreagents type and also the mineral surface properties. It is believed that for microorganisms the adhesion mechanism is controlled by electrostatics interactions, especially for calcite and hematite. For quartz and apatite beside physical interactions (electrostatic), chemical adsorption (hydrogen bonding, chemical interactions forces) would be also involved. The last would explain the floatability results observed at pH where the mineral surfaces were negatively charged. It is believe that biosurfactants have anionic character, due to the presence of a negatively-charged carboxylate ion, thus during the mineral-biosurfactant interaction several mechanism would be involved (specific and non-specific). The adsorption/adhesion of the bioreagents is related to the modification of the zeta potential profile of the mineral, and as a consequence the modification in their surface properties. Apparently an extensive surface modification was produced by microorganism cells and thus high flotation rates were expected. Following the same thought the interaction of the biosurfactants, which modified the zeta potential profile of minerals in a less extension, would promote lower flotation rates. However, the flotation results showed low floatability values and long flotation times for the

microorganisms and higher floatability values with shorter flotation times for the biosurfactants. Thus, the previous indicate a higher performance of the biosurfactants and a stronger mineral collector character when compare with the microorganisms.

Finally, the microflotation of pure minerals can support to identify pH-concentration regions for a selective separation of different minerals, which was tested and satisfactory proven during the flotation of a real ore. Thus, it was possible to increase the concentration of hematite using the BS-*R.opacus* as a collector, with no necessity of the addition of frothers or chemical modifiers. It means that the BS-*R.opacus* presented a high selectively for hematite and can be successfully used as a collector. It is necessary to consider that these are preliminary studies and much more research is required in order to better understand the fundaments and behavior of these kind of bioreagents and just then we can thing about their feasibility and applicability in mineral processing.

Acknowledgements:

The authors gratefully acknowledge CNPq, ITV-VALE, CAPES and FAPERJ for supporting this research.

References

1. Sharma, P. K., Rao, K. H., Forssberg, K. S. E., Natarajan, K. A. (2001) ´Surface chemical characterisation of Paenibacillus polymyxa before and after adaptation to sulfide minerals´, International Journal of Minerals Processing. 62, 3-25,
2. Natarajan, K. A. (2006) ´Microbially-induced mineral flotation and flocculation: prospects and challenges´, Proceedings of XXIII International Mineral Processing Congress, 2006, 487-498,
3. Farahat, M., Hirajima, T., Sasaki, K., Aiba, Y., Doi, K. (2008) ´Adsorption of SIP E. coli onto quartz and its applications in froth flotation´. Minerals Engineering 21, 389-395,
4. Merma, A.G., Torem, M.L., Moran, J.V., Monte, M.B.M. (2013) ´On the fundamental aspects of apatite and quartz flotation using a gran positive strain as a bioreagent´, Minerals Engineering. 48, 61–67,
5. Sanwani, E.; Chaerun, S.; Mirahati, R.; Wahyuningsih T. 2016. Bioflotation: Bacteria-mineral interaction for eco-friendly and sustainable mineral processing. Procedia Chemistry, 19, 666 – 672. Elsevier.
6. Kim, Gahee; Choi, J.; Silva, R.A.; Song, Y.; Kim, H. 2017.Feasilibity of bench-scale selective bioflotation of copper oxide minerals using R. opacus. Hydrometallurgy, 168, 94 – 102. Elsevier.
7. Martin, F.; Kracht, W.; Vargas, T. 2018. Biodepression of pyrite using Acidithiobacillus ferroxidans in seawater. Minerals Engineering. 117, 127 – 131. Elsevier.
8. Silva, C.A., Cara, D.V.C., Silva, E.M.S., Leal, G.S.; Machado, A.M.; Da Silva, L.M. 2018. Apatite flotation using saponified baker´s yeast cells (saccharomyces cerevisiae) as a bioreagent. Journal of materials research and technology (article in press). ABM.

9. Mesquita, L.M.S., Lins, F.A.F., Torem, M.L., (2003) ´Interaction of a hydrophobic bacterium strain in a hematite–quartz flotation system´, International Journal of Mineral Processing 71, pp. 31–44.
10. Botero, A.E.C., Torem, M.L., Mesquita, L.M.S., (2007) ´Fundamental studies of Rhodococcus opacus as a biocollector of calcite and magnesite´. Minerals Engineering 20 (10), pp. 1026–1032.
11. Botero, A.E.C., Torem, M.L., Mesquita, L.M.S. (2008) ´Surface chemistry fundamentals of biosorption of Rhodococcus opacus and its effect in calcite and magnesite flotation´, Minerals Engineering. 21, 1, pp. 83–92.
12. Vilinska, A., Rao, K.H., (2008) ´Leptosririllum ferrooxidans-sulfide mineral interactions with reference to bioflotation and bioflocculation´, Transaction Nonferrous Material Society China 18, pp. 1403–1409.
13. Rao, K.H., Vilinska, A., Chernyshova, I.V., (2010) ´Minerals bioprocessing: R & D needs in mineral biobeneficiation´, Hydrometallurgy. 104, pp. 465–470
14. Farahat, M., Hirajima, T., Sasaki, K., Doi, K., (2009) ´Adhesion of Escherichia coli onto quartz, hematite and corundum: Extended DLVO theory and flotation behavior´. Colloids and surfaces B: Biointerfaces, 74, pp. 140–149.
15. Farahat, M., Hirajima, T., Sasaki, K., (2010) ´Adhesion of Ferroplasma acidiphilhum onto pyrite calculated from the extended DLVO theory using the van Oss-Good-Chaudhury approach´. Journal of colloids and interface science. 29, pp. 594–601.
16. Sarvamangala, H., Natarajan, K.A., (2011) ´Microbially induced flotation of alumina, silica/calcite from haematite´, International Journal of Minerals processing. 99, pp. 70–77.
17. Sarvamangala, K. A. Natarajan, S. T. Girisha. (2012) ´Biobeneficiation of Iron ores´, International Journal of Mining Engineering and Mineral processing. 1, 2, pp. 21–30.
18. Sarvamangala, H., Natarajan, K.A., Girisha, S.T., (2013) ´Microbially-induced pyrite removal from galena using Bacillus subtilis´, International Journal of Minerals processing. 120, pp. 15–21.
19. Pakudone, S.U., Natarajan, K.A.,(2011) ´Microbially induced separation of quartz from calcite using Saccharomyces cerevisiae´, Colloids and surfaces B: Biointerfaces. 88, pp. 45–50.
20. Khoshdast, H.; Sam, A.; Vali, H.; Noghabi, K.A. 2011. Effect of rhamnolipid biosurfactants on performance of coal and mineral flotation. International Biodeterioration & Biodegradation, 65, 1238 – 1243. Elsevier.
21. Subramanian, S., Santhiya, D. and Natarajan, K.A., (2003) ´Surface modification studies on sulphide minerals using bioreagents´, International Journal of Mineral Processing. 72, pp. 175-188.
22. Vasanthakumar, B., Ravishankar, H., Subramanian, S. (2013) ´Microbially induced selective flotation of sphalerite from galena using mineral-adapted strains of Bacillus megaterium´, Colloids and Surfaces B: Biointerfaces. 112, pp. 279 – 286.
23. Mehrabani, J.V., Noaparast, M., Mousavi, S.M., Dehghan, R., Rassoli, E., Hajizadeh, H., (2010) ´Depresion of pyrite in the flotation of high pyrite low-grade lead-zinc ore using Acidithiobacillus ferrooxidans´ Minerals Engineering. 23, 1, pp. 10–16.

24. Elmahdy, A. M., El-Mofty, S. E., Abdel-Khalek, M. A., Abdel-Khalek, N. A., El-Midany, A. A. (2013) ´Bacterially induced phosphate-dolomite separation using amphoteric collector´. Separation and Purification Technology. 102, 94-102,
25. Abdel-Khalek, M.A., El-Midany, A.A. (2013) ´Adsoprtion of Paenibacillus polymyxa and its impact on coal cleaning´, Fuel Processing Technology. 113, pp. 52–56
26. El-Midany, A.A., Abdel-Khalek, M.A. (2014) ´Reducing sulfur and ash from coal using Bacillus subtilis and Paenibacillus polymyxa´. Fuel 115, pp. 589–595.
27. Puelles, J.G.S. 2016. Hematite flotation using a crude biosurfactant extracted from R. opacus. Master Dissertation. Chemical Department, Pontifical Catholic University of Rio de Janeiro.
28. Schmitt, J.; Flemming, H.C. 1998. FTIR-spectroscopy in microbial and material analysis. International Biodeterioration & Biodegradation 41, 1 – 11.
29. Puzey, K.A.; Gardner, P.J.; Petrova, V.K.; Donnelly, C.W.; Petrucci, G.A. 2008. Automated species and strain identification of bacteria in complex matrices using FTIR spectroscopy. Proceedings of SPIE - The International Society for Optical Engineering (Proceedings of SPIE). 3, 1 – 9. Society of Photo-optical Instrumentation Engineers.
30. Naumann, D. 2000. Infrared Spectroscopy in Microbiology. Encyclopedia of Analytical Chemistry (R.A. Meyers), 102 – 131. Jhon Wiley & Son.
31. Garip, S., Gozen, A.C., Severcan, F., 2009. Use of Fourier transform infrared spectroscopy for rapid comparative analysis of Bacillus and Micrococcus isolates. Food Chem. 113 (4), 1301–1307. Elsevier.
32. Yang H, Li T, Chang Y, Luo H, Tang Q. 2014. Possibility of using strain F9 (Serratia marcescens) as a bio-collector for hematite flotation. Int J Miner Metall Mater. 21, 3, 210–5. Springer.
33. Rao, K.H., Subramanian, S., (2007) ´Bioflotation and bioflocculation of relevance to minerals bioprocessing´, In: Microbial processing of metal sulfides (Edgardo R. Donati e Wolfgang Sand), pp. 267–286
34. Olivera, C.A.C. 2018. Hematite-quartz system flotation using the soluble biosurfactant extracted from R. erythropolis. Doctoral Thesis. Chemical Department, Pontifical Catholic University of Rio de Janeiro.
35. Yang, H., Tang, Q., Wang, C., Zhang, J., (2013) ´Flocculation and flotation response of Rhodococcus erythropolis to pure minerals in hematite´, Minerals Engineering 45, pp. 67–72.
36. Barros, A.F. Luiz, Ferreira, Eliomar E., Peres, Antonio E.C., (2008) ´Flotability of apatites and gangue minerals of an igneous phosphate ore´. Minerals Engineering 21, pp. 994–999.
37. Kou, J., Tao, D., Xu, G., (2010) ´Fatty acid collectors for phosphate flotation and their adsorption behavior using QCM-D´ International Journal of Mineral Processing 95, pp. 1–9.
38. Lopez, L.Y.; Merma, A.G.; Torem, M.L.; Pino, G.H. 2015. Fundamental aspects of hematite flotation using the bacterial strain Rhodococcus ruber as bioreagent. Minerals Engineering, 75, 63-69. Elsevier.

39. Sun, J.; Wu, Z.; Cheng, H.; Zhang, Z.; Frost, R.L. 2014. A Raman spectroscopic comparison of calcite and dolomite. Spectrochimica Acta Part A: Molecular and Biomolecular Spectroscopy. 117, 158 – 162. Elsevier.
40. Azizi, D.; Larachi, F. 2018. Surface interactions and flotation behavior of calcite, dolomite and ankerite with alkyl hydroxamic acid bearing collector and sodium silicate. Colloids and Surfaces A: Physicochemical and Engineering Aspects. 537, 126-138. Elsevier.
41. Nan, N.; Zhu, Y.; Han, Y. 2019. Flotation performance and mechanism of α-Bromolauric acid on separation of hematite and fluorapatite. Minerals Engineering, 132, 162-168. Elsevier.
42. Cao, Q.; Zou, H.; Chen, X.; Wen, S.; 2019. Flotation selectivity ofN-hexadecanoylglycine in the fluorapatite–dolomitesystem. Minerals Engineering, 131, 353 – 362. Elsevier.
43. Liu, X.;. Li, C.; Luo, H.; Cheng, R.; Liu, F. 2017. Selective reverseflotation of apatite from dolomite in collophanite oreusing saponified gutter oil fatty acid as a collector. International Journal of mineral processing, 165, 20-27,
44. Wengang, L.; Wenbao, L.; Xinyang, W.; Dezhou, W.; Hao, Z.; Wei, L. 2016. Effect of butanol on flotation separation of quartz from hematitewith N-dodecyl ethylenediamine. International journal of mining science and technology. 26, 1059 – 1063. Elsevier.
45. Peçanha, H. R., Albuquerque, M. D. F., Simão, R. A., Leal Filho, L. S., Monte, M. B. M. (2019) Interaction forces between colloidal starch and quartz and hematite particles in mineral flotation. Colloids and surfaces A, 562, 79-85.

XIII International Mineral Processing and Recycling Conference
Belgrade, Serbia, 8-10 May 2019

University of Belgrade, Technical Faculty in Bor
Vojske Jugoslavije 12, 19210 Bor, Serbia
Tel. +381 30 424 555 Fax +381 30 421 078

RECYCLING OF THE CRITICAL RAW MATERIALS FROM WASTE ELECTRONICS

Željko Kamberović #
University of Belgrade, Faculty of Technology and Metallurgy,
Belgrade, Serbia

ABSTRACT

The rising criticality of technologically inevitably metals and the continuous growth of the waste electronics promotes a scientific need for development of innovative recycling process, both efficient and selective. Experimental results showed primarily that by pyrometallurgical treatment it is difficult to achieve selectivity, and secondary that the distribution of metals in melting products is too complicated, deviating from the experiential and expected. Therefore, application of an integral pyro - hydrometallurgical treatment is suggested for improved raw materials efficiency. Successful implementation of the developed state-of-art technological process, guarantee more efficient approach to recycling processes, production of new materials which supports the concepts of sustainable development and cleaner production. Proposed technological solution is applicable in industry with relatively low investments compared to expected revenues, allowing companies to become competitive in the regional market and beyond, which is particularly important for small and medium enterprises with lower operating capacities. This lecture explains measures for the further development of the recycling industry as a part of circular economy strategy in Serbia.

Key words: metallurgy, recycling, WEEE, circular economy

corresponding author: kamber@tmf.bg.ac.rs

SECTION LECTURE

XIII International Mineral Processing and Recycling Conference
Belgrade, Serbia, 8-10 May 2019

University of Belgrade, Technical Faculty in Bor
Vojske Jugoslavije 12, 19210 Bor, Serbia
Tel. +381 30 424 555 Fax +381 30 421 078

OBTAINING THE APPLICABLE MATERIAL FROM THE FFW AND ZEOLITIC TUFF

Mira Cocić [1, #], Mihovil Logar [2]
[1]University of Belgrade, Technical Faculty in Bor, Bor, Serbia
[2]University of Belgrade, Faculty of Mining and Geology, Belgrade, Serbia

ABSTRACT – This paper presents the characteristics of synthesized glass-ceramics obtained by sintering the mixture of final flotation waste (FFW) with zeolite tuff (originated from Igroš near Brus, Serbia). The investigation were conducted with the aim of finding the possibility of using FFW (waste material) originating from RTB Bor Company (Zijin Bor Copper DOO, Serbia).
By the thermal treatment of T20 (20 % of zeolite fuff, 80 % FFW) and T40 (40 % of zeolite tuff, 60 % FFW) blends on temperature up to 1260 °C over a period of 7 hours, the glass-ceramics of dendritic structure were synthesized. Synthesized glass-ceramics consists of two phases: iron oxide crystals (maghemite, magnetite and hematite) and glass with an approximate phases ratio of 68/32 (T20) and 77/23 (T40). Relatively low shrinkage of synthesized material (up to 7 %) provides reliable control when designing a given shape, which indicates that such glass-ceramics can be used as basis for the building materials.

Key words: FFW, zeolite tuffs, sintering, glass-ceramics, phase composition, microstructure.

INTRODUCTION

In the process of concentration the copper ore, and also, during the processing of copper concentrate, waste materials are generated [1]. Mining and flotation waste deposits and molten slag depots represent large areas of degraded land and permanent sources of pollution of the surrounding soil, water and air [1 - 4]. That is the main reason why recycling of industrial waste materials is often topic of many papers.

Vitrification of waste originating from the copper [5, 6] and zinc [7] industry produces glass-ceramic, chemically stable materials, with the significantly better characteristics than traditional ceramics and natural building materials. Also, slags from high-pressure furnaces are used as additives for cementitious materials [8, 9] and as additives to building materials [9, 10]. By mixing such materials with quartz sand, aluminum silicate glass with a low dielectric constant and low dielectric loss can be obtained [11].

corresponding author: mcocic@tfbor.bg.ac.rs

Since ancient times, the application and use of zeolitic tuffs for lightweight construction stone have been known [12]. Particularly zeolite clinoptilolite has a wider application in construction [12]. Further, it was used as a pucolan in the production of cement [13 - 15], and as a supplement to the concrete mixture [16, 17] for the production of lightweight concrete. Also it was used as a thermal insulation material [18]. By melting of the copper flotation slag (30 %), slag of high furnace (30 %) and zeolite tuff (40 %) in electric furnaces for 30 min at 1400 °C, a mixture of high degree of crystallization was obtained, suitable for the production of glass ceramics [5].

Zeolite tuff in certain relationships with the FFW may have an application for the production of glass-ceramic material [4, 19]. This paper describes the research of the potential application of FFW mixture with tuff for obtaining the glass-ceramic materials. The glass-ceramics was synthesized by sintering the FFW mixture with zeolite tuff (Igroš near Brus, Serbia). The aims of our research were investigating the dynamics of liquid phase development, to lower the sintering temperature, sintering interval, and density.

MATERIALS AND METHODS

In the process of flotation the slag from the copper smelting, the final flotation waste (FFW) is created. In order to investigate the possibility of using FFW as a raw material for the production of glass-ceramic materials, a sample of FFW was taken prior to transport to the landfill [4, 19, 20]. The site from which the sample of zeolite tuff was taken (Igroš - Vidojevići), Serbia is about 8 km east of Brus and 3 km northeast of Rasina. The zeolite tuff is interstratified in the Miocene-Pliocene series of marble green clays, which make up the bottom and brown clay and sandbags that make up a draw. The layer of zeolite tuff is light gray to white (Figure 2a), 1-4 m thick, with general east-west distribution [21].

The tests are divided into two parts. The first part covered the characterization of the starting materials (FFW and tuff) where the chemical composition, phase composition (polarization microscope, X-ray diffraction, DTA analysis, and infrared spectroscopy) and thermal properties (sintering, softening and melting interval) were examined [4, 19, 20].

The second part of the study involved the process of obtaining and characterizing synthesized glass-ceramics from a mixture of FFW with tuff: T20 (20 % tuff, 80 % FFW) and T40 (40 % tuff, 60 % FFW) at 1260 °C / 7 h [4].

The sintering temperature was designed based on thermal characteristics of the raw materials and, also, based on data from the literature [5, 6, 22-25].

The glass-ceramic material was obtained by sintering the samples in the presence of a liquid phase. The sintering interval of the FFW is difficult to control, so that, this requires a type of filler. The material to be synthesized should bear the physical properties of the added material (zeolite tuff), while the FFW should provide the liquid phase needed to achieve the synthesis.

RESULTS AND DISCUSSION

Chemical and phase composition of raw materials (FFW and zeolite tuff) obtained by XRPD and XRF method is shown in Table 1. In the chemical composition of FFW

dominates iron and oxides of silicon, while in the zeolite tuff, oxides of silicon and aluminum are most present ingredients.

The phase composition of FFW is calculated based on X-ray diffraction analysis (Fig. 1a) and chemical composition using theoretical, stoichiometric formulas of magnetite and fayalite (given in Table 1). FFW consists of: fayalite (40 %), magnetite (25 %) and glass (35 %), which represents an important basis for the production of glass-ceramics. Zeolite tuffs are built from the clinoptilolite, plagioclase, biotite, and smectite (Figure 3a) [4, 19].

Figure 1b shows the DTA diagram. As a result of the loss of adsorbed moisture, endothermic reaction is pronounced at the 110 °C. As a result of the oxidation of magnetite into hematite γ -Fe_2O_3 (on the surface of the grain) (reaction 1) an exothermic reaction occurs at the 400 °C. As a result of oxidation of magnetite into hematite γ -Fe_2O_3 (in the grain core), an exothermic reaction also occurs at 575 oC [26]. An exothermic reaction of the γ -Fe_2O_3 transition to α-Fe_2O_3 (reaction 1) arose at a temperature of 705 °C.

$$Fe_3O_4 \rightarrow \gamma Fe_2O_3 \rightarrow \alpha Fe_2O_3 \quad (1)$$

Microscopic examination of the zeolite tuff (Fig. 2b) show that it was mainly built from fine-grained amorphous volcanic ash, which is largely zeolitized, ie, transformed into clinoptilolite and fragments of minerals: biotite, plagioclase and quartz, and quite rarely amphibians, just after some zirconium grain. Plagioclase is well preserved with developed polysynthetic lamellas and sometimes zonal. Quartz grains are sloping, arched, broken, with frequent undulatory eclipse. Foxes of biotite are sometimes deformed. The grain size of the listed minerals belongs to class of above 0.06 mm.

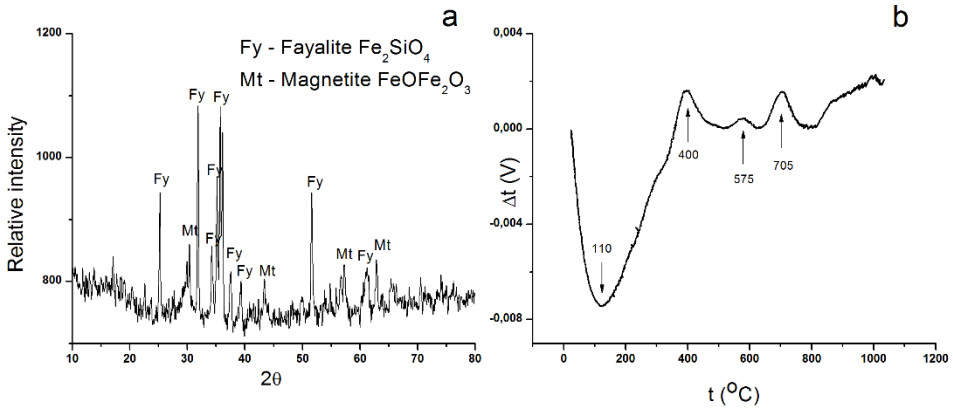

Figure 1. a) X-ray powder diffraction diagram of FFW [4]; **b)** DTA diagram of FFW

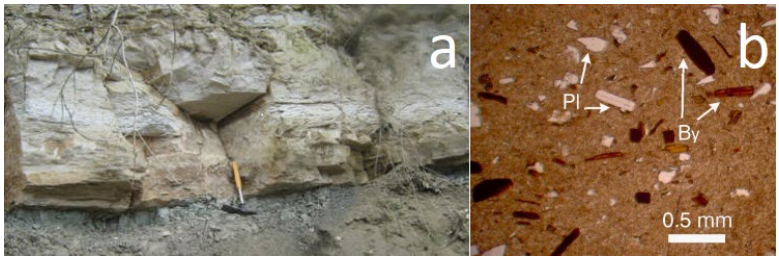

Figure 2. a) Zeolite tuff (Igroš - Vidojevići); **b)** Micro photography of zeolite tuff (Pl - plagioclase, By - biotite)

Table 1. Chemical and phase composition of raw materials and glass-ceramics (T20 and T40)

Oxides	Share (%)						
	FFW				Zeolite tuff	T20	T40
		Mt	*Fy*	*Glass*			
SiO_2	34.27	-	13.64	20.63	57.91	41.11	46.13
TiO_2	0.36	-	-	0.36	0.54	0.42	0.49
Al_2O_3	4.89	-	-	4.89	11.44	6.47	7.82
Fe_2O_3	52.1	25.34	25.97	0.78		44.43	37.61
FeO		-	-		4.54		
Mn_3O_4	0.07	-	-	0.07			
MgO	0.79	-	-	-	1.47	1.10	1.17
CaO	4.58	-	0.79	4.58	5.11	4.80	5.21
Na_2O	0.31	-	-	0.31	0.95	0.41	0.64
K_2O	1.2	-	-	1.22	0.72	1.12	1.06
P_2O_5	0.07	-	-	0.07			
SO_3	0.5	-	-	0.5			
CuO	0.49	-	-	0.49			
H_2O^+					14.43		
H_2O^-					3.6		
sum %	**100.44**	25.34	40.4	34.7	**100.71**	**99.86**	**100.13**
Phase composition	**Fy, Mt, glass**				**Kp, Pl, By, Sm**	**Mhm, Mt, Hm**	**Mhm, Mt, Hm**

Legend: **FFW** - Final flotation waste, **Fy** - fayalite (Fe_2SiO_4), **Mt** - magnetite ($FeFe_2O_4$), Kp - clinoptilolite $(Ca,Na,K)_{2\text{-}3}Al_3(Al,Si)_2Si_{13}O_{36} \times n(H_2O)$, Pl - plagioclase, By - biotite ($K(Mg,Fe)_3AlSi_3O_{10}(OH,F)_2$), Sm - smectite, Mhm - Maghemite ($Fe^{3+}{}_2O_3$), Hm - Hematite (Fe_2O_3)

The infrared spectrum of the zeolite tuff is shown in Figure 3b. A series of absorption maxima in the shown spectrum corresponds to clinoptilolite. The strips at 3595 cm^{-1} and 3427 cm^{-1} originate from the valence vibrations of OH groups, and the band at 1630 cm^{-1} of the H_2O molecule is in removable structural positions characteristic of zeolites. The absorption peaks between 800 and 1300 cm^{-1} are due to the vibration of the Si-O-Si lattice.

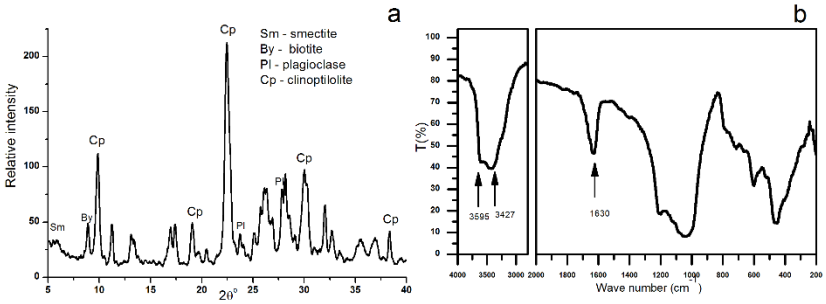

Figure 3. a) X-ray powder diffraction diagram of zeolite tuff (Igroš - Vidojevići), **b)** IR spectra of zeolite tuff

The results of testing the thermal properties of the row materials, determined by the thermal microscope at a 12 °/min regime, are shown in Figure 4 (together with the mixing diagrams) and in Table 2. Zeolite tuff has several temperatures of beginning and end of sintering, but it has less change in volume (5.4), and significantly narrower sintering interval (20) compared with the FFW.

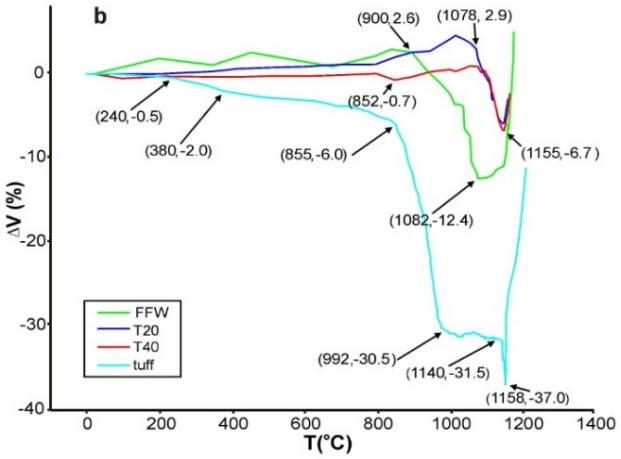

Figure 4. Changes in the volume of row materials as a function of temperature (T, ΔV)

Due to the dehydration of clinoptilolite (which is the dominant mineral in the zeolite tuff) at 240 - 350 °C, the shrinkage occurs (2 %). A large contraction caused by the collapse of the clinoptilolite structure occurs within a temperature range from 850 to 950 °C. The development of the liquid phase begins at 1140 °C, which is the beginning of sintering. The end of the sintering occurs at 1160 °C, together with the sample deformation [4, 19].

The mean chemical composition (fields) of the FFW mixture with the zeolite tuff (T20 and T40) obtained by SEM-EDS analysis is shown in Table 1. The analyses were made to total iron, and the results in Table 1 were converted to Fe_2O_3.

Table 2. Thermal characteristics of raw materials and mixtures

Thermal characteristics	Samples			
	Raw materials		FFW mixtures with zeolite tuff	
	FFW	Zeolite tuff	T20	T40
Start of sintering (℃)	900	1,140	1,080	1,080
End of sintering (℃)	1.090	1,160	1,160	1,160
Interval of sintering (℃)	190	20	80	80
Change in volume (%)	13	5.5	7	7

By the thermal treatment of the FFW mixtures with zeolite tuff (T20 and T40) to a temperature of 1260 ℃ over a period of 7 hours a glass-ceramics was synthesized, consisting of glass phase and iron oxide crystals, as shown in Figure 5. The morphology of obtained glass-ceramics is typical for the hematite crystals, due to subhedral rhombohedral crystals. X-ray diffraction analysis identified hematite, maghemite, and magnetite (Figure 6) indicating a structural variation [4, 19].

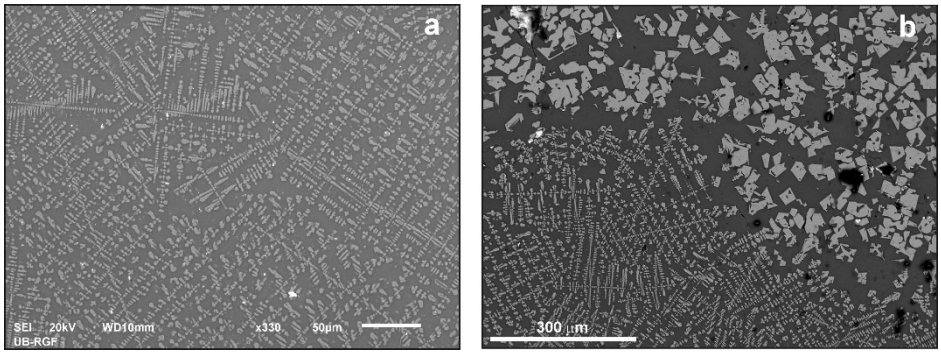

Figure 5. Microphotography of the glass-ceramics (SEM) obtained from: **a)** T20, and **b)** T40

In the T20 samples (Figure 5a), a microstructure with homogeneous fully crystalline material is formed in the form of small rounded crystals of iron oxide in the size lesser than 1 μm. The crystals grow in the form of an interconnected dendritic grid [4, 19]. The same microstructure of the glass was presented in [27].

When the crystals grow, its internal free energy is exchanged with the environment, and if the temperature gradient between the crystal and the environment is large, the diffuse heat exchange ceases to be operational. In such cases, convection is seen as an energy transfer mechanism which produces a dendritic structure [28]. Dendritic crystals in glass represent a kind of structural reinforcement and can improve the general mechanical properties of glass-ceramics such as, elasticity, which is important because the brittleness is weakness of glass-ceramics.

In the T40 samples (Figure 5b), the iron-oxide crystals form dendrites, which are concentrated in one part of the sample, while in another part of sample they appear as individual crystals. Probably the sample wasn't cooled homogeneously. In the zones that are at short distances, there was a difference in the cooling rate, so

dendrites and crystals appear. The crystals appear in subhedral and euhedral forms, and the rhombohedral forms are also noticed [4, 19].

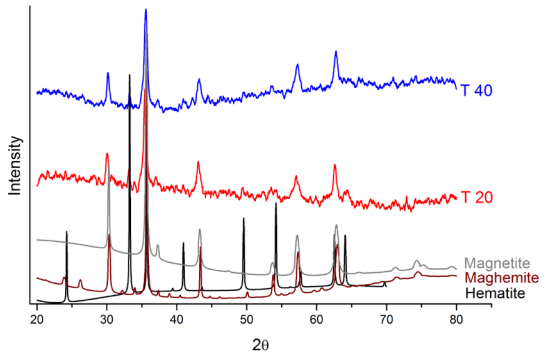

Figure 6. X-ray powder diffraction diagrams of the obtained glass-ceramics

The content of the crystals in the synthesized glass-ceramics is determined by integration with the digital image analysis, based on the surface they occupy in the observed cross-section. The content of the crystals in T20 samples is 32.3 %, and in T40 is 23.3 %. Contrary to expectations, the content of crystals does not increase with the increase of the concentration of zeolite tuff. The reason for this may be the choice of the integrated surface, because only one field of view was used for the integration. The changes in dimension of samples as a function of temperature are shown in Figure 4 and Table 2.

FFW mixtures with zeolite tuff (T20 and T40) do not show a contraction caused by the collapse of the clinoptilolite structure (850 to 900 °C) as happens to pure zeolite tuff. This effect is absent because the temperature range coincides with the development of liquid phase of FFW. The reaction of the FFW particles with the clinoptilolite dominated zeolite tuff particles does not allow its structural collapse. Minimum contraction (-0.7 %) is observed at 850 °C (T40) indicating the onset of collapse of the clinoptilolite structure. The temperature of start of sintering, for both the mixtures, is close to start of sintering of FFW (1080 °C). The end of sintering temperature for T20 and T40 coincides with the end of sintering of the pure zeolite tuff (1160 °C) [4, 19].

CONCLUSION

The glass-ceramic material obtained by sintering the mixture of FFW and zeolitic tuff T20 (20 % tuff, 80 % FFW) and T40 (40 % tuff, 60 % FFW) at a temperature of 1260 °C for 7h, consists of iron-oxide crystals (maghemite, magnetite, and hematite) and glass. An approximate ratio of phases was 32/68 (T20) and 23/77 (T40). Crystals mostly appear in the form of dendritic aggregates, which represent kind of the structural reinforcement and improve the general mechanical properties of glass-ceramics. A relatively small shrinkage of synthesized material (about 7 %) provides reliable control in obtaining a given shape. This indicates that such material can be used as a basis for building materials.

Acknowledgements:

This work is partly funded by the Grant of the Ministry of Education, Science and Technological Development of the Republic of Serbia, project 176010: 'Composition, genesis, application and contribution to the environmental sustainability'.

References

1. Dimitrijevic, M., Kostov, A., Tasic, V., Milosevic, N. (2009) J. Hazard. Mater., 164, 892-899,
2. Stanojlović, R., Stirbanovic, Z., Sokolovic, J. (2008) JMM, 44, 44-50,
3. Bogdanovic, G., Trumic, M., Trumic, Maja, Antic, D. (2011) ROR, 4, 37-43,
4. Cocić, M. (2012) Application of the flotation waste from the RTB Bor for glass-ceramics. PhD thesis, University of Belgrade, Faculty of Mining and Geology, Belgrade, Serbia,
5. Karamanov, A., Aloisi, M., Pelino, M. (2007) J. Hazard. Mater., 140, 333-339,
6. Coruh, S., Nuri, E. O., Cheng, T. (2006) Waste Manage. Res., 24, 234-241,
7. Pelino, M. (2000) Waste Manage., 20, 561-568,
8. Alp, I., Deveci, H., Sungun, H. (2008) J. Hazard. Mater., 159, 390,
9. Gorai, B., Jana, R. K., Premchand (2003) Resour. Conserv. Recy., 39, 299,
10. Asokana, P., Saxena, M., Asolekar, S. R. (2007) Build. Environ., 42, 2311,
11. Li, S., Huang, S., Liu, H., Wu, F., Chang Z. Yue, Y. (2015) JOM, 67, 2754,
12. Margeta, K., Farkaš, A., Glasnović, Z. (2011) Građevinar, 63, 1009,
13. Ahmadi, B., Shekarchi, M. (2010) Cement Concrete Comp., 32, 134,
14. Bilim, (2011) Constr. Build. Mater., 25, 3175,
15. Sasnauskas, V., Rinkevičius, G., Martinavičius, D., Vaičiukynienė, D. Ivanauskas, E. (2015) JSACE 2, 11,
16. Ramezanianpour, A., Kazemian, A., Sarvari, M. Ahmadi, B. (2013) J. Mater. Civ. Eng., 25, 589,
17. Karakurt, C., Kurama, H., Bekir, T. I. (2010) Cement Concrete Comp., 32, 1,
18. Djambazov, S., Yoleva, A., Chervenliev, P., Georgiev A., J. (2015) Chem. Technol. Metall., 50, 520,
19. Cocić, M., Logar, M., Erić, S., Tasić, V., Dević, S., Cocić, S., Matović. (2017) B. Sci. Sinter. 49 (4), 431-443,
20. Cocić, M., Logar, M., Matović, B., Dević, S., Volkov-Husović, T., Cocić, S., Tasić V. (2016) Sci. Sinter., 48 (2) 197-208,
21. Obradović, J. (1977) Geol. Anali Balk. Pol., XLI, 293-302,
22. Karamanov, A., Arrizza, L., Ergul, S. (2009) J. Eur. Ceram. Soc., 29, 595,
23. Karamanov, A., Taglieri, G., Pelino, M. (1999) J. Am. Ceram. Soc., 82, 3012,
24. Rincon, M., Càceres, J., Gonzàles-Oliver, C. J., Russo, D. O., Petkova, A. Hristov, H. (1999) J. Therm. Anal. Calorim., 56, 931,
25. Karamanova, A., Ergul, S., Akyildiz, M. Pelino, M. (2008) J Non-Cryst. Solids., 354, 290,
26. Ivanova, V. P., Kasatov, B. K., Krasavina, T. N., Rozinova, E. L. (1963) Kolterman&Miller, Termijska analiza minerala i rudnih minerala,
27. Romero, M. Rincon, J. Ma. (1998) J. Eur. Ceram. Soc., 18, 153,
28. Badillo, A., Ceynar, D., Beckermann, C. (2007) J. Cryst. Growth, 309, 197.

PAPERS BY SECTIONS

XIII International Mineral Processing and Recycling Conference
Belgrade, Serbia, 8-10 May 2019

University of Belgrade, Technical Faculty in Bor
Vojske Jugoslavije 12, 19210 Bor, Serbia
Tel. +381 30 424 555 Fax +381 30 421 078

DETERMINATION OF SURFACE MOISTURE AND PARTICLE SIZE DISTRIBUTION OF COAL USING ON-LINE IMAGE PROCESSING

Piyush Khatri [1], Puneet Choudhary [1], Brahma Deo [1,#], Parimal Malakar [2], Sourav Saran Bose [2], Gyanranjan Pothal [2], Partha Chattopadhyaya [2]
[1]School of Minerals, Metallurgical and Materials Engineering IIT Bhubaneswar, Odisha, India
[2]TATA Sponge Iron Limited (TSIL), Joda, Odisha, India

ABSTRACT – Experiments on laboratory scale and subsequently on the moving conveyor belt in the plant are carried out so as to determine the optimal conditions of simultaneous determination of moisture and particle size for the first time in a sponge iron plant using rotary kilns; the -3mm particle size in coal varies from 20-65%, approximately; variation in moisture in coal is from 8-15%, approximately. The pixel intensity information is used to find the moisture content in the coal using MATLAB. Similarly, a MATLAB program is used to determine particle size distribution from the gray scale images obtained under LED light.

Key words: coal, size distribution, moisture content, image processing, rotary kiln

INTRODUCTION

The rotary kiln for sponge iron production uses iron ore (62-65% Fe) and poor quality coal (up to 25% ash, -3mm fines reaching up to 60%, and moisture up to 15%). There are three rotary kilns at TATA sponge with a total production capacity of 4.20,000 tons per year at present. In a plant situation, apparently for the reasons of economy, there is little choice over control of particle size and moisture and the raw materials have to be used (both iron ore and coal) as procured. Present work focuses on determination of particle size and moisture in coal only. In the earlier plantpractice the samples of coal were analyzed on 8 hour basis, but a study showed that the variations were large even on hourly basis. For a good control of kiln operation it is necessary to know coal particle size distribution and the moisture in it so that the related operating parameters can be adjusted accordingly.

A specific size range of coal is desired for the reduction of iron ore to sponge iron. Coal is fed both from feed side and from injection side. A large fraction of fine particles in coal adversely affect the quality of sponge iron produced, as also shown

corresponding author: bdeo@iitbbs.ac.in

in Fig. 1. In addition to this, part of the fine coal (7-10% of coal added from feed side of kiln) is physically entrained in high velocity exhaust gases and hence swept out of kiln without being used. Thisincreases coal consumption per ton of sponge iron produced. Coal is the costliest raw material added to the kiln.

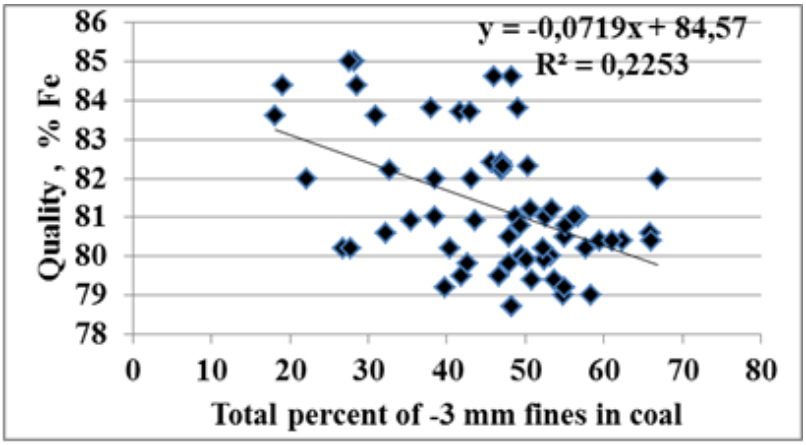

Figure 1. Effect of percentage of -3mm fraction in coal on temperature at T9 location in kiln

Moisture in coal also affects the quality of sponge iron produced. At high temperature, the moisture present in the coal reacts with carbon and produce carbon monoxide and hydrogen by an endothermic water gas reaction.

$$H_2O_{(g)} + C \rightarrow CO_{(g)} + H_{2(g)} \quad (1)$$

Even though the reducing gases (CO + H_2) are produced and hydrogen is a more efficient reducing agent for iron oxide, the temperature of reduction goes down which directly reduces the quality of product.

The use of image processing for particle size and moisture determination is widely practiced [1-9]. The property which is used for moisture determination is the variation in reflectivity of coal surface with moisture content.

A special feature of the present work is that the image processing experiments have been done with LED lights to determine particle size and moisture in coal simultaneously, from single image, online, on the shop floor, automatically, at short time intervals. The camera and the lights are placed just before the coal enters (through conveyor belt) the coal injection facility of the kiln. Optimal height for best and simultaneous determination of moisture and particle size is found out by rigorous experiments. The information obtained on moisture and particle size is fed to process control models of rotary kiln which have already been developed at TATA sponge [10]. The models are used for advising appropriate actions to be taken for adjusting the control parameters like air flow rate, coal feed rate, rotation speed of kiln, ore coal ratio, etc. The objective is to minimize accretions and maximize kiln productivity. It constitutes a part of the overall program at TATA sponge devoted to implementation of “Industry 4.0” (or “smart factory”).

LABORATORY EXPERIMENT ON DETERMINING PARTICLE SIZE DISTRIBUTION OF COAL

A typical analysis of coal used in present work is moisture: 8.3%, +20 mm: 2.1%, +18 mm: 1.5%, +15mm: 3.2%, +8mm: 14.7%, +5mm: 12.1%, +3mm: 9.7%, +2mm: 10.3%, +1mm: 12.9%, -1mm: 33.5%. The objective of image analysis is only to find out the total % of -3 mm fractions in coal and not the entire particle size distribution. Initial laboratory experiments to investigate the applicability of technique were doneat a fixed height of camera of 40 cm placed normal to the sample surface. Image (194x176 pixels) was taken under LED flashlight and wasused for particle size distribution analysis. For the sake of verification, conventional sieve analysis was also done.

The analysis of imageis done by using MATLAB. A simple code "imread (image)" is used to load the image in the workspace of MATLAB. The image in the workspace is cropped using "imcrop" function. The 3D part of the cropped image is converted to 2D using "graythresh" function. The image in the workspace of MATLAB will be RGB image and it is converted to the binary image so that detection of the particle can be done in the image. Morphological operations are performed on the binary image using "bwmorph" function to draw the boundary of particles in the image. To distinguish the particles from the binary image, the "watershed" function is used. This function detects the particle from a binary image by treating it as a surface where light (white) pixels represent high elevations and dark (black) pixels represent low elevations.

The area of the detected particles is calculated using "regionprop" function. Initially, the image of the particle with size 3mm is loaded in the code and average area of the detected particle was calculated. The image of the reference sample was taken at 40 cm from the sample and the average area of the particle with size 3 mm is taken as reference for further calculation. Now, the image of the mixed sample which was taken from the coal feeder is read in the MATLAB code and the area of the particles in the image is calculated. All the areas of detected particles of the mixed sample from the image are divided into two groups: (a) particles with size less than 3 mm and (b) particles with size equal and larger than 3 mm. These groups are represented graphically with their percentage of size distribution in the image. As an example, the image of particles is shown in Fig. 2(a) and its binary image is shown in Fig. 2. (b). Graphical distribution is shown in Fig. 3. A small error is inbuilt in this procedure because the overlap of particles has not been considered [6].

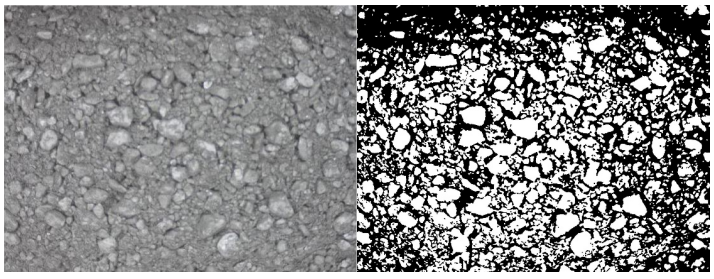

Figure 2. (a) Image of coal sample from the feeder of coal (RHS) and (b) its binary image (LHS)

The area of the detected particles was calculated and using this we plotted the percentage distribution of different size ranges of coal.

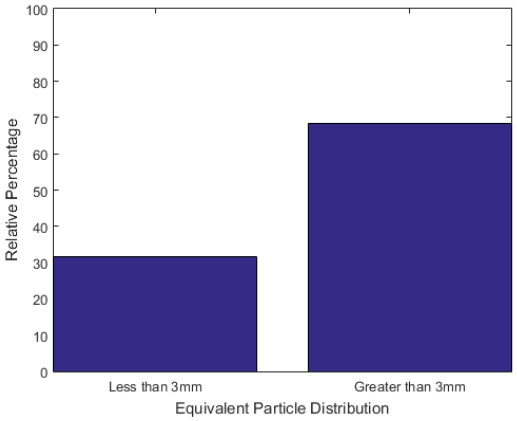

Figure 3. Particle size distribution of coal using image processing;
- 3 mm fraction is 30 %

LABORATORY EXPERIMENTS ON DETERMINING SURFACE MOISTURE CONTENT OF COAL

The reflectance of coal varies with its surface moisture content. This difference in reflectivity of coal with different surface moisture content will have different pixel intensity information in its image. This pixel intensity information can be used to predict the moisture content in the coal. The intensity information of the two images was calculated using the MATLAB code. The difference in intensity information of two coal samples with different moisture contents is seen in Fig. 4 (a) and4 (b).

All the images are made up of three primary colours, namely red, green and blue. The variation of intensity information with surface moisture was studied by formulating two different MATLAB models. When the image is loaded in the workspace of MATLAB, it is uploaded as a 3-D matrix of red, green and blue intensity information of each pixel of the image. In the first model, we convert the RGB image into a grayscale image in which the 3-D matrix is converted to an equivalent 2-D matrix. This 2-D matrix of a grayscale image is used to predict the surface moisture content in coal.

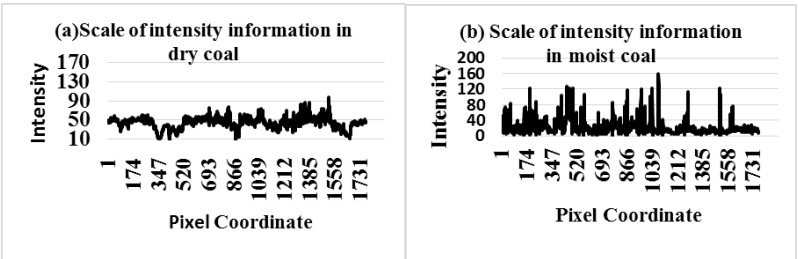

Figure 4. Images were taken in flash light: (a) scale of intensity information for dry coal and (b) scale of intensity information for moist coal

In the second model, instead of converting the RGB (3-D matrix) of the image to an equivalent 2-D matrix, the red, green and blue intensity information is directly used to predict the surface moisture of coal. From the red, green and blue intensity, DN (Digital number) [9] values are calculated. The DN value of each pixel with red, green and blue intensity as r, g, and b respectively is given as:

$$DN = (0.2999 \cdot r) + (0.5870 \cdot g) + (0.1140 \cdot b) \quad (2)$$

These DN values are used to predict the surface moisture of coal. No significant difference was observed in the results of gray scale image and RGB image for coal samples used in this work, with former being slightly more accurate.

Three different light sources, namely LED flashlight, normal light (tube light 40 watts) and IR lamp were used to find the best one. In each case a sample of 20 gm coal with moisture varying from 0% (dry coal), 2-3%, 7-8%, 12-13%, 17-18% and 22-23% were prepared in laboratory. Five images of each sample were taken with a camera normal to the surface at a height 40 cm under light source and their variation of intensity information in the image with its respective moisture content was studied. In normal light saturation effects started to show after 15% moisture, Fig. 5 (a). No saturation occurred with LED and IR lamps. As an example, sum of intensities under LED light is shown in Fig. 5 (b).

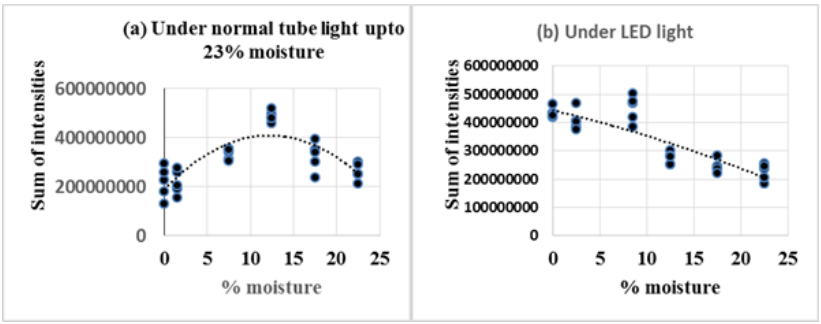

Figure 5. Sum of intensities under (a) normal and (b) LED light

It can be seen from Fig 5 (b) that the results of image analysis with LED when compared with actual values, agree within 15% of the moisture value up to 25% moisture in coal. This LED light sources with gray scale image analysis (Model 1 described above) was therefore adopted for industrial trials on shop floor for simultaneous determination of particle size and moisture.

SHOP FLOOR TRIALS FOR SIMULTANEOUS DETERMINATION OF PARTICLE SIZE AND MOISTURE CONTENT

In the laboratory trials, as described above, a constant height of 40 cm camera was used. The environment on shop floor is rough and not so clean. Also, the coal bed is in constant motion. A special sturdy but flexible arrangement was designed to hold the camera and the lights sources and this arrangement fixed above the bed. The camera height was changed from 20-50 cm. At each height at least two images were

taken. On comparing the results of actual versus predicted (for both moisture and particle size) the best height of camera was decided. Now, extended trails were conducted with LED lights at a fixed height of camera. Images were every 30 minutes and altogether 124 samples were collected. Simultaneously, coal samples were collected for analysis by conventional methods of powder particle size and moisture analysis. The results of powder particle size are shown in Fig. 6; the -3 mm fraction in the range of could be determined with an accuracy of ±9%.

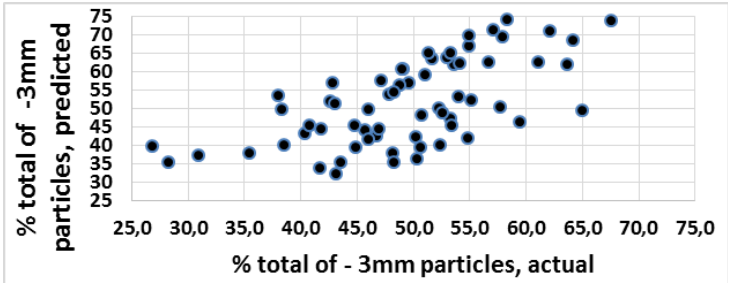

Figure 6. Comparison of actual versus predicted total percentage of -3 mm fraction in coal charged in kiln

During the period of experimentation, the actual moisture in coal varied from 7.54±0.52% and the accuracy of moisture determination in these samples was ±0.88%. Extended trials for moisture accuracy of moisture determination will be conducted in rainy season. The simulated laboratory trials have already shown that accuracy of moisture determination is within 15% of the moisture value.

CONCLUSION

The application of image analysis to predict particle size distribution and surface moisture analysis is tested first on laboratory scale and tried on industrial scale. Optimal placement and height of lights and camera were determined experimentally such that both moisture and particles sizes can be determined from a single image. The percentage of particles of – 3mm size can be determined with inaccuracy of ±9%. Moisture content on the surface of coal, varying in the range of 0-25%, can be determined with an accuracy of ±15% the moisture value under LED light source.

Acknowledgment

Authors (PC, PK, BD) from IIT Bhubaneswar are grateful to the management of TSIL for giving an excellent opportunity to work and carry out experiments at TSIL and for receiving all the guidance from plant personnel.

References

1. Heyduk, A. (2018) Machine Vision Monitoring and Particle Size Feed Analysis. Mining - Informatics, Automation and Electrical Engineering, 4 (533) (1), 7,
2. Igathinathane, C., Ulusoy, U. (2012) Particle Size Distribution Analysis Of

Ground Coal By Machine Vision Volume Approach. 26th International Mineral Processing Congress, IMPC 2012: Innovative Processing for Sustainable Growth - Conference Proceedings, (924), 5581–5593,

3. Kumara, G.J.J. (2016) Image Analysis Techniques On Evaluation Of Particle Size Distribution Of Gravel. International Journal of Geomate, (1999),
4. Sakti, M.B.G., Ariyanto, D.P. (2018) Estimating soil moisture content using red-green-blue imagery from digital camera. In IOP Conference Series: Earth and Environmental Science, 200(1), 012004. IOP Publishing,
5. Shanthi, C., Porpatham, R.K., Pappa, N. (2014) Image Analysis for Particle Size Distribution. International Journal of Engineering and Technology, 6(3), 1340-1345,
6. Thurley, M.J. (2009) Automated online measurement of particle size distribution using 3D range data. IFAC Proceedings Volumes, 42(23), 134-139,
7. Zhang, Z. (2016) Particle overlapping error correction for coal size distribution estimation by image analysis. International Journal of Mineral Processing, 155, 136-139,
8. Bai, X., Lu, G., Bennet, T., Sarroza, A., Eastwick, C., Liu, H., Yan, Y. (2017) Combustion behavior profiling of single pulverized coal particles in a drop tube furnace through high-speed imaging and image analysis. Experimental Thermal and Fluid Science, 85, 322-330,
9. Zhu, Y., Wang, Y., Shao, M., Horton, R. (2011) Estimating Soil Water Content From Surface Digital Image Gray Level Measurements Under Visible Spectrum. Canadian Journal of Soil Science, 91(1), 69–76,
10. Shah, C., Choudhary, P., Deo, B., Malakar, P., Sahoo, S.K., Pothal, G., Chattopadhyay, P. (2018) Conventional and AI Models for Operational Guidance and Control of Sponge Iron Rotary Kilns at TATA Sponge. In Soft Computing for Problem Solving (pp. 461-469). Springer, Singapore.

XIII International Mineral Processing and Recycling Conference
Belgrade, Serbia, 8-10 May 2019

University of Belgrade, Technical Faculty in Bor
Vojske Jugoslavije 12, 19210 Bor, Serbia
Tel. +381 30 424 555 Fax +381 30 421 078

DEVELOPMENT AND MECHANICAL PROPERTIES OF THE PELLETIZED FLY ASH

Sonja Milićević [1,#], Sanja Martinović [2], Vladimir Jovanović [1], Milica Vlahović [2], Ndue Kanari [3], Ana Popović [1], Marija Kojić [2]

[1]Institute for Technology of Nuclear and Other Mineral Raw Materials, Belgrade, Serbia

[2]University of Belgrade, Institute of Chemistry, Technology and Metallurgy, Belgrade, Serbia

[3]Université de Lorraine, UMR 7359 CNRS, CREGU, GeoRessources Laboratory, 2, rue du doyen Roubault, BP 10162, 54505 Vandoeuvre-lès-Nancy, France

ABSTRACT – This paper covers results of pelletizing fly ash in order to obtain pellets, with the satisfied mechanical properties, that can be used in wastewater treatments. Serbian fly ash from "Nikola Tesla" power plant was used as a low cost sorbent. Fly ash was subjected to the elementary and XRD analysis. Portland cement was used as pelletizing agent along with the plastification agent. Mechanical properties of pellets were investigated using different methods such as: pressure resistance, impact resistance, resistance to abrasion and disintegration in water. Best results were obtained with addition of 10 % of cement along with the plasticizer.

Key words: fly ash, pellets, mechanical properties.

INTRODUCTION

Recent investigations are focused on possibility of waste utilization as potential adsorbents in wastewater treatments. Industrial by-products and wastes are almost zero-cost materials and at the same time their utilization could contribute to the solution of their management problem improving the material efficiency within the several industrial activities.

Fly ash has potential application in wastewater treatment because of its major chemical components (alumina, silica, ferric oxide, calcium oxide, magnesium oxide and carbon), and its physical properties such as porosity, particle size distribution and surface area. Besides, the alkaline nature of fly ash makes it a good neutralizing agent [1, 2]. Namely, fly ash as a potential hazardous solid waste produced like a by-product in power plants worldwide in million tonnes has attracted researches

corresponding author: s.milicevic@itnms.ac.rs

interest for years. Fly ash material solidifies while suspended in the exhaust gases and is collected by electrostatic precipitators or filter bags. Since the particles solidify rapidly while suspended in the exhaust gases, fly ash particles are generally spherical in shape and range in size from 0.5 μm to 300 μm. Therefore, the hydraulic properties of fly ash are the one that present major obstacle for its application in wastewater treatments.

The problem of micronized fly ash particles that are not useful in wastewater treatments can be overcome through the agglomeration process such as pelletization. Pelletization is a form of tumble growth agglomeration, whereby material fines are "grown" through a tumbling motion and the addition of water or a binding agent [3]. This process is a non-pressure method of agglomeration that allows production of new materials and use of waste resources with significant environmental and economic impact.

This paper is focused on processing and valorization of industrial waste - fly ash in order to obtain new adsorption material with good mechanical properties and removing capacity for heavy metals from acid mine wastewaters.

EXPERIMENTAL

Materials

Fly ash originates from power plant Nikola Tesla (Tent B) and the chemical composition is presented in Table 1.

Table 1. Chemical composition of the fly ash

Content (%)							
SiO_2	Al_2O_3	Fe_2O_3	CaO	MgO	K_2O	Na_2O	TiO_2
47.80	30.53	5.47	8.69	2.29	1.49	0.25	1.02
Cd	Pb	Zn	Cu	Cr	Ni	Mn	IL*
0.005	0.04	0.021	0.005	0.022	0.03	0.045	1.45

IL * - Ignition lost

Chemical composition places the investigated fly ash to the class F that is characterized with pozzolanic properties.

The mineralogical composition of fly ash was primarily quartz with small amounts of mullite and plagioclase as determined by X-ray powder diffraction analysis (Philips, PW-1710).

Particle size distribution (Figure 1), determined using laser diffraction method (Helos (H1597) & Sucell R4, Sympatec GmbH) show the major size fraction mass content (60 %) of the class below 100 μm.

Cement used in these investigations belong to group of Portland cement and is produced by the Lafarge (PC 42.5R Lafarge).

Plasticizer is applied as chemical additive with a purpose to absorb on the cement particles and build the network of the cement particles. Plasticizer used in this paper belongs to the group of the highly efficient superplasticizer (hyperplasticizer) Cementol Hiperplast 463, produced by the TKK, Slovenia. The effect of the plasticizer depends, mainly, on the type and the amount of the cement. Frame dose of the plasticizer is 0.2 - 1.5 kg plasticizer / 100 kg cement. The mixing

time, after the addition of the plasticizer should be at least 1 min, where the optimal time is 3 min.

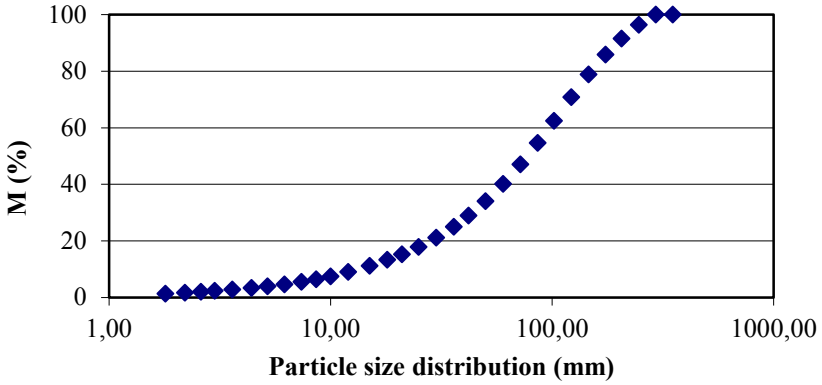

Figure 1. Particle size distribution of the fly ash

Table 2. Chemical composition of the Portland cement

Content (%)							
SiO_2	Al_2O_3	Fe_2O_3	CaO	MgO	K_2O	Na_2O	P_2O_5
21.10	5.42	2.38	63.18	2.35	0.74	0.23	0.12
SO_3 < 4 %	Cl	Na_2O_{eq}	ZnO	Mn_2O_3	SrO	TiO_2	/
3.56	0.0386	0.72	0.038	0.11	0.099	0.245	/

Pelletization

Fly ash pelletizing was conducted on ''Ünal'' disc pelletizer with vibratory feeder, (plate diameter 40 cm, edge height 10 cm, plate inclination angle of 50 °, rotary speed 15 rpm).

The initial samples of fly ashe and cement were homogenized. This is a precondition that must be met in order to obtain pellets of uniform composition during pelletizing. Fly ash is homogenized with the required amount of cement as a binder, without adding any water. After that, the homogenized samples are by vibratory feeder continuously fed on to the pelletizing plate, where the necessary amount of water is added using sprayers. During pelletizing experiments, in some samples, precisely defined amount of plasticizer was added, also. The plate inclination angle (50 °) and the number of revolutions (15 rpm) were constant, while the quantity of the binder varied.

Four composite samples were formed by mixing Fly ash, cement as binder and plasticizer with the Fly ash to cement mass ratio presented in Table 3.

Table 3. Content of the materials used for the production of pellets

Mark	Fly ash	Cement	Plasticizer
P10p	90 %	10 %	0.15 ml
P10	90 %	10 %	/
P5p	95 %	5 %	0.07 ml
P5	95 %	5 %	/

Number next to the letter P indicates the percentage of the cement in the sample and the presence of letter ''p'' in subscript implies the addition of the plasticizer.

Formed pellets were stored for 72 h at the 90 % moisture saturated atmosphere and then dried at 40 °C .

RESULTS AND DISCUSSION

After drying process, pellets were sieved and four different fraction sizes were obtained, as presented in Figure 2.

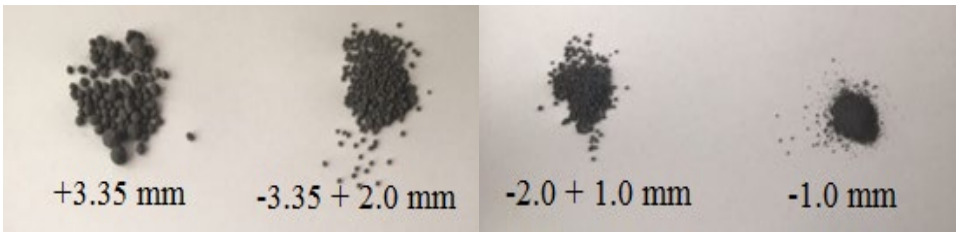

Figure 2. Different fraction sizes of the obtained pellets

Particle size distribution, presented in Figure 3, indicate the largest presence (41 %) of the class - 2.0 + 1.0 mm. This particle size along with the class of - 3.35 + 2.0 mm (17 %) and class of - 7.0 + 3.35 mm (24 %) are the preferred size of the pellets for their application in the dynamic (column) systems. The percentage of the undesirable class of - 1.0 mm below 20 % is a very good result.

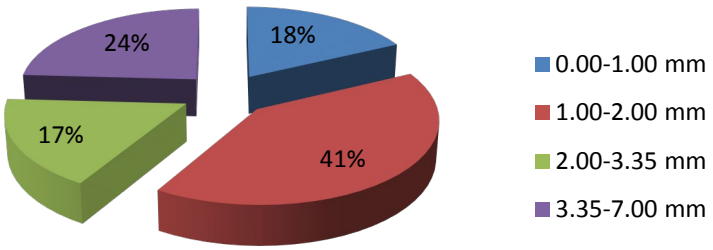

Figure 3. Particle size distributions of the pellets

The purpose of fly ash pelletization, in this paper, is to obtain the material that is more suitable for the application in the wastewater treatments than the parenting one (micronized fly ash). In generally, the pellets are produces to improve the

hydraulic properties of the fly ash. However, from the transport and handling point of view, there are certain mechanical properties that pellets need to satisfy. Tests for pellet mechanical properties include: impact resistance, compressive strength, abrasion resistance and the time required for the pellet to disintegrate completely in water.

Impact resistance is tested by dropping a 100 g pellet sample 25 times from the height of 457 mm on to a 9 mm thick steel plate, after which the sample is sieved on a corresponding screen, whereat the mass of screen undersize should not exceed 5 % (more rarely 10 %) of the total mass of the sample [4]. Obtained results are presented in Table 4.

Table 4. Dependence of the pellets impact resistant on binder content

	1.0 - 2.0 mm	2.0 - 3.35 mm	3.35 - 7.0 mm
	%		
P10p	10.5	9.3	9.2
P10	19.3	16.1	14.6
P5p	65.8	47.1	34.6
P5	81.1	78.3	75.4

According to the results, the dosage of the binder and the addition of the plasticizer, both, highly influence this mechanical property of the pellets. Only pellets with the 10 % of cement and addition of plasticizer meet the requested demand for this mechanical property.

Compressive strength is tested on 10 pellet samples using a standard laboratory hydraulic press in order to determine the maximum pressure that the pellet can withstand without breaking. Pellets should be able to withstand a minimum of 0.5 kg/pellet, which is considered as satisfactory for further handling [4]. Obtained results are presented in Table 5.

Table 5. Dependence of the pellets compressive strength on binder content

	1.0 - 2.0 mm	2.0 - 3.35 mm	3.35 - 7.0 mm
	kg/pellet		
P10p	0.45	0.60	1.12
P10	0.32	0.51	0.73
P5p	0.15	0.32	0.45
P5	0.09	0.15	0.21

From the results in Table 5 it's obvious that the dosage of the cement highly influences this property. Pellets with 10 % of cement, regardless the addition of plasticizer, mostly meet the requested demand, and the compressive strength increases with increasing the particle size.

Pellet abrasion resistance is tested by sieving a 100 g pellet sample on a laboratory mechanical device, i.e., a corresponding screen, for a period of 5 min. After that it was possible to determine that the mass fraction of screen undersize should not exceed 5 % of the total mass of the sample [4]. Obtained results are presented in Table 6.

Table 6. Dependence of the pellets abrasion resistance on the binder content

	1.0 - 2.0 mm	2.0 - 3.35 mm	3.35 - 7.0 mm
P10p	0.52	3.13	3.17
P10	1.59	4.86	4.98
P5p	2.65	17.5	11.95
P5	5.2	21.3	25.4

Pellets with 10 % of cement, regardless the addition of plasticizer and particle size distribution meet the requested demands.

The disintegration of pellet in water is tested by immersing three pellet samples from each group into the water, at room temperature and measuring the time required for the pellet to completely disintegrate in water. Obtained results are presented in Table 7.

Table 7. Average time required for pellets to disintegrate in water depending on binder dosage

	1.0 - 2.0 mm	2.0 - 3.35 mm	3.35 - 7.0 mm
	h		
P10p	0.52	3.13	3.17
P10	1.59	4.86	4.98
P5p	2.65	17.5	11.95
P5	5.2	21.3	25.4

All investigated pellets, regardless the cement dosage, addition of plasticizer and the particle size distribution meet this demand.

CONCLUSION

Fly ash can be efficiently pelletized using cement as binder. Under the investigated pelletizing conditions, more than 80 % of the obtained pellets are suitable for the application in continuous systems, from the particle size distribution point of view. For the production of the pellets with the satisfying mechanical properties, required amount of the cement as binder is 10 %. The dose of the plasticizer, up to 3 % in relation to the amount of the cement, additionally improves the mechanical properties, especially impact resistance.

Acknowledgements:

This research has been part of the investigations on the bilateral project N° 40808RM (project registration number: 451-03-01963/2017-09/08) between the France and Serbia (Pavle Savic program). It has been financed by the Ministry of Education, Science, and Technological Development of Republic of Serbia as part of the project TR 033007 "Implementation of new technical, technological and environmental solutions in the mining and metallurgical operations RBB and RBM". Part of the investigations were financially supported through the ''Green fond'' financed by the Ministry of Environmental Protection of Republic of Serbia. The authors would like to express their gratitude for this support.

References

1. Milicevic, S., Boljanac, T., Martinovic, S., Vlahovic, M., Milosevic, V., Babic, B. (2012) Removal of copper from aqueous solutions by low cost adsorbent-Kolubara lignite. Fuel Processing Technology, 95, 1-7,
2. Papandreou, A., Stournars, C. J., Panias, D. (2007) Copper and cadmium adsorption on pellets made from fired coal fly ash. Journal of Hazardous Materials, 148 (3), 538-547,
3. Mehos, G., Kozicki, C. M. (2017) Choosing agglomeration equipment. Chemical Engineering, 124 (10), 51-57,
4. Albert, K. B., Langford, D. (1998) Pelletizing limestone fines, Mars Mineral, Mars, PA, 12-29,
5. Jovanović, V., Knežević, D., Dekulić, Ž., Kragović, M., Stojanović, J., Mihajlović, S., Nišić, D., Radulović, D., Ivošević, B., Petrov, M. (2017) Effects of bentonite binder dosage on the properties of green limestone pellets. Hemijska Industrija, 71 (2), 135-144.

XIII International Mineral Processing and Recycling Conference
Belgrade, Serbia, 8-10 May 2019

University of Belgrade, Technical Faculty in Bor
Vojske Jugoslavije 12, 19210 Bor, Serbia
Tel. +381 30 424 555 Fax +381 30 421 078

CHARACTERIZATION OF TWO TYPES OD NICKEL ORES AND ANALYSIS OF THE PROSPECTS OF NICKEL CONCENTRATION

Maja Pačeškoska [1], Ružica Manojlović [1,#], Jarmila Trpčevska [2]
[1]University "Ss. Cyril&Methodius", Faculty of Technology and Metallurgy, Skopje, Republic of North Macedonia
[2]Metallurgy and Recycling, Technical University, Faculty of Materials, Košice, Slovakia

ABSTRACT – Characterization of two types of nickel-rich ores – from Guatemala and Albania – was performed. XRF, XRD and SEM/EDS methods were applied, as well as several methods of separation: gravimetric; dry three-staged low-intensity magnetic; dry three-staged high-intensity magnetic and wet magnetic separation. The results showed that the Guatemalan ore contains 1.83 % Ni and 10.13 % Fe and the Albanian ore 0.88 % Ni and 40.24 % Fe. Regarding the mineralogical composition, the Albanian ore is composed of Fe_2O_3, α-$Fe_4O_8H_4$, $Ca_{1.9}Al_{3.8}Si_{8.2}O_{24}$ and $Mg_{3-x}Si_2O_5(OH)_{4-2x}$, whereas the Guatemalan ore consists of $(Mg,Fe)_3Si_2O_5(OH)_4$, $Ni_3Si_2O_5(OH)_4$, $Mg_3Si_2O_5(OH)_4$, $Fe_{2.95}Si_{0.05}O_4$ and $CaAl_2Si_2O_8 4H_2O$. From the applied separation methods, the greatest efficiency was observed with dry high-intensity three-staged magnetic separation, especially in the case of Guatemalan ore.

Key words: nickel, nickel ores, methods for beneficiation of ore, gravimetric separation, magnetic separation

INTRODUCTION

The use of ferronickel alloys with lower nickel content is becoming an ever-increasing occurrence. Worldwide, the percent of nickel in alloys used for production of ferronickel ranges from very low – 0.2 % Ni (Outukumpu, Finnish mine) to 12 % Ni, in Australian mines [1]. After the closing of the mine Rzanovo, the company Euro Nickel Industries imports ore from different countries, with varying nickel content. The ores used by Euro Nickel Industries in Kavadraci, Macedonia, have a nickel content raging from 0.7 to 1.49 % Ni [2]. Recently, efforts have been made for employing an array of beneficiation methods, in order to enable the use of ore with poorer quality for the production of ferronickel [3-5]. In this work, characterization of two types of nickel-rich ores – from Guatemala and Albania – was performed.

corresponding author: ruzica@tmf.ukim.edu.mk

Special attention was given to the investigation of the possibility for nickel concentration by applying several physical methods [6-9].

MATERIAL AND METHODS

Two types of ore were analyzed – ore from Guatemala, type Guaxilan, and ore from Albania, type TMC. The appearance of the ores is shown on Fig.1. After the preparation, which includes drying and crushing characterization of the ores was made. For the characterization of the ores, XRF, SEM/EDS and XRD methods were used. With the use of these methods, the chemical and mineralogical composition of the ores was determined.

For investigation the possibilities for ore concentration, several methods for separation were used: gravimetric; dry three-staged low-intensity magnetic; dry three-staged high-intensity magnetic and wet magnetic separation. Various methods were applied in order to determine the most efficient one.

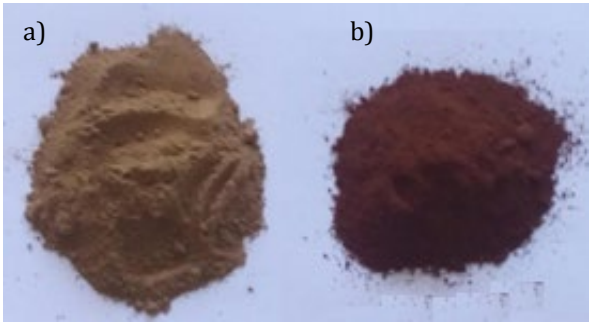

Figure 1. Appearance of the ores **a)** „Guaxilan" from Guatemala, **b)** „TMC" from Albania

RESULTS AND DISCUSSION

The results from the analysis of the chemical composition of the ores, performed by XRF analysis, are given in Table 1. The data for their moisture, bulk density and specific gravity are included in it, as well.

Table 1. Chemical composition, moisture, bulk density and specific gravity of the ores

Type of ore	Chemical composition, %					Moisture, %	Bulk density g/cm^3	Specific gravity, g/cm^3
	Fe	Ni	CaO	MgO	SiO_2			
Guatemala	10.13	1.83	1.23	25.9	39.29	34.8	0.95	2.22
Albania	40.24	0.88	4.52	1.93	10.52	11.01	1.90	3.63

As can be seen from Table 1, the Guatemalan ore is richer in Ni content than the Albanian, for 0.9 %, which is 51.9 % more, whereas the Albanian ore is almost four times richer in Fe (3.97 times), but with lower Mg and Si content.

The results of the analysis of the mineral composition of the ores are shown on Fig.2.

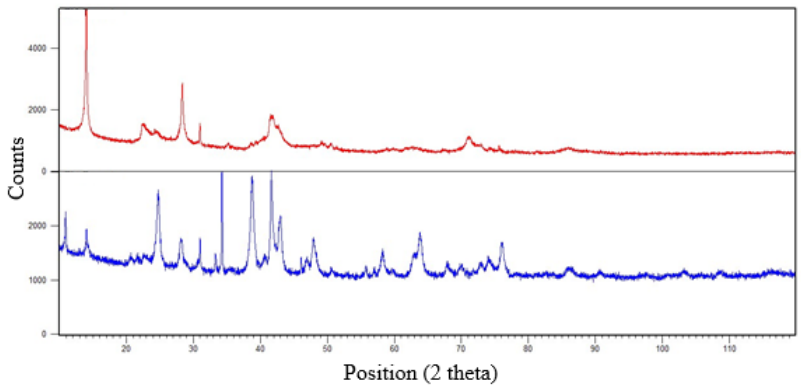

Figure 2. X-ray diffractogram of Guatemala ore (up) and Albania ore (down)

With the help of XRD analysis the precise mineralogical composition of the ores was determined. The Guatemalan ore contains hydroxides and, to a lesser extent, oxides. More precisely, it contains iron silicate hydroxide (serpentine), $(Mg,Fe)_3Si_2O_5(OH)_4$, nickel silicate hydroxide (neoputine, serpentine, kaolin), magnesium silicate hydroxide (chrysotile, white asbestos), $Ni_3Si_2O_5(OH)_4$, $Mg_3Si_2O_5(OH)_4$, iron silicate oxide, $Fe_{2.95}Si_{0.05}O_4$ and calcium aluminum silicate, $CaAl_2Si_2O_84H_2O$. The Albanian ore contains mostly oxides and, to a lesser extent, hydroxides: hematite, Fe_2O_3, goethite, α-$Fe_4O_8H_4$, calcium aluminum silicate (zeolite), $Ca_{1.9}Al_{3.8}Si_{8.2}O_{24}$, and magnesium silicate hydroxide (antigorite), $Mg_{3-x}Si_2O_5(OH)_{4-2x}$.

Selection of the results yielded by the SEM/EDS method analysis is presented in the following section. Fig.3 shows morphology of Guatemalan ore samples, and on Fig.4 the EDS spectra of the same ore is given. The Albanian ore samples are represented on Figs. 5 and 6 – SEM microphotographs and EDS spectra, respectively.

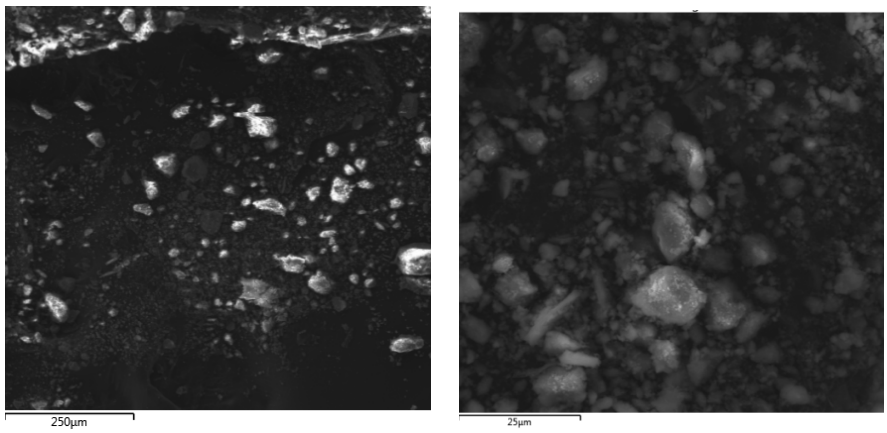

a) b)

Figure 3. SEM microphotography of „Guaxilan" ore from Guatemala
a) sample 1, b) sample 2

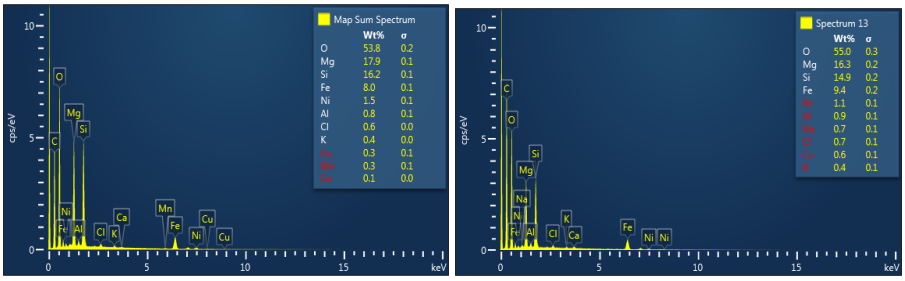

a) b)

Figure 4. EDS spectra of the ore from Guatemala a) sample 1, b) sample 2

The microphotographs of the Guatemalan ore reveal small-grain, cluster, amorphous, isotropic and porous structure, with uneven distribution of the elements through the entire sample. The Ni content varies from 1.1 % to 1.5 %, whereas the Fe content varies from 8 % to 9.4 %.

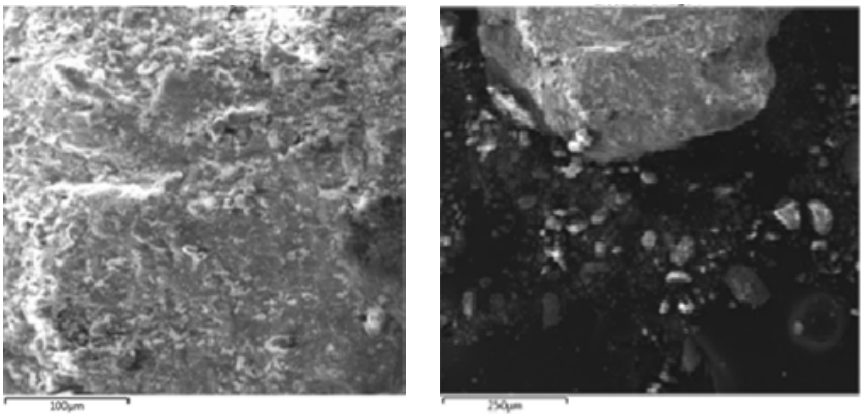

a) b)

Figure 5. SEM microphotography of TMC ore from Albania
a) sample 1, b) sample 2

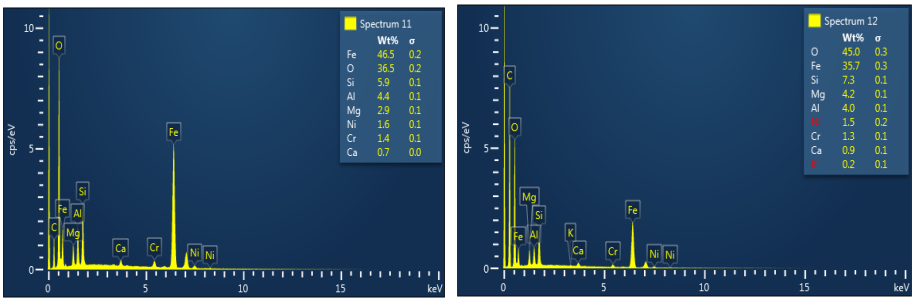

a) b)

Figure 6. EDS spectra of the ore from Albania a) sample 1, b) sample 2

The microphotographs show a compact, amorphous and isotropic ore structure. The Fe content varies from 46.5 % to 35.7 %, while the Ni content varies from 1.5 % to 1.6%, in the analyzed samples.

Both ores were subjected to several methods of concentration: gravimetric; dry, three-staged low-intensity magnetic; dry three-staged high-intensity magnetic and wet magnetic separation.

The **hydrocyclone method for gravimetric analysis** served to determine the granulation and the chemical composition, as well as the concentration of Fe and Ni in different fractions. It was performed in 5 cyclones, with 5 fractions, with particle granulation from 294 to 13 μm. In the case of the Guatemalan ore, the reduction of the particle size continuously increased the content of Fe and Ni. Thus, going from the largest fraction (-294+56 μm) to the smallest (-19+13 μm), the Fe content has increased from 10.13 % to 18.06 %, whereas the Ni content – from 1.83 % to 2.02 %.

In the case of the Albanian ore, going from the first to the fifth cyclone, the Fe content is larger in the larger fraction cyclones and it ranges from 40.27 % to 33.16 %. The Ni content is lowered towards the fifth cyclone, but not significantly – from 0.88 % to 0.84 %.

The **dry three-stage low-intensity magnetic separation** was performed with magnetic separators with permanent low-intensity magnets. The samples from both ores were crushed and then screened and separated in 5 classes. The class distribution during the screening is presented on Figure 7.

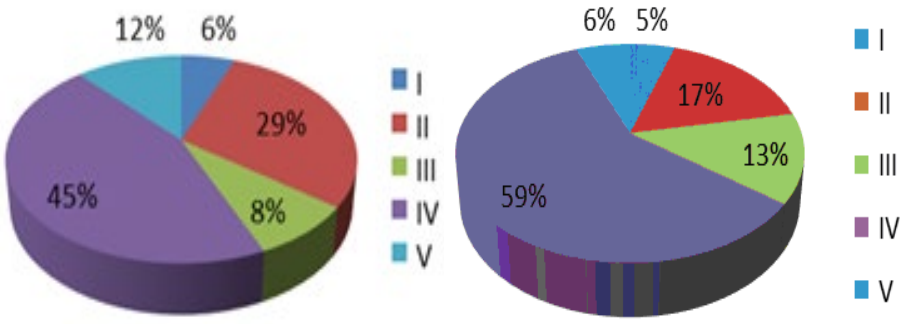

a) b)

Figure 7. Class distribution during the screening of the ore from a) Guatemala, b) Albania

The results from the performed magnetic separation of the Guatemalan ores are given in Table 2, whereas the ones from the Albanian ore are given in Table 3.

As can be seen on Fig.7, class IV has the greatest contribution in both ores (45 % and 59 %), and the least – class I (6 % and 5 %). After the dry three-stage low-intensity magnetic separation of the Guatemalan ore (Table 2) the Fe content has increased in the magnetic part, from 10.12 % to 24.47 %, i.e., for 37.4 %, and the Ni content – from 1.8 % to 1.9 %, i.e., for 5.55 %. In the nonmagnetic part, the Fe content has increased from 10.13 % to 17.14 %, and the Ni content – from 1.83 to 2.03 %.

Table 2. Fe and Ni content after magnetic separation of the ore from Guatemala

Class	Magnetic part		Nonmagnetic part	
	Fe, %	Ni, %	Fe, %	Ni, %
I	10.12	1.80	10.13	1.83
II	18	1.8	13.78	2.01
III	18.91	1.83	11.59	1.85
IV	21.91	1.67	16.2	1.92
V	24.47	1.9	17.14	2.03

Table 3. Fe and Ni content after magnetic separation of the ore from Albania

Class	Magnetic part		Nonmagnetic part	
	Fe, %	Ni, %	Fe, %	Ni, %
I	48.88	1.02	46.29	0.7
II	47.43	0.9	38.41	0.83
III	47.64	1.03	41.7	0.79
IV	45.67	1.02	40.82	0.83
V	41.62	1.1	36.86	0.97

In the case of the Albanian ore (Table 3) the magnetic part is characterized by the reduction of the Fe content from 48.88% to 41.62% and increase of the Ni content from 1.02% to 1.1%. The nonmagnetic part is also characterized by the decrease of the Fe content from 46.29% to 36.86%, whereas the Ni content has increased from 0.7% to 0.97%. In summary, the dry three-stage low-intensity magnetic separation yielded lower effects in the case of the Guatemalan ore.

The results from the **dry three-stage high-intensity magnetic separation** are given in Table 4.

Table 4. Fe and Ni content in the magnetic and nonmagnetic part after dry three-stage high-intensity magnetic separation

Guatemalan ore				Albanian ore			
Magnetic part, 31.54 %		Nonmagnetic part, 68.46 %		Magnetic part, 62.74 %		Nonmagnetic part, 37.26 %	
Fe, %	Ni, %	Fe, %	Ni, %	Fe, %	Ni, %	Fe, %	Ni, %
16.34	2.01	19.83	2.05	42.34	0.79	40.56	0.9

As can be seen in Table 4, the Guatemalan ore yielded a magnetic part of 31.54 % and nonmagnetic part of 68.46%. The increase of the Fe content in the magnetic part is 61.3 % and 95.76 % in the nonmagnetic part, whereas the Ni content increased for 9.84% in the magnetic part, and for 12.02 % in the nonmagnetic part.

In the case of the Albanian ore, the magnetic part is 62.74 %, while the nonmagnetic part is 37.26 %. The effects of the dry three-stage low-intensity magnetic separation are lesser when compared to the Guatemalan ore. Namely, the Fe content in the magnetic part increased for 5.22%, and for 0.79% in the nonmagnetic part, whereas the Ni content in the nonmagnetic part increased for 2.27%.

The wet magnetic separation was performed with the variation of the electrical current from 0.3A, 0.6A and 1.5A and the intensity of the magnetic field from 1000Gs, 1350Gs and 3000Gs, with 9 analyses of the both ores. The results had shown that the increase of the current increases the share of the magnetic part, in the case of the Albanian ore for 89%, whereas for the Guatemalan ore for 7.8 times more. Regarding the Fe content in the nonmagnetic part, the best results were achieved with highest values for the intensity of the magnetic field and the electrical current in the case of the Albanian ore – its share was 1.23 times greater. However, the Ni content is only slightly increased, in both ores, both in the magnetic and nonmagnetic part.

CONCLUSION

1. The chemical composition of the ores was determined. The Guatemalan ore, when compared to the one from Albania, is richer in Ni for 51.9%, but has a lower content of Fe, nearly four times.

2. From a mineralogical point of view, the Guatemalan ore is richest in hydroxides and contains oxides to a lesser extent, i.e. it contains $(Mg,Fe)_3Si_2O_5(OH)$, $Ni_3Si_2O_5(OH)_4$, $Mg_3Si_2O_5(OH)_4$, $Fe_{2.95}Si_{0.05}O_4$ и $CaAl_2Si_2O_84H_2O$. The Albanian ore is rich in oxides and slightly lower in hydroxides – it contains Fe_2O_3, α-$Fe_4O_8H_4$, $Ca_{1.9}Al_{3.8}Si_{8.2}O_{24}$ and $Mg_{3-x}Si_2O_5(OH)_{4-2x}$.

3. The Guatemalan ore is characterized by small-grained, clustered, amorphous and porous structure, with Fe content from 8 % to 9.4 % and Ni content from 1.1 % to 1.5 %. The ore from Albania has a compact, amorphous and isotropic structure, with Fe content from 35.7 % to 46.5 % and Ni content up to 1.6 %.

4. Among all four methods of concentration: gravimetric; dry three-staged low-intensity magnetic; dry three-staged high-intensity magnetic and wet magnetic separation, the dry three-stage high-intensity magnetic separation had shown the greatest efficiency. The implementing of this method in the process of Euro Nickel Industries would prove to be an efficient and profitable investment in the long term.

References

1. A.M. Evans, Ore Geology and Industrial Minerals, 3rd edition, Blackwell Publishing, 1993,
2. T. Serafimovski, A.V. Volkov, B. Boev, G. Tasev, Ržanovo metamorphosed lateritic Fe-Ni deposit, Republic of Macedonia, Geology of Ore Deposits, Vol. 55, Issue 5, (2013), 383–398,
3. B. Altansukh, K. Haga, A. Shibayama, Recovery of Nickel and Cobalt from a Low Grade Laterite Ore, Resources Processing, Vol. 61, No. 2 (2014), 100-109,
4. N.W. Brand, C.R.M. Butt, M. Elias, Nickel laterites: Classification ad f eatures,

AGSO Journal of Australian Geology&Geiophysics, 17 (4), (1998), 81– 88,
5. J.A. Finch, Column Flotation: A Selected Review - Part IV: Novel Flotation
6. *R.S. Young*, *Chemical analysis in extractive metallurgy*, Charles *Griffin, London, 1971,*
7. P.E. Ostapenko, Theory and Practice of Magnetite Ores Dressing, Nedra, Moscow, 1985,
8. *M.A. Bikbov*, V.V. Karmazin, A.A. Bikbov, Low-Intensity Magnetic Separation: Principal Stages of a Separator Development – What is the Next Step?, Physical Separation in Science and Engineering, Vol. 13, 2, (2004), 53–67,
9. J. Stener, Wet low-intensity magnetic separation: measurement methods and modelling, Doctoral Thesis, Lulea University of Technology, Lulea, Sweden, 2015.

XIII International Mineral Processing and Recycling Conference
Belgrade, Serbia, 8-10 May 2019

University of Belgrade, Technical Faculty in Bor
Vojske Jugoslavije 12, 19210 Bor, Serbia
Tel. +381 30 424 555 Fax +381 30 421 078

A CASE STUDY OF HEAVY MEDIA CYCLONE EFFICIENCY IMPROVEMENT AT TATA STEEL WEST BOKARO - A NOVEL APPROACH

Farookh Sekh [1,#], Vineet Kumar [2]
[1]Tata Steel Limited, India
[2]Nalco, An Ecolab Company, India

ABSTRACT – From the literature reviews it was found that rheological parameters viscosity and stability of heavy media suspension largely affects the performance of the HMC. As a joint improvement initiative, TSL and Nalco team has initiated lab scale evaluation of newly developed Dispersant to assess its effects on the rheology and stability of magnetite suspension. This Dispersant alter the particle-particle interaction of magnetite thus increasing the media stability and decreasing the apparent viscosity. It was evident from the tests that it is possible to have both a very stable suspension and a low viscosity of heavy media by using this dispersant.

Key words: rheology, dispersant, heavy media cyclone, viscosity, coal, magnetite stability

INTRODUCTION

Tata Steel, Jamshedpur, Jharkhand, India owns captive mines and washeries at West Bokaro which supplies 40 % coking coal requirements for its integrated steel making operations. In the washeries, The ROM coal after being crushed and screened at 0.5 mm, the (-)13 mm to + 0.5 mm fraction is treated in Dense Media Cyclone (called the coarse circuit) ant the - 0.5 mm in a flotation circuit (called the fines circuit). The +0.5 mm coal is fed to the primary cyclones, which produces rejects at a higher relative density of separation (1.54 - 1.58). The overflow flow from the primary cyclones form the feed to the secondary cyclones which in turn produce clean coal and middling at a lower relative density of separation (1.32 - 1.38). The magnetite recovery circuit is a typical circuit that exists in any coal washing plant and is shown in Fig.1. The dense medium and clean coal (middlings or rejects, as the case may be) is laundered to sieve bends and one set of drain-and-rinse screens. The sieve bends and the first section of each drain-and-rinse screen are used to drain medium.

Form the coal, the media is collected in screen under pass and returned to the primary cyclone sump via the primary cyclone medium distribution box. The second

corresponding author: farookh@tatasteel.com

section of the screens is used to rinse and drain the coal free of adher in medium.

The spray water containing the dense-medium rinsed from the coal is collected in the second section of the screen under-pans and returned to the dilute medium sump for subsequent magnetite recovery. The level of magnetite water slurry in the dilute media sump can be adjusted using PID (Proportional, Integral, Derivative 3-term controller) loop provided for level control and the modulating Splitter actuator. When the slurry levels in the sun rises, the splitted actuator would drivert the flow away form the system to maintain balance. The indication loop also generates high and low alarm levels within the control system. The dilute medium thus collected in the dilute medium sump is pumped to magnetic separators, which produce the recovered magnetite as over-dense medium and arejecttailings circuit. The over-dense medium is returned to the over-dense medium sump and distributed to the dense-medium washing circuits as make up. Magnetic separator tailings are used as product rinsing water.

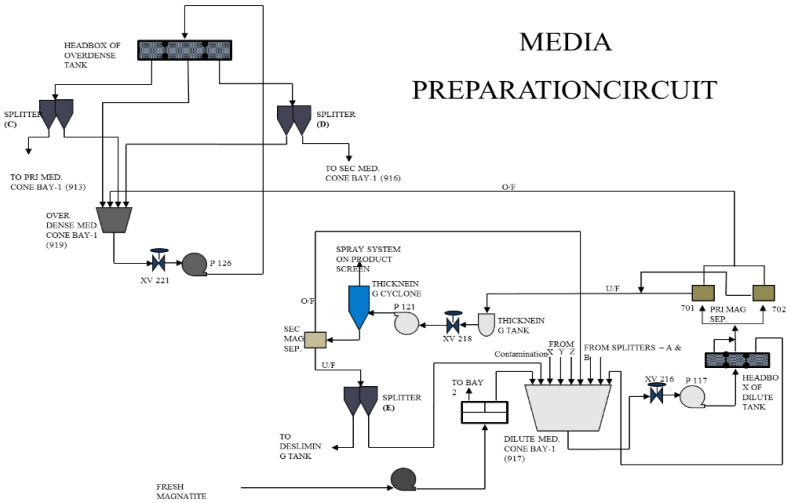

Figure 1. Media Circuit Diagram

Tata Steel West Bokaro always encouraged improvement initiatives. With depletion of high grade coal seams and subsequent processing of low grade ores having poor separation in cyclone, possibility of adherence of clay on the coal surface that deteriorate the separation performance always loomed large. These seams have wider variation in ash percentage with poor floatability characteristics resulting into lower fine clean coal recovery.

The availability of indigenous Coal has been drastically increased to cater to the increased requirement after expansion project at Tata Steel Jamshedpur. The supply of indigenous coal at lower ash level has always been a priority for Tata Steel West Bokaro in order to reduce the import requirement of clean coal from overseas considering the economics associated with it.

With the possibility of enhancing yield keeping the concentrate ash % in specified limits by usage of Dispersant, and as a developmental initiative Nalco has worked to develop the New Dispersant Freevis 9939. Preliminary testing was conducted at

Nalco lab and the results were quite encouraging in terms magnetite suspension.

STUDY OF EFFECT OF FREEVIS ON MAGNETITE SUSPENSION IN LABORATORY TEST

Comprehensive lab tests were conducted to check the effect of new developed Freevis on the magnetite suspension. Sample was collected from secondary media head box having sp. Gravity 1.35. for test work, 1 litre of magnetite slurry was taken and 0.5 ml of Freevis was dosage. Magnetite suspension was observed with time.

Figure 2. Comparative Test to check the effect of Freevis in magnetite suspension

From the test results and observation, it was quite evident that the with usage if Freevis the magnetite suspension stability increase significantly. The idea can be use in Heavy Media Cyclone process to increase the magnetite stability in cyclone which will help in better separation thus the recovery of clean coal.

Plant trial with freevis 9939

Based on the encouraging indication in laboratory test, a small-scale plant scale trial was conducted for one shift in Tata Steel west Bokaro washery 3 on 28th February 2019.

Trial philosphy and kpi

- The check the effect of the chemical pre and trial data will be compared.
- During the Trial all variable parameters like Coal Seam, Plant Throughput, Flotation Reagents dosage, Flotation Cell Parameters will be kept same.
- Dosing of the Chemical will be done in Neat (100 % Conc @ 250 ml/min) at Primary head Box of BAY I Circuit.
- The Data will be captured in a template which will be used for analysis purpose.
- The Main KPI of the trial will be to reduce the misplacement of clean coal in Middling's.

Dosage and feeding:

Chemical will be done in Neat (100 % Conc @ 250 ml/min) at Primary head Box of BAY I Circuit.

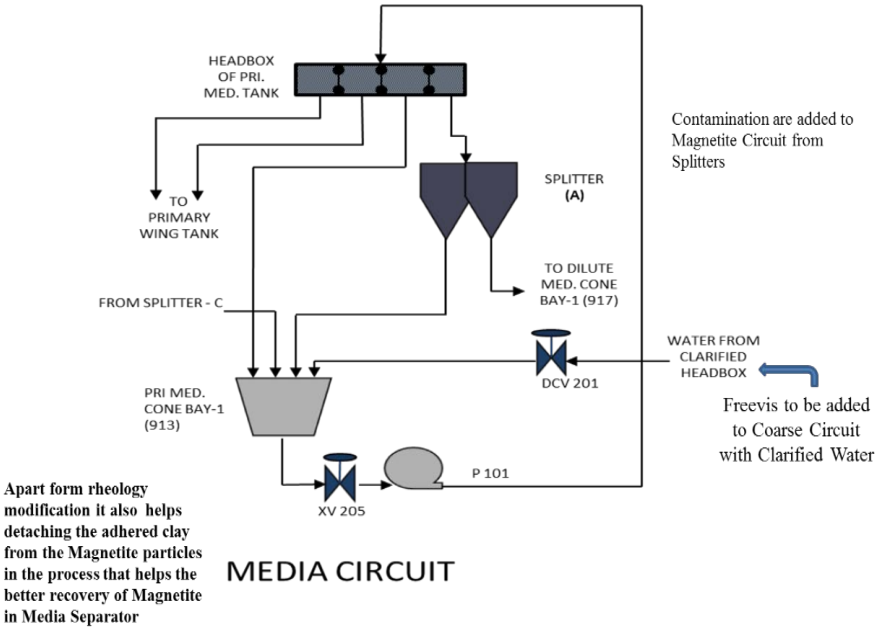

Figure 3. Nalco Freevis 9939 effect in Magnetite Stability

SAMPLING AND RESULTS

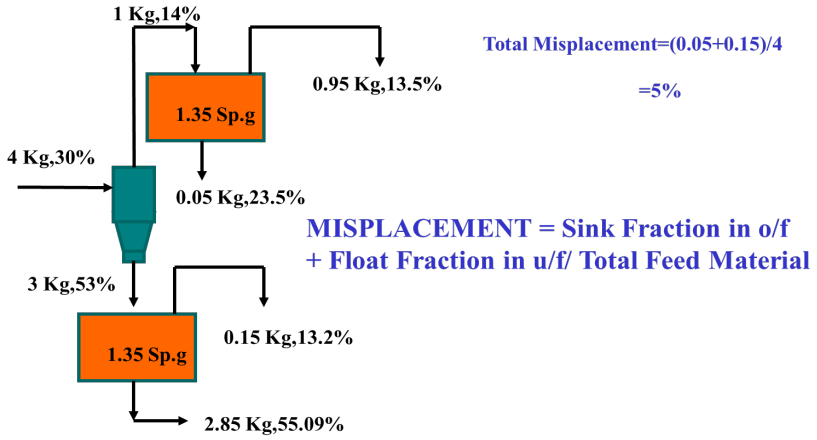

Figure 4. Sample Misplacement Example

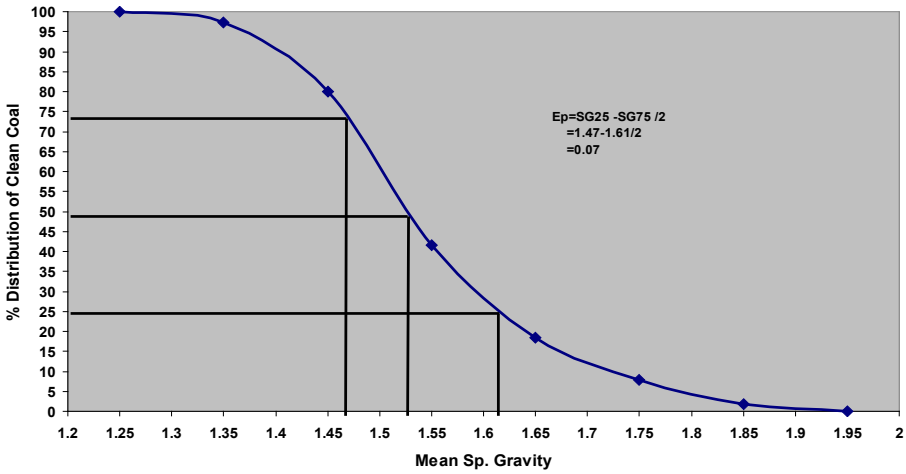

Figure 5. Ep Curve for Clean Coal Distribution

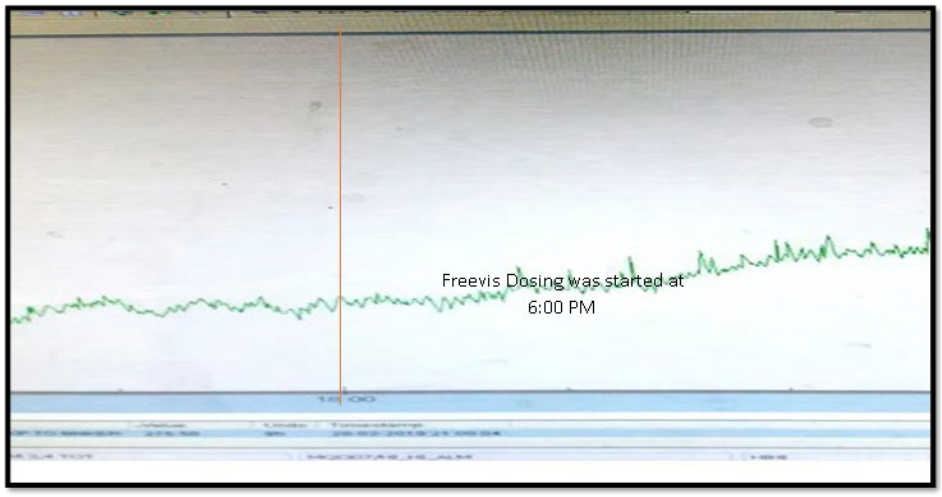

Figure 6. Snap taken from Control room DCS For Yield trend. Freevis was started ta 6:00 PM on 28th February and it is seen from the graph that the yield is increasing after the dosing of Freevis

Table 1. Misplacement of clean coal in middling: without chemical

TIME	5.00 to 5.30			TIME	5.30-6.00			TIME	6.00 to 6.30		
1	WT	WT %	ASH %	2	WT	WT %	ASH %	3	WT	WT %	ASH %
FT at 1.50	0.352	18.66	37.27	FT at 1.50	0.456	20.61	34.83	FT at 1.50	0.171	9.09	32.29
Sk at 1.50	1.534	81.34	36.06	Sk at 1.50	1.756	79.39	37.37	Sk at 1.50	1.711	90.91	39.46
AVG	1.886	100	36.29	AVG	2.212	100.00	36.85	AVG	1.882	100	38.81

Table 2. Misplacement of clean coal in middling: with chemical

TIME	7.20 to 7.50			TIME	7.50-8.20			TIME	7.50-8.20		
4	WT	WT %	ASH %	5	WT	WT %	ASH %	6	WT	WT %	ASH %
FT at 1.50	0.140	7.83	31.69	FT at 1.50	0.34	18.06	34.92	FT at 1.50	0.252	14.18	33.33
Sk at 1.50	1.649	92.17	43.06	Sk at 1.50	1.543	81.94	34.81	Sk at 1.50	1.525	85.82	35.99
AVG	1.789	100	42.17	AVG	1.883	100	34.83	AVG	1.777	100	35.61

CONCLUSION

The small-scale plant trial was quite encouraging, and it is giving indication that with the use of Freevis there is a good scope of yield improvement and there is any adverse effect on the circuit. However, to quantify the benefits and to check the commercial feasibility a longer trial is needed. Based on the encouraging trend a week trial is planned in March'19.

References

1. Collins, B., Napier-Munn, T.J., Sciarone, M. (1974) The production, properties and selection of ferrosilicon powders for dense-medium,
2. Project report on TSL, West Bokaro by R. Sripriya, A. Dutta, P.K. Dhall, M. Narasimha.

XIII International Mineral Processing and Recycling Conference
Belgrade, Serbia, 8-10 May 2019

University of Belgrade, Technical Faculty in Bor
Vojske Jugoslavije 12, 19210 Bor, Serbia
Tel. +381 30 424 555 Fax +381 30 421 078

CHARACTERISTICS OF RESIDUE OBTAINED FROM RED OPALITE WITH CHEMICAL ACTIVATION

Blagica Cekova [1,#], Viktorija Bezhovska [2], Afrodita Ramos [1]
[1]MIT University, Faculty of Environmental Resources Management, Skopje, Republic of North Macedonia
[2]University St. Cyril and Methodius, Faculty of Technology and Metallurgy, Skopje, Republic of North Macedonia

ABSTRACT – The material that is taken for examination is from the site "Gorni Stubol" in Probistip. From the chemical analysis we can conclude that the raw material is with a pinkish – red color resulting from a large amount of Fe_2O_3 oxide (12.80 %). The chemical activation of the red opalite was carried out with a 10 % solution of HCl with a Fe_2O_3 content of 2.24 %. The chemical analysis of the residue is given in tables 1 and 2. For our tests was taken material with particle sizes over 0.063 mm and 0.063 mm below. The adsorption characteristics were investigated by a static – gravimetric method, and the B.E.T equation for multilayer adsorption was used to calculate the specific surface area.

Key words: red opal, residue, chemical analysis, adsorption, B.E.T equation.

INTRODUCTION

The natural raw material red opalite is polymineral raw material that acts massively and compactly. In addition to the opalescence, lemonitisation was performed from which the rock is pigmented with a pinkish-ceramic pigment which is probably limonistic. The rock represents a tuffite that is intensely hydrothermal altered or the rock has an tuffite character.

Based on the characteristics and tests carried out on the red opalite it can be concluded that it can not be used in obtaining new products. The amount of Fe_2O_3 oxide is detrimental to the synthesis of new products.

Chemical activation of red opalite was performed with 10 % HCl solution. The extraction was carried out on a material with a particle size above 0.063 mm and below 0.063 mm.

In this paper will be given the chemical composition of the residue after the extraction and examination of its adsorption properties using the static – gravimetric method.

corresponding author: cekovab@yahoo.com

MATERIAL AND METHODS

As a material, red opalite with granulation above 0.063 mm and below 0.063 mm was used. Concentration of HCl is 10 %. The mixture is placed in a glass reactor. The suspension after extraction is filtered into vacuum and the residue was washed with distilled water.

Chemical activation allowed us to reduce the percentage of iron from 12.80 in the red opal to 1.71 - 2.04 % depending on the size of the particles, but taking care that the present clay components in the red opalite remain completely with their structures. [1, 2]

The chemical composition of the residue with a particle size above 0.063 mm is given in Table 1, while the chemical composition of the residue with a particle size below 0.063 mm in Table 2.

Table 1. Chemical composition residue with a particle size above 0.063 mm

Components	Participation (%)
SiO_2	60.22
Al_2O_3	24.19
Fe_2O_3	1.71
MgO	-
CaO	0.72
K_2O	0.55
Na_2O	0.50
Loss of mass	12.06

Table 2. Chemical composition of the rest with a particle size below 0.063 mm

Components	Participation (%)
SiO_2	60.94
Al_2O_3	23,33
Fe_2O_3	2.04
MgO	-
CaO	0.72
K_2O	0.15
Na_2O	0.10
Loss of mass	12.72

The absorption properties of the residue are determined by water vapor at a temperature of 288 K. The adsorption isotherms depending on the temperature and particle size are given in Figures 1 and 2. While the linear shape of the adsorption isotherms in Figures 3 and 4. The adsorption isotherm defines the monolayer capacity using the equation for multilayer adsorption of B.E.T. to determine the specific area. [3]

Determined specific surface area of the residue with a particle size below 0.063 mm is 39.92 m^2 / kg 10^3, and for the residue, with a particle size above 0.063 mm, it is 37.01 m^2 / kg 103.

The monolayer capacity for the remainder with a particle size exceeding 0.063 mm is 0.5121 mol / kg, and for the residue with a particle size below 0.063 mm am = 0.5523 mol / kg.

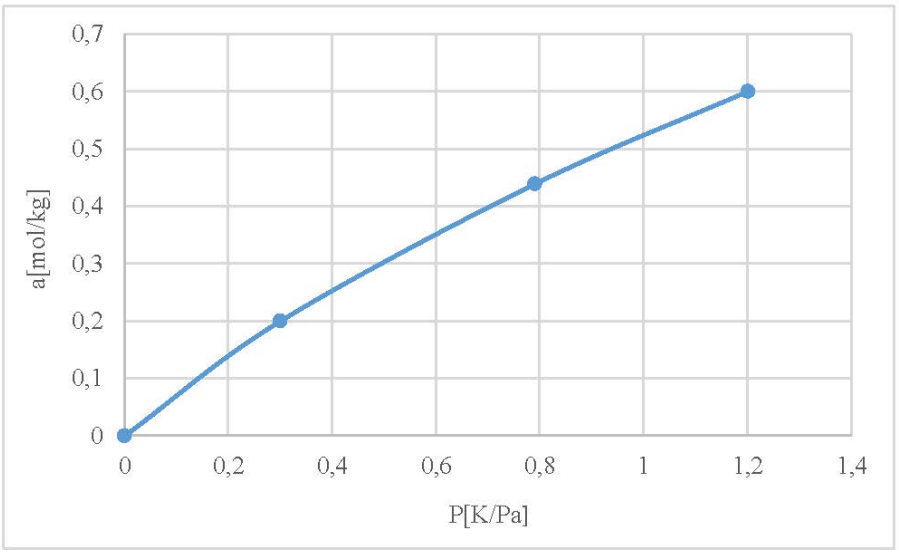

Figure 1. The adsorption isotherm of water vapor on the residue with particle size below 0.063 mm

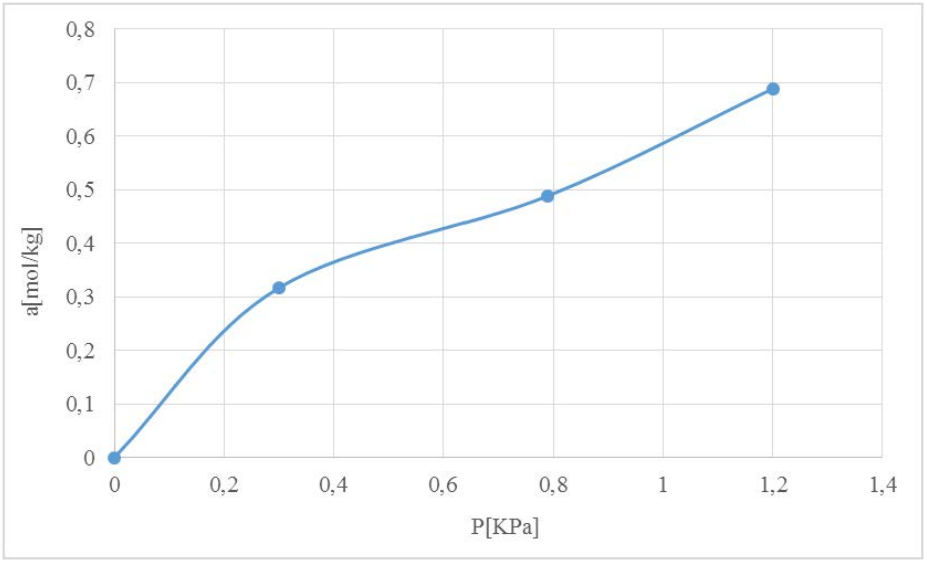

Figure 2. Adsorption isotherm of water vapor over the residue with particle size over 0.063 mm

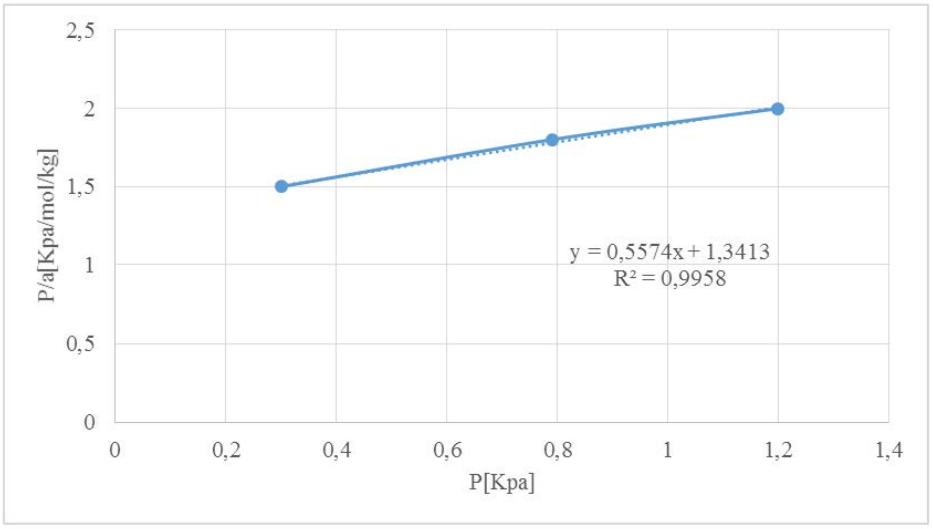

Figure 3. Linear form of the adsorption isotherm on the residue with particle size below 0.063 mm

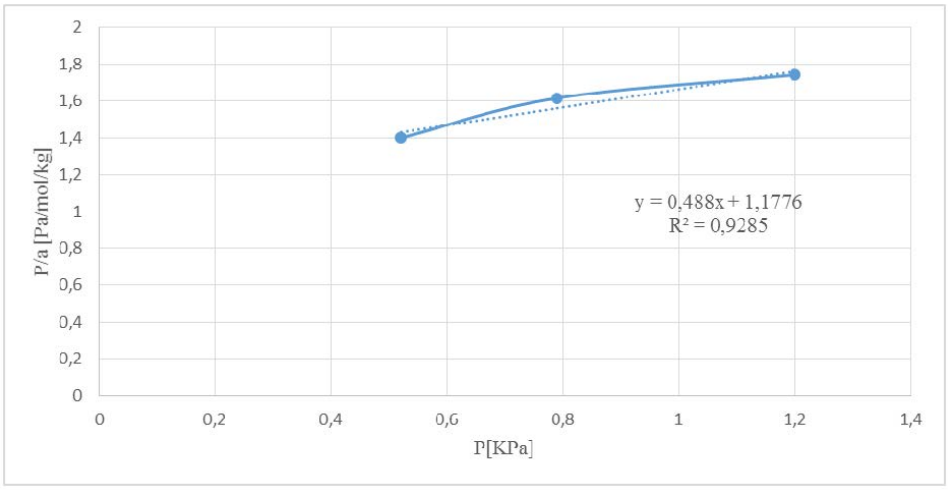

Figure 4. Linear form of the adsorption isotherm on the residue with particle size over 0.063 mm

CONCLUSION

From the performed tests, the obtained results can be concluded that the residue with a small percentage of Fe_2O_3 oxide can be used in the ceramic industry, the synthesis of dead material and the absorption of heavy metals in contaminated soils and wastewater.

References

1. Цекова, Б. (1983) Синтеза на зеолит од тип 4А поаѓајки од остатоците по лужење на алунит од алунитисан туф. Универзитет „Кирил и Методиј“, Центар за Математичко - технички науки ООЗТ Технолошки фалкултет - Скопје,
2. Nano, G. V., Strathmann, T. J. (2006) Ferrous sorption by hydrous metal oxides. Journal of Colloid and Interface Science, 297 (2), 443-454,
3. Gregg, S., Sing, K. (1982) Adsorption surface area and porosity. Academic Press, London.

XIII International Mineral Processing and Recycling Conference
Belgrade, Serbia, 8-10 May 2019

University of Belgrade, Technical Faculty in Bor
Vojske Jugoslavije 12, 19210 Bor, Serbia
Tel. +381 30 424 555 Fax +381 30 421 078

CHARACTERIZATION OF MINING AND PULP INDUSTRY SIDE STREAMS: PARTICLE CHARACTERISTICS AND CHEMICAL COMPOSITIONS

Küçük Mehmet Emin #, Kinnarinen Teemu, Häkkinen Antti
LUT University, LUT School of Engineering Science, Lappeenranta, Finland

ABSTRACT – This paper presents characterization study of various secondary materials including fly ash, bottom ash, green liquor dregs, steel slag, demolition waste and mine tailings that were carried out to understand their reutilization potential as construction materials in the form of geopolymer composites. Particle sizes, particle morphologies, elemental and mineral compositions and specific surface areas of the solid materials were revealed. Most of the materials were observed to have a considerable amorphous content, low concentrations of possibly hazardous trace elements, Al_2O_3 and SiO_2. The results suggest that some of these materials can be utilized in preparation of geopolymer composites after efficient pre-treatment processes.

Key words: particle size distribution, fly ash, tailings, green liquor dregs, geopolymer.

INTRODUCTION

In 2016, 5 tons of waste were produced per inhabitant in European Union (EU), from which only 38 % were recycled, while 46 % were landfilled [1]. Landfilling, as a method of disposal, causes pollution in the air, soil, and water, and it restricts the recovery of valuable secondary materials from the waste. Industries of pulp & paper, mining & quarrying, and construction constitute more than 60 % of the overall waste [2]. Recycling and re-utilization of these industrial side streams play a very critical role for sustainable waste management and circular economy. On the other hand, construction industry is responsible for 5 - 8 % of the overall CO_2 due to its energy-intensive processes, such as cement production [3]. For reduction of this large emission, environmentally friendly inorganic composites have been developed through polymerization of materials with high aluminosilicate contents. These materials are called geopolymer composites, and they can be applied in construction industry as an alternative to ordinary concrete as they provide good mechanical, thermal and chemical properties [4, 5]. Due to their high aluminosilicate concentrations, ash [4, 5], steel slag [6], demolition and construction wastes [7], and mine tailings [8] have been utilized by the construction industry. However,

corresponding author: Mehmet.Kucuk@lut.fi

information is needed about other properties of the streams, including physical, chemical and particle properties. This study focuses on the characterization of local side streams in Finland originated from pulp & paper, iron & steel, mining, and construction industry to understand their reutilization potential in geopolymer composites.

MATERIAL AND METHODS

Origin of the samples

Names, notations, and origins of the characterized eight side streams within the scope of this study are presented in Table 1. Samples FA2 and BA originate from the same incinerator, FA2 being the biomass fly ash, while the biomass bottom ash is BA.

Table 1. Types and origins of the samples

Sample	Notation	Origin of the sample
Fly ash sample 1	FA1	Bark boiler from pulp mill
Fly ash sample 2	FA2	Co-incineration plant from pulp mill
Fly ash sample 3	FA3	Coal power plant
Bottom ash	BA	Co-incineration plant from pulp mill
Green liquor dregs	GLD	Kraft pulp mill
Mine tailings	MT	Carbonate mine
Demolition waste	DW	Waste combustion plant
Steel slag	SS	Electric arc furnace slag

Analyses

Particle sizes of the streams were measured with Malvern Mastersizer 3000, equipped with Hydro EV particle dispersing unit (Malvern Instruments, UK). Scanning electron microscope (SEM) was applied for investigating the surface morphology of the samples while elemental compositions were obtained by energy-dispersive X-ray spectroscopy (EDS) mappings with a Hitachi SU 3500 scanning electron microscope. Samples BA, MT, and DW were manually crushed before SEM and EDS analyses. X-ray diffraction with Bruker D8 Advance was used for mineral composition analyses. The specific surface areas (SSA) of the solids were measured with Micrometrics 3Flex BET surface area analyzer and concentrations of trace elements were determined by using inductively coupled plasma – optical emission spectroscopy (ICP-OES). ICP-OES analyses were performed after digestion by using standardized 4-acid digestion and peroxide smelt digestion methods.

RESULTS AND DISCUSSION

Particle Sizes

Particle sizes of the samples are shown in Table 2. Tailings and the demolition waste were found to contain the largest particles. The particle size of the bottom ash was not measured as it exceeded the measurement limit of the equipment.

Table 2. Particle sizes of the samples

Sample	d_{10}, µm	d_{50}, µm	d_{90}, µm
FA1	11.3	53.7	159
FA2	7.3	30.7	116
FA3	3.7	26.5	108
GLD	7.3	34.7	103
MT	35.6	147	311
DW	5.5	84.8	481

Specific surface areas (SSA)

Specific surface areas of the samples determined with BET measurement method are shown in Table 3. As expected, higher specific surface area values were found for samples consisting of smaller particles.

Table 3. Specific surface areas of the samples

Sample	FA1	FA2	FA3	BA	GLD	MT	DW
BET SSA (m^2/g)	8.1	1.7	14	0.1	9.3	0.3	7.4

Surface morphologies

Morphologies of the materials are shown in SEM images in Fig. 1. BA consists of elongated and angular-shaped particles with larger size. Fly ash solids are mainly predominated by spherical and irregular-shaped particles with different size ranges, which is in good accordance with other studies [5, 9]. Large particles of the carbonate mine tailings confirm the particle size data presented in Section 3.1.

Elemental compositions

The concentrations of the elements in the streams are presented in Table 4. These results show that the element concentrations vary greatly for different solids. Major elements observed in the samples were C, O, Ca, Si and Al. Concentrations of Al, Si and Si/Al vary over a ten-folded range. It is important to determine the Si/Al ratio and concentrations of Al and Si, because they affect the microstructure and mechanical strength of the geopolymer composites [10]. Ca concentration also plays an important role in geopolymer composites as there is a direct proportion between Ca content and the mechanical strength and acid resistance of the final product [5]. Finally, being a ferrous residue, steel slag sample (SS) contains high concentrations of iron compared to all other samples.

Table 4. Elemental compositions of the samples obtained by EDS

Sample	Element	C	O	Na	Mg	Al	Si	P	S	Cl	K	Ca	Ti	Mn	Fe	Zn
FA1	(w -%)	6	36	2	1	6	6	1	3	1	4	31	0	1	1	0
FA2	(w -%)	4	35	4	1	3	6	1	7	3	3	27	1	1	2	1
FA3	(w -%)	35	36	1	0	7	15	0	0	0	1	2	1	0	2	0
BA	(w -%)	2	47	2	0	6	30	0	0	0	3	7	1	0	2	0
GLD	(w -%)	10	47	10	5	0	1	0	2	0	0	23	0	2	1	0
MT	(w -%)	8	44	1	3	1	16	0	0	0	0	27	0	0	1	0
DW	(w -%)	10	42	1	1	2	7	0	12	0	1	24	0	0	2	0
SS	(w -%)	4	24	0	1	3	6	0	0	0	0	34	0	4	21	0

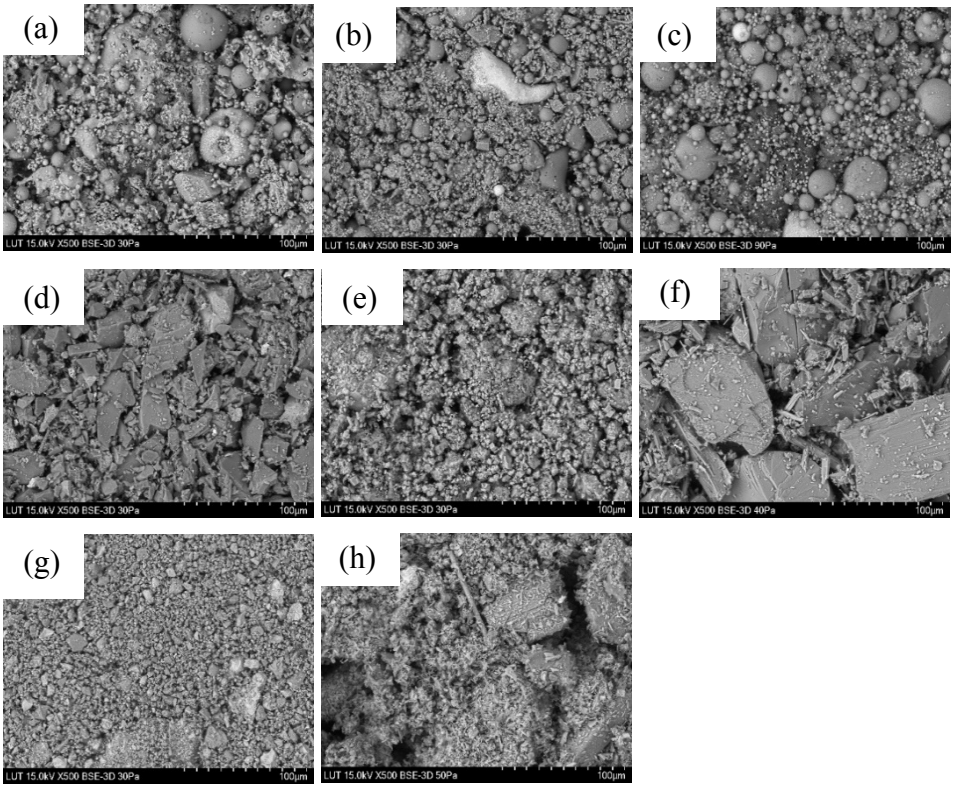

Figure 1. SEM images of the samples (a) FA1, (b) FA2, (c) FA3, (d) BA, (e) GLD, (f) MT, (g) DW, (h) SS

Mineral compositions

Table 5 presents the mineral compositions of the secondary materials. What cannot be observed in Table 5 is that most of the samples contained a considerable amount of amorphous material. The most frequently occurring minerals in the side streams were quartz, anhydrite and calcite. Si and Ca elements were found to be present in different forms of sulphates, oxides and silicates in the ash samples. The coal fly ash sample (FA3) contained quartz and mullite minerals, which was also reported in other studies [4]. Dahl et al. [12] identified anhydrite, lime and quartz in biomass fly ash in their study. The presence of portlandite, calcio-olivine and calcite were found in other studies [13]. De Boom and Degrez [14] identified gehlenite when they studied the mineral composition of biomass fly ash. The bottom ash (BA) sample contained various phases of silicate: albite, microcline and quartz, which were previously detected [11]. Binary, ternary and quaternary phases containing Ca, Fe and Si were detected in steel slag (SS) including, larnite, wuestite and srebrodolskite. The presence of larnite and wuestite were found before in other studies [6].

Trace element concentrations

Table 6 shows the potentially hazardous trace element concentrations of the side streams obtained with ICP-OES analyses. The great variance of the concentrations is due to the different design of incineration plants, and fuel incinerated. When FA2 and BA are compared, concentrations of potentially hazardous trace elements in bottom ash are often detected lower than the ones in fly ash samples, similar to other studies [12].

Table 5. Mineral compositions of the samples

Sample	Mineral
FA1	Anhydrite ($Ca(SO)_4$), Gehlenite ($Ca_2Al_2SiO_7$), Lime (CaO), Portlandite ($Ca(OH)_2$), Quartz (SiO_2)
FA2	Anhydrite ($Ca(SO)_4$), Calcite ($Ca(CO)_3$), Calcio-olivine (ɣ-Ca_2SiO4), Gehlenite ($Ca_2Al_2SiO_7$), Lime (CaO), Quartz (SiO_2)
FA3	Mullite ($Al_6Si_2O_{13}$), Quartz (SiO_2)
BA	Albite ($NaAlSi_3O_8$), Microcline ($KAlSi_3O_8$), Quartz (SiO_2)

Table 6. ICP-OES results of the samples (mg/kg; d.w.)

Metal	FA1 ppm	FA2 ppm	FA3 ppm	BA ppm	MT ppm	SS ppm
Cd	6.2	11	< 2	< 2	< 2	< 2
Co	4.2	32.5	30.9	11.4	3.1	3.9
Cr	58	199	71	111	24	7690
Cu	76	1910	65	1970	9	129
Ni	24	112	84	56	11	52
Pb	20	770	30	165	< 10	< 10

CONCLUSION

Eight different side streams including biomass fly ash, biomass bottom ash, coal fly ash, carbonate mine tailings, demolition and construction waste, steel slag, and green liquor dregs were characterized to understand their utilization potential in geopolymer composites. BA was found to have the largest particle size, followed by tailings and demolition waste with D50 values of 147 and 85 μm, respectively. Fly ash samples were found to consist of spherical and irregularly-shaped particles in a wide size range, while morphologies of bottom ash, demolition waste, green liquor dregs and tailings were predominated by more irregularly-shaped particles. EDS analyses revealed that fly ash and bottom ash streams contain the highest concentrations of aluminum and silicate (3 - 30 w -%). Lower concentrations of calcium were observed in bottom ash and coal fly ash, while steel slag contained over 20 w-% iron. Major minerals identified in the samples were anhydrite and quartz in addition to carbonates, silicates and oxides of aluminum, calcium, iron, potassium and sodium for some samples. These findings suggest that the investigated ash samples, mine tailings and steel slag could be used as sustainable construction materials after pre-treatment and further separation processes.

References

1. European Commission, Environment, Waste. Available from: http://ec.europa.eu/ environment /waste/index.htm, Accessed on February 2, 2019,
2. European Comission, Eurostat, Waste generation, (2016) Available from: https://ec.europa.eu/eurostat/statistics-explained/index.php/Waste_statistics#Total_waste_generation, Accessed on February 2, 2019,
3. Deja, J., Uliasz-Bochenczyk, A., Mokrzycki, E. (2010) CO2 emissions from Polish cement industry. International Journal of Greenhouse Gas Control 4 (4), 583-588.
4. Kaja, A. M., Lazaro, A., Yu, Q. L. (2018) Effects of Portland cement on activation mechanism of class F fly ash geopolymer cured under ambient conditions. Construction and Building Materials, 189, 1113-1123,
5. Zhao, X., Liu, C., Zuo, L., Wang, L., Zhu, Q., Wang, M. (2018) Investigation into the effect of calcium on the existence form of geopolymerized gel product of fly ash based geopolymers, Cement and Concrete Composites.,
6. Santamaria, A., Faleschini, F., Giacomello, G., Brunelli, K., San José, J., Pellegrino, C., Pasetto, M. (2018) Dimensional stability of electric arc furnace slag in civil engineering applications. Journal of Cleaner Production, 205, 599-609,
7. Robayo-Salazar, R. A., Rivera, J. F., Mejía de Gutiérrez, R. (2017) Alkali-activated building materials made with recycled construction and demolition wastes. Construction and Building Materials 149, 130-138,
8. Ahmari, S., Zhang, L. (2012) Production of eco-friendly bricks from copper mine tailings through geopolymerization. Construction and Building Materials, 29, 323-331,
9. Camerani, M.C., Steenari, B., Sharma, R., Beckett, R., 2002, Cd speciation in biomass fly ash particles after size separation by centrifugal SPLITT, Fuel 81, 1739-1753.
10. Davidovits, J. (2015) Geopolymer Chemistry and Applications. 4th edition, Institut Géopolymère, France, 179-187,
11. Valmari, T., Kauppinen, E. I., Kurkela, J., Jokiniemi, J. K., Sfiris, G., Revitzer, H. (1998) Fly ash formation and deposition during fluidized bed combustion of willow. Journal of Aerosol Science, 29 (4), 445-459,
12. Dahl, O., Nurmesniemi, H., Pöykiö, R., Watkins, G. (2010), Heavy metal concentrations in bottom ash and fly ash fractions from a large-sized (246 MW) fluidized bed boiler with respect to their Finnish forest fertilizer limit values, Fuel Processing Technology, 91 (11), 1634-1639,
13. Höllen, D., Berneder, I., Capo Tous, F., Stöllner, M., Philipp Sedlazeck, K., Schwarz, T., Aldrian, A., Lehner, M. (2018) Stepwise treatment of ashes and slags by dissolution, precipitation of iron phases and carbonate precipitation for production of raw materials for industrial applications, Waste Management 78, 750-762,
14. De Boom, A., Degrez, M. (2015) Combining sieving and washing, a way to treat MSWI boiler fly ash, Waste Management 39, 179-188.

XIII International Mineral Processing and Recycling Conference
Belgrade, Serbia, 8-10 May 2019

University of Belgrade, Technical Faculty in Bor
Vojske Jugoslavije 12, 19210 Bor, Serbia
Tel. +381 30 424 555 Fax +381 30 421 078

VALIDATION OF ICP–OES PROCEDURE FOR MAJOR AND TRACE ELEMENTS DETERMINATION IN THE LEACHATES OF FLY ASH AND FLY ASH BASED COMPOSITES

Nevenka Mijatović [1,#], Anja Terzić [1], Ljiljana Miličić [1], Dragana Živojinović [2]
[1]Institute for Materials Testing, Belgrade, Serbia
[2]University of Belgrade, Faculty of Technology and Metallurgy, Belgrade, Serbia

ABSTRACT – The novel global trends for waste materials processing and recycling, as well as new European standards for sampling and testing of these materials, require better performances of analytical methods for the chemical analysis and improvements regarding their matrices. In this study, a new method for optical emission spectrometry with inductively coupled plasma (ICP-OES) has been developed and subsequently validated for determination of 35 elements comprised in leachates of fly ash and composites based on fly ash, i.e. cement pastes and mortars. Validation performances and the uncertainty measurement were determined and calculated via three different routes: validation method, participation in proficiency testing schemes and standard method. It is proved that this method is acceptable for the determination of all 35 elements in this matrix. The obtained results highlight a new simple and effective analyzing route for quantity determination of undesired trace elements in fluids upon conducted leaching test.

Key words: analytical procedures, waste materials, industrial byproducts, leaching test, environmental safety.

INTRODUCTION

Fly ash, a byproduct of coal combustion in power plants, is one of the major causes of environmental pollution. The application of fly ash in the building industry is important for the reduction it its disposed quantities [1]. Fly ash contains hazardous substances such as heavy metals [2]. Heavy metals are prone to mobility in an aqueous medium, which might lead to their leaching into soil and groundwater [3]. Leaching test in the laboratory simulates the natural leaching of heavy metals to the environment [4].

Validation of the analytical method is a procedure which provides accuracy and precision of the results during the long-term use of the method. Validation is achieved by a high degree of reliability and confidence, because validation can

corresponding author: nevenka.mijatovic@institutims.rs

determine the causes of potential problems during application methods [5, 6]. The validation performances for evaluation of analytical method are: selectivity, accuracy, precision, detection limit, limit of quantification, sensitivity, working range and linearity, robustness and recovery [7]. The ICP-OES method is an analytical technique for chemical elements determination. The information regarding the method validation is not easy to find. Statistical tools and analytical methods for the validation [8-10] represent a relatively new method for the interpretation of the data obtained via this instrumental technique. Laboratories also use mathematical tools for the calculation of the measurement uncertainty.

Three solutions for calculation of the measurement uncertainty are presented in this paper - one by in-house validation and two by top-down approaches (data of participation in proficiency testing (PT) schemes and data given in standard method). All necessary steps for evaluation of the measurement uncertainty and validation of determination of 35 elements (Al, Ve, Cd, So, Cr, Cu, Fe, Mn, Mo, Ni, V, Mo, Zn, Pb, Bi, Si, Zr, W, As, Se, Sb, Sn, Ti, Ba, B, Ag, Mg, Ca, K, Na, S, P, Ga, In, Li) in the fly ash and cementitious materials leachates are established.

MATERIALS AND METHODS

Five different materials were used in the leaching test: fly ash, Portland cement paste, Portland cement paste with fly ash, cement mortar and cement mortar with fly ash. CEM I 42.5R (Lafarge) was used for preparation of the cement pastes and mortars. A lignite coal combustion ash from power-plant plant "Kolubara" (Serbia) was employed in the experiment. Fly ash was used in 30 % of cement mass quantity in the composite mixtures.

The samples for the leaching test were prepared according to Standard EN 12457-4. The leachability of heavy metals from fly ash was carried out by mixing the fly ash sample with deionized water in water to binder ratio: 1:10. The mixture was subsequently shaken in a laboratory mixer at room temperature for the next 24 hours. The leachate was then filtered, and metal concentrations were determined by ICP-OES method.

Calibration standards were prepared from Merck standard solutions, i.e. multi-element standard for determination of 22 elements (values given in $mg \cdot dm^{-3}$): Al-998 ± 10, Cd-1001 ± 10 , Co-1000 ± 10, Cr-998 ± 10, Cu-997 ± 10, Fe-1003 ± 10, Mn-1001 ± 10, Ni-1000 ± 10, Sr-1000 ± 10, Zn-998 ± 10, Pb-1002 ± 10, Bi-1001 ± 10, Ba-998 ± 10, B-1003 ± 10, Ag-1001 ± 10, Mg-998 ± 10, Ca-1003 ± 10, K-1000 ± 10, Na-1001 ± 10, Ga-998 ± 10, In-998 ± 10, Li-998 ± 10. Standard solution for the determination of SO42-, P, Se, Sb, Mo, As, Si, Ti, Be, Sn, V, Zr, W were (values given in $mg \cdot dm^{-3}$): SO_4^{2}-1000 ± 2; P-1000 ± 6, Se-992 ± 8; Sb-971 ± 7; Mo-1003 ± 5; As-987 ± 5; Si-9492 ± 70; Ti-1000 ± 2; Be-1000 ± 2; Sn-1000 ± 2; V-1000 ± 2; Zr-1000 ± 2; W-1000 ± 2, respectively. Stock solutions were prepared by a single dilution or series of dilutions to acquire the working concentration set in the range from 0.50 $mg \cdot dm^{-3}$ to 100.00 $mg \cdot dm^{-3}$ for each element, except for Ca and S. Concentration ranges of Ca and S were 0.50 $mg \cdot dm^{-3}$ to 1000 $mg \cdot dm^{-3}$. Deionized distilled water was used in all mentioned solutions.

Preparation of the matrix spike standards for all 35 elements (Al, Be, Cd, Co, Cr, Cu, Fe, Mn, Mo, Ni, V, Sr, Zn, Pb, Bi, Si, Zr, W, As, Se, Sb, Sn, Ti, Ba, B, Ag, Mg, Ca, K, Na, S, P, Ga, In, Li) was conducted by adding standard solutions with known

concentration to real samples, i.e. leachates.

An ICP analyzer, Spectro Genesis with a plasma generator working at 27.12 MHz was used in all experiments. Power generator is 1.700 KW. The consumption of argon (high purity argon - 99.9999 %) is used during analysis is 16 l per minute. A holographic grating is 2400 point/mm. The plasma is positioned radially with the range of wavelength of 175 – 775 nm. The results are determined via Smart Analyzer Vision software.

RESULTS AND DISCUSSION

According to EURACHEM 1998, the validation was performed by evaluation of the selectivity i.e. the ability to unequivocally assess the analyte in the presence of components that are expected to occur in the solution (Matrix effect), limit of detection (LoD), limit of quantification (LoQ), precision (repeatability and reproducibility) and accuracy. Parameters of calibration lines are: wavelength of the emission line (λ), limits of detection (LoD), limits of quantification (LoQ), correlation coefficients (R), Y-intercepts, slopes of linear function, proportion of two slopes calibration lines, one of the original standard solution and another derived spike standard solution and working ranges are given in Figure 1.

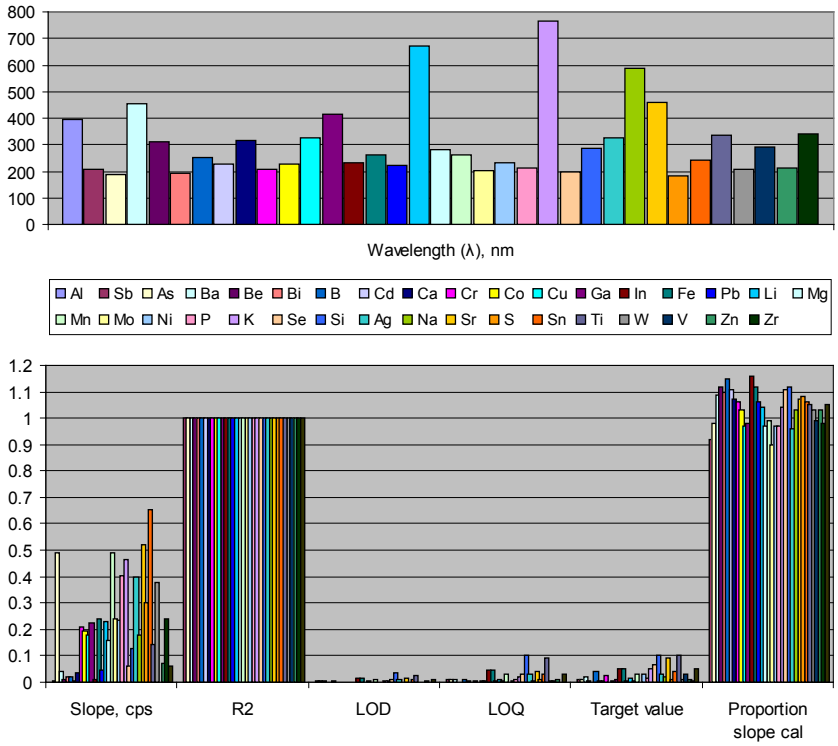

Figure 1. Data for selectivity and linearity for ICP analysis of fly ash leachate.*

* Slope (cps $dm^3 \cdot mg^{-1}$); LOD ($mg \cdot dm^{-3}$); LOQ ($mg \cdot dm^{-3}$); Target value ($mg \cdot dm^{-3}$))

Parameters of linearity and selectivity were determined using Merck standard

stock solutions with the concentration range from 0.50 to 100.00 mg·dm^{-3}. Four of the most sensitive lines were selected for each element from a software wavelengths library. The working wavelength with a minimum of spectral interference and the matrix effects of the sample were selected by comparing slopes of the proportion of two calibration lines - one of the original standard solution and the other derived from the spike standard solution. The selected wavelength from the available specter/database of wavelengths is one in which ratio of these slopes is the closest to 1.00. After selecting the appropriate wavelengths, the quantitative determination method is carried out manually. The background for each of the selected line was corrected in order to achieve many possible relationships with the signal intensity, which was derived from the background element and the signal itself. LoD, LoQ, correlation coefficients, Y-intercepts and slopes of linear function are automatically calculated by Smart Analyzer Vision software.

If the correlation coefficient is close to 1 then the linearity of the method is better. Fig. 1 shows that the correlation coefficients are higher than 0.99. This emphasizes the fact that the methods applied within the selected range of the concentrations gave the results that are directly proportional to the concentration of elements in the sample. LoD and LoQ showed that the targeted performances were achieved by this method.

The accuracy and the precision of proposed method were tested by the determination of the content of each analyzed elements and by comparison of these values with the concentration of the certified standard solutions. This validation step was determined by the contents of each of the analyzed elements using Merck standard stock solutions. The concentration of the 2.00 mg·dm^{-3} was applied for the all elements, except for Ca, S, Al, Si, K and Na. For Ca and S were used standard stock of the 100.00 mg·dm^{-3}, while for Al, Si, K and Na were used 20.00 mg·dm^{-3}. This standard solution was selected to determine the accuracy and precision of all the elements of this method because that is due to the approximate contents of all elements in real samples. The precision could be expressed mostly by repeatability and reproducibility. The repeatability and reproducibility were assessed on daily basis. The variations between daily measurements were estimated. The results obtained for repeatability were conducted on six parallel samples by a single operator using the same equipment. Precision (repeatability) was expressed as % RSD. Accuracy is given as the difference in recovery of the CRM target value and the obtained value (Fig. 2).

The results provided in Fig. 2 show that the recoveries for all elements were in range of approximately ±7 % of target values. For concentrations of the 2.00 mg·dm^{-3}, RSD was below 5 %. For concentrations of the 20.00 mg·dm^{-3}, RSD was below 1 %. For concentration of the 100.00 mg·dm^{-3}, RSD for Ca and S were 0.3 %.

Measurement of the uncertainty was calculated by Nord test concept, i.e. recovery test approach [11]. In this approach, the sources of uncertainty are grouped into the two major components: precision and trueness. These two major components in the single laboratory validation and QC approach are the within-laboratory reproducibility and bias (Eq. 1).

$$u_c\ (\%) = \sqrt{u(R_w)^2 + (u(Bias)^2)} \quad (1)$$

u_c is combined standard uncertainty, $u(R_w)$ - uncertainty of the estimate within-

laboratory reproducibility, $u(Bias)$-uncertainty of the estimate of the laboratory and the method bias.

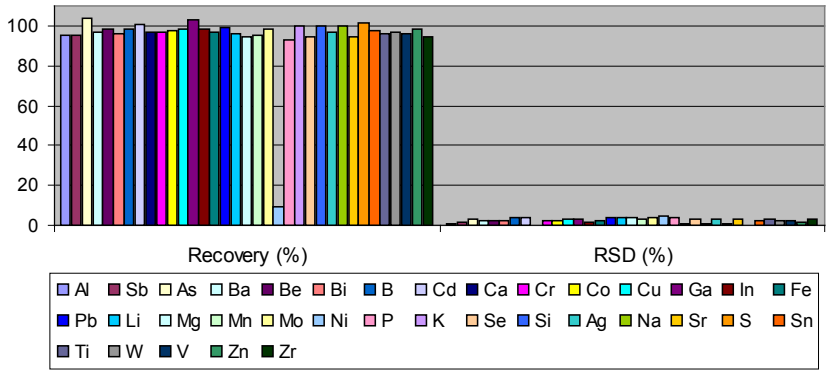

Figure 2. Accuracy and precision for ICP analysis of fly ash leachate

The uncertainty component for within-laboratory reproducibility $u(R_w)$ was estimated using repeated measurements of a control sample (similar matrix and concentration as the test samples) over a long period of time. R_w includes repeatability and between-days (runs).

$Bias$ includes both - laboratory and procedural bias. In this case, uncertainty of $Bias$ was calculated from the validation data (accuracy) of the spike recovery, data from the certificate of calibration of the reference materials and volumetric glassware (Eq. 2).

$$u(Bias) = \sqrt{RMS_{Bias}{}^2 + u(Cref)^2} \tag{2}$$

$u(Bias)$ - uncertainty of the estimate of the laboratory and the method bias.

Main sources of uncertainty measurement in this case were: uncertainty of the calibration of reference materials, uncertainty of measured intensities of the reference solutions, uncertainty of delivered volumes and recovery of the method. Recovery eliminates possible interferences in the method for the samples of selected matrix. After estimation, all sources of uncertainty were combined and converted to combine the standard uncertainty $u(x)$. The final result was given as the expanded uncertainty $U(x)$, which was calculated as $U(x) = k \cdot u(x)$, where k is the coverage factor corresponding to a 95 % confidence level. Calculations were made by using the Mathcad software which was checked and validated before use. The results of the measurement of uncertainty by data of validation for 35 elements in fly ash leachate sample are given in Figure 3.

One of the easier ways to calculate measurement uncertainty is by using data of the participation in proficiency testing (PT) schemes. In such case, s_R from inter-laboratory comparisons were used directly for each compared element as an approximation of $u(x)$. The expanded uncertainty calculated $U(x) = 2 \cdot s_R$, for each element. The results of the measurement of uncertainty for 17 compared elements are also provided in Fig. 3. This method may over-estimate the uncertainty

depending on the quality of the laboratory. It may also under-estimate the uncertainty due to the sample inhomogeneity or matrix variations. In this case, s_R, given in standard method was directly used and the expanded uncertainty was calculated $U(x) = 2 \cdot s_R$ for each element. The results of uncertainty measurements calculated by data given in standard method are given in Fig. 3.

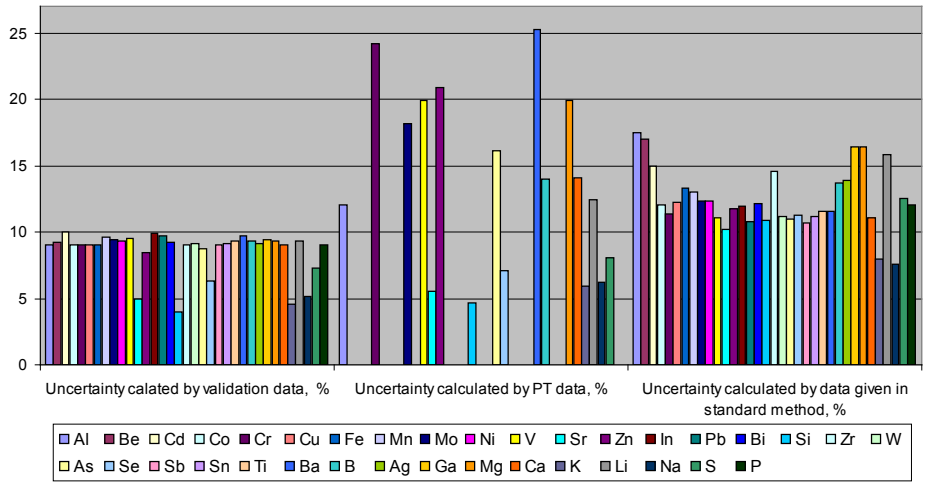

Figure 3. ICP method uncertainty measurement upon analysis of fly ash leachate * * Working range for Al-Ga: 0.05-10, Mg-P: 0.1-100

Values of extended measurement uncertainty calculated by data of validation are lower than 10 %. These values are less than values obtained in measurement uncertainty calculated by data of (PT) and measurements uncertainty calculated by data given in standard method. The measurement uncertainty should be smaller than the target value. If the target uncertainty is not defined in a regulation or specification it is considered that additional tolerance can be in a range of 20-30 % in order to allow the variability of the uncertainty estimation process. All values in Fig. 3 are below 30 %.

The concentrations of 35 elements in the fly ash leachate were compared to the values obtained on the samples of cement pastes and mortars (standard pastes/mortars and those with 30 % addition of fly ash). The contents of heavy metals contained in the leachate from composites that comprised fly ash were much higher than those found in standard cement pastes and cement mortars. However, concentrations of heavy metals in leachates of standard binders as well as binders with addition of fly ash were significantly lower than concentrations of these elements in fly ash leachate. This is explained by the fact that during hydration heavy metals are immobilized by the crystalline structure of the cement minerals.

CONCLUSION

A fully validated method for ICP-OES analysis of the fly ash leachate is presented. This method enables the quantification of 35 selected metals. The validation results

satisfy the criteria for waste water (EN ISO 11885:2011). All uncertainty results were below 30 %. It was concluded that different approaches can be selected for the evaluation of measurement uncertainty, depending on the purpose and available data. The development of this method facilitates and speeds up the process of trace metals in the leachate from fly ash as the waste material, which is widely used in construction industries.

Acknowledgements:

This investigation was supported by the Serbian Ministry of Education, Science and Technological Development and it was conducted under the project III 45008.

References

1. Terzić, A., Pezo, L., Mijatović, N., Stojanović, J., Kragović, M., Miličić, Lj., Andrić, Lj. (2018) The effect of alternations in mineral additives (zeolite, bentonite, fly ash) on physico-chemical behavior of Portland cement based binders. Construction and Building Materials, 180, 199-210,
2. Terzic, A., Đorđevic, N., Mitric, M., Markovic, S., Đordjevic, K., Pavlović, V. (2017) Sintering of Fly Ash Based Composites with Zeolite and Bentonite Addition for Application in Construction Materials. Science of Sintering, 49 (1), 23-37,
3. Terzić, A., Radojević, Z., Miličić, Lj., Pavlović, Lj., Aćimović, Z. (2012) Leaching of the potentially toxic pollutants from composites based on waste raw material. Chemical Industry and Chemical Engineering Quarterly, 18 (3), 373-383,
4. Manoj T., Samir, B., Dewangan, U., Raunak, K. (2015) Suitability of leaching test methods for fly ash and slag: A review. Journal of Radiation Research and Applied Sciences, 8 (4), 523-527,
5. ISO 8402:1994. Quality management and quality assurance – Vocabulary,
6. ISO 3534-1:2006. Statistics - Vocabulary and symbols - Part 1: General statistical terms and terms used in probability,
7. ISO/IEC 17025:2017 – General requirements for the competence of testing and calibration laboratories,
8. Sereshti, H, Far, A. R., Samadi, S. (2012) Optimized Ultrasound-Assisted Emulsification-Microextraction Followed by ICP-OES for Simultaneous Determination of Lanthanum and Cerium in Urine and Water Samples. Analytical Letters, 45 (11), 1426-1439,
9. Biata, N., Dimpe, K., Ramontja, J., Nomngongo, P. (2018) Determination of thallium in water samples using inductively coupled plasma optical emission spectrometry (ICP-OES) after ultrasonic assisted-dispersive solid phase microextraction. Microchemical Journal, 137, 214-222,
10. Capra, L., Manolache, M., Ion, I., Ion, A. (2016) Validation of a method for determination of antimony in drinking water by ICP-OES. UPB Scientific Bulletin, Series B: Chemistry and Materials Science, 78 (3), 103-112,
11. Magnusson, B., Näykki, T., Hovind, H., Krysell, M. (2013) Handbook for Calculation of Measurement Uncertainty in Environmental Laboratories. Edition 2, Nordtest report, Espoo, Finland.

XIII International Mineral Processing and Recycling Conference
Belgrade, Serbia, 8-10 May 2019

University of Belgrade, Technical Faculty in Bor
Vojske Jugoslavije 12, 19210 Bor, Serbia
Tel. +381 30 424 555 Fax +381 30 421 078

INVESTIGATION AND DEVELOPMENT OF RECYCLED WATER CONDITIONING BY THE ENRICHMENT OF COPPER-MOLYBDENUM ORES

Irina Pestriak [1,#], Valery V. Morozov [1], Galina P. Dvoychenkova [2], Erdenetuya Otchir [3]

[1]National University of Science and Technology "MISiS", Moscow, Russia
[2]Research Institute of Comprehensive Exploitation of Mineral Resources Academy of Sciences, Moscow, Russia
[3]Erdenet Mining Corporation, Erdenet city, Mongolia

ABSTRACT – Accumulations in the circulating water of ion-molecular components leads to lower efficiency of enrichment and processing of copper-molybdenum ores. The objective of the investigation is to determine the maximum allowable concentrations of ions and molecules as well as the choice of conditions for the deposition or adsorption. First of our experiences was to decrease the concentration in the circulating water of the copper ions and fatty acids. For reducing the concentration of copper ions and fatty acids in the recycled water is investigated the operation of pre-mixing of water flows with the highest concentrations of these ions. The results to be achieved consist not only in ensuring of the achievement of the concentrations of the ions of copper and iron, however, significantly reducing the amount of oxidized copper, make it possible to use the united sewage as current water for flotation process. Based on the research findings, as applied to Erdenet MC, maintaining pH range of 7.2 - 7.8 was been recommended for the being treated wastewater of complex chemistry. Mixing and adding in recycled water the filtrate of tailings, discharges of urban wastewater treatment and effluent of ash pit CHP provides increase in capacity of water flow at the enrichment plant by 15-17 %.

Key words: copper-molybdenum ores, enrichment, recycling water, conditioning, flotation.

INTRODUCTION

An important task being solved for circulating water supply system at mining and processing plants is the cleaning and conditioning of the circulating waters up to the level that supports the enrichment technology at a high level, which achieved by using of natural water [1]. Part of this task is maximal using wastewater complicated chemical composition, formed by atmospheric oxidation of dumps and tailings stockpiled [2].

Effective way to reduce the negative impact of tailings effluent to surface water

corresponding author: spestryak@mail.ru

and groundwater is the application of chemical methods of binding the heavy metal ions and fatty acids in insoluble compounds that not only allows you to drastically reduce the concentration of harmful substances, but also extract the valuable components contained in wastewater [3, 4].

INVESTIGATION OF THE CHEMICAL DEPOSITION OF IONIC COMPOUNDS IN WASTEWATER

To conduct flotation studies used the reverse water - draining tailings of Erdenet mining corporation (Erdenet MC). Before carrying out a process of collective flotation it was added copper sulfate in an amount necessary to achieve the desired concentration of copper ions. The circulating water was applied in the grinding process of copper-molybdenum ore and the classification operation. Procedure reagents conform to the regime adopted at the factory.

Thermodynamic modeling methods for computation of the state of copper compounds in detail in the book [5]. Analysis of the results of calculation and validation of precipitation indicates that the interaction with ions of copper, accompanied by the formation of normal copper oleate occurs with the presence of separation of ions and compounds of oleic acid with total concentration of more than 10^{-6} mol/l (0.3 mg/l). Reaction takes place in acidic and neutral environment. When the concentration of ions of copper and oleic acid reduce the formation of copper oleate doesn't occur. The increasing of pH level to alkalescent turns the copper oleate into hydroxide-carbonate copper [6].

As seen from Table 1, the effluents from the tailings storage facility-settling pond of Erdenet MC are alkaline and characterized by high concentration of carbonate ions and low concentrations of heavy metals. The seepage waters, collected from the aquifers beneath the embankment foundation, are weakly acid and with marked contents of heavy metals. The municipal treatment plant sewage contains fair quantities of various organic compounds, including fats, fatty acids, synthetic surfactants and other.

Table 1. Chemistry and properties of the wastewaters of mining and benefication combine "Erdenet"

Type of wastewaters	Concentration, mg/l					
	pH	$[Cu^{2+}]$	[Fe]	$[HCO_3^-]$	[OR]	$[Ca^{2+}]$
Tailings of processing plant	9.1-10.1	< 0.01	< 0.01	125-160	12.5-14	310-420
Flows from the tailings ponds	7.8-8.3	< 0.04	< 0.02	125-160	7-8	160-200
Dams filtrate - seepage waters	6.4-7.0	1.8-4.5	0.3-1.5	150-180	6-7.5	145-234
Sewage of urban wastewater treatment plants	7.1-7.6	< 0.01	0.03-0.04	165-340	25-50	120-150
Sewage of dam ash CHP	7.5-8.9	< 0.01	< 0.01	178-230	0.9-1.5	140-300

[OR] - organic compounds

To provide maximum decreasing the concentrations of the heavy metal cations at

combining all these wastewaters, mechanism of the proceeding reactions in this process should be determined. This will enable to select and justify the optimum conditions for the reactions.

As the initial components of the wastewaters and filtrates, we took into account copper and calcium ions, ion-molecular species of carbonic and oleic acids, hydrogen and hydroxyl ions. As sediments, all stable compounds, formed in the course of the components interaction, are considered.

To determine conditions of the insoluble compounds formation, thermodynamic analysis of chemical interaction of copper and calcium ions with the other components of the liquid phase was implemented. The calculation technique is described in studies [4].

In the modeling process, we took into account the actual concentrations of the ion-molecular components (species) in the wastewaters and requirements to recirculating waters for reuse (of the purified waters) in the production process. The previous studies determined the requirements to the ion composition of the recirculating waters: maximum permissible concentration (MPC) for copper ions: 0.4 mg/l, for ions of unsaturated fatty acid series C_{17} – C_{21}: 0.6 mg/l [7]. The special computer program was applied for calculating and plotting the thermodynamic stability diagrams, presenting the inter-phase transition boundaries, confining the compound stability fields at any given concentration of the ion-molecular components.

Review of the calculation results and check of the sediments composition showed that common copper oleate is formed in weakly-acid or neutral media. With growing pH to faintly alkaline reaction, copper oleate transformed in copper hydroxycarbonate. Decreasing pH is undesirable, because this results in dissolving copper oleate with formation of copper cations and oleic acid molecules in the solution.

Notice that in presence of both oleic acid and carbonate components (ions and molecule), the copper deposition form depends on concentrations of the species and pH. At low concentrations of carbonate ions, copper oleate is predominantly formed. With increasing pH, copper oleate is transformed into copper hydroxide and, with increasing carbonate concentration, into copper hydroxidecarbonate.

The implemented calculations and checks of the sediments composition showed that, in the wastewaters, active interaction of oleate ions and calcium ions takes place and results in insoluble calcium oleate formation. This reaction goes at pH ranging 5 to 8. Decreasing the concentrations of calcium ions and oleic acid below 10^{-4} mol/l prevents calcium oleate formation. Increasing pH up to alkaline medium results in conversion of calcium oleate into calcium carbonate. At pH above 8, the only stable form of calcium is calcium carbonate. In acidic medium (pH below 6), calcium oleate is decomposed to form calcium ions and oleic acid.

In natural conditions (exposed to air), in the pH range from 6 to 11, deposition of copper from the wastewater occurs in the form $(CuOH)_2CO_3$. Ingress of oleate ions into the recirculating water enables precipitating copper in the form of copper oleate also. The remaining copper ions are after-precipitated to form copper hydroxycarbonate. In natural conditions, in the same pH range, calcium precipitates in the form of $CaCO_3$, whereas in the presence of oleate ions, calcium oleate primarily originates. After precipitating calcium oleate or with increasing the concentration of

carbonate ions, in alkaline medium calcium carbonate is formed.

The developed model of the precipitation processes enables determining the compounds of copper and calcium (also of other metals in the long term), which are stable at different concentrations of carbonate ions and other aqueous species (ion-molecular components). At the same time, this model enables determining the boundary conditions for precipitation removal of adverse components at any given parameters of recirculating water.

$$lg[HCO_3^-] = 12.36 - 2\,lg[Ca^{2+}] - 3\,pH \qquad (6.36 \le pH \le 10.34) \qquad (1)$$

This constraint equation is the result of the conversion of the equilibrium constant for the resulting reaction, describing calcium oleate formation process in the conditions of copper oleate stability:

$$2Ca^{2+} + 2Cu(Ol)_2 + HCO_3^- + 2H_2O = (CuOH)_2CO_3 + 3H^+ + 2Ca(Ol)_2 \qquad (2)$$

After substituting the average values of the ion concentrations into equation 4, the analytical constraint equation was obtained for the variable parameters of the thermodynamic stability diagrams describing the conditions for the simultaneous binding of oleate ions in copper and calcium oleate. These constraint equations are designed to select the optimal conditions for recirculating water treatment. For example, using the data on the actual concentration of bicarbonate ions in the recirculating waters ($10^{-4.5}$ – 10^{-4} mol/l), the optimal pH range (7.0 - 7.23), in which the most complete oleate ion precipitation is achieved with high degree of copper ion precipitation, is determined.

RESEARCH AND TESTING OF WATER RECYCLING SCHEMES TO ERDENET MINING AND PROCESSING PLANT

The calculation results are satisfactorily confirmed by the data of industrial researches of the recirculating water at Erdenet mining and processing combine, Mongolia that gives the evidence of applicability of the developed scientific approach and physic-chemical model for precipitation of metal cations and fatty acid compounds from the wastewater of complex chemical composition.

Based on the research findings, as applied to Erdenet MC, maintaining pH range of 7.2 - 7.25 was been recommended for the being treated wastewater of complex chemistry. The proposed wastewater treatment flow sheet and the process procedure provides for combined treatment of the seepage water with the municipal treatment plant sewage and the power building ash dump effluents. For instance, this is possible by mixing the wastewaters in the following ratio: seepage water - 1, the municipal treatment plant sewage - 0.8, the power building ash dump effluents - 0.2.

For a more complete and stable capture of unwanted ions, it was proposed to apply a method of their deposition using limestone as a regulator of the medium. The analysis of the nature of the dependences shows that with the use of $Ca(OH)_2$ with an increase in pH, the concentration of copper ions decreases more intensely than with the use of NaOH (Fig. 1). The dependence of the change in the concentration of oleate ions on pH using $Ca(OH)_2$ is similar in nature, but has a wider pH range in

which the minimum measured concentrations of fatty acids are maintained in the pH range from 6.5 to 7.8, which corresponds to the results of thermodynamic modeling conditions for the binding of oleate ions to calcium oleate in the specified pH range.

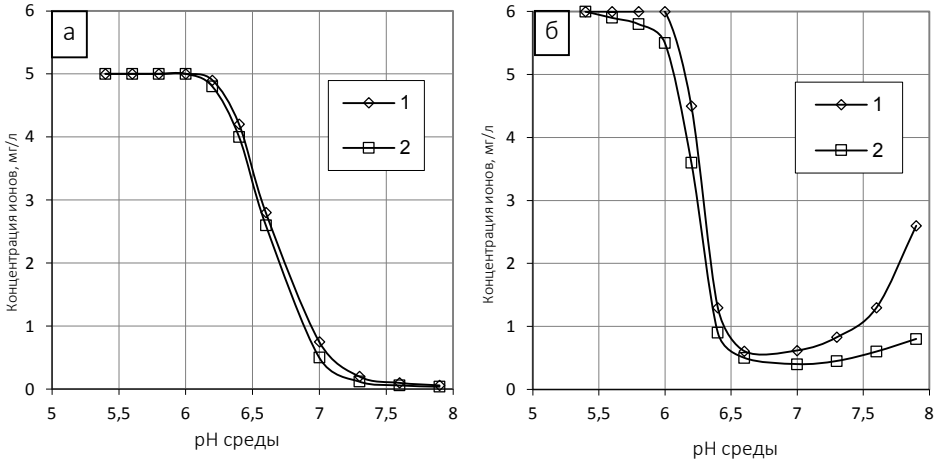

Figure 1. Dependence of changes in the concentrations of copper ions **(a)** and oleic acid **(b)** while regulating the pH of the combined drainage water and domestic waste water using NaOH (1) and $Ca(OH)_2$ (2)

The research findings make it possible to use the combined wastewaters as the recirculating water for the flotation process, as evidenced by the implemented industrial tests of the existing flotation flow sheet for processing of the copper-molybdenum ores.

The test results showed that the use of the water, produced by the extended water circulation flow sheet (Fig.2), including pre-mixing the seepage water, the municipal treatment plant sewage and the power building effluents in the predetermined ratio of their volumes and when adding lime, improves the copper-molybdenum ore concentration performance in comparison with the design layout of the recirculating water supply system expansion (Table 2).

The copper-molybdenum ore concentration performance data, for the option of applying the developed flow sheet and procedure of recirculating water supply, presented in Table 2, evidence that, while maintaining the level of copper and molybdenum recovery, grade of the copper and molybdenum concentrates is markedly increased by 0.4 and 0.6 %, respectively.

Adding in recycled water the filtrate of tailings, discharges of urban wastewater treatment and effluent of ash pit CHP provides increase in water flow by 15-17 %.

Applying the developed water treatment process procedure also provided decreasing heavy metal ions concentrations in the subsurface groundwater used by people for domestic needs. As is seen from Table 3, applying the developed flow sheet and water treatment procedure has provided decreasing the concentration of copper ions in the subsurface waters downstream (beneath) the tailings storage facility (pit № 1) by 40 %, that of fatty acids - in 2 times.

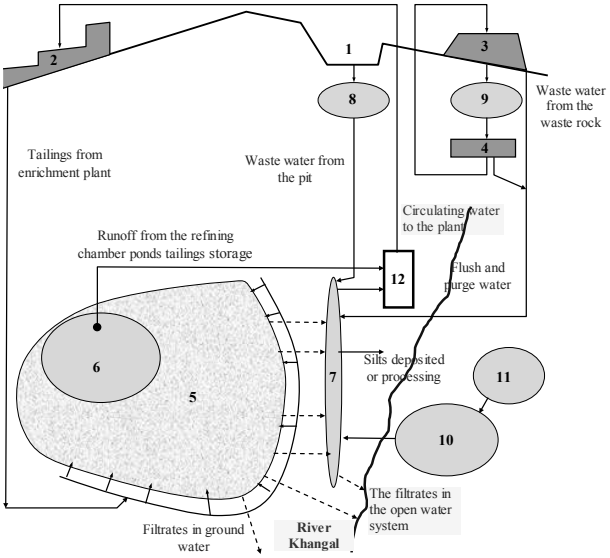

Figure 3. Schematic diagram of the water cycle recommended for Erdenet MC: **1** - quarry; **2** - enrichment plant; **3** - leach pad; **4** - hydrometallurgical plant; **5** - tailings; **6** - lake; **7** - filtration channel; **8**, **9** - collections of waste; **10** - urban waste water treatment plant; **11** - ash dump of Energy division; **12** - sludge collection

Table 2. The recirculating water parameters and the concentration performance using the extended water circulation layouts for the Erdenet processing plant

Experimental conditions of circulating water	pH	Concentrations in circulating waters, mg/l		Content in concentrate, %		Recovery in concentrates, %	
		Cu	fatty acids	Cu	Mo	Cu	Mo
Mixing flows from the tailings ponds and filtrate dam	8.2 - 8.35	0.65	0.25	21.5	49.0	86.23	36.3
Mixing the filtrate dam and sewage urban wastewater treatment plants	6.3 - 7.6	0.55	1.35	20.5	49.1	85.01	35.5
Mixing flows from the tailings ponds, waste rock, dams filtrate, urban plant and sewage CHP wastewater treatment when adding lime	7.5 - 7.8	0.15	0.4	21.9	49.6	86.24	36.8

Table 3. Chemistry and properties of the wastewaters and the natural waters before and after applying the water treatment process with combining the highly contaminated wastewaters

Product	Concentration, mg/l					
	pH	[Cu]	[Fe]	[OR]	[SO_4^{2-}]	[Cl^-]
The tailings storage facility seepage water	6.4 - 7.0	0.8 - 4.5	0.3-1.5	6 - 7.5	625 - 1000	20 - 30
Pit №1 (subsurface waters beneath the seepage zone) without combining the wastewaters	7.0 - 7.2	0.1 - 0.25	0.01 - 0.02	1 - 2	600 - 870	20 - 35
Pit №1 (subsurface waters beneath the seepage zone) after combining the wastewaters	7.2 - 7.8	0.05 - 0.07	< 0.01	1.5 -2.9	650 - 750	25 - 45
Seepage water (before combining the wastewaters)	6.8 - 7.1	1.0 - 2.5	0.02 - 0.04	5 - 6.5	600 - 950	20 - 35
Seepage waters (after combining the wastewaters)	7.6 - 8.2	0.05 - 0.1	0.01 - 0.02	1.5 -2.5	600 - 950	25 - 40

OR - organic compounds

CONCLUSION

The procedure for highly contaminated wastewater treatment, included in the mining and benefication combine "Erdenet" recirculating water supply system, not only solves the process task of reducing fresh water consumption and losses of the valuable components, but also provides environmental benefit: decreasing the concentration and discharge of the regulated contaminants into the subsurface waters within the combine industrial site.

References

1. Baimakhanov, M. (2011) System of internal-drainage water rotation at concentrating plants of nonferrous metallurgy with simultaneous perfection of their technology. Nonferrous Metals, 1, 56-60,
2. Radić, R., Milošević, Ž., Jurić, S., Čudić, S. (2016) Flotation of ores and waste waters. Metalurgija, 55 (4), 832-834,
3. Morozov, V., Avdokhin, V. (1999) Scientific basis for purification of wastewaters and treatment of recirculating waters of ore mining and processing enterprise with valuable component utilization. Mining Informational and Analytical Bulletin, 6, 14-16,
4. Leay, G, Smart, R. S., Skinner, W. M. (2001) The impact of water quality on flotation performance. The Journal of The South African Institute of Mining and Metallurgy, 101, 69-75,

5. Abramov, A. (2010) Flotation. Physico-chemical modeling of the processes, Mir gornoy krnigi, Moscow, 672,
6. Erdenetuyaa, O., Pestryak, I., Morozov, V. (2012) Development of reagent-free method for recirculating water treatment at Erdenet ore mining and processing enterprise. Mining Informational and Analytical Bulletin, 8, 133-136,
7. Pestriak, I., Morozova, O. (2013) Research and development of water treatment technologies for processing of copper-molybdenum. Proceedings of the XV Balkan Congress on Mineral Processing. Sozopol, Bulgaria, 345-349.

XIII International Mineral Processing and Recycling Conference
Belgrade, Serbia, 8-10 May 2019

University of Belgrade, Technical Faculty in Bor
Vojske Jugoslavije 12, 19210 Bor, Serbia
Tel. +381 30 424 555 Fax +381 30 421 078

EXAMINATION OF ADSORPTIONAL ABILITY TO THE NATURAL RAW MATERIAL - PERLITE FROM R. MACEDONIA

Blagica Cekova [1, #], Viktorija Bezhovska [2], Afrodita Ramos [1], Filip Jovanovski [2]

[1]MIT University, Faculty of Enviromental Resources Management, Skopje, Republic of North Macedonia

[2]University St. Cyril and Methodius, Faculty of Technology and Metallurgy, Skopje, Republic of North Macedonia

ABSTRACT – Perlite as a raw material is an interesting material, so it is the object and purpose of our research. Perlite is examined as a substrate, and it finds application in horticulture and construction. There are two types of perlite crude and expanded perlite. The perlite is an amorphous volcanic glass and is usually formed by hydration of an obsidian (a rock formed by a rapid cooling of a volcanic lava). The obtained chemical analyzes show that SiO_2 is dominant oxide with 75.47 mass % and Al_2O_3 12.77 mass %, small amount of Fe_2O_3, 0.94 mass % and a very small percentage are present oxides of sodium, potassium, magnesium and calcium. In this paper, the specific surface of the perlite with a static gravimetric method will be determined and then tested as an absorbent. The results will be shown graphically with adsorption isotherms.

Key words: perlite, adsorption, adsorption isotherm, specific surface area.

INTRODUCTION

The Republic of Macedonia has a large number of non-metallic raw materials that can be used to obtain new products that find a variety of aplication. One of these raw materials is the perlite of the Kavadarci region of the Republic of Macedonia. Perlite as a raw material is an interesting material, so it is the object and purpose of our research. Perlite is examined as a substrate, and it finds application in floriculture and construction. There are two types of perlite crude and expanded perlite. The expanded perlite is the most used and used as a substrate in the soil. The perlite has a glass structure, since it originates from glassy magmatic rocks.

Essentially perlite and vermiculite are used in the horticultural industry because they both provide aeration and drainage, they can retain and hold substantial amounts of water and later release it as needed, they are sterile and free from diseases, they have a fairly neutral pH (especially perlite which is neutral), and they

corresponding author: cekovab@yahoo.com

are readily available, non-toxic, safe to use, and relatively inexpensive. As a rule of thumb, perlite tends to last longer, has a more neutral pH, and functions much better in hydroponics, outdoor applications, lawns and gardens (in part because it is stronger). Nevertheless, for decades they both have been used by professionals, dedicated amateurs and gardeners. [1, 2]

MATERIAL AND METHODS

For the tests, is used natural material - perlite, the size of the particles is 0.063 mm. The composition of the perlite is determined by silicate analysis, the structural tests are performed by an IR method, and the thermal transformations with DTA and TGA analysis.

RESULTS AND DISCUSSION

The test sample is taken from perlite (Figure 1) with particle size of 0.063 mm. A silicate analysis was performed with alkaline melting. The results are presented in Table 1.

Table 1. Chemical analysis of perlite

Components	Quantity expressed in %
SiO_2	75.47
Al_2O_3	12.77
K_2O	4.51
CaO	0.61
Fe_2O_3	0.94
Na_2O	3.04
MgO	0.10
TiO_2	0.20
Loss of mass	2.36
Total	100 %

Figure 1. Sample of perlite

From the results obtained from the chemical analysis, it can be concluded that the SiO_2 component is dominant, in relation to other components. The presence of colored materials is in small quantities, so the perlite is white. The presence of the elements: Ni, Pb, Mn, As, Cr, B, Cu, Cd and Zn is insignificantly small and is > 0.1 ppm.

The results obtained for the perlite of the Republic of Macedonia were determined by chemical analysis of the perlite of the Republic of Poland, and it was concluded that there are no major deviations and differences in these perlites. The components SiO_2 and Al_2O_2 dominate in all analyzes. [3, 4]

The structure is determined by Infrared Spectroscopy (IR) and the resulting spectrum is shown in Figure 2.

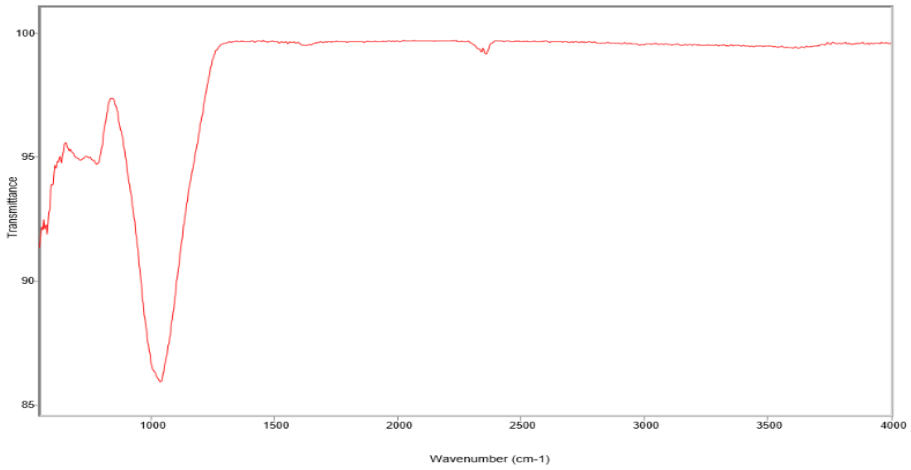

Figure 2. IR spectrum of perlite

With the assignment of the IR spectrum, the following was noted:

- In the area of 2250 - 2500 cm^{-1}, a tape emerges as a result of the molecular valence vibrations of valentine water.
- The tape hat appears in the 1000 - 1200 cm^{-1} area is the SiO_2 bond with the perlite.
- In the area of 500 - 600 cm^{-1}, vibrations emerge from plagioglysis and quartz. [5, 6]

The thermal transformations of the perlite are given in Fig. 3.

Where DTA, TG and DTG curves are given at a temperature of 850 - 900 °C, the water quickly exits the structure of the perlite. The DT curve at 110 °C produces a crystalline mullite with porous structure. The expanded perlite is modified with an aluminum-silicate gel. The TGA curve gives the mass loss and it is 2.36 g / mass. DTG is a mathematical function of DTA and TGA curves. The specific surface of the perlite is determined by a static gravimetric method.

Various concentrations of H_2SO_4 in a thermostat are used for this test. The results are given by the adsorption isotherm in Figure 4, the linear shape of Figure 5, the specific surface of the perlite is determined from the linear shape by applying the BET equation.

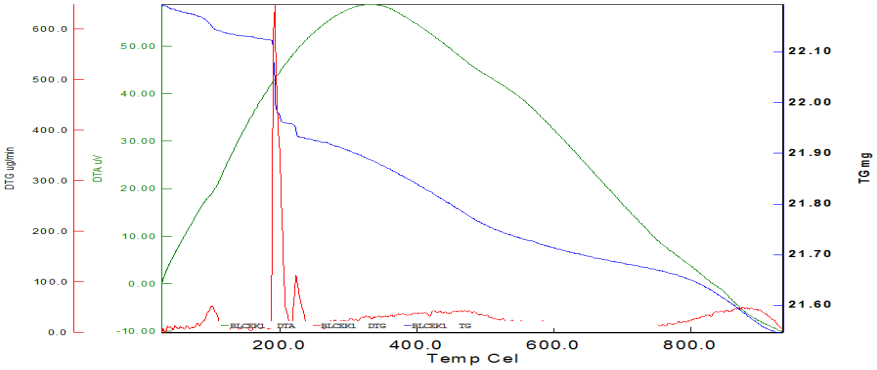

Figure 3. DTA range of Perlite

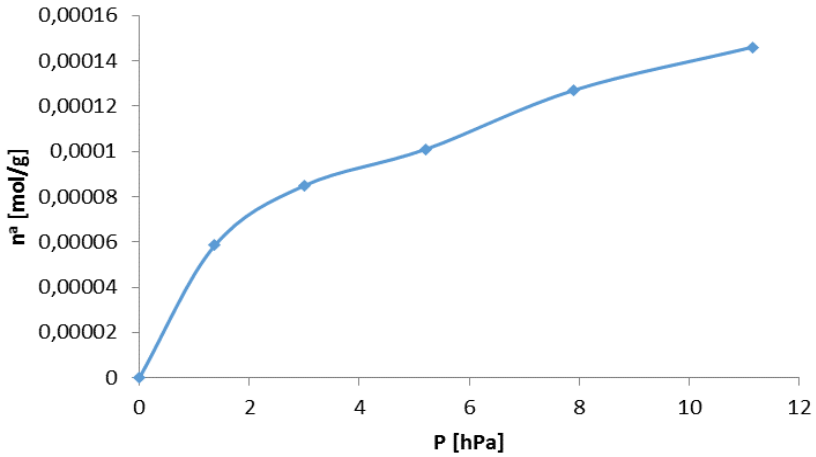

Figure 4. Adsorption Isotherm of perlite

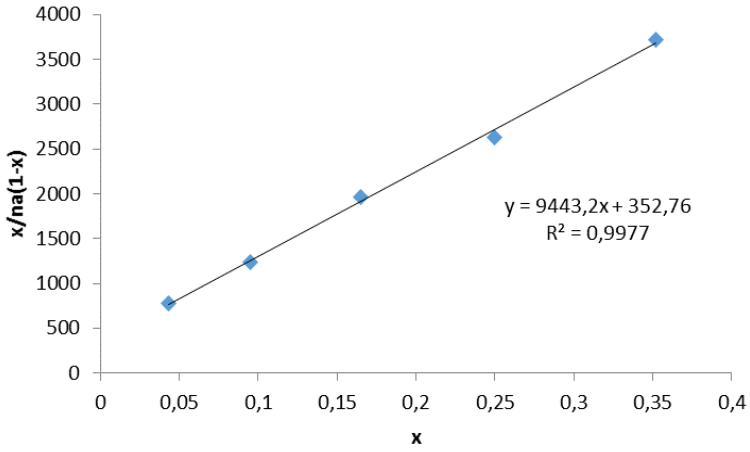

Figure 5. Linear shape of the BET equation

Certain specific area is 6.51 m^2/g. On the perlite examinations were carried out for its application in the synthesis of porous materials.

CONCLUSION

The perlite as a raw material from the Republic of Macedonia finds a variety of applications, it has been initially tested for porous materials, in the construction industry it can be tested as an insulator and large amounts of perlite are used as substrates in agriculture. The advantage is great because as a raw material is clean, environmentally friendly, there is the possibility of adsorption of heavy metals from water and soil.

References

1. Allen, R. L. (1988) False pyroclastic textures in altered silicic lavas, with implications for volcanic associated mineralization. Economic Geology, 83 (7), 1424-1446,
2. Bolen, P. W. (2009) Perlite. USGS Minerals Yearbook, United States Patent 4940497,
3. Koukouzas, N., Dunham, A. (1994) Genesis of a Volcanic Industrial Rock. Trachilas perlite deposit, Milos island, Greece,
4. Orhun, O. (1969). Perlit, Madenciler, 8 (4), 213-222,
5. MTA. (1985) Türkiye Perlit Envanteri. Ankara: Maden Tetkik ve Arama Genel Müdürliğü Yayınları,
6. Tkalchel, E. (1980) Emajl - keramika - staklo, 1-2.

XIII International Mineral Processing and Recycling Conference
Belgrade, Serbia, 8-10 May 2019

University of Belgrade, Technical Faculty in Bor
Vojske Jugoslavije 12, 19210 Bor, Serbia
Tel. +381 30 424 555 Fax +381 30 421 078

SET PLAN AND CRITICAL METALS

Marinela Ivanova Panayotova [1, #], Vladko Toforov Panayotov [2]
[1]University of Mining and Geology, Sofia, Bulgaria
[2]Academy of Sciences, Sofia, Bulgaria

ABSTRACT – The Strategic Energy Technology Plan (SET-Plan) of the EU aims to transform the way we produce and use energy by accelerating the deployment of low-carbon technologies, thus contributing to: securing energy supply for EU, increasing competitiveness of EU companies, and fight against climate changes. Studies have pointed five metals (tellurium-Te, indium-In, gallium-Ga, neodymium-Nd and dysprosium-Dy) as critical with respect to SET-Plan implementation. The paper presents the use, demand, reserves, classical production ways of Te, In, Ga, the possibilities for their recycling, substitution in SET-Plan technologies and extraction from non-traditional sources, such as tailings, slag and other techogenic waste.

Key words: gallium, indium, tellurium, metals from tailings and technogenic waste

INTRODUCTION

To stop dangerous climate changes, greenhouse gas emissions must decrease rapidly. To solve this task, EU facilitates developing the low-carbon energy technologies. The EU's SET Plan considers implementation of six low-carbon energy technologies, namely nuclear (fission), solar (PV and CSP), wind, bio-energy (including biofuels), carbon capture and storage and smart electricity grids. A study of the Joint Research Centre (JRC) at the European Commission identified 5 metals as a bottle-neck for the SET plan realization: Nd, Dy, In, Te and Ga [1]. Another study of the JRC [2] devoted to metals needed for the decarbonisation of the EU energy sector classified as 'critical' 8 metals (Dy, Eu, Tb, Y, Pr, Nd, Ga and Te). Four materials (graphite, Re, In and Pt) are classified as 'near critical'. Rare earths have different properties and production ways and due to the limited paper length are left out of the paper's scope. Since Ga, In and Te are pointed as important metals by the both studies, this paper is devoted to them. The SET-Plan Te requirements for 2020 are estimated at 30.0% of current world supply, those for In - at 10.8% and for Ga - at 2.3% [1].

corresponding author: marichim@mgu.bg

GALLIUM

Applications, demand

The electrical and electronic equipment (EEE) sector in Europe is the major user of Ga (95% of the element use) [3]. In the USA, 70% of consumed Ga is used in integrated circuits (ICs) and 30% for optoelectronic devices (laser diodes, LEDs, photodetectors, and solar cells) [4].

The global LED market in 2016 was 21% higher than in 2015. The value of worldwide GaAs device consumption increased in 2016 compared to 2015 due to a growing wireless telecommunications. In 2017, the GaN radio frequency device market increased by 14% and by 23% (compared to 2016 and to 2015). These tendencies are expected to continue [4].

Production, resources

Around 90% of primary Ga is obtained as a by-product of aluminium (Al) extraction from bauxite. The remaining amount is produced as by-product of zinc (Zn) processing [5]. Gallium presents in bauxite in average concentration of 50 g/t, and could reach the same concentrations in some Zn ores. Gallium contained in world resources of bauxite is estimated to over 1 million tons. A considerable quantity could be contained in world Zn resources [4]. During alumina production, around 70% of the Ga available in bauxite is leached into the Bayer liquid and can be subsequently extracted. However, less than 10% of the Ga present in bauxite and Zn ores is recoverable [4], and the factors controlling the recovery are proprietary. This is considered as the major bottleneck in world's Ga supply.

Coals are thought to be the largest resources of Ga. However, the Ga concentration (0.01%÷0.1%) is considered uneconomic to treat coals for the extraction of Ga [6].

China's primary low-grade Ga production capacity has expanded to approximately 600 tons per year and the production of low-grade Ga was 300 tons in 2017, 20% more than in 2016. China accounted for over 80% of worldwide primary low-grade Ga capacity in 2017. Other producers were Japan, the Republic of Korea, Russia, and Ukraine. The main producers of refined Ga in 2017 were China, Japan, Slovakia, the UK, and the USA [4].

Possibility for substitution

Liquid crystals made of organic compounds are used in visual displays as substitutes for Ga-containing LEDs but so far, they are not competitive in terms of price and durability [7]. Silicon based metal-oxide semiconductor power amplifiers compete with GaAs power amplifiers in smart phones. Indium phosphide components can be substituted for GaAs-based infrared laser diodes in some wavelength implementations, and helium-neon lasers compete with GaAs in visible laser diode uses. Silicon (Si) or silicon-based substrates are used as substitutes for GaAs or GaN substrates. However, it can only be for a limited number of applications, as Si presents a lesser electron mobility and consequently it is significantly less efficient [7]. In addition, Si and In are also classified as critical metals [8].

ICs based on GaAs are used in many defense-related applications because of their unique properties, and no effective substitutes exist for GaAs in these applications.

Recycling, use of technogenic waste

Gallium is recovered from technological scrap from the manufacturing of GaAs-based devices - in Canada, China, Japan, Germany, Belgium, the UK, and the USA. The production scrap recycling has reached an efficiency of 90%. High efficiency has also been achieved for LEDs processing. Umicore recovers Ga from production scrap from CIGS thin film solar cells.

It is estimated that approximately 900 t of Ga are accumulated in landfills over the last 20 years in the EU [3]. The Ga content in semiconductors is highly dispersed due to their use in printed circuit boards (PCBs) and LEDs. Separation methods for the recovery of metals from PCBs are available. However, many metals contained in the PCBs, including Ga, are disposed of as slag, mainly because sufficient quantities are not easily collected to make recycling feasible. Current recycling processes of waste EEE containing Ga favour the recovery of precious metals or copper (Cu), while Ga ends up as an impurity in recycled metals or in waste slags [7]. At present, practically no recycling of Ga at industrial scale from post-consumer products is known to take place [3]. UNEP estimated that less than 1% end-of-life Ga is recycled [9]. Between 2 and 8 million t of PV waste is estimated to be generated in EU in 2030. The figures are expected to reach 60 - 75 million t till 2050 [3]. Due to the similarities in the materials and composition of thin film solar cells and LCD flat screen, recycling companies are examining the possibility of joint recycling process for the both products, which could make soon the process feasible.

Gallium is enriched in the residues during the coal ashing process and could be extracted from them. By applying hydrometallurgical technologies, recovery of Ga from coal gasification fly ash from the Puertollano Integrated Coal Gasification Combined Cycle Power Plant (Spain) has been proposed [10]. Ga presents as trace element in phosphate rock and could potentially be extracted as by-product [11].

It is estimated that the extractive waste (in situ /tailings) reported over the last 20 years in EU contain approximately 100 t Ga. A good example in this line is the BRAVO (Bauxite Residue and Aluminium Valorization Operations) project in Ireland which is targeted to the recovery of critical raw materials CRMs (among them – Ga) from red mud, simultaneously bringing environmental benefits due to the additional treatment of the red mud [3].

INDIUM

Applications, demand

Most of the global In consumption is for production of indium tin oxide (ITO). ITO thin film coatings are used for electrical conductive purposes in a variety of flat panel displays (liquid crystal displays - LCDs). Other uses of In include alloys and solders, compounds, electrical components and semiconductors (including copper indium gallium (di)selenide - CIGS), and research [4].

Japan and the Republic of Korea accounted for most of global consumption for the production of ITO. Indium consumption is expected to grow due to the continued ITO demand for LCD screens and the growth of the emerging IGZO (Indium Gallium Zinc Oxide) display market.

Production, resources

Indium is usually recovered from sphalerite - 95% of the refined metal [7]. The In content of Zn deposits is in the range of <1÷100 ppm [4]. Indium is obtained through processing waste products generated during the Zn refining process, such as dusts, fumes, residues, and slag. These materials are leached with HCl or H_2SO_4 to dissolve In. The obtained solution undergoes a solvent extraction to increase the concentration of In in the solution. Then In is removed from the solution by cementation, and the resulting In sponge is cast into anodes for electrolytic refining to produce In metal of standard-grade purity (99.97 or 99.99%).

It is estimated that only 25% of In contained in mined Zn ores is refined due to fact that not all In containing Zn ores are processed by refineries capable to extract In. At the smelters that include In-processing circuits, the average In recovery rate is about 50% (from 30 to 80%) [12]; this is considered to be the major bottleneck in In supply. The production of In depends heavily on the Zn production. Production of In contributes only to a small amount of the profit of Zn producers but requires investment in refining technology and active sourcing of In-containing Zn concentrates to ensure that the overall In content would be sufficient to justify its recovery. In order to give grounds for its economic recovery, minimum In content in concentrate of around 100 ppm is required. Indium occurs in trace amounts in other base-metal sulfides, particularly chalcopyrite and stannite but most deposits of these metals are sub-economic for In. However, In contained in smelting wastes is potentially available for recovery in the future.

The main world producers of refined In are China, Republic of Korea, Japan, Canada, and in Europe - France and Belgium. Exact quantitative estimates of reserves are not available [4]. Global resources and reserves of In calculated from global Zn resources and reserves using an average Zn ore In content of 50 g/t, have been estimated at 95000 t and 12500 t, respectively in 2012. When considering recoverable In in Cu deposits and using an average In content of 10 g/t, total resources and reserves amounted to 125000 t and 18800 t in 2012 [7].

Possibility for substitution

Alternatives to ITO coatings have been developed: antimony tin oxide and zinc oxide nanopowder - for LCDs; carbon nanotube - for flexible displays, solar cells, and touch screens; poly (3,4-ethylene dioxythiophene) - for flexible displays and organic LEDs. Graphene has been developed to replace ITO electrodes in solar cells. Gallium arsenide can substitute for indium phosphide in solar cells and in different semiconductor applications.

However, some losses in product characteristics may be observed. Tin-indium alloys can be replaced by tin-bismuth alloys in a number of low temperature bonding and soldering applications. Lead-based alloys could replace In and indium-tin alloys used in sealing at cryogenic temperatures but at the expense of the possibility of environmental pollution. In addition, some substitutes are also critical metals for EU, e.g. antimony (Sb), Ga, bismuth (Bi).

Recycling, use of technogenic waste

Indium is usually recovered from ITO-producing scrap in Japan and the Republic

of Korea [4]. The classical ITO sputtering technology is very inefficient; only 40% of the material is used in the process leaving large amounts available for recycling. The reclaim process is with recovery yields up to 95%, with turn-around times of fewer than 15 days [13]. Indium is also recovered from pre-consumer solar CIGS production waste. This is economically viable due to the high concentrations of metal found in these materials and the large quantities (around 50%) of scrap formed during production.

It is estimated that approximately 80 t of In are accumulated in landfills over the last 20 years in the EU [3]. On the worldwide basis only 1% of In from end-of-use waste is recovered [9]. This is due to the In dissipative use, the lack of an appropriate technology, or low economic incentives compared to recycling costs. Several research projects were aimed at In recycling from LCDs, based on different approaches: chloride-induced vaporization, pyrolysis followed by acid immersion, acid leaching followed by DEHPA extraction, using sub-critical water.

As mentioned above, only small part of In, available in mined ores, is extracted and refined. About 25-30% of mined-out In accumulates in residues [14]. Tailings and residues were estimated to contain 15000 t of reserves of In [15]. It is estimated that the extractive waste (in situ /tailings) reported over the last 20 years in EU contain approximately 10 t of In [3]. Therefore, there is an opportunity to increase In production from tailings. However, recovery from tailings is difficult due to the low concentrations of critical metals and high amounts of other metals and contamination. Improvements in technology have made this recovery feasible for In under good market conditions [16]. In order to justify its economic recovery, a minimum In content of around 100 ppm in tailings is required [17].

Promising studies on In extraction from Cu-smelting ash, Zn smelter slag and leaching residue were conducted by different Chinese scientists. Extraction of Ga and In from the concentrated brine, rejected by a desalination unit based on RO has been proposed. It is based on application of several extraction steps, evaporation, chlorination, hydrolysis and reduction with hydrogen. Indium with a purity of 97.4% and Ga with a purity of 99.8% were recovered [18]. It has been found that seafloor massive sulfides, especially those in arc and back-arc settings, are enriched in Ge and In, and could be used as source of those metals [19].

TELLURIUM

Applications, demand

Tellurium is used in the production of cadmium-tellurium-based solar cells. Global consumption estimates for the end use of Te are as follows: 40% solar, 30% thermo-electric production (refrigerators and water dispensers), 15% metallurgy, 5% rubber applications, and 10% other [4]. World production of Te in 2017 was about 420 t, increased with 20 t compared to 2016 [4]. The need to realize the EU Energy roadmap, especially implementation of solar PV applications leads to expectations of further increase in the Te demand.

Production, resources

Tellurium is produced mainly (>90%) from anode slimes from the electrolytic Cu

refining [4]. The remainder is derived from skimmings at lead (Pb) refineries and from flue dusts and gases from the smelting of Bi, Cu, and Pb-Zn ores. Gold telluride is a potential source, however, gold telluride projects might be viable as gold mines, since a higher Te price is required to support Te recovery [17]. The anode slimes contain 1- 4% Te, although 8 - 9% Te have been reported at some refineries. These numbers ensure a recovery rate of approximately 50% of the available Te within the slimes [20].

The biggest world Te producer is China, recovering Te from anode slimes and industrial waste produced in Cu, Pb, Zn, Ni, and precious metals smelting processes and from Te mining. Other producers are Sweden, Japan, Russia, and Canada. Estimated world reserves, which include only Te contained in Cu resources, were 31000 t in 2017. The estimates assume that >1/2 of the Te contained in unrefined Cu anodes is recoverable. Data on Te resources are not available [4]. The only certain present-day primary sources for Te ore are the Kankberg VMS deposit in Sweden, which produces about 10% of the world's Te, and the Dashuigou and Majiagou deposits in China, which together produce from 2-7% of the world's Te [20]. The availability of Te depends on the production of smelted Cu. Since Te is recovered only from the electrolytic refining of smelted Cu, the increased use of the leaching - solvent extraction - electrowinning processes for Cu extraction, which does not capture Te, limits the future supply of Te [20].

Possibility for substitution

Several materials can replace Te in most of its uses, but usually with losses in production efficiency or product characteristics. Concerning substitutions relevant to SET plan technologies, amorphous Si and copper indium gallium selenide are the two principal competitors to CdTe in thin-film PV power cells. However, Si, In and Ga are classified as critical for Europe metals [8].

Recycling, use of technogenic waste

In the production of CdTe solar cells the material utilization rates of the deposition of CdTe range from 35 to 90%. The material loss is collected and its recycling is feasible. The Te recycling rate from end-of-life products was less than 1% in 2011 [9]. For traditional metallurgical and chemical uses, there was little or no old scrap from which to extract Te because these uses are highly dissipative. A very small amount of Te is recovered from scrapped selenium-tellurium photoreceptors employed in older plain paper copiers in Europe.

A plant in the US recycles Te from CdTe solar cells; however, CdTe solar cells are relatively new and had not reached the end of their useful life [4]. Pilot recycling facilities recover 95% of semiconductor material and can provide feedstock for future production of photovoltaic solar panels [20]. The company First Solar installed in Germany the first recycling plant for used thin film solar cells based on CdTe. Generally, for Te recycling, two types of processes have been proposed - pyrometallurgical and hydro-metallurgical. Pyrometallurgical processes are more suitable for centralized recycling, whereas hydro-metallurgical processes are more likely feasible for small de-centralized operations. There is a potential for Te recovery from electronic scrap, if the scrap is processed in appropriate smelting

plants.

CONCLUSION

The important sustainable strategies to address bottlenecks in the supply of critical metals, needed for SET plan realization are: higher material use efficiency and reuse, substitution, recycling, and increasing European mine production and by-product extraction. All four strategies have their place, but also - their specific limitations.

Use of less material and reuse are limited by the technical specifications of the equipment, needed for the SET Plan. Implementation of substitution is complex issue due to the need specific technical requirements to be met and the fact that often the substitute is also critical metal. In recycling, metal recovery from end-of-life products is limited by economic and technological restrictions. The recycling cannot provide large secondary volumes of Ga, In and Te in the short-term since the scrap bearing these metals will only enter the recycling circuit many years later.

The problem with insufficiency of minor metals can be effectively mitigated by reducing the loss rates in mining and using technogenic waste (by-products, tailings, slags, waste and retentate from water treatment facilities) as source. Support to geological prospecting and mining, incentives to encourage byproduct recovery in zinc, copper and aluminium refining in Europe would also be part of the efficient solution of the problem.

References

1. Moss, R.L., Tzimas, E., Kara, H., Willis, P., Kooroshy, J. (2011) Critical metals in strategic energy technologies. JRC-scientific and strategic reports, European Commission Joint Research Centre Institute for Energy and Transport, Luxembourg,
2. Moss, R.L., Tzimas, E., Willis, P., Arendorf, J., Tercero-Espinoza, L. (2013) Critical metals in the path towards the decarbonisation of the EU energy sector. Assessing rare metals as supply-chain bottlenecks in low-carbon energy technologies. JRC Report EUR, 25994,
3. Mathieux, F., Ardente, F., Bobba, S., Nuss, P., Blengini, G., Alves Dias, P., Blagoeva, D., Torres De Matos, C., Wittmer, D., Pavel, C., Hamor, T., Saveyn, H., Gawlik, B., Orveillon, G., Huygens, D., Garbarino, E., Tzimas, E., Bouraoui, F., Solar, S., (2017) Critical Raw Materials and the Circular Economy – Background report. JRC, Publications Office of the European Union, Luxembourg,
4. Ober, J. A. (2018) Mineral commodity summaries 2018. US Geological Survey,
5. Zhao, Z., Yang, Y., Xiao, Y., Fan, Y. (2012) Recovery of gallium from Bayer liquor: A review. Hydrometallurgy, 125, 115-124,
6. Jaskula, B. W., (2011) Minerals Yearbook - 2011, Gallium, USGS, USA,
7. Deloitte Sustainability, British Geological Survey, Bureau de Recherches Géologiques et Minières, Netherlands Organisation for Applied Scientific Research, (2017) Study on the review of the list of Critical Raw Materials Criticality Assessments Final Report, Directorate-General for Internal

Market, Industry, Entrepreneurship and SMEs Raw Materials, European Union, Luxembourg,
8. Communication from the Commission to the European Parliament, the Council, the European Economic and Social Committee and the Committee of Regions on the 2017 list of Critical Raw Materials for the EU Brussels, 13.9.2017 COM (2017) 490 final,
9. Graedel, T., Allwood, J., Birat, J., Reck, B., Sibley, S., Sonnemann, G., Buchert, M., Hagelüken, C., (2011) Recycling rates of metals - a status report, Working group on global metal flows, UNEP,
10. Font, O., Querol, X., Juan, R., Casado, R., Ruiz, C., Lopez-Soler, A., Coca, P., Pena, F., (2007) Recovery of gallium and vanadium from gasification fly ash, Journal of Hazardous Materials A139, 413–423,
11. Chen, M., Graedel, T.E., (2015) The potential for mining trace elements from phosphate rock, Journal of Cleaner Production, 91, 337–346,
12. Shanks, W., Kimball, B., Tolcin, A., Guberman, D., (2017) Germanium and indium, chap. I of Schulz, K., DeYoung, J., Seal, R., Bradley, D., eds., Critical mineral resources of the United States—Economic and environmental geology and prospects for future supply, USGS Professional Paper 1802, I1–I26,
13. Murez, C., (2012) ITO rotary target: a game changer for the indium market, Minor Metals Conference, http://www.umicore.com/,
14. Ad hoc Working Group, (2014) Report on critical raw materials for the EU, Critical raw materials profiles, May 2014, DG ENTR, European Commission,
15. Harrower, M., (2010) Indium Sources and Applications, Minor Metals Conference, 28.02.2012 Brussels, Metal Bulletin Events, www.metalbulletinstore.com,
16. Tolcin, A.C., (2010) Minerals Yearbook - 2010, Indium, USGS, USA,
17. Willis, P., Chapman, A., Fryer, A. (2012) Study of by-products of copper, lead, zinc and nickel. A report prepared by Oakdene Hollins, Aylesbury, Buckinghamshire, for International Lead and Zinc Study Group, International Nickel Study Group, and International Copper Study Group,
18. Le Dirach, J., Nisan, S., Poletiko, C. (2005) Extraction of strategic materials from the concentrated brine rejected by integrated nuclear desalination systems. Desalination, 182(1-3), 449-460,
19. Hein, J.R., Mizell, K., Koschinsky, A., Conrad, T.A. (2013) Deep-ocean mineral deposits as a source of critical metals for high-and green-technology applications: Comparison with land-based resources. Ore Geology Reviews, 51, 1-14,
20. Goldfarb, R., Berger, B., George, M., Seal, R., (2017) Tellurium, chap. R of Schulz, K., DeYoung, J., Seal, R., Bradley, D., eds., Critical mineral resources of the United States—Economic and environmental geology and prospects for future supply, USGS Professional Paper 1802, R1– R27.

XIII International Mineral Processing and Recycling Conference
Belgrade, Serbia, 8-10 May 2019

University of Belgrade, Technical Faculty in Bor
Vojske Jugoslavije 12, 19210 Bor, Serbia
Tel. +381 30 424 555 Fax +381 30 421 078

MICRO - TO NANOSCALE TEXTURES OF ORE MINERALS: METHODS OF STUDY AND SIGNIFICANCE

Aleksandar Pačevski [1, #], Janez Zavašnik [2], Aleš Šoster [3], Andreja Šestan [2], Aleksandar Luković [4], Ivana Jelić [1], Aleksandar Kremenović [1], Alena Zdravković [1], Suzana Erić [1], Danica Bajuk-Bogdanović [5]

[1]University of Belgrade, Faculty of Mining and Geology, Belgrade, Serbia
[2]"Jožef Stefan" Institute, Ljubljana, Slovenia
[3]University of Ljubljana, Faculty of Natural Science and Engineering, Ljubljana, Slovenia
[4]Nature History Museum, Belgrade, Serbia
[5]University of Belgrade, Faculty of Physical Chemistry, Belgrade, Serbia

INTRODUCTION

Investigations of ore minerals, and mineralogical studies of the ore deposits in general, are not only crucial for the interpretation of ore-forming processes and genesis of ore deposits but also have a significant impact on the exploitation efficiency and subsequent extractive metallurgy. Additionally, such researches also comprise crystal chemistry and transformation processes in minerals (especially sulphides) and thus providing a prominent contribution to the understanding of presence and liberation of toxic elements in mining waste materials and their impact on the environment. Simultaneously, by the oxidation processes precious metals (Au and Ag) can be also liberated from the sulphides.

Key words: mineral textures, ore deposits, EMPA, FIB, TEM, XRD, Raman microprobe.

METHODS

Routine mineralogical investigations of ore minerals and textures start with proper sample preparation and initial research using the polarising microscope in reflected light (ore microscope) extended by scanning electron microscopy (SEM) combined with electron microprobe analysis (EMPA). In some cases, X-ray diffraction (XRD), electron backscattered diffraction (EBSD) and Raman microprobe can be used to obtain additional data of the mineral textures. Nevertheless, with

corresponding author: aleksandar.pacevski@rgf.bg.ac.rs

stated methods, we can typically obtain textural and chemical information from a millimeter scale to the spatial resolution of ≈ 1-2 μm. Recent advances in electron microscopy, combined with sample preparation using focused ion beam (FIB) offer an opportunity to address mineral textures down to the nano- and atomic-scale using transmission electron microscopy (TEM). Combining all these instruments and methods it is possible to resolve very important questions about: i) crystal chemistry of minerals, i.e. whether a particular chemical impurity is bound in the crystal structure or form nanoscale inclusions, and ii) micro- to nanoscale mineral textures (decomposition of solid solutions causing exsolution textures, replacement processes, etc.), reflecting ore-forming and other geological processes.

RESULTS AND CONCLUSIONS

The proposed new approach in mineralogical studies is aimed to establish combined microscopic and microprobe methods and proceedings which would enable comprehensive examinations of ore and rock samples from a field and macroscopic observation down to the atomic scale. Using the proposed techniques, some of our most notable results obtained in the last years consider: 1) accommodation of chemical impurities (Cu, Pb, As and Ag) in pyrite from the Čoka Marin polymetallic deposit. Copper is structurally bound in this Fe-sulphide (up to 8 wt. % Cu) [1] and more, regarding predominant presence of pyrite in this deposit, it should take in mind the possible losses in copper during the exploitation and mineral processing. On the other side, Pb, As and Ag forms nanoscale inclusions in this mineral [2]. Part of the silver also can be lost during an explatation and, by oxidation of pyrite in mining waste material toxic elements Pb and As can be liberated, which would affect the environment; 2) beside micrometer grains, occurrence of also „invisible gold" in arsenopyrite from the Gokčanica locality and Au liberation during arsenopyrite oxidation (Jelić et al, in prep); 3) occurrence of Pb,Cu-bearing sulphates and other products of sulphide oxidation on waste rock damps at the Pb-Zn Rudnik mine and Ag liberation during galena oxidation [4, Zdravković, in prep.]; 4) combined chemical and textural evolution study of native placer Au grains from sedimentary deposits of Drava river (SLO) and interpretation of the provenance (Zavašnik et al, in prep); 5) distinction of residual and authigenic (sedimentary) REE minerals (monazite and xenotime) and TiO2 polymorphs (rutile and anatase) in sedimentary rocks [3, Pačevski et al, in prep.]. Identification of minerals which are REE carriers and aforementioned distinction, based on both textural and chemical properties of minerals, are especially important for future studies of potential REE extraction from bauxites; 6) interpretation of complex nanoscale aggregates in nickeliferous laterite ores in Phthiotis (GR), enriched in ΣREE, Sc and Co for potential exploitation (Zavašnik et al, in prep.); 7) breakdown of crystal structure and exsolution processes of hematite-ilmenite solid solution in the andesites of Bor metallogenic district, controlled by the magma ascent (Luković et al, in prep); 8) re-evaluation of old data from an abandoned mine in Litija (SLO), and identification of Hg- and Cd-bearing phases overlooked by optical microscopy during the time of operation (Šoster et al, in prep.).

Acknowledgements:

This study was supported by the project OI176016 of the Ministry of Education,

Science and technological development of the Republic of Serbia and by the bilateral project between Serbia and Slovenia: "Micro- to nanoscale textures of ore minerals: methods of study and significance".

References

1. Pačevski, A., Libowitzky, E., Živković, P., Dimitrijević, R., Cvetković, Lj. (2008) Copper-bearing pyrite from the Čoka Marin polymetallic deposit, Serbia: Mineral inclusions or true solid-solution? The Canadian Mineralogist, 46 (1), 249-261,
2. Pačevski, A., Moritz, R., Kouzmanov, K., Marquardt, K., Živković, P., Cvetković, Lj. (2012) Texture and composition of Pb-bearing pyrite from the Čoka Marin polymetallic deposit, Serbia, controlled by nanoscale inclusions. The Canadian Mineralogist, 50 (1), 1-20,
3. Radusinović, S., Jelenković, R., Pačevski, A., Simić, V., Božović, D., Holclajtner-Antunović, I., Životić, D. (2017) Content and mode of occurrences of rare earth elements in the Zagrad karstic bauxite deposit (Nikšić area, Montenegro). Ore Geology Reviews, 80, 406-428,
4. Zdravković, A., Cvetković, V., Pačevski, A., Rosić, A., Šarić, K., Matović, V., Erić, S. (2017) Products of oxidative dissolution on waste rock dumps at the Pb-Zn Rudnik mine in Serbia and their possible effects on the environment. Journal of Geochemical Exploration, 181, 160-171.

XIII International Mineral Processing and Recycling Conference
Belgrade, Serbia, 8-10 May 2019

University of Belgrade, Technical Faculty in Bor
Vojske Jugoslavije 12, 19210 Bor, Serbia
Tel. +381 30 424 555 Fax +381 30 421 078

MICRO - TO NANOSCALE TEXTURE OF GOLD-BEARING ARSENOPYRITE FROM THE GOKČANICA LOCALITY, SERBIA

Ivana Jelić [1, #], Janez Zavašnik [2], Predrag Vulić [1], Aleksandar Pačevski [1]
[1]University of Belgrade, Faculty of Mining and Geology, Belgrade, Serbia
[2]"Jožef Stefan" Institute, Ljubljana, Slovenia

INTRODUCTION

Arsenopyrite (FeAsS) is generally undesirable mineral in the ore deposits, as has no economic significance for exploitation and due to the high toxicity of arsenic, released during oxidation of mining dumps. However, significant amounts of gold can be associated with this mineral and even, arsenopyrite and As-bearing pyrite most readily act as hosts for "invisible gold" [1]. In some gold deposits, Au-bearing arsenopyrite represents one of the main ore mineral. Consequently, it can be used as an indicator of gold-bearing mineralisations. Considering of nonstoichoimetry in As:S ratio in this mineral depending on temperature of deposition, arsenopyrite can serve as geothermometer [2].

Key words: arsenopyrite, reflected light, SEM, etching, invisible gold, scorodite, Gokčanica.

MATERIAL AND METHODS

Within Šumadija-Kopaonik ore district arsenopyrite is often associated with Pb-Zn and other ores, while in some mineralizations and deposits it is even predominant mineral. In our study, several types of ore deposits and mineralizations of different stages of deposition across Šumadija-Kopaonik ore district, containing considerable amounts of arsenopyrite, were sampled and investigated in detail: Golijska reka (magmatic stage - granitoides), Jurija (pneumatolytic to high-temperature hydrothermal stage), Rudnik and Trepča (metasomatismin limestones (skarns) to high-temperature hydrothermal stage), Gokčanica and Sastavci (hydrothermal – vein type in fault zones). We analysed arsenopyrite samples from abovementioned localities by reflected light microscopy, X-ray diffraction and scanning electron microscope equipped with an energy-dispersive spectrometer (SEM-EDS). Our initial results show that only arsenopyrite from Gokčanica are gold-bearing;

corresponding author: iljubojevic@gmail.com

therefore, these samples were further additionally studied by etching method.

RESULTS

Studied samples from the Gokčanica locality contain arsenopyrite and pyrite as predominant sulphides, while bismuthinite, bismuth, chalcopyrite, sphalerite, pyrrothite and gold occur in lesser extent. Arsenopyrite occurs in the form of coarse anhedral to subhedral grains up to 4 mm in sized and coarse-grained aggregates which are often cataclized and cemented by quartz and secondary arsenates (scorodite and Bi-arsenates). Gold occurs in both forms micrometer- ("visible gold") to nanometer-scale ("invisible gold"). Beside nanoscale inclusions of gold, "invisible gold" can be present also as structurally bound Au in arsenopyrite [3]. In this study, nanosized gold were well-revealed after etching of the sample surface with nitric acid and were re-analysed by SEM-EDS. Generally, we found three different types of gold within arsenopyrite grains and aggregates: 1) gold embedded in the grains of arsenopyrite, 2) gold in cracks and cavities between arsenopyrite grains and, 3) in the secondary oxidation products of arsenopyrite, bismuthinite and native bismuth (scorodite and Bi-arsenates). Scorodite is predominant secondary mineral which occurs mainly as alteration rim along grain boundaries and fractures in arsenopyrite, while Bi-arsenates, i.e. the oxidation products of bismuth and bismutinite, are present to a lesser extent.

DISCUSSION AND CONCLUSIONS

Although Gokčanica locality mineralisation has no particular economic importance, the deciphering the gold occurrence in this type of mineralisation could help in the general understanding of gold migration and precipitation in the whole magmato-volcanic system of Šumadija-Kopaonik ore district. The main results of our investigation: gold particle size, chemical form (structurally bound or nano-inclusions of gold), association with other minerals, etc. all have a substantial impact on metallurgical treatment and Au liberation from As-bearing ores and can be extended and applied on any similar type of deposit. Forthcoming question to be answered is: whether formation of visible gold in secondary oxidation products and in cracks and cavities is associated with weathering alteration of arsenopyrite or by alteration caused by subsequent hydrothermal fluids during a later stage of mineralization? Cook et al., 2013 [4] suggested that abovementioned kind of gold has originated from remobilization of Au incorporated within arsenopyrite rather than by supplying from later hydrothermal fluids.

Acknowledgements:

This study was supported by the project OI176016 of the Ministry of Education, Science and technological development of the Republic of Serbia and by the bilateral project between Serbia and Slovenia: "Micro - to nanoscale textures of ore minerals: methods of study and significance".

References

1. Cook, N. J., Chryssoulis, S. L. (1990) Concentrations of "invisible gold" in the

common sulphides. The Canadian Mineralogist, 28, 1-16,
2. Kretschmar, U., Scott, S. D. (1976) Phase relations involving arsenopyrite in the system Fe-As-S and their application. Canadian Mineralogist, 14, 364-386,
3. Cabri, L. J., Newville, M., Gordon, R. A., Crozier, E. D., Sutton, S. R., McMahon, G., Jiang, D.-T. (2000) Chemical speciation of gold in arsenopyrite. The Canadian Mineralogist, 38 (5), 1265-1281,
4. Cook, N. J., Ciobanu, C. L., Meria, D., Silcock, D., Wade, B. (2013) Arsenopyrite-pyrite association in an orogenic gold ore: tracing mineralization history from textures and trace elements. Economic Geology, 108 (6), 1273-1283.

XIII International Mineral Processing and Recycling Conference
Belgrade, Serbia, 8-10 May 2019

University of Belgrade, Technical Faculty in Bor
Vojske Jugoslavije 12, 19210 Bor, Serbia
Tel. +381 30 424 555 Fax +381 30 421 078

INSTRUMENTAL METHODS FOR CHARACTERIZATION OF ZEOLITE

Vladimir Nikolić #, Milan Trumić, Maja S. Trumić
University of Belgrade, Technical Faculty Bor, Bor, Serbia

ABSTRACT – The paper presents a short overview of instrumental methods that are suitable for monitoring all changes that occur after grinding, in the microstructure and the phase composition of zeolite. Modern physicochemical methods used to determine the composition, microstructure and surface structure of the raw material are intended to give a positive response to the increasingly complex requirements of material testing to meet the technical requirements for testing individual parameters. For example, the structural analysis of zeolites, particularly their pore structure, can be determined by scanning electron microscopy (SEM). The phase composition of zeolites and individual properties can be determined by X-ray fluorescence analysis (XRF), X-ray diffraction analysis, IR spectrometry (IR), cation exchange capacity (CEC), differential thermal analysis (DTA), thermogravimetric analysis (TGA), and differential scanning calorimetry (DSC). An overview of the practical application of these methods on zeolite are presented in this paper.

Key words: zeolite, instrumental methods, thermal analysis, DTA, TGA, DSC, X-ray, IR, SEM.

INTRODUCTION

Zeolites are crystalline alumosilicates, meshy structures, composed of a large number of cavities connected by channels [1]. The basic building unit of zeolite is the tetrahedron TO4, where T represents Si or Al (less Ge, Ga, P, Fe, B) [2, 3]. Tetrahedra are interconnected by common oxygen atoms located in structural nodes, and their characteristics vary due to variations in the control structure and the Si / Al ratio [4]. By interconnecting the tetrahedron, through a common oxygen atom (the so-called "oxygen bridge"), secondary building units are obtained, and by their further connection, they are obtained by polyhedra [5]. This joining, which gives a three-dimensional mesh structure, can be accomplished in many ways, and hence a great diversity of zeolite structures [3, 6].

The fascinating properties of zeolite, such as ion exchange, separation, and catalysis are determined by their unique structural characteristics, such as the correct three-dimensional micropore network, Si / Al ratio as well as the nature and amount of out-network cations. Well-defined micropores give zeolites the properties of molecular sieves, linking them to micropores and cavities. [7, 8] Another feature

corresponding author: vnikolic@tfbor.bg.ac.rs

of zeolite is the possession of acidic centers (Bronsted and Lewis) that result from negative network charge, which gives zeolites the ability for heterogeneous catalysis. Bronsted acid positions are derived from protons that are attached to network oxygen, which are connected to aluminum in the grid, while Lewis acidic sites originate from out-of-network aluminum [9].

INSTRUMENTAL METHODS FOR DETERMINATION OF CHARACTERIZATION, IDENTIFICATION OF PHASE COMPONENT AND MICROSTRUCTURE OF ZEOLITE

Methods for testing phase composition and structure of materials can be divided into: methods of thermal analysis, spectrochemical methods and methods of microscopic analysis. In the case of zeolites, the most common are differential thermal analysis (DTA), thermogravimetric analysis (TGA), differential scanning calorimetry (DSC), X-ray diffraction analysis (X-ray method), infrared spectrometry (IR), scanning electronic microscopy (SEM), as well as determining the capacity of the cation exchange. Some of these methods will be described in this paper.

Determination of cation exchange capacity

Cation-exchange capacity (CEC) is defined as the amount of exchangeable cations that the mineral can adsorate at a certain pH value. It represents a measure of total negative charge and includes: (1) negative charge resulting from isomorphic substitution within the grid, (2) free bond at the edges and on the outer surface, (3) available disassociated hydroxyl groups. The last type of charge is pH dependent. [10]

The cation exchange capacity of most natural zeolites ranges from 100 to 300 mmol M + / 100 g. [11, 12] Several methods have been developed to determine the capacity of the cation exchange. The methods used for determination are based on the complete exchange of existing cations with other cations such as: ammonium chloride method, ammonium acetate method, sodium acetate method.

Thermal analysis methods

The term thermal analysis (TA) refers to the monitoring of changes in any physical properties of the test substance during its exposure to a particular heat treatment with strict temperature control. The physical properties that are most often followed are:

- enthalpy (and its related property, thermal capacity) - the appropriate thermal analysis method is called calorimetry,
- mass - the thermal analysis method is thermogravimetry (TG). [13]

Differential Thermal Analysis - DTA

Differential thermal analysis is based on the measurement of the temperature difference ΔT of the test sample and the thermal material during heating or cooling at constant speed, under the same other conditions. The DTA curve records these differences during the reaction in the sample, showing thermal effects as deviations

from the zero line. Different temperature changes are the result of unwinding of a process in the sample (change in the crystal structure, boiling, evaporation, dehydration reactions, dissociation, oxidation, reduction, destruction of the crystal lattice and others). The reactions are followed either by releasing or absorbing heat, and therefore the exothermic and endothermic peaks are identified on the diagram. [8, 15]

Table 1. Split Thermal Analysis Method [14]

Thermal analysis method	The property	Shortened name of the method
Analysis of faulty heating / cooling	temperature	-
Differential Thermal Analysis	temperature change	DTA
Differential scanning calorimetry	amount of heat	DSC
Thermogravimetric analysis	mass	TGA
Thermomechanical analysis	dimensions / mechanical properties	TMA
Thermoelectric analysis	electrical properties	TEA
Thermometric analysis	pressure	-
Thermomagnetic analysis	magenetic properties	-
Thermo-optical analysis	optical properties	TOA
Thermoacoustic analysis	acoustic properties	TOA

Thermogravimetric analysis (TGA)

Thermogravimetric analysis is one of the most commonly used methods used to measure the change in sample mass, which occurs during programmed heating or cooling of the sample, with well-defined experimental conditions [16]. The temperatures at which these processes take place are characteristic of individual minerals and serve to identify them and determine their presence in the sample.

Thermogravimetry is a convenient method for monitoring all physical-chemical changes in the sample in which the mass change occurs. The increase or decrease in mass in the sample is due to evaporation, sublimation, dehydration, dehydroxylation, combustion, reactions with atmospheric gases where non-volatile products are produced, etc. Thermogravimetric analysis is used to determine the differences in the crystallographic properties of zeolites by monitoring the mass loss of material [17]. Studies have shown that for zeolites, mass losses up to 300 °C are caused by the dehydration of three types of water, poorly bound, tightly bound and zeolite water [18]. Differences in the amount of lost water can be attributed to variations in the size of non-framework cations, in the presence of smaller cations corresponding to higher quantities of zeolite water [19, 20]. Above 500 °C mass loss is the result of dehydroxylation of hydroxyl groups associated with defect sites within the zeolite [20]. This reaction can be continued up to 800 °C, but generally slowed down due to strong bonds of molecules removed at high temperatures and cages of zeolite [20].

Differential scanning calorimetry

Differential scanning calorimetry (DSC) is a technology that registers the energy

(energy flux) required to maintain the zero temperature difference between the test sample (S) and the reference material (R) at a predefined rate of heating (cooling), assuming that both materials are located under the same conditions [16] The difference in energy required for maintaining the sample and the reference material at the same temperature is the measure of energy changes in the test sample (relative to the reference material). DSC is often used as a quantitative measurement method that provides the possibility of determining important thermal parameters, such as: melting and boiling temperatures, transition temperature from glass to viscous, percentage of crystallized fractions, thermal stability, phase transformation identification, and the like.

SPECTROCHEMICAL METHODS

These methods are based on the property of atoms and molecules to emit radiation of a certain wavelength, when they are brought into an induced state, or to absorb radiation of a certain wavelength, when this radiation is passed through a sample of a material. The spectrochemical methods for determining the chemical nature of a sample of a material are based on the examination of the spectral composition of the radiation of that material.

X-ray fluorescence analysis (XRF)

X-ray fluorescence analysis is a very powerful analytical method for the spectrochemical determination of almost all the elements of the periodic system present in the sample. XRF radiation is induced when photons of sufficiently high energy, emitted from the X-ray source, are struck in the test material. Primary X-radiation interacts with the analyte atoms. [21]

The most important feature of the XRF analysis is that this technique allows qualitative and quantitative analysis of almost all visible elements in the X-ray spectrum (Be-U) present in an unknown sample. The analysis is not destructive in principle, it has high precision and accuracy, it is possible to determine several elements at the same time, requires a short time of irradiation so that it is possible to analyze a large number of samples in a short time; Online analysis is also possible, and the costs are low. [21]

Rendgenic diffraction is a non-destructive method that has wide application for the characterization of crystalline materials [22]. X-ray diffraction techniques are based on their dissipation in matter. Due to Rendgenic diffraction analysis - X-ray

Their wavelengths, scattered X-rays interact with each other so that the distribution of intensity depends on the angle of wavelength and incident and on the atomic structure of the sample. Distribution of the diffused x-ray is called the diffraction image. The atomic structure of the material can be determined by analyzing the diffraction image. The two main X-ray diffraction techniques are: single-crystal x-ray diffraction (SCD) diffraction and x-ray powder diffraction (XRPD)diffraction.[23, 24]

By comparing the diffraction image of the examined material with the catalog of recorded samples (ASTM cards), identification of unknown materials is performed. There is no possibility that more substances have the same same diffractogram. When analyzing zeolite, a complex diffractogram is obtained and its analysis is more

complex, but the identification is carried out in the same manner described above.

Infrared Spectrometry (FT-IR)

Infrared spectrometry is a non-destructive analytical method for the identification of organic materials. The method is based on the fact that atoms in the molecule are in a state of continuous vibration. Depending on its complexity and geometry, each molecule is characterized by a number of vibration types (with a vibration frequency that depends on the mass of the atoms and the strength of the bonds between them). Some of the molecular vibrations are characteristic of molecules as a whole, while others reflect the presence of certain functional groups in them. Vibration frequencies are usually expressed as a wave number whose unit is cm^{-1}. Expressed in this way, the frequency is the reciprocal value of the wavelength, λ. [25]

METHODS FOR THE EXAMINATION OF MICROSTRUCTURE

Microscopic methods of material testing enable the determination of parameters related to structure, texture, morphology, and the like. These parameters allow the assessment of material behavior in application conditions. Microscopic tests can also provide quantitative relationships in the microstructure of the material.

Scanning electron microscopy (SEM)

Scanning the electronic microscope (SEM) is one of the most popular and useful instruments that displays an image that reveals a surface topography of the sample [26], serves for the examination and analysis of the morphological microstructure and the characterization of the chemical composition [27]. It also has wide application for displaying the structural characterization of materials and devices, especially in the field of nanotechnology. In SEM, incident electrons interact with atoms that make samples that produce signals that contain information on the morphology of the sample surface, composition, and other physical and chemical properties. Scanning electron microscopy can magnify 10 to 500,000 times, which is about 250 times the best light microscope. The observed elements on the micrograph correspond to the observed details up to the order of 1 nm. [28]

The basic conditions that must be met in order to give a sample could be recorded by scanning electron microscopy are that the sample is non-volatile in order to achieve and maintain a high vacuum inside the microscope and that the sample is electroconductive. In order for samples with low electrical conductivity to be recorded in order to improve the contrast on the sample, it is necessary to fill them first with some of the conductive materials such as carbon, gold-palladium alloy, tungsten, copper, aluminum or some other conductive metal or alloy. [28]

CONCLUSION

The most important properties of materials for their application depend on their physico-chemical, mineralogical characteristics, phase composition, microstructure, etc. Therefore, methods for determining these characteristics have a very important role in the characterization of the material. Each method used in scientific research

gives the user very valuable information on the tested material. All of these techniques are mostly used in combination, and in this way very detailed and detailed information related to the characterization of materials is obtained, which is difficult or almost impossible to obtain using any analytical methods. By developing the technology of today's instrumental method, they enable very fast measurements and extremely quick and simple interpretation of the results obtained.

References

1. Loiola, A. R., Andrade, J. C. R. A., Sasaki, J. M., da Silva, L.R.D. (2012) Structural analysis of zeolite NaA synthesized by a cost-effective hydrothermal method using kaolin and its use as water softener. Journal of Colloid and Interface Science, 367, 34-39,
2. Calzaferri, G., Li, H. (2008) Mimicking the antenna system of green plants. Photochemical and Photobiological Sciences, 7 (8), 879-910,
3. Mojović, D. Z. (2009) Aluminosilicates with incorporated metallic custers of transitional metal groups Ib and IVb-VIII as electrocatalytic materials, University of Belgrade, Faculty of Physical Chemistry, Belgrade,
4. Terzić, A., Volkov-Husović, T., Jančić-Heineman, R., Pavlović Lj. (2008) Application of instrumental methods in the investigation of properties and microstructure of construction concretes. Metallurgical & Materials Engineering, 14 (4), 253-270,
5. Željko, T. (2016) Possible application of synthetic zeolite CR-100(Crystal-Right™) in ammonia adsorption fromground water of Banat aquifer. University of Novi Sad, Faculty of Technology, Novi Sad,
6. Charkhi, A., Kazemian, H., Kazemeini, M. (2010) Optimized experimental design for natural clinoptilolite zeolite ball milling to produce nano powders. Powder Technology, 203, 389-396,
7. Akhtar, F., Andersson, L., Ogunwumi, S., Hedin, N., Bergström L. (2014) Structuring adsorbents and catalysts by processing of porous powders. Journal of the European Ceramic Society, 34 (7),1643-1666,
8. Flanigen, M. (2011) Zeolites and molecular sieves: An historical perspective. Introduction to Zeolite Science and Practice, 137, 11-35,
9. Radulović, M. A. (2013) The influence of inclusions on phase transformations of framework aluminosilucates. University of Belgrade, Faculty of Physical Chemistry, Belgrade,
10. Ranđelović, M. (2012) Interaction of electrochemicaly active, microalloyed and structurally modified composites, based on alumosilicate matrix, with certain ionic and colloidal species of harmful ingredients in synthetic waters. University of Niš, Faculty of Science and Mathematics, Niš,
11. Ming, W. D., Dixon, B. J. (1987) Quantitative determination of clinoptilolite insoils by a cation exchange capacity method. Clays and Clay Minerals, 35 (6), 463-468,
12. Ćurković, L., Trgo, M., Rožić, M., Vukojević-Medvidović N. (2011) Kinetics and thermodynamics study of copper ions removal by natural clinoptilolite. Indian Journal of Chemical Technology, 18 (2), 137-144,
13. Mićić, D. M. (2016) Chemical and thermal analysis of berry seeds. University

of Belgrade, Faculty of Physical Chemistry, Belgrade,
14. Földvári M. (2011) Handbook of thermogravimetric system of minerals and its use in geological practice. Geological Institute of Hungary, Budapest,
15. Klančnik, G., Medved, J., Mrvar, P. (2010) Differential thermal analysis (DTA) and differential scanning calorimetry (DSC) as a method of material investigation. RMZ - Materials and Geoenvironment, 57 (1), 127-142,
16. Brown, E. M. (1998) Handbook Of Thermal Analysis And Calorimetry. Volume 1, Principles and Practice, Elsevier Science, Amsterdam,
17. Pane, I., Hansen, W. (2005) Investigation of blended cement hydration by isothermal calorimetry and thermal analysis. Cement and Concrete Research, 35 (6), 1155-1164,
18. Knowlton, G. D., White, T. E. D. R., Mckague, H. L. (1981) Thermal study of types of water associated with clinoptilolite. Clays and Clay Minerals, 29 (5), 403-411,
19. Alver, B. E., Sakizci, M., Yörükoğullari, E. (2009) Investigation of clinoptilolite rich natural zeolites from Turkey: a combined XRF, TG/DTG, DTA and DSC study. Journal of Thermal Analysis and Calorimetry, 100 (1), 19-26,
20. Khaleghian-Moghadam, R., Seyedeyn-Azad, F. (2009) A study on the thermal behavior of low silica Xtype zeolite ion-exchanged with alkaline earth cations. Microporous and Mesoporous Materials, 120 (3), 285-293,
21. Gauglitz, G., Vo-Dinh, T. (2003) The Handbook of Spectroscopy. WILEY-VCH Verlag GmbH & Co. KGaA, Weinheim,
22. Veselinović, M. Lj. (2010) X-ray analysis of nanostructural calcium phosphate powders obtained by new synthesis procedures. University of Belgrade, Faculty of Mining and Geology, Belgrade,
23. He, B. B. (2009) Two-Dimensional X-Ray Diffraction. John Wiley & Sons, Inc., Hoboken, New Jersey,
24. QingQing, P., Ping, G., Jiong, D., Qiang, C., Hui, L. (2012) Comparative crystal structure determination of griseofulvin: Powder X-ray diffraction versus single-crystal X-ray diffraction. Chinese Science Bulletin, 57 (30), 3867-3871,
25. Griffiths, R. P., de Haseth, A. J. (2007) Fourier Transform Infrared Spectrometry. Second Edition, Wiley Interscience, New Jersey,
26. Zhu, Y., Inada, H. (2016) Encyclopedia of Nanotechnology. Springer Netherlands, Dordrecht,
27. Zhou, W., Apkarian, P. R., Wang, Z. L., Joy, D. (2007) Scanning Microscopy for Nanotechnology. Springer, New York, NY, USA,
28. Egerton R. F. (2005) Physical principles of electron microscopy: an introduction to TEM, SEM, and AEM. Springer Science, New York.

XIII International Mineral Processing and Recycling Conference
Belgrade, Serbia, 8-10 May 2019

University of Belgrade, Technical Faculty in Bor
Vojske Jugoslavije 12, 19210 Bor, Serbia
Tel. +381 30 424 555 Fax +381 30 421 078

IMPROVEMENT OF OPTICAL METHODS ANALYSIS OF ORE GRADE AT OPTIMATION OF MINERAL PROCESSING PROCESSES

Valery V. Morozov [1, #], Ganbaatar Zorigt [2], Delgerbat Lodoy [2], Y. P. Morozov [3]

[1]National University of Science and Technology "MISiS", Moscow, Russia
[2]Erdenet Mining Corporation, Erdenet city, Mongolia
[3]Urals State University of Mines, Ekaterinburg, Russia

ABSTRACT – To improve the efficiency of ore composition determination, new methods and tools are proposed. At in-stream analysis, the special systems were tested, such provide highly accurate in-stream measurements of ore properties. A special flatbed facility for optical spectrum-based estimation of fine-crushed ore composition has been developed, being incorporated into the existing system of ore sampling and analysis. Application of the flatbed facility renders possible a high accuracy of determining ore mineralogical composition. Modern systems for optical spectrum-based estimation of ore grade provide a basis for effective automated control of ore benefication processes, based on the principle of advanced ore grade control. The systems implemented contributed to increasing copper and molybdenum recovery at the "Erdenet" mining and processing plant (Mongolia).

Key words: copper-molybdenum ores, image analysis, estimation of ore grade, control of flotation, process optimization.

INTRODUCTION

In-stream ore grade analysis is a new and effective method control of ore benefication processes. This is realised based on radiometric measurements in the X-ray and visible spectrum regions, in which mineral components of the initial ore [1] or the benefication products become apparent [2]. An important advantage of such methods is in-stream measuring ore parameters, including mass fractions of individual minerals, which makes it possible to use the information obtained in the processes of automated control [3].

Other studies have proven the feasibility of the processed ore grade estimation based on the results of measurements of the elemental composition of the initial ore and products of its flotation, using X-ray fluorescence analysers. Adequate estimation of the ore grade is only possible with in-stream measurement of the mineralogical composition parameters, such as the degree of ore oxidation and the

corresponding author: dchmggu@mail.ru

ratio of the major mineral phases [4].

METHOD OF OPTICAL SPECTRUM-BASED ESTIMATION OF ORE GRADES

Estimation of ore grade can be implemented on the basis of continuous measurement of the mineralogical composition directly in-stream, i.e. at a conveyor, or using sampling with the following analysis of colored images.

Reliable separate determination of minerals in ore is possible using modern formats of colour image recognition. For primary colour image processing, the RGB format (presenting any colour as a combination of red, green and blue) is the most suitable. Other parameters, the most important of which are the spectral characteristics, hue and saturation (HSV), are determined based on these three basic parameters [5].

Initially, a database of the system was filled with video images of all major minerals of the deposit. Via image software processing, computer databases of individual minerals were created. The spectral characteristics of minerals in visible light are the source of information for optical spectrum based-estimation of ore mineralogical composition.

As can be seen from Fig. 1, the spectral characteristics of minerals become more resolvable when using the two-parameter recognition system "colour - saturation" in HSV format. Full-scale application of the HSV format capabilities considerably increases the feasibility of determining the minerals, which reaches 0.95, even for complex systems such as chalcopyrite - pyrite or chalcocite - covellite, bornite.

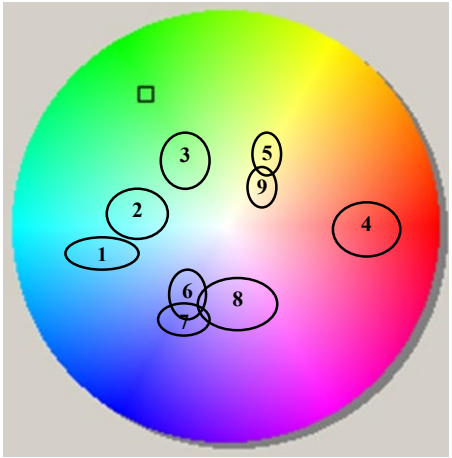

Figure 1. Colour characteristics of minerals in HSV format (hue - saturation):
1 - azurite; **2** - turquoise, **3** - malachite; **4** - cuprite; **5** - chalcopyrite; **6** - chalcocite; **7** - bornite; **8** - covellite; **9** - pyrite

Based on the optical spectrum-based mineralogical estimation, mass fractions of oxidised minerals, primary and secondary copper sulphides, pyrite, quartz, sericite, and other minerals, the presence and ratio of which characterises ore grade, can be determined. Same time, the proportion of talc, mica, schists and other minerals,

which has an effect on the flotation process, is measured.

The optical spectrum-based estimation technique is very advantageous when assessing the ore oxidation level. The ore oxidation level is defined as the ratio of the mass fraction of copper in the oxidised minerals to the total mass fraction of copper. In the optical spectrum-based estimation method, the ore oxidation level is calculated as the ratio of total intensity of the reflected light from the oxidised minerals to the total intensity of the reflected light from all the copper minerals. Similarly, based on the optical spectrum-based mineralogical analysis, the ratio of primary (chalcopyrite) and secondary (bornite, chalcocite, covellite) copper sulphide minerals is determined.

The task of determining the grade of ore, entering into processing, is to determine its similarity to the main technological types of ores [4]. In the algorithm we have adopted, the ultimate goal of ore grade determination consists of determining its composition in terms of proportions of the main technological types of ores. As the initial data, the ore analysis system uses readings of X-ray fluorescence material composition analysers and video image analysis sensors.

The calculation of ore grade was carried out using a multi-criteria method for affiliation shares calculations. Of the area for finding the desired solution to this task is presented by images of the typical ores. Ore is presented as a mixture of the five types of ores; the contribution (i.e. mass fraction) of each ore type to the ore should be determined. The system mathematical model provides for calculation of the incoming ore affiliation by six (or more) significant parameters (for instance, copper, molybdenum and iron contents in the ore, the proportions of oxidised copper minerals, secondary sulphide copper minerals, primary copper minerals (chalcopyrite) and sericite in the ore). One can use other parameters, e.g. the size of impregnation of valuable minerals in the ore.

The solution consists of determining the share of affiliation of the given point to a specific set of points in multidimensional space. The essence of calculation of the shares of ore affiliation to a certain type consists of the fact that, for the incoming ore, the degree of "similarity" to each of the five known ore types can be determined, and, proportionally to this degree (affiliation), fractions of each of these five types in the incoming ore can also be determined. For this purpose, distances between the point, the coordinates of which describe the incoming ore parameters, and points, the coordinates of which describe the ore types, identified as basic by technologists, are initially determined (Fig. 2).

The normalised difference (Si) between the parameters of the ore mixture (Zn) and the parameters of the ore types (Zni) is calculated as

$$Si = (|Zn-Zni|)/Zni \text{ , at } i=1\text{-}5 \quad (1)$$

The normalised values of “similarity” of the ore mixture with the typical ore parameters are calculated as

$$Di = 1/Si, \quad at\ i=1\text{-}5 \quad (2)$$

where Si – normalised difference between the parameters of the ore mixture and the parameters of the typical ores.

Then, after normalising and evaluation of the parameters' significance, the mass fractions of the ore types in the ore, incoming to processing, are determined. The mass fractions of the specific ore types (γ i) in the ore mixture are calculated as

$$\gamma i = kDi/\sum(kDi),\ ati = 1\text{-}5 \quad (3)$$

where k - factors of significance of the specific measured ore parameters.

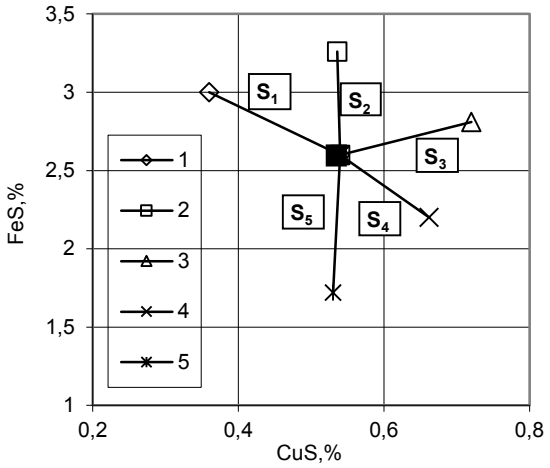

Figure 2. An example of ore composition assessment in two-dimensional space: 1, 2, 3, 4, 5 – the ore types; 6 (■) - currently produced ore; S_1, S_2, S_3, S_4, S_5 - differences between the parameters of the currently produced ore and the parameters of the ore types 1, 2, 3, 4, 5

The factors of significance of the specific measured ore parameters are adaptively adjustable parameters. The starting base for their adjustment is the checking information on the actual ore [4].

The ore grade operation is repeated after a specified period of time. The final results of the processed ore grade analysis reflect changes in the processed ore composition.

TECHNIQUE FOR THE OPTICAL ORE ANALYSIS SYSTEM

The systems of the crushed ore visual metering analysis were tested in many processing plants. However, no significant progress in recognition of ore mineralogical composition was reached. At the "Erdenet" processing plant (Mongolia), a new facility for advanced ore diagnostics, based on optical analyser of mineral composition, was tested. The optical spectrum-based analysis system was installed above the conveyor for feeding ore to the grinding operation.

The system of video image analysis (Fig. 3) provided the ore digital video image. It was created based on modern telemetry and software and hardware tools. The system provided information on the ore mineralogical composition and type. The system also provides data on the particle size distribution of the ore, being delivered

to the grinding operation, and the impregnation of minerals.

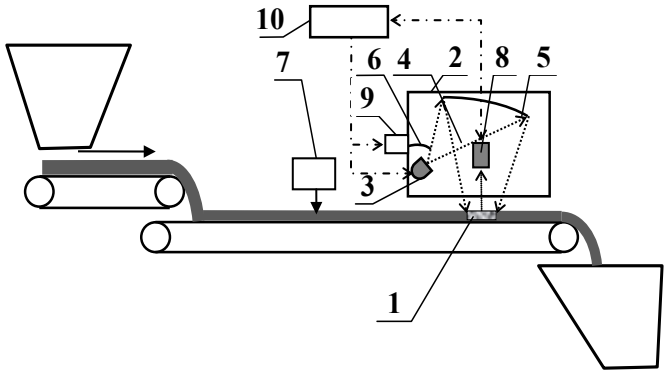

Figure 3. Facility for telemetrical estimation of the ore size and grade:
1 - measurement area; **2** - case, **3** - light source, **4** - light flux; **5**, **6** - main and additional reflectors; **7** - spraying apparatus; **8** - video camera; **9** - reflector drive; **10** – processor

The facility operates in dual-alternating mode. In the first mode, reflector 5 forms diffused lighting, providing even illumination of the sample. In the second mode, reflector 6 forms plane light flux. This contributes to the maximum "contrast" of the image that is necessary for measuring the ore particle size distribution [6].

The ore scanning on the conveyor belt is carried out continuously. The information obtained by the system is processed and averaged. Then, using the aforementioned algorithm, recognition of the ore grade is carried out.

The disadvantage of the in-stream (on conveyor) ore analysis is the low accuracy of the measurements due to bad definition of the obtained images. This is due to the non-uniformity of the sample and the infeasibility of adjustment for definition for the entire surface of the ore.

At the Erdenet processing plant, the new method for the ore diagnostics, based on the mineralogical composition analysis using the flatbed facility, was tested. High precision of the optical spectrum-based estimation is achieved using special devices, installed in the sampling and the sample analysis flow sheet, applied by the technical control department.

For this analysis, the special facility was developed [7]. The facility includes a table for placing the sample, made of transparent glass, light flux source, optical system and optical converter (Fig. 4).

The measurement technique involves preparing the ore sample, forming the measurement area in the form of a flat portion of the sample, illumination and capture of the images of the formed flat portion of the sample in the visible spectrum range. The sample illumination and image capturing is carried out bottom-upwards in the two-dimensional scanning mode. Due to the sample "flattening", the sample roughness is considerably decreased. As a result, an almost planar parallel surface with uniform illumination without shaded areas is formed. This provides the high definition of the images with subsequent high accuracy of the mineral determination.

The duration of the operations for the analysis and calculation does not exceed 10 minutes, which is quite acceptable for the automatic control of the grinding and flotation processes.

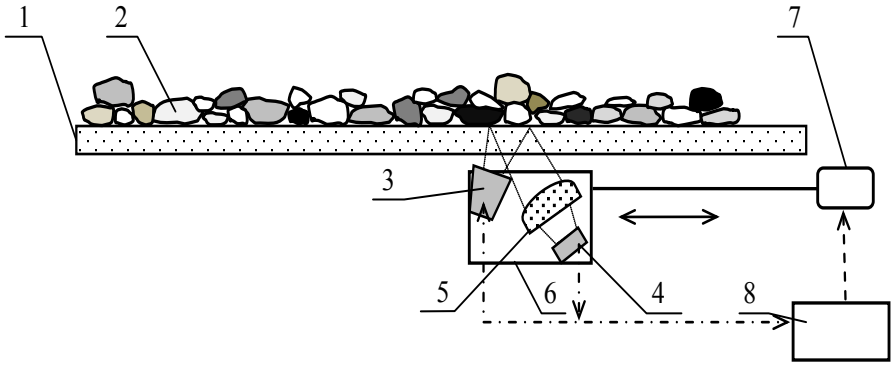

Figure 4. Design of the flatbed facility for optical spectrum-based estimation of ore grade: **1** - table for placing the sample; **2** - sample; **3** - light flux source; **4** - optical converter; **5** - optical system; **6** - carriage; **7** - drive; **8** - processor

BENEFICATION PROCESS CONTROL BASED ON ORE GRADE ESTIMATION

The process of ore process control is initially carried out at the stages of ore extraction and transportation. This provides both control of ore averaging on-stream and division of the primary stream into two streams: of predominantly sulphide and predominantly mixed ores.

The first stage consists of ore sampling and mineralogical analysis directly in the course of mining. The criteria (parameters) of the ore grade used are “Ore oxidation level” and “Primary ore share”. The criterion “Ore oxidation level” numerically corresponds to the proportion of copper in the form of oxidised minerals (i.e. azurite, cuprite, malachite, chrysocolla and others). The criterion “Primary ore share” is calculated as the percentage of copper in the form of chalcopyrite (i.e. primary copper sulphide mineral). Depending on the values of these parameters, streams of the oxidised ore, going to leaching, primary and mixed ores, going to beneficiation, are formed.

To calculate the required parameters of grinding and flotation, special studies were carried out on the most pronounced samples of the typical ores, and the process diagrams for their grinding and flotation were developed. Given the infeasibility of obtaining samples representing a given ore type by 100 %, statistical analysis of the results and simulation of benefication modes for the “typical” ores was implemented. The simulation results made it possible to select the following ore types: - Massive Primary Ore (MPO); - Mixed Secondary Sulphidised Ore (MSSO); - Lean Pyritised Ore (LPO); - Mixed Seriticitised Ore (MSO) and Mixed Oxidised Ore (MOO).

At the same time, the simulation results enabled calculation of the optimum parameters of the process mode for each ore grade (Table 1).

The value of the pre-set function SF for each parameter of the process was calculated as a weighted average of the parameters values for each “typical” ore type

(SFi) taking into account the contribution of the given type in the ores mixture using Equation (4):

$$SF = \Sigma\gamma i SFi \quad (4)$$

where γi - relative weight fraction of an ore type i in the ore mixture incoming to processing.

Table 1. Preset functions in the grinding and flotation processes control systems

Process variable - set of control functions	MPO	MSSO	LPO	MSO	MOO
Grinding size, % of -74 μm grain size	67.5	64.5	67.0	66.0	66.0
Water supply to the mill, t/m^{3}h	1.65	1.74	1.71	1.75	1.75
Pulp density %	43.5	41.0	41.5	40.0	40.0
Collector consumption	10.0	12.0	13.0	17.5	10.0
Frother consumption	13.0	16.0	16.0	19.0	13.0
Lime consumption	1,100	1,300	1,300	1,300	1,100

When calculating the reagent consumption, the effects of mutual impact of co-processing ores of the different technological types ("the typical ores") must be taken into account.

The predefined functions were used as baseline in the local systems of automatic control of grinding and flotation processes at the Erdenet processing plant (Fig.5).

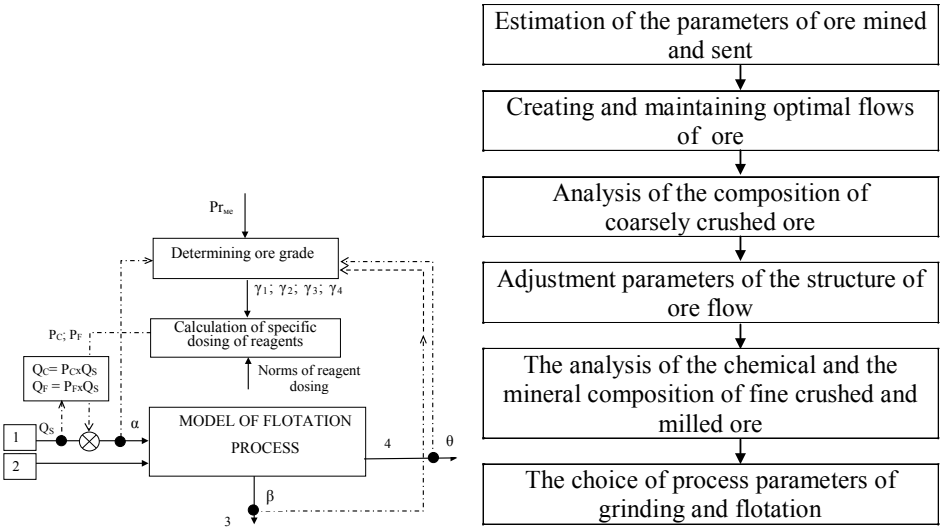

Figure 5. Scheme and algorithm of estimation of ore quality and automatic control of ore enrichment process

Using the procedure for ore grade determination increases the automatic control stability, as it allows a fast response to changes in the incoming ore grade. Applying the ore grade estimation algorithm enabled an increase of the control stability by

5-7 %. Maintaining the optimum degree of grinding and reagent consumption in the flotation of the currently extracting ore provides increasing recovery of copper and molybdenum into concentrates by 0.3 % and 1.1 %, respectively, as well as decreasing the consumption of reagents by 2-3 %.

CONCLUSION

At the processing plant of Erdenet mining corporation (Mongolia), new systems and algorithms of flotation process control, based on an advanced system of estimating the processed ore grade, have seen further progress. The new methods and facilities for automatic in-stream measurement of the ore mineralogical composition (at the conveyor belt) and in-stream sampling with later analysis were tested. The control algorithm uses data of ore grade and the accumulated information about the optimal process parameters for grinding and flotation. The introduction of this system reduces losses of valuable components and reagent consumption.

References

1. Kongas, M. (2010) New features in on-stream XRF analysis for flotation circuit management and control. Non-ferrous metals, Russia, 34-37,
2. Haavisto, O., Hyötyniemi, H. (2010) Reflectance spectroscopy in the analysis of mineral flotation slurries. Journal of Process Control, 21 (2), 246-253,
3. Morozov, V., Bokani, L., Ulitenko K., Stolyarov V, Ganbaatar Z.,Delgerbat L. (2010) Modern systems of control of technological processes. In: Proceedings of the 18th Mediterranean conference on control and automation, IEEE (ed.), Marrakech, 237-242,
4. Morozov, V., Davaasambuu, D., Ganbaatar, Z., Delgerbat, L., Topchaev, V., Sokolov, I., Stolyarov, V. (2013) Modern systems of automatic control of processes of grinding and flotation of copper-molybdenum ore. In: Automation in Mining, Minerals and Metal Processing, 16th IFAC Symposium, IFAC (ed.), Mission Bay, San Diego, Part 1, 166-171,
5. Albiol, A., Torres, L., Delp, E. (2001) Optimum color spaces for skin detection, Proceedings of the International Conference on Image Processing (ICIP), 122-124,
6. Morozov, V. V., Shek, V. M., Morozov, Y. P., Lodoy D. (2017) Method visiometrics quality analysis of flow of ore and device for its implementation. Patent RF № 2620024, IPC G01N 21/85, Publ. 22.05.2017, Bul. No. 15,
7. Morozov, V. V., Lodoi, D., Morozov Y. P., Scheck, V. M. (2017) Method visiometrics analysis of the quality of the ore and the device for implementation. Patent RF № 2620103 IPC B03B 13/00, V07C 5/34, Publ. 23.05.2017, Bul. No. 15.

XIII International Mineral Processing and Recycling Conference
Belgrade, Serbia, 8-10 May 2019

University of Belgrade, Technical Faculty in Bor
Vojske Jugoslavije 12, 19210 Bor, Serbia
Tel. +381 30 424 555 Fax +381 30 421 078

OBTAINING FILLERS BASED ON LIMESTONE FROM DEPOSIT "BRIJEG"-ULCINJ FOR APPLICATIONS IN VARIOUS INDUSTRIES

Dragan S. Radulović [1, #], Ljubiša Andrić [1], Milan Petrov [1], Darko Božović [2], Marko Pavlović [3]

[1]Institute for Technology of Nuclear and other Mineral Raw Materials, Belgrade, Serbia
[2]Geological survey, Podgorica, Montenegro
[3]University of Belgrade, Faculty of Technology and Metallurgy, Belgrade, Serbia

ABSTRACT – Paper presents results of investigations of the possibility of using "Brijeg"-Ulcinj limestone as filler in various industries. Micronization, granulometric composition, oil and water absorption and degree of whiteness were investigated, and chemical and thermal analyses were performed.
Physico-chemical properties of this sample classify it among high quality carbonate raw materials with high $CaCO_3$ content of 98.21%, with low contents of $MgCO_3$ 0.88 % and SiO_2 0.16 %. Its quality satisfies requirements of standards on using of calcium carbonate as filler in next industries: paints and coatings; rubber and PVC; glass; foundry ; sugar industry production of mineral fertilizers and metallurgy.

Key words: limestone, filler, industrial use, standards.

INTRODUCTION

Republic of Montenegro has big reserves of limestone in coastal area and in south of the territory [1]. Even though deposits are huge, limestone is mainly used in construction as construction stone, and to some extent as architectural stone [2]. Since calcium carbonate as filler is much more expensive than construction stone, relevant institutions of Montenegro initiated investigations of the possibility of using limestone as filler [3]. On the basis of the obtained results it was evaluated whether it can be used as filler in accordance with standards (SRPS) in various industry branches [4-6].

"Brijeg"-Ulcinj deposit consists of carbonate sediments, mostly limestone ones, and less dolomitic sediments. Ore reserves are estimated at about 3,000,000 t of limestone [1]. The aim of investigations presented in this paper was to determine the

corresponding author: d.radulovic@itnms.ac.rs

possibility of using raw material as filler in various industry branches.

EXPERIMENTAL

Materials and methods

Starting limestone sample used in investigations was from "Brijeg" - Ulcinj deposit. First, its specific volumetric weight (density) was measured by pycnometer, and granulometric composition were determined by Tyler screen [7]. Granulometric composition of the micronized sample was determined by sieve size 63 μm, classification on Cyclosizer and Bach elutriator. Limestone filler quality was determined by chemical analysis. Thermal (DT/TG) analysis of the sample was performed using Netzsch-Simultaneous Thermal Analysis- STA 409 EP device, with heating speed of ΔT = 10 °C /min, in temperature interval from 20 to 1000 °C. Degree of whiteness was determined by whiteness meter, according to MgO 100 % standard.

Investigation of physical properties of starting sample

Specific volumetric weight of the starting sample is γ= 2.712 g / cm^3. Based on data from the table 1 is drown a diagram of particle size distribution shown in Figure 1, for samples of limestone Brijeg. In Figure 1, shows the direct curve of particle size distribution and cumulative curves and average sample of outflow and flow limestone deposits "Brijeg"-Ulcinj. From the intersection of cumulative curves average outflow and flow determined that the average diameter of the sample of limestone d_{50}=4.93 mm, and upper size limit of the sample was 14.76 mm.

Table 1. Granulometric-composition of the initial sample Brijeg- Ulcinj

Size class [mm]	M, %	↓∑ M, %	↑∑ M, %
- 19.1 + 15.9	2.66	2.66	100.00
- 15.9 + 12.7	8.58	11.24	97.34
- 12.7 + 9.52	17.22	28.46	88.76
- 9.52 + 7.93	8.06	36.52	71.54
- 7.93 + 5.0	12.89	49.41	63.48
- 5.0 + 3.36	16.28	65.69	50.59
- 3.36+ 2.38	5.13	70.82	34.31
- 2.38+ 1.6	6.74	77.56	29.18
- 1.6+ 1.19	5.08	82.64	22.44
- 1.19+ 0.63	6.96	89.60	17.36
- 0.63 + 0.4	3.03	92.63	10.40
- 0.400 + 0.300	1.57	94.20	7.37
- 0.300 + 0.200	1.51	95.71	5.80
- 0.200 + 0.000	4.29	100.00	4.29
Input	100.00	/	/

Technological investigations

For investigations of the possibility of using limestone as filler in various industry branches limestone was micronized, and thus obtained product were subjected to the following physico-chemical characterization: -chemical analysis, thermal

(DT/TG) analysis, determination of granulometric composition, degree of whiteness and absorption of oil and water.

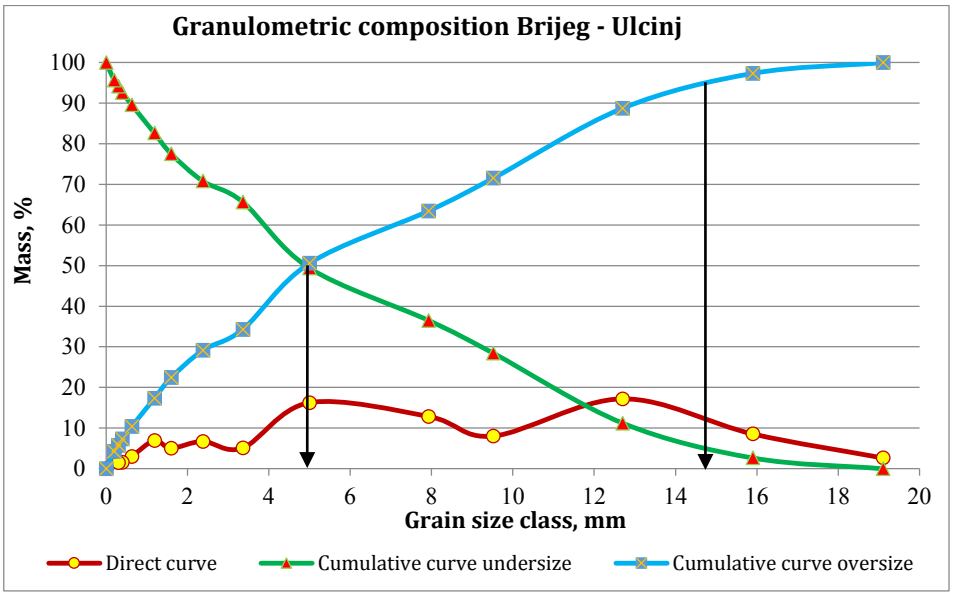

Figure 1. The curves of particle size-composition of the starting sample "Brijeg"-Ulcinj

Determining granulometric composition of micronized sample

Granulometric composition of the micronized products is represented in Table 2, and showed that upper size limit is 85 μm, and that the finest class - 5.7 μm content is around 11 %.

Table 2. Granulometric composition of grinded sample Brijeg

Size class [μm]	M, %	↓∑ M, %	↑∑ M, %
+ 63	33.32	33.32	100.00
-63+44	5.27	38.59	66.68
-44+33	7.13	45.72	61.41
-33+23	5.80	51.52	54.28
-23+15	4.07	55.59	48.48
-15+11	3.87	59.46	44.41
-11+5.7	29.4	88.86	40.54
-5.7+0	11.14	100.00	11.14
Input	100.00	/	/

Determining the degree of whiteness

Whiteness was assessed on three samples of the limestone from deposit "Brijeg", and the result is shown in Table 3.

Table 3. The degree of whiteness the limestone samples

No	mark of the sample	whiteness according MgO - 100 %
1.	Brijeg-1	85.90
2	Brijeg-2	84.80
3	Brijeg-3	85.80
	Average value	85.50

Determination of absorption water and oil

In order to determine absorption water and oil are also used three samples of the limestone from deposit "Brijeg", and the results are shown in Tables 4 and 5.

Table 4. Absorption of the oil of samples of limestone

No.	mark of the sample	absorption of the oil, %
1.	Brijeg-1	13.42
2.	Brijeg-2	13.65
3.	Brijeg-3	13.52
	Average value	13.53

Table 5. Absorption of the water of samples of limestone

No.	mark of the sample	absorption of the water, %
1.	Brijeg-1	18.51
2.	Brijeg-2	18.77
3.	Brijeg-3	18.67
	Average value	18.65

Thermal (DT/TG) analysis

Results of thermal (DTA/TG) analysis of the micronized sample “Brijeg” limestone are presented as a diagram in Figure 2.

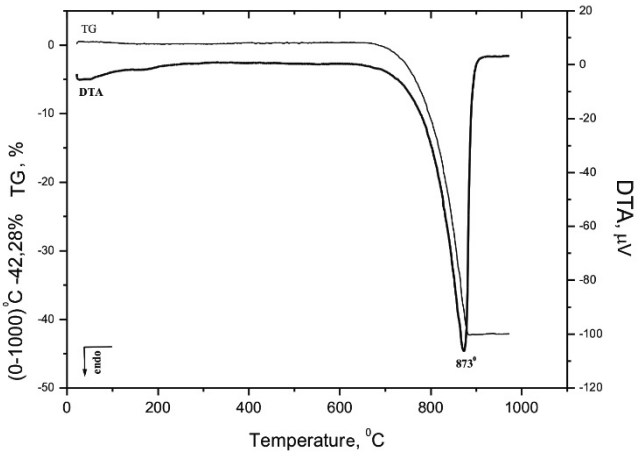

Figure 2. DTA/TG diagram of ”Brijeg” limestone sample

In Figure 2 are presents the TG and DTA diagrams of the initial sample of limestone. DTA diagram (Figure 2.) shows endothermic peak with maximum at 873 °C, which is attributed to phase transformation of calcite ($CaCO_3$) into CaO, according to the following reaction:

$$CaCO_3 \rightarrow CaO + CO_2 \quad (1)$$

This phase transformation is accompanied by weight loss of 42.28 % (TG diagram, Figure 2) in the temperature range from 650 °C to 900 °C.

Chemical analysis

Results of chemical analysis of the micronized limestone with contents of main components and damaging components are presented in Tables 6 and 7.

Table 6. Chemical composition of main components of limestone sample

Component	Cont., %
CaO	55.03
$CaCO_3$	98.21
CO_2	43.19
MgO	0.88
Fe_2O_3	0.028
Al_2O_3	0.022
R_2O_3	0.048
SiO_2	0.16
K_2O	0.0052
Na_2O	0.025
TiO_2	< 0.02
P_2O_5	< 0.005
LOI	43.62

Table 7. Chemical composition of damaging components of limestone sample

Component	Cont., %
Cu	9
Mn	27
S	< 0.01
P	< 25
Ni	21
Cr	6
Mo	< 50
Pb	25
Cd	4
pH	9.28
Fe solu.	200
As	/
Hg	/

Results of physico-chemical characterization of "Brijeg" limestone sample and the required filler quality (Standards) lead to conclusion that this limestone is of good quality. Namely, its $CaCO_3$ content is high - 98.21 %, and $MgCO_3$ (1.84 %) and silicates (SiO_2 0.16 %) content low. However, relatively high content of heavy metals was found, above all Cu (9 ppm), Pb (25 ppm), Ni (21 ppm) and Cd (4 ppm).

RESULTS AND DISCUSSION

Limestone filler quality for each industry branch is defined by appropriate standards or requirements of manufacturers who use limestone as raw material in their production cycle. Limestone quality requirements are defined as content of useful and damaging components, i.e. as chemical composition, as well as the necessary size class.

Evaluation of "Brijeg" limestone filler quality based on chemical composition

According to the results presented above, limestone from "Brijeg" – Ulcinj deposit can be used in the following industries:

- in industry of paints and coatings; it is among high quality raw materials in accordance with market and standard requirements (SRPS B.B6.032);
- in paper industry; it is among A, B quality, while for the C and highest D quality its whiteness degree is not satisfying (SRPS B.B6.033);
- in rubber and PVC industry; it satisfies the highest quality standards and market requirements (SRPS B.B6.031);
- in foundry industry; it belongs to the highest class I in accordance with market requirements imposed by standard (SRPS B.B6.012);
- in sugar industry; due to the increased MgO content it is in quality class II in accordance with market and standard requirements (SRPS B.B6.013);
- in metallurgy; it is in the highest class I in accordance with market requirements imposed by standards (SRPS B.B6.011);
- in production of glass; due to the increased MgO content it is in quality category IV and V in accordance with market requirements imposed by standards (SRPS B.B6.020);
- in production of phosphate mineral nutrients, in accordance with market requirements strictly defined for use ("Official Gazette of the Republic of Serbia" 31/78, 6/81, 2/90, 20/00).

Limestone from "Brijeg" – Ulcinj deposit cannot be used:

- in pharmaceutical and cosmetics industry because its low whiteness degree and increased content of heavy metal Cd relative to market requirements defined by standard (SRPS B.B6.034);
- for production of mineral fertilizers because of the increased MgO content, which is strictly defined by manufacturer's requirements (Azotara Pančevo);
- in production of cattle feed because of the increased content of heavy metals Pb and Cd, which is very strictly defined for this use ("Official Gazette of the Republic of Serbia" 31/78, 6/81, 2/90, 20/00);
- for neutralization of acidic soils; because of the increased content of MgO, P2O5 and Cu as biogenic elements and heavy metals, Ni and Cd, the contents of which are very strictly defined ("Official Gazette of the Republic of Serbia" 60/2000).

Evaluation of "Brijeg" – Ulcinj limestone filler quality based on users' requirements for the necessary raw material size (fineness)

Some industries require finely micronized limestone, while others require raw

material of larger particle size, sometimes even coarse. Following industries use ground and micronized limestone:

- for paints and coatings industry; A quality 99.5 % of - 20μm, B quality 97 % of - 20μm and 0.01 % of + 44 μm;
- for paper industry for all quality categories (A, B and C) the required fineness is 100 % of - 45 μm, where for A quality 75 % of -10 μm, for B quality 80 %, and for C quality the required fineness is 95 % of -10 μm and 90 % of - 2 μm; rubber and PVC industry requires for A and B quality raw material to be 99.5 % of - 45 μm, while for C and D quality upper limit limestone size is 45 μm;
- for glass industry, since "Brijeg" limestone corresponds to quality IV and V according to its chemical composition, there is predefined granulometric composition for these quality classes, subdivided into six subclasses in size range from - 1 + 0.1 mm;

Following industries demand larger sizes and coarse limestone:

- for foundry industry, raw material should be size - 50 + 30 mm, with class - 30 mm content up to 5 %;
- for sugar industry, limestone is to be classified into six subclasses in size range from - 215 + 63 mm, with maximum fine content in each subclass up to 8 %;
- metallurgy uses limestone consisting of five subclasses in size range from - 70 + 0.1 mm.

CONCLUSION

Limestone from "Brijeg"- Ulcinj deposit according to its physico-chemical properties belongs to high quality carbonate raw material with high content of $CaCO_3$ of 98.21 %, and low content of $MgCO_3$ of 0.88 % and silicates (SiO_2 0.16 %). It meets the requirements of standards for using calcium carbonates as fillers in industry of paints and coatings; paper industry, rubber and PVC industry; foundry industry; sugar industry and metallurgy. According to market demand and standards it belongs to high quality raw material in industry of paints and coatings, rubber and PVC, foundry industry and metallurgy. However, for the sugar industry and the production of glass, it does not comfor with the highest standards.

Because of increased MgO content "Brijeg" limestone cannot be used in fertilizers industry. Due to high content of heavy metals Pb (25 ppm), Ni (21 ppm) and Cd (4 ppm), as well as biogenic elements MgO (0,88 %) and Cu (9 ppm), "Brijeg" limestone cannot be used in pharmaceutical and cosmetics industry, in production of cattle feed and for neutralization of acidic soils. Obtaining of wide range of fillers for various industry branches would provide products which are more expensive per mass unit than products that have been used until now up to 10 times.

Acknowledgements:

This paper is a result of investigations under projects TR31003 and TR 34013,

financed by the Ministry of Education and Science of the Republic of Serbia from 2011-2014.

References

1. Report on the limestone testing from the territory of Montenegro, for application as a filler in different branches of industry, (2011) ITNMS Archive, Belgrade,
2. http://geology.com/usgs/limestone/
3. Božović, M. D., Simić, M. V., Radulović, S. D., Abramović, B. F., Radusinović, S. S. (2016) Carbonate filler resources of the Bjelopavlici area, Montenegro, Hemijska industrija. 70 (5), 493-500,
4. Sekulić, T. Ž. (2011) "Kalcijum karbonatne i kvarcne sirovine i njihova primena", Monografija, ITNMS, Beograd, 21-75,
5. www.patentgenius.com/patent/4026762"Use of ground limestone as a filler in paper"
6. http://minerals.usgs.gov/minerals/pubs/commodity/stone_crushed/mcs-2010-stonc.pdf
7. Milosavljević, R. (1974) "Metode ispitivanja mineralnih sirovina u pripremi mineralnih sirovina", Rudarsko-geološki fakultet Beograd.

XIII International Mineral Processing and Recycling Conference
Belgrade, Serbia, 8-10 May 2019

University of Belgrade, Technical Faculty in Bor
Vojske Jugoslavije 12, 19210 Bor, Serbia
Tel. +381 30 424 555 Fax +381 30 421 078

EFFICIENCY OF ZEOLITE GRINDING AND ITS POTENTIAL APPLICATION

Katarina Balanović [#], Milan Trumić, Maja Trumić
University of Belgrade, Technical Faculty in Bor, Bor, Serbia

ABSTRACT – Procedures such as adsorption, ion exchange, membrane processes, etc. are suitable for the removal of heavy metals from industrial wastewater. Natural zeolites are often used as adsorbents and ion exchangers because they are simply and cheaply exploited, and because of their high porosity and large specific surface. By reducing the zeolite grain size, the metal adsorption rate increases, which does not have effect on zeolite adsorption capacity. Zeolite comminution leads to the generation of various surface defects and increase of surface energy, which increases its chemical reactivity. For this reason, the zeolite grinding test should be carried out. In this paper, the zeolite grinding kinetics in a ball mill with charge of different ball size was analyzed. By analyzing the obtained results, it was observed that the highest value of the zeolite grinding efficiency (narrow range of zeolite particle size) was achieved by using the charge with the ball smallest diameter.

Key words: zeolites, grinding, ball mill, charge

INTRODUCTION

The use of natural zeolites as adsorbents and ion exchangers has become a widely used method for the removal of heavy metals from wastewaters because they are simply and cheaply exploited, and because of their high porosity and large specific surface [1, 2]. Natural zeolites are especially suitable for purification wastewater because they are not toxic (contain non-toxic compounds K, Ca, Na, and Mg) they have no smell and are harmless to the environment [1, 3]. In this way wastewater containing lead, chromium, cadmium, nickel, copper, mercury, silver as well as acid mine drainage, can be treated [4]. For this purpose, zeolites with a wide range of particle size, - 5 + 0 mm, can be used [5].

By reducing the zeolite grain size, the metal adsorption rate increases, which does not have effect on zeolite adsorption capacity [2]. The longer the grinding time, the zeolite particle size will be smaller, but the volume of the pores and surface area increases [6, 7]. Zeolite comminution leads to the generation of various deformations on the surface, which increases its chemical reactivity [7].

For this reason, in this paper, the zeolite grinding test was performed. The zeolite grinding kinetics in a ball mill with charge of different ball size was analyzed. The

[#] corresponding author: kbalanovic@tfbor.bg.ac.rs

equation of the grinding kinetics law for the first order grinding was used. The differential form of the first order grinding kinetics equation is [8]:

$$\frac{dR}{dt} = -kR \tag{1}$$

where is: $\frac{dR}{dt}$ – grinding speed of a large class,
R – the content of the wide class in the mill at the moment (t),
t – grinding time,
k – grinding rate constant.

The integral form of equation (1) is:

$$R = R_0 \cdot e^{-kt} \tag{2}$$

Equation (2) can be written in the form:

$$ln\, R_0 - ln\, R = kt \tag{3}$$

Or otherwise:

$$ln\frac{R_0}{R} = kt \tag{4}$$

Equation (4) represents the equation of the linear line in the coordinate system [t; $ln(R_0/R)$], with the coefficient of direction (k):

$$k = tg\alpha = \frac{Y}{X} = \frac{ln\frac{R_0}{R_2} - ln\frac{R_0}{R_1}}{t_2 - t_1} \tag{5}$$

MATERIALS AND METHODS

The test was carried out on samples of zeolite from the deposit "Igroš"- Kopaonik. The chemical composition of zeolite was tested in the Institute for Technology of Nuclear and Other Mineral Raw Materials in Belgrade and is shown in Table 1. The zeolite density is 2186 kg/m^3, and the Bond working index is Wi = 9.20 kWh/t.

Three samples of 200 g (narrow range of particle size - 0.850 + 0.600 mm) were formed. Grinding kinetics were monitored at the following time intervals: 0.5 min, 1 min, 2 min, 4 min, 8 min, 15 min, same as in paper in which were monitored grinding kinetics of the same sample but wide range of particle size [9].

Grinding experiments were carried out in a laboratory ball mill with the following characteristics:

- mill diameter: D = 158 mm,
- mill length: L = 198 mm,

- relative rotational rate of the mill: $\Psi = 0.85\ n_k$,
- coefficient of ball mill loading: $\varphi = 0.40$,
- inside surface of cylinder mill: ribbed,
- grinding method: dry.

Table 1. Chemical composition of the zeolite sample [9]

Component	Content (%)
SiO_2	64.05
TiO_2	15.29
Fe_2O_3	4.82
Al_2O_3	2.52
MgO	1.33
Na_2O	1.27
K_2O	0.77
Other	9.95

The ball mill (Fig. 1) is rolling using a roller device (Fig. 2). Inside surface of mill is ribbed to prevent sliding of the ball during operation of the mill (Fig. 3).

Figure 1. Outside view of the mill

Figure 2. Device with rollers

Figure 3. Ribbed inside surface of the mill

Balls were made from steel: S4146, extra high quality, having hardness 62 ± 2 HRC according to Rockwell. The mill ball loading was constant in all grinding experiments and amounted to 40 % by volume. Three different charge of balls were used (Fig. 4), where each individual charge was composed of balls of the same diameter. The ball charge characteristics are given in Table 2.

Table 2. Characteristics of ball charge

Ball diameter in charge (mm)	Charge mass (g)	Number of balls in charge	Ball mass (g)
10	6775.8	1562	4.34
15	6945.1	482	14.41
24	6921.8	127	54.50

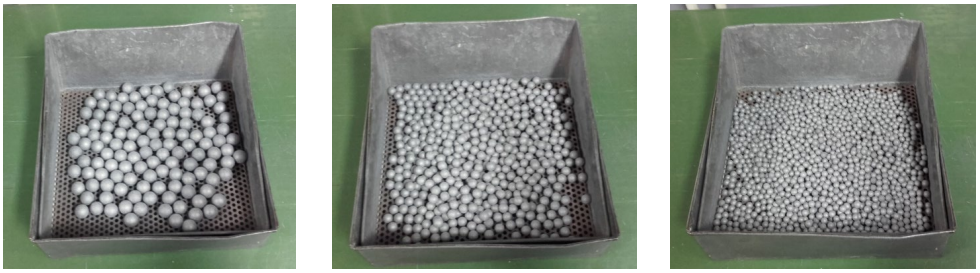

Figure 4. Three different charge made of balls of diameter 24, 15 and 10 mm

RESULTS AND DISCUSSION

The results of the zeolite sample grinding kinetics with a 24 mm ball diameter charge, are shown in Figure 5. In Table 3, the values of the grinding rate constant and the correlation coefficients, are given.

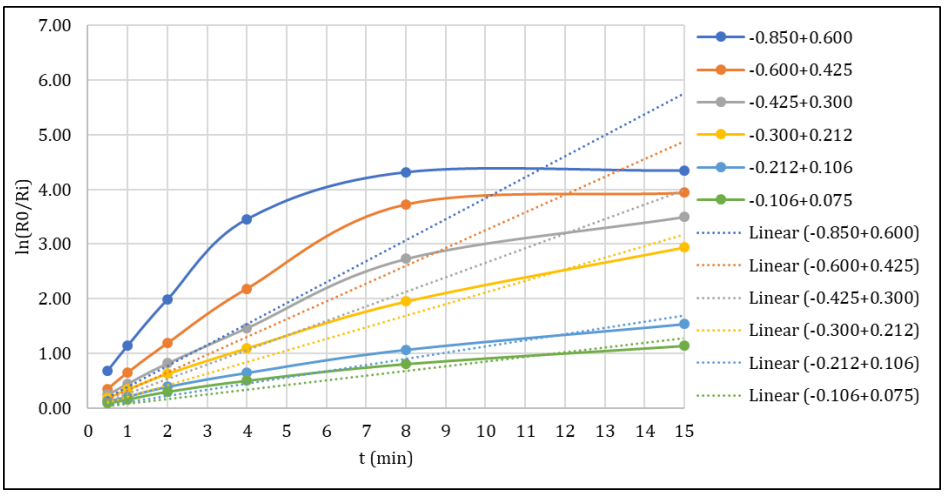

Figure 5. Zeolite grinding kinetics with 24 mm ball diameter in charge

Table 3. Grinding rate constant and the correlation coefficients obtained by the zeolite grinding with 24 mm ball diameter in charge

Size fraction, d (mm)	Grinding rate constant, k	Correlation coefficient, R^2
- 0.850 + 0.600	0.384	0.2608
- 0.600 + 0.425	0.325	0.7199
- 0.425 + 0.300	0.266	0.8963
- 0.300 + 0.212	0.212	0.9549
- 0.212 + 0.106	0.113	0.9148
- 0.106 + 0.075	0.085	0.8936

By analyzing the values from Table 3, it can be noticed that the grinding rate constant with 24 mm ball diameter in charge decreases with the reduction zeolite

sample size. The highest grinding rate constant was obtained at the largest size fraction - 0.850 + 0,600 mm. The correlation coefficient for the narrow size class - 0.850 + 0.600 mm is smaller than the minimum correlation coefficient that is R^2_{min}=0.569 [10], which means that this model cannot describe the grinding kinetics for this narrow class.

In Figure 6, the results of the zeolite sample grinding kinetics with 15 mm ball in a charge are shown. In Table 4, the values of the grinding rate constant and the correlation coefficients, are given.

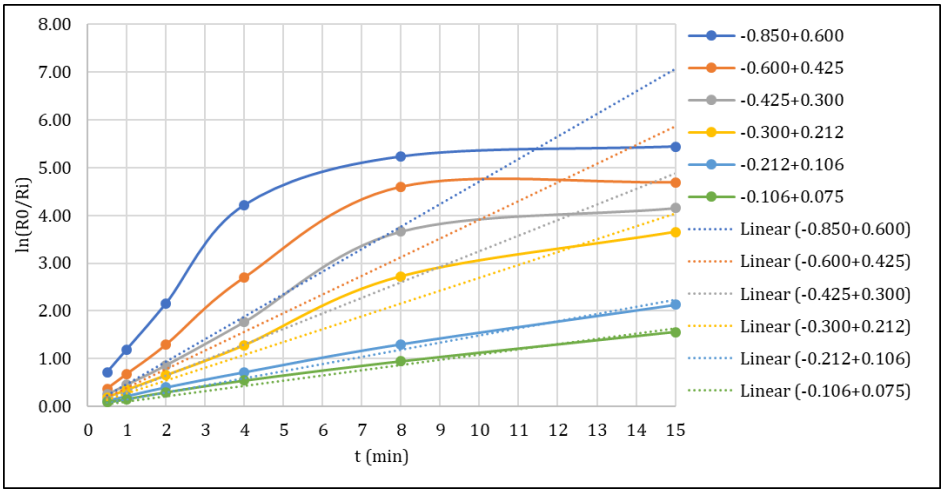

Figure 6. Zeolite grinding kinetics with 15 mm ball diameter in charge

Table 4. Grinding rate constant and the correlation coefficients obtained by the zeolite grinding with 15 mm ball diameter in charge

Size fraction, d (mm)	Grinding rate constant, k	Correlation coefficient, R^2
- 0.850 + 0.600	0.471	0.4178
- 0.600 + 0.425	0.391	0.7177
- 0.425 + 0.300	0.326	0.8606
- 0.300 + 0.212	0.269	0.9452
- 0.212 + 0.106	0.150	0.9822
- 0.106 + 0.075	0.110	0.9779

The values in Table 4 show that in case of grinding with 15 mm ball diameter in charge, the values of the grinding rate constant are reduced by decreasing zeolite sample size, same as at grinding with 24 mm ball diameter in charge. The highest grinding rate constant was achieved with the largest size fraction - 0.850 + 0,600 mm. The correlation coefficient for the narrow size class - 0.850 + 0.600 mm is smaller than the minimum correlation coefficient that is R^2_{min}=0.569 [10], which means that this model cannot describe the grinding kinetics for this narrow class.

In Figure 7, the results of the zeolite sample grinding kinetics with 10 mm ball diameter in charge are shown. In Table 5, the values of the grinding rate constant and the correlation coefficients, are given.

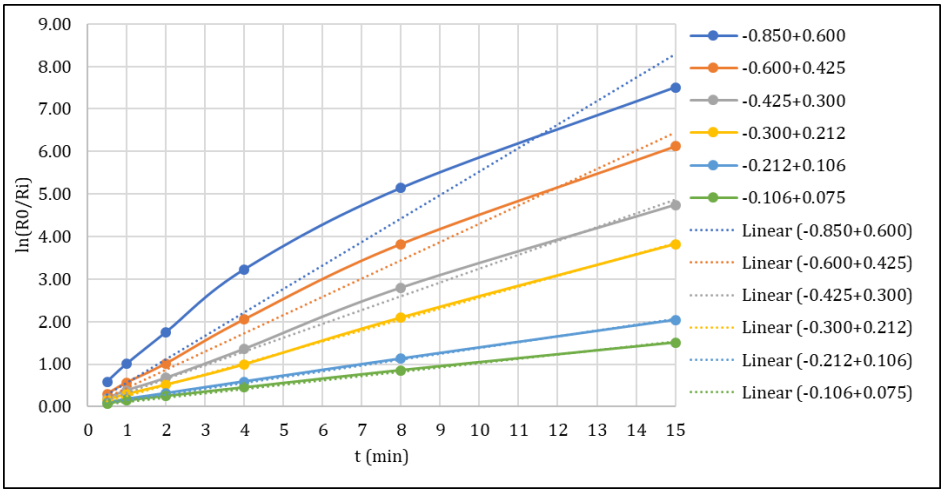

Figure 7. Zeolite grinding kinetics with 10 mm ball diameter in charge

Table 5. Grinding rate constant and the correlation coefficients obtained by the zeolite grinding with 10 mm ball diameter in charge

Size fraction, d (mm)	Grinding rate constant, k	Correlation coefficient, R^2
- 0.850 + 0.600	0.553	0.9207
- 0.600 + 0.425	0.430	0.9840
- 0.425 + 0.300	0.325	0.9958
- 0.300 + 0.212	0.256	0.9995
- 0.212 + 0.106	0.138	0.9974
- 0.106 + 0.075	0.103	0.9952

In this case, as in the previous two, the value of the grinding rate constant decreases with the decrease in the sample size. The highest grinding rate constant was achieved with the size fraction - 0.850 + 0,600 mm.

In Table 6 and Figure 8, grinding kinetics with a different ball diameter in charge is given for each narrow size class, which were produced from comminution of a size class - 0,850 + 0,600 mm.

Table 6. Grinding rate constant of narrow size classes with a different ball diameter in charge

Size fraction, d (mm)	Ball diameter in charge (mm)		
	24	15	10
- 0.850 + 0.600	0.384	0.471	0.553
- 0.600 + 0.425	0.325	0.391	0.430
- 0.425 + 0.300	0.266	0.326	0.325
- 0.300 + 0.212	0.212	0.269	0.256
- 0.212 + 0.106	0.113	0.150	0.138
- 0.106 + 0.075	0.085	0.110	0.103

By comparing the results of grinding with 24 mm, 15 mm and 10 mm ball

diameter in charge, the highest value of the grinding rate constant, for larger size fraction, is obtained with 10 mm ball diameter in charge. With reducing the size fraction the highest value of the grinding rate is obtained with 15 mm ball diameter in charge. The smallest value of the grinding rate constant is obtained with 24 mm ball diameter in charge.

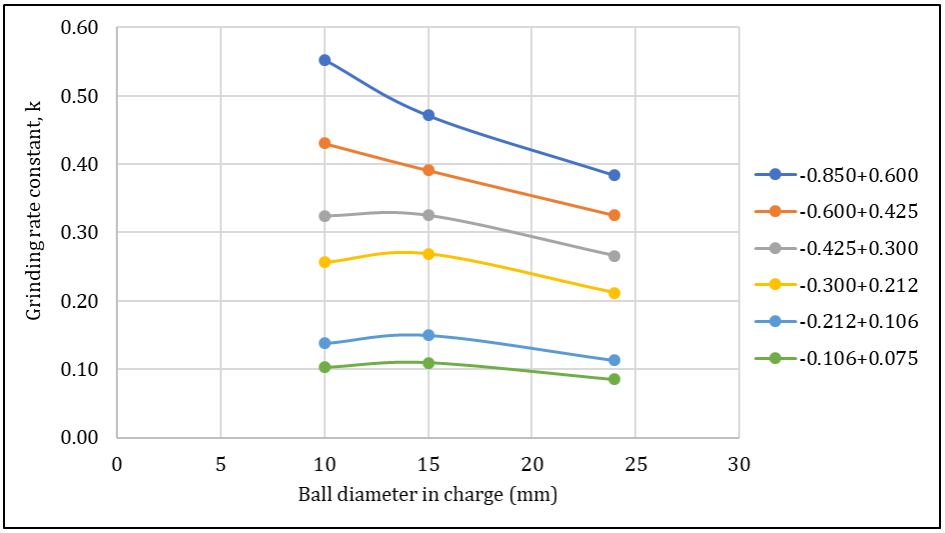

Figure 8. Grinding rate constant of narrow size classes with a different ball diameter in charge

Also, from Figure 8, we can see that each narrow size class has the corresponding optimal ball diameter in the charge, which is shown in table 7.

Table 7. The optimal ball diameters that are determined over the grinding rate constant

Size fraction, d (mm)	The optimal ball diameter (mm)
- 0.850 + 0.600	10
- 0.600 + 0.425	10
- 0.425 + 0.300	13
- 0.300 + 0.212	13.5
- 0.212 + 0.106	14
- 0.106 + 0.075	14

CONCLUSION

Based on all obtained results it is concluded that the grinding rate constant, with different ball diameter in charge (24 mm, 15 mm and 10 mm), decreases with the reduction zeolite sample size. The highest grinding rate constant, in all cases, was obtained at the largest size fraction - 0.850 + 0,600 mm.

For each narrow size class, there is an optimal ball diameter that gives the highest grinding rate constant.

References

1. Vukojević Medvidović, N., Perić, J., Trgo, M. (2006) Column performance in lead removal from aqueous solutions by fixed bed of natural zeolite–clinoptilolite. Separation and Purification Technology, 49(3), 237-244.
2. Trgo, M., Vukojević Medvidović, N., Perić, J., Svilović, S., Čačija, G. (2015) Influence of zeolite particle size and initial lead concentration on sorption kinetic study by batch experiments. The holistic approach to environment, 5(3), 105-118.
3. Wang, W.P., Wang, W., Zhou, Y.Q. (2012) Adsorption characteristics of natural zeolite on ammonia nitrogen. Advanced Materials Research, 599, 501-504.
4. Pansini, M. (1996) Natural zeolites as cation exchangers for environmental protection. Mineralium deposita, 31(6), 563-575.
5. Sekulić, Ž., Kolonja, B., Knežević, D. (2013) Defining the size class as the quality parameter of zeolite assortment of products. Mining and Metallurgy Engineering Bor, (3), 13-32.
6. Widayanti, S.M., Syamsu, K., Warsiki, E., Yuliani, S. (2016) Effect of natural Bayah zeolite particle size reduction to physico-chemical properties and absorption against potassium permanganate ($KMnO_4$). AIP Conference Proceedings, 1710(1), 030029.
7. Czapik, P., Czechowicz, M. (2017) Effects of natural zeolite particle size on the cement paste properties. Structure and Environment, 9(3), 180-190.
8. Magdalinović, N. (1999) Usitnjavanje i klasiranje, Nauka Beograd, 195-205.
9. Balanović, K., Trumić, M., Trumić, M. (2018) Comminution of Zeolite and its Potential Application. International V4 Waste Recycling 21 Conference, Miskolc, Hungary, Proceedings, 53-61.
10. Volk, W. (1965) Statystyka stosowana dla inżynierów. Wydawnictwa Naukowo-Techniczne.

XIII International Mineral Processing and Recycling Conference
Belgrade, Serbia, 8-10 May 2019

University of Belgrade, Technical Faculty in Bor
Vojske Jugoslavije 12, 19210 Bor, Serbia
Tel. +381 30 424 555 Fax +381 30 421 078

PRODUCTION OF GLASS - CERAMICS FROM COAL FLY ASH AND LIMESTONE

Veljko Savić [1, #], Vladimir Topalović [1], Srdjan Matijašević [1], Jelena Nikolić [1], Snežana Zildžović [1], Sonja Smiljanić [2], Snežana Grujić [2]
[1]Institute for Technology of Nuclear and Other Mineral Raw Materials, Belgrade, Serbia
[2]Faculty of Technology and Metallurgy, Belgrade, Serbia

ABSTRACT – The results of laboratory scale experiments of vitrification of fly ash collected from the coal fired power plant are presented. The final glassy material was obtained by melting a mixture of ash and limestone at T= 1450 °C and quenching the melt in air. To convert the waste into useful and environmentally acceptable material the crystallization of fly ash glass was performed by powder route processing. The properties of the resultant glass-ceramic indicate a potential various application such as building materials, ceramics tiles, etc.

Key words: vitrification, fly ash glass, glass-ceramic

INTRODUCTION

The increasing production of fly ashes from carbon combustion in thermal power plants has compounded environmental and economical problems worldwide. Many efforts have been made to improve the environmental quality of residues from coal combustion and to recycle or utilise at least part of it.

The recovery of waste matrices otherwise destined for disposal allows to save resources, reducing the need for natural raw materials. Considering that recycling has priority over disposal/deposition in landfill sites and the use of secondary raw materials reduces costs and conserves resources, it is a need in the processing of waste materials into utilisable secondary raw materials [1-3].

Coal combustion generate large amounts of ashes, which are disposed in open pits or landfills. Usually, fly ashes contain appreciable amounts of heavy metals (Pb, Hg, Cd, Cr, etc.) which can be accumulated in surrounding soil and water sources causing a huge environmental damage. Unfortunately, only small amount of fly ashes were recycled and reused and therefore, it is necessary to seek new options to solve this problem. Over the past few decades, coal fly ash has mainly been used in concrete

corresponding author: v.savic@itnms.ac.rs

[4], cement [5], paper making [6], steam-cured bricks [7], ceramics and other related industries. Because the chemical contents of coal fly ash are close to those of ceramic raw materials, research into using fly ash in applications similar to other ceramic products has attracted much attention. As one of promising solution the vitrification of fly ashes could be considered.

By this process the waste toxic components are bonded within the glass structure and the obtained durable material is environmentally stable for a long time. Also, the vitrification greatly reduces the volume of waste and by using appropriate technologies the waste can be converted to useful materials. As reported earlier the different fly ashes without or with addition of other waste inorganic materials, can be transformed in glasses by melting technique. It has been demonstrated that is possible to prepare a glass-ceramics with good chemical and mechanical durability by controlled crystallization of the parent waste fly ash glasses [8-10].

This paper reports the results of vitrfication of waste fly ash collected from the open pit near the TPS „Nikola Tesla" - Republic of Serbia. Also, the possibility of obtaining the glass-ceramics by sintering and crystallization of powder parent vitrified fly ash was presented.

MATERIALS AND METHODS

The raw sample of fly ash was dried and then analyzed. To determine chemical composition of fly ash a wet chemical method and AAS (Perkin Elmer 703) were employed. The phase composition was defined by the XRD - Philips PW-1710 automated diffractometer with a Cu K_α radiation tube operating at 40 kV and 32 mA.

The grain size was determined using Warman cyclosizer M4. Vitrification procedure was realized by melting of the mixture of fly ash and powdered raw limestone (60:40) at T = 1450 °C for 2 h in an electrical furnace Carbolite BLF 1700 using zirconate crucible. As confirmed by XRD the melt which was cooled in air on steel plate solidified as a homogenous black glass.

For DTA measurement the powder glass was prepared by crushing and grinding the bulk glass in agate mortar, and then sieving it up to grain size of < 0.038 mm. Netsch STA 409 EP DTA device was used, and sample (100mg) was heated at v = 10 °C min^{-1} up to T = 1000 °C.

For the crystallization experiments the glass powders (< 0.074 mm) were pressed at P = 50 MPa in the form of pellets (d = 5mm). The test samples were sintered in an electric furnace at the temperature of 1000 °C for 2 h. The phase composition of the resultant glass-ceramics was examined by XRD using Philips PW- 1710 automated diffractometer.

RESULTS AND DISCUSSION

The chemical composition of the fly ash sample is shown in Table 1.

Table 1. Chemical composition of the fly ash sample

Oxides	SiO_2	Al_2O_3	CaO	MgO	Na_2O	K_2O	$(Fe_2O_3)_u$	TiO_2	P_2O_5	S	L.o.i
Mass %	58.52	24.03	3.31	2.11	0.32	1.08	6.23	0.87	<0.02	0.33	3.16

The XRD and microscopic analyses revealed a complex phase composition of fly ash. The glassy phase (> 30 %) appears in the sample in a form of pearls of different colors with dimension up to 1mm. The large porous aggregates (> 40 %) belong to the burned clay (chamotte) with inclusions of coal and iron oxides. As can be seen from the XRD patterns (Figure 1), the crystalline phases determined in the sample are: quartz, feldspar, mullite, melilite, crystoballite and anhydrite.

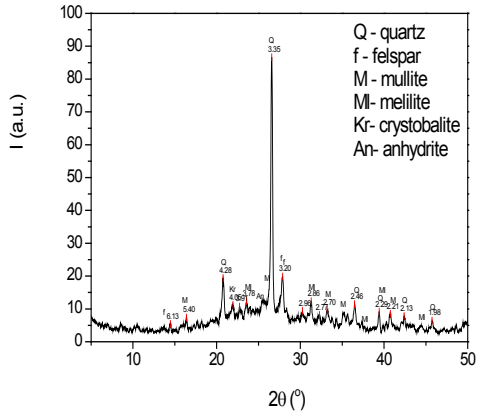

Figure 1. XRD patterns of the fly ash sample

The grain size of the fly ash is shown in Figure 2.

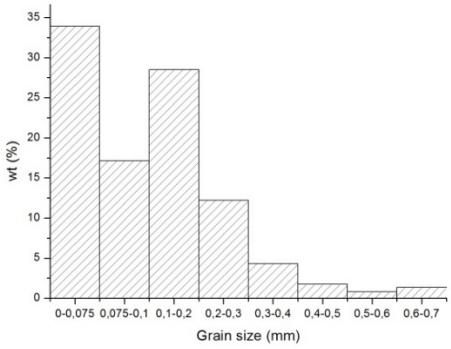

Figure 2. Grains size analysis of the fly ash sample

The melting experiments have shown that is not possible to obtain an appropriate melt of the raw fly ash at temperatures $T \leq 1500$ °C. At $T = 1500$ ˚C, the melt remains highly viscous and could not be cast. To vitrify the fly ash properly, the mixture of limestone and fly ash was melted at $T = 1450$ °C for 2 h. The parent homogenous black glass was obtained by melt casting on steel plate and it is shown in Figure 3. The chemical composition of the glass sample is shown in Table 2, and DTA curve in Figure 4.

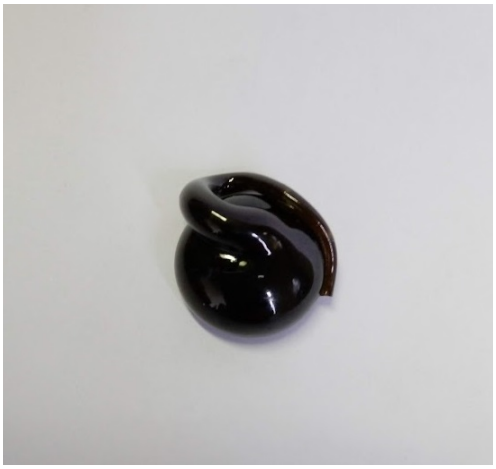

Figure 3. Parent glass sample

Table 2. Chemical composition of the parent glass sample

Oxides	SiO_2	Al_2O_3	CaO	MgO	Na_2O	K_2O	$(Fe_2O_3)_u$	TiO_2	L.o.i
Mass %	46.83	18.97	26.33	1.49	0.29	0.67	4.18	0.68	0.58

The cations of heavy metal of fly ash were bonded into the parent glass network structure. From the DTA curve (Figure 4), the glass transformation temperature T_g = 740 °C and the peak crystallization temperature T_p = 966 °C were determined.

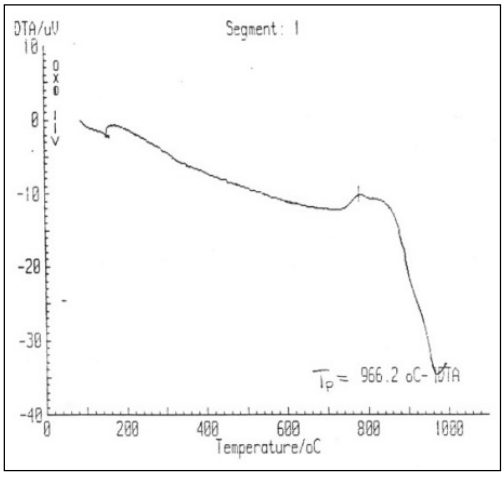

Figure 4. DTA curve of the parent glass sample

The results of sintering showed that the glass pellets shrink significantly during heating. The appearance of the untreated cold pressed sample and sintered at T = 1000 °C for 2h is present in Figure 5.

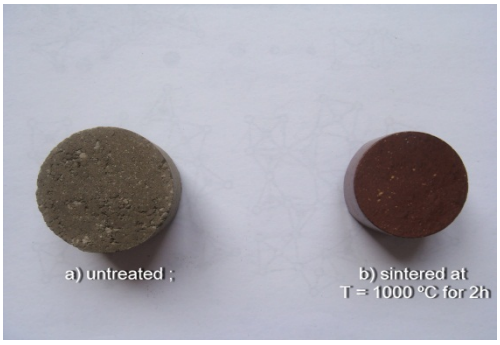

Figure 5. Appearance of glass pellets

By sintering process a dense dark-brown body with glassy appearance was obtained. The XRD analysis showed the crystallization of the sample. The extent of crystallization is small and only one crystalline phase (anorthite) was determined in the sintered sample (Figure 6).

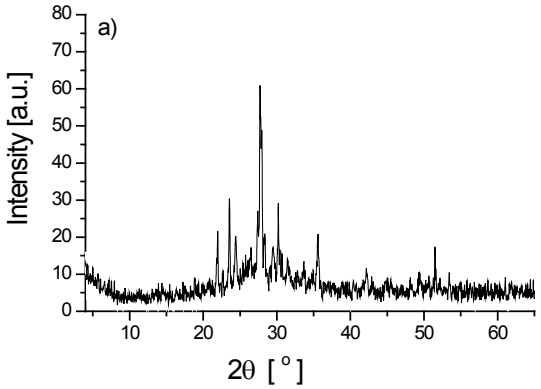

Figure 6. XRD patterns of the sample sintered at T = 1000 °C for 2h

This result demonstrated that the sintering and crystallization processes take place simultaneously during heating of sample. These glass-ceramic material could be applied for production of building materials, ceramics tiles and waste disposal matrix.

CONCLUSION

The subject of this study was the vitrification of waste coal fly ash from thermo-power station. The results of laboratory experiments have shown that the vitrification process can be considered as promising solution for waste management. This process enables the conversion of toxic and environmentally dangerous waste material into a inert glass which can be used for production of useful glass-ceramics with potential wide application.

Acknowledgements:

The authors are grateful to the Ministry of Education and Science, Republic of Serbia for financial support (Projects TR 34001 and OI 172004).

References

1. Barbieri, L., Manfredini, T., Queralt, I., Rincon, J and Romero, M., Vitrification of fly ash from thermal power station., *Glass Technology*, 38 (1997) 165,
2. Barbieri, L., Lancelloti, T., Manfredini, T., Queralt, I., Rincon, J and Romero, M., Glasses and glass-ceramics from coal fly ashes., *Fuel* 78 (1999) 271,
3. L. Maccarini Schabbac, F. Andreola, E. Karamanova, I. Lancellotti, A. Karamanov, L. Barbieri, Integrated approach to establish the sinter-crystallization ability of glasses from secondary raw material, *Journal of Non-Crystalline Solids* 357 (2011) 10–17,
4. W. Wang, C. Lu, G. Yuan, Y. Zhang, Effects of pore water saturation on the mechanical properties of fly ash concrete, *Constr. Build. Mater.* 130 (2017) 54–63,
5. M. Rafieizonooz, J. Mirza, M.R. Salim, M.W. Hussin, E. Khankhaje, Investigation of coal bottom ash and fly ash in concrete as replacement for sand and cement, *Constr. Build. Mater.* 116 (2016) 15–24,
6. M. Zhang, Q. Li, S. Song, N. Hao, G. Liu, Increase of paper strength and bulk by co-flocculation of fines and fly ash-based calcium silicate, *Bioresources* 11 (2016) 7406–7415,
7. Qian, G., Song, Y., Zhang, Y., Xia, Y., Zhang, H., Chui, P., Diopside based glass-ceramics from MSWI fly ash and bottom ash, *Waste Management.*, 26 (2006) 1462,
8. Park, Ch., Yoon, S., Yun, Y., The characterization of glass-ceramics made from waste glass and fly ash, *J. Ceram . Process. Res*., 8 (2007) 435,
9. Kim, J., Kim, H., Processing and properties of a glass-ceramic from coal fly ash from a thermal power plant through an economic process, *J. Eur. Ceram. Soc.,* 24 (2004) 2825,
10. Leroy, C., Ferro, M., Monteiro, R., Fernandes, M., Production of glass-ceramics from coal ash, *J. Eur. Ceram.Soc*., 21 (2001) 195.

XIII International Mineral Processing and Recycling Conference
Belgrade, Serbia, 8-10 May 2019

University of Belgrade, Technical Faculty in Bor
Vojske Jugoslavije 12, 19210 Bor, Serbia
Tel. +381 30 424 555 Fax +381 30 421 078

THE POSSIBILITY OF USING THE FLY ASH FROM THERMAL POWER PLANT "STANARI" DOBOJ IN THE DEVELOPMENT OF GEOPOLYMERS

Ilhan Bušatlić, Nadira Bušatlić #
University of Zenica, Faculty of Metallurgy and Technology, Bosnia and Herzegovina

ABSTRACT – When producing one ton of cement, about one ton of CO_2 is emitted into the atmosphere. Because of this, new materials called geopolymers began to be used as substitute for cement. Geopolymers are inorganic polymers, which result from the geopolymerization of alumosilicate oxides and alkali metal solutions. The raw material for making geopolymer can be any material with a high content of oxides of silicon and aluminum, regardless of its origin. In this paper the possibility of using the fly ash from thermal power plant "Stanari" Doboj for the production of geopolymer was examined. The fly ash from thermal power plant "Stanari" Doboj is supplied in bag filters when coal burning. 12M NaOH solution and water glass were used as alkaline activators. The compressive strength of the samples was tested after 1, 7 and 28 days.

Key words: geopolymers, fly ash, alkaline activator, compressive strength

INTRODUCTION

Cement is a material that has wide application in construction. World cement production is 4.2 billion tons a year. When producing 1 ton of cement, about 1 ton of CO2 is emitted into the atmosphere. In order to reduce CO_2 emissions and utilize reserves of technogenic waste materials, the beginning of the 20th century began the development of new inorganic alumosilicate materials resulting from the polymerization reaction. These materials are called geopolymers. The name of geopolymer was proposed by Joseph Davidovitsz in 1978. According to Davidovitsz, geopolymers are inorganic, solid stable polymeric materials which are transform, polymerize and hardening at low temperatures, in the presence of acidic or alkaline activators.

Geopolymerization involves a heterogeneous chemical reaction between solid aluminosilicate oxides and alkali metal silicate solutions at highly alkaline conditions and mild temperatures yielding amorphous to semicrystalline polymeric structures, which consist of Si–O–Al and Si–O–Si bonds [2]. Geopolymerization is a geosynthesis

corresponding author: nadira.busatlic@gmail.com

(reaction that chemically integrates minerals) that depend on the ability of the aluminium ion (6-fold or 4-fold coordination) to induce crystallographical and chemical changes in a silica backbone [3].

THE RAW MATERIALS FOR THE PREPARATION OF GEOPOLYMER

The raw materials for preparation of geopolymer can be any natural or unnatural (waste) materials with high content of silicon and aluminum. As natural raw materials most commonly used are different types of clay, and from unnatural raw materials are used fly ash, blast furnace slag and their combinations.

When milled coal burning in thermal power plants, particles of ash are collected together with flue gases, which are collected in bags and electro filters. These particles are called fly ash. From the total amount of ash generated in thermal power plants, about 85 % is fly ash [1].

World production of fly ash is about 400 million tons a year, while only 10-30 % of this waste material is again used in the production of cement, concrete and fillers. [1]

Since fly ash particles are very small, they quickly cool down and their structure is mostly amorphous (60 – 90 %). Very small content of particles have a crystalline structure. The chemical composition of fly ash depends on the content of the impurities present in the coal used, and the combustion regime of that coal in the furnace of the thermal power plants.

Fly ash F class has a lower content of CaO and contains several compounds combined between oxides of aluminum, silicon and iron. Fly ash class C contains a high percentage of CaO.

An important role in the geopolymerization process has a raw component that is an activator of the process. Such a raw material component has been called the "alkaline activator" since the reaction takes place in a highly alkaline medium. Various combinations of alkaline solutions can be used, and all alkaline activators, as Glukovsky systematized them, can be divided into six groups:

- Hydroxides: MOH,
- Salts of weak acids: M_2CO_3, M_2SO_3, M_3PO_4,
- Silicates: $M_2O \cdot nSiO_2$,
- Aluminates: $M_2O \cdot nAl_2O_3$,
- Alumosilicates: $M_2O \cdot Al_2O_3 \cdot (2\text{-}6)SiO_2$,
- Salts of strong acids: M_2SO_4,

where the letter M represents an alkali cation.

Palomo et al. (1999) concluded that the type of activator plays an important role in the polymerization process. The reactions take place at a high speed when the alkaline activator contains soluble silicates, either sodium or potassium silicate, compared to the use of only alkaline hydroxides. [4]

A study by Xu and Van Deventer (2000) showed that the addition of a sodium silicate solution to sodium hydroxide solution as an alkaline activator improved the reaction between the source material and the solution. [4]

Tempest et al. (2009) state that the sodium silicate activator dissolves rapidly and

begins to bond particles of fly ash. Pores are quickly filled with gel as soon as the liquid phase succeeds in reaching ash particles. The liquid phase is important as a fluid transport medium that allows the activator to reach the fly ash particles and reacts with them. [4]

The geopolymerization mechanism is not yet completely clear, but it is assumed that Si and Al atoms in the original raw material begin to dissolve during the action of hydroxyl ions. After that, the dissolved ions Si and Al are transported, orientated and condensed into monomers. The resulting monomers bind to polymeric structures at mildly elevated temperatures by polycondensation / polymerization.

PREPARATION OF SAMPLES AND TEST METHODS

In this paper the possibility of using the fly ash from thermal power plant "Stanari" Doboj for the production of geopolymer was examined, as well as the influence of the temperature of activation of samples on the compressive strength. The fly ash from TPP Stanari, BiH, 12M NaOH solution and commercially water glass are used as material.

The testing work of Thermal Power Plant Stanari started at the beginning of 2016. This is the first TPP that combusts crushed coal, not pulverized coal. In this TPP, coal is burned in a fluidizing layer at a lower temperature (850 to 870 °C), from the temperature of the furnace for pulverized coal. Fly ash is collected on a bag filter and then deposited in a fly ash silo. The chemical analysis of the fly ash TPP Stanari is shown in Table 1, and its granulometric composition is shown in Figure 1.

Table 1. Chemical composition of fly ash from TPP Stanari, B&H

Component	SiO_2	Al_2O_3	Fe_2O_3	CaO	MgO	MnO	Na_2O	K_2O	CO_2	SO_3	LOI
Content (%)	48,38	23,49	7,51	11,48	2,76	0,117	0,69	1,79	0,09	2,15	1,543

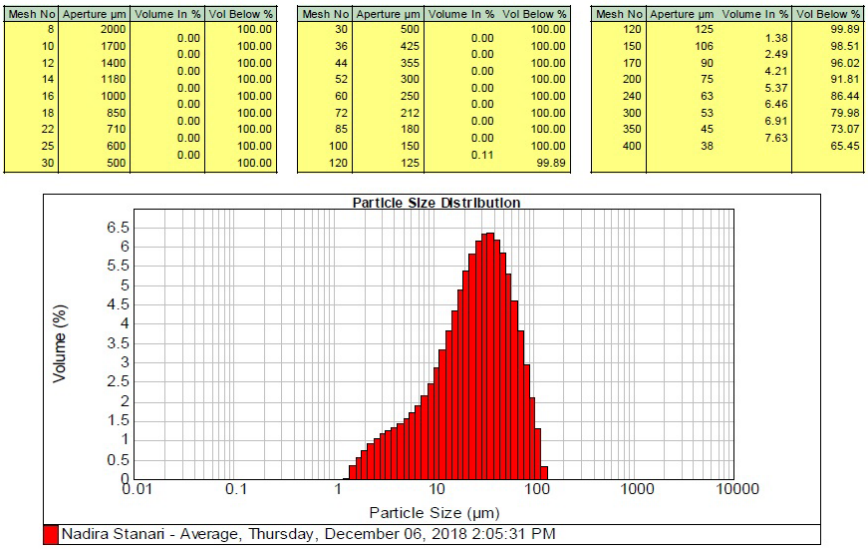

Mesh No	Aperture µm	Volume In %	Vol Below %
8	2000	0.00	100.00
10	1700	0.00	100.00
12	1400	0.00	100.00
14	1180	0.00	100.00
16	1000	0.00	100.00
18	850	0.00	100.00
22	710	0.00	100.00
25	600	0.00	100.00
30	500	0.00	100.00

Mesh No	Aperture µm	Volume In %	Vol Below %
30	500	0.00	100.00
36	425	0.00	100.00
44	355	0.00	100.00
52	300	0.00	100.00
60	250	0.00	100.00
72	212	0.00	100.00
85	180	0.00	100.00
100	150	0.00	100.00
120	125	0.11	99.89

Mesh No	Aperture µm	Volume In %	Vol Below %
120	125	1.38	99.89
150	106	2.49	98.51
170	90	4.21	96.02
200	75	5.37	91.81
240	63	6.46	86.44
300	53	6.91	79.98
350	45	7.63	73.07
400	38		65.45

Figure 1. Granulometric composition of fly ash

From Figure 1 it can be seen that particles of fly ash range from 1 to 100 microns. The most of particles is about 50 microns in size.

12 M NaOH solution was made in the Laboratory for Analytical Chemistry of the Metallurgical and Technology Faculty in Zenica.

Commercially water glass are used in the examination whose characteristics are shown in Table 2.

Table 2. Characteristics of commercially water glass

Characteristics	**Values**
SiO_2(%)	25.0 – 27.5
Na_2O (%)	11.5 – 12.5
Al_2O_3 + Fe_2O_3(%)	Max 0.3
Fe (%)	Max 0.02
Density (g/cm^3)	1.40 – 1.45
Insoluble substances in water	Max 0.15
Module (SiO_2/ Na_2O)	2.0 – 2.4

For the preparation of the samples, the ratio AA / FA = 0.8 was used, while the Na_2SiO_3 / NaOH ratio was 2. The samples were manually blended and vibrated on a vibrating table for 10 minutes. The binding process is exothermic so the samples must be hermetically closed. After 24 h, the samples were taken out of the mold and wrapped in nylon bags, as shown in Figure 2. The wrapped samples were kept in the oven for 24 hours at activation temperatures of 60, 70 and 80 °C.

Figure 2. Prepared of samples

After temperature activation, the samples were taken out from the bags and kept at room temperature. The compressive strength of the samples was tested after 1, 7 and 28 days after thermally treated. The results of the compressive strength are shown in Table 3, and in Figure 4.

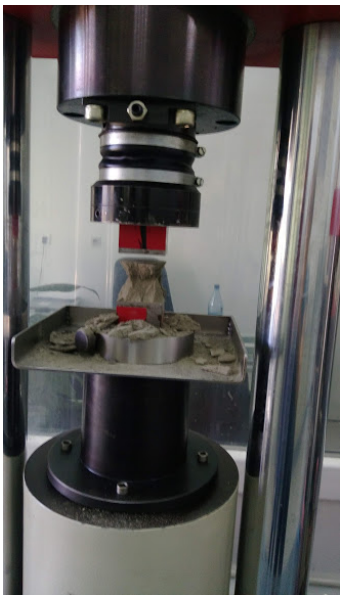

Figure 3. Testing the compressive strength of the samples

Table 3. The results of compressive strength of geopolymers

Temperature (°C)	**Compressive strength (MPa)**		
	1 day	7 days	28 days
60	26,70	17,80	19,60
70	27,50	21,85	32,40
80	24,70	21,66	20,8

From Figure 4 it can be seen that all samples have a satisfactory compressive strength after 1 day. After 7 days, the compressive strength of the samples slightly falls, and then its grow again. The samples thermally activated at 70 °C have the highest compressive strength of 27.5 MPa after 1 day and 32.4 MPa after 28 days. From the above, it can be concluded that the temperature of 70 °C is the optimum geopolymer activation temperature at which the maximum values of the compressive strength are achieved.

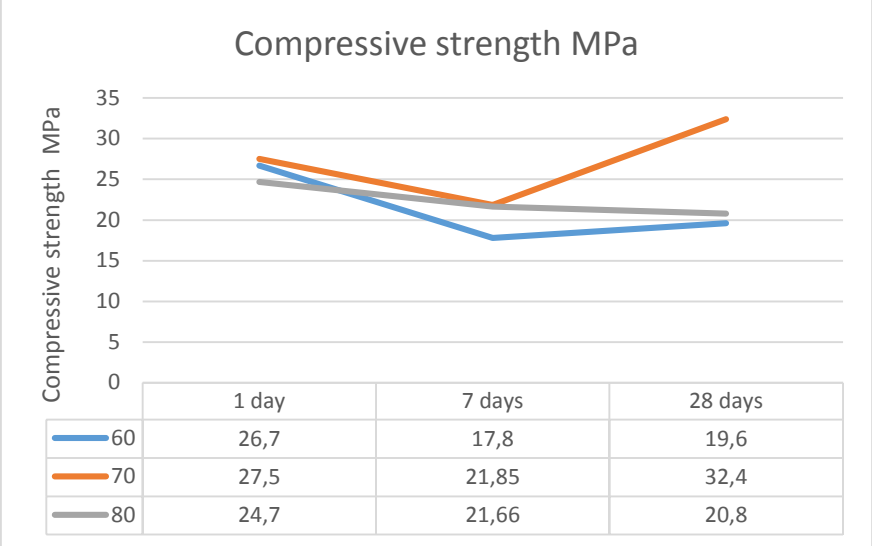

Figure 4. Dependency of the compressive strength of the activation temperature and the geopolymer test time

CONCLUSION

The paper presents the possibility of using the fly ash from TPP Stanari, which is collected in bag filters, for the production of geopolymer. The influence of the activation temperature of the samples on the compressive strength was also examined. From the above examination, the following can be concluded:

• Because of very fine particles of the fly ash tested, it is necessary to use a ratio of AA / LP of 0.8 and more.

• When the samples are cured, before and during the thermal treatment, they must be hermetically closed because of the exothermic reaction of the geopolymerization.

• The compressive strength of the samples after 1 day is satisfactory high at all three temperatures and ranges from 26.7 MPa to 60 °C, 27.5 MPa at 70 °C and 24.7 MPa to 80 °C.

• The highest values of the compressive strength after 1, 7 and 28 days show the samples are thermally activated at temperatures of 70 °C for 24 h.

References

1. Bušatlić, N. Bušatlić, Cementne sirovine u Bosni i Hercegovini, Štamparija Fojnica d.d. Fojnica, 2018,
2. D. Dimas, I. Giannopoulou and D. Panias, Polymerization in sodium silicate solutions: a fundamental process in geopolymerization technology, J. Mater Sci., 44 (2009), 3719- 3730,
3. J. Davidovits, The polysialate terminology: a very useful and simple model for the promotion and understanding of green-chemistry, In geopolymer,

green chemistry and sustainable development solutions: proceedings of the world congress geopolymer 2005, Davidovits J., Geopolymer Institute, Saint-Quentin, France. Ed., (2005), 9-12,

4. M. M. A. Abdullah, K. Hussin, M. Bnhussain, K. N. Ismail, W. M. Ibrahim, Mechanism and Chemical Reaction of Fly Ash Geopolymer Cement-A Review, Internation Journal of Pure and Applied Sciences and Technology, 2011,
5. M. Mustafa Al Bakri, H. Kamarudin, M. Bnhussain, I. Khairul Nizar, A.R. Rafiza, Y. Zarina, The Processing, Characterization and Properties of Fly Ash Based Geopolymer Concrete, 2011,
6. C. D. Budh, N. R. Warhade, Effect of Molarity on Compressive Strength of Geopolymer Mortar, India 2014,
7. F. Škvara, L. Kopecky, L. Myškova, V. Šmilauer, L. Alberovska, L. Vinšova, Aluminosilicate Polymers – Influence of Elevated Temperatures, Efflorescence, Czech Republic, 2009,
8. Bušatlić I., Dodaci cementu, Fakultet za metalurgiju i materijale, Zenica, 2013.

XIII International Mineral Processing and Recycling Conference
Belgrade, Serbia, 8-10 May 2019

University of Belgrade, Technical Faculty in Bor
Vojske Jugoslavije 12, 19210 Bor, Serbia
Tel. +381 30 424 555 Fax +381 30 421 078

IDENTIFYING CHEMICAL COMPOSITION OF CATHODE MATERIALS IN LITHIUM-ION BATTERIES

Dragana Medić #, Snežana Milić, Boban Spalović, Ivan Đorđević
University of Belgrade, Technical Faculty in Bor, Bor, Serbia

ABSTRACT – Lithium-ion (Li-ion) batteries are electrochemical devices which enable chemical energy to turn into electricity. After a while, a battery loses its functionality and cannot be used any more. Such batteries are considered waste and require special treatement, i.e. recycling. Spent lithium-ion batteries are classified as dangerous waste and, if not treated in accordance with regulations, can be a serious threat to the quality of the environment and human health. There are no battery-recycling facilities in The Republic of Serbia. Moreover, a system for collecting and sorting batteries in an organized way has not been developed. Current way of managing electronic waste makes it difficult for scientists who atempt to contribute in optimizing the recycling process. In this paper, batteries were sorted based on the chemical composition of cathode materials. ICP-OES (Inductively coupled plasma - optical emission spectrometry) was used for the sorting process.

Key words: Lithium-ion batteries, Cathode material, ICP-OES

INTRODUCTION

By the end of 1970s, Armand came up with the idea to make batteries whose electrodes consisted of intercalated materials with different electrode potentials. Because of the intercalation of lithium between electrodes, this type of battery is often called "the rocking chair battery" [1]. However, it was only in 1991 that the Sony company commercialized the Li-ion battery in which the cathode was made of $LiCoO_2$, while the anode was made of carbon [2, 3, 4]. Out of safety reasons, Co was in time replaced with other metals, such as: Ni, Al, Ga, Mg and Ti. In 1996, Goodenough et al. suggested to replace cathode material which was used than, with $LiFePO_4$, while Chiang et al. improved the properties of the material by doping it with aluminum, niobium and zirconium [2].

Today, thanks to their excellent electrochemical properties, Li-ion batteries are widely used in various electronic devices, such as: mobile phones, laptops, digital cameras, electric vehicles, hybrid vehicles and other home and industrial appliances [5, 6,7]. Yue et al. [8] indicate two major problems which appear as a consequence of the increase use of Li-ion batteries. The first problem is related to an increased

corresponding author: dmedic@tfbor.bg.ac.rs

number of spent batteries. Namely, the structure of Li-ion batteries has toxic components whose piling in the environment can have serious consequences to the ecosystem. The second problem is related to the shortage or resources for the production of Li-ion battery. The increased production of Li-ion batteries exhausts the natural supplies of metal which it consists of, especially lithium and cobalt.

Bernandes et al. [9] in their paper presented a few alternatives to the final disposition of batteries. They indicate that the most common way of disposing primary batteries is on sanitary land fills. Lack of such treatment of electronic waste means mobility of dangerous and harmful supstances in the environment. In order for that to be prevented, waste stabilisation should be implemented. Because of the high cost of the stabilisation process, batteries are discarded without prior treatement. One of the ways to remove batteries from the environment is to burn them. However, the burning process may cause mercury, cadmium, lead and dioxins emissions to the environment. Recycling imposes as the best solution for spent battery treatement [9].

Acording to United States Geological Survey, up to 20 % of batteries available for recycling gets recycled. Meanwhile, the International Resources Panel reports that less than 1 % Li is valorized in the process of recycling Li-ion batteries. Complete lack of an efficient classification and management is sited as the main obstacle in the development of economical and eco-friendly industrial battery recycling processes [10]. There is a wide range of battery types in the market, which differ in size and chemical composition. Large companies developed machines which sort batteries based on their magnetic properties, mass and size. However, such devices are still not available to a wider scientific community.

In this paper, classification of Li-ion batteries was done based on the chemical composition of cathode material. This classification will facilitate future laboratory research which aims to find the best process in the valorization of valuable metals.

EXPERIMENTAL

Materials and reagents

Twenty laptop Li-ion batteries of different manufacturers were gathered from local secondary material collectors. Concentrated nitric and hydrochloric acid were used for disolving cathode materials in a ratio of 1:1, all of them with analytical grade.

Equipment

ICP-OES (Inductively coupled plasma - optical emission spectrometry, Perkin Elmer Optima 8300) was used to determine the composition of Li, Co, Mn, Ni, Al, Cu and Fe. The operating conditions employed for ICP-OES determination were 1300 W RF power, 8 L/min plasma flow, 0.5 L/min auxiliary flow, 0.75 L/min nebulizer flow, 2 mL/min sample uptake rate. Axial view was used for metals determination, while 2-point background correction and 4 replicates were used to measure the analytical signal. The emission intensities were obtained for the most sensitive lines free of spectral interference. The calibration standards were prepared by diluting the stock multi-elemental standard solution (1000 mg/L) in 0.2 % (v/v) nitric acid. The calibration curves for all the studied elements were in the range of 1 to 100 mg/L.

Experimental procedure

After the plastic battery cases were removed, 22 different types of cells were separated by a visual inspection. Visual identification was based on the color of the plastic cell covering, the ring around the positive contact and model number. The cells were sequentally numbered from 1 to 22 and then discharged using resistive wire of 5.5 Ω.

Following the procedure described in the Dorella and Mansur paper [11] manual dismantling of the cell was performed. The material inside the cell was separated into cathode, anode, separator and metallic shell. In order to separate cathode material from the aliminium foil, the cathode was heat treated for 10 minutes on 580 °C.

With the goal of removing carbon and organic solvents, cathode dust was additionally heated for 12 h on 650 °C. After that, 0.5 g of cathode powder from each cell was disolved in 20 ml of concentrated HCl and HNO_3 (1:1), and then 15 ml of the sample was taken via a pipette and transfered into a 100 ml volumetric flask and filled up to the mark with demineralized water. The samples were filtered, 1 ml of solution was taken and filled up to 25 ml with 1 % HNO_3. The solution of cathode powder from 22 cells is shown in Figure 1.

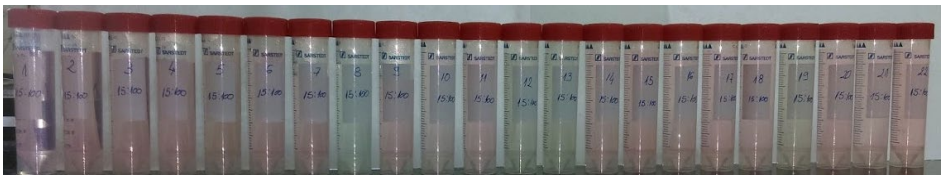

Figure 1. Disolved cathode material in HNO_3 and HCl (1:1)

The pink color of the solution indicates that a high concentration of cobalt ions is present. Since there is no pink color in samples 8, 12, 13 and 19, it can be concluded that in these aforementioned samples the cobalt is not present or is present in low concentrations, which the ICP-OES method confirmed.

Figure 2 shows every individual step which preceded the chemical identification of cathode material.

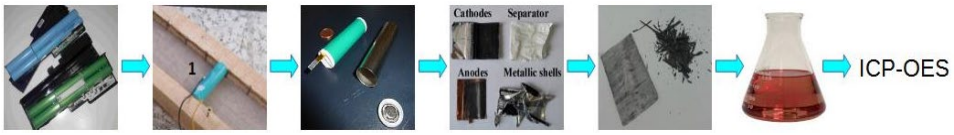

Figure 2. Pre-treatment of Li-ion battery

RESULTS AND DISCUSSION

Table 1 presents identified cells, out of which 17 cathode materials contained $LiCoO_2$, while in only 5 types of cells, the cathode material is made from $LiNiMnCoO_2$.

Table 1. Sorting of Li-ion batteries

Sample's serial number	Model	Chemistry	Color (Wrap)	Color (Ring)	Image
1.	ILIFJT7	$LiCoO_2$		Red	
2.	IFOH2	$LiCoO_2$		Blue	
3.	MICFK56	$LiCoO_2$		Green	
4.	GKCFHH2	$LiCoO_2$		White	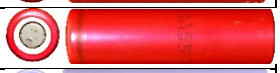
5.	CGR18650 CF	$LiNiMnCoO_2$		White	
6.	CGR18650 HG	$LiCoO_2$		Black	
7.	LGDS218650	$LiCoO_2$		White	
8.	/	$LiNiMnCoO_2$		White	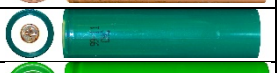
9.	SF US18650GR	$LiCoO_2$		Black	
10.	US18650GR	$LiCoO_2$		Black	
11.	US17670GR	$LiCoO_2$		Black	
12.	ICR18650-22F	$LiNiMnCoO_2$		White	
13.	ICR18650-22H	$LiNiMnCoO_2$		White	
14.	CGR18650A	$LiCoO_2$		White	
15.	ICR18650-22E	$LiCoO_2$		White	
16.	ICR18650-22B	$LiCoO_2$		Blue	
17.	LGR18650P	$LiCoO_2$		White	
18.	LGDS318650	$LiCoO_2$		White	
19.	CGR17670A	$LiNiMnCoO_2$		White	
20.	CGR18650C	$LiCoO_2$		White	
21.	ICR18650-20B	$LiCoO_2$		White	
22.	ICR18650-20	$LiCoO_2$		White	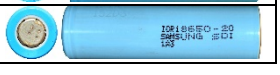

This method of sorting Li-ion batteries according to their cathode material is

considered a destructive battery identifying method, because it is necessary to open the each individual battery in order for the chemical composition of cathode materil to be determined. Another disadvantage of this method is that it consumes a lot of time and uses plenty of chemicals.

Chen i Shen [12] cite that by repairing the cells, a profit of 2.5 $ can be made, while by recycling metal from cells only achieves the economic gain of 0.5 $. For this reason, the functionality of the cell should be checked, if there is a possible for their repair. However, the current way of packaging battery cells is inadequate due to the difficulty of replacing the nonfunctional cells. Researchers will face a great challenge in making the battery recycling process economically viable and, at the same time, environmentally friendly. First of all, a thorough dedication should be given to every step of the recycling process, starting from the organized collection and sorting of batteries.

In Sweden, the battery collection boxes are attached to paper recycling containers. That way, trucks can transport paper along with spent batteries. This system of collecting waste is also being used in Germany and Portugal. The Neatherlands separates the spent batteries from mixed household waste by using magnets. In certain countries, consumers dispose of batteries together with electronic devices [9].

In The Republic of Serbia, 4 companies posses a permit to collect and transport spent batteries. However, there is no organized battery sorting system, or facilities for spent battery treatement. As a part of the Clean up Serbia initiative, a Collection Project for Spent Batteries was created, within which boxes for collecting them were placed in large supermarkets [13].

CONCLUSION

Identification of Li-ion batteries was done with ICP-OES method which provides reliable information on the chemical composition of cathodic material. However, the method's disadvantage is that it requires a lot of time and chemical reagents. Since visual identification was proven as a reliable and quick method of sorting, an automated cell recognition system could be used for industrial purposes using a digital camera. If greater reliability of identification is desired, other chemical methods, which are much faster than the above mentioned and sufficiently reliable, can be used.

Acknowledgment

Authors are grateful to the Ministry of Education, Science and Technological Development of Serbia for financial support (Projects No. 172031).

References

1. Blomgren G. (2017) The Development and Future of Lithium Ion Batteries, Journal of The Electrochemical Society, 164, A5019−A5025,
2. Heelan J., Gratz E., Zheng Z., Wang Q., Chen M., Apelian D., Wang Y. (2016) Current and Prospective Li-Ion Battery Recycling and Recovery Processes, The Minerals, Metals & Materials Society, 68, 2632−2638,

3. Natarajan S., Aravindan V. (2018) Recycling Strategies for Spent Li-Ion Battery Mixed Cathodes, ACS Energy Letters, 3, 2101–2103,
4. Bankole O.E., Gong C., Lei L. (2013) Battery Recycling Technologies: Recycling Waste Lithium Ion Batteries with the Impact on the Environment In-View, Journal of Environment and Ecology, 4, 14–28,
5. Yu L., Shu B., Yao S. (2015) Recycling of Cobalt by Liquid Leaching from Waste 18650-Type Lithium-Ion Batteries, Advances in Chemical Engineering and Science, 5, 425–429,
6. Nayl A.A., Elkhashab R.A., Badawy S.M., El-Khateeb M.A. (2015) Acid leaching of mixed spent Li-ion batteries, Arabian Journal of Chemistry, 10, S3632–S3639,
7. Chen W-S., Ho H-J. (2018) Recovery of Valuable Metals from Lithium-Ion Batteries NMC Cathode Waste Materials by Hydrometallurgical Methods, Metals, 8, 1–16,
8. Yue Y., Wei S., Yongjie B., Chenyang Z., Shaole S., Yuehua H. (2018) Recovering Valuable Metals from Spent Lithium Ion Battery via a Combination of Reduction Thermal Treatment and Facile Acid Leaching, ACS Sustainable Chemistry & Engineering, 6, 10445–10453,
9. Bernardes A.M., Espinosa D.C.R., Tenório J.A.S. (2004) Recycling of batteries: a review of current processes and technologies, Journal of Power Sources, 130, 291–298.
10. Lv W., Wang Z., Cao H., Sun Y., Zhang Y., Sun Z. (2018) A Critical Review and Analysis on the Recycling of Spent Lithium-Ion Batteries, 6, 1504–1521,
11. Dorella G., Mansur M.B. (2007) A study of the separation of cobalt from spent Li-ion battery residues, Journal of Power Sources, 170, 210–215,
12. Chen H., Shen J. (2017) A degradation-based sorting method for lithium-ion battery reuse, PLoS ONE, 12, 1–15,
13. Lokalni plan upravljanja otpadom grada Beograda 2011-2020. SEPA (2011), http://www.sepa.gov.rs/download/UpravOtpad/RPUO_Beograd.pdf, *Accessed on*: 06 March 2019.

XIII International Mineral Processing and Recycling Conference
Belgrade, Serbia, 8-10 May 2019

University of Belgrade, Technical Faculty in Bor
Vojske Jugoslavije 12, 19210 Bor, Serbia
Tel. +381 30 424 555 Fax +381 30 421 078

APPLICATION OF WASTE GLASS IN PRODUCTION OF INSULATORS

Zoran Štirbanović [1, #], Predrag Mitrović [2], Zoran Stević [1], Jovica Sokolović [1], Zoran Milkić [2]
[1]University of Belgrade, Technical faculty in Bor, Bor, Serbia
[2]Measurement Transformers Factory Zaječar, Zaječar, Serbia

ABSTRACT – In this paper are presented the results of the study of applying waste borosilicate glass in the production of insulators. Different types of insulators were made: IPC-1; IPA-3,6; IPB-A2; PIA-1b and IPU-12A, by casting into molds mixture of epoxy resins with different weight ratio of quartz flour and borosilicate glass powder as fillers. After casting, all insulators were tested by measuring partial discharge in order to determine their quality. Electrical testing has shown the good quality of all insulators.

Key words: insulators, quartz flour, borosilicate glass powder, partial discharge

INTRODUCTION

The history of glassmaking, according to some sources, dates back more than 5000-6000 years [1, 2]. There are many definitions of glass, and one of them says that glass is "inorganic product of fusion that has been cooled to a rigid condition without crystallizing" [1]. Glass is usually made of silicon dioxide (SiO_2), but in recent years a large number of non-silicate glasses were recognized, such as polymers and metals that can also be formed as glasses, as well as large number of non-oxide, inorganic compositions [3].

Glass is a material used in many areas of life and industry and as such vast amounts of glass are being produced every year. In 2007 approximately 115 million tons of glass was produced in the world [4]. Good characteristic of glass is that it can be recycled numerous times without losing its quality [5]. Recycling glass uses 3.3 MJ/kg less energy than landfilling and also reduces emissions of CO_2 by 0.39 kg CO_2e/kg [6]. Waste glass can be used for reproduction of glass, but also it is widely used for building materials [5], in concrete and cement production [7,8], for production of different polymers [9,10], etc.

corresponding author: zstirbanovic@tfbor.bg.ac.rs

Besides large quantities also different types of glasses are being produced, such as: flat glass, container glass, continuous filament glass fiber, domestic glass and special glass [4]. One of the special types of glasses is borosilicate glass that can be used for laboratory glassware, household cooking ware, industrial piping, bulbs for hot lamps and electronic tubes of high wattage such as X-ray tubes, etc., and all due to its characteristics such as: lower thermal expansion than soda-lime silica glasses, have good chemical resistance, high dielectric strength and a higher softening temperature than soda-lime silica glasses [11].

In this paper are presented the results of the study of using waste borosilicate glass in production of insulators. Measurement Transformers Factory in Zaječar is producing a variety of measuring transformers, but also different types of insulators. Insulators are usually made by casting into molds mixture of epoxy resins and high purity quartz [12]. Quartz is being used as filler for upgrading some of the characteristics of the products [13], but also for lowering their price. Since borosilicate glass mainly consists of quartz [8] and as it was mentioned before has high dielectric strength, in this study quartz was replaced with 25%; 50%; 75% or 100% waste borosilicate glass in weight. The obtained insulators were subsequently tested by measuring partial discharges and obtained results were compared to the same results for insulators made of quartz.

EXPERIMENTAL

Materials

For production of insulators following components were being used: epoxy resin CY 5962, hardener HY 918, flexibilizer DY 040, colouring pastes DW 0136 and accelerator DY 062, all by Huntsman Corporation. As fillers were used quartz flour Millisil W12, produced by Quarzwerke GmbH, and borosilicate glass powder Boruvit B140 produced by Ziegler Minerals.

Chemical composition

Chemical compositions of quartz flour Millisil W12 and borosilicate glass powder Boruvit B140 (given by the producer) are shown in Table 1.

Table 1. Chemical compositions of quartz flour and of borosilicate glass powder

Material	SiO_2	CaO	MgO	Na_2O	K_2O	Fe_2O_3	Al_2O_3	B_2O_3	ZrO_2
Quartz flour	98,38 %	<0,01 %	<0,01 %	<0,02 %	0,02 %	0,022 %	0,14 %	/	/
Borosilicate glass powder	77-80 %	/	/	4-5 %	1 %	/	2-4 %	11-13 %	0-1 %

When fillers are being used in production of insulators there are some limitations in terms of their chemical composition such as: min. 98,5 % SiO_2; max. 0,75 % Al_2O_3; max. 0,05 % Fe_2O_3; max. 0,1 % CaO+ MgO; max. 0,1 % Na_2O+ K_2O. It must be emphasized that these limitations are prescribed by Measurement Transformers Factory Zaječar and they relate to technology used in this factory.

As it can be seen from Table 1, the content of SiO_2 in quartz flour is slightly under prescribed value, but the difference is insignificant, and since all other values are in the prescribed range it can be said that quartz flour Millisil W12 meets all the

necessary requirements. As the borosilicate glass powder Boruvit B140 is concerned, it can be seen that the content of SiO_2 is much under prescribed value, and the values of Al_2O_3 and Na_2O+ K_2O are much above prescribed values.

Grain size composition

Grain size composition of the filler is also one of characteristic that is very important in the process of producing insulators. It is recommendable that grain size of the material used as filler should be 100 % under 60 μm.

In Figure 1 are shown grain size compositions of quartz flour Millisil W12 and borosilicate glass powder Boruvit B140.

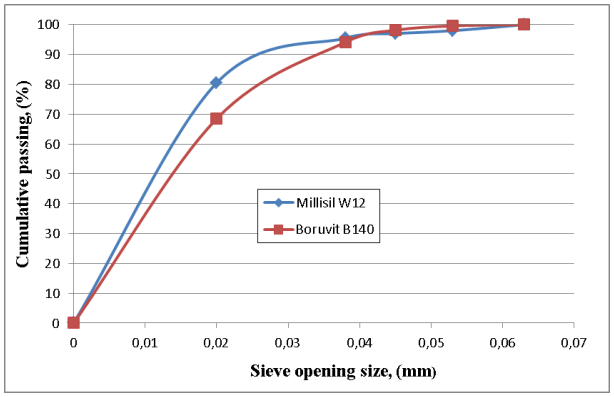

Figure 1. Grain size compositions of quartz flour Millisil W12 and borosilicate glass powder Boruvit B140

As it can be seen from Figure 1, grain size compositions of both materials fulfill needed requirement, i.e. 100% under 60 μm. Also, it can be noted that content of grain size under 20 μm is higher for quartz flour, approximately 80%, so it can be said that this material is finer grinded.

CASTING OF INSULATORS INTO MOLDS

The mixture of epoxy resin and other components with filler is initially put into mixer, so all the components are properly mixed, warmed up and vacuumed, and later it is discharged into the vessel. Just before the casting, a precisely measured quantity of accelerator is added. The mass is then poured into molds that have been previously well-heated at 70 °C and lubricated. The pouring of the mass must be slow and in a thin layer so all the air is out of the molds. Molds with a mass are then left in the furnace for 15 minutes at a temperature of 120 °C to 150 °C, and then the insulators are removed from the molds and left at room temperature for at least 12 hours.

Following types of insulators were made: IPC-1; IPA-3,6; IPB-A2; PIA-1b and IPU-12A (Figure 2). Each of these insulators were made with different weight ratio of quartz flour and borosilicate glass powder:

- 100 % quartz flour;

- 75 % quartz flour and 25 % borosilicate glass powder;
- 50 % quartz flour and 50 % borosilicate glass powder;
- 25 % quartz flour and 75 % borosilicate glass powder;
- 100 % borosilicate glass powder.

Also, two samples of each of these insulators were made.

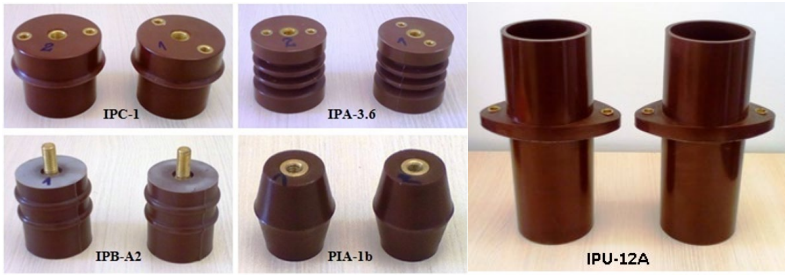

Figure 2. Insulators after casting

ELECTRICAL TESTING OF INSULATORS

After casting, insulators were tested in Laboratory for testing electrical properties in Measurement Transformers Factory in Zaječar by measuring their partial discharge (Figure 3). Partial discharge represents the occurrence of currents in insulator due to local breakthroughs within the inhomogeneity or presence of cavities in insulation mass, which can cause significant degradation to the insulator [14]. The measured values of partial discharge should be as low as possible, indicating the good quality of insulators.

Figure 3. Measuring partial discharge of insulators

RESULTS AND DISCUSSIONS

In addition to the quality of the mass and the method of casting, the amount of partial discharges through the insulator at a tested voltage also depends on the type of insulator tested, ie, its dimensions, as well as the distance of the connections in the insulator.

In Table 2 are presented the results of measuring partial discharge of different types of insulators with different ratio of quartz flour and borosilicate glass powder.

Table 2. The results of measuring partial discharges of insulators

Content of fillers		IPC-1		IPB-A2		IPA-3,6		PIA-1b		IPU-12A	
		[κV]	[pC]	[κV]	[pC]	[κV]	[pC]	[κV]	[pC]	[κV]	[pC / nC]
100% quartz flour	sample 1	20.6	38	14	350	17.6	42	20	5	4.5 5 5.5	6.5 pC 40-50 pC 200-250 pC
	sample 2	28	40	16.5	245	24	190	34	38	4.4 4.4 5.5	4 pC 200 pC 500-700 pC
75 % quartz flour 25 % borosilicate glass powder	sample 3	28	3	7 28	17 785	28	3	28	3	2 4 10	3 pC 1800 pC 2 500 pC
	sample 4	28	3	4 28	3 550	23 28	6 92	28	5	2 6 8	4 pC 1500 pC 4 nC
50 % quartz flour 50 % borosilicate glass powder	sample 5	28	3	25 28	6 30	23 28	6 24	28	4	2 4 10	3 pC 1600 pC 2 800 pC
	sample 6	21 28	6 80	25 28	7 23	28	3	28	3	6 8 10	1800 pC 5 nC 6.7 nC
25 % quartz flour 75 % borosilicate glass powder	sample 7	20 28	2.9 164	11 25	490 730	28	26	20 25	4 4	5.7 6.7 8.3	500 pC 1.4 nC 4 nC
	sample 8	20 35	3 3.2	15 25	60 164	14 25	62 70	20 25	4 4	4.4 6 8.9	670 pC 2.3 nC 4.5 nC
100 % borosilicate glass powder	sample 9	18 20	4 ≈200	20	580	12 20	5 45	50	3	5.5 6 7	4 pC 400-600 pC 650-850 pC
	sample 10	25	3	20	380	10 20	5 44	10 12	4 25	3.5 3.7 5.5	3 pC 80-130 pC 700-850 pC

In Table 2 are also given the values of voltages causing initial partial discharge to appear. As it can be seen, all insulators have shown good quality in terms of partial discharge values. There are no big deviations of partial discharge of insulators with borosilicate glass powder compared to insulators with only quartz flour, thus proving the possibility of using this type of glass as filler in the production of insulators. Initial values of partial discharge for insulators IPB-A2 and IPU-12A are higher compared to other insulators because their dimensions, as well as dimensions and layout of their connections, are much different.

CONCLUSION

Insulators are made by using epoxy resin with mineral filler, usually quartz. Substitution of natural material with waste material has benefits in terms of preserving natural resources and preventing environmental degradation by landfilling vast amounts of different waste materials.

The aim of this study was to substitute quartz with waste glass in the production of insulators. Borosilicate waste glass was used because of its preferable characteristics, especially high dielectric strength.

Different types of insulators were made, by casting into molds mixture of epoxy resins with different weight ratio of quartz flour and borosilicate glass powder as fillers, and after that they were tested by measuring partial discharge in order to determine their quality. Electrical testing has shown the good quality of all insulators, thus proving the possibility of using borosilicate waste glass as filler in the production of insulators.

References

1. Zanottoa, E. D., Mauro J. C., (2017.) The glassy state of matter: Its definition and ultimate fate, Journal of Non-Crystalline Solids 471, 490–495,
2. Mauro J. C., Zanottoa, E. D., (2014.) Two Centuries of Glass Research: Historical Trends,Current Status, and Grand Challenges for the Future, International Journal of Applied Glass Science 5 (3), 313–327,
3. Shelby, J. E., (2004.) Introduction to Glass Science and Technology, Second Edition, The Royal Society of Chemistry, Cambridge, UK,
4. Wintour N., (2015.)The glass industry: Recent trends and changes in working conditions and employment relations, International Labour Office, Sectoral Policies Department. - Geneva: ILO,
5. Heriyanto, Pahlevani, F., Sahajwalla, V., (2018.) From waste glass to building materials – An innovative sustainable solution for waste glass, Journal of Cleaner Production 191, 192–206,
6. Vossberg, C., Mason-Jones, K., Cohen B., (2014.) An energetic life cycle assessment of C&D waste and container glass recycling in Cape Town, South Africa, Resources, Conservation and Recycling 88, 39–49,
7. Shi, C., Zheng, K., (2007.) A review on the use of waste glasses in the production of cement and concrete, Resources, Conservation and Recycling 52, 234–247,
8. Han, W., Tao Sun, T., Li, X., Sun, M., Lu Y., (2016.) Using of borosilicate glass waste as a cement additive, Nuclear Instruments and Methods in Physics

Research B 381, 11–15,
9. Rivera, J. F., Cuarán-Cuarán, Z. I., Vanegas-Bonilla, N., Mejía de Gutiérrez, R., (2018.) Novel use of waste glass powder: Production of geopolymeric tiles, Advanced Powder Technology 29, 3448–3454,
10. Žlebek, T., Hodul, J., Drochytka, R., (2017.) Experimental testing suitability of the waste glass into the polymer anchor materials based on epoxy resin, Procedia Engineering 195, 220-227,
11. Konijnendijk, W. L., (1975.) The structure of borosilicate glasses, Technische Hogeschool Eindhoven, Eindhoven, Netherlands,
12. Gallot-Lavallée, O., Teyssedre, G., Laurent, C., Rowe, S., (2006.) Space charge behavior in an epoxy resin: the influence of fillers, temperature and electrode material. <hal-00019785>,
13. Kouloumbi, N., Ghivalos, L. G., Pantazopoulou, P., (2003.) Effect of quartz filler on epoxy coatings behavior, Journal of Materials Engineering and Performance 12 (2), 135–140,
14. Jahoda, E., Kúdelčík, J., (2017.) Internal partial discharge in cavity of polyurethane, Procedia Engineering 192, 365 – 369.

XIII International Mineral Processing and Recycling Conference
Belgrade, Serbia, 8-10 May 2019

University of Belgrade, Technical Faculty in Bor
Vojske Jugoslavije 12, 19210 Bor, Serbia
Tel. +381 30 424 555 Fax +381 30 421 078

SILVER NANOPARTICLE SYNTHESIS AND USES IN SEPIOLITE-ALGINATE NANOCOMPOSITES FOR PROTECTIVE COATINGS

Buket Kabacaoğlu [1, #], Birgül Benli [2]
[1]Istanbul Technical University, Chemical Engineering Dept., 34469, Turkey
[2]Istanbul Technical University, Mineral Processing Engineering Dept., 34469, Turkey

ABSTRACT – This study aims to investigate biodegradable protective coatings enhanced with green synthesized AgNPs using alginate and ascorbic acid. Before being used as a fibrous additive, natural sepiolite clay first beneficiated using gravity separation and high speed mixer. The composites were evaluated using several in common disc diffusion method on gram$^-$ E. coli and gram$^+$ S. aureus bacteria tests. 1.24 % wt. of synthesized AgNPs is enough to show good antibacterial activity nearly 1.5 times higher zones than medical antibiotic discs. Synthesized nanoparticles present opportunity for utilization of clay nanocomposites from drug-delivery to enhanced coatings, i.e. corrosion protection and protective polymeric coating.

Key words: silver nanoparticle, alginate, sepiolite, AFM imaging, protective coating

INTRODUCTION

Clay minerals based nanocomposites and coatings have potential for three dimensional scoldfolds, wound dressings and drug release due to stability in aqueous environments such as human body fluid [1]. Protective coatings have also proven to be one of the most effective surface modification methods to slow down corrosion of metal implants [2]. Compared to inorganic coatings, biodegradable polymeric coatings are more prominent for their protective properties as well as biomedical applications [3] and antibacterial coating systems [4]. Antibacterial coatings are important because of their ability to hinder bacterial growth on biomedical surfaces and cure the development of infections conditions [5].

Growing exceptionally fast amongst other nanotechnology products, silver nanoparticles are broadly applied in the medicine field for their antibacterial and anti-inflammatory properties [6]. Chemical reduction, photo-physical, photochemical and electrochemical methods are commonly utilized to synthetically produce silver nanoparticles in a wide size range of 2-100 nm [7]. Despite chemical

corresponding author: buketkabacaoglu@gmail.com

and physical methods being used for metal nanoparticle production for a long time, the importance of creating a green process is evident from the toxicity issues that may occur with hazardous chemicals being absorbed to the nanoparticle surface due to the use of hydrazine and sodium borohydride, some of the most commonly used reducing agents.

Nanoparticle biosynthesis requires a reducing and a stabilizing agent, both can be fulfilled by carbohydrates such as starch and its constituents due to their chemical structure [8]. Moreover, carbohydrates can be utilized to overcome the problem of agglomeration of silver nanoparticles in aqueous solutions. Therefore, these carbohydrates based nanoparticles synthesis could be useful for the polymers as stabilizing agents as well. Some examples can be given for these polymers such as alginate, chitosan, PVA and PVP for their extensive use in the biomedical cooperation with silver nanoparticles. Alginate, which is a natural polymer extracted from brown algae, is known to form hydrogels with cations that have a valence of two, like Ca^{+2}, in its aqueous form through crosslinking. This hydrophilic, biocompatible and biodegradable gels shape can easily be manipulated which makes it useful not only in biomedicine but also in drug release, wound dressings, food industry and more [9]. Silver nanoparticles' catalytic property and diffusion can be advanced by taking advantage of porous materials' high surface areas and channels that can be self-organized [8]. Clays, especially fibrous sepiolite are important solid porous materials.

Sepiolite is an important industrial clay mineral with the ideal chemical formula $Si_{12}Mg_8O_{30}(OH)_4(OH_2)_4.8H_2O$ and composed of magnesium octahedral layer sandwiched between silica tetrahedral sheets [10,11]. These three-layer sheets are bonded to each other only by van der Waals forces. Figure 1 shows the unique fiber structure of sepiolite that has many micro-pores and channels during fiber elongation [12]. Preliminary molecular dynamics (MD) simulation of sepiolite interfacial water structure clearly illustrated that natural sepiolite fibers have anisotropic surfaces composed of hydrophobic/hydrophilic ribbons [13].

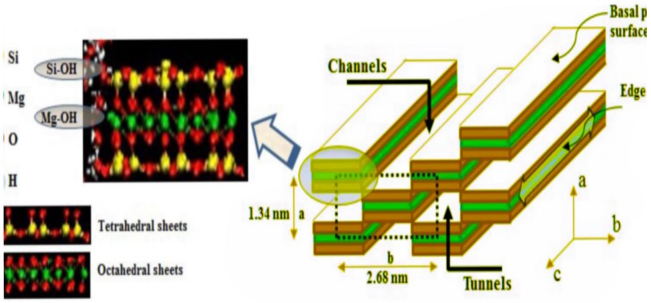

Figure 1. The structure of hydrophobic/hydrophilic ribbons of fibrous sepiolite

In this work, we present a green and optimized method to synthesize silver nanoparticles that can be incorporated into alginate-sepiolite films that could be have potential usage for biodegradable magnesium implants. First, we aimed to choose a green method to synthesize silver nanoparticles with preliminary laboratory work. After choosing alginate as the matrix for silver nanoparticle

formation, we designed an experiment using Minitab's Box-Behnken response surface design to see which factors affect the particle size of AgNPs the most and proceeded to optimize the experiment to target producing the smallest particles possible using the Assistant function of Minitab according to the responses obtained from UV-VIS spectrophotometer and Zetasizer.

After combining these results, the AgNP solutions representing 3 different particle sizes between 5 to 75 nm were chosen and these three solutions were mixed with alginate and sepiolite solution. The final mixed solutions were turned into films and were left to wait in a $CaCl_2$ solution. The final AgNP-alginate and AgNP-composite films were then send to AFM image analysis.

There have been reports about utilizing different biodegradable polymers to stabilize AgNPs using chemical reduction. Also, applying DOE to synthesizing AgNPs has been done before. However, there have not been a study that applied DOE to green methods of AgNP synthesis. In addition, the AgNPs were added to polymeric films that were further tested in simulated body fluid for the purpose of being used in biodegradable body implants.

MATERIALS AND METHODS

Materials

The raw sepiolite sample consisted of 85±3 % sepiolite was obtained from AEM Co., Turktaciri region of Turkey. Quantitative chemical analyses were carried out by ICP (inductively coupled plasma) spectrophotometry in the ACME Analytical Lab. (Canada), and the main constituents were defined as 49.85 wt. of SiO_2, 2.38 wt. of Al_2O_3, 0.87 wt. of Fe_2O_3, 2.65 wt. of CaO and 20.15 wt. of MgO. Mineralogical characterization of the sample with a Shimadzu XRD-6000 equipped with a Cu X-ray tube (λ= 1.5405 Å) showed that major mineral impurity is dolomite along with illite, palygorskite, calcite, smectite, dolomite, quartz, crystobalite and feldspar.

As silver precursor, silver nitrate (Merck grade) was used. Alginic acid sodium salt from brown algae, sodium alginate, obtained from Fluka was used as both stabilizing and reducing agent. Ascorbic acid was also used as reducing agent. The other chemicals used in this study are Merck grade and did not receive any further purification. All solutions were prepared with distilled water.

BENEFICIATION STUDIES OF SEPIOLITE FIBERS

Due to very fine particle sizes (<2 mm), the removal of impurities is still a problem without making any breaks in the fibers of sepiolite. The most convenient method to separate impurities from sepiolite can be based on their specific gravities using a Mozley Table like a quick and powerful compact shaking table which offers many advantages especially in small capacities. Two-step concentration by Mozley table was performed and between these two steps, the products were dried as intermediate step to show the effect of drying on the separation efficiency of sepiolite fibers.

Sepiolite samples were first reduced up to a particle size less than 5 mm. Then, two-step Mozley table tests contain the following procedures: preconcentrated fractions were recirculated on the gravity separator (Mozley table) several times; the last recirculated fractions were dried in an oven at 60 °C for 24 h; dried sepiolite

samples were ground to a particle size less than 2 mm; concentrated fractions were recirculated on Mozley table and dried at 60 °C for 24 h. Finally, these concentrated samples were used for the adsorption, antibacterial and electric currency tests.

ATOMIC FORCE MICROSCOPY (AFM) MEASUREMENTS

AFM images of sepiolite fibers were performed using XE-70E (Park Systems Corp., Suwon, Korea) in contact mode by NSC36/Cr–Autype cantilevers with 0.5 Hz scanning speed. (AFM,). The AFM measurements were carried out under moisture controlled medium ambient conditions (22±2 °C). Cantilevers were exposed to UV/O3 (UV Cleaner, Bioforce Nanosciences) for 15 min prior to each experiment to remove any possible contamination on each probe. In order to quantify the size of sepiolite fibers on AFM images, all images were processed by XEI Image Processor (Park Systems Corp., Suwon, Korea).

ANTIBACTERIAL SUSCEPTIBILITY TESTING BY DISK DIFFUSION METHOD

Escherichia coli (ATCC 25922) and *Staphylococcus aureus* (ATCC 25923) were obtained from Center for Culture Collections and Microorganisms, Istanbul Faculty of Medicine, Turkey. Luria-Bertani broth (LB, Merck) was used as a growth medium.

25 grams of Luria-Bertani Broth (Powder, Merck) was added into 1000 ml of deionized water at room temperature, stirred vigorously for 30 minutes to dissolve equally. 500 ml of this solution transferred to autoclavable glass bottles, for preparing LB Agar 15 gr. of Agar agar (Powder, Merck) added into the other half of the solution and stirred vigorously 30 minutes more. Bottles autoclaved (Nüve OT 100 V) at 1.5 atm, 121 °C for 20 minutes. Bottles were collected then cooled to 50 °C. 15 ml of LB agar poured in plates to solidify. Bacterial suspensions were prepared by growing the bacteria overnight at 37 °C in LB broth (20 ml). The bacterial suspensions were diluted with a sterile saline solution to a final concentration of 1.5×108 CFU/ml (0.5 McFarland turbidity).

Antibacterial activity of the raw, Ag^+ and silver nanoparticles added sepiolite films were tested on *E.coli* and *S.aureus*. 0.1 ml of each bacteria suspension that adjusted to 0.5 McFarland turbidity used to inoculate the surface of LB agar plate. By the use of a drigalski-spatula bacterial suspension spread evenly on agar plates while rotating the plate to ensure homogeneous growth. 0.2 gram of the raw and ion exchanged samples, were pressed into pellets (7 mm diameter) and placed over the surface of the agar plates. Then all plates are incubated at 37 °C overnight. For comparing the results Ampicillin/sulbactam (SAM) antibiotic discs and raw samples were used as control samples. After an overnight incubation, the bacterial growth around each disc is observed. If the test isolate is susceptible to a particular antibacterial agent, no growth or the zone of inhibition will be observed around the disk. This zone is then measured in mm and results compared with control groups.

RESULTS AND DISCUSSION

Table 1 presents the experiments used for the determine optimization of AgNPs preparation. Box-Behnken Response surface design (3 parameters) by Minitab 18 were selected as 15 runs with 3 replicates. Three parameters that influence the size of AgNPs were followings: the amount of $AgNO_3$ and ascorbic acid as well as the pH

of the AgNP solution. 3 center points were applied to the following high and low values of the parameters; 11 and 5 for pH, 1.2 and 0.4 ml for ascorbic acid and 0.8 and 0.4 ml for the amount of $AgNO_3$. As the first selected response is UV absorbance peaks observed between the range 200-600 nm by UV-VIS spectrophotometer. Table 1 also shows their particle sizes and their zeta potential (mV) with respect to the obtained AgNPs.

Table 1. Particle size diameters and zeta potentials of AgNPs using Box-Behnken response surface design by Minitab

Run	pH	$AgNO_3$ (mL)	Ascorbic acid (mL)	Response λ (nm)	Particle Size Diameter (nm)	Zeta Potential (mV)
1	-	-	0	250	0	0
2	+	-	0	260	0	0
3	-	+	0	420	5.6	-54.1
4	+	+	0	400	52.5	-65.7
5	-	0	-	420	2.5	-54.1
6	+	0	-	420	6.2	-54.1
7	-	0	+	450	13	-40
8	+	0	+	400	52.5	-65.7
9	0	-	-	475	24.3	-24.9
10	0	+	-	475	24.3	-24.9
11	0	-	+	470	24.3	-24.9
12	0	+	+	470	24.3	-24.9
13	0	0	0	510	24.3	-24.9
14	0	0	0	470	24.3	-24.9
15	0	0	0	470	24.3	-24.9

The selected AgNP solutions (Figure 2 (a)) are runs 4, 6 and 9 of the Minitab set. Figure 2 (b) is the following UV spectrophotometer peaks at 400, 420 and 470 λ. After adding sepiolite and mixing with the appropriate amount of alginate polymer mixing, composite films were encapsulated with $CaCl_2$ solution to form crosslinking with Ca-egg-box mechanism. Figure 2 (c) shows the AFM image of the dried films.

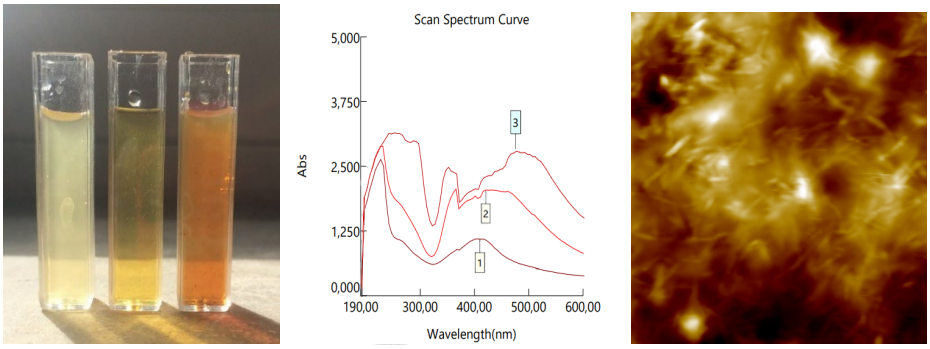

Figure 2. From leftto right, Minitabruns 6, 4 and 9. (a) colors, (b) UV absorbance, (c) AFM image of AgNPs-sepiolite addedalginate compositefilms

Alginate-AgNP beads were made with AgNPs made according to optimization of Minitab results at λ = 420 nm. Comparing the water swelling of alginate beads that were left in 20 % wt. $CaCl_2$ solution for different amounts of times before staying in distilled water for 24 hours, the beads that stayed in the $CaCl_2$ solution for 30 minutes had twice as much water swelling compared with beads that stayed in $CaCl_2$ solution for 24 hours. Additionally, Alg-AgNP beads that stayed in the same $CaCl_2$ solution from 0 minutes to 24 hours were left to dry for 4 days. As a result, it is found that beads that spent 30 minutes had lost the most weight (96.75 %) while the beads that stayed 24 hours had the least weight loss (49.12 %). Later, another swelling test was conducted using simulated body fluid (SBF) made according to Jalota's SBF recipe (NaCl, $NaHCO_3$, KCl, Na_2HPO_4, $MgCl_2.6H_2O$, HCl, $CaCl_2.2H_2O$, Na_2SO_4, TRIS) that has 1.5 times more ion concentration than regular SBF, which has an accelerating effect [14]. According to results, the dry beads that previously spent 30 minutes in $CaCl_2$ solution and 24 hours in distilled water had 378 % SBF swelling in 3 days. However, no swelling was observed for the wet beads using SBF. Beads that only stayed in $CaCl_2$ solution for 30 minutes lost 23.5 % of their weight in SBF solution in 3 days meanwhile beads that stayed additionally in distilled water for 24 hours had only 2 % dissolving in SBF.

According to antibacterial tests, composite films that contain 1.24 % wt. silver had 1.5 times better antibacterial activity than medical antibiotic discs. Comparing different AgNP solutions that were used in films, the Minitab run 6 had the best antibacterial activity while Minitab run 4 had the least antibacterial activity in both alginate-sepiolite composite and alginate only films.

CONCLUSION

The antibacterial property of composite films was confirmed and it was found that the best antibacterial activity was performed by AgNPs that had a peak of λ= 420 nm according to disc diffusion test. The AgNP solution that was prepared with Minitab to optimized conditions at λ= 420 nm, was used in the sepiolite added particles and then mixed with alginate biopolymer to prepare the composite films. 1.24 % wt. of silver nanoparticles were even enough to obtain 1.5 times better antibacterial activity than medical antibiotic discs. Stability tests in SBF were tested in beads form during 3 days. In terms of shape and appearance these particles are very stable. The dry particles swell nearly over 300% in SBF; whereas, no significant degradation/swelling observed for wet beads after being submerged in SBF solution. This phenomenon could be similar to the "salting out" effect of the electrolytes.

Acknowledgements:

The authors would like to acknowledge the Engineering Research Group of the Scientific and Technological Research Council of Turkey (TUBITAK, Project No. MAG-217M275) for their full financial support.

References

1. Yan, Q., Dong, H., Su, J., Han, J., Song, B., Wei, Q. & Shi, Y. (2018). A Review of 3D Printing Technology for Medical Applications, Engineering, 4(5), 729-742,

2. Chakraborty Banerjee, P., Al-Saadi, S., Choudhary, L., Harandi, S., & Singh, R. (2019). Magnesium Implants: Prospects and Challenges. Materials, 12(1), 136,
3. Li, L.-Y., Cui, L.-Y., Zeng, R.-C., Li, S.-Q., Chen, X.-B., Zheng, Y., & Kannan, M. B. (2018). Advances in functionalized polymer coatings on biodegradable magnesium alloys – A review. Acta Biomaterialia, 79, 23–36,
4. Chen, Z., Li, Z., Li, J., Liu, C., Lao, C., Fu, Y., … He, Y. (2019). 3D printing of ceramics: A review. Journal of the European Ceramic Society, 39(4), 661–687,
5. Cloutier, M., Mantovani, D., & Rosei, F. (2015). Antibacterial Coatings: Challenges, Perspectives, and Opportunities. Trends in Biotechnology, 33(11), 637–652,
6. Liu, J., & Jiang, G. (Eds.). (2016). Silver Nanoparticles In The Environment. Springer-Verlag Berlin An. doi:10.1007/978-3-662-46070-2,
7. Alarcon, E. (Ed.). (2015). Silver Nanoparticle Applications. Springer International Publishing. doi:10.1007/978-3-319-11262-6_7,
8. Luque, R., & Varma, R. S. (Eds.). (2012). Sustainable preparation of metal nanoparticles methods and applications. Cambridge: Royal Society of chemistry,
9. Armentano, I., & Kenny, J. M. (Eds.). (2013). Silver nanoparticles : synthesis, uses and health concerns,
10. Lemić, J., Tomašević-Čanović, M., Djuričić, M., & Stanić, T. (2005). Surface modification of sepiolite with quaternarya mines. Journal of Colloid and Interface Science, 292(1), 11–19,
11. Sabah, E. (1998). Adsorption mechanisms of various amines on sepiolite. Ph.D. thesis. Osmangazi University, Eskişehir, Turkey,
12. Benli, B., & Yalın, C. (2017). The influence of silver and copper ions on the antibacterial activity and local electrical properties of single sepiolite fiber: A conductive atomic force microscopy (C-AFM) study. Applied Clay Science, 146, 449–456,
13. Benli, B., Du, H., & Celik, M. S. (2012). The anisotropic characteristics of natural fibrous sepiolite as revealed by contactangle, surface free energy, AFM and molecular Dynamics simulation. Colloids and Surfaces A: Physicochemical and Engineering Aspects, 408, 22–31,
14. Jalota, S., Bhaduri, B. and Tas, A. C. (2006). "Effect of Carbonate Content and Buffer Type on Calcium Phosphate Formation in SBF Solutions", Journal of Materials Science: Materials in Medicine, 17, 697–707. doi: 10.1007/s10856-006-9680-1.

XIII International Mineral Processing and Recycling Conference
Belgrade, Serbia, 8-10 May 2019

University of Belgrade, Technical Faculty in Bor
Vojske Jugoslavije 12, 19210 Bor, Serbia
Tel. +381 30 424 555 Fax +381 30 421 078

PROCESSING EXPERIMENTS OF FELDSPAR RAW MATERIAL USING COMBINED MAGNETIC AND GRAVITY CONCENTRATING SEPARATIONS

Tomáš Vrbický [1,#], Jiří Botula [2], Richard Přikryl [1]
[1]Charles University in Prague, Faculty of Science, Institute of Geochemistry, Mineralogy and Mineral Resources, Prague, Czech Republic
[2]Technical University of Ostrava, Faculty of Mining and Geology VŠB, Ostrava - Poruba, Czech Republic

ABSTRACT – Feldspar-rich leucogranite formed by metasomatic / hydrothermal alteration of original granite makes one of the key resources of feldspar raw material for ceramic / glass industries in the Czech Republic. Studied material is composed by prevailing albite and quartz accompanied with small amounts of minor / accessory phases (Fe, Mn, Ti-rich phases partly with complex mineralogical binding with Nb-Ta, Li-micas, and apatite). These phases represent the major harmful components which can cause colour changes in final product.
Previous study focused on laboratory and small-scale trials aiming to increase purity of the raw material and to evaluate potential use of by-product(s). By studying various separation techniques, combination of dry magnetic separation and air gravity concentrating table proved to be very effective.
The above mentioned trials lead to the formulation of the feldspar raw material processing flow-chart which has been applied on full-scale in the recent study. By using several tons of input material, magnetic separation followed by air-gravity concentrating table has been applied. The end-products of the separation process were tested for their chemical composition (XRF) and for their properties in ceramic / glass industry (specifically experimental burning and colorimetric measurements). Such an approach allows for realistic evaluation of the beneficiation flow-chart prior to its implementation on the industrial scale of feldspar raw material processing.

Key words: feldspar, by products, magnetic separation, gravity separation

INTRODUCTION

Feldspar-rich leucogranite formed by metasomatic / hydrothermal alteration of its granitic precursors in the Horní Slavkov - Krásno ore district (making part of Slavkov crystalline unit located in the western part of the Bohemian Massif, Czech Republic – Blecha a Štemprok 2012) [1] presents the largest exploited deposit for industrial feldspars in the Czech Republic.

Extracted material is used primarily in local ceramic and/or glass industry, but

corresponding author: t.vrbicky@seznam.cz

substantial portion of production is exported to Poland and Germany.

Figure 1. View on the Krásno open pit quarry from the north

The exploited raw material is composed of prevalent feldspar minerals, specifically albite [2], accompanied with quartz [3]. Minor components are represented by Li-rich micas, being classified as zinnwaldite [4] and apatite [5]. Nb-Ta-rich rutile presents common accessory. Some other rare minerals occurring at this locality were previously acknowledged by mineralogists [6, 7, 8].

Presence of harmful colourants (Nb-Ta-rich rutile, iron oxides/oxyhydroxides, and partly also Li-micas in the case of studied material) is the most restrictive factor influencing final use of exploited feldspar raw material.

To increase the quality of the final product, certain portions of the exploited material with increased content of colourants were processed by using magnetic separation. According to preliminary studies of the authors, the incipient separate (currently classified as waste) contains minerals such as Nb-Ta-rich rutile, Li-micas, and apatite. Although extensive processing leading to separation of colourants is not commonly used in practice, we have made full-scale trials in order to increase purity of the feldspar raw material and to evaluate raw material potential of by-product.

MATERIALS AND METHODS

The experimental study was performed by using FKS 0-5 material, which is the most common standard product of the quarry being crushed to 0/5 mm granulometry. About 150 tons of the material was used for the processing trial which was composed of magnetic separation followed by air-gravity concentrating table.

Particle size distribution of samples was measured by Laser diffraction (Malvern Panalytical). The initial material and the end-products of the separation process were tested for their chemical composition by using XRF and SEM-EDS. For selected samples, content of specific light elements (e.g., of Li) was determined by wet silicate analysis.

RESULTS AND DISCUSSION

Currently, the part of feldspar raw material is processed by dry magnetic separation. Previous experiments have shown that the magnetic separate can be further processed to obtain a mica concentrate (by using high intensity dry magnetic separation) and a heavy mineral concentrate (by air gravity concentration table). Due to small size of minerals grains, the recommended granulometry of processed material is 0.2/0.5 mm. By using air gravity concentration table, it was impossible to it adjust to the material containing substantial amount of grains smaller than 0.2 mm because of the dust. Concerning material with granulometry above 0.5 mm, the separation of colourants from the final product was impossible due to grain size of the rock-forming phases. In such a case, the efficiency of separation method significantly decreases.

In general, the separate from the proposed processing scheme consists of a (1) light fraction and (2) heavy fraction. The preliminary results of the composition of these fractions is as follows:

1) Light fraction - magnetic part: This separate is composed predominantly of Li-rich mica (zinnwaldite) with a LiO_2 content of 2.1 % on average.
2) Heavy fraction: This fraction represents the material obtained as a heavy fraction on air gravity concentration table. It consists mainly of Fe-, Mn-, Ti-, Nb-phases containing Nb_2O_3 up to several percent.

Figure 2. Photograph illustrating two final products after air gravity concentration table (light fraction on the left and heavy fraction on the right)

The Li-rich mica concentrate could be directly utilized for Li enriching. Concerning the case of heavy fraction, further investigation is necessary focusing on finding an economically viable way on how to separate Nb-Ta-rich phases from the accompanying minerals.

CONCLUSION

The combination of magnetic separation and air gravity concentration table proved to be a very effective way on how to separate Nb-Ta-rich phases and Li-mica from processed feldspar raw material represented by hydrothermally altered granites. Due to grain size of constituent minerals, the processing appeared to be most effective for 0.2/0.5 granulometry. Based on the amount of raw material which is exploited and processed annually, up to several tons of separate with economic value can be obtained.

Acknowledgements:

Financial support for the project from the Grant Agency of Charles University in Prague (GAUK 1352218) is gratefully acknowledged.

References

1. Blecha, V., Štemprok, M. (2012): Petrophysical and geochemical characteristics of late Variscan granites in the Karlovy Vary Massif (Czech Republic) – implications for gravity and magnetic interpretation at shallow depths. Journal of Geosciences, 57, 65–85,
2. Nosek, P. (1997): Přehodnocení ložiska Krásno - Vysoký Kámen. Surovina: živcové suroviny. Nepublikovaná zpráva, Gekon, s.r.o., Praha 9. P051561,
3. Jarchovský, T. (2006): The nature and genesis of greisen stocks at Krásno, Slavkovský les - western Bohemia, Czech Republic. Jurnal of the Czech Geological Society, 3-4, c. 51, 201–216,
4. Hron, M., Kottnauer, R. Punčochář, M. (2007): Krásno - ložiskový průzkum 2006, etapa průzkumu: podrobná, číslo úkolu 2700981. závěrečná zpráva. Nepublikovaná zpráva,
5. Pauliš, P. (1990): Autunit z Vysokého kamene (Krásno) u Horního Slavkova. Casopis pro mineralogii a geologii, 35, c. 1, 105–106,
6. Beran, P. (1999): Nerosty cíno-wolframových ložisek Slavkovského lesa. Okresní muzeum a knihovna Sokolov,
7. Sejkora, J., Ondruš, P., Fikar, M., Veselovský, F., Mach, Z., Gabašová, A. (2006b): New data on mineralogy of the Vysoký Kámen deposits near Krásno, Slavkovský les area, Czech Republic. Journal of the Czech Geological Society, 51, c. 1-2, 43–55,
8. Pauliš, P., Ludvík, J., Pour, O., Malíková, R. (2014): Hollandit z Vysokého Kamene u Krásna. Minerál, 6, c. 22, 530–532.

XIII International Mineral Processing and Recycling Conference
Belgrade, Serbia, 8-10 May 2019

University of Belgrade, Technical Faculty in Bor
Vojske Jugoslavije 12, 19210 Bor, Serbia
Tel. +381 30 424 555 Fax +381 30 421 078

ECO-TECHNOLOGY FOR COMPLEX PROCESSING OF ORES AND INDUSTRIAL WASTE

Yrii Chugunov, Vladyslav Ivanchenko #
National Academy of Sciences of Ukraine, Ukraine

ABSTRACT – Traditional methods of ore dressing extract useful minerals from ores, and nonmetallic minerals are sent to waste. High humidity, residual amounts of flotation reagents, other chemicals and mixed mineral composition of the waste make it difficult to further enrich and use. The authors have developed and tested an innovative technology and equipment for the processing of mineral raw materials by the vortex air-mineral flow. A gradient of density, magnetic and electrostatic properties, differences in morphology, internal structure, hardness of mineral individuals and strength of aggregates were used. Simultaneously during ore preparation process selective destruction of intergrowths was performed and electrostatic charges were removed from the surface of the particles. The morphology and the internal structure of grains were transformed purposefully. Separation was carried out in narrow granulometric classes. During the processing of ores several (3-4 or more) useful products were produced. Samples of modern building materials were made from dry waste, cleared from ore minerals. Various ferrous, non-ferrous, noble and rare metalsores, as well as solid industrial waste were processed by using this technology and equipment. Water, flotation reagents and other chemicals for separation were not used. There was also no enrichment waste. The works were carried out according to the requirements of occupational health and environmental protection. Taking into account these factors, the proposed technical solutions are attributed to eco-technologies.

Key words: dry separation, vortex air-mineral flow, complex processing, ecology.

INTRODUCTION

Currently, there is a tendency to replace traditional enrichment methods with complex ores processing without accumulation of waste [1, 4, 5]. The principal difference between new technologies is: a) the production and transfer to consumers of several market products; c) the complete absence of waste; c) integration of all technological operations in one cycle; d) it is assumed that the product of the previous stage is technologically coordinated with the subsequent stage of processing. Thus, it is possible to increase the profitability of production, the negative impact on the environment is reduced and many social issues are resolved. This paper presents an innovative technology of waste-free processing of mineral raw materials, developed and tested in the National Academy of Sciences of Ukraine.

corresponding author: vvivanchenko@ukr.net

It is based on the achievements of solid state physics and nanomineralogy. The processes are implemented in a vortex air-mineral flowand are accompanied by a profound transformation of the morphology and properties of the mineral particles of the processed raw materials.

MATERIALS AND METHODS

For more than 10 years, the authors studied ores of ferrous, non-ferrous, rare and precious metals from Ghana, Bulgaria, Bolivia, Kazakhstan, Peru, Philippines, Russia, Ukraine, slags from ferrous and non-ferrous metallurgy, incineration plants, electronic scrap and other industrial wastes. In total more than 100 samples weighing from 10 to 50 kg are processed. Laboratory studies were aimed at developing, as far as possible, a universal technology for the processing of mineral raw materials without producing enrichment waste. The stage ended with the development of a technology for the complex processing of natural and technogenic raw materials in a vortex air-mineral flow and the creation of a laboratory unit for its implementation [2, 3].

The equipment includes a rotor mill, an air cyclone, a set of dust precipitation chambers, a bag filter, an exhaust fan and a control unit. The device has a loading unit for the supply of material and air and 12 unloading units. Additionally, magnetic and gravity air separators are used. Most of the installation is designed and manufactured by the authors themselves.

RESULTS

The processing of mineral raw materials is carried out as follows (Fig. 1). Ore or industrial waste is loaded into the rotor mill through the loading unit along with air. The air flow is created by an exhaust fan and additionally rotor blades. The destruction of the material occurs under the impact of the rotor blades, as well as due to the collisions of pieces between themselves and the mill armor. The dust with the air flow is carried out through the cyclone and dust precipitation chambers and accumulates in the bag filter. As the pieces break down and ore minerals are released from intergrowths, nonmetallic minerals are removed from the working chamber and are precipitated in a cyclone and dust precipitation chambers, followed by unloading materials into several storage hoppers. Metals and ore minerals are moved to the lower part of the working chamber of the rotor mill and unloaded into a separate drive.

At the next stage, the material from each hoppers is subjected to separation (if necessary) in an electrostatic, magnetic or gravitational field, depending on the mineral composition of the natural ore or industrial waste.

THE DISCUSSION OF THE RESULTS

Permanent removal of dust from the working chamber ensures the removal of electrostatic charges from the surface of metal particles, ore and minerals.

In turn, this significantly increases the separation efficiency of the granular material in the physical fields of all types.

The destruction and self-destruction of pieces of the ore and industrial waste

occurs due to numerous short but very dynamic bangs. This leads to the formation of isometric particles. Microscopic and electron microscopic studies of ground material indicate that the isometric shape of particles is maintained in all size classes, up to several microns. The cubic isometric shape of the grains has a positive effect on the separation results.

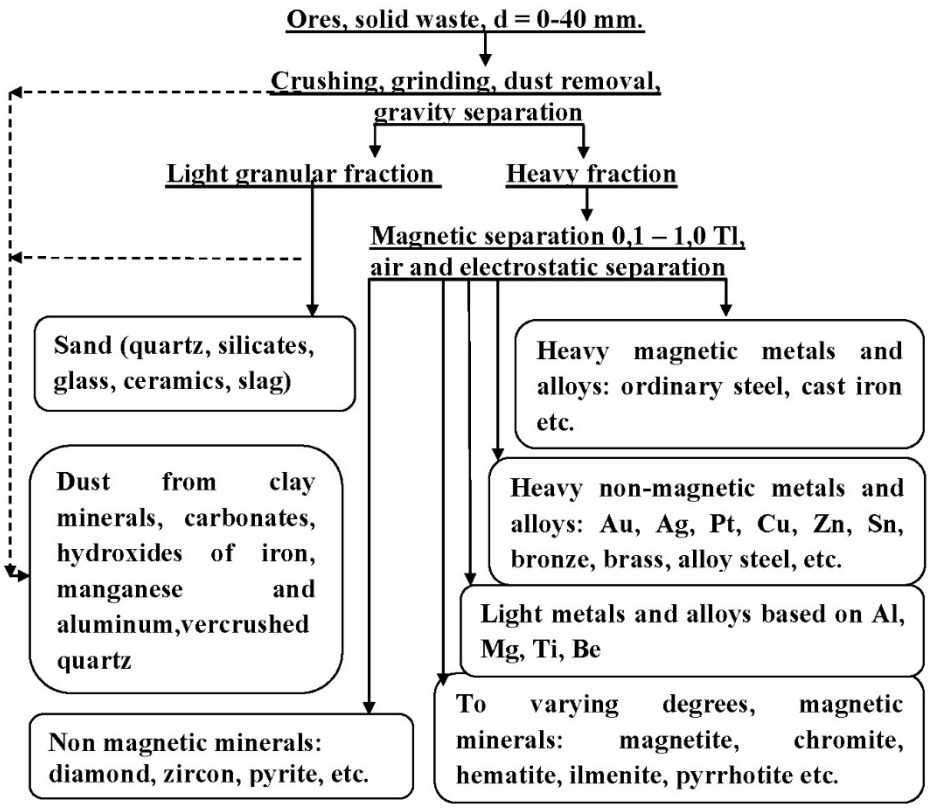

Figure 1. Scheme of complex processing of ores and solid industrial wastes in a vortex air-mineral flow

Circular motion in the vortex air-mineral flow of the working chamber of the mill leads to the transformation of malleable metal particles of various shapes into rounded spherical grains. At the same time, metals are cleaned from inclusions of nonmetallic minerals and slag, compacted and effectively divided into separate products. This additional factor is important for the extraction of metals from ores and slags.

CONCENTRATES AND OTHER PROCESSED PRODUCTS

The authors used the above technology for the integrated processing of various industrial waste and natural ores. As a result, products with a metal content ranging from 30 % (gold) to 95-98 % (ferrous and non-ferrous metals, bronze, brass and

other alloys) are produced (Fig. 2). In ash and slag waste of incineration plants and electronic scrap there are compounds of parts and agglomerates consisting of ferrous, non-ferrous, precious and rare metals. In order to avoid the loss of valuable metals, complex polymetallic products were produced from this raw material for their further separation in chemical-metallurgical processes (Fig. 2d).

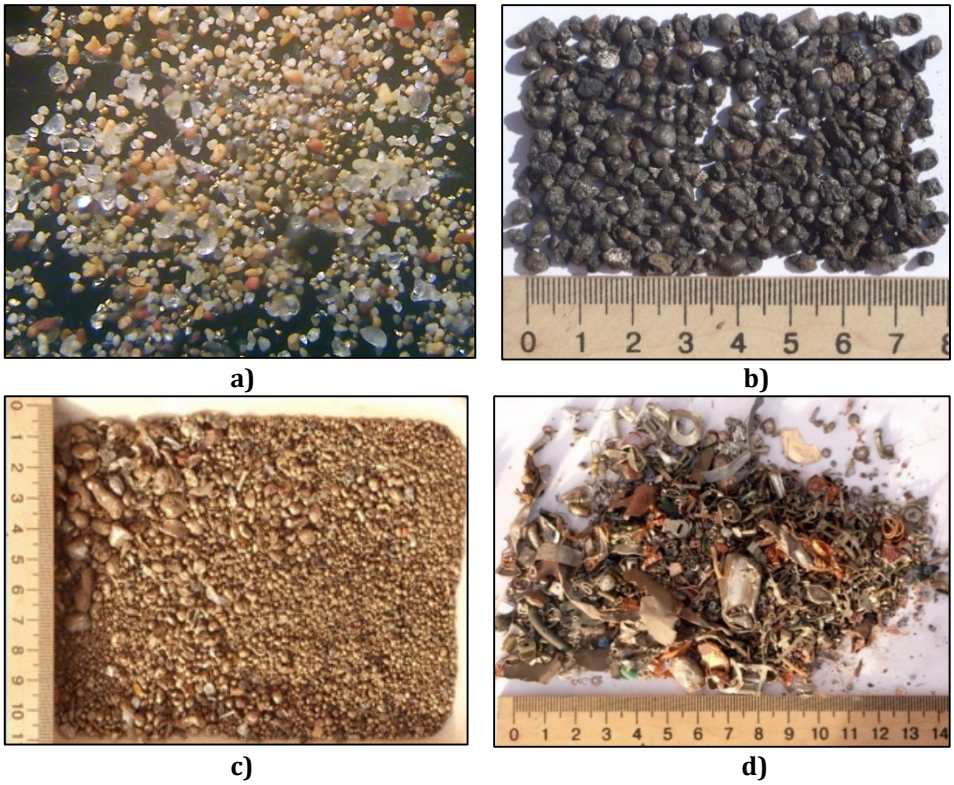

Figure 2. Extracted metals: **a)** - gold from natural ores (microscope, magnification 80^{X}); **b)** - steel from slags of ferrous metallurgy; **c)** - bronze from slags of nonferrous metallurgy; **d)** - ferrous, non-ferrous and precious metals from electronic scrap

High quality is also characteristic of concentrates: magnetite and goethite-hematite (Fig. 3), manganese, ilmenite, rutile garnet and others.

The metals content in the remaining fine-grained mass does not exceed the accepted norms. This allows to use them in construction and other areas (Fig. 4a-4c). Positive results were also obtained when cleaning coal (Fig. 4d) and iron ore from ballast and harmful impurities (Si, Al, Na, K, S, P). All products are produced without incineration (electronic scrap), without flotation and chemical reagents and without the participation of water.

a) **b)**

Figure 3. Produced concentrates: **a)** - magnetite from the tailings of magnetite quartzite; **b)** - hematite from dump oxidized ferruginous quartzites

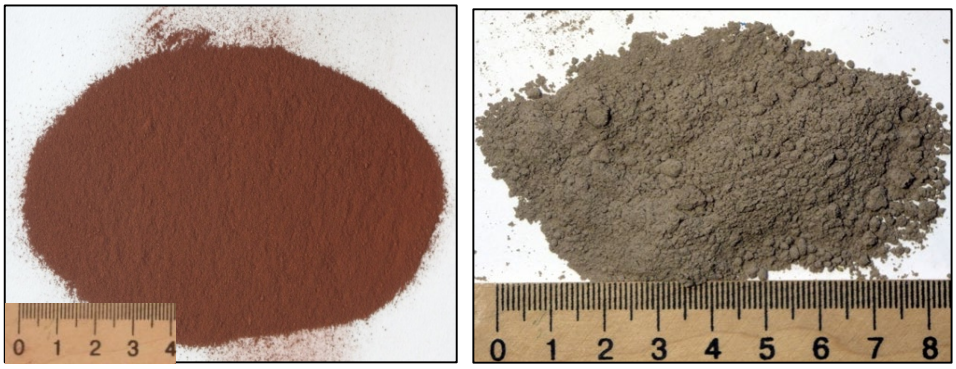

a) **b)**

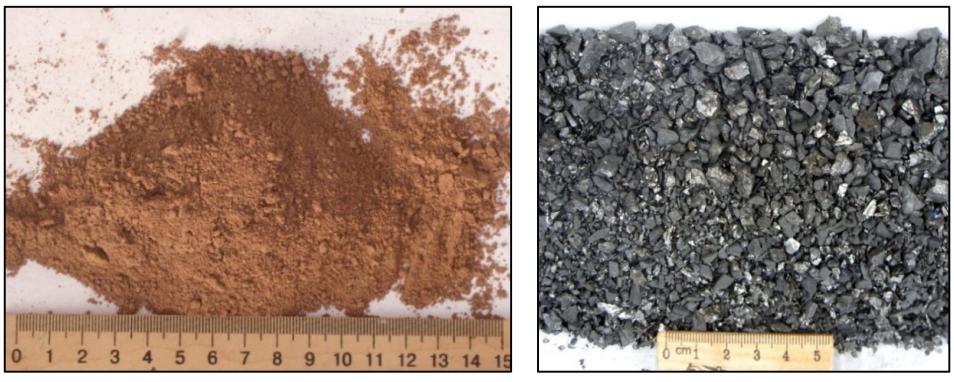

c) **d)**

Figure 4. Non-metallic materials produced from industrial waste: **a)** - dry paint from hematite quartzite; **b)** - raw materials for the manufacture of cement from scrubbed slags from waste incineration plants; **c)** - fine-grained textolite from electronic scrap, separated from metals; **d)** - cleaned from ash coal

CONCLUSION

Wasteless processing of natural and man-made ores in a vortex air-mineral flow is an alternative to many mineral processing technologies, especially “wet”.

Preliminary removal of electrostatic charges from the surface of particles, purposeful transformation of the morphology and internal structure of metals, ores and nonmetallic grains provide effective subsequent separation in both water and air. However, air separation has many technological, economic and environmental benefits.

The authors will be grateful for the opportunity to test new types of ores and solid industrial waste for waste-free processing using the proposed innovative technology.

References

1. Bajare, D., Bumanis, G., Korjakins, A. (2014) New porous material made from industrial and municipal waste for building application. Materials Science (Medžiagotyra) 20 (3), 1392-1320,
2. Chugunov, Y., Ivanchenko, V. (2015) Technology for enrichment and reprocessing of slag waste incineration plants. Proceedings of the XVI Balkan Mineral Processing Congress. Mining Institute Belgrade, Academy of Engineering Sciences of Serbia, University of Belgrade, Belgrade, Serbia, Volume 2, 859-860,
3. Ivanchenko, V., Chugunov, Y., Ivanchenko, A. (2015) Mineralogy and dry concentration of the ores of hematite and goethite. Proceedings of the XVI Balkan Mineral Processing Congress. Mining Institute Belgrade, Academy of Engineering Sciences of Serbia, University of Belgrade, Belgrade, Serbia, Volume 1, 219-222,
4. Lottermoser, B. (2010) Mine Wastes: Characterization, Treatment and Environmental Impacts. Springer, Verlag Berlin Heidelberg, 400.

XIII International Mineral Processing and Recycling Conference
Belgrade, Serbia, 8-10 May 2019

University of Belgrade, Technical Faculty in Bor
Vojske Jugoslavije 12, 19210 Bor, Serbia
Tel. +381 30 424 555 Fax +381 30 421 078

PROCESSING OF CHROMITE PLANT TAILINGS

Symbat Dyussenova #, Bagdaulet Kenzhaliyev, Rinat Abdulvaliyev, Sergey Gladyshev
Satbayev University, Institute of Metallurgy and Ore Beneficiation, JSC, Kazakhstan

ABSTRACT – At present, the importance of solving the problem of involving in the processing of tailings of enrichment of chromite-containing ores is connected not only with ecology, but also with the need to increase chromium production. Modern gravity enrichment technologies make it possible to efficiently produce chromium concentrates from large and medium fractions of chromite-containing ores, while finely divided sludge is practically not enriched due to the difficulty of separating complex minerals into concentrates and waste rock. This paper presents the results of studies on the gravity processing of tailings. The technology includes the enrichment of the fine fraction - 0.2 +0 mm of tailings of the dressing plant of chromite-containing ores by gravity methods using a KNELSON centrifugal separator. In technology, the efficiency of the operation of gravity enrichment is provided by the preliminary activation of the fine fraction in a solution of sodium bicarbonate ($NaHCO_3$). With gravitational enrichment, a total chromite concentrate was obtained containing 51.3 % Cr_2O_3. The output of concentrate was 41.7 %. Extraction of Cr2O3 in the concentrate was 68.1 %.

Key words: chromite-containing ore, gravity concentration, tailings, concentrate

INTRODUCTION

The importance of solving the problem of involving in processing tailings is connected not only with the environment but also the need to increase the production of chromium [1-3]. Modern gravity separation technology can effectively get chrome concentrates large and medium fractions of chromium ores and fine sludge is hardly enriched because of the difficulty of separation of complex minerals concentrates and waste rock [5].

MATERIAL AND METHODS OF WORK

Technology for processing tailings chrome ore includes benefication of the fine fraction - 0.2 + 0 mm of the beneficiation plant tailings by gravity methods using a KNELSON centrifugal separator.

corresponding author: dusenova_s@mail.ru

Table 1 and 2 show the chemical and phase composition of the original sample.

Table 1. Chemical analysis of tailings

Element	Content %	Element	Content %
Cr_2O_3	25.47	Cu	0.008
Fe_2O_3	9.1	Pb	0.05
SiO_2	21.53	As	0.025
Al_2O_3	1.51	Sb	0.23
H_2O	7.8	K	0.05
CaO	0.75	Na	0.05
MgO	29.4	P	0.008
MnO_2	0.053	C	< 0.2
S	0.1	Ag, г/т	< 2.0
Zn	0.1	Au, г/т	< 0.05
Co	0.02	Ni	0.28

Table 2. X-ray phase analysis of tailings

Phase name	Formula according to PDFII2012 database	The content of the phase %
Antigorite	$Mg_3Si_2O_5(OH)_4$	41.8
Clinochrysotile	$Mg_3Si_2O_5(OH)_4$	5.1
Lizardite-1T	$(Mg,Al)_3(Si,Fe)_2O_5)(OH)_4$	12.5
Aluminum Ferrous magnesite	$MgAl_6Fe_{1.4}O_4$	8.7
Chromite	$(Fe_{0.52}Mg_{0.48})Cr_{0.72}(Al_{0.28})O_4$	15.3
Clinohlore	$Mg_6Si_4O_{10}(OH)_8$	5.6
Aluminum Magnesium Silicate	$Ca_{23.20}Mg_{22.4}(Al_{92}Si_{100}O_{384})$	11.0

RESULTS AND DISCUSSION

Before gravitational enrichment, a preliminary chemical activation of the tailings was carried out in a solution containing 120 g / dm^3 of $NaHCO_3$ at temperatures of 100 - 240 °C, duration 90 minutes, and the ratio L: S = 10.0 [6, 7].

Analysis of the resulting sludge activation showed (Figure 1) that the chemical composition of the samples varies slightly, but, as follows from X-ray phase analysis, their phase composition changes (Figure 2).

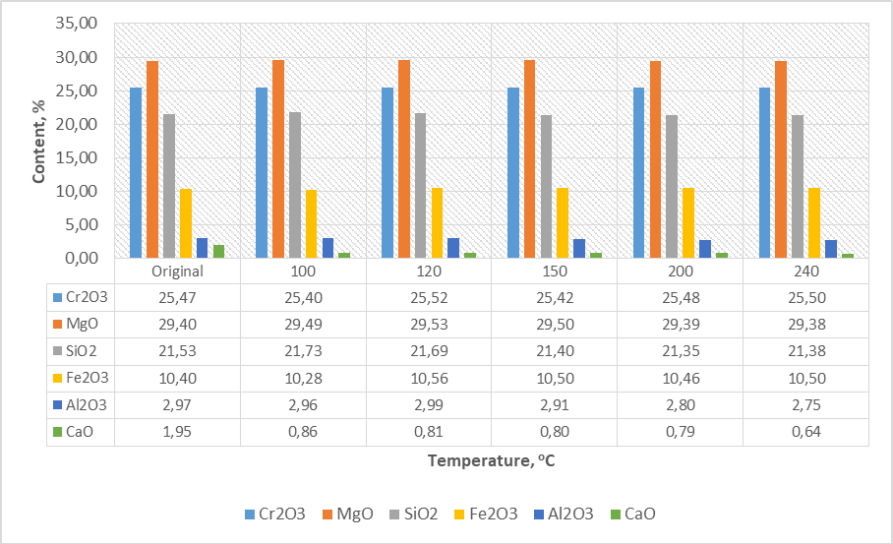

	Original	100	120	150	200	240
Cr2O3	25,47	25,40	25,52	25,42	25,48	25,50
MgO	29,40	29,49	29,53	29,50	29,39	29,38
SiO2	21,53	21,73	21,69	21,40	21,35	21,38
Fe2O3	10,40	10,28	10,56	10,50	10,46	10,50
Al2O3	2,97	2,96	2,99	2,91	2,80	2,75
CaO	1,95	0,86	0,81	0,80	0,79	0,64

Figure 1. The chemical composition of the sludge after activation at a temperature of from 100 to 240 °C

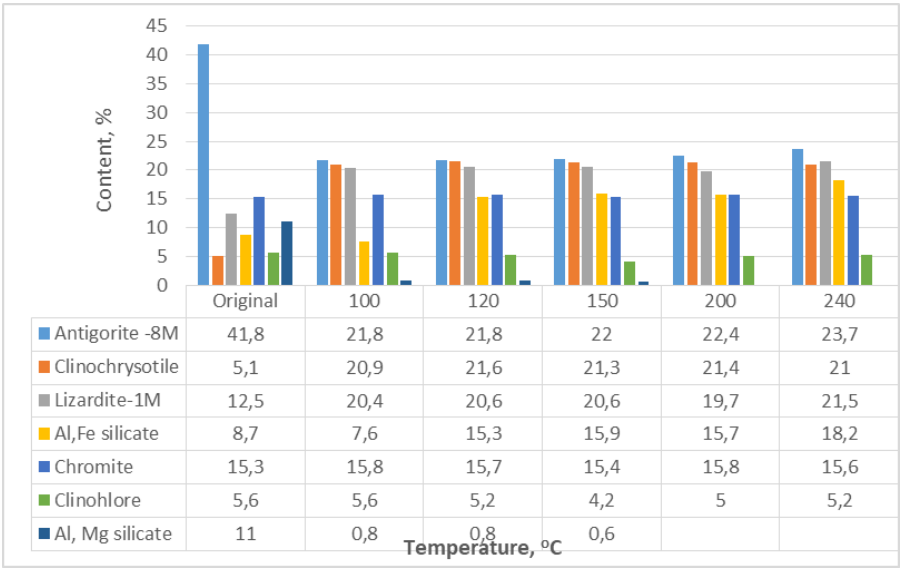

	Original	100	120	150	200	240
Antigorite -8M	41,8	21,8	21,8	22	22,4	23,7
Clinochrysotile	5,1	20,9	21,6	21,3	21,4	21
Lizardite-1M	12,5	20,4	20,6	20,6	19,7	21,5
Al,Fe silicate	8,7	7,6	15,3	15,9	15,7	18,2
Chromite	15,3	15,8	15,7	15,4	15,8	15,6
Clinohlore	5,6	5,6	5,2	4,2	5	5,2
Al, Mg silicate	11	0,8	0,8	0,6		

Figure 2. The phase composition of the sludge after activation at a temperature of from 100 to 240 °C

Analysis of the dependence of the phase composition of the sludge on the

activation temperature shows that at a temperature of 120 °C, almost all the main changes are over.

After pre-activation, at 120 °C, the sludge was sent to gravity concentration (Figure 3).

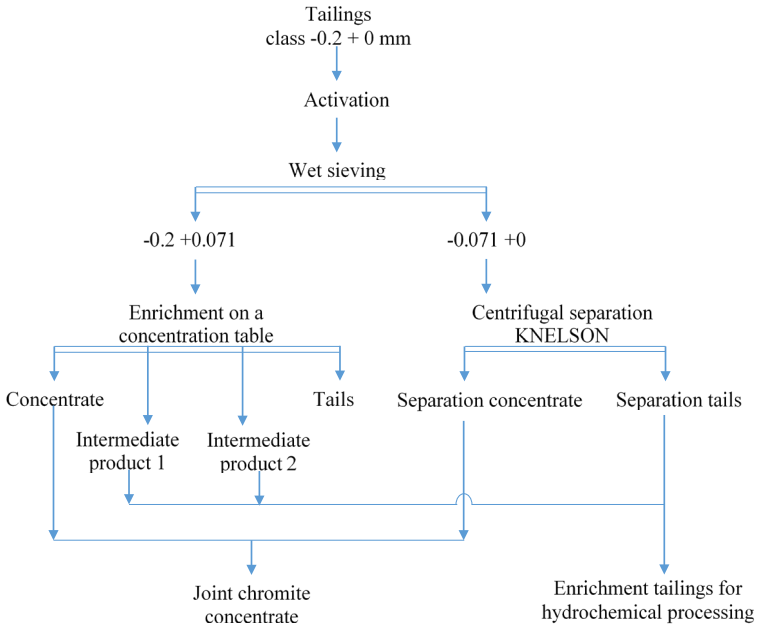

Figure 3. Scheme of gravity concentration

As a result of concentration of sludge class -0.2 +0.071 mm, a concentrate with a Cr_2O_3 content of 52.33 % was obtained at a concentration table (table 3).

Table 3. The results of the concentration of sludge after activation on the concentration table

Name	Output, %	Content of Cr_2O_3, %	Extraction of Cr_2O_3, %
Concentrate	26.42	52.33	68.51
Intermediate product 1	58.11	9.07	26.14
Intermediate product 2	8.36	5.83	2.42
Tails	7.11	8.33	2.93
Total:	100.0	20.17	100.0

The results of the concentration of sludge class -0.071 +0 mm on a KNELSON centrifugal separator are shown in table 4.

Table 4. The results of the concentration of sludge after activation on a centrifugal separator KNELSON

Name	Output, %	Content of Cr_2O_3, %	Extraction of Cr_2O_3,%
Separation concentrate	41.3	51.22	63.15
Separation tails	58.7	21.03	36.85
Total:	100.0	33.49	100.0

From classes -0.2 + 0.071 mm and -0.071 + 0 mm was obtained the combined concentrate with a Cr_2O_3 content of 51.3 % with a yield of 41.7 %. Extraction of Cr_2O_3 in the combined concentrate was 68.1 %.

References

1. Ryabin V.A., Popilsky M.Ya., Soloshenko A.A. 1997. Modern technologies of chrome ore processing, neutralization and utilization of toxic waste // Abstracts of reports. Int. scientific tech. conf. on rer. technog. formations. - pp. 59-61. – Ekaterinburg, Russia,
2. Garkunova N.V., Plyshevsky Yu.S. 2003. Use of industrial wastes containing olevin-serpentine rocks for the production of magnesium compounds // Proc. Int. ex. conf. “Uralecology - Technogen-2003”. – 320 p. – Ekaterinburg, Russia,
3. Leontiev, L.I., Sheshukov, O.Yu., Nekrasov, I.V. 2014. Analysis of the processing and use of industrial wastes of metallurgical production // Complex use of mineral raw materials. - № 4. - pp. 8-25. – Almaty, Kazakhstan,
4. Analysis of the global chrome market. [Electronic resource]. URL:http://www.metalresearch.ru/world_chromium_analysis.html,
5. Semidalov S.Yu., Nevsky Yu.N., Bushueva N.Yu., Sergeev G.I., Melnichenko A.F., Rogov V.M. 1999. A method of enrichment of chrome-containing waste ferroalloy production / publ. 10.09.99, Byul. - №4. Patent 2136376. – Russia,
6. Abdulvaliyev R.A., Abdykirova G.Zh., Dyussenova S.B., Imangalieva L.M. 2017. Enrichment of chromite-containing sludges // Enrichment of ores. - № 6. - pp. 27-31. – Saint-Peterburg, Russia,
7. Gladyshev, S.V., Abdulvaliev, R.A., Kenzhaliev, B.K., Dyusenova, S.B., Imangaliyeva, L.M. 2018. Getting chromite concentrate from tailings // Complex use of mineral raw materials - №1. - pp. 12 - 17. – Almaty, Kazakhstan.

XIII International Mineral Processing and Recycling Conference
Belgrade, Serbia, 8-10 May 2019

University of Belgrade, Technical Faculty in Bor
Vojske Jugoslavije 12, 19210 Bor, Serbia
Tel. +381 30 424 555 Fax +381 30 421 078

OPTIMIZATION OF THE PROCESS OF ELECTROCHEMICAL OXIDATION OF CERIUM IN THE PROCESSING OF RARE METALS RAW MATERIALS

O. V. Yurasova [1], T. A. Kharlamova [2,#], A. A. Gasanov [1], A. F. Alaferdov [2]
[1]State Research and Design Institute of the rare metal industry (JSC Giredmet), Moscow, Russia
[2]National University of Science and Technology "MISiS" (NUST MISIS), Moscow, Russia

ABSTRACT – The Russian rare earth raw metals (REM) are complex materials to contain up to 57% of cerium in the total amount of lanthanides. Authors recommended to separate cerium at the first stages of rare earth concentrate treatment by combined methods of electrochemical oxidation and liquid extraction. The process has been suggested to optimize by using up-to-date equipment, including a diaphragm-type electrolyzer of OXITRON-58L-O2 type. Investigations have been performed over process solutions prepared out of Solikamsk Magnesium Plant concentrates extracted out of loparite. Conditions have been created to achieve oxidation level $Ce^{+3} \geq 99\%$ in terms of electric power consumption less than 0.8 kW/h per 1 kg of CeO_2.

Key words: rare-earth materials; cerium (III) and (IV); oxidation; electrolysis; electrolyzer; extraction

INTRODUCTION

Today, it is difficult to find innovation technology that does not use REE as components of application, e.g. development of superconducting materials, special alloys, super magnets, accumulators, catalysts and etc. After the USSR dissolution, Russia lost leadership in the production of rare earth metals (REM), and majority of plants and feedstock sources of REM appeared to be outside Russia. Today, the world REM market is dominated by China which possesses sufficiently rich and easy transformable feedstock of REM. This enables China to fix metal prices and terms of sale.

Nowadays in Russia, under support of the Russian Government the industrial production of REM is revived. Note that mineral feedstock and technogenic waste has been reputed to be a source of REM. Approximate compositions of rare earth concentrates (REC) and ores for industrial processing are presented in Table 1.

Each source of REM is unique by its composition (REM and impurities content)

corresponding author: 9168787573@mail.ru

and structure. Specific feature of domestic feedstock of REM is the predominant content of cerium in it - up to 57% of total amount of rare earth metals. Therefore, in the traditional technological scheme of rare-earth metals production the extraction of cerium from other lanthanides makes up the first stage. The process is based on cerium oxidation in the tetravalent state by chemical (oxidation by O_2, ozone, potassium permanganate or hydrogen peroxide) or electrochemical method with subsequent cerium separation from rare earth metals by precipitation, ion exchange or extraction method.

The work analyzes factors capable of optimizing the process of electrooxidation cerium through the use of diaphragm-type electrolyzer. Technological parameters and optimal conditions of process have been studied.

Table 1. Approximate compositions of REC and ores which are promising for development of industrial processing in Russia

REE composition in ore% mass.	Loparite	Apatite	Phosphogypsum	Eudialyte	Tomtor ore
	32.4	0.98	0.52	2.0	13.67
Ln_2O_3			$\sum Ln_2O_3$ – 100% in concentrate		
La_2O_3	21.11	27.2	20.86	9.8	23.31
CeO_2	57.72	43.55	46.75	26.0	42.68
Pr_6O_{11}	5.36	5.8	5.15	4.0	4.14
Nd_2O_3	14.4	14.3	17.31	12.0	16.72
Sm_2O_3	0.89	1.9	2.38	4.2	2.46
Eu_2O_3	0.18	0.5	0.63	0.6	0.79
Gd_2O_3	0.15	1.8	1.80	4.2	1.67
Tb_4O_7	0.02	0.2	0.07	0.6	–
Dy_2O_3	0,11	0.7	0.96	3.3	0.83
Ho_2O_3	0.02	–	0,14	0.6	0.15
Er_2O_3	–	0.15	0.27	2.5	0.57
Tm_2O_3	–	–	–	0.4	0.06
Yb_2O_3	–	–	0.10	1.8	0.24
Lu_2O_3	–	–	–	0.3	–
Y_2O_3	0.023	3.9	3.56	30.0	6.37

EXPERIMENTAL

Studies have been pursued on a model and afterwards in technological nitrate solutions prepared out of rare earth concentrate of Solikamsk Magnesium Plant. Rare earth concentrate was prepared out of loparite concentrate containing 293.6 to 345.5 g/l of rare earth oxide (REO). The composition of the prepared rare earth concentrate is shown in Table 2.

Model solutions were prepared by dissolution of CeO_2 in the nitric acid to contain 50-100 g/l of HNO_3 and 140-160 g/l of Ce_2O_3. In turn, rare earth element solutions were prepared by dissolution of carbonates in the nitric acid. Note that REE ions in solutions were determined by titration method with complexing agent EDTA in the presence of indicator. Cerium ions were detected by titration using mohr's salt and potassium permanganate solution.

Composition study of aqueous and solid phases has been carried out by inductively coupled plasma atomic emission spectrometry with the help of ICAP 6300 JY-38 spectrometer (Thermo Fisher Scientific) and roentgen-fluorescent method by means of ARL OPTIM'Xspectrometer (Thermo Fisher Scientific) according to standardized procedures as set forth in "Giredmet".

Table 2. Composition of prepared rare earth concentrate

Compound	Composition, mass %
La_2O_3	26.1
CeO_2	54.2
Pr_6O_{11}	5.0
Nd_2O_3	13.0
Sm_2O_3	0.97
CaO	0.06
SrO	0.04
Fe_2O_3	0.001
SiO_2	0.02
Cl	0.05

Required concentration of acid in aqueous phase was maintained by adding HNO_3. Acid concentration was measured by volume or potentiometric titration.

Coulomb efficiency *BT* was calculated according to the following equation:

$$BT = (\frac{Q_{exp}}{Q_t}) * 100\% \quad (1)$$

where Q_{exp} and Q_t are electrical charges (A∗ h) consumed in oxidation process, defined experimentally and calculated by Faraday's laws of electrolysis, correspondingly. Values of electrical charges were determined according to equations below:

$$Q_t = C_{Ce^{4+}} * \frac{V}{q} \quad (2)$$

where $C_{Ce^{4+}}$ is current concentration of Ce^{+4} (g/l); V is a volume of treated solution (l); q = 5.224 (g – eqv / A∗h) is electrochemical equivalent; t – time (h).

$$Q_{exp} = I * t \quad (3)$$

where I is current supplied to electrochemical reactor (A), t – time (h).

Degree of cerium oxidation was calculated according to the following equation:

$$\alpha = \left(\frac{C_{Ce^{4+}}}{C_{Ce_0}}\right) * 100\% \quad (4)$$

where C_{Ce_0} is total concentration of cerium in the processed solution (g/l).

Studies were conducted in way of electrochemical oxidation of cerium (III).

RESULTS AND DISCUSSION

Membrane and diaphragm-type electrolyzers have been considered [5–8] to conduct experiments on electrochemical oxidation of cerium. It should be noted that the diaphragm material is resistant to high temperatures, easily regenerated, adjustable and has no limitations on current density, a diaphragm-type electrolyzer OXITRON-58L-O2 was chosen [9]. The diaphragm-type electrolyzer is manufactured in LLC "Delfin Aqua" and applied for electrochemical synthesis of strong oxidizers. Electrochemical setup is shown in Fig. 1. A main part of laboratory setup is an electrochemical reactor MB-26-21-15K shown in Fig. 2.

Figure 1. Laboratory electrochemical setup

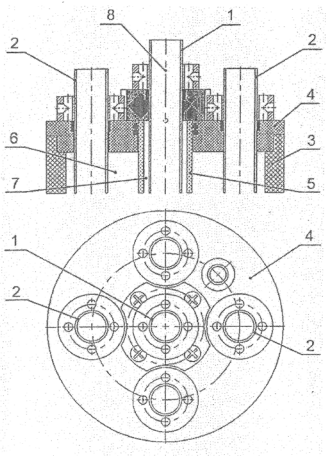

Figure 2. Electrochemical reactor MB-26-21-15K: 1 – cathode, 2 – anode, 3 – reactor vessel, 4 – plug, 5 – diaphragm, 6 – anode chamber, 7 – cathode chamber, 8 – perfs

Note that a reactor vessel consists of 4 platinizing titanic anodes and 1 titanic cathode of cylindrical shape while electrode spaces are divided by ceramic diaphragm made of aluminum oxide and zirconium. Two types of circulation are provided in the reactor vessel: external/ internal circulation for anolyte and external one for catholyte.

External circulation rate is 30 l/h and the internal one is 100 l/h. Hydrodynamics in reactor provides the mixing of electrolyte in the whole volume of anode space of reactor and gives equiprobable access of electro-oxidized reagent to the total anode surface. Therefore, in the whole volume of anode space of reactor the same constant concentration of oxidizable cerium is settled. A pressure regulator mounted on the reactor vessel makes it possible to regulate pressures in electrode chambers. Technical features of setup are shown in Table 3.

Technological process of electrochemical cerium oxidation initially has been analyzed in model solutions which contained 136 to 150 g/l of Ce^{+3} and 50 to 120 g/l of HNO_3. As a catholyte, aqueous solutions of nitric acid and cerium nitrate are considered. After determination of optimal modes of electrolyzer operation on model solutions the further investigations were conducted in technological solutions of REM concentrates. For this purpose, cathode and anode chambers of reactor were pumped with technological solutions. Then, electrolyte external circulation and anolyte internal circulation preheated up to 50°C was switched on in such a way that circulation rate of anolyte proved to be higher 3 times as compared to the circulation rate of catholyte.

The use of pressure regulator made it possible to create a positive pressure of 0.3 atm in the cathode chamber. After that, current was supplied and electrolysis conducted at the constant current density. While in catholyte, a certain quantity of nitric acid was added at regular intervals (~15 min) to maintain its concentration at 50-70 g/l. After completion of operating cycle, the current supply was suspended, pumps switched off and drain valves open to sample catholyte and anolyte for further analytical control.

Table 3. Technical features of OXITRON-58L-O2 setup

Parameter	Units of measurement	Value
Feed rate of solution	l/h	
- in cathode chamber		10–40
- in anode chamber		10–40
Electrode potential in reactor	V	3–30
Strength of current in reactor	A	3–30
Pressure	MPa	
- in cathode chamber		0–1.0
- in anode chamber		0–1.0
Mass of setup	Kg	50
Dimensions (height×width×depth)	Mm	890×480×500
Maximal time of operating mode stabilization	Min	15

Studies have been carried out in technological solutions to show the possibility of achieving high degree of oxidation Ce^{+3} (≥ 99 %) at power consumption less than 0.8 kW·h per 1 kg of CeO_2. Kinetics of oxidation process in salt concentrates with ∑REM and Ce_2O_3 ~ 53 % content is given in Table 4.

Mass balance of Ce^{+3} oxidation process at certain operating mode of electrolyzer is shown in Table 5.

Table 4. CeO_2 concentration vs. electrolysis time

Time, hours	Concentration, g/l	
	CeO_2	HNO_3
1	35.5	66.88
2	63.6	69.98
3	95.1	63.6
4	123.1	56.4
5	142.3	59.9
6	151.1	62.1
7	155.1	66.8
8	155.9	62.4

Note: average indicator BT=76.4%, current density is 2.3 A/dm², electrolyze time – 8 hours.

Table 5. Mass balance of electrolysis process

Anolyte	∑REE, g/l	Ce^{+3} concentration, g/l	Ce^{+4} concentration, g/l	Cerium mass, g
Before electrolysis	300	159.0	0	477
After electrolysis	300	0.5	158.5	477

Table 5 shows that the level of Ce^{+3} oxidation consists of 99.68%. Further extraction and purification of oxidized cerium from REM solutions were conducted by means of extraction techniques.

CONCLUSION

Analysis of the results of ceric electrochemical oxidation in the MB-26-21-15K electrochemical reactor showed that the proposed design of the electrolyzer is quite promising from the point of view of industrial application. Despite the complex multicomponent composition of the feedstock, the proposed design of the electrolyzer provides a degree of cerium extraction> 99% with an energy consumption of not more than 0.8 kWh / kg CeO2 and can be used in the technology for extracting cerium based on a combination of electrochemical and extraction methods for REM- processing of various cerium-containing raw materials.

References

1. Mikhailichenko, A.I., Mikhlin, E.B. (1987) Rare earth metals. Metallurgiya, 232,
2. Korovin, S.S., Zimina, G.V. Reznik, A.M., Bukin, V.I., Korkushko, V.F. (1996) Rare and Disseminated Elements. Chemistry and Technology, 1, 376,

3. Lokshin, E.P., Sedneva, T.A., Kalinnikov, V.T. (2008) The method of producing cerium dioxide, Russian Patent, Appl. 2341459,
4. Morais, C.A., Benedetto, J.S., Ciminelli, V.S.T. (2003) Recovery of cerium by oxidation/hydrolysis with $KMnO_4$–Na_2CO_3. Proceedings of the 5th International Symposium "Honoring Professor Ian M. Ritchie. TMS", Vancouver, 1773,
5. Sedneva, T.A., Tikhomirova, I.A. (2002) The oxidation of cerium in the membrane electrolyzer. Apatity: ICTREMRM KSC RAS, 1-11,
6. Ayers, A., Cormak, A., Gray, J., Schneider, A., (1973) Apparatus for electrolytic oxidation or reduction, concentration, and separation of elements in solution, USA Patent, Appl. 3.770.612,
7. Pozdeev, S.S., Kondrat'eva, E.S., Gubin, A.F., Kolesnikov, V.A. (2014) Electrooxidation of ions cerium (III) in an electrolytic cell of the membrane type. Uspekhi v khimii i khim. Tekhnologii, 8(5), 98-100,
8. Gasanov, A.A., Yurasova, O.V., Kharlamova, T.A., Alaverdov, A.F. (2015) Construction of electrolyzers for oxidation of cerium. Non-ferrous metals, 8, 50-54,
9. Petrovsky, T.G., Bakhir, V.M., Kharlamova,T.A. (2015) Electrolytic cell for carrying out electrochemical redox processes of liquid mediums containing metals of variable valency, Russian Patent for useful model, Appl. 161511,

XIII International Mineral Processing and Recycling Conference
Belgrade, Serbia, 8-10 May 2019

University of Belgrade, Technical Faculty in Bor
Vojske Jugoslavije 12, 19210 Bor, Serbia
Tel. +381 30 424 555 Fax +381 30 421 078

THE ALTERATIONS OF THE CALCIFEROUS MINERALS SURFACE PROPERTIES AND FLOATABILITY UNDER THE IMPACT OF HIGH - POWER ELECTROMAGNETIC PULSES

Valentine A. Chanturiya, Igor Zh. Bunin, Maria V. Ryazantseva #
Institute of Comprehensive Exploitation of Mineral Resources Russian Academy of Sciences named after academician N.V. Mel'nikov, Russia

ABSTRACT – The modification of structural chemical properties of natural fluorite, scheelite and calcite under the impact of high – power electromagnetic pulses (HPEMP - treatment) were studied with help of adsorption of acid – base indicators. It was determined that the HPEMP - treatment during the of 30 seconds (3×10^3 pulses) resulted in the intensification of fluorite surface 'electron – donating ability and acceptor properties of calcite and scheelite surfaces. Single mineral flotation tests has allowed to determine that treatment by high-power electromagnetic pulses resulted in the improvement of the calciferous minerals floatability. The rising of the scheelite recovery was 10–12%, for fluorite it was 5–6%, for calcite –7–8%.

Key words: calcite, fluorite, scheelte, floatability, high - power electromagnetic pulses

INTRODUCTION

A detailed study of the relationship between the parameters of the treatment by high - power electromagnetic pulses (HPEMP - treatment) and the surface properties of calciferous minerals is of high relevance for the development and refinement of the existing understanding of the processes involved in the interaction between strong electromagnetic fields and geomaterials of various origin, for the development of a scientific framework for the application of HPEMP - treatment for directed modification of the structure and properties of mineral, and for solving practical problems aimed primarily at improving of the efficiency of calciferous minerals processing [1-4].

This paper presents the findings of a study of the effects of high-power electromagnetic pulses (HPEMP) parameters on the structural and chemical state of the surfaces of calcite, fluorite, and scheelite and their sorption and flotation properties.

corresponding author: ryzanceva@mail.ru

MATERIALS AND METHODS

In this study, natural calciferous minerals were used – calcite ($CaCO_3$ > 98%), scheelite ($CaWO_4$ > 98%),) and fluorite (CaF_2 > 98%), size fraction -80+50 μm. Distilled water (MeS / H_2O = 10 / 1) was added to the samples before they were treated with high – power electromagnetic pulses (HPEMP - treatment).

HPEMP - treatment of the samples was performed on a lab scale in air by a series of pulses between 5 to 10 ns long. The electrical field component was 30 kV with a pulse frequency of 100 Hz. The pulse energy was approximately 0.1 J and the integral treatment pulse number varied from $5 \cdot 10^2$ to $1.5 \cdot 10^4$ pulses. Pulse parameters were kept constant and the number of pulses was controlled by varying the treatment duration between 5 s and 150 s.

To identify and study the acid - base properties of the mineral surfaces, the Hammett indicator adsorption method from aqueous media was adopted [5].

The adsorption of oleate was determined using UV spectroscopy according to the residual concentration of oleate ion in the pulp filtrate after contact of the mineral sample with the reagent solution (SU 1322130). Sorption of sodium silicate was determined by the residual concentration of silicon (C_{Si}) in the pulp filtrate by the method (PND 14.1.: 2.215 - 06), based on the interaction of silicic acid with ammonium molybdate in an acidic medium.

Flotation test conditions: monomineral sample fraction ($CaCO_3$, CaF_2, $CaWO_4$) sized -80 +50 μm, 1.00 g; pH = 10.0; contact time of the mineral with water (S:L = 1:6) 1 min, with sodium silicate (100 g / t) 3 min, sodium oleate (300 g / t) 3 min, flotation time - 1.5 min. Reagent treatment was defined to achieve the highest possible recovery in the flotation of untreated scheelite sample.

RESULTS AND DISCUSSION

Acid - base properties of the surface As seen in Figure 1a, the surface of calcite ($CaCO_3$) in the native state is mainly composed of Broensted acidic sites (BAS) with pKa = 1.3 (55.4×10^{-3} μmol/g); neutral sites (pKa = 7.3, n= 15.4×10^{-3} μmol/g), base Lewis (pKa = - 4.4, n = 13.4×10^{-3} μmol/g), and Broensted (pKa = 12.8, n = 16.6×10^{-3} μmol/g) sites also constitute a major share. The number of sites with pKa = 4.1 and pKa = 6.4 is 0.5×10^{-3} and 3.3×10^{-3} μmol/g, respectively.

As a result of HPEMP - treatment of the duration $t_{treatment} \sim$ 10 - 30 sec ($N \sim 10^3$-3×10^3 pulses), a reduction was identified in Broensted base sites from 19.3×10^{-3} to 2.8×10^{-3} μmol/g, an increase in the concentration of aprotonic electron donor Lewis sites with pKa = -4.4 by ~1.2 times (from 13.4×10^{-3} μmol/g to 16.7×10^{-3} μmol/g) and proton donor Broensted sites with pKa = 1.3 and pKa = 4.1 by ~1.2 and 5.2 - 8.6 times, respectively.

Increasing the treatment duration to $t_{treatment} \geq$ 50 sec ($N \geq 5 \times 10^3$) resulted in a consistent increase in the number of Broensted base sites with pKa = 12.8 by a factor of 10 - 19.5 (surface hydroxylation) and a decrease in the number of Lewis base (pKa = -4.4) and Broensted acid sites with pKa = 1.3 and 4.1. (Fig. 1b). Concentration of neutral sites (pKa = 7.3 and pKa = 6.4) did not change during the treatment.

Analysis of the calcite data reveals two key findings. The first one is the antibate change in the concentration (μmol/g) of sites with pKa = 12.8 and pKa = 1.3 depending on the duration of the pulse treatment, which may be interpreted as the

conversion of Broensted base and acid sites indicating a change in the donor - acceptor equilibrium and stronger acceptor properties of the surface at $t_{treatment} \leq 30$ sec (3×10^3 pulses), followed by weakening with increasing treatment time. The second one is that the increase in the number of sites with pKa = 4.1 and pKa = - 4.4 may be the result of accumulation and annihilation of structural defects.

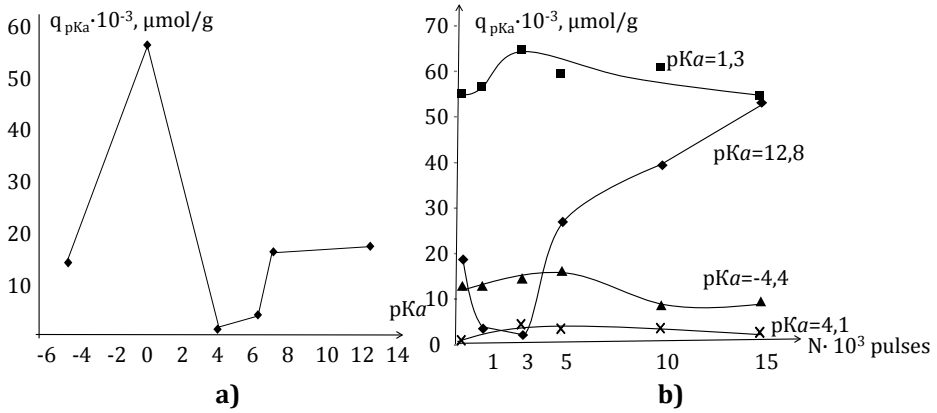

Figure 1. The distribution of the adsorption centers throughout the pK*a* values for the initial calcite sample **(a)**; the dependence of the active centers with pK*a* = -4.4; 1.3; 4.1; 12.8 on the number of pulses **(b)**

Distribution of the adsorption sites on the original sample surface of ***fluorite*** (CaF_2) is shown in Figure 2 a. The original mineral surface is dominates by Broensted (pKa = 12.8, n = 195.6 x 10^{-3} µmol/g) and Lewis (pKa = -4.4, n = 79.4 x 10^{-3} µmol/g) base sites. Besides, Broensted acid (pKa = 4.1, n = 48.2 x 10^{-3} µmol/g; pKa = 1.3, n = 21.9 x 10^{-3} µmol/g), neutral, and base (pKa = 7.3, n = 0.79 x 10^{-3} µmol/g, pKa = 8.8, n = 0.87 x 10^{-3}) sites have been identified.

As can be seen in Figure 2, treatment of the the mineral for $t_{treatment} \sim 10$ sec ($N \sim 10^3$) reduced the number of sites with pKa = -4.4 by more than an order of magnitude (from 83.21 x 10^{-3} µmol/g to 8.19 x 10^{-3} µmol/g) and increased the number of sites with pKa = 1.3 (from 21.9 x 10^{-3} µmol/g to 118.59 x 10^{-3} µmol/g) and 4.1 (from 48.2 x 10^{-3} µmol/g to 58.2 µmol/g), i.e. by ~5.5 and 1.2 times, respectively.

Further increase in the duration of pulse treatment to $t_{treatment} \sim 30$ sec had the opposite effect, resulting in a significant increase in the sites with pKa = -4.4 and a decrease in the sites with pKa = 1.3; after the treatment, the concentration of the sites with pKa = -4.4 was nearly three times that in the original sample surface.

HPEMP treatment for 50 seconds (5 x 10^3 pulses) resulted in a decrease by a factor of at least 11 in the concentration of base sites with pKa = -4.4. Importantly, the increase in Broensted acid sites with pKa = 1.3 was not proportional (from 87.57 x 10^{-3} µmol/g to 96.10 x 10^{-3} µmol/g); sites with pKa = 4.1, to the contrary, decreased by a factor of 1.2 and the concentration of sites with pKa = 7.3, 8.8, and 12.8 did not change over the entire examined range of HPEMP values.

Based on the data from the fluorite samples, one can conclude that HPEMP treatment over 10 sec (10^3 pulses) results in a decrease of Lewis basicity with the

conversion of Lewis base sites (pKa = -4.4) to Broensted acid sites (pKa = 4.1 and 1.3), which indicates stronger electron-donor properties of the surface. At $t_{treatment}$~ 30 sec, an explosive growth in Lewis base sites combined with a parallel decrease in Broensted acidity were observed, which apparently is a result of both defect formation and deprotonation and/or dehydroxylation of the sites with pKa = 4.1 and 1.3. Considering the ambiguity of the accumulation mechanism of Lewis base sites (deprotonation indicates stronger acceptor properties, while dehydroxylation indicates the opposite), the effects of this treatment stage on the donor and acceptor properties cannot be conclusively identified. However, increasing the treatment time to 50 seconds caused a sharp decrease in the number of Lewis base sites with a minor share converting to proton donor Broensted sites; the latter indicates some increase in the donor ability of the mineral surface.

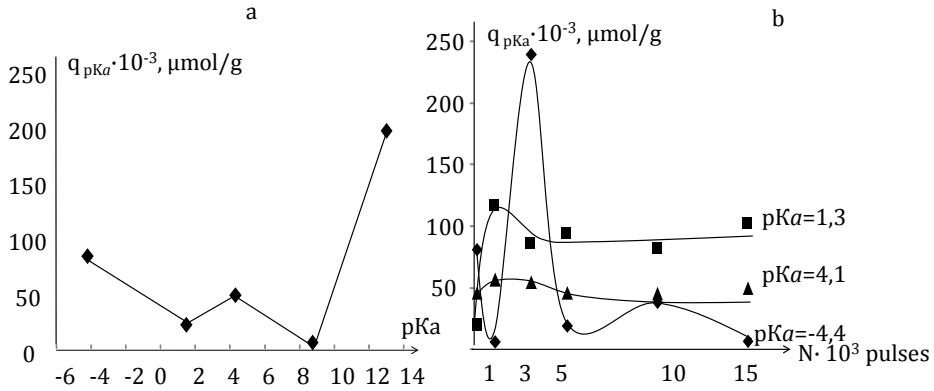

Figure 2. The distribution of the adsorption centers throughout the pK*a* values for the initial fluorite sample **(a)**; the dependence of the active centers with pK*a* = -4.4; 1.3; 4.1 on the number of pulses **(b)**

The surface of the original sample of ***scheelite*** $CaWO_4$ is mainly composed of proton donor Broensted sites with pKa = 1.3 (n = 45.72 x 10^{-3} μmol/g), with 13.16 x 10^{-3} μmol/g and 19.82 x 10^{-3} μmol/g sites with pKa = 4.1 and 6.4, respectively. The concentration of Lewis (pKa = -4.4) and Broensted base sites is not that high: 3.33 x 10^{-3} μmol/g and 5.52 x 10^{-3} μmol/g, respectively (Fig. 3a).

Using the indicator method, it was demonstrated that the concentration of acid sites with pKa = 1.3, 6.4, 7.3 and pKa = 8.8 did not change as a result of the HPEMP treatment. At the same time, the number of Broensted base sites with pKa = 12.8 increased by a factor of 4.8 - 6 (from 5.5 x 10^{-3} μmol/g in the initial surface to 33.11 x 10^{-3} μmol/g as a result of the HPEMP treatment of t_{tr}~ 150 sec). However, at $t_{tr} \leq$ 100 sec, there is a decrease in the number of proton donor Broensted sites with pKa = 4.1 (Figure 3b), resulting in an increased number of Lewis base sites and the concentration of proton donor Broensted sites falling from 13.16 x 10^{-3} μmol/g in the original sample to 6.07 x 10^{-3} μmol/g in the sample after $t_{treatment}$ ~ 100 sec.

In other words, in scheelite, the main changes in the acid and base surface properties are associated with the increase in the number of Broensted alkaline sites.

Considering the fact that the concentration of acid and neutral (pKa = 1.3, 6.4, 7.3, 8.8) sites does not change, the increase in Broensted basicity may be logically explained by the stronger acceptor properties of the surface - activation of sites with pKa ≥ 14 accompanied by dissociative adsorption of water leading to growth in the number of sites with pKa = 12.8. The conversion of sites with pKa = -4.4 to sites with pKa = 4.1 indicates weaker donor properties of the surface.

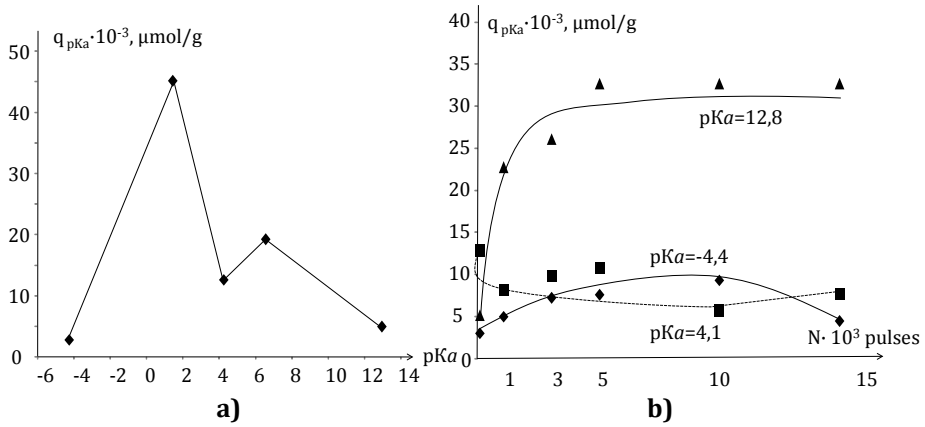

Figure 3. The distribution of the adsorption centers throughout the pK*a* values for the initial scheelite sample **(a)**; the dependence of the active centers with pK*a* = -4.4; 1.3;4.1 on the number of pulses **(b)**

The sorption activity of calcium minerals towards oleate was investigated by UV - spectroscopy based on the residual concentration of oleic acid in in the pulp after the contact of the mineral with the reagent solution. The obtained dates are presented in Figure 4, as it can be seen the preliminary HPEMP - treatment activated the sorption of the collector on the surface of calciferous minerals.

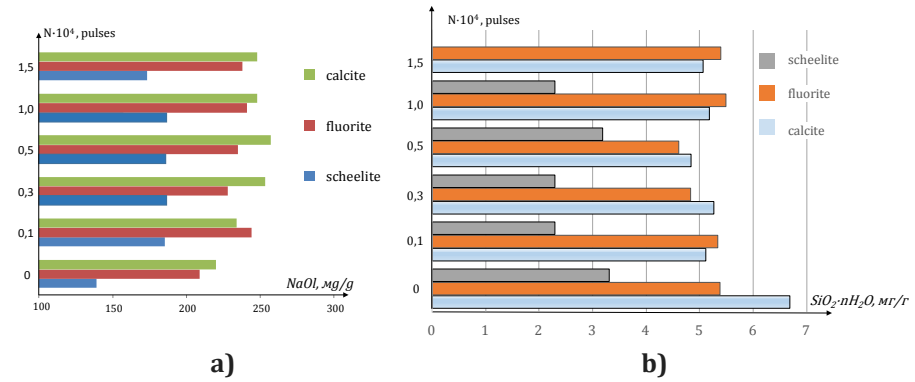

Figure 4. The influence of HPEMP - treatment ($N_{imp.}$ = 10³ – 1,5×10⁴) on the quantity (mg / g) of oleic acid adsorbed on the surface of calcite, fluorite and scheelite **(a)**; the influence of the HPEMP – treatment on the sodium silicate sorption pon the surface of shelite, fluorite and calcite **(b)**

For scheelite samples HEMP – treatment results to the increasing of the adsorbed oleate quantity (μg / g) by a factor of 1.2–1.3 times: from 139 μg / g (the mineral in the initial state) to 173 – 185 μg / g (the sample after the HPEMP – treatment, $N_{pules} = 3 \times 10^3–10^4$). For fluorite and calcite, the increasing of the adsorbed reagent quantity is 10 – 17%: the reagent adsorption for fluorite increased from 209 μg / g (initial state) to 238 – 244 μg / g ($N_{pules} = 3 \times 10^3–10^4$). For calcite samples, the rising of the sorption quantity was about 15 %: from 229 μg / g (initial sample) to 260 – 269 μg / g for the mineral after HPEMP - treatment ($N_{pules} = 3 \times 10^3–10^4$).

The study of the HPEMP – treatment influence on adsorption of sodium silicate at the minerals surface demonstrates the decreasing in the quantity (mg / g) of the adsorbed reagent by 10–25% (Figure). In the case of scheelite and fluorite, the decreasing in the amount of adsorbed sodium silicate quantity was 10 – 14%: for scheelite — 3.2 mg / g (mineral in the initial state), 2.1 - 2.2 mg / g for samples after the HPEMP - treatment ($N_{pulses} = 10^3 - 3 \times 10^3$). The influence is more effective for calcite: the decreasing in the quantity of adsorbed sodium silicate was ~ 20 - 25% as compared to the to the sample in the initial state (6.7 mg / g) and 4.8 - 5.1 mg / g for the sample after the HPEMP - treatment ($N_{pulses} = (3 - 5) \times 10^3$)).

Flotation test results Figure 5 illustrates the relationship between the floatability of monomineral fractions of calcite, fluorite, and scheelite and the duration of HPEMP - treatment.

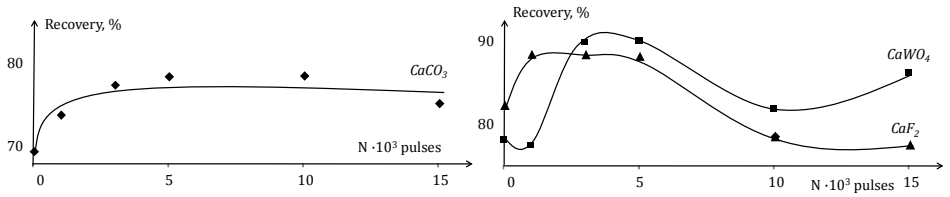

Figure 5. Floatability of calcite, fluorite and scheelite as function of the number of pulses

It can be seen that, in the studied minerals, there is an increase in the froth yield as a result of a short ($t_{tr} \leq 50$ sec) HPEMP treatment - the largest increase in recovery achieved was 8% in calcite, 6% in fluorite, 12% in scheelite.

CONCLUSIONS

1. Using the Hammett color indicator adsorption method, following key evolution mechanisms were identified of the acid-base sites in calcium mineral surfaces exposed to high-voltage nanosecond pulses: stronger electron-donor properties of ***fluorite*** surfaces and stronger acceptor properties of ***scheelite*** surfaces as a result of HPEMP treatment; mutual conversion at $t_{обр} \leq 30$ sec of Broensted base and acid sites in ***calcite*** surfaces resulting in weaker donor properties and stronger acceptor properties of the mineral surfaces, and then, at $t_{обр} > 30$ sec, recovery (strengthening) of the donor properties of the surfaces.
2. It was determined that HPEMP – treatment of calciferous minerals causes the

increasing in their sorption activity towards a fatty acid collector (sodium oleate) and a decrease in the quantity (mg / g) of adsorbed depressor (sodium silicate). The increasing of adsorbed sodium oleate quantity for scheelite was 20 –30% as compared with the initial sample; for calcite and fluorite, the increasing of the adsorbed reagent quantity was about 10 – 20%. The decreasing in the quantity of adsorbed sodium silicate (mg / g) was 10 – 15% for scheelite and fluorite and 20–25% for calcite.

3. In monomineral flotation of calcite, fluorite, and scheelite, the optimal parameters of the HPEMP - treatment were identified ($t_{treatment}$~ 10-50 sec) and the reagent treatment was optimized for scheelite recovery, resulting in an increase of recovery of 8% in calcite, 6% in fluorite, and 10-12% in scheelite.

References

1. Chanturia, V. A., Bunin, I. Z., Ryazantseva, M. V., Khabarova, I. A. (2012) Influence of nanosecond electromagnetic pulses on phase surface composition, electrochemical, sorption and flotation properties of chalcopyrite and sphalerite. Journal of Mining Science, 48(4), 155 – 164,
2. Chanturia, V. A., Bunin, I. Z., Ryazantseva, M. V., Khabarova, I. A. (2013) X-Ray photoelectron spectroscopy-based analysis of change in the composition and chemical state of atoms on chalcopyrite and sphalerite surface before and after the nanosecond electromagnetic pulse treatment. Journal of Mining Science, 49(3), 489-498,
3. Chanturia, V. A., Bunin, I. Z., Ryazantseva, M. V., Khabarova, I. A., Koporulina, E. V., Anashkina, N. E. (2014) Surface activation and induced change of physicochemical and process properties of galena by nanosecond electromagnetic pulses. Journal of Mining Science, 50(3), 573-586,
4. Ryazantseva, M. V., Bunin, I. Z. (2015) Modifying acid–base surface properties of calcite, fluorite and scheelite under electromagnetic pulse treatment. Journal of Mining Science, 51(5), 1016-1020,
5. Nechiporenko, A., Burenina, T., Koltsov, S. (1985) Indicator method for the investigation of solid-surface acidity. Russian journal of general chemistry, 55(9), 1907-1912.

XIII International Mineral Processing and Recycling Conference
Belgrade, Serbia, 8-10 May 2019

University of Belgrade, Technical Faculty in Bor
Vojske Jugoslavije 12, 19210 Bor, Serbia
Tel. +381 30 424 555 Fax +381 30 421 078

OPTIMIZATION OF FLOTATION GRINDING PROCESSES USING MODEL-BASED CRITERIA

Erdenezul Jargalsaikhan #, Valery Morozov
National University of Science and Technology "MISiS", Moscow, Russia

ABSTRACT - This paper is developed control algorithm of grinding and flotation processes. It was assumed consecutive realization method of estimation the grade ore and optimization of economic-based technological processes. In order to increase the efficiency of enrichment of copper-molybdenum ores, it was proposed to measure and take into account the concentration of nonionic collector in the aqueous phase of the pulp when choosing the grinding and flotation regimes. Based on the data on the grinding fineness and the concentration of the collector in the aqueous phase of the pulp, a model has been obtained that relates the extraction of metals to process parameters. The control algorithm of grade consists in the formation of ore model coming for processing, as a mixture to certain types of ores, and the choice modes of enrichment based on the obtained information about the grade of the ore being processed. An economic criterion is used as an efficiency criterion, the sum of the cost of most metals and the costs of improving the quality of the concentrate. Account the ore grade and the response to the metal content allow to better take into account the objective characteristics of processed ore. Using the obtained model and the economically oriented optimization objective, the optimal grain size of grinding of copper-molybdenum ores was determined. Application of the developed control algorithm allows increasing the technical and economic efficiency of the whole complex of copper-molybdenum ore plant of Erdenet in Mongolia.

Keywords: copper-molybdenum ores, grinding, flotation, modeling, ore grade, optimization criteria

INTRODUCTION

The perspective direction of algorithms is the development and application of model-oriented criteria of optimization [1, 2]. One such example is developed at the GOK "Erdenet" Plant control algorithm processes of enrichment for the grade of the ore [3, 4]. Also, the promising direction is the application of criteria based on economic estimates, the complex criterion in particular of reducing the losses of valuable components [5, 6]. The combination of these methods is a good platform for creating a complex control algorithm that takes into account the properties of processed raw materials to the greatest extent.

METHOD OF THE CONTROL ALGORITHM

Along with the use of the method of managing process parameters based on the

corresponding author: zul479@gmail.com

ore grade assessment, algorithms for controlling the parameters of the beneficiation processes should use economic optimization criteria. To develop efficient and sustainable control algorithms for the beneficiation processes, it was proposed to select and maintain the parameters of the technological mode, calculated using an economically oriented model of the beneficiation process.

Control algorithm developed the grinding and flotation processes, shown in Figure 1, assumes a consistent implementation of methods for estimating the grade ore and the economically-based optimization of technological processes.

This control algorithm is implemented in two circuits. The first circuit regulates the productivity taking into account the ore grinding size. The second level - the regulation of lime and collector. The regulatory objective was maintained optimal conditions for milling and collective flotation operations.

The layout of flotation process control algorithms is based on the principle of two-level control when the optimally calculated parameters of the grinding and flotation processes are based estimation of grade ore, and the determination of the main parameters for typical ores is carried out using economic-based optimization criteria.

The control algorithm is described in detail in the grade of ore [7, 8] and consists in the representation of ore supplied for processing, mixtures ores of certain grades, and choice of mode enrichment based on information about the processed grade ore.

The optimal parameters of grinding and flotation processes are calculated taking into account the contribution of each metal to the cost of commercial products.

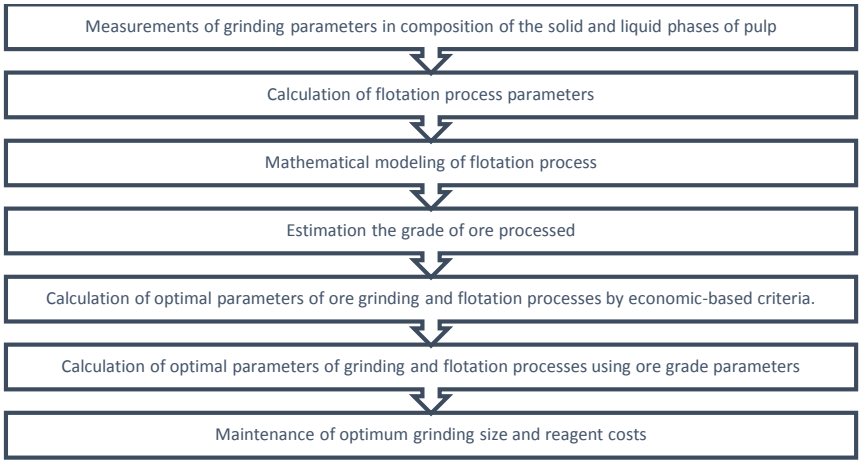

Figure 1. The general control algorithm for the flotation process by ore grade of estimation procedure and economically-based optimization criteria

As a criterion of efficiency, it is advisable to use a special economic criterion-the loss function, expressed as the cost of lost metals, and the cost of improving the quality of the concentrate:

$$Q_t = \varepsilon^*_{Cu} C_{Cu} \alpha_{Cu} + \varepsilon^*_{Mo} C_{Mo} \alpha_{Mo} + \varepsilon^*_{Py} C_{Py} \alpha_{Py} \quad (1)$$

where: **ε***;C;α- loss, price and content in the ore of copper (Cu), molybdenum (Mo), pyrite (Py). Under the price of pyrite is understood to be the cost of extracting pyrite from copper concentrate in a selective cycle.

This criterion was justified and proposed in [9]. A special feature is the control algorithm developed and described in this paper. The fact is that the optimal parameters of the grinding and flotation processes are initially calculated for individual ore grades.

RESULTS OF EXPERIMENTS

In Figure 2 shows the dependence of extraction of metals and the optimization criterion in the collective copper-molybdenum flotation of various ores. It shows that for certain parameters (recovery of copper, molybdenum and iron) are impossible to improve for determining process conditions. In this research, for the improving conditions process used Q_t function, the dependence of which on size of grinding is seen in Figure 2.

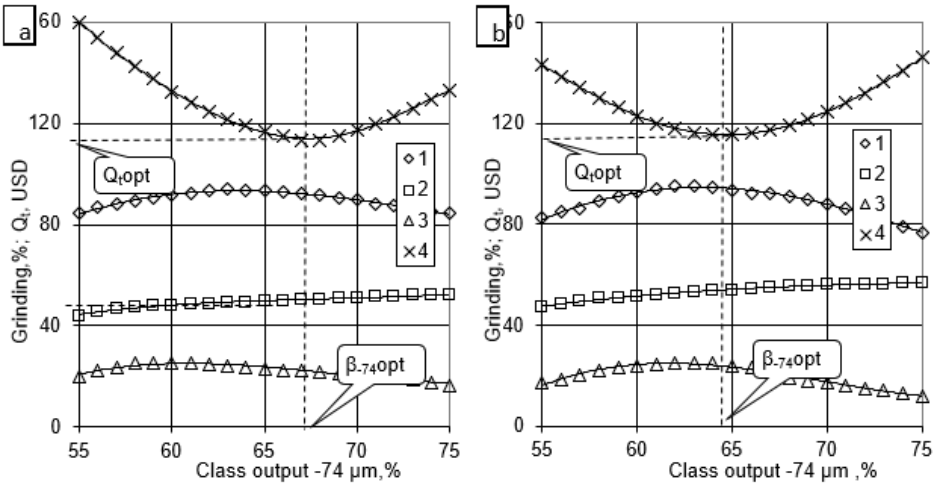

Figure 2. Dependence of copper (1) molybdenum (2) and iron of pyrite (3) recoveries in collective concentrate and optimization criterion Qt (4) at the size of grinding for massive primary ore (a) and mixed secondary sulfidized ore (b)

Analysis represented Figure 2 dependencies show that the improvement of technological parameters was determined by the behavior of all ore components and optimal grinding conditions for different types of ores. In these tests, for massive primary ore, the function is low, reduce losses at size grinding of 67.5%, class output -74 μm, and for mixed secondary sulfidized ore at the size of grinding 64.5%, class -74 μm.

It can be seen from Figure 3 that the dependence of the optimization criterion for collective copper-molybdenum flotation of different types of ores also makes it possible to determine the improvement of technological conditions.

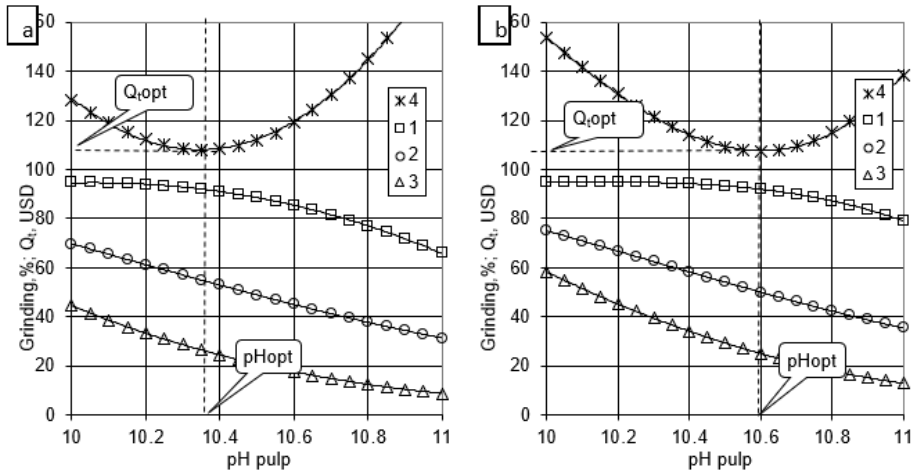

Figure 3. The dependence of copper recoveries (1) molybdenum (2) iron of pyrite (3) in collective concentrate and optimization criterion Q_t (4) from the pH collective flotation of massive primary ore (a) and mixed secondary sulfidized ores (b)

Figure 3 shows the analysis of the dependencies that the improvement of technological parameters are determined by the behavior of all ore components and optimal flotation conditions for different types of ores.

Thus, for massive primary ore, the minimum loss function is observed at pH=10.36, and for mixed secondary sulfidized ore-at pH=10.59.

The results in the Table1 show that calculations of the optimal parameters of the grinding and flotation processes are basis for calculation of grinding and flotation automatic control systems.

Table 1. Values of technological parameters set points in control systems of grinding and classification processes

№	Process of parameter	MPO	MSSO	PPO	MOO	MSO
1	Size of the grinding - class output – 74 μm, %	67.5	64.5	67.0	66.0	66.0
2	pH of pulp in flotation	10.36	10.59	10.50	10.31	10.55

MPO - massive primary ore; MSSO- mixed secondary sulfidized ores; PPO – poor pyrite ore; MOO- mixed oxidized ores; MSO - mixed sericitized ore.

CONTROL ALGORITHM TESTING AND ANALYSIS OF RESULTS

The algorithm developed an existing when tested in ASTPC of enrichment factory. It can be seen from Table 2, the use of model-based control algorithm to grinding and flotation processes. This makes possible to increase the indicators of enrichment in the collective flotation cycle and at the enrichment factory. Characteristically, the average size of grinding ore has not changed. However, the interval of varying size of the grinding ore has expanded. It is connected to the variation of the setting function

in the control system. Consumption of the collector and lime also has not changed (Table 2). Similarly, the interval of variation expenses of reagents has expanded.

Table 2. Parameters and test results of the model-based control algorithm of grinding and flotation processes at the GOK "Erdenet" plant

The parameter of the process	Ordinary mode of control		New control algorithm	
	Interval of variation	Average value	Limits of variation	Average value
Productivity, t/h	856-911	878	848 – 918	918
Size of crushed ore, % class-74 μm	64.5- 65.3	65.0	64.0 – 65.9	65.0
Consumption of collector, g/t	13.8 – 15.8	14.81	13.5 – 16.0	14.83
Consumption of lime, kg/t	1.34 – 1.55	1.45	1.30 – 1.60	1.46
pH liquid phase	10.3 – 10.45	10.37	10.3 – 10.46	10.38
Copper recovery in collective concentrate, %		91.6		92.2
Copper recovery in product concentrate, %		88.7		90.1
Molybdenum recovery in collective concentrate, %		59.1		60.1
Molybdenum recovery in product concentrate, %		51.6		52.7
Loss function (Qt) in the collective flotation concentrate, USD/t		11.1		10.8
Loss function (Qt) as a whole by the factory, USD /t		13.2		12.9

CONCLUSION

The average value and interval of variation pH have not changed. In general, these results suggest that using model-based criteria does not change the average parameters of the mode. However, the account of grade ore and responding to the content of metals allow better objective characteristics of the processed ore. Consequently, using a new algorithm allowed to achieve an increase in metal extraction and further, reduce the cost of copper and molybdenum.

The results finding of this study indicate that using economic-based criteria can make possible to improve the technical and economic efficiency complex of enrichment copper-molybdenum ore.

Acknowledgments

The authors would like to thank the GOK "Erdenet" Plant in Mongolia.

References

1. Bartolacci, G., Pelletier Jr, P., Tessier Jr, J., Duchesne, C., Bossé, P. A., Fournier, J. (2006) Application of numerical image analysis to process diagnosis and physical parameter measurement in mineral processes—part I: flotation control based on froth textural characteristics. Minerals Engineering, 19(6-8), 734-747,

2. Sbárbaro, D., Del Villar, R. (Eds.). (2010) Advanced control and supervision of mineral processing plants. Springer Science & Business Media, 376,
3. Delgerbat, L. (2002) Investigation, modeling and optimization of grinding processes and collective flotation of copper-molybdenum ores. Mining Information and Analytical Bulletin, Moscow, 226-230,
4. Ganbaatar, Z. et al. (2011) The enrichment of copper-molybdenum ores using integrated radiometric assay grade ore. Mining information-analytical bulletin, 176-182,
5. Schena, G., Gochin, R. (1995) Application of engineering economics methods to decision making in mineral processing. Proceedings of the XIX International Mineral Processing Congress, San Francisco, USA, Volume 1, 267 – 272,
6. Morozov, V.V., Zhargalsaikhan, E. (2017) Optimization of the flotation process using economic criteria. Proceedings of the 11th Congress of the Enrichers of the CIS Countries, Moscow, 1, 161-164,
7. Morozov, V., Avdokhin, V., Topchaev, V., Ulitenko, K., Stolyarov, V., Ganbaatar, Z., Mergenbaatar, N. (2008) Modern algorithm and system for monitoring and control of milling and flotation process. Preprints of the 18th IFAC World Congress, IFAC (ed.), Seoul, 222-228,
8. Morozov, V., Davaasambuu, D., Ganbaatar, Z., Delgerbat, L., Topchaev, V., Sokolov, I., Stolyarov, V. (2013) Modern systems of automatic control of processes of grinding and flotation of copper-molybdenum ore. 16th IFAC Symposium on Control, Optimization, and Automation in Mining, Minerals and Metal Processing, Volume 15, Part1, IFAC (ed.), 166-171,
9. Ganbaatar, Z. et al. (2017) Management of the processes of copper-molybdenum ores enrichment using advanced quality control. Mining sciences and technologies, 40-48.

XIII International Mineral Processing and Recycling Conference
Belgrade, Serbia, 8-10 May 2019

University of Belgrade, Technical Faculty in Bor
Vojske Jugoslavije 12, 19210 Bor, Serbia
Tel. +381 30 424 555 Fax +381 30 421 078

ENHANCEMENT OF FLOTATION KINETICS THROUGH APPLICATION OF MODIFIER

Bijay Shankar Tiwari #, Amit Ranjan, Ashwani Kumar, Bhalla Srinivas Rao
Tata Steel Limited, Jamshedpur, Jharkhand, India

ABSTRACT – Jamadoba Coal Processing Plant (JCPP) produces coking coal at 18.5% targeted Ash level from high feed ash of raw coal of captive UG mines of Jamadoba Group of collieries Dhanbad , Jharkand ,India) . In JCPP, Fines circuit beneficiates finer fraction (-0.5mm) of around 20 % of the raw coal using physico-chemical froth floatation method. In recent years, due to deterioration of Raw Coal washability and Characteristics, drop in Clean coal yield was observed at JCPP particularly from FF cell. The surface of fine coal particles (-0.5 mm) is usually coated with minerals, making the particles hydrophilic and preventing the adsorption of flotation collectors onto the mineral surfaces, which hinders mineral (gangues) separation. There have been many studies conducted to investigate the negative effects caused by fine particles. A trial with Modifiers in FF cell was conducted at Laboratory and plant scale to study the effect of modifiers on performance of Froth Flotation Cell. An increase in Overall Clean Coal yield by 0.53 % on Raw Coal basis was observed during the trial tests and also increase in Separation Efficiency by 4.86 % and increase in Tailings ash by 3.56 (from 40.40 % to 43.96 %) were observed in comparison to flotation performance without application of Modifier. Modifiers modify the colloidal interactions between particles by creating electrostatic and/or steric repulsion which counter balances the contribution of the van der Waals attraction to the total net force.

Key words: UG :Underground, FF Cell : Froth Flotation Cell, JCPP : Jamadoba Coal Preparation Plant, CC : Clean Coal

INTRODUCTION

Coal flotation is known to be very sensitive to changes in feed characteristics, such as, size consist, ash content, extent of oxidation, content of ultra fines and clay, coal rank etc. and also to operational parameters, such as, pulp density, reagent type and dosage, reagent impurities, conditioning time, wetting time, air flow rate, impeller speed, froth height, etc .

Prime coking coal is about to become the primary feedstock of the existing coking coal washeries of Tata steel Jharia division and synthetic collector is being used as

corresponding author: bijay.tiwari@tatasteel.com

coal collector as a flotation reagent. Due to the depletion of high grade prime coking coal from upper seam subsequent processing of lower seam coal having poor floatability. The natural hydrophobicity of coal makes froth flotation an appealing beneficiation process for fine coal.

However, due to the heterogeneous nature of coal, significant variations in hydrophobicity and floatability exist even for coals of similar rank. Even the different organic constituents (macerals) may respond differently to flotation by froth flotation. It is a highly versatile method for physically separating particles based on differences in the ability of air bubbles to selectively adhere to specific mineral surfaces in mineral/water slurry.

JCPP process raw coal of captive mines and produce clean coal after reducing the ash percentage in raw coal (28.0 % - 34.0 % ash in raw coal is reduced to ~18.5 % ash in clean coal).

Due to depletion of good coal in the upper coal seams of the mines, Jharia collieries are now left with inferior coal reserves in lower seams. The coal from lower seams has wider variation in ash percentage with poor wash ability characteristics resulting into lower clean coal yield. This coal causes destabilization and process inefficiency in the beneficiation plants.

The beneficiation of the sized raw coal is done through two circuits, Coarse Circuit (dense media cyclones) and Fines Circuit (froth flotation). Coarse fraction comprising of approximately 80 % of the Coarse raw coal (13 mm to 0.5 mm) is beneficiated through the coarse circuit using gravity separation method and fines fraction (<0.5 mm size coal) comprising of 20 % of the raw coal is beneficiated through the fines circuit using physico-chemical method.

With these two processes, the ash of the raw coal is reduced to the customer's requirement level at 18.5 %. The deteriorating Raw Coal quality and washability characteristics adversely effects operation of FF cell resulting in deterioration of grade and quality of coking coal produced from FF cell.

Efficiency of the flotation process depends on efficiency of collector apart from other several parameters as mention above. Increasing collector efficiency, modifier was selected as one of the surfactants for laboratory & Plant Trials.

Modifiers/Dispersants are widely used in most of coal washeries to modify the colloidal interactions between particles by creating electrostatic and/or steric repulsion which counter balances the contribution of the van der Waals attraction to the total net force. Modifiers are used extensively in flotation practice to modify the action of collectors, either by intensifying or reducing the hydrophobic effect of collectors on particle surfaces.

Modifiers may act directly on the mineral surface and change its chemical composition. Modifiers are reagents which facilitate collector attachment to a mineral, or increase the amount of collector which can be attached, or may reduce mineral surface hydration.

Before plant trial, detail lab test was conducted in which raw coal of size less than 15 mm was collected & screened at 0.5 mm. Standard procedure was followed from sample collection to analysis.

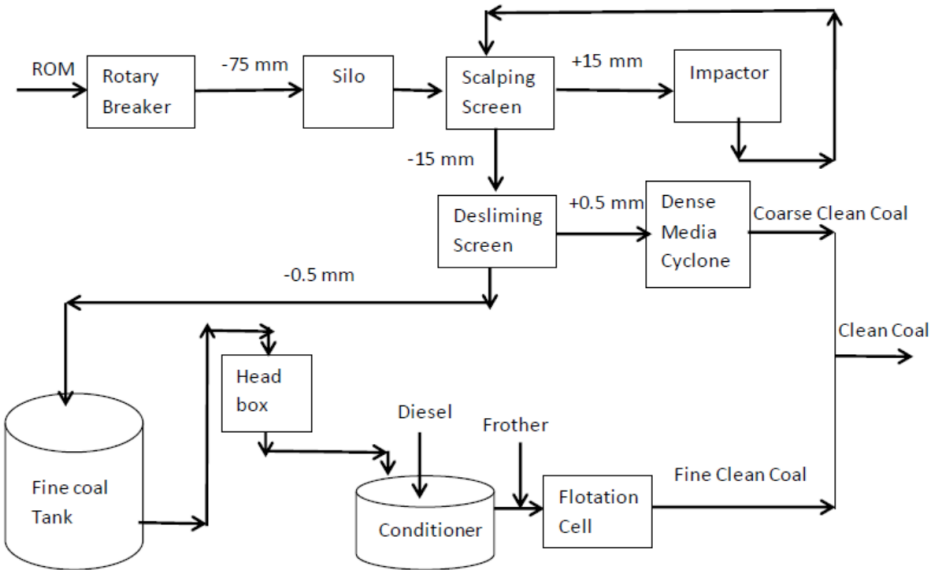

Figure 1. Process flow of JCPP

Figure 2, Figure 3 and Figure 4 show the deterioration Raw Coal Ash & its impact on Clean Coal Yield & Separation Efficiency:

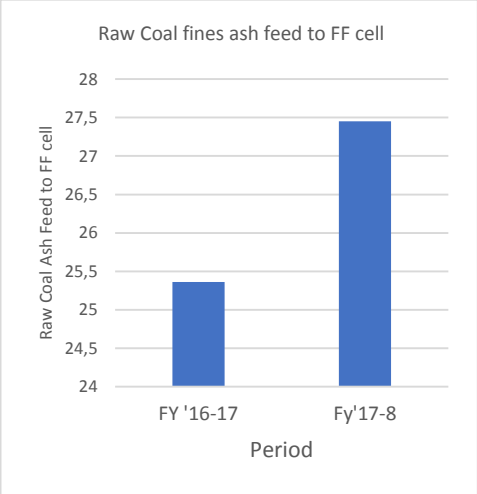

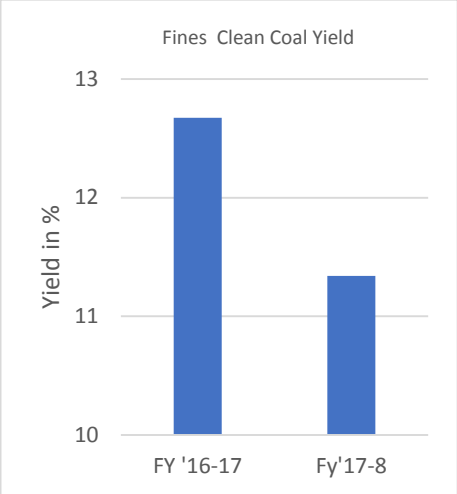

Figure 2. Showing Raw Coal ash Feed to FF cell

Figure 3. Showing Fines Clean Coal Yield

Figure 2, shows that Raw Coal feed to FF cell has deteriorated, resulting in lower Clean coal yield from FF Cell (Fig-3) and also adverse impact on Separation Efficiency of FF cell (Fig-4).

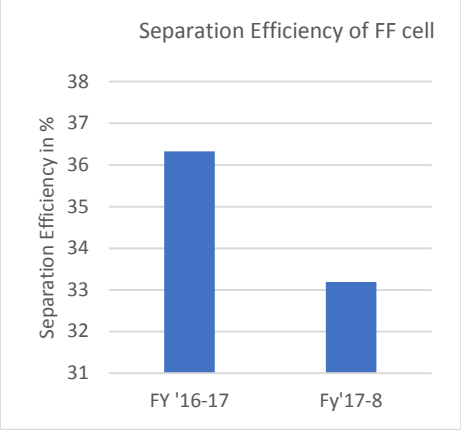

Figure 4. Seperation Efficiency of FF cell

PLANT TRIAL

Prior to Plant test Flotation tests were carried out in lab model flotation cell having 3 liter capacity. Reagent dosage (Collector & Frother) was maintained based on actual dosing rates in plant. Laboratory FF Cell test was carried out at different Modifier dosing rates as shown in Table-2. Flotation concentrate and tailings were collected, dried, weighed, pulverized and their ash contents were determined. Tap water was used throughout the experiments. Flotation Test was conducted with following fixed parameters as Shown in Table-1.

Table 1. Parameters in Flotation tests

Fixed Parameters	Level
Feed Size in mm	0.5
Pulp density	10 % solid by weight
Conditioning timing	1 minute each with collector and frother
Slurry pH	8.1
Impeller Spped	750 RPM
Synthetic collector Dosing in Kg/ton	0.54
Frother Dosing rate in kg/ton	0.015

Table 2. S Laboratory Test Results at different Modifier Dosing rates

Modifier Dose rate in kg/ton	Fines Clean coal Yield	Fines Clean Coal ash in (%)	Tailings Ash (%)
0.14	9.33	14.55	37.63
0.16	9.61	14.60	37.97
0.18	9.94	14.51	41.09
0.21	9.97	15.30	42.21

Based on Clean Coal Yield, Grade of product (Ash limit 13.5 % to 14.5 % max) andtailing ash (Minimum ash required more than 40 %), modifier Dosing rate 0.18

kg /ton or 100cc/min was selected for plant test.

METHODOLOGY FOR PLANT SCALE TRIAL TEST

1. Plant Data of last three months before staring Plant Test were collected as shown in Table- 3 as without modifier for comparing the plant test results with without modifier.
2. Plant Test work was conducted for one month Period.
2. Quantity of Modifier Triton X 100 for one month Plant Tests were arranged.
3. Sample of Raw Coal Feed to FF cell, Fines Clean Coal from conveyor belt and Tailings from FF cell Launder were collected in each shift.
4.Sample analysis were carried out for Raw Coal ash, Tailings ash , and Fines Clean coal ash of samples collected by in -house geological testing facility.
5. Clean Coal yield was calculated on ash basis, and separation efficiency and Combustible recoveries were calculated and were tabulated as shown in Table-3.
6. Comparative study with and without application of Modifier were done.

Table 3. Showing Plant Test Results in Plant

Parameters	Froth Flotation Product ash %			Yield on Unit Basis* (%)	Separation Efficiency (%)	Combustible Recovery (%)
	Feed	Froth	Tailings			
With Modifier	28.24	14.00	43.60	51.38	36.38	62.06
Without Modifier	28.44	13.89	40.40	48.23	30.60	56.89
Difference	0.20		3.20	3.15	5.78	5.17

*Yield calculated on Ash Basis.

RESULTS AND DISCUSSION

- FF cell Tailing ash increased by 3.20 % with Application of Modifier during plant Test.
- Fines Clean coal yield from Froth Flotation Cell increased by 3.15 % on Raw Coal on unit basis.
- Overall Clean coal yield gain 3.15 % (from FF cell) from plant was observed.
- Froth Flotation Cell Separation Efficiency increased by 5.78 %
- Combustible recovery from FF Cell increased by 5.17 %.

CONCLUSION

Based on Test Results, Application of Modifier along collector and frother in FF cell were regularized in plant on regular basis.

References

1. Froth Flotation, The Adhesion of Solid Particles to Flat Interfaces and Bubbles. Chemical Engineering Society 12: 133-141.by Nutt, C. Published in 1960,
2. Mineral Processing. 3rd edition. ElsevierPublishing Co., Essex, England. By Pryot, E. J. Published in 1965.

XIII International Mineral Processing and Recycling Conference
Belgrade, Serbia, 8-10 May 2019

University of Belgrade, Technical Faculty in Bor
Vojske Jugoslavije 12, 19210 Bor, Serbia
Tel. +381 30 424 555 Fax +381 30 421 078

INVESTIGATION OF THE FLOTATION PARAMETERS FOR THE ORE FROM THE ''CEROVO-C2'' DEPOSIT – CEMENTATION ZONE

Jelena Čarapić #, Vladan Milošević, Branislav Ivošević, Dejan Todorović, Zoran Bartulović, Vladimir Jovanović, Sonja Milićević
Institute for Technology of Nuclear and Other Mineral Raw Materials, Belgrade, Serbia

ABSTRACT – The part of the results, obtained during the technological investigations of the ore from the deposit ''Cerovo-C2'' deposit - Cementation zone, are presented in this paper. Investigations were undertaken at different flotation conditions (three collectors and grinding fineness) in order to define possibility and optimal conditions for processing the ore from this deposit. Obtained results indicate the possibility for producing the copper concentrate with the commercial quality. Best results were obtained with the collector Flomin C4132 and grinding fineness of 80 % below 0.074 mm, where the copper content in the rough concentrate was 4.64 % and the copper recovery was 81.74 %..

Key words: flotation, collectors, grinding fineness, copper recovery.

INTRODUCTION

The copper deposit "Kraku Bugaresku-Cementation" belongs to the basic type of porphyry deposits, as well as subgroups of deposits that are characterized by secondary sulphide enrichment (cementation subtype).

Based on the concentration degree of the mineral composition and the mutual relations of individual elements in the deposit, a certain vertical zonality is observed. From the surface of the terrain to the depth can be distinguished: the oxidation zone, the cementation zone or the secondary sulphide enrichment and the primary zone.

Below the level of groundwater, a secondary sulphide enrichment zone (a zone of cementation) is created. The zone of cementation is characterized by processes which are reflected in the delivery of components and somewhat more pronounced caolinization, relative to hypogenic mineralization. The thickness of this zone is predominantly about 30 meters. For this zone, it is characteristic partly, rather than completely, converting chalcopyrite into coveline and chalcocite. The depth intervals of the zones are conditioned by the locally present tectonics.

In the deposit Cerovo C2 dominant minerals are sulphide copper minerals with

corresponding author: j.carapic@itnms.ac.rs

the tolerant presence of the oxide fractions from the aspect of their processing in flotation concentration.

Laboratory technological investigations were carried out in order to examine the possibilities of processing this type of ore by the mean of flotation concentration. Investigations were carried out at different grinding fineness and different flotation reagents in order to define the possibilities and optimal conditions for processing the ore from this deposit.

EXPERIMENTAL

Characteristics of ore sample

Ore samples from the deposit Cerovo C2 derives from the boreholes and were taken during the investigating activities. Samples were grinded and homogenized in order to obtain composite sample.

Moisture content in the composite sample was 3.5 %.

Chemical composition of composite sample is given in Table 1.

Table 1. Chemical composition of ore sample

Content							
Cu_{uk}	**Cu_s**	**Cu_{ox}**	**S**	**Fe**	**Au**	**Ag**	**Pt**
%					**ppm**	**ppm**	**ppm**
0.265	0.233	0.032	2.90	2.35	0.03	1.10	15.0
SiO_2	**Al_2O_3**	**CaO**	**MgO**	**Fe_2O_3**	**K_2O**	**Na_2O**	**TiO_2**
%							
61.86	18.62	1.08	2.04	3.36	3.24	0.41	0.17

* Ignition Lost - I.L.= 5.98 %

X-ray diffraction was used to determine the phase composition. The XRD patterns were obtained using a PW 1710 automated diffractometer (Philips) using a Cu tube operated at 40 kV and 30 mA. The instrument was equipped with a diffracted beam curved graphite monochromator and a Xe-filled proportional counter. All the XRD measurements were performed at room temperature in a stationary sample holder. The presence of minerals pyrite, chalcopyrite, digenite, coveline, chalcocite, digenite, coveline, luzonite, sphalerite, galenite, molibdenite, native gold, rutile, magnetite, Cu-oxsides, gangue minerals are determined in samples [1].

Cu-oxides are: Cu- limonite, azurite i malachite. Gangue minerals are: quartz and silicates.

Technological conditions

Laboratory technological testing the conditions of flotation concentration included a change of relevant technological parameters [2]:

- Tests were carried out through three series of experiments of rough flotation,
- Each series consisted of three experiments:

  I series - three different collectors with grinding fineness 60.0 % - 0.074 mm,

II series - three different collectors with grinding fineness 70.0% - 0.074 mm,
III series - three different collectors with grinding fineness 80.0 % - 0.074 mm.

- pH value of the pulp was 10.5 in each experiment,
- Pulp density during grinding in all experiments was 60% solid phase,
- Pulp density during flotation in all experiments was 25% solid phase,
- D-250 was used as a frother in all experiments with recommended consumption by the manufacturer.

In all experiments, the conditioning time was 10 minutes; the time of rough flotation was 20 minutes. Collectors were added in three doses, one dose in conditioning and two doses in rough flotation.

Consumption of individual collectors by series of experiments is given in Table 2.

Table 2. Consumption of collectors

Series of experiments	Grinding fineness	Consumption of collectors [g/t dry ore]		
		PEX	MX5193+PEX	C4132
I	60.0 % -0.074 mm	70.0	10.0+10.0	11.0
II	70.0 % -0.074 mm	70.0	10.0+10.0	11.0
III	80.0 % -0.074 mm	70.0	10.0+10.0	11.0

RESULTS AND DISCUSSION

The dependence of the total copper content in the rough concentrate, for all investigated collectors, on the grinding fineness is graphically presented at Figure 1. The diagram shows that the total copper content in the rough concentrate increases with the growth of the grinding fineness for all investigated collectors.

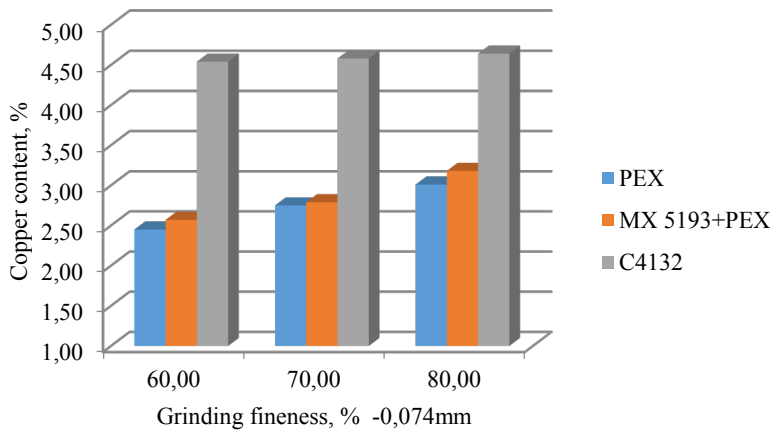

Figure 1. Influence of the grinding finenness on the total copper content in the rough concentrate

The smallest copper content, for all grinding fineness, was achieved using the Potassium Ethyl xanthate (PEX) collector, while the highest content of total copper (4.64 %) for grinding fineness 80 % - 0.074 mm was in experiments in which Flomin C4132 was used as a collector.

The copper recovery in the rough concentrate, for all investigated collectors, on the grinding fineness is numerically given in Table 3 and graphically presented at Figure 2.

From the presented results it can be noted that the copper recovery in the rough concentrate increases with the growth of the grinding fineness for all investigated collectors.

Table 3. The copper recovery in the rough concentrate

Series of experiments	Grinding fineness	Copper recovery, %		
		PEX	MX5193+PEX	C4132
I	60.0 % -0.074 mm	73.91	79.05	74.55
II	70.0 % -0.074 mm	77.07	80.89	76.43
III	80.0 % -0.074 mm	83.77	84.19	81.74

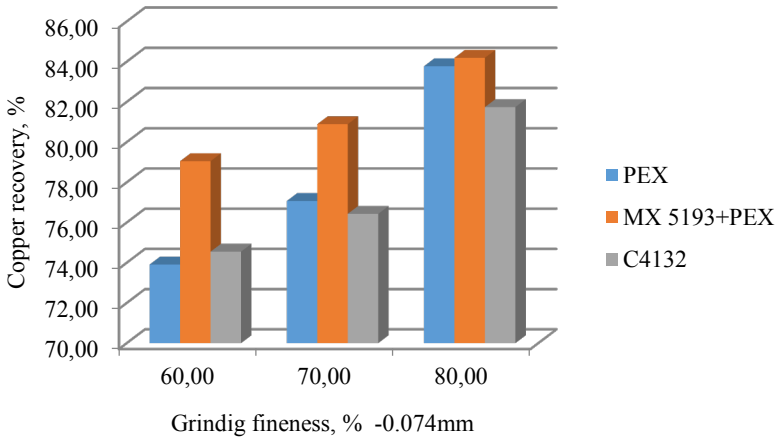

Figure 2. Influence of the grinding finenness on the copper recovery in the rough concentrate

Obtained values of the copper recovery are satisfying, specially from the point of view that this investigation present only preliminary tests. This results can be used as the guideline for the further, more detailed flotation concentration investigations, that should result in the process optimization. Additionally, the presence of the oxide particles are the one that also limited the copper recovery by the flotation concentration process. Therefore, the expactations concerning the copper recovery cannot be the same like in a case of processing the pure sulphide ore.

The higher values of copper recovery in the rough concentrate obtained when applying the PEX as a collector and the combination of the MX 5193 and PEX collectors relative to the tests in which the Flomin C4132 collector is used are explained by the large mass fraction of the rough concentrate.

By the usage of the much more selective collector Flomin C4132, the presence of a limiting factor for the application of xanthates, such as pyrite and sludge particles, is completely eliminated [3]. This collector is designed to collect only copper particles and in this case gives the best results, especially if we take in account all the related parameters: mass fraction of the rough concentrate, the content of the copper in the rough concentrate (~ 4.5 % Cu), copper recovery in the rough concentrate (74 - 82 % Cu), but also and the applied dosage of the collector.

Consumption of collector Flomin C4132 is much lower compared to the other used collectors.

Additionally, Flomin C4132 also has froth properties, and its usage also reduces the dosage of the froth.

CONCLUSION

Investigations of the copper minerals flotation, under different conditions, that were undertaken, show some differences in the effects of their application.

The results of the experiments indicate that the copper content and copper recovery of the rough concentrate increase with the growth of the grinding fineness. In some cases, significant differences in flotation effects for different grinding fineness were observed and these differences range from 0.2 to 1 % for the total copper content and 4 to 10 % for the copper recovery in the rough concentrate. Therefore, it can be concluded that by increasing the grinding fineness and the degree of raw material liberation, increase the probability of successful hydrophobization of mineral grains [4]. By increasing the specific surface area of the raw material, more favorable conditions for the flotation process are achieved and technological indicators of this process are improved.

For the range of these investigations, the most favorable technological results were achieved for 80 % of the class 0.074 mm.

The results of testing the flotation procedure for the concentration of copper minerals from the Cerovo C2 cementation zone samples unambiguously indicate the possibility of applying this technological operation for the successful valorization of copper minerals from the ore.

Acknowledgements:

These investigations were conducted under the Project 33007, “Implementation of new technical, technological and environmental solutions in the mining and metallurgical operations RBB and RBM”, funded by the Ministry of Science and Technological Development of the Republic of Serbia.

References

1. Stojanovic, J. (2018) Kvantitativna mineraloška analiza rude ležišta Cerovo C2, ITNMS, Belgrade,
2. Milosevic, V. et al, (2018) Elaborat-Tehnološka laboratorijska ispitivanja uzoraka rude iz rudnog tela Cerovo-Cementacija 2, ITNMS, Belgrade
3. Bulatovic, S. (2010) Handbook of Flotation Reagents: Chemistry, Theory and Practice. 1st Edition, Elesevier Science and Technology Books, 230,
4. Magdalinovic, N. (1991) Usitnjavanje i klasiranje, Naučna knjiga, Beograd.

XIII International Mineral Processing and Recycling Conference
Belgrade, Serbia, 8-10 May 2019

University of Belgrade, Technical Faculty in Bor
Vojske Jugoslavije 12, 19210 Bor, Serbia
Tel. +381 30 424 555 Fax +381 30 421 078

THE EFFECT OF DIFFERENT COLLECTORS ON THE FLOTATION RESULTS IN THE COPPER MINE MAJDANPEK

Jovica Sokolović [1,#], Rodoljub Stanojlović [1], Ljubiša Andrić [1,2], Zoran Štirbanović [1], Nikola Ćirić [3]

[1]University of Belgrade, Technical Faculty in Bor, Bor, Serbia
[2]Institute for Technology of Nuclear and other Mineral Raw Materials, Belgrade, Serbia
[3]Zijin Bor Copper d.o.o, Copper Mine Majdanpek, Majdanpek, Serbia

ABSTRACT – This paper present comparative study between different collectors on the flotation results of copper ore from the deposit „North revir" in the Copper Mine Majdanpek. Various collectors and combinations of them were used for experimental study in the flotation of copper ore and the results showed that collectors dosages of 20 g/t Z11, 8 g/t AP3404 and 8 g/t SKIK BZ 2000 produced the maximum Cu recovery (84.96 %).

Key words: copper, ore, Majdanpek, flotation, collectors.

INTRODUCTION

Copper flotation is a process strongly influenced by many factors related to the copper ore (grade, particle size distribution, surface properties, degree of liberation etc.) and with the process variables (reagent type and dosage, pH, froth speed etc.).

Collectors play a critical role in the flotation of copper ores. For many decades, the most commonly used collector alone or combinations were those of xanthate and dithiophosphate, or of xanthate and dialkyl thionocarbamate. Xanthate collectors were introduced in 1925, and are still widely used, especially for easy-to-treat copper ores. However, in the past 10-15 years, a large number of new collector has been developed and introduced by Cytec [1].

Various collectors and combinations of them were used for experimental study in the flotation of copper ore from the Copper Mine Majdanpek (RBM), which is a part of Zijin Bor Copper d.o.o. (formerly known as RTB Bor).

corresponding author: jsokolovic@tfbor.bg.ac.rs

EXPERIMENTAL

Material

The copper ore sample was collected from the flotation plant of the Copper Mine Majdanpek in Serbia. It is a composite of copper ore samples from the "North Revir" deposit. The sample was ground on a laboratory jaw crusher into a closed cycle with 3.37 mm sieve.

Mineralogical analyses

Mineralogical analyses of copper ore were determined by ore microscopy. Qualitative mineralogical analysis was performed in reflected light in air and immersion (cedar oil), on Carl Zeiss-Jena, JENAPOL-U microscope and system for microphotography "STUDIO PCTV" (Pinnacle) with identification of ore and non-ore minerals. Objective magnification was from 10 to 50x (exceptionally 100x in oil immersion).

Mineralogical analyses of copper ore are shown in table 1 [2, 3].

Table 1. Mineralogical analyses of copper ore

Mineral	Chemical formula	Content (%)
Quartz	SiO_2	49.10
Dolomite	$CaMgC_2O_6$	15.50
Calcite	$CaCO_3$	13.60
Albite	$NaAlSi_3O_8$	11.50
Pyrite	FeS_2	7.30
Chlorite	$Al_{0,865}\ Fe_{0,255}\ H_4Mg_{2,292}\ O_9Si_{1,588}$	3.10
Chalcopyrite	$CuFeS_2$	0.80
Chalcosine, magnetite, sphalerite	Cu_2S; Fe_3O_4; ZnS	0.20

Mineralogical analysis indicated the presence of following minerals: pyrite, chalcopyrite, chalcocite, bornite, covellite, cuprite, magnetite, rutile, limonite, sphalerite, galena, tailings minerals.

The main copper mineral is chalcopyrite, which is compared to the ore minerals, represented by about 10 %, while other ore minerals account for about 2 %. Pyrite is the most abundant mineral in relation to other ore minerals.

Chemical analyses

The average chemical composition is presented in table 2 [3].

Table 2. Chemical analyses of copper ore

Elements	Cu^{tot} (%)	Cu^{sul} (%)	Cu^{ox} (%)	S (%)	Pb (%)	Zn (%)	Ag (g/t)	Au (g/t)
Content	0.273	0.253	0.02	4.63	Ø	0.08	1.20	0.20

Chemical analyses showed that average copper content was 0.273 % with a dominant portion of sulfide copper (0.253 %). The content of precious metals (Au

and Ag) in the ore was 0.2 g/t and 1.2 g/t, respectively.

Grinding tests

The grinding test was carried out in a cylindrical laboratory ball mill, dimension (DXL) = (400x125 mm) with a 65 % (in weight) of solid in pulp. Grinding time was 685 s. Grain size composition and distribution of copper and sulphur in the grinding product of copper ore is given in table 3 [3].

Table 3. Chemical analyses of the product of grinding

Grain size (μm)	Mass (%)	Cu (%)	Cu^{ox} (%)	S (%)	Distribution	
					Cu (%)	S (%)
+ 147	16.13	0.20	0.01	3.54	11.49	12.33
- 147 + 74	26.81	0.26	0.01	6.70	21.86	37.28
- 74 + 37	15.67	0.34	0.02	6.31	21.28	21.36
- 37 + 0	41.39	0.36	0.06	3.51	45.36	29.03
Total:	100.00	0.273	0.02	4.63	100.00	100.00

It can be seen from table 3 that the highest average copper content (0.36 %) is in the finest grain size below 37 microns.

Flotation tests

After grinding, copper ore samples with 65 % of grain size fraction - 74 μm were submitted to flotation. Flotation tests were carried out using a laboratory flotation machine DENVER DR-12 with a cell volume of $2.7 \cdot 10^{-3}$ m^3.

A technological scheme of laboratory flotation test is given in figure 1.

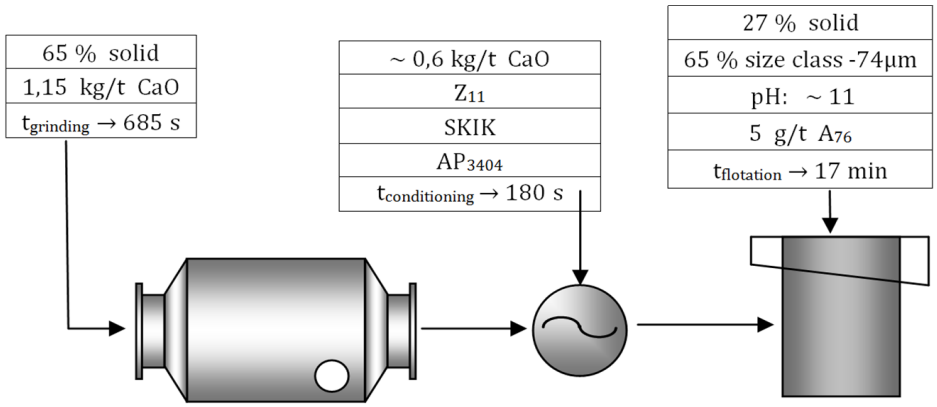

Figure 1. Technological scheme of laboratory flotation tests

In the flotation test are used the next collectors: Z11, Aerophine 3404 (AP3404) and SKIK.

Z11 (sodium isopropyl xanthates) was obtained from Chemical Industry Župa Kruševac (Serbia).

Aerophine 3404 promoter (dialkyl dithiophosphinates) is a Cytec collector. It is an effective primary collector in the selective flotation of lead/gold/silver minerals with low copper content. Aerophine 3404 promoter is highly selective against iron [1].

SKIK, a new collector with corrosion inhibition properties, was obtained from Metoha Tehnology Novi Sad (Serbia).

AEROFROTH 76A was used as a frother in all experiments.

The flotation tests were carried out with different collectors (alone or combination) and with different collectors dosage. Type and dosage of collectors (g/t) in the flotation tests is given in table 4 [3].

Table 4. Type and dosage of collectors (g/t) in the flotation tests

Collector	No 1.	No 2.	No 3.	No 4.	No 5.	No 6.	No 7.	No 8.	No 9.	No 10.
Z_{11}	25	35	45	-	-	-	20	18	18	20
AP_{3404}	-	-	-	25	35	45	8	10	12	16
SKIK	-	-	-	-	-	-	8	8	6	-
A_{76}	5	5	5	5	5	5	5	5	5	5

In the all experiments, the conditioning time was 6 minutes, and the flotation time was 17 minutes. Pulp pH values was 11, defined as optimal values [3].

RESULTS AND DISCUSSION

Results of flotation tests of copper ore are shown in table 5 [3].

Table 5. Results of flotation tests of copper ore

Test No.	Mass yield (%)	Content		Recovery	
		Cu (%)	S (%)	Cu (%)	S (%)
1	16.39	1.39	19.87	83.45	70.34
2	14.63	1.55	21.58	83.06	68.19
3	15.61	1.42	22.72	81.19	76.60
4	14.08	1.54	15.99	79.43	48.63
5	14.44	1.58	17.92	83.57	55.89
6	17.31	1.32	20.32	83.70	75.97
7	15.26	1.52	24.81	84.96	81.77
8	14.88	1.50	21.92	81.76	70.45
9	14.09	1.57	23.43	81.03	71.30
10	14.82	1.55	22.83	84.14	73.08

The effect of different collectors on copper (Cu) and sulphur (S) recovery is given on figure 2, as well as on copper (Cu) and sulphur (S) grade is given on figure 3 [3].

It can be seen that the collectors dosages of 20 g/t Z11, 8 g/t AP3404 and 8 g/t SKIK BZ 2000 produced the maximum Cu recovery (84.96 %). Copper grade was 1.52 %.

The results also show that when Z11 (sodium isopropyl xanthate) is used alone, even in smaller dosage, very good flotation results are achieved, while the use of

Aerophine AP3404 in the flotation of copper ore requires a significantly higher dosage to achieve more efficient flotation.

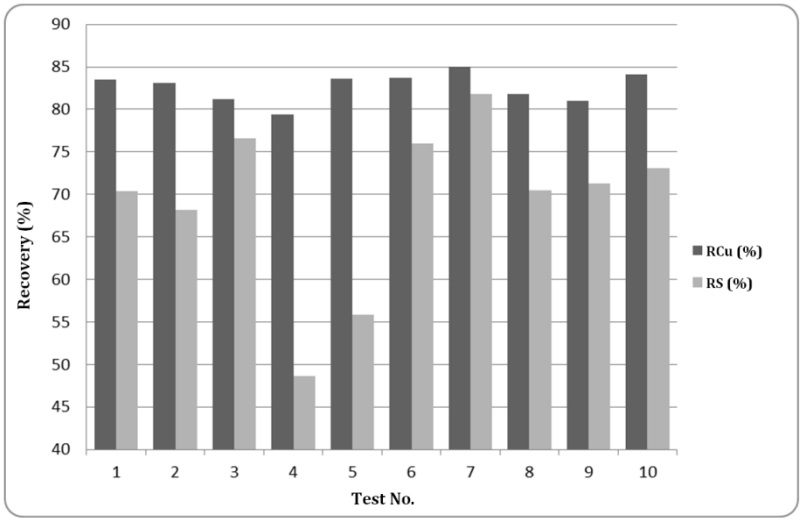

Figure 2. Effect of different collectors on copper (Cu) and sulphur (S) recovery

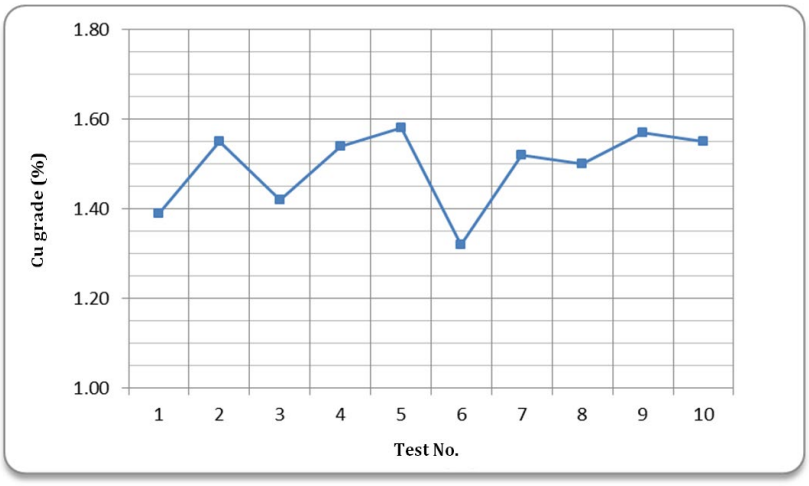

Figure 3. Effect of different collectors on copper (Cu) and sulphur (S) grade

It can be noticed that in the experiments in which 25 g/t of both collectors were used, the following, noticeably different results of copper recovery were obtained: Z11 (test no. 1) – 83.45 %; and AP3404 (test no. 4) – 79.43 %.

It was found that copper recovery increased from 79.43 % to 83.70 % with increasing dosage of AP3404 collector from 25 to 45 g/t. These results were achieved with a collector distribution pattern of 100 %.

Slightly better results were achieved with combination of both collectors such as: 20 g/t Z11 and 16 g/t AP3404 (test no. 10). Achieved copper recovery was 84.14 % with 1.55 % copper concentrate grade. Result of this study also show that the average copper grade in the rough concentrate was from 1.39 % (test no. 1) to 1.58 % (test no. 5).

Compared obtained result with result of previous study [4] it can be seen that the better flotation result was achieved in the laboratory flotation test than in the industrial flotation plant of the Copper Mine Majdanpek (copper recovery was 78.58 %)[4].

CONCLUSION

On the basis of obtained results, it can be concluded next:

- The results show that the distribution of collectors Z11, AP3404 and SKIK BZ 2000 (56 %, 22 %, 22 %) can produce the highest recovery (84.96 %).
- Copper grade in the rough concentrate was 1.52 %.
- The optimal dosages to achieve maximum recovery were found to be 20 g/t Z11, 8 g/t AP3404 and 8 g/t SKIK BZ 2000.
- In order to achieve better results in the industrial conditions, it is necessary introduction of new collectors and optimization of the dosage for copper flotation in the flotation plant of Copper Mine Majdanpek.

Acknowledgements:

This paper presents the results of the Projects TR 33007 and TR 33038 funded by the Ministry of Education, Science and Technological development of the Republic of Serbia. The authors are grateful to the Ministry for financial support.

References

1. Mining Chemicals Handbook, (2002) Cytec Industries Inc, www.cytec.com,
2. Stanojlović, R., Sokolović, J., Ćirić, N. (2015) Mineralogical analysis of the copper ore from the deposit "Severni revir" of Copper Mine Majdanpek, In: 47th International October Conference on Mining and Metallurgy - IOC 2015, October 04-06, 2015, Bor Lake, Bor, Serbia, Proceedings, 135-140,
3. Ciric, N. (2014) Investigating possibilities of improving technological process parameters of the basic flotation of copper ore from deposit "Severni revir" in the Copper Mine Majdanpek, Master thesis, University of Belgrade, Technical faculty in Bor, Bor, Serbia,
4. Stanojlovic, R., Sokolovic, J., Ciric, N. (2014) Technological requirements of new copper smelter of RTB Bor, a great challenge for the mining profession and science, Mining and Metallurgy Engineering Bor, (4) 49-64.

XIII International Mineral Processing and Recycling Conference
Belgrade, Serbia, 8-10 May 2019

University of Belgrade, Technical Faculty in Bor
Vojske Jugoslavije 12, 19210 Bor, Serbia
Tel. +381 30 424 555 Fax +381 30 421 078

A CASE STUDY OF EMULSIFYING THE COLLECTOR IN COAL FLOTATION TO IMPROVE THE SEPARATION EFFICIENCY OF FLOTATION CELL

Vineet Kumar [1, #], B. V. Sudhir Kumar [2]
[1]Nalco, An Ecolab Company, India
[2]Tata Steel Limited, India

ABSTRACT – Studies indicate that proper dispersion of flotation reagent improves the efficiency of the reagent and the flotation performance. Considering the same, an effort is been made by Nalco water in consultation with Tata Steel Limited to use newly developed emulsifier to emulsifying collector before being dosed into the floatation feed, so that the collector gets properly dispersed into the fines pulp and improved flotation performance can be achieved. The emulsifier provided better mixing of chemical with coal slurry. It helped to better coating of chemical on coal particles which helped in better recovery of clean coal (approx. 0.17% yield improvement).

Key words: mechanical emulsifier, coal, flotation, collector, recovery

INTRODUCTION

IN Wasehry#2, West Bokaro after De Sliming Screen the fines coal fraction (-0.5 mm to 0 mm) is sent to fines sump, from the sump the fines slurry is sent to conditioner through pump. Collector is being added to suction of the Pump and Frother is added in the conditioned and thoroughly mixed. After that the fines slurry is sent to Froth Flotation Cell through Pulp Density adjusting Tank. Froth is skimmed and mechanically removed from cell through with the help of froth paddle and collected in the Froth head box. There are four cells and each cell have 4 compartments. It is observed that the froth formation and froth stability in first compartment is very good but gradually it's get deteriorating towards last compartment. To improve the recovery from the third and fourth compartment of the cells, study of multidosing od collector and frother in third and fourth compartment was done with the below modalities and data was analyzed.

corresponding author: vkumar@ecolab.com

FEASIBILITY OF ENVISAGING MULTI DOSAGE POINTS OF COLLECTOR AND FROTHER IN FLOTATION CELL PLANT TRIAL

Trial Modalities

- Spilt Dosing of Frother and Collector was tried separately in the plant
- The trial was planned on two Provision
    - Equal spilt dosing across Conditioner and four compartments
    - 50% of the reagent was dosed in the conditioner and rest 50% was equally split in four compartments
- Samples were collected with single point dosing and split dosing
- Samples Collected: Feed, Froth and Tailings
- Separation efficiency and Yield on Ash basis will be the criteria to access the benefit.

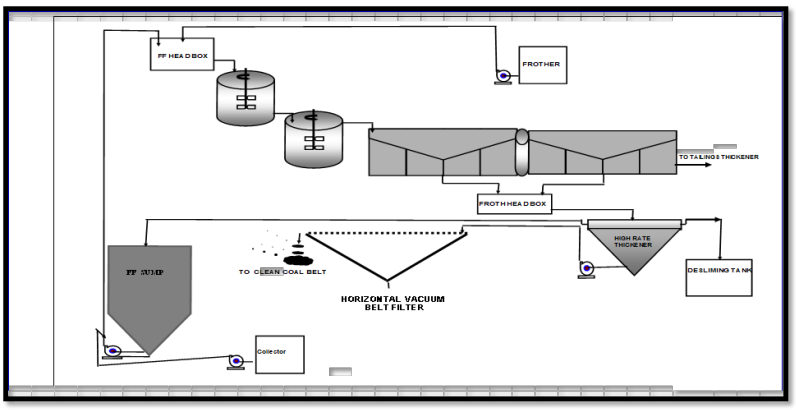

Figure 1. Schematic Diagram of Flotation circuit at Tata Steel West Bokaro, Washery II

Kpi

- KPI Impact: Improvement in Separation Efficiency of flotation of Coal.
- Potential Saving (In Crore): 1% increase in separation efficiency will led to 1% increase in fines yield. 1 Crore.

Table 1. Split Dosing of Frother Result and Observation

	Feed	Froth	Tailings	Yield on Ash Basis	Separation Efficiency
Single Dosing	22.2	10.7	34.9	52.5	31.2
Split Dosing	22.2	10.1	35.4	52.1	32.85

- No any significant yield improvement observed.
- Due to excess froth generation, water clarity from thickener deteriorated. Observed TSS was approx. 200 ppm as against plan of maximum 150 ppm.

Table 2. Split Dosing of Collector Result and Observation

	Feed	Froth	Tailings	Yield on Ash Basis	Separation Efficiency
Single Dosing	24.1	11.8	37.8	52.8	31.3
Split Dosing	24.1	11.7	37.3	53.6	31.1

- No any yield improvement observed.
- Due to excess froth generation, water clarity from thickener deteriorated. Observed TSS was approx. 200 ppm as against plan of maximum 150 ppm

EMULSIFICATION OF COLLECTOR DOSAGE TO IMPROVE THE SEPARATION EFFICIENCY OF FLOATATION CELL

As the split/multi dosing of any reagent (Collector/Frother) not given the expected result, then we explored the idea of emulsification of collector. A newly developed emulsifier is aimed emulsify the collector before being dosed into the floatation feed, so that the collector get properly dispersed into the fines pulp and improved flotation performance can be achieved. Two nos. Of Emulsifier unit were imported from Australia and installed in washery2.

Emulsifier: Installation and Working Philosophy

Flotation reagents Collector and Frother are normally Oil derivatives and they can't mix in water properly. A Mechanical emulsifier apparatus uses High speed and high shearing mixing process to emulsify the flotation reagents into water.

Figure 2. Emulsifier

The emulsifier works with water entering at "A" (25 mm male British Standard Pipe [BSP] thread), frother or collector entering at "C" (19 mm female BSP thread) and the emulsified solution exiting at "B" (19 mm male BSP thread).

Some checkpoints:

1. The water flow through "D" should be >10 m/sec to generate nano bubbles. To test this - if it sprays 15-20 metres out of the nozzle then the water pressure is sufficient.
2. If the water volume is too high and flows back out of "C" then try to add some down slope to syphon the emulsion out of the unit. The nozzle can be made smaller but then the concentration of the emulsion increases – however this may still be necessary. Emulsion of any sort is better than no emulsion but nano bubbles are the best.
3. The unit is at atmospheric pressure so the delivery cannot rise above point "C" otherwise the emulsified water will flow out of "C".
4. The frother or collector is added at "C". This is opened to the atmosphere and a vacuum is generated. Smell is draw into the vacuum.
5. The pipe from "C" to "B" allows a mixing chamber after the nozzle orifice and also delivers an attachment mechanism for cable ties etc along a hand rail.

PLANT TRIAL WITH EMULSIFICATION OF COLLECTOR

The trial was taken at Washery # 2 which comprise of 4 cells. The Emulsifier unit was installed in the section of Flotation Cell feed pump and collector is being dosage at the existing rate through the emulsifier. Following modalities is being adopted during the trial.

Trial Modalities:

1. The emulsifier is installed at Collector dosing pump discharge side, with a provision to bypass it as & when required so that the flexibility is received for on/off states.
2. Water line taken from High pressure pump line.
3. The ratio of Water: Collector will be maintained adequately.
4. The trial was started maintaining all the dosage parameters same.
5. The comparative results in terms of Feed, Froth & Tailing ash & yield was monitored and tabulated.
6. All the controlling parameters of the flotation were monitored.

KPI:

1. Flotation clean coal yield improvement by 1% (on ash balance basis) in Fine Coal Circuit.
2. Base Line: Fine coal yield 7.61% on Raw Coal Basis (Dry Basis).
3. Target: Fine Coal Yield 7.76% on Raw Coal Basis (Dry Basis).

Trial Observation and Results

Statististical Analysis of the data generated from trial was anaylised and summary of the analysis indicates significant improvement in plant trhoughput. Summary of the Trial ***tonnage per hours is as below.***

Table 3. Trial tonnage per hours

	Feed Ash	Froth Ash	Tailings Ash	Separation Efficiency	% Yiled (Dry Basis)
Pre - Trial	24.03	13.41	39.86	28.65	7.61
Trial-Emulsification	25.45	13.69	40.62	29.4	7.78

- There was not any process disturbance during the trial.
- Pre-Trial data is of May Month and post-trial data is of July and August'17.
- Separation Efficiency increased by about 1%.
- Yield on raw coal basis increase by 0.17% against the base line. (7.78% against the baseline 7.61% and against target 7.76%).

Table 4. Monthly Dashboard of Yield Gain through Emulsification of Collector

SRM Project : Feasibility of envisaging multi dosage points for process optimization											
Plant Location	Project Id	Project Owner	KPI	Unit of KPI	Base Line	Target	Annual Potential Saving (In Crore)	Project Start	Project Finish	Month in which saving accrual is expected	Project Status
West Bokaro	ASPIRE/SIP/47051	Mr. Rajeev Ranjan	Fine coal yield	%	7.61	7.76	1	Jan-17	Jul-17	Jul-18	Project completed in Sept'17
Project Outcome Dashboard											
	Sept* 17	Oct'17	Nov'17	Dec'17	Jan'18	Feb'18	Mar'18				
Fine Coal Yield Improvement (%)	0.15% (294 Mt of C Coal)	0.22% (377 MT of C Coal)	0.09 %(176MT of C Coal)	0.14%M 177MT of C Coal)	0.11%(288 MT of C Coal)	0.08% (143 MT of C Coal)	0.13% (249 MT of C Coal)				

CONCLUSION

The installation of emulsifier provides better mixing of chemical with coal slurry. It helped to better coating of chemical on coal particles which helped in better recovery of clean coal. The approximate 0.17% yield improvement is gained and considering Rs/- 5000 per ton effective price of C Coal and 2.2 million ton per annum the net saving will be Rs/- 165 lacs.

References

1. Project report on "Feasibility of envisaging multi reagent dosage points for process optimization in flotation cell at Washery II, Tata Steel, West Bokaro" by R K Ranjan,
2. Trial Report on "Emulsifying of Collector for Separation Efficiency Improvement in Flotation Cell at Tata Steel, West Bokaro Washery" By Nalco, An Ecolab Company.

XIII International Mineral Processing and Recycling Conference
Belgrade, Serbia, 8-10 May 2019

University of Belgrade, Technical Faculty in Bor
Vojske Jugoslavije 12, 19210 Bor, Serbia
Tel. +381 30 424 555 Fax +381 30 421 078

INFLUENCE OF REAGENTS ON PHYSICAL AND MECHANICAL PROPERTIES OF MINERALS

Degodya Elena Yurevna, Shavakuleva Olga Petrovna #
FSBEI HPE Nosov Magnitogorsk State Technical University, Department of Geology, Mine Surveying and Mineral Dressing, Magnitogorsk, Russia

ABSTRACT – There are reagents that are widely used in the processing of mineral raw materials, but their effect is not fully understood. The paper studies in detail the effect of the reagent-liquid glass on the physical and mechanical properties of titanomagnetite, magnetite ore and metallurgical waste. The results prove that the interaction of liquid glass with the surface of minerals changes the properties of ore, which affect the enrichment parameters. The presented results reflect its novelty.

Key words: ore dressing, ore, liquid glass, grinding.

RESULTS AND DISCUSSION OF THE RESULTS

Liquid glass is one of the most common reagents used in the processing of mineral raw materials. The main valuable properties of liquid glass is non-toxic, environmentally friendly, inexpensive, non-deficient and affordable reagent.

A large amount of research is devoted to liquid glass, while there is currently no single theory that adequately reflects which form of liquid glass is the most active [1]. Considering that the majority of authors have conducted studies on the effect of liquid glass on various minerals and in various conditions using different processes, it can be assumed that there is no single mechanism of action of liquid glass - common for various minerals and various conditions. Probably, the mechanism of action of liquid glass and actively depressing or activating forms will be determined by the nature of the mineral and the process conditions. To clarify the mechanisms of action of liquid glass, we conducted studies and obtained certain results reflecting the novelty of the work.

The effect of liquid glass was studied to intensify the process of grinding iron-containing ores, such as magnetite ore from the Maly Kuibas deposit and titanium-magnetite ore from the Kopan deposit.

The influence of reagents on the grinding of titanium magnetite ore was studied. The following reagents were used: soda ash, sodium oleate, sodium tripolyphosphate and tall oil [2, 3]. The results of grinding of titanomagnetite ore for 40 min with the

corresponding author: shavakylevao@yandex.ru

addition of various reagents show that of all the studied reagents, the greatest influence on the grinding process of titanomagnetite ore is exerted by liquid glass. At a reagent concentration of 160 mg/dm^3, the increase in the finished class - 0.071 mm was 12 %.

The results of grinding magnetite ore showed that the greatest effect on the efficiency of destruction of minerals has a liquid glass, so the concentration of the reagent 120 mg/dm^3 increase in the finished class - 0.071 mm was 23 %.

The work also conducted experiments with metallurgical slag. The results obtained show that at a reagent concentration of 120 mg/dm^3, the increase in the finished class of - 0.071 mm in crushed slags was 21 %.

The use of liquid glass in grinding gives an increase in the growth class - 0.071 mm in the crushed product by fixing the reagent on the surface of minerals, which leads to a decrease in the specific free surface energy on the interface.

The specific free surface energy, that is, the energy spent on the formation of a unit of surface is equal to [4]:

$$\sigma = \frac{E_s}{2 \cdot S} \tag{1}$$

E_s - the energy to rupture, Joules;
S - breaking the surface, cm^2.

For a crystal containing N atoms (n is the Avogardo number) with a coordination number ν for each atom, the number of bonds will be, since one bond falls on 2 neighboring atoms. The energy of a single bond (e) will be equal to the atomization energy (E) divided by the total number of bonds [4]:

$$e = \frac{2 \cdot E}{\nu \cdot N} \tag{2}$$

In a magnetite crystal with a face-centered cubic lattice, when the discontinuity surface passes through the plane (III), the energy of formation of the surface unit (1 cm^2) is equal to:

$$\sigma = \frac{2 \cdot K \cdot E}{\nu \cdot N} \tag{3}$$

К - coefficient of proportionality.

The number of bonds per unit surface will be proportional, where R is the interatomic distance. Thus:

$$\sigma = \frac{K \cdot E}{R^2} \tag{4}$$

From formulas (1) to (4), we can conclude about the proportionality of the magnitude of the surface energy and the energy of atomization. Thus, the fixed ions

and molecules of reagents reduce the strength of minerals, as the atomization energy of the crystal decreases. Thus, in the case of liquid glass ions SiO_3^{2-}, $HSiO_3^-$ and H_2SiO_3 molecules, fixed on the surface of minerals, reduce the symmetry of the system, which leads to a decrease in the stability of the crystal lattice, the destruction of which requires less energy.

The results of studies of the effect of liquid glass on the performance of wet magnetic separation of titanium magnetite ore showed that at a liquid glass concentration of 160 mg/dm^3, the mass fraction of iron in the concentrate increases from 57.90 to 64.16 %, and the extraction of iron into the magnetic fraction - from 86.00 to 91.48 % of the operation. The mass fraction of titanium dioxide is reduced from 11.32 to 5.84 %, and extraction - from 69.52 to 34.43 %.

CONCLUSION

The results allow us to draw the following conclusions:

1. The use of liquid glass leads to an increase in the amount of the resulting class - 0.071 mm in crushed iron-containing products.
2. Liquid glass reduces the magnitude of the coercive force and substantially dampens the magnetic properties of the minerals that improves the quality of the concentrate in the subsequent magnetic cleaning out.

References

1. Eigeles, M. A. (1977) Reagents - Regulators in the Flotation Process. Nedra, Moskow, 216,
2. Chizhevsky, V. B. Quality Improving of Iron-Vanadium Concentrate in Processing of Titanium-Magnetite Ores"/V.B. Chizhevsky, N. A. Sedinkina, O.P. Shavakuleva //Progressive Methods of Dressing and Integrated Utilization of Natural and Technogenic Raw Minerals (Plaksinsky Scientific Conference -2014): Materials of International Scientific and Practical Conference under general editorship of the RAS Academician V.A. Chanturiya. – Almaty, LLP "Arko", Karaganda, 2014. 582-584,
3. Shavakuleva, O. P. (2006) Effect of Grain Size of Ferromagnetic Minerals on the Magnetic Properties. Mining Information and Analytical Bulletin, 1, 340-342,
4. Urus, V. S. (1975) Energy crystal chemistry. 335.

XIII International Mineral Processing and Recycling Conference
Belgrade, Serbia, 8-10 May 2019

University of Belgrade, Technical Faculty in Bor
Vojske Jugoslavije 12, 19210 Bor, Serbia
Tel. +381 30 424 555 Fax +381 30 421 078

A CASE STUDY OF FLOWABILITY IMPROVEMENT USING SUPER ABSORBENT POLYMER AT TATA STEEL NOAMUNMDI NDCMP

Parveen Kumar Dhal [1], Himanshu Sarangi [1], Ranjan Kumar [1, #], Parag Mukherjee, Vineet Kumar [2]
[1]Tata Steel Limited, Noamundi, India
[2]Nalco Water India Ltd., Kolkata, India

ABSTRACT – The flowability of iron fines largely depends on the particle size, particle distribution and its shape and the moisture content of the material also have considerable influence on the flowability. The flowability of iron ore fines have always been an issue and during monsoon season the issues gets exacerbated because of high moisture content (> 9.5%) in ores and production gets hampered badly. To cater the flowability issue in Tata Steel, Noamundi iron ore mines NDCMP and Nalco team used super absorbent polymer in their circuit and the application helped significantly to increase the flowability and hence the production.

Key words: flowability, super absorbent polymer, critical moisture, iron ore, stickiness

INTRODUCTION

TSL-Dry Plant designed capacity is 1000 MT/hr which produces -10 mm product in order to cater the requirement of TSL-Jamshedpur Pallet and Sinter Plant. The Dry plant is in two part, 1. New DCMP and 2. 1000TPH Plant. 1. In New DCMP, The ROM (-1000 mm) is dumped into primary crusher (Set Size-150 mm) and subjected to screened through double decker screens. The underflow of DDS, -40 mm is directly sent into DC1E conveyor. The DDS oversize material (150x40 mm) is taken through DC-1C conveyor for secondary crushing after that -40 mm product is sent for further crushing to 1000TPH Plant.

In 1000TPH Plant, the underflow of single deck and double deck screen, i.e. -10 mm material is directly sent to product surge bin through NDC11, NDC12 and NDC20 conveyor. The single deck and double deck screen over size (40x10 mm) material taken through NDC9 for Tertiary Crushing and after that -10 mm material sent to product surge bin through NDC18, NDC19, NDC12 and NDC20 conveyors. From surge bin -10 mm materials sent to Stackyard for further processing.

The flowability of iron ore fines have always been an issue and due to this flowability issue DRY plant was facing major challenges in production especially in

corresponding author: ranjan.kumar@tatasteel.com

monsoon season. the flowability of iron fines largely depends on the particle size, particle distribution and its shape and the moisture content of the material also have considerable influence on the flowability. During monsoon season the issues gets exacerbated because of high moisture content (> 9.5%) creating the binding of clays into the ore surface resulting in the flowability issue. These includes:

- Poor screening Efficiency leading to FFS high current.
- High recycle load due to poor screening in Multi flow screens.
- Material deposition in transfer chute and Bunker choking issue.
- Material deposition in arm guards of HP 4 crushers which leads to premature failure of U seal and T seal.

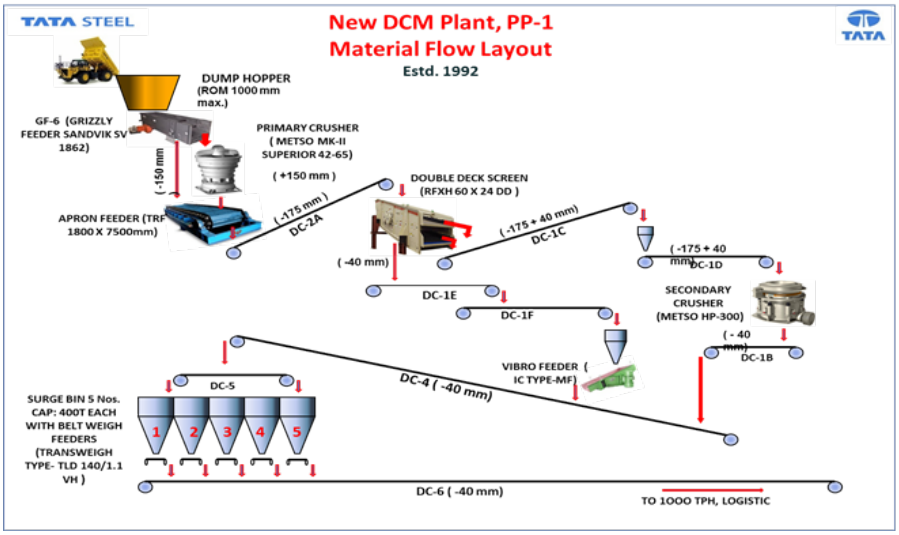

Figure 1. Flow Sheet of New Dry Circuit Material Plant- Noamundi Mines, TATA STEEL

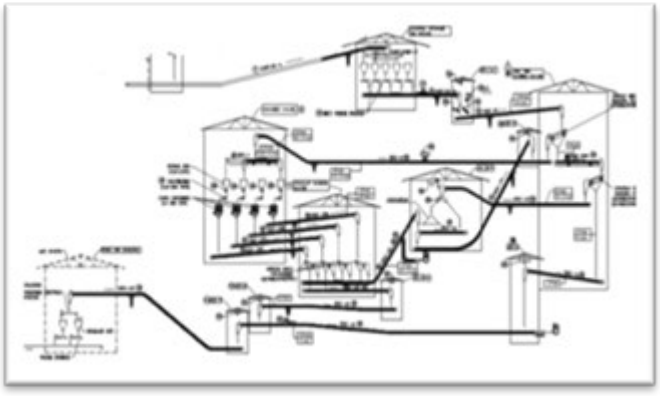

Figure 2. Flow Sheet of Dry Circuit Material Plant (1000TPH)- Noamundi Mines, TATA STEEL

To cater the flowability issue Nalco emulsion moisture absorbent was initially used, and the application helped significantly to increase the iron ore fines flowability and hence the production. To improve further, Nalco to use its product Release Ez, which is a Super absorbent polymer in powder form and in general the powder SAPs have higher absorption ratio (amount of water absorbed per gm of SAP).

RELEASE EZ 81609: WORKING PRINCIPLE AND MECHANISM

Nalco Release Ez is a very high molecular mass, crossed linked polyelectrolytes polymers and it can absorb and retain extremely large amount of water or any liquid relative to their own weight. This class of polymers are known as super absorbent polymer (SAP) and it is one of the best commercially available SAP in market. It exhibits quick and high absorption capacity.

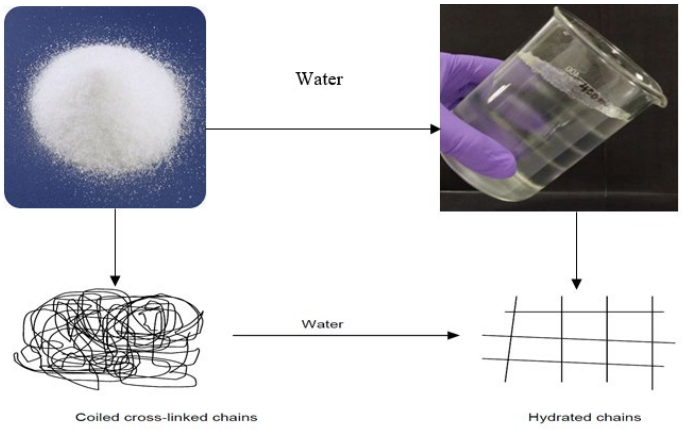

Figure 3. How the Cross-linked Chains get opened after absorbing water

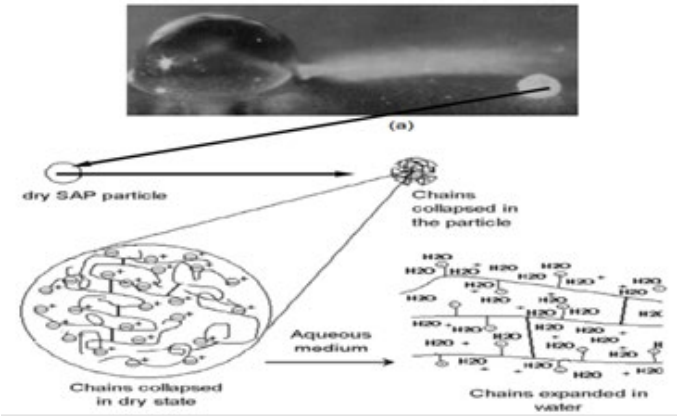

Figure 4. What really happens

HOW ABSORPTION RATIO IS CALCULATED

Following test protocol can be used to check the absorption ratio of the chemical.

1. 1.0 g of polymer used for each set of experiment
2. 50 ml to 500 ml of water added to 1.0 g of polymer
3. Stopwatch was started immediately
4. Shake the solution for 20 to 30 secs with glass rod
5. Then allowed to form the gel naturally. This gel formation starts from bottom of beaker
6. Time was measured, and photos was taken for each set of experiment.

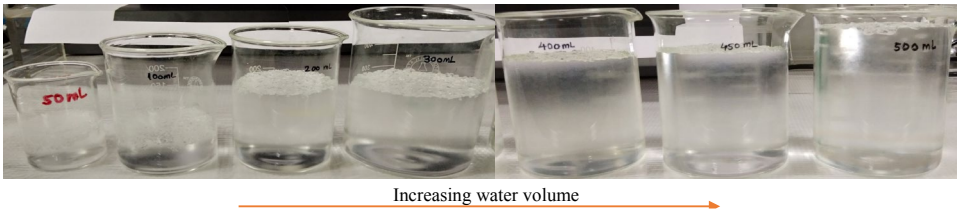

Figure 5. ReleasEZ 81609 Absorption Study

– 1 gm of Release Ez 81609 can adsorb 650 ml or more water. Whereas common SAP present in market can adsorb only 200-250 ml of water.

TEST WITH IRON ORE

A comprehensive test was conducted with -10 mm iron fines to check the efficacy of the chemical and find out the optimized dosage range. The test was conducted with varying moisture content (8.98% -12.43%) in iron ore fines and it was evident from the test results that chemical was instantly absorbing the inbound moisture from the fines and after mixing the chemical ore is looks completely dried up. The optimum dosage range was found in the range of 40 gpt to 80 gpt depending upon the moisture content in iron ore.

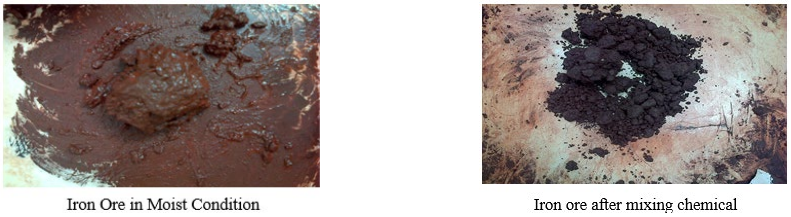

Figure 6. Effect of chemical with moist Iron ore

PLANT SCALE TRIAL

To check the efficacy of the chemical during adverse situation and with extremely sticky ore it was decided that the trial will be doen at extreme rainy season. A two-week trial with Nalco ReleasEZ 81609 at New DCMP Noamundi started from 28th August in Monsoon season. The Trial was started with following DOE and KPI

- Dosing of the Nalco chemical will be done at only one point at Apron Feeder and dosage rate will be start from 30 Gpt.
- Only trained operator having valid permanent gate pass will be involve in the Trial.
- Main KPI will be to increase the throughput (average TPH) of the plant from its existing level to at its optimum level at minimal chemical dosage.

Figure 7. Chemical Dosing System and Dosing Points

TRIAL OBSERVATION

- Trial duration was for two weeks at New DCMP Noamundi from 28th August till 11th September. September'18 to check the efficacy of the New powder flowability aid.
- After starting of the trial it was observed that the Nalco ReleasEZ 81609 was very hygroscopic (Moisture absorbing capacity) and it was absorbing moisture from atmosphere instantly. That was affecting the performance of the chemical. To cater the situation, we installed heating arrangement with the dosing system and run the trial.
- Our entire focus in this trial was to maintain the throughput under extreme conditions. After initial stabilising period there was no jamming/choking issue during entire trial period even in the peak monsoon period.
- There was continuous heavy rain fall for last five days of the trail, but no choking/jamming issue was reported. The average TPH in both the plants were above 1000 TPH (rated Capacity).
- The consumption pattern in normal condition was about 28-35 GPT, which in extreme situation with very sicky ores, went up to 70-75 GPT in heavy rain period.

PLANT SCALE TRIAL DATA ANALYSIS

Statististical Analysis of the data generated from trial was anaylised and summary of the analysis indicates significant improvement in plant trhoughput. Summary of the Trial ***tonnage per hours is as below***:

Table 1.

Average	Median	Maximum	Minimum	Std Dev
1022	1022	1359	727	120

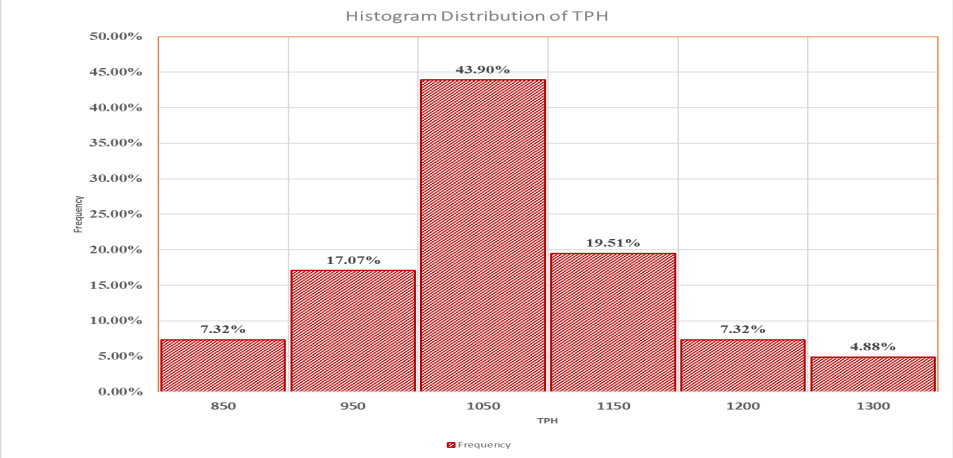

Figure 8. Histogram Distribution of Tonnage per Hour

From the graph it is evident that 75% times during the trial the average TPH was above 950. Approximately 50% the plant TPH was above the rated capacity of 1000 TPH.

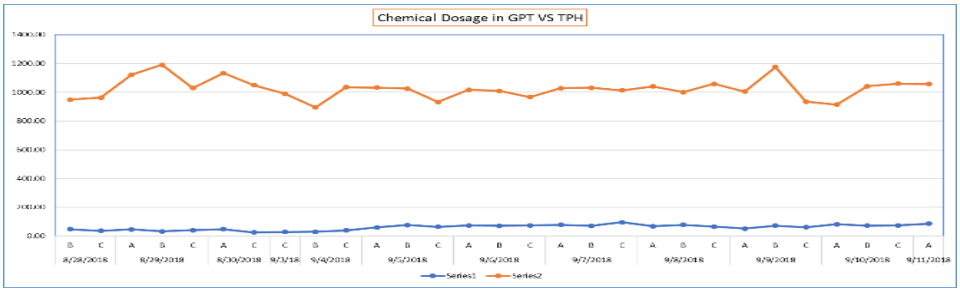

Figure 9. Chemical Dosage VS TPH profile

The graph shows that the TPH was almost at 1000TPH maintained but afterwards chemical consumption has been increased.

Figure 10. TPH Profile during the Trial

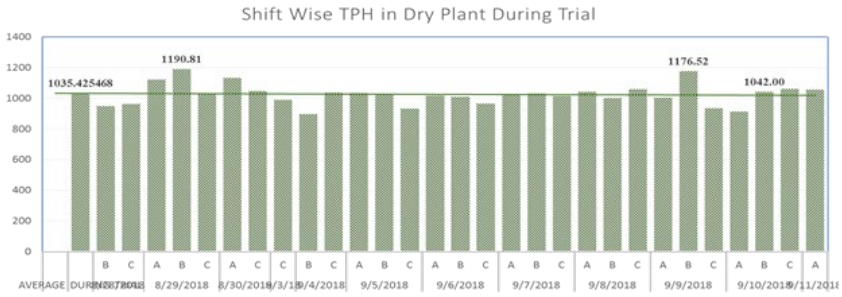

Figure 11. Shift wise THP in dry plant during trial

CONCLUSION

Statististical Analysis of the data generated from the trial are analysed for trial. Summary of the stastiscal analysis indicate that there is an average gain of 80 TPH production increase due to the addition of Release Ez 81609 flowability Aid. More Importantly we could maintain the optimum throughput of the plant under extreme conditions.

References

1. Quintero, E., Marino, N. (1990). The Venezuelan bauxite project. Light Metals 1990, 5-10,
2. Faneitti, M., Fernandez, E., Romero, J., Franquiz, N., Gross, A.E. (1994). Wet Bauxite Ore Handling Control. Light Metals 1994, 11-13,
3. Gross, A.E., Owen, D.O. (1993). Development of a Bauxite Dust Control and Ore Handling Agent. Light Metals 1993, 5-8,
4. Flow properties of iron ore with additive N-85810, R&D Centre, NMDC Limited, April-2014,
5. Grima, A., Wypych, P. (2014) Flow Property Testing of Joda East Iron Ore and Development of EDEM Material Models, Project No. BME-1423,
6. Pal, B.K., Nayak, N.P. Feasibility of Beneficiation of Low Grade Iron Ore Fines/Slimes, 2-4,
7. Pradip. (2006) Processing of alumina-rich Indian iron ore slimes. International Journal of Mineral, Metals and Materials Engineering, 59(5), 551-568.

XIII International Mineral Processing and Recycling Conference
Belgrade, Serbia, 8-10 May 2019

University of Belgrade, Technical Faculty in Bor
Vojske Jugoslavije 12, 19210 Bor, Serbia
Tel. +381 30 424 555 Fax +381 30 421 078

EFFECT OF SODIUM OLEATE ON HYDROPHOBICITY OF CALCITE

Ilker Acar [#], Ozkan Acisli
Ataturk University, Faculty of Earth Sciences, Oltu, Turkey

ABSTRACT – In this study, surface modification of calcite was examined using sodium oleate as a modifying agent. Effect of the modifier dosage was studied by a laboratory stirred ball mill in wet condition. The modification efficiency was evaluated mainly by floating test. Thermogravimetric analysis was also carried out to determine the amount of sodium oleate on the modified calcite surface. Overall results have shown that natural hydrophilic calcite can be easily made hydrophobic using sodium oleate, and the optimum active ratio of 99 % was achieved with the dosage of only 5 kg/ton.

Key words: surface modification, calcite, hydrophobicity, sodium oleate

INTRODUCTION

Calcium carbonate ($CaCO_3$) is the most widely used filler in the industries of plastics, rubber, paper, paint and ink mainly due to its broad availability in readily usable form and low cost [1, 2]. Due to its ideal properties like superior whiteness, inertness and incombustibility, and besides low oil-adsorbency and water adsorption, ground calcium carbonate (GCC) constitutes more than 80 % of the total $CaCO_3$ consumption. GCC is extensively used in polymer composites to improve physical properties and workability, provide numerous functionalities and reduce cost [3, 4].

Despite their desirable properties, hydrophilic $CaCO_3$ particles are also very adhesive and easy to agglomerate, causing poor dispersion in organic matrices and detrimental effects especially on impact strength. Therefore, it is necessary to make surface of the calcite filler hydrophobic using a surface modification process to improve the dispersibility, water resistance, mechanical properties and reinforcement in a polymer composite [3, 4, 5].

Mechano-activated surface modification is a method which utilizes mechano-chemical effect during ultrafine grinding. Since dry processes require comparatively longer time and much more energy, surface modification in wet ultrafine grinding system is the preferred method used to produce high quality mineral powder.

Nowadays, wet-stirred ball milling, which combines ultrafine grinding together

[#] corresponding author: ilker.acar@atauni.edu.tr

with surface modification, is the most commonly used method for this purpose [6, 7]. Of the various surface modifiers, such as silanes, phosphates, titanates, zirconates, etc, fatty acids and their salts are the most frequently used to improve calcite's compatibility with, and dispersion in, polymers [4, 5].

In this study, surface modification of natural ground calcite was examined by wet-stirred ball milling using a fatty acid salt, sodium oleate as a modifying agent. Modification efficiency was evaluated mainly by floating test, and also using thermogravimetric (TG) analysis.

EXPERIMENTAL AND MATERIALS

The ground calcium carbonate (GCC) was prepared by crushing and grinding of a natural calcite sample. A fatty acid surfactant, sodium oleate (oleic acid sodium salt) was used for the surface modification. The main chemical composition of the GCC sample was determined by X-ray fluorescence (XRF) spectrometry. The loss on ignition (LOI) test was carried out in an air oven at 1050 ^{o}C for 4 h. Laser size analysis was used for the particle size measurement. The specific gravity measurement was done using a water pycnometer. Table 1 shows the basic chemical composition and physical properties of the GCC sample.

Table 1. The main chemical composition and basic physical properties of the sample

Chemical composition	
Constituent	**%**
CaO	55.30
SiO_2	0.18
MgO	0.60
Fe_2O_3	0.11
LOI (CO_2)	43.66
Physical properties	
Average particle size, d_{50} (μm)	7.32
Specific gravity	2.64

According to Table 1, chemical composition of the GCC sample is almost completely constituted by $CaCO_3$ (CaO + CO_2) content, which is totally 98.96 %, since the weight loss during the LOI test is resulted from the evaporation of CO_2 from the sample.

METHODS

The surface modification tests were conducted by a laboratory scale Union Process HD-01/HDDM-01 Attritor in wet condition. Non-metallic media was used as the grinding medium. Sodium oleate dosage was selected as the experimental variables, whereas 60 g of the GCC sample, 50 % pulp density, 15 min of the residence time, 1000 rpm of the rotary speed and 280 mL of the grinding media were kept

constant through the modification tests. At the end of each test, the modified GCC was separated from the grinding media and the aqueous phase, followed by washing with distilled water and drying at 50 °C.

Floating test was used mainly to evaluate the modification efficiency. It measures the active ratio, which can be calculated using the following formula:

$$AR\ (\%) = \frac{M_F}{M_T} \cdot 100 \quad (1)$$

In this equation, AR is the active ratio (%), and M_F and M_T are the masses of the floated product and the total mass of the sample, respectively. According to the related literature, the higher the active ratio, the better the modification effect is.

Thermogravimetric (TG) analysis, which is an adequate technique for determining organic component adsorbed on the calcite surface, was also used to further evaluate the modification process. It was conducted using a temperature range 30-700 ^{o}C in N_2 atmosphere.

RESULTS AND DISCUSSIONS

Effect of sodium oleate dosage

The surface modification tests were performed in the natural pH of about 9. Figure 1 shows the relationship between the Na-oleate dosage and the active ratio, which is calculated by means of the floating tests. As seen from this figure, the active ratio values, indicating the degree of hydrophobicity, increased with increasing modifier dosage up to 100 % for 7.5 kg Na-oleate per ton of the GCC sample. The active ratio values decreased substantially beyond this point down to 33.63 % for 15 kg/ton as a result of the tail to tail arrangement because of the excess amount of the Na-oleate. Although the best result was obtained with 7.5 kg/ton, the optimum result which is 99 % of active ratio was achieved using only the Na-oleate dosage of 5 kg/ton.

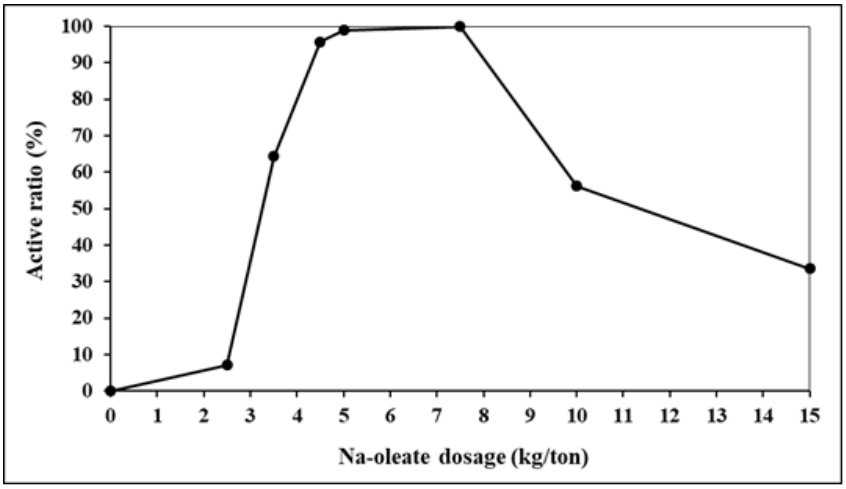

Figure 1. Effect of sodium oleate dosage on hydrophobicity of the calcite

Thermogravimetric (TG) analyses

TG analysis is a common method used for detecting organic component on calcite surface and determining its amount. TG analyses for the unmodified calcite and the calcite modified with different dosages of Na-oleate can be seen from Figure 2.

In this figure, some codes were given to the unmodified and modified samples, namely O for the unmodified calcite and SO5 for the GCC sample treated with 5 kg/ton Na-oleate. In addition, similarly, SO7.5, SO10 and SO15 represent the GCC sample treated with Na-oleate dosages of 7.5, 10 and 15 kg/ton, respectively.

According to Figure 2, the GCC samples modified with Na-oleate gave larger weight losses at 200-400 °C compared to the unmodified sample due to the thermal decomposition of Na-oleate adsorbed on the GCC samples.

Figure 3 illustrates the relationship between Na-oleate dosage and weight loss at 200-400 °C. As seen from this figure, there is a very strong relationship between the Na-oleate dosage adsorbed on the GCC samples and the weight loss. The R^2 value of 0.9945 was obtained from this relation, indicating that TG analysis is an effective and easily applicable method to determine the adsorbed amount of organic component on calcite surface.

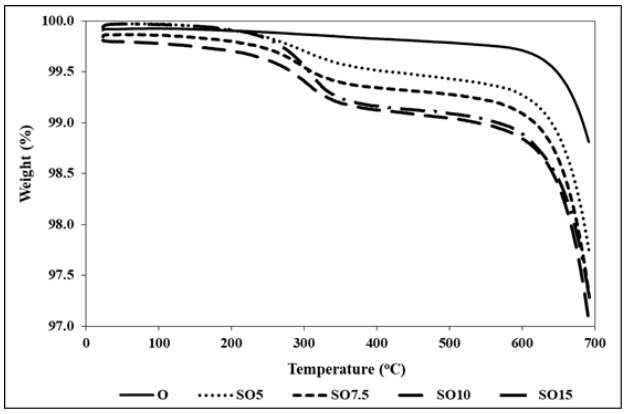

Figure 2. TG analyses of the unmodified and modified calcite samples

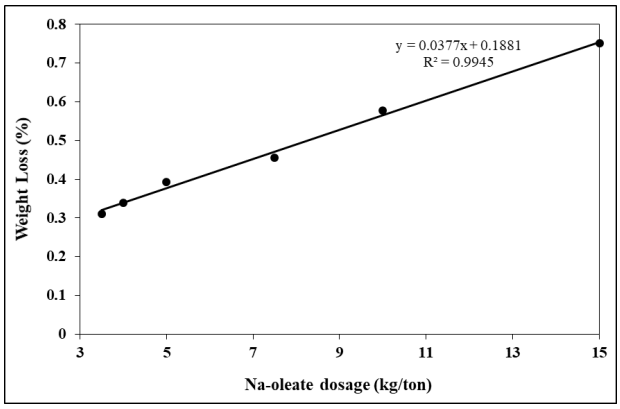

Figure 3. Relationship between Na-oleate dosage and weight loss

Figure 3 also clearly pointed out that the amount of weight loss increased sequentially with increasing Na-oleate dosage adsorbed on the modified samples.

CONCLUSION

In this study, surface modification of calcite by wet-stirred ball milling was examined using sodium oleate as a modifying agent. Modification efficiency was evaluated mainly by floating test, and also using thermogravimetric (TG) analysis. The active ratio values, which represent hydrophobicity of the modified samples, of 99 and 100 % were obtained with Na-oleate dosages of 5 and 7.5 kg/ton, respectively. The active ratio values decreased substantially beyond this point down to 33.63 % for Na-oleate dosage of 15 kg/ton due to the excess amount. TG analysis was also used for determining Na-oleate adsorbed on the calcite surface. As well understood from the TG analyses, there is a very strong relationship between the Na-oleate dosage and the weight loss at 200-400 °C, indicating the effectiveness of the method for determining the adsorbed amount of organic component on calcite surface. Overall results have indicated that natural hydrophilic calcite can easily be made hydrophobic using sodium oleate, but the dosage must be carefully controlled for the maximum efficiency.

References

1. Rungruang, P., B. P. Grady and P. Supaphol (2006). Surface-modified calcium carbonate particles by admicellar polymerization to be used as filler for isotactic polypropylene, Colloids and Surfaces a-Physicochemical and Engineering Aspects 275(1-3): 114-125,
2. Yang, Y. C., S. B. Jeong, S. Y. Yang, Y. B. Chae and H. S. Kim (2009). "The Changes in Surface Properties of the Calcite Powder with Stearic Acid Treatment." Materials Transactions 50(3): 695-701,
3. Jeong, S. B., Y. C. Yang, Y. B. Chae and B. G. Kim (2009). "Characteristics of the Treated Ground Calcium Carbonate Powder with Stearic Acid Using the Dry Process Coating System." Materials Transactions 50(2): 409-414,
4. Liang, Y., K. Yu, Q. Zheng, J. Xie and T.-J. Wang (2018). "Thermal treatment to improve the hydrophobicity of ground CaCO 3 particles modified with sodium stearate." Applied Surface Science 436: 832-838,
5. Mihajlovic, S., Ž. Sekulic, A. Dakovic, D. Vucinic, V. Jovanovic and J. Stojanovic (2009). "Surface Properties of Natural Calcite Filler Treated with Stearic Acid." Ceramics-Silikáty 53(4): 268-275,
6. Ding, H., S. C. Lu, Y. X. Deng and G. X. Du (2007). "Mechano-activated surface modification of calcium carbonate in wet stirred mill and its properties." Transactions of Nonferrous Metals Society of China 17(5): 1100-1104,
7. Yogurtcuoglu, E. and M. Ucurum (2011). "Surface modification of calcite by wet-stirred ball milling and its properties." Powder Technology 214(1): 47-53.

XIII International Mineral Processing and Recycling Conference
Belgrade, Serbia, 8-10 May 2019

University of Belgrade, Technical Faculty in Bor
Vojske Jugoslavije 12, 19210 Bor, Serbia
Tel. +381 30 424 555 Fax +381 30 421 078

UTILIZATION OF HYDROGEN BUBBLES IN ELECTROFLOTATION OF FINES OF IRON ORE TAILINGS USING A BIOSURFACTANT

Taissa Felisberto Rosado, Ronald Rojas Hacha, Mauricio Leonardo Torem #, Antonio Gutierrez Merma
Pontifical Catholic University of Rio de Janeiro, Department of Chemical and Materials Engineering, Gávea, Rio de Janeiro, Brazil

ABSTRACT – Iron ore mining produces considerable amounts of fine particles, such particles are not recovered by conventional flotation processes due mainly to the low probability of bubble/particle collision and adhesion. In order to solve the problem of low particle recovery, several flotation technologies have been developed to increase bubble/particle collision efficiency. Among these technologies the electroflotation process stands out for increasing bubble/particle collision efficiency. The present work aims to study the recovery of fines of iron ore tailings using hydrogen bubbles by electroflotation using a biosurfactant obtained from Rhodococcus opacus strain. The study was carried out in a modified Patridge-Smit binary cell, the iron grade of the ore tailing was around 14 %, and the particle size was - 38 + 20 μm. Electrophoretic mobility measurements (Zeta potential) and infrared spectroscopy analysis were carried out with the objective of evaluating any mineral surface modification before and after biocollector-minerals interactions. Subsequently, electroflotation tests were performed with hydrogen bubbles to evaluate the effect of pH and biocollector concentration on the iron recovery. The results showed an iron recovery around 80 % and iron grade of 55 % at pH 3.

Key words: electroflotation, microbubbles, phodococcus opacus, biosurfactant, iron ore fines.

INTRODUCTION

Processing of iron ores generate large amounts of tailings, these tailings are composed of a large proportion of slimes (fine particles) of a difficult recovery. The recovery of fine particles, it is difficult to perform by conventional concentration processes, and, therefore, end up being discarded in tailings dams. The difficulties of fine particle recovery are mainly related to the low probability of collision and adhesion bubble/particle [1, 2]. Electroflotation process presented as an alternative to solve the low recovery of fine particles since the generation of hydrogen and oxygen microbubbles (< 100 μm) increases the probability of collision and adhesion bubble/particle. This process presents greater flexibility in the control of bubble size by modifying some parameters, such as pH, current density, electrolyte

corresponding author: torem@puc.br

concentration, and electrode material and geometry [3, 4]. Electroflotation process addresses the problems related to the low recovery of fines presented by conventional flotation processes, however, it does not address the problems related to the toxicity of the synthetic collectors. A biotechnological alternative to reduce the impact of using synthetic reagents in the concentration process is the use of microorganisms. Different microorganisms such as bacteria, yeasts and fungi have surfactant properties, which can be used in the mineral industry, directly in the form of cells or indirectly through the use of their surfactant components [5, 6, 7, 8].

MATERIALS AND METHODS

Preparation of ore samples

A sample of iron ore tailings was used to carry out the electroflotation tests, this sample was prepared and classified, the particle size selected for this study was - 38 + 20 μm. The chemical analysis to quantification of iron was carried out by volumetry with potassium dichromate as titrant. The quantification of the mineralogical phases of the tailing was performed by X-ray diffraction.

Zeta Potential measurements and

Zeta potential measurements were performed on the hematite and quartz, and after interaction with bioreagent. These studies were performed in a Malvern Zetasizer Nano microelectrophoresis apparatus at the Mineral and Environmental Technology Laboratory at PUC-Rio.

Fourier transform infrared spectroscopy - FTIR

FTIR spectra were obtained on the FTIR Scientific Nicolet 6700 FTIR spectrophotometer using the KBr pellet method. The spectra were obtained with the objective of identifying the functional groups present in bioreagent and biosurfactant. The pellets were obtained from a sample mixture with KBr. The sample and KBr ratio was 1/100 (wt/wt).

Preparation and obtaining of bioreagent and biosurfactant

The bioreagent was prepared from the bacterial strain R. opacus obtained from the Brazilian Collection of Environment and Industry Microorganisms (CBMAI - UNICAMP). The bacterial strain was cultured in liquid medium in 250 mL Erlenmeyer flasks and incubated in a rotating shaker at 28 °C for 72 h. The culture medium used was yeast malt glucose (YMG; glucose: 10 g/L, meat peptone: 5 g/L, malt extract: 3 g/L, yeast extract: 3 g/L) at pH 7.20. After growth, the cell suspension was centrifuged at 4,500 RPM for 10 min, and the centrifuged concentrate containing the bacterial cells was washed twice with deionized water, followed by resuspension in a solution of 0.001mol/L NaCl. Finally, the concentrated suspension obtained was autoclaved at 1.0 atm. pressure and 121 °C temperature for 20 min (vertical autoclave) to inactivate the bacteria, the concentrate was used as the bioreagent. The biosurfactant was extracted from a bioreagent cultured for a time of 168 h (7 days) following the same steps of preparation of the previously detailed bioreagent. This

new bioreagent was centrifuged and suspended in alcohol (95 °) for 24 h. Further new centrifugation was performed to separate the soluble material of the insoluble material, the insoluble material was discarded. The soluble material was dried in an oven at 50 °C for 24 h with the aim of volatilizing the alcohol. The material obtained was solubilized in water deionized for use as biosurfactant.

Electrodes

Platinum electrodes with 99.95 % purity were used as both cathode and anode. Platinum wires were woven in knitted form and coated on a rubber edge. The total surface area of the electrode was 14.10 cm^2, the wire diameter was 0.002 cm, and the spacing between the wires was 0.002 cm.

Electroflotation test

The electroflotation test was performed in two Partridge-Smith modified semi-cells of 380 mL usable volume (Figure 1). These cells were made of glass and had an external diameter of 50 mm, an internal diameter of 46 mm, and a height of 215 mm. The semi-cells were connected by a saline bridge of 44 mm in external diameter. The saline bridge housed two Millipore plates of 40 mm in outside diameter. The semi-cells contained electrodes and the electrolyte solution (Na_2SO_4). Platinum electrodes were used as the anode (O_2 bubbles) and cathode (H_2 bubbles). The voltage variation at the half cells was controlled by a voltage source. After the generation of the bubbles, the desired operating conditions were stabilized in the semi-cells, mainly by pH adjustment. Then, the iron ore tailing was conditioned with the collector (bioreagent and biosurfactant) for 5 min in a becker. After conditioning, the conditioned sample was introduced into the semi-cell (cathode) and then the solution volume was complete to 360 mL to initiate electroflotation for 5 min. The experimental conditions of the electroflotation tests were performed to current density (22.18 mA/cm^2), electrolyte concentration (0.2 mol/L) and 1g of tailing sample.

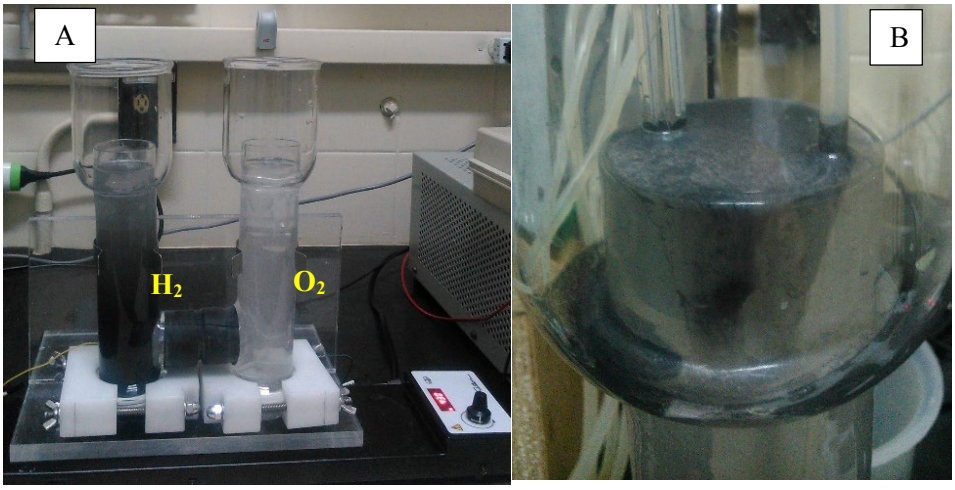

Figure 1. Electroflotation process. A: Modified Partridge-Smith cell. B: Iron recovery

RESULTS AND DISCUSSION

Iron ore sample

The results of the chemical analysis by volumetry with potassium dichromate showed an iron grade of 14 %. The X-ray diffraction analysis revealed the presence of hematite and quartz as the main minerals present in the tailing.

Zeta potential

Figure 2 shows the zeta potential profiles of hematite, quartz, and the interaction with R. opacus for the purpose of evaluating the types of interactions. The zeta potential profile of hematite indicates an IEP of about pH 5 (Figure 2A). The values of the zeta potential demonstrate the relative stability of the hematite particles at values close to 15mV in the acidic range and values around -25mV in the alkaline range. After contact of the hematite with R. opacus, a change in the surface properties of the mineral was observed. The hematite showed a displacement of the IEP (pH 5 to 4), which indicates a possible electrostatic interaction between R. opacus and hematite particles. On the other hand, the zeta potential profile of quartz has not IEP in the range evaluated (pH 2-11) (Figure 2B). These zeta potential values demonstrate the relative stability of the quartz particles in suspension, reaching values close to -50mV in the alkaline range. After contact of the quartz with R. opacus, significant changes were not observed in the superficial properties of the mineral in the evaluated range.

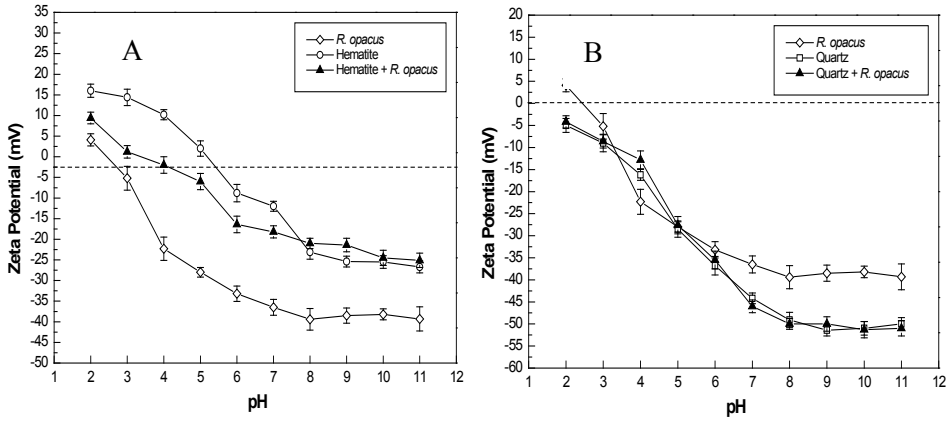

Figure 2. Zeta Potential measurement for hematite and quartz before and after interaction with R. opacus

Fourier transform infrared spectroscopy

Figure 3A shows the absorption bands corresponding to the bioreagent, it is possible to observe the absorption band around 3,291.58 cm^{-1} corresponding to the stretching vibration of the O-H and N-H groups of polysaccharides and proteins [9]. Bands of lower intensity of 2,924.73 and 2,853.69 cm^{-1} belonging to the asymmetric and symmetric vibrations of the CH_2 radicals that are present in the lipids, proteins,

carbohydrates and nucleic acids [10]. The absorption band near 1,745.14 cm^{-1} corresponds to the vibration of the stretching of the functional group C=O found in lipids and triglycerides. There is also a region between 1,633.51 and 1,543.90 cm^{-1} associated with the vibration of amide I and amide II groups [6]. The absorption band 1,460.99 cm^{-1} belongs to the symmetrical vibration of the CH_2 radicals. The absorption band 1,399.09 cm^{-1} corresponds to the asymmetric vibration of the COO- group. The absorption bands 1,236.61 and 1,066.92 cm^{-1} represent the asymmetric vibrations of present in phospholipids and nucleic acids [10]. Figure 3B shows the absorption bands of biosurfactant, it is possible observe the absorption band 3,291.58 cm^{-1} corresponding to the stretching of the O-H and N-H groups of polysaccharides and proteins, also observed the absorption band 2,853.69 cm^{-1} belongs to the symmetrical vibration of the CH_2 radicals. Finally, it is possible to observe the absorption bands 1,633.51 and 1,399.09 cm^{-1} corresponding to the groups C=O and COO^-.

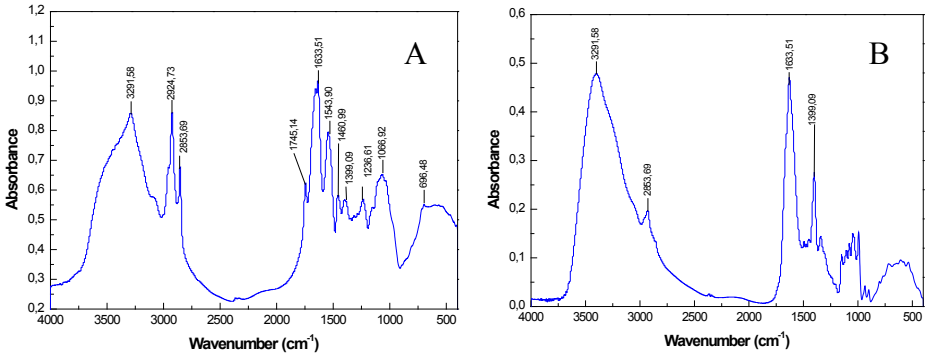

Figure 3. FTIR spectroscopy of biorreagent and biosurfactant

Electroflotation

Effect of pH

Changes in the system pH leads to significant changes in the mineral surface and of the biocollector (bioreagent and biosurfactant), consequently, this may favor or inhibit the mineral interaction mineral/biocollector [11]. Figure 4 shows the effect of pH on iron recovery and grade for the biocollector. In the case of the bioreagent (Figure 4A), the increase of pH favored the iron recovery and grade up to pH 6, above this pH value a decrease was observed. The same effect was not observed in the case of biosurfactant (Figure 4B), in this case, the pH increase did not favor iron recovery and grade. These phenomena may be related to the behavior of the different surfactants species present in the bioreagent and biosurfactant which can be activated or inhibited by the medium pH. The biosurfactant had a better performance responding a recovery around 80 % and Fe grade of 55 %.

Effect of bioreagent and biosurfactant concentration

The increase biocollector concentration may favor the recovery and content of the concentrated material, some counter effect may occur when the critical micellar

concentration (CMC) is reached or when the formation of agglomerates occurs decreasing the effective area of adsorption [12]. Under the conditions evaluated the increase of the bioreagent concentration does not influence substantially in the iron recovery and grade (Figure 5A). In the case of the biosurfactant an increase in the recovery caused by increase of the biosurfactant concentration was observed (Figure 5B).

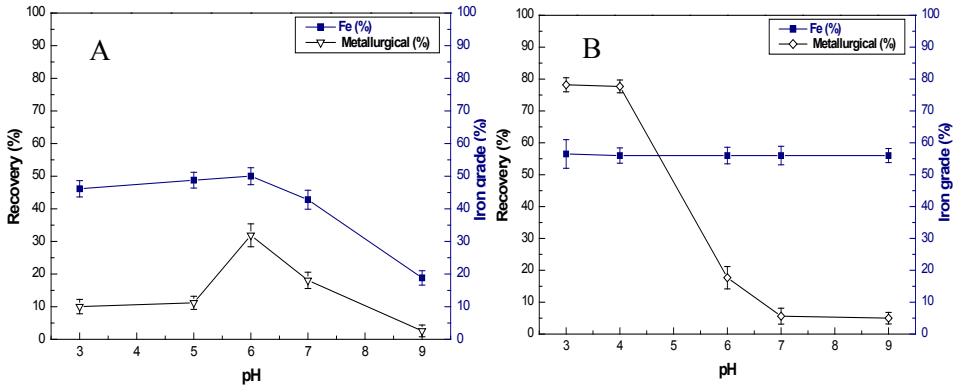

Figure 4. Effect of pH in recovery and Fe grade. A: biorreagent; B: biosurfactant

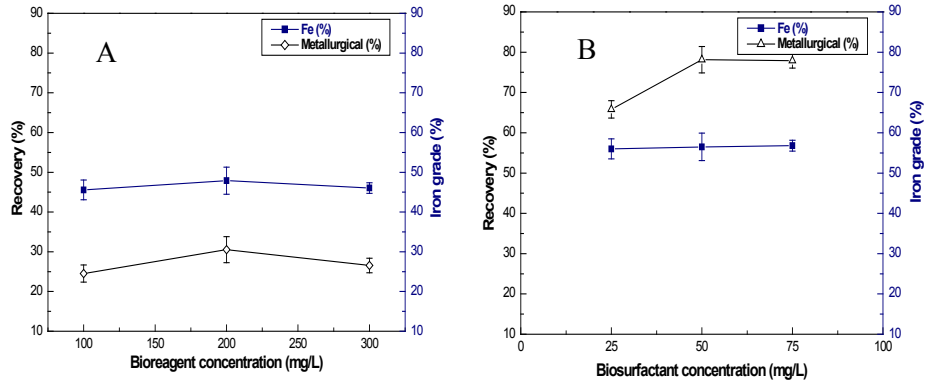

Figure 5. Effect of biocollector concentration. A: biorreagent; B: biosurfactant

CONCLUSION

The results of the electroflotation tests using the bioreagent and biosurfactant showed potential to separation of fines of iron ore tailings. The biosurfactant presented better recovery and iron content when compared to the bioreagent. This can be attributed to the presence of groups C=O and COO^- present in the biosurfactant with greater intensity. Under the conditions evaluated the bioreagent presented a recovery around 35 % and iron grade of 50 % at pH 6. The biosurfactant presented a recovery approximately 80 % and iron grade of 55 % at pH 3.

Acknowledgements:

The authors acknowledge PUC-Rio (Pontifical Catholic University of Rio de Janeiro), CNPq (Conselho Nacional de Desenvolvimento Científico e Tecnológico), and CAPES (Coordenação de Aperfeiçoamento de Pessoal de Nível Superior) for financial support.

References

1. Trahar, W. J. (1981) A rational interpretation of the role of particle size in flotation. International Journal of Mineral Processing, 8 (4), 289-327,
2. Peng, Y., Liang, L., Tan, J., Sha, J., Xie, G. (2015) Effect of flotation reagent adsorption by different ultra-fine coal particles on coal flotation. International Journal of Mineral Processing, 142, 17-21,
3. Sun, W., Ma, L., Hu, Y., Dong, Y., Zhang, G. (2011) Hydrogen bubble flotation of fine minerals containing calcium. Mining Science and Technology (China), 21 (4), 591-597,
4. Ren, L., Zhang, Y., Qin, W., Bao, S., Wang, P., Yang, C. (2014) Investigation of condition-induced bubble size and distribution in electroflotation using a high-speed camera. International Journal of Mining Science and Technology, 24 (1), 7-12,
5. Mesquita, L. M. S., Lins, F. F., Torem, M. L. (2003) Interaction of a hydrophobic bacterium strain in a hematite-quartz flotation system. International Journal of Mineral Processing, 71 (1-4), 31-44,
6. Bueno, B. Y. M., Torem, M. L., Molina, F. A. L. M. S., De Mesquita, L. M. S. (2008) Biosorption of lead (II), chromium (III) and copper (II) by R. opacus: Equilibrium and kinetic studies. Minerals engineering, 21 (1), 65-75,
7. Kim, G., Park, K., Choi, J., Gomez-Flores, A., Han, Y., Choi, S. Q., Kim, H. (2015) Bioflotation of malachite using different growth phases of R. opacus: Effect of bacterial shape on detachment by shear flow. International Journal of Mineral Processing, 143, 98-104,
8. Olivera, C. A. C., Merma, A. G., Puelles, J. G. S., Torem, M. L. (2017) On the fundamentals aspects of hematite bioflotation using a Gram positive strain. Minerals Engineering, 106, 55-63,
9. Melin, A. M., Allery, A., Perromat, A., Bébéar, C., Déléris, G., de Barbeyrac, B. (2004) Fourier transform infrared spectroscopy as a new tool for characterization of mollicutes. Journal of microbiological methods, 56 (1), 73-82,
10. Robert, P., Marquis, M., Barron, C., Guillon, F., Saulnier, L. (2005) FT-IR investigation of cell wall polysaccharides from cereal grains. Arabinoxylan infrared assignment. Journal of Agricultural and Food Chemistry, 53 (18), 7014-7018,
11. Sanwani, E., Chaerun, S., Mirahati, R., Wahyuningsih, T. (2016) Bioflotation: bacteria-mineral interaction for eco-friendly and sustainable mineral processing. Procedia Chemistry, 19, 666-672,
12. Ekmekyapar, F., Aslan, A., Bayhan, Y. K., Cakici, A. (2006) Biosorption of copper (II) by nonliving lichen biomass of Cladonia rangiformis hoffm. Journal of Hazardous Materials, 137 (1), 293-298.

XIII International Mineral Processing and Recycling Conference
Belgrade, Serbia, 8-10 May 2019

University of Belgrade, Technical Faculty in Bor
Vojske Jugoslavije 12, 19210 Bor, Serbia
Tel. +381 30 424 555 Fax +381 30 421 078

BIOSORPTIVE FLOTATION OF NICKEL AND COBALT BY *RHODOCOCCUS ERYTHROPOLIS*

Antonio Gutiérrez Merma, Maurício Leonardo Torem #, Vinicius de Jesus Towesend, Caroline D. Grossi
Pontifical Catholic University, Department of Chemical Engineering and Materials, Gávea, Rio de Janeiro, Brazil

ABSTRACT – The treatment of wastewater produced during mining process is a technological challenge due to their complexity. The removal of metals, at low concentrations, from these kinds of effluents, in order to reach the standards required by current legislation, has been a challenge for some metal species. Biosorptive flotation can be defined as a physicochemical process that removes substances from an aqueous solution by the combination of two processes, the biosorption and the flotation. The sorbent is a biological matrix as bacteria, which have sorbent and frother properties due to the functional groups presented on their cell wall. In this work the biosorptive capacity of the *Rhodococcus erythropolis* in the removal of Ni (II) and Co (II) in aqueous solutions was studied. The appropriate pH value for biosorption was around 7 for both metals. The results of the uptake capacity of the biosorbent were well adjusted to the Langmuir isotherm model, where the maximum capture capacities were 22.5 mg/g for Ni (II) and 14.6 mg/g for Co (II). The surface properties of the biosorbent were evaluated before and after the interaction of the metals in order to determine the possible mechanisms of biosorption, through electrokinetic measurements, infrared spectroscopy and scanning electron microscopy. The biosorptive flotation results confirmed that *R. erythropolis* presents properties as a bioreagent for metals uptake; removal percentages of 40.20 % and 23.52 % were obtained for nickel and cobalt, respectively. The results show that *R. erythropolis* present an alternative for metal removal in low concentration effluents.

Key words: *Rhodococcus erythropolis*, biosorption, bioreagent.

INTRODUCTION

Heavy metals are introduced into the environment through natural phenomena and anthropic activities, resulting in the contamination of environment. The discharge of Wastewater into water bodies is a major environmental problem worldwide, because it contains toxic heavy metals and other organic and inorganic pollutants. Industrial wastewater often contains heavy metal ions which are non-biodegradable and many of them are soluble in aqueous media and easily available to living organisms [1]. Heavy metals are among the most common pollutants found in industrial effluents. Even at low concentrations these metals can be toxic to

corresponding author: torem@puc.br

organisms including humans [2]. Heavy metals such as Ni and Co are common constituents of wastewater from mining operations, urban stormwater runoff, and industrial effluents. Although in small concentrations they are essential to life, excessive levels may be detrimental. Therefore, heavy metals in wastewater should be minimized [3].

Numerous physico-chemical methods have been utilized for the removal of heavy metals from aqueous solutions including: metal extraction, ion exchange process, chemical precipitation of metals in form of insoluble salts and membrane separation. These methods have several difficulties included in their high operating costs, lack of selectivity, imperfect removing of metal ions, in addition to the production of wastes during their production [4]. New technologies, with acceptable costs, are necessary to reduce the concentration of heavy metals, presents in wastewaters, in the environment to acceptable levels [5].

Biosorption is a physical-chemical process, simply defined as the removal of substances from solution by biological material. This is a property of both living and dead organisms (and their components), and has been heralded as a promising biotechnology because of its simplicity, analogous operation to conventional ion-exchange technology, apparent efficiency and availability of biomass and waste bio-products [6]. All kinds of microbial, plant and animal biomass, and derived products, are investigated in a variety of forms, and in relation to a variety of substances [7]. A large number of reviews are already available, dealing with elimination of heavy metals using various kinds of biosorbents [2].

In this work, the *Rhodococcus erythropolis* (RE) was used as biosorbent for the removal of Ni (II) and Co (II) from aqueous solutions, the aim of this work was the evaluation of the biosorption capacity of the biosorbent in uptake of Ni (II) and Co (II) at various pH values. The Langmuir and Freundlich models were used to fit the experimental data. Electrophoretic studies were carried out in order to evaluate the influence of metal speciation on the biosorbent.

METHODOLOGY

Microorganism, media and growth

Rhodococcus erythropolis was cultivated in tryptic soy broth (TSB) culture medium. The TSB culture medium is composed of pancreatic digest of casein 17.0 g/l, papaic digest of soybean 3.0 g/L, dextrose 2.5 g/L, sodium chloride 5.0 g/L and dipotassium phosphate 2.5 g/L. Stocks of the bacteria were prepared using a solid medium in Petri plates and saving them in a refrigerator at 4° C to later be inoculated in liquid medium. After the bacterial inoculation in liquid medium, the flasks were disposed on a rotary shaker, maintained at 150 rpm and 28 °C until it reaches its maximum concentration. Thereafter, the bacterial suspension was centrifuged and the obtained biomass was twice washed with deionized water, then the cells were re-suspended in a 10^{-3} mol/L NaCl solution. Finally, the bacterial concentrate was autoclaved in order to avoid further bacterial development. For the measurement of cell concentration in suspension, the dry weight method.

Metal solutions

Synthetic solutions were prepared with distilled water from stock solutions of

1000 mg L^{-1} of Nickel and Cobalt, separately, from the corresponding Chloride salts. All reagents were of analytical grade. Both reagents were diluted in distilled water in the appropriate proportions for each case. The pH of the solutions was adjusted to a desired value with 0.1 mol/L HCl and 0.1 mol/L NaOH.

Batch biosorption studies

The Experiments were conducted in 125 mL Erlenmeyer flasks containing nickel(II) or cobalt(II) synthetics solutions of known concentrations and doses of biosorbent fixed in 1 g/L. Flasks were agitated on a shaker at a constant shaking rate of 120 rpm for 30 min to ensure that equilibrium. The amount of metal adsorbed was calculated by:

$$q = \frac{v(C - Ce)}{m} \quad (1)$$

where C and Ce are the initial and equilibrium concentrations of metal (mg/L), M is the dry weight of biomass (g) and V is the solution volume (L). The regression coefficient (R^2) was used to measure the goodness-of-fit.

Effect of solution pH

The pH of wastewater has a large influence on the extent of biosorption. The adsorption capacity of both biosorbents was investigated using solutions with a fixed nickel(II) and cobalt(II) concentration of 20 mg/L and pH varying from 4.0 to 8.0. The final concentrations of the solutions were measured by atomic absorption.

Zeta potential measurements

Zeta potential were measuremented for both biosorbents, before and after interaction with nickel (II) and cobalt(II) at different pH's. Were carried out on the micro-electrophoresis apparatus "Zeta Meter System 4.0". NaCl as used as indifferent electrolyte with a concentration of 10^{-3} mol/L. The pH was adjusted using diluted HCl and NaOH solutions.

Equilibrium modelling

To study the equilibrium of biosorption the most frequently used approach consists of measuring the uptake capacity, which represents the quantity of metal removed (q) against the equilibrium concentration of metal ion in solution. Classical adsorption models (Langmuir e Freundlich) were used to describe the equilibrium between adsorbed metal ions onto biossorbents and metal ions in solution a constant temperature [8].

The Langmuir model suggests that uptake occurs on a homogeneous surface by monolayer sorption without interaction between adsorbed molecules and is expressed by the following equation.

$$q = \frac{qmax\ B\ Ce}{1 + B\ Ce} \quad (2)$$

The empirical Freundlich model can be applied to non-ideal adsorption on heterogeneous surfaces as well as multilayer adsorption and is expressed by the following equation.

$$q = Kf\ Ce^{\frac{1}{n}} \quad (3)$$

RESULTS AND DISCUSSION

Adsorption isotherms

One of the most critical parameters of the biosorption process is pH, because, it affects the charge of surface active sites on the biomass [9]. Fig. 1 shows the effect of pH value in removal of Ni (II) And Co (II) by biosorption process with both biosorbants.

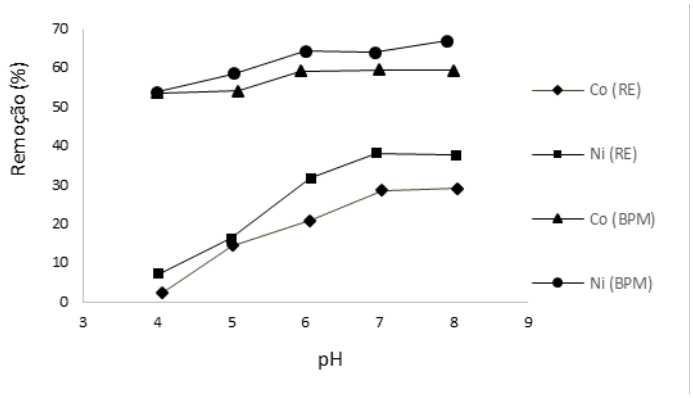

Figure 1. Effect of solution pH for Ni(II) and Co (II) and both biosorbents (initial concentration of biosorbent: 1gL^{-1}; concentration metals; 20mg L^{-1}; stirring speed: 120 rpm; temperature: 25 °C and contact time 30 min)

The maximum Ni (II) adsorption was around 38 %, at pH 7.0 and 66 %, at pH 8 for RE and BPM, Respectively. Nevertheless, to avoid the formation of complexes or metal precipitation was considered for BPM, pH 7 with adsorption around 64 %. Akar et al. [10] found that the *Phaseolus vulgaris* adsorbed nickel at range of pH 7, also, Pal et al. [11] found that fungi biomass adsorbed cobalt at pH 7. According to the surface complexation theory (Stumm and Morgan, 1996), the improvement in metals removal as pH increased can be explained on the basis of a reduction in competition between proton and metal species for the surface sites.

Adsorption isotherms

Text Equilibrium sorption studies determine the capacity of the sorbent, which can be described by a sorption isotherm, characterized by certain constants whose values express the surface properties and affinity of the sorbent. The Langmuir equation (Eq.2) can be rearranged to the following linear form:

$$\frac{Ce}{q} = \frac{Ce}{q_{max}} + \frac{Ce}{q_{max}\ B} \quad (4)$$

So The slope of the graphical representation of Ce/q versus Ce equals $1/q_{max}$ and the intersection is equal to $1/(q_{max}\ B)$. The logarithmic form of Freundlich equation (Eq.3) is:

$$logq = logKf + \frac{1}{n} log\ Ce \tag{5}$$

The slope of the graphical representation of log q versus log Ce equals 1/n and the intersection is equal to log K*f*.

Figs. 2 show the linearized isotherms with Langmuir and Freundlich models, respectively, for both biosorbent for Ni(II) and Co (II). The Langmuir and Freundlich parameters for the biosorption of Ni(II) and Co (II) are listed in Table 1. It is indicated that both of the isotherm models fit well when R^2 values are compared.

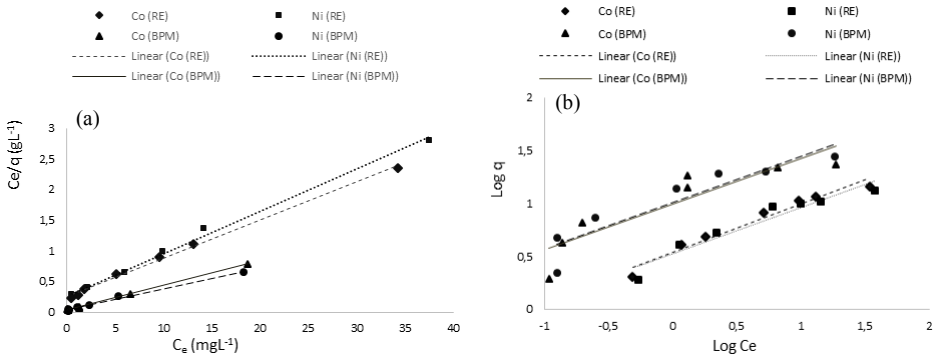

Figure 2. Linearized Langmuir isotherm (a) and linearized Freundlich isotherm (b) for Ni(II) and Co (II) both biosorbents (initial concentration of biosorbent: 1 g L^{-1}; stirring speed: 120 rpm; temperature: 25 °C and contact time 30 min)

Table 1. Isotherm model constants for the biosorption of Ni(II) and Co (II) onto RE and BPM

Metal	**Isotherm**						
	Langmuir				**Freundlich**		
	q_{max}	B	R^2		Kf	n	R^2
	BPM						
Nickel	29.359	0.805	0.991		10.265	2.293	0.920
Cobalt	24.719	1.262	0.998		9.865	2.322	0.962
	RE						
Nickel	14.469	0.264	0.995		3.394	2.289	0.859
Cobalt	16.068	0.240	0.996		3.478	2.182	0.813

Table 1 show uptake capacity (q_{max}) of *R. Erythropolis* was obtained 14.469 mg g^{-1} for Nickel and 16.068 mg g^{-1} for Cobalt. For BPE q_{max} was obtained 29.359 mg g^{-1} for Nickel and 24.719 mg g^{-1} for Cobalt. BPM indicated higher q_{max} values. For the cases of Freundlich isotherm, the adsorption feature is defined by both K*f* and n values, where K*f* value represents the adsorption coefficient and n value is related to the effect of concentration of metal ions. As shown in **Table 1**, for the *R.Erithropolis*

as biosorbent the K*f* value of nicke was 3.394 and 3.478 for cobalt. For the BPE as biosorbent the K*f* value of nicke was 10.265 and 9.865 for cobalt. A BPM indicated higher K values. Based on the R^2 correlation prediction, one may suggest that adsorption both biosorbents follow the Langmuir model, precisely with a higher R^2 value in contrast to the Freundlich model.

Zeta potential measurements

Figure 3a shows the zeta potential curve for *R. Erythropolis*, before and after interaction with Ni (II) and Co (II). A change is observed in the surface properties of RE after interaction with metal ions. The isoelectric point was shifted to pH value around 3.1. One can attribute the shift in the isoelectric point value to a specific adsorption of the metallic species. **Fig. 3 (b)** shows the zeta potential curve for *R. Erythropolis*, before and after interaction with Ni (II) and Co (II). A change is observed in the surface properties of BPM after interaction with metal ions. Surface charge is negative in any pH range without an isoelectric point before and after interaction. Therefore, the surface charge of the BPM shifted to less negative values, this can be attributed to the electrostatic adsorption of the metals.

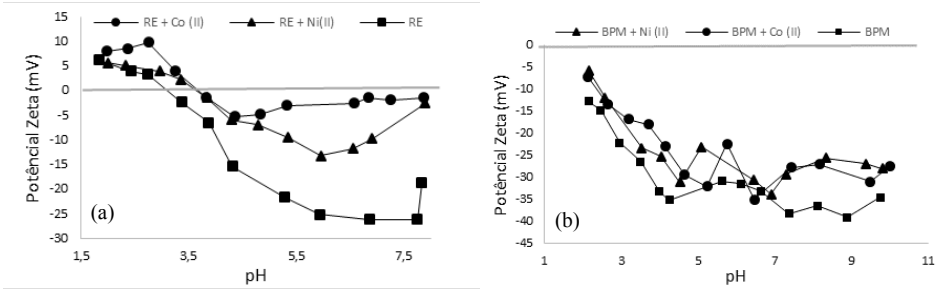

Figure 3. Zeta potential of RE (a) Zeta potential of BPM (b) in NaCl: 10^{-3} M, Co (II) and Ni(II) concentration: 20mgL^{-1} And biosorbent concentration: 1mgL^{-1}

CONCLUSION

Results showed that BPM has more adsorption capacity for Ni(II) and Ni(Co) uptake than *R.Erythropolis*. The isotherm model that ajusted best the biosorption data was Langmuir model with larger R^2 for both biosorbentes. The biosorption of metal ions dependent on pH. pH 7 were found to be the most suitable for Ni (II) and Co (II) biosorption in both cases. RE exhibited positively charged surface below pH 3.1 and negatively charged surface above this value. This explains its highest efficiency in the metal removal at pH 7. BPM exhibited negatively charged surface in all pH range, but they present more negative values in the range of pH 7 and 8, this explains its highest efficiency in the metal removal at pH 7.0. Thus, it is suggested that RE and BPM could be considered as a low cost, novel and abundant bioreagent for the removal of nickel and cobalt ions from aqueous solutions.

Acknowledgements:

The authors gratefully acknowledge CNPq, CAPES and FAPERJ for supporting this research.

References

1. Ali, A. (2017). 'Removal of Mn (II) from water using chemically modified banana peels as efficient adsorbent'. Environmental Nanotechnology, Monitoring & Management, 7, 57-63.
2. Veneu, D. M., Torem, M. L., & Pino, G. A. (2013). 'Fundamental aspects of copper and zinc removal from aqueous solutions using a Streptomyces lunalinharesii strain'. Minerals Engineering, 48, 44-50.
3. Triantafyllou, S. (1999) 'Removal of Nickel and Cobalt from Aqueous Solutions by Na-Activated Bentonite', Clays and Clay Minerals, 47,5, 567–572.
4. Sadeek, S. A., Negm, N. A., Hefni, H. H. H. e Wahab, M. M. A. (2015) 'Metal adsorption by agricultural biosorbents: Adsorption isotherm, kinetic and biosorbents chemical structures', International Journal of Biological Macromolecules, 81, 400–409.
5. Bueno, B. Y. M., Torem, M. L., de Carvalho, R. J., Pino, G. A. H. e de Mesquita, L. M. S. (2011) 'Fundamental aspects of biosorption of lead (II) ions onto a Rhodococcus opacus strain for environmental applications', Minerals Engineering, 24,14, 1619–1624.
6. Abdel-Ghani, N. e El-Chaghaby, G. (2014) 'Biosorption for Metal Ions Removal From Aqueous Solutions: a Review of Recent Studies', Mnkjournals.Com, 3, 1, 24–42.
7. Gadd, G. M. (2009) 'Biosorption: critical review of scientific rationale, environmental importance and significance for pollution treatment', Journal of Chemical Technology & Biotechnology, 84, 1, 13–28.
8. Febrianto, J., Kosasih, A.N., Sunarso, J., Ju, Y., Indraswati, N., Ismadji, S. (2009) 'Equilibrium and kinetic studies in adsorption of heavy metals using biosorbent: a summary of recent studies', Journal of Hazardous Materials 162, 616–645.
9. Farooq, U., Kozinski, J.A., Khan, A., Athar, M. (2010) 'Biosorption of heavy metal ion using wheat based biosorbents – a review of recent literature', Bioresource Technology 101, 5043–5053.
10. Akar, T., Kaynak, Z., Ulusoy, S., Yuvaci, D., Ozsari, G., & Akar, S. T. (2009), 'Enhanced biosorption of nickel (II) ions by silica-gel-immobilized waste biomass: biosorption characteristics in batch and dynamic flow mode' Journal of Hazardous Materials, 163(2), 1134-1141.
11. Pal, A., Ghosh, S., & Paul, A. K. (2006) 'Biosorption of cobalt by fungi from serpentine soil of Andaman', Bioresource Technology, 97(10), 1253-1258.

XIII International Mineral Processing and Recycling Conference
Belgrade, Serbia, 8-10 May 2019

University of Belgrade, Technical Faculty in Bor
Vojske Jugoslavije 12, 19210 Bor, Serbia
Tel. +381 30 424 555 Fax +381 30 421 078

THE INFLUENCE OF pH VALUE ON DEINKING FLOTATION

Dragana Marilović [1, #], Maja Trumić [1], Milan Trumić [1], Ljubiša Andrić [2]
[1]University of Belgrade, Technical Faculty in Bor, Bor, Serbia
[2]Institute for Technology of Nuclear and other Mineral Raw Materials, Belgrade, Serbia

ABSTRACT – The effect of pH values and flotation time on deinking flotation was investigated in order to obtain the best results of toner and fiber recovery. These results shows that this raw material does not required longer flotation time of 4 minutes. Under the investigated conditions, the values over 90 % for toner and fiber recovery are not achieved. The highest recovery was achieved after 4 minutes in high acid conditions pH 3 (It = 62.69 %; Im = 93.08 %) and slightly alkaline conditions pH 9 (It = 81.01 %; Im = 80.87 %).

Key words: deinking flotation, oleic acid, offset paper, ink

INTRODUCTION

Recycling aims to restore the used product with the same characteristics as it had at the beginning of its use. Paper is a material which consists of fibers, fillers and colors [1]. The paper can be recycled up to seven times because of the loss of quality after every recycling circle [2]. For the treatment of secondary fibers, several procedures such as screening, cleaning and flotation can be applied [3] depending on the type and characteristics of the paper and ink. The most effective and commonly applied process is deinking flotation [4, 5].

DEINKING FLOTATION

Flotation is a widely used separation method in many industries. It is selective separation process based on physicochemical properties differences between the ink and fibre, where hydrophobic toner particles are separated from an aqueous paper suspension by adhesion to air bubles and has many similarities as flotation of mineral raw materials [6]. Deinking flotation process consists of two steps. Detachment of the ink particles from cellulose fibers and the removal of the detached ink particles from the pulp slurry. First step is disintegration and forming pulp where paper fibers and color particles are separated. Chemicals required in the flotation

corresponding author: dmarilovic@tfbor.bg.ac.rs

steps, such as collectors, pH regulators, dispergants, etc., are usually added at the pulping stage to ensure good mixing and dissolution and to enhance fibre swelling and ink detaching. Fibre swelling is promoted at high pH (8-11) [7,8].

Adhesion of air bubbles to ink particles depends of the reagents which are adsorbed on the particle surface making them hydrophobic. Regular choice of reagents promotes the selectivity of ink separation [9]. Because of the low sensitivity to water hardness, in deinking flotation under neutral conditions are often used non-ionic surfactants [10].

MATERIALS AND METODS

For experiments were used synthetic samples formed of white unprinted offset paper and toner cartridge from a laser printer. Paper were mechanicaly cutted in shredder into pieces and with the added distiled water heated on 40 °C disintegrated in an blender, and then soaked in for 17 hours. In order to obtain a realistic synthetic sample, the toner from the cartridge was thermally treated in an oven at 100 °C for 60 min. After cooling, toner was crushed and screened on the sieve openings 212, 150 and 106 μm.

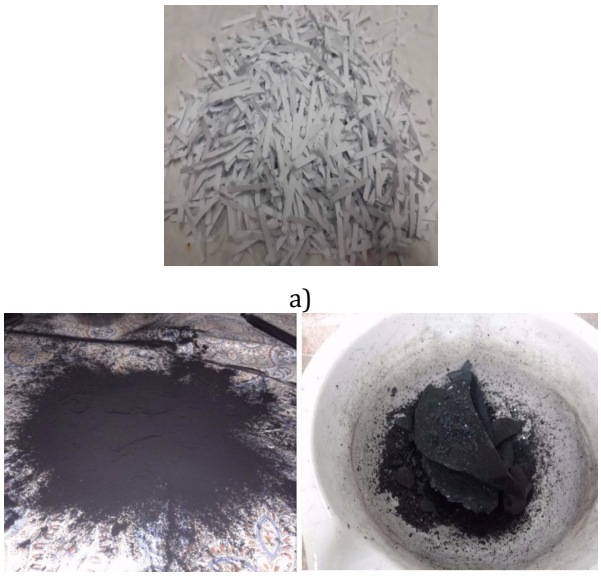

a)

b) c)

Figure 1. a) cutted paper b) toner before thermal treatment, c) toner after thermal treatment

FLOTATION EXPERIMENTS

Experiments were carried out in a 2.2 l laboratory scale flotation machine Denver D-12 (Figure 2) in a glass flotation cell. The operating conditions of the flotation were constant for all experiments. The agitation speed was 1100 rpm, consistency 1 %, temperature 23 °C, air flow 270 dm^3/h. The collector was added during conditioning stage, the conditioning time was 15 min. Using collector was oleic acid

($C_{17}H_{33}$-COOH) dosage 125 g/t. pH values in experiments were different, from 3 to 12. To study the kinetics during the flotation process, the samples were extracted from the froth at 2, 4 and 20 min. The fiber from suspension products were filtered through a Buchner funnel, then dried at the room temperature and weighed to determine the fiber recovery.

The ink particles from froth products were filtered throw filter pads. To determinate the ash content, dried froth filter pads were heated at 550 °C in a furnance. Then, the ash was analysed for iron by XRF analyser to determine toner recovery.

Figure 2. Flotation machine

RESULTS AND DISCUSSION

The results of deinking flotation experiments are shown in Table 1.

Table 1. Results of deinking flotation under different conditions

Flotation time t (min)	**2**		**4**		**20**	
pH	**It (%)**	**Im (%)**	**It (%)**	**Im (%)**	**It (%)**	**Im (%)**
3	60.60	94.90	62.69	93.08	62.99	89.77
5	28.03	95.10	31.26	91.95	31.33	88.19
7	50.23	94.75	53.40	92.52	53.93	88.32
9	75.56	88.82	81.01	80.87	84.24	64.99
12	48.37	90.22	49.03	81.90	49.31	77.02

Table 1 shows the flotation results of toner and fiber recovery for all conditions.

From results can be seen the greater impact of pH value on the toner recovery than on fiber recovery. The fiber recovery of 88 % was achieved after 20 minutes flotation in acid and neutral conditions at pH 3, 5, and 7, and after 2 min of flotation in alkaline conditions at pH 9. Considering the results of fiber recovery obtained under different conditions, the highest fiber loss is achieved after 20 minutes in slightly alkaline conditions at pH 9 where Im was 65 %.

In shorter time of flotation, after 2 minutes in slightly acid conditions, toner recovery was 28.03 %. Compared with the results in slightly alkaline conditions where toner recovery was 75.56 %, it can be seen that toner recovery was higher for 47 %. At high alkaline conditions at pH 12, after 2 minutes of flotation, toner recovery decreases for 12 % (It = 48.37 %) than in high acidic conditions at pH 3 (It = 60.60 %).

Maximum values for toner recovery for every conditions was achieved after 4 minutes of flotation and this value remains constant until the end of the flotation time. Toner recovery in slightly acidic conditions was reduced as much as 53 % (It = 31.06) compared to results obtained in slightly alkaline conditions at pH 9.

This results indicate the influence of pH values at the rate of separation toner particles into the foam product under shorter and extended flotation time. The highest recovery was achieved after 4 min of flotation in high acid conditions at pH 3 where fiber recovery was 93 % and toner recovery achieved 63 % and in slightly alkaline conditions at pH 9 where fiber and toner recovery was 81 %, but not achieved value of recovery under 90 %. This results may indicate that flotation of such a raw material requires a shorter flotation time and potential change in conditions of flotation process.

CONCLUSION

The paper presents the results of the deinking flotation using the oleic acid as reagents in different conditions. As it can be observed, the removal of ink particles depends on several parameters. pH value and flotation time have got an essential role in deinking flotation. The results shows that the highest recovery was achieved after 4 minutes in high acid and slightly alkaline conditions, but not achieved value of recovery under 90 % which indicates the success of the process separation and obtaining a new products of appropriate quality. Based on the data, it can be said that the pH value is not negligible, but in addition, flotation time is one of the most important factors. With a longer flotation time toner recovery does not increase and it can only have a negative impact on the process because of the loss fibers in the foam.

References

1. Saurabh K., (2012), Deinking pulp fractionation: characterization and separation of fines by screening. Chemical and ProcessEngineering. Université de Grenoble, Dissertation,
2. Bajpai P., Recycling and Deinking of Recovered Paper, 1st Edition (2014), Elsevier insights, 304,
3. Zhao Y., Deng Y., Zhu Y., (2004), Roles of surfactants in Flotation Deinking, Progress in Paper Recycling, 14, 1, 41-45,

4. Borchardt J.K., Miller J.D., Azevedo M.A.D., (1998), Office paper de-inking, Applications in chemistry/chemical engineering, 360-367,
5. Tutak D., Modified deinking of digitally printed paper with water based inkjet ink, Cellulose Chemistry and Technology, 51 (5-6), 483-488 (2017),
6. Trumić M. S., Antonijević M., Trumić M. Ž., Bogdanović G., (2016), The application of mineral processing techniques for the printed paper recycling, Recycling and Sustainable Development, 9 (1), 47-57,
7. Azevedo M.A.D., Drelich J., Miller J.D., (1999), The effect of pH on Pulping and Flotation of Mixed office wastepaper, Journal of pulp and paper science, vol 25, no 9, 317-320,
8. Trumić S. M., Trumić Ž.M., Vujić B., Andrić Lj., Bogdanović G., Results of fibre and toner flotation depending on oleic acid dosage, Waste Management & Research (2016), Vol. 34(9) 969–974,
9. Pauck W. J., (2003), The role of sodium silicate in newsprint deinking, Master, University of Natal, Durban, 21-30,
10. Svensson R., (2011), The influence of surfactant chemistry on flotation deinking, Dissertation, University of Technology, Sweden, 12-31.

XIII International Mineral Processing and Recycling Conference
Belgrade, Serbia, 8-10 May 2019

University of Belgrade, Technical Faculty in Bor
Vojske Jugoslavije 12, 19210 Bor, Serbia
Tel. +381 30 424 555 Fax +381 30 421 078

RECOVERY OF HEMATITE FROM IRON ORE TAILING USING A BIOSURFACTANT FROM THE *RHODOCOCCUS OPACUS* STRAIN AS A COLLECTOR

Andreza Rafaela Morais Pereira, Ronald Rojas Hacha, Antonio Gutierrez Merma, Mauricio Leonardo Torem #
Pontifical Catholic University of Rio de Janeiro, Department of Chemical and Materials Engineering, Gávea, Rio de Janeiro, Brazil

ABSTRACT – Bioflotation employs bacterias and/or their metabolic products that can act as collectors, depressants or frothers. Thus, the objective of this article was to study the possibility of hematite concentration from the iron ore tailings using the biosurfactant extracted from the *Rhodococcus opacus* strain as biocollector and sodium silicate as a depressor of silica gangue. Zeta potential test was used to detect the interaction of the biosurfactant on the mineral surface. The physicochemical properties of biosurfactant were determined by surface tension. Microflotation tests were conducted at Partridge-Smith cell were carried out at different pH, biosurfactant concentrations and depressor concentrations. According to the results, the zeta potential of hematite shifted after interaction with the biosurfactant showing the adhesion of the biosurfactant on the hematite surface. The surface tension of the deionized water was reached around 36 mN/m at 0.16 g.L-1 (1,000 g/t) of biosurfactant concentration, the critical micellar concentration (CMC) was reached with the concentration of approximately 1 g.L-1 (6,000 g/t). Microflotation tests the highest iron recovery was (37 %) and iron grade (36.80 %) with the 6,000 g/t biosurfactant concentration at pH 3 without sodium silicate.

Key words: bioflotation, flotation, Rhodococcus opacus, hematite, iron ore tailings.

INTRODUCTION

With the increasing demand for minerals and the depletion of high grade mineral deposits, mineral research is increasingly focusing on the beneficiation of low grade ores to produce material suitable for a global market [1].

Biotechnology has been studied as an alternative for the future. Recent developments in the field of biotechnology have given promise not only to aid in mineral processing but also in metallurgy operations [2].

The use of bacterias and/or their metabolic substances in mineral processing has achieved more enhance in last decades. The developed studies show that they can be used as collectors, depressants or frothers agents in the mineral flotation. [4 -6].

corresponding author: torem@puc.brmm

Biosurfactants, surface-active compounds of biological origin, are of increasing interest for many industries because of their chemical diversity, multifunctional characteristics, and low toxicity in comparison to synthetic petrochemical-derived surfactants [7].

Therefore, the present work studies the use of the biosurfactant from the bacterial strain *Rhodococcus opacus* as a hematite biocollector in the direct flotation of the iron ore tailings. Initially, the iron ore tailing was characterized to know the chemical composition, followed by fundamental tests such as zeta potential, surface tension. Lastly, the variables (biocollector concentrations, depressor concentrations, and pH) were analyzed using microflotation tests in Patridge-Smith cell.

MATERIALS AND METHODS

Sampling

Iron ore tailing samples were collected from an industrial plant after a reverse iron ore flotation process. The samples were homogenized, dried (30 ± 5 ºC) and quartered for further flotation tests and X-ray fluorescence (XRF). For zeta potential, hematite samples were dry-ground in a porcelain mortar to the desired particles sizes.

Sample characterization

Elemental quantification of iron ore tailings was performed by volumetric titration and (XRF) realized for the determination of Fe. The determination of SiO_2, Si, Fe_2O_3 was made by difference.

Microorganisms and biosurfactant

The biosurfactant obtained from *Rhodococcus opacus* was used as a biocolector in the flotation of iron ore tailings. This bacterial strain was obtained from the Chemical, Biological and Agricultural Pluridisciplinary Research Center (CPQBA UNICAMP). The bacterial strain was cultured in liquid medium in 250 mL Erlenmeyer flasks and incubated in a rotating shaker (CIENTEC CT-712) at (28 ± 2 °C) for 72 h. The culture medium used was yeast malt glucose (YMG, Table 1). After growth, the cell suspension was centrifuged at 4,500 rpm for 8 min (CIENTEC CT-5,000), and the centrifuged concentrate containing the bacterial cells was washed once with deionized water and centrifuged again for discarding the remaining culture medium. After the centrifuged cells were re-suspended in ethanol (95 %), and autoclaved at 1.2 atm for 20 min. The insoluble part was removed by centrifugation at 4,500 rpm for 8 min) and the soluble part was dried at (50 ± 5 ºC) for 24 h. The dried material was dissolved in deionized water and the insoluble part was discarded. The solution with the soluble biosurfactant was kept at (4 ± 2 ºC) in a refrigerator for further analysis.

Zeta potential

Zeta potential studies were performed in a Malvern Zetasizer Nano microelectrophoresis apparatus at the Mineral Technology Center in Rio de Janeiro.

The suspensions of the mineral were prepared using KCl as the indifferent electrolyte at concentrations of 0.01 and 0.001 mol/L and deionized water. The pure hematite was conditioned at concentrations of 0.16 g/L equivalent to 1,000 g/t of biosurfactant. The desired pH value for the measurement was adjusted with dilute solutions (0.01 mol/L) of HCl and NaOH. The samples were obtained from the floated minerals, after drying in an oven at (50 ± 2 °C) for 8 h.

Table 1. Culture medium Yeast Malt Glucose (YMG)

Component	Liquid (g/L)	Solid (g/L)
Glicose	20	20
Peptone	5	5
Malt extract	3	3
Yeast extract	3	3
Agar	--	20
pH	7.2	7.2

Surface tension

Surface tension measurements were performed using the DC 200 Surface Electro Optics tensiometer by the Nöuy ring method at (21 ± 2 ºC). At pH 3 were studied different biosurfactant concentrations.

Microflotation tests

Microflotation tests were conducted in a Partridge-Smith cell in order to verify the influence of pH, biosurfactant concentration and the depressor concentration. It was used during a microflotation tests a rotameter, a bubblemeter, a magnetic stirrer, a vacuum-compressor. The detailed operating conditions used in the microflotation tests are presented in Table 2.

Table 2. Operation conditions microflotation tests

Conditions	Values
pH	3, 5, 7, 9, 11
Biosurfactant concentration	1000, 2000, 4000, 6000, 8000 g/t
Depressor concentation	100, 300, 600, 900, 1200 g/t
Iron ore tailings	5 g
Agitation	Magnetic
Volume	270 mL
Conditioning time	5 min.
Flotation time	5 min

RESULTS AND DISCUSSION

Sample characterization

The results of the chemical analysis by volumetric titration of the iron ore tailings sample showed a grade of 13.85 % Fe and 80.20 % SiO_2. X-ray Fluorescence (FRX) analysis corroborate the results of the volumetric titration with a grade of 13.8 % Fe and 80.3 % SiO_2 (Table 3).

Table 3. Chemical composition of iron ore tailing of the volumetric analysis

Compositions (%)	SiO_2	Fe_2O_3	Fe	Si
Volumetric Titration	80.20	19.80	13.85	37
FRX	80.30	19.73	13.8	37.53

Zeta potential

Figure 1.a shows the zeta potential curves of hematite in different concentrations of potassium chloride (indifferent electrolyte) and deionized water. As the concentration of KCl increased, a decrease in the magnitude of the hematite potential was observed, without altering the isoelectric point found that was around pH 6.2. This decrease is associated with the compression effect of the double electric layer caused by the increase of ionic strength in the solution [8-9].

Figure 1.b shows the zeta potential curve of hematite before and after interaction with the biosurfactant with an indifferent electrolyte concentration (10-3 M KCl). Before the interaction with the biosurfactant the zeta potential of the hematite presented values close to 15 mV in the acidic range and values around -7 mV in the alkaline range. After the interaction of the hematite with the biosurfactant the zeta potential of the hematite presented values close to 13 mV in the acidic range and values around -35 mV in the alkaline range, showing stability of the particles after the interaction. The hematite also shows a decrease in the value of its potential, as well as the displacement in the pH value corresponding to the PIE (pH 6.2 to pH 3.9).

The adsorption on the mineral surface can occur via electrostatic forces, since the hematite presents a positive charge and the mineral biosurfactant. Puelles [5], emphasizes that the biosurfactant is not composed only of trehalolipids. It can be composed of different organic substances, such as polysaccharides, fatty acids, phospholipids and even there may be soluble amino acids, and different substances may be adsorbed depending on the pH.

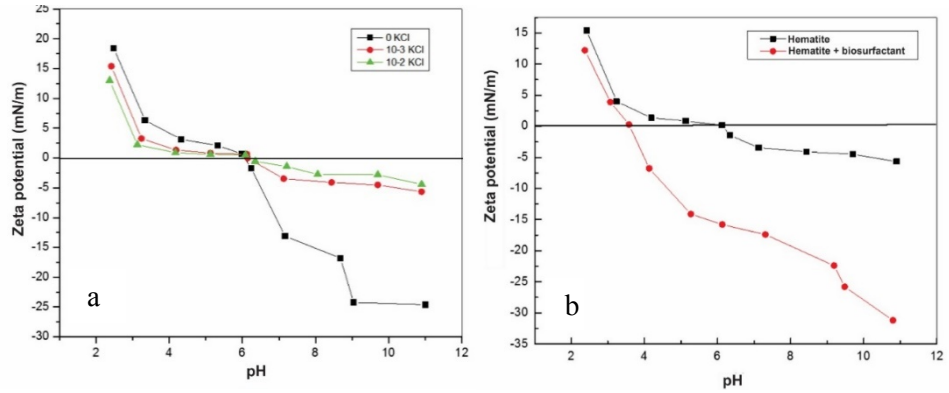

Figure 1. a) Zeta potential curves of pure hematite with indifferent eletrolytes, **b)** Zeta potential curves of hematite before and after its interaction with biosurfactant (electrolytic support: NaCl 10-3 mol/L)

Surface tension

Figure 2 shows the curve of surface tension versus biosurfactant concentration at pH 3. The surface tension of the deionized water presented a value around 71 mN/m; after the addition of 0.16 g.L-1 (1,000 g/t) of the biosurfactant concentration, the surface tension reached around 36 mN/m. The critical micellar concentration (CMC) was reached with the concentration of approximately 1 g.L-1(6,000 g/t) biosurfactant, the surface tension remaining constant after this concentration.

The *Rhodococcus* genus produces trehalose containing glycolipids, this reduction in surface tension can be attributed due to the presence of these surfactant substances at the liquid-gas interface. Most of the biosurfactants found in the *Rhodococcus* genus were reported to low the surface tension of water from 72 mN/m to values between 19 and 43 mN/m at CMC between 17 and 37 ppm [10].

Rufino et al. [11] studied the surface tension of the biosurfactant produced by *Candida lipolytica* UCP 0988. The authors observed that the reduction of water surface tension decreases gradually from 70 mN/m to 25 mN/m with increasing biosurfactant concentration.

Didyk and Sadowsky [12] studied the biosurfactants produced by biosurfactants *Bacillus circulans* and *Streptomyces sp.* they were used for biomodification of the serpentinite and quartz surfaces. The biosurfactants produced by the bacteria were able to decrease the surface tension of water from 72 to 28.6 mN/m (*Bacillus circulans*) and to 29.3 mN/ m (*Streptomyces sp.*).

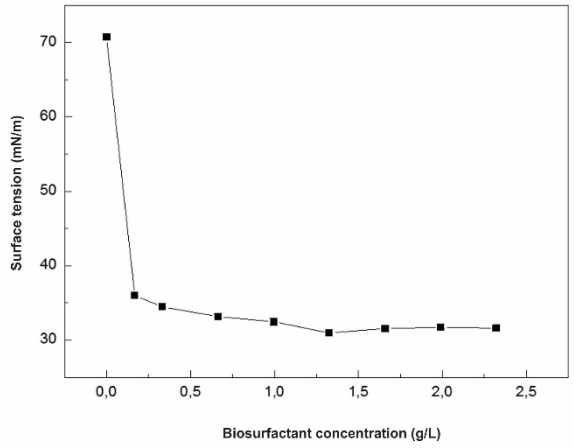

Figure 2. Surface tension versus biosurfactant concentration (pH 3)

Microflotation tests

Figure 3. shows the results of the pH effect on iron recovery and iron grade with biosurfactant concentration of 4,000 g/t. It was observed in the results that iron recoveries and iron grades decreased with pH variation, suggesting that pH is an important variable in flotation tests. Specifically, lower values of iron recovery and iron grade were observed at pH 4 and 5 (pH 4, iron recovery 9.61 % and iron grade 39.24 %, pH 5, iron recovery 4.23 % and iron grade 44,21 %, respectively), while pH

2 and 3 showed higher values (pH 2, iron recovery 34.28 % and iron grade 34.85 %, pH 3, iron recovery 28.41 % and iron grade 37.08 %). The results obtained are in agreement with the surface tension tests, that the lowest surface tension measurements occurred in low pH values, indicating that there may be greater adsorption of the biosurfactant in the mineral and with the tests of zeta potential that showed the reversal of mineral load after interaction with the biosurfactant.

Puelles [5] studied the floatability of hematite with the use of biosurfactant from Rhodococcus opacus in Hallimond tube and observed that the highest floatability occurred at pH 3, close to the hematite PIE after the interaction with the biosurfactant.

Oliveira [6] studied the floatability of hematite with the use of biosurfactant from Rhodococcus erythropolis in Hallimond tube and observed that the highest floatability occurred at pH 3, close to the hematite PIE after the interaction with the biosurfactant. The author explains that this result can be attributed to the different functional groups with hydrophobic character present in the biosurfactant.

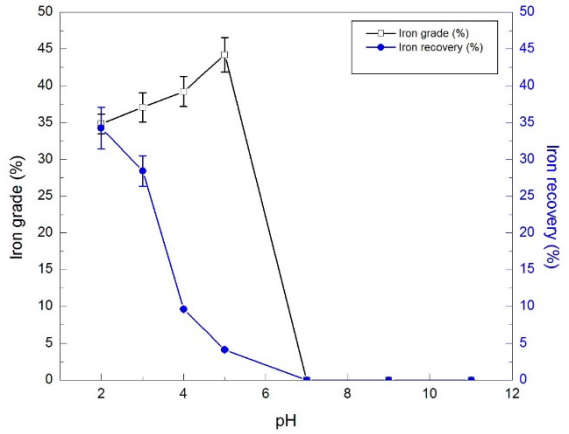

Figure 3. pH effect on iron recovery and iron grade (biosurfactant conc. at 4,000 g/t.)

Figure 4. a) shows the results of the effect of biosurfactant concentration on iron recovery and iron grade at pH 3. The increase of biosurfactant concentration caused a decrease in iron recovery and iron grade. This result is in agreement with the test of surface tension realized in this work that presents the critical micellar concentration (CMC) was reached with the concentration around 6,000 g/t remaining the surface tension constant after that concentration. The critical micelle concentration (CMC) is the concentration of surfactant in which organized molecular assemblies known as micelles are formed, decreasing the interactions of the biocollector with the mineral surface and, consequently, negatively affecting the flotation recovery [13-14]. It was observed in the results that the biosurfactant concentration in 6,000 g/t obtained the highest iron recovery (36.80 %) and the highest iron grade (36.97 %).

Figure 4. b) shows the results of the effect of sodium silicate concentration on iron recovery and iron grade with a concentration of 4,000 g/t of biosurfactant at pH 3. With the increase of the sodium silicate concentration, there was a decrease in iron

recovery and the iron grade. The hematite depression occurs due to adsorption of the sodium silicate on the mineral surface. Yang et al. [15] explained that at low pH values, negatively charged silicate anions and neutral species begin to prevail in solution and are active adsorbate species.

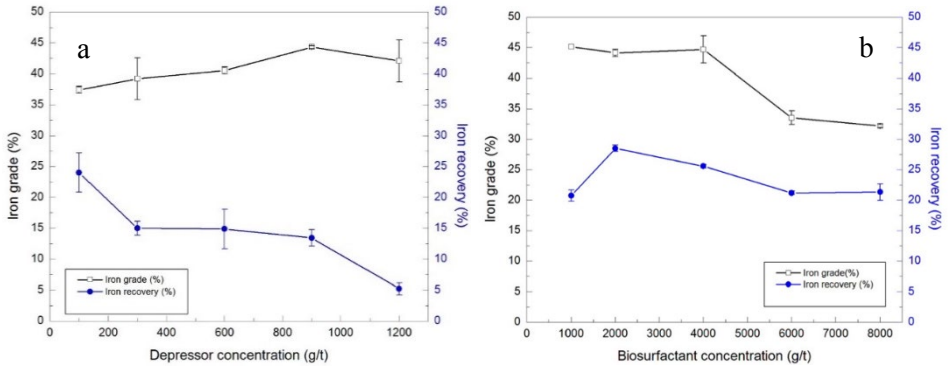

Figure 4. a) Effect of biosurfactant concentration on metallurgical recovery and iron content at pH 3; **b)** Effect of sodium silicate concentration on iron recovery and iron grade (biosurfactant concentration at 4,000 g/t and pH 3)

CONCLUSION

Zeta potential evaluation of hematite particles before and after interaction with bacterial cells showed a shift of the hematite IEP towards acidic pH, which indicates adhesion of biosurfactant onto the mineral surface.

Surface tension measurements showed that with the minimum biosurfactant concentration the surface tension of the deionized water was reached around 36 mN/m. The reduction of the surface tension facilitates the interaction between the mineral and air bubble. The critical micellar concentration (CMC) was reached with the concentration of approximately 1 g.L-1(6,000 g/t).

Microflotation tests presented that the highest iron recovery (36.80 %) and the highest iron grade (36.97 %) was obtained in the concentration of biosurfactant at 6,000 g/t. With the increase of the sodium silicate concentration, there was a decrease of the iron recovery and the iron grade, impairing the hematite flotation. This occurs due to monomeric species that adsorb on the surface of the hematite by electrostatic forces and make the mineral hydrophilic.

Acknowledgements:

The authors acknowledge Instituto Tecnológico Vale - ITV, PUC-Rio (Pontifical Catholic University of Rio de Janeiro); CNPq (National Council for Scientific and Technological Development); CAPES (Coordination for the Improvement of Higher Level Personnel); FAPERJ (Rio de Janeiro State Research Foundation) and CETEM (Mineral Technology Centre) for financial and technological support.

References

1. Dwyer, R., Bruckard, W. J., Rea, S., Holmes, R. J. (2012) Bioflotation and bioflocculation review: microorganisms relevant for mineral beneficiation. Mineral Processing and Extractive Metallurgy (Transactions of the institutions of Mining and Metallurgy: Section C, 121, 65-71,
2. Smith, R. W., Misra, M., Dubel, J. (1991) Mineral bioprocessing and the future. Minerals Engineering, 4 (7-11), 1127-1141,
3. Zouboulis, A. I., Matis, K. A., Lazaridis, N. K., Golyshin, P. N. (2003) The use biosurfactants in flotation: application for the removal of metal ions. Minerals Engineering, 16 (11), 1231-1236,
4. Khoshdast, H., Sam, A., Manafi, Z. (2012) The use of rhamnolipid biosurfactants as a frothing agent and a sample copper ore response. Minerals Engineering, 26, 41-49,
5. Puelles, J. G. S. (2016) Hematite flotation using a crude biosurfactant extracted from Rhodococcus opacus. Master's Dissertation - Materials Engineering, Chemical and Metallurgical Processes, Pontifical Catholic University of Rio de Janeiro, Rio de Janeiro, 112,
6. Oliveira, C. A. C. (2018) Flotation of the hematite-quartz system using the soluble biosurfactant produced by Rhodococcus erythropolis. PhD Thesis - Chemical and Materials Engineering, Pontifícia Universidade Católica do Rio de Janeiro, Rio de Janeiro, 148,
7. Maier, R. (2003) Biosurfactants: Evolution and Diversity in Bacteria. Advances in Applied Microbiology, 52, 101-116,
8. Hunter, R. J. (1981) Zeta Potential in Colloid Science - Principles and Applications. Academic Press Inc., (Colloid science series),
9. Fuerstenau, D. W., Pradip. 2005. Zeta potentials in the flotation of oxide and silicate minerals. Advanced Colloid Interfacial Science, 114, 9-26,
10. Christova, N., Stoineva, I. (2014) Trehalose Biosurfactants. In: Biosurfactants Research Trends and Applicactions, CRC Press, Boca Raton, 183-190,
11. Rufino, R. D., Luna, J. M., Takaki, G. M. C., Sarubbo, L. A., (2014) Characterization and properties of biosurfactant by Candida lipolytica UCP 0988. Eletronic Journal of Biotechnology, 17, 34-38,
12. Didyk, A. M., Sadowski, Z. (2012) Flotation of serpentinite and quartz using biosurfactants. Physicochemical Problems of Mineral Processing, 48 (2), 607-618,
13. Santos, D. K. F., Rufino, R. D., Luna, J. M., Santos, V. A., Sarubbo, L. A. (2016) Biosurfactants: Multifucntional biomolecules of the 21st century. International Journal of molecular sciences, 17, 1-31,
14. Hacha, R. R., Torem, M. L., Merma, A. G., Coelho, V. F. S. (2018) Electroflotation of fine hematite particles with Rhodococcus opacus as a biocollector in a modified Partridge-Smith cell. Minerals Engineering, 126, 105-115,
15. Yang, X., Roonasi, P., Holmgren, A. (2008) A study of sodium silicate in aqueous solution and sorbed by synthetic magnetite using in situ ATR-FTIR spectroscopy. Journal of Colloid and Interface Science, 328, 41-47.

XIII International Mineral Processing and Recycling Conference
Belgrade, Serbia, 8-10 May 2019

University of Belgrade, Technical Faculty in Bor
Vojske Jugoslavije 12, 19210 Bor, Serbia
Tel. +381 30 424 555 Fax +381 30 421 078

INNOVATIVE FLOCCULATION PROCESS FOR TREATING DISPERSED IRON TAILINGS BEARING WATERS

H. A. Oliveira, A. Azevedo, J. Rubio #
Federal University of Rio Grande do Sul-Brazil, Departamento de Engenharia de Minas, Rio Grande do Sul, Brazil

ABSTRACT

The disaster at the Fundão Tailings Dam (Samarco Mine-Brazil) is considered one of the largest in the world, in terms of volume of tailings dumped and magnitude of overall damages. Iron mining tailings, commonly stored in dam impoundments, are mixtures of crushed rock and suspensions of particles rejected from processing of reverse flotation and desliming. Risks related to these dams are a threat to sustainable development of the mining industry due to the toxic qualities and high volumes of the tailings, which may cause failures that contaminate ecosystems. More than 43 million m^3 of iron ore tailings caused environmental damage, polluting 668 km of watercourses from the Doce River Basin towards the Atlantic Ocean. Very fine tailing particles caused severe changes in the water quality of this river and estuarine region, increasing turbidity levels up to 6,000 times (600,000 NTU) higher than the upper limit established by law. The tailings consist predominantly of quartz, with secondary amounts of 12 - 28 % hematite (Fe_2O_3); 2.7 - 13 % goethite (FeO(OH)), and some trace minerals of Mn (Mn oxide) and Al (Gibbsite). The mud plume contaminated water sources making it difficult to treat to potable levels with existing installations, affecting 12 cities and 424,000 inhabitants around the Doce River basin.

Treatment stations were interrupted after the dam accident, but they are gradually coming back on line - with higher treatment costs (reagents, filters cleaning, etc.). The removal of the suspended solids by settling, without affecting the Gualaxo River water quality, requires low costs, non-toxic sustainable flocculation reagents. The polyacrylamides highly employed usually contain monomers and degraded molecules, both considered toxic when expose to humans and aquatic fauna. Accordingly, this work studied alternatives to remove the dispersed solids by a novel eco-friendly flocculation-settling technique. A survey of flocculation schemes was conducted and the best route found was employing ferric hydroxide precipitates

corresponding author: jrubio@ufrgs.br

and a natural flocculant, such as gelatinized corn starch. Physical and chemical characterization and solid/liquid separation of turbid waters from a river affected by an iron tailing rupture disaster (Gualaxo River, Brazil) were studied at bench scale.

Parameters such as turbidity, pH, surface tension, electrical conductivity, total suspended solids (TSS), particle size distribution (micro and nanoparticles) and zeta potential were analyzed from samples collected at three different river depths. The results in all samples showed the presence of micro and nanoparticles, ranging in diameters from 100 nm to 200 μm. Best results for flocculation and settling were obtained at pH 7.5, through an innovative combination of eco-friendly reagents: i. ferric hydroxide precipitates (10 mg/L Fe^{3+}) to trap the dispersed solids; ii. and gelatinized starch (5 mg/L) to form large flocs. The results showed removals between 90 - 100 % of total suspended solids (micro and nanoparticles), resulting in clear water with residual turbidity < 7 NTU. It is believed that this alternative has a high potential for treating the turbid water at Gualaxo River, assisting the water treatment stations.

Key words: flocculation, iron mining, tailings.

XIII International Mineral Processing and Recycling Conference
Belgrade, Serbia, 8-10 May 2019

University of Belgrade, Technical Faculty in Bor
Vojske Jugoslavije 12, 19210 Bor, Serbia
Tel. +381 30 424 555 Fax +381 30 421 078

SELECTIVE BIOFLOCCULATION OF HEMATITE USING THE YEAST *CANDIDA STELLATA*

Marcelo Carneiro Camarate, Maurício Leonardo Torem #, Antonio Gutierrez Merma, Ronald Rojas Hacha
Pontifical Catholic University, Department of Chemical Engineering and Materials, Gávea, Rio de Janeiro, Brazil

ABSTRACT – One of the biggest problems in the mineral recovery industry is related to the loss of ultrafine particles during the concentration process. The use of biological raw material in the flotation, coagulation and flocculation processes has been used as an alternative to solve this problem, however, there are few studies related to the recovery of ultrafine hematite particles by bioflocculation. Thus, this research aims at a fundamental study of the processing of ultrafine hematite particles using the biosurfactant extracted from the yeast *Candida stellata*. The hematite bioflocculation will be evaluated by jar-test assay, evaluating the influence of pH. The interaction of the bioreagent onto the mineral surface will be evaluated by FTIR (Fourier Transform Infra-red), evaluating the functional groups adsorbed and surface tension measurements. This study will aim at an alternative route for the recovery of ultrafine hematite particles using a biodegradable material that don't causes damages for the environment with high efficiency, meeting with the requirements demanded for this purpose.

Key words: biossurfactant, bioflocculation, yeast, hematite, quartz.

INTRODUCTION

Particle size is a very important variable in the operational performance of mineral processing operations. These concentration processes work well for particles of a limited size range, this limit depends on the mineral type, beyond which its efficiency reduces substantially. In iron ore flotation particles finer than 10 μm are not effectively and selectively separated by traditional froth flotation, because they tend to follow liquid streamlines around the bubble due to their low inertia, reducing the probability of collision and adhesion between particles and bubbles [1], others factors can be considered as difficulty of overcoming the energy barrier, high adsorption of reagents, low selectivity and mineralogical changes [2, 3, 4]. According to literature a promising ultrafine particles separation technique lies in flocculation, where a selective flocculant adsorbs on the surface particle [5]. These flocculants can be microorganisms and their byproducts, which adsorb onto the mineral surface and

corresponding author: torem@puc.br

induce a change in surface properties, e.g. reduce their electrostatic charge or promote hydrophobic interaction between the hydrophobized particles [6, 7, 8]. In this work, flocculation of hematite and quartz by the biosurfactant extracted from the *Candida stellata* yeast has been evaluated by jar tests; the aim of the work is to find a selectively window pH to separate hematite form quartz. Moreover, the adsorption of the biosurfactant onto the mineral surface was evaluated by FTIR and surface tension.

MATERIALS AND METHODS

Sample preparation

Quartz sample (> 95 % SiO_2) was provided by a local supplier (Belo horizonte, Minas Gerais State), the sample was comminuted in a jaw crush and screened to - 3 mm and then dry-ground in a porcelain mortar and wet screened to obtain a particle size with a P_{80} around 5 μm; the hematite sample was provided by Sigma Aldrich (Hematite powder, < 5 μm, > 96 %).

Microorganism, media, growth and biosurfactant extraction

Candida stellate strain was obtained from the collection of Reference Bacteria on Health Surveillance (CBRVS) - Oswaldo Cruz foundation. The maintenance solid medium consist of 20.0 g/l glucose, 5.0 g/l peptone, 3.0 g/l malt extract, 3.0 g/l yeast extract, and 20 g/l agar. The broth composition is the same except for agar. The incubation time was six days in a rotatory shaker at 151 rpm, 28 °C, then, the cells were separated from the culture medium by centrifugation at 3,200 g for 8 min. following by re-suspending twice with deionized water. The biosurfactant extraction followed the procedure from Moreau et al.[9], where the cells were centrifuged and then re-suspended in ethanol (500 ml for 1 L of broth), and autoclaved at 1 bar and 121 °C for 20 min. The insoluble part was removed by centrifugation (3,200 g), and then the soluble part was dried at 45 °C for 24 h. After this time, this material was dissolved in water, the insoluble part was separated from the soluble part by centrifugation (3,200 g) and filtration (8 μm). The final solution is the crude biosurfactant solution and the biosurfactant concentration was determined by dry-weight measurement.

FTIR analysis and Surface tension measurements

For the characterization studies, we used a Nicolet FTIR 2000 spectrophotometer (Attenuated total reflection); sample pre-treatment requires a drying temperature of 50 °C. The analyses were done before and after interacting with the biosurfactant. The surface tension of the biosurfactant solution was determined using a DCA-200S tensiometer (Surface Electro optics). The pH solution was adjusted using HCl and NaOH aliquots and the biosurfactant concentration ranges from 0 to 400 mg L^{-1}. Additionally, the intersection of the two tangents at the minimum and maximum surface tension values gives the critical micelle concentration (CMC).

Flocculation tests

A desired quantity of the mineral sample was conditioned with a desired

concentration (100 mg L^{-1}) of the biosurfactant inside a 500 mL graduated cylinder at a desired pH value, during 5 min., then the suspension was vigorously mixed during 20 min., after this time the mixer was turned off and allow mineral to settle for 5 to 120 min. The height of clarified liquid versus sedimentation time was recorded.

RESULTS AND DISCUSSION

Bioflocculation of hematite and quartz

Figures 1 and 2 show the flocculation of hematite and quartz, before and after interacting with the crude biosurfactant, respectively. The formation of agglomerate (coagulation-flocculation) depends on the balance of attractive and repulsive forces between the particles, before interacting with the biosurfactant the minerals particles carry a surface charge and are keep in suspension by electrostatic repulsion. Hence, the higher flocculation of hematite is expected at its isoelectric point (IEP), which according to literature is around 7 [10, 11] (Fig. 1). The same was not observed for quartz (Fig. 2), since experiments were conducted at pH higher than its IEP (below than 2). At pH 3 the recovery of hematite (~ 52 %) was lower than the quartz´s (~ 68 %) probably due to a lower surface charge of the quartz because of the proximity of its IEP.

After interacting with the biosurfactant the flocculation profile for both minerals suffered a modification, this evidences adsorption of the biosurfactant. The higher increment (about 40 %) in the flocculation of hematite particles was observed at acidic conditions (pH 3), achieving a recovery higher than 90 %. At pH 7 the effect of the biosurfactant was unnoticeable, it could be probably related to no adsorption of the biosurfactant. The last will be confirmed with adsorption experiments in futures works.

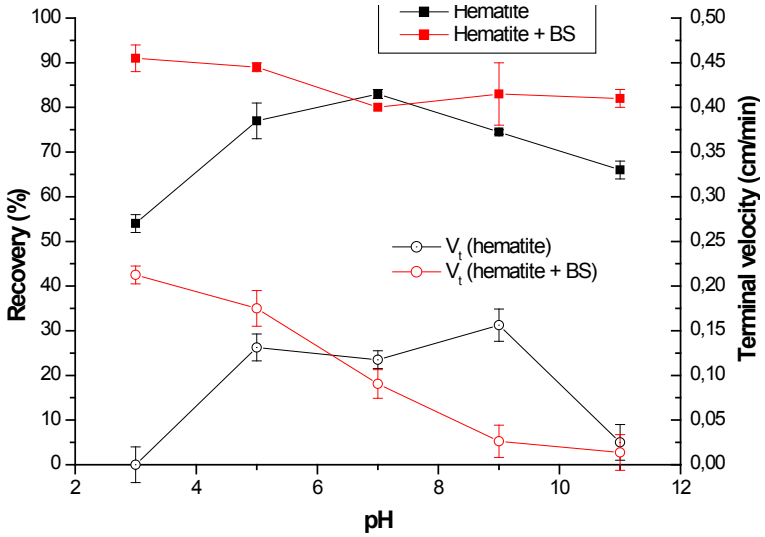

Figure 1. Recovery and terminal velocity of hematite particles before and after interacting with the biosurfactant, biosurfactant concentration: 100 mg/L, time: 120 min

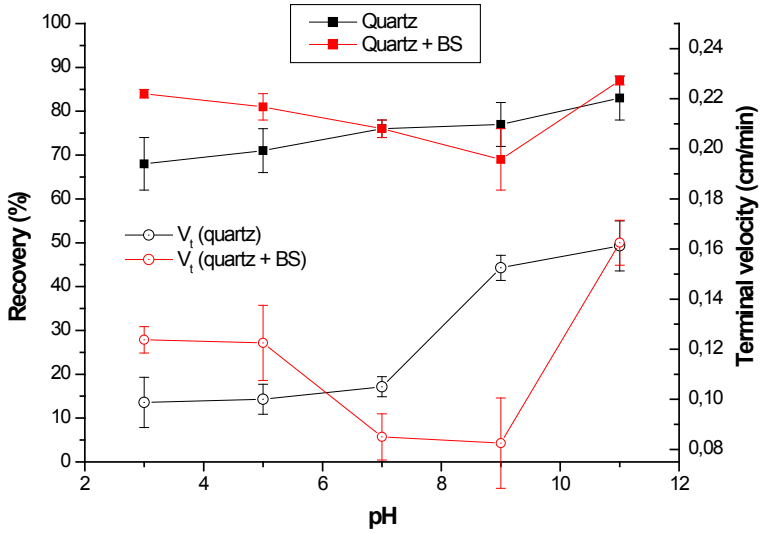

Figure 2. Recovery and terminal velocity of quartz particles before and after interacting with the biosurfactant, biosurfactant concentration: 100 mg/L, time: 120 min

The bioflocculation of quartz presented a similar behavior (Fig. 2), higher recovery at pH 3 and lower at pH 7. This could be related to the adsorption of the biosurfactant, being maximum at pH 3 and minimum at pH 7. Although, a high recovery of quartz was achieved (around 83 %), a lower increment was observed after interacting with the biosurfactant (around 15 %) when compared with bioflocculation of hematite.

The objective of this work is to find a selectively window to separate hematite from quartz, apparently this window was present at pH 3. At this pH the recovery of hematite and quartz were ~ 92 % and ~ 83 %, respectively, these values are very close and a selectively separation looks impracticable. However, the terminal velocity of the minerals particles (Fig. 1 and Fig.2) could help to elucidate the separation; at acidic conditions both minerals presented an increase of their terminal velocity, after interacting with the biosurfactant, this increase was higher for hematite at pH 3. Thus, at pH 3 the terminal velocity of quartz and hematite presented values around 0.12 and 0.22 cm min^{-1}, respectively, (values achieved after 40 and 20 min., respectively), and hence, the separation of hematite from quartz could be obtained, during the first minutes of the operation.

FTIR analysis and Surface Tension

The composition of biosurfactants derived from microorganisms is complex, and present several functions groups, which can be observed in the region of the infrared spectrum between 3,500 and 1,000 cm^{-1}. Thus, knowing that the characteristic bands for hematite and quartz are found below 1,000 cm^{-1} [12, 13, 14], the infrared spectrum studied was between 3,500 and 1,000 cm^{-1}.

Figures 1 and 2, show the ATR-FTIR spectra of hematite and quartz particles before and after interacting with the crude biosurfactant at pH 3, respectively. The

FTIR spectra evidences adsorption of the crude biosurfactant onto the hematite surface (Fig. 3), according to literature [10] this result suggested a chemisorption driven force, we have to remark that in order to remove weak attached substances the samples were rinsed twice with deionized water. No changes were observed in the FTIR spectra of quartz after interacting with the biosurfactant (Fig. 4), this could evidence a weak adsorption of the biosurfactant and hence a higher selectivity of the biosurfactant to adsorb on the hematite surface. The FTIR spectra of hematite after the interaction presents several peaks i.e. 2,924, 2,853 correspond to alkyl C-H stretch, peak between 1,780 and 1,630 correspond to carbonyl stretching absorption (aldehyde, carboxylic acid, ketone, amide and ester). Finally, the peak at 1,090 corresponds to phosphate group in teichoic acid. [15, 16].

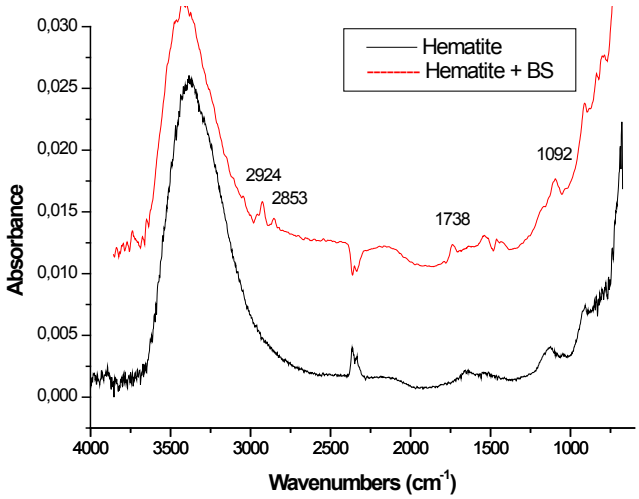

Figure 3. FTIR spectra of hematite before and after interacting with the biosurfactant, pH 3

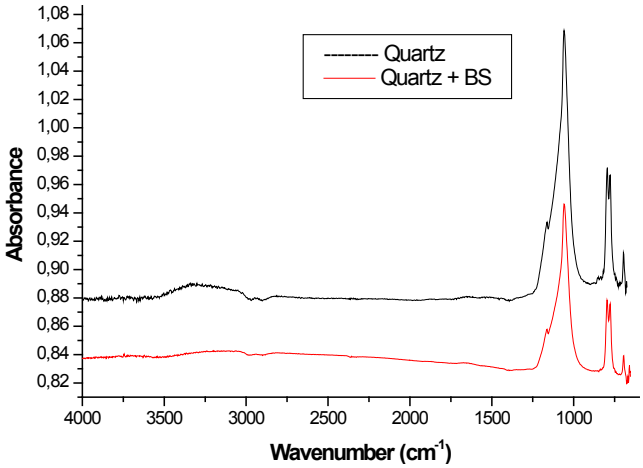

Figure 4. FTIR spectra of quartz before and after interacting with the biosurfactant, pH 3

Figure 5 shows the surface tension of the crude biosurfactant-water interface as a function of concentration. The estimated critical micellar concentration, after mathematical regression, is approximately 250 mg/L, and the surface tension decreased to 42 mN/m. These results are similar to previous works [10, 11].

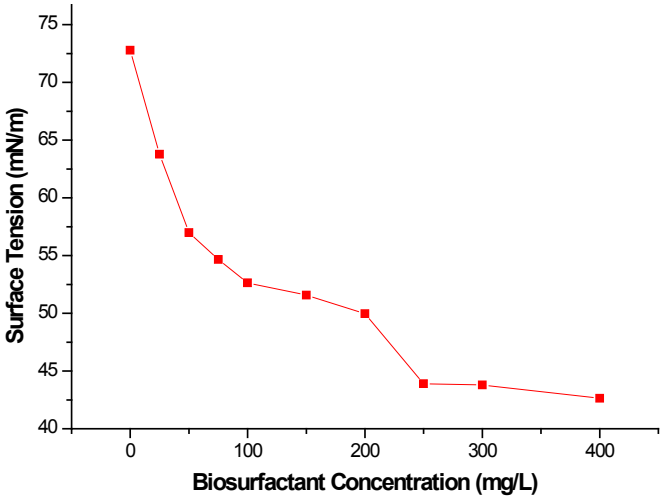

Figure 5. Surface tension of the biosurfactant as a function of biosurfactant concentration

CONCLUSION

It was observed that it is possible to flocculate hematite and quartz using the biosurfactant extracted from Candida stellate yeast. The interaction of the mineral with biosurfactant provoked a higher recovery of hematite (90 %) via flocculation, this effect was higher at pH 3. Recovery of quartz was lower (85 %) at the same experimental conditions, however, the terminal velocity of hematite was higher (0.22 cm min^{-1}) than of the quartz (0.12 cm min^{-1}), which would be an indicative of a potential region for selective separation. The main factor that affect the process are the pH and the biosurfactant concentration. The biosurfactant affected the surface properties of the minerals and the surface tension of air/water interface, achieving up to ~ 40 mNm^{-1}. Thus, this biosurfactant presents a higher potential for mineral processing.

References

1. Tadesse, B.; Albijanic, B.; Makuei, F.; Browner, R.; 2018. Recovery of fine and ultrafine mineral particles by electroflotation- A review. Mineral Processing and Extractive Metallurgy Review, 1-15, Taylor and Francis.
2. Hacha, R.R.; Torem, M.L., Merma, A.G.; Coelho, V.F. 2018. Electroflotation of fine hematite particles with R. opacus as a biocollector in a modified Partridge-Smith cell. Minerals engineering, 126, 105 – 115. Elsevier.
3. Rubio, J., Capponi, F., Matiolo, E., Rosa, J.J., 2004. Advances in flotation of copper and molybdenum sulphide ore fines. In: XXI National Meeting of Ores

Treatment and Extractive Metallurgy, vol. 2, pp. 69–78. Florianópolis-SC.
4. Peng, Y., Liang, L., Tan, J., Sha, J., Xie, G., 2015. Effect of flotation reagent adsorption by different ultra-fine coal particles on coal flotation. Int. J. Miner. Process. 142, 17–21. Elsevier.
5. Zhang, J.; Sun, W.; Gao, Z.; Niu, F.; Wang, L.; Zhao, Y.; Gao, Y. 2018. Selective flocculation separation of fine hematite from quartz using a novel grafted colopymer flocculant. Minerals, 8, 227, 1 – 11. MDPI.
6. Harajima, T.; Aiba, Y.; Farahat, M.; Okibe, N.; Sasaki, K.; Tsuruta, T.; Doi, K. 2012. Effect of microorganisms on flocculation of quartz. International Journal of Mineral Processing, 102-103, 107 – 111. Elsevier.
7. Vilinska, A.; Rao, H. 2010. Leptosririllum ferrooxidans-sulfide mineral interactions with reference to bioflotation and bioflocculation. Trans. Nonferrous Met. Soc. China, 18, 1403 – 1409. Science Press.
8. Selim, K.A.; Rostom, M. 2018. Bioflocculation of (iron oxide-silica) system using Bacillus cereus bacteria isolated from Egyptian iron ore surface. Egyptian Journal of Petroleum, 27, 235 – 240. Elsevier.
9. Moreau, R., Powell, M. J., Singh, V., 2003. Pressurized Liquid Extraction of Polar and Nonpolar Lipids in Corn and Oats with Hexane, Methylene Chloride, Isopropanol, and Ethanol. Journal of the American Oil Chemists' Society, 80, 1063–1067.
10. Puelles, J.G.S. 2016. Hematite flotation using a crude biosurfactant extracted from R. opacus. Master Dissertation. Chemical Department, Pontifical Catholic University of Rio de Janeiro.
11. Olivera, C.A.C. 2018. Hematite-quartz system flotation using the soluble biosurfactant extracted from R. erythropolis. Doctoral Thesis. Chemical Department, Pontifical Catholic University of Rio de Janeiro.
12. Wang, Y.; Maramatsu, A.; Sugimoto, T.; 1998. FTIR analysis of well-defined α-Fe2O3 particles. Colloids and Surfaces. A: Physicochemical and Engineering Aspects, 134, 281-297. Elsevier.
13. Maity, D., Agrawal, D.C., 2007. Synthesis of iron oxide nanoparticles under oxidizing environment and their stabilization in aqueous and non-aqueous media. J. Magn. Magn. Mater. 308 (1), 46–55.
14. Liu W, Liu W, Wei D, Li M, Zhao Q, Xu S. 2017. Synthesis of N,N-Bis (2-hydroxypropyl) laurylamine and its flotation on quartz. Chem Eng J.; 309:63–9.
15. Garip, S., Gozen, A.C., Severcan, F., 2009. Use of Fourier transform infrared spectroscopy for rapid comparative analysis of Bacillus and Micrococcus isolates. Food Chem. 113 (4), 1301–1307. Elsevier.
16. Hacha, R.R.; Torem, M.L.; Merma, A.G.; Coelho, V.F. 2018. Electroflotation of fine hematite particles with Rhodococcus opacus as a biocollector in a modified Partridge-smith cell. Mineral Engineering, 126, 105 – 115. Elsevier.

XIII International Mineral Processing and Recycling Conference
Belgrade, Serbia, 8-10 May 2019

University of Belgrade, Technical Faculty in Bor
Vojske Jugoslavije 12, 19210 Bor, Serbia
Tel. +381 30 424 555 Fax +381 30 421 078

EVOLUTION OF COAL PROCESSING PRACTICES AT TATA STEEL

Arun Misra #, Debaprasad Chakraborty, Bhargav Dhavala
Tata Steel Limited, Jamshedpur, Jharkhand, India

ABSTRACT – Tata Steel meets its coal requirement for coke making from two captive coal mines: Jharia (underground) and West Bokaro (open cast). Indian coals are high in ash content owing to their drift origin and come under 'difficult-to-wash 'category. Hence, coal produced from the captive mines cannot be used directly for coke making. To make it suitable for coke making, it must be processed to lower down its mineral matter. In 1951/52, Tata Steel became a pioneer in Asia by setting up its first coal washery in West Bokaro & Jharia to produce clean coal with 19 % ash using Chance Cone process, feed size being 75*6 mm. Fine coal (-6 mm) was used directly without beneficiation. To keep abreast with the technology trends, Chance Cone process was eventually replaced by Dense Media Cyclones and mechanical flotation cells in 1982. 1990s witnessed the replacement of DSM cyclones with scrolled evolute cyclones having higher efficiency and capacity followed by introduction of pump fed cyclones and replacement of flat-bottom flotation cells with U-bottom ones. Technological improvements between 2000-2018 touch-based most of the critical unit operations in a beneficiation plant: Comminution (*Introduction of Sizers to improve liberation*), Classification (*Replacement of Elliptical screens with Banana screens to improve the desliming efficiency*), Flotation (*Introduction of 'Advanced new-generation mixing mechanism' & substitution of Diesel with green reagents*) and Dewatering (*Replacement of Screen bowl centrifuges with Vacuum Belt Filter to capture the ultra-fine clean coal otherwise getting lost with the centrifuge effluents*). Focus was also put on automation of the technological processes: *PGNAA based real-time ash monitoring system to ensure consistency in the product quality*. Increase in demand of coking coal and the deteriorating raw coal quality demand that we continuously scan the world & adopt best technologies to become a technology leader in the business. Down the line, Tata Steel aims to have: (a) Intermediate size beneficiation to mitigate the limitations DMC/Flotation have in processing finer/coarser size fractions, (b) Superior technologies for fine coal beneficiation/difficult-to-float coals and (c) Advanced measurement and control systems in place.

Key words: dense media cyclone, flotation, banana screen, vaccum belt filter, intermediate size beneficiation

INTRODUCTION

Tata Steel meets its coal requirement for coke making from two captive coal mines: Jharia (underground) and West Bokaro (open cast) located in the state of Jharkhand. Indian coals are high in ash content (~35%) owing to their drift origin and come under 'difficult-to-wash 'category due to high Near Gravity Material (~40-

corresponding author: arun.misra@tatasteel.com

50%). Hence, coal produced from the captive mines cannot be used directly for coke making. To make it suitable for coke making, it is beneficiated in a washery and the washed coal is then used for coke making. Tata Steel became a pioneer in Asia by setting up its first coal washery in West Bokaro & Jharia in 1951 & 1952, respectively. The journey of coal beneficiation practices at Tata Steel in a nutshell is shown in Figure 1 and the story behind each step is explained in detail subsequently.

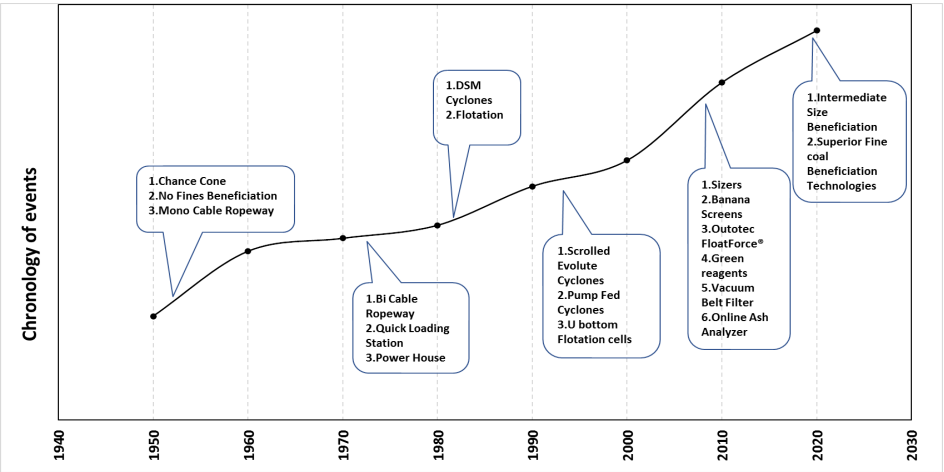

Figure 1. Technological Improvements – chronology of events

TECHNOLOGICAL IMPROVEMENTS IN COAL BENEFICIATION AT TATA STEEL

1950S – 1970s (chance cone process)

Raw coal having an ash content of 20-23% was crushed and reduced to -75 mm size followed by screening at 6 mm. 75*6 mm size fraction of coal was beneficiated in Chance Cone process (a dense media separator utilizing sand as media) whereas the finer fraction (-6 mm) was directly added without beneficiation to the washed coal and used (Figure 2). The composite clean coal having an ash of 19% was transported to the railway siding via. a mono-cable ropeway. Yield of clean coal varied from 65-90% and most of the equipments were manually controlled. Until early 1970s, only top seams were worked and fed to the washery. In the late 1970s, the middle and lower seams having comparatively higher ash were also mined, a bi-cable ropeway for transportation of washed coal from the washery to the railway siding, a quick loading system at the railway siding and a power house were also added.

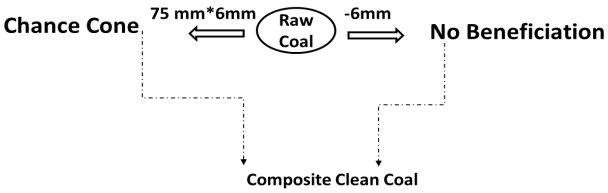

Figure 2. Flowsheet in 1950-1970s

1980S (dense media cyclones and froth flotation)

Advent of new technologies, continuous deterioration in the mined raw coal quality supplemented by the poor performance of Chance Cone process was witnessed. Earlier, the coal washeries did not have any fines treatment circuits; they were simply blended with the washed coarser coals owing to the very good quality. However, with time, quality of fines deteriorated significantly and it was practically impossible to maintain the quality of washed coal by direct mixing. Detailed studies were carried out to arrive at the correct feed top size to the washery to optimize the clean coal yield at a desired ash. Eventually, Chance Cone process was replaced with Dense Media Cyclones for processing coarser raw coal fraction: 13 to 0.5mm and mechanical flotation cells for processing finer raw coal fraction: -0.5mm (Figure 3).

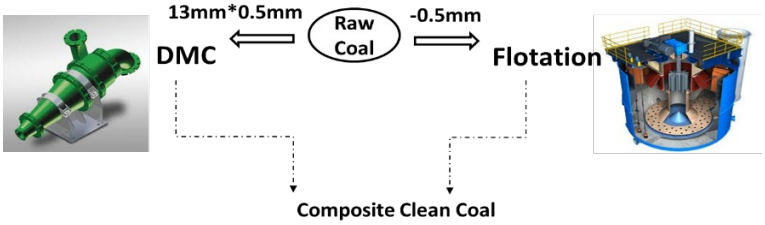

Figure 3. Flowsheet in 1980s

1990s

Low Ep Scrolled Evolute Cyclones: In the year 1998-99, Washeries switched over from Dutch State Mines (DSM) design cyclones to scrolled evolute design cyclones. Process performance improved as the Ep obtained was 0.02-0.025 as against 0.035-0.040 in the DSM cyclones. These cyclones are also of larger capacity thereby helping in increasing the plant throughput.

Introduction of Pump Fed Cyclones & High –Low Concept in Cyclone Circuit: At West Bokaro washery#3, parallel modular streams in cyclone circuit along with pump fed cyclones were introduced. Pump feeding system has its own share of pros and cons. Gravity feeding requires higher footprint but achieves a more consistent flow, less pump wear and feed degradation.

There are two stages of cyclone washing in which the primary cyclones are operated at higher specific gravity to discard the rejects. The second stage cyclones are operated at lower specific gravity for separation of clean coal & middlings. These cyclones have V/f converters for maintaining the required inlet pressure thereby reducing the capital costs in comparison to a conventional gravity fed cyclone.

Replacement of flat-bottom flotation cells with U-bottom ones: U-bottom cells minimize the sanding/silting phenomenon. Sanding is high in flat-bottom cells due to lack of velocity in the un-agitated zones thereby allowing the larger particles to settle down.

2000-2018

Introduction of Sizers to improve liberation: Crushing and liberating coal to the correct size is of prime importance as it would improve the performance of the

coal washery. Sizers were introduced in place of roll crushers to get optimum liberation at reduced noise and dust.

Replacement of Elliptical screens with Banana screens to improve the desliming efficiency: Earlier, elliptical screens were used for desliming raw coal at 0.5 mm. Screening efficiency of these screens was found to be poor- it was observed that a substantial quantity of undersize i.e. (-) 0.5 mm reported to the screen oversize. These finer coal particles create difficulties in maintaining the cut density inside the cyclone thereby impacting the efficiency. These screens were eventually replaced with robust Banana Screens.

Introduction of 'Advanced new-generation mixing mechanism 'in Flotation cells: At West Bokaro Washery-3, significantly high (20-25% by wt.) proportion of plus 0.5 mm size coal particles report in the flotation cell feed. This was always a concern as most of these particles report to the flotation tailings. To improve the fines circuit performance, Tata Steel incorporated a new generation mixing mechanism- Outotec FloatForce® in one flotation bank to start with. This mechanism creates more turbulent energy and generates finer bubbles as it has separate chambers for air and slurry in the rotor assembly of the flotation cell (Figure 4). In the conventional mixing mechanism, the design of rotor-stator assembly is such that there is a single passage for both slurry and air and hence, air mixing with slurry is not fully effective. Outotec FloatForce® has also been found to be more effective in floating relatively coarser particles and pushing more coal slurry as compared to the conventional mixing mechanism.

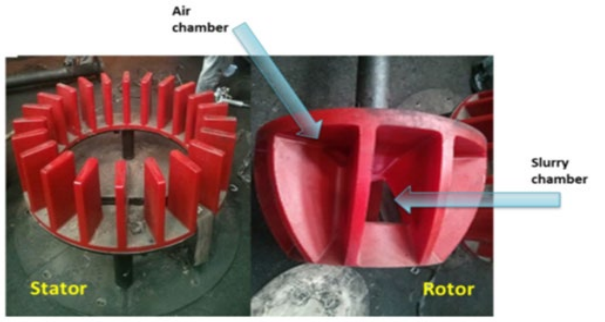

Figure 4. New generation mixing mechanism Outotec FloatForce®

Substitution of Diesel with green reagents in Flotation: For ages, Diesel is being used as a collector in coal flotation. With the stringent environmental regulations and policies, replacement of diesel with a reagent that is environment friendly as well as technically & economically competent became inevitable. Diesel is also highly inflammable and prone to pilferage and hence, poses safety as well as environmental hazards. A Joint improvement initiative was taken with Nalco Chemicals for the development of a synthetic collector which not only gives technically competent results but also is economical, safe and environment friendly.

Introduction of Vacuum Belt Filter for dewatering fine clean coal: Initially, Screen Bowl Centrifuges were used for dewatering fine clean coal: < 0.5 mm. However, it was observed that ultra-fine coal particles were getting lost with the centrifuge effluents. To capture such low ash ultra-fine clean coal, Horizontal

Vacuum Belt Filters (HVBF) were installed. The belt filter installed at West Bokaro washery#3 is also the world's largest HVBF with an effective filtration area of 145 m^2 for coal slurry.

On Line Ash Analyzers for consistency in product quality: Taking representative samples from conveyor belt and analyses for effective quality monitoring & control was time consuming. As a result, corrective actions could not be taken timely resulting in in variations in the clean coal ash. To overcome the mentioned problems, online ash analyser based on Prompt Gamma Neutron Activation concept was introduced. Use of online analyzer to monitor ash has resulted in minimization of shift wise standard deviation in the clean coal ash.

2018+ (some already established, some need to be established)

Intermediate size beneficiation: It has been observed through process audits that recovery of 0.5-0.25/0.15 mm size fraction is the lowest of the lot in froth flotation process and 0.5 mm is not the ideal top size for flotation. To improve the recovery of 0.5-0.25/0.15 mm size fraction, intermediate size beneficiation in a Reflux Classifier (RC) has already been implemented at Jamadoba washery and would be replicated across the remaining coal washeries of Tata Steel in the near future (Figure 5).

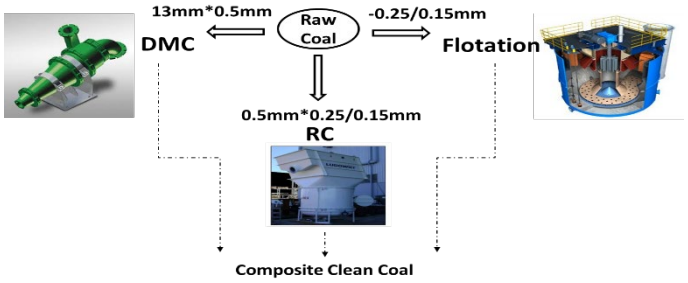

Figure 5. Futuristic Flowsheet

Superior technologies for fine coal beneficiation/difficult-to-float coals: Flotation is a complex process controlled by factors which can be divided into three facets: coal characteristics, chemistry and machine characteristics. Factors within the coal and chemistry areas are dynamic and hence, need to be dealt with by personnel on an ongoing basis in normal plant operations. However, the most important characteristic of any flotation technology is air bubble generation and the size of air bubbles produced as this controls flotation kinetics and dictates the carrying capacity of the machine. Several technologies have come up for fine coal beneficiation such as Column cells, Jameson cells and Jet flotation cells which have been found superior to the conventional mechanical flotation cells.

Step-by-step approach to a fully automated plant: In the age of Digitalization, IoT and Industry 4.0, it is equally important to have automation – basic & advanced measurement systems & control systems in the technological processes to achieve higher yields at the same grade and to become a technology leader in the business as shown in Figure 6.

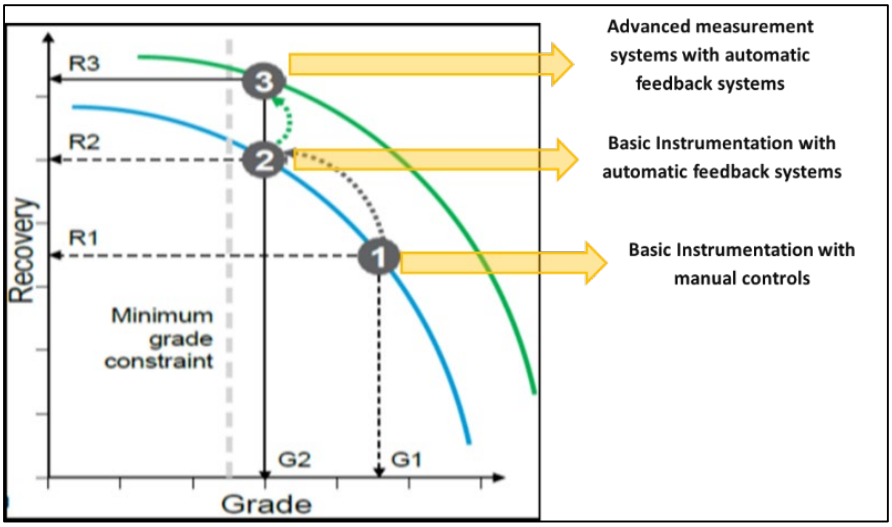

Figure 6. Automation in technological processes

CONCLUSIONS & WAY FORWARD

Increase in demand of coking coal and the deteriorating raw coal quality demand that we continuously scan the world & adopt best technologies to become a technology leader in the business.

References

1. Rao, P.S., Khattri, P., Krishna, C.G., Rao, S.M. (2012) Technological advancements in coal processing at Tata Steel. International Mineral Processing Congress – IMPC. Delhi, India, Proceedings, 4426,
2. Khattri, P., Krishna, C.G., Rao, P.S., Banerjee, P.P., Rao, S.M. (2012) Gammametry-a technological intervention for optimization & process control at coal washeries. International Mineral Processing Congress – IMPC. Delhi, India, Proceedings, 2403,
3. Prasad, L., Safyi, S.M., (1985) Some aspects of coal flotation at washeries of Tata Steel. Eprints NML,
4. Rao, T.C., Prasad, L., Singh, K. (1978) Some aspects of beneficiation of coal slimes in India. Paper presented at Seminar on coal washing organised by the Bureau of Public Enterprises. New Delhi, India,
5. Chakraborty, D.P., Sen, S., Ray, P.R., Kumar, A., Tata Steel Limited (2015) Augmenting supplies of metallurgical coal to steel mills by upgrading low and medium coking coals. CPSI J, 66–72,
6. Ahmed, N. (1989) The New Washery at Tata Steel's West Bokaro Colliery. Tata Tech. Vol. 5.

XIII International Mineral Processing and Recycling Conference
Belgrade, Serbia, 8-10 May 2019

University of Belgrade, Technical Faculty in Bor
Vojske Jugoslavije 12, 19210 Bor, Serbia
Tel. +381 30 424 555 Fax +381 30 421 078

UNDERGROUND COAL ENRICHMENT

Viktor Atrushkevich #
Moscow Mining Institute of the National University of Science and Technology MISiS, Russia

ABSTRACT – Evolution of mining technological systems is the constantly and multifactorial process having for an object to intensify mining in various geological conditions with person and nature safety growing requirements. Here is some results of cooperation of Moscow mining institute and Scientific and Production Association "Hydrotechnology" dealing with creation and implementation of clean coal technological systems of mining coal deposits by the opencast, underground and hybrid method with use of also hydraulically mechanized equipment. Technology options with processing and complete mineral enrichment at mining enterprises are also presented. Technical solutions that improve quality of coal products and mining safety are given.

Key words: clean coal technology, ash content, hydro-transport, water jets, safety of mining

INTRODUCTION

The trend of mining enterprises towards higher efficiency is improvement of end product quality by partial or complete processing of minerals. The authors have developed clean coal technology and equipment for integrated processing of coal in technological system of mining enterprises on the basis of hydromechanization.

Underground hydro mechanized coal mining technology had higher technical and economic indicators in comparison with "dry" traditional coal mining especially in complicated mining-and-geological conditions. However, for wide introduction of hydraulic mining in the coal industry was interfered by high capital intensity and power consumption of this technology, considerable operational losses, need of constructing of special factories for coal dewatering, aggravating an ecological situation, high labor input and cost of dewatering of coal and purification of technological water.

MATERIAL AND METHODS OF WORK

Mine experiment and industrial testing of technology in various mining and geological conditions were used as the main research method.

To eliminate the abovementioned shortcomings, we could use the created by

corresponding author: iugi@mail.ru

Scientific and Production Association "Hydrotechnology" highly effective, non-polluting coal mining hydro-mechanical technology, which simplify coal mining process. Use of the expensive longwall mechanized complexes inherent in traditional technological systems is excluded. Basis of new hydraulic mining technology, created by dr. Habil., professor Arkadiy Atrushkevich, [1] is the underground closed hydro-transport system including a complex of the equipment for underground dewatering and enrichment of coal, purification of technological water and supplying it in cleared working and development faces (fig. 1).

Specified technology feature and degree is lack of lakes-clarifiers and any polluted water evacuation in open reservoirs on a surface impairing the ecological situation.

Development of new level hydraulic technology confirmed its high efficiency on experimental hydraulic mines "Nagornaya-1" and "Nagornaya-2" in Kuzbuss (Russia) in production process (Table 1).

Table 1. Main progress data of work of "Nagornaya-1" and "Nagornaya-2" hydraulic mines

№	Indicator name	Dimension	Value of an indicator
1	Labor productivity of the worker: - on ordinary coal, - on a concentrate	 t/month t/month	 350 250
2	Ash-content of extracted coal	%	10
3	Coal ash-content on the next mines with traditional technology of production	%	22-26
4	Hydraulic mine construction term with volume of production of 360-500 thousand tone/year	month	6-10
5	Capital investments for equipping of hydraulic mine construction in different (including – complicated) mining-and-geological conditions	million $ USA	8-12

The technological structure and engineering new technology of hydraulic mining, which provides for high progress data, characterized by existence of technological processes limited number that defines its: simplicity, low capital expenditure and ecological purity. New technology includes the following processes:

- mechanical-hydraulic roadways drivage (using of this technology for mechanical-hydraulic roadways drivage at the experimental Scientific and Production Association "Hydrotechnology" hydraulic mines in Kuzbass allowed, during the drivage of roadways with cross-sectional area of 8-10 square meters in coal seams, to achieve a speed of 40 meters per day);
- mechanical-hydraulic coal extraction in room and pillar system (fig. 2);
- gravity free-flow non-pressure hydro-transport of coal to the dewatering room;
- underground closed complex of coal dewatering and enrichment, purification

of technological water and supplying in coal and development faces;
- dewatered coal delivery and warehousing on the surface of the mine;
- coal additional enrichment (if required) on surface and concentrate loading in vehicles.

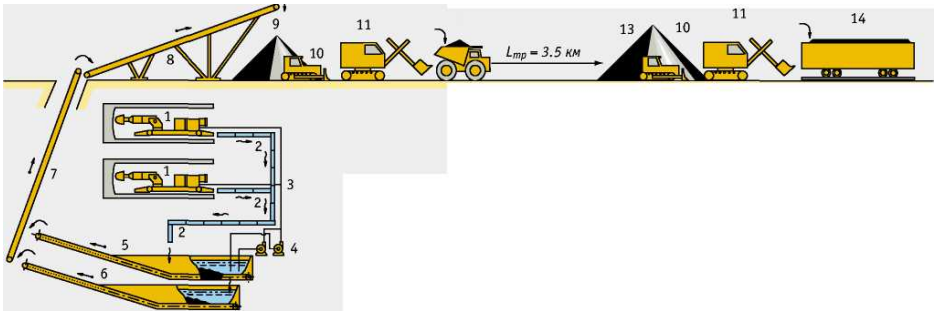

Figure 1. Mine technological scheme with mechanic-hydraulic technology of coal mining Symbols: 1-roadheader; 2-chute; 3-low-pressure head pipeline; 4-low-pressure head pump; 5-unit of dewatering of coal; 6-unit of purification of water; 7-conveyor; 8-trestle conveyor; 9-intermediate coal warehouse; 10-bulldozer; 11-excavator (loader); 12-truck motor transport; 13-main coal warehouse of a concentrate; 14-main railway transport

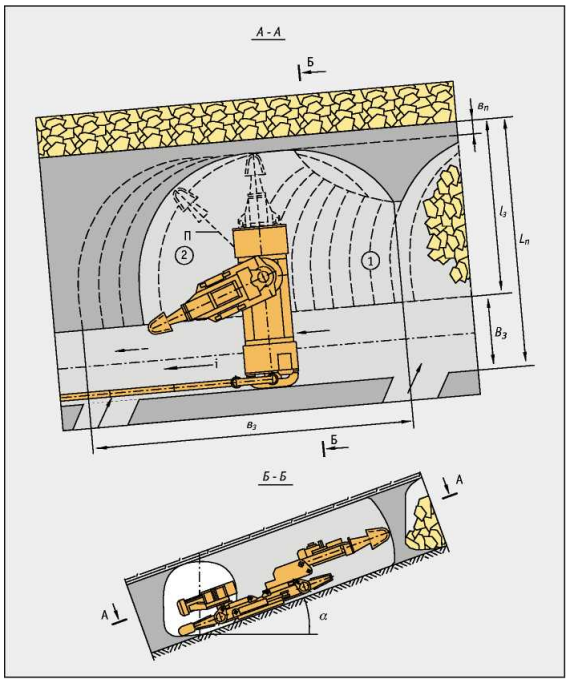

Figure 2. Scheme version of mechanical-hydraulic extraction during continuous coal mining with support pillars leaving by remotely control walking roadheader

Mining in coal and development faces is carried out by support-walking roadheader KPA-3M (fig. 3) [2], equipped for work with hydraulic transportation. Technological water in volume of 150-250 m^3/h is supplied to development face on a flexible pressure head sleeve in diameter of 80-120 mm for pulp transportation on the floors of room and drift when the angle of floors greater than 5%, and on metal chutes (trenches) when it is 3-4%. Coal extraction is carried out selectively, that due hydrotransport excludes presence of large pieces of rock layers and roof in a stream of pulp.

It is necessary to note that the mechanical-hydraulic method of roadways drivage can be used in coal mines with traditional technology of production with separate local system of coal dewatering (fig. 4).

Coal extraction in coal working faces is also provided by the remotely controlled support-walking roadheader (fig. 2,3). It especially worked actively due: to compact size, high stability, and the possibility of parallel movement.

Reduction of ash content of the coal produced is achieved by selective extraction and enrichment in gravity free-flow non-pressure hydro-transport. Dewatered coal moves along an inclined shaft by scraper or belt conveyor to the surface warehouse.

On fig. 5 technological scheme of coal mining by mechanical-hydraulic method on "Anzherskaya-Yuzhnaya-3" mine is shown.

Figure 3. Remotely controlled support-walking roadheader (model KPA-3M)

Practice of construction and operation of five coal-mining enterprises with use of offered technology allow to note, except economic advantages, its following additional advantages: lack of dust in mine atmosphere since it is localized directly in formation places; decrease mining enterprises harmful emission to minimum; more complete useful mineral dredging at the expense of possibility of local mining of coal reserves and wrong configuration mine fields, mineral product high quality not demanding its enrichment; decrease mine waters pollution as a result of water closed cycle use. In our view, the main advantage of this technology is the high work safety, since high humidity of mine air minimizes the possibility of methane and coal dust explosion [3]. In this understanding, it really is Non-Blasting and high safety technology.

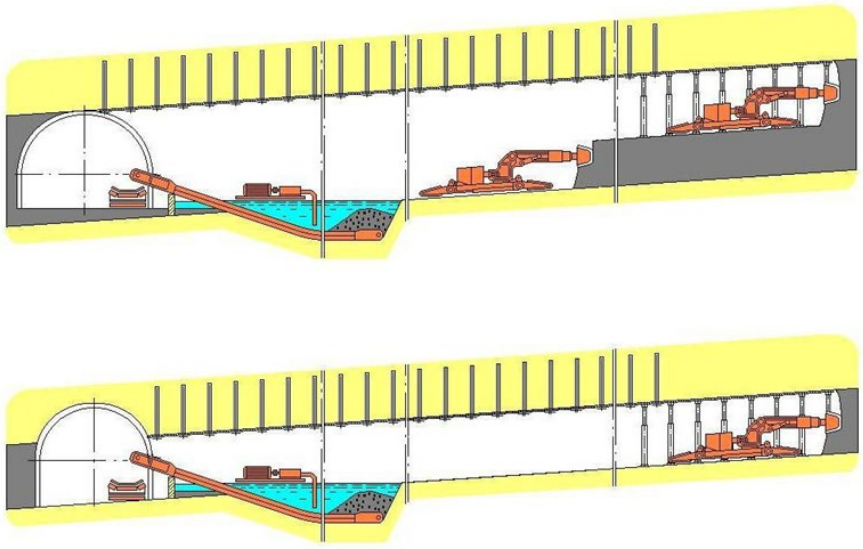

Figure 4. Continuous driving (drifts) technology by mechanical-hydraulic support-walking roadheader with local application of hydraulic transportation and coal dewatering in “dry” mines conditions: (a) – roadway drivage technology in thick seams; (b) – roadway drivage technology in thin seams

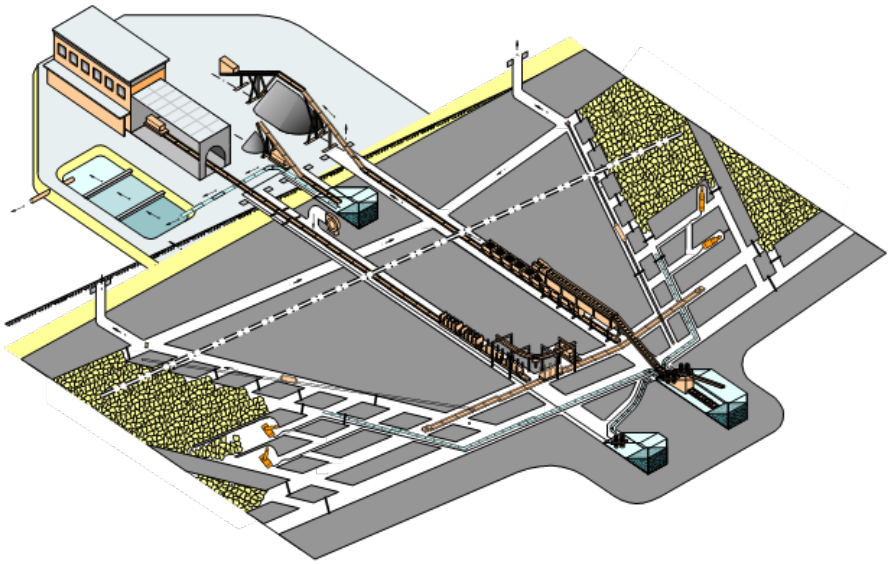

Figure 5. Technological scheme of mining by mechanical-hydraulic method on "Anzherskaya-Yuzhnaya-3" mine with underground enrichment of coal

RESULTS AND DISCUSSION

Absence analogs of hydraulic integrated technology of coal mining and underground enrichment (clean coal technology) open good prospects for its widespread use, including mining of another mineral [4-6].

Development and realization of new technologies are especially actually for design, construction and maintenance of medium-sized and small mining enterprises. Though, in existing variety of mining-and-geological, economic and social conditions of development of concrete deposits or their sites to "small" it is possible to refer the enterprises not only with limited stocks, but also with "limited" investments.

CONCLUSION

High adaptive hydro mechanized technology of hybrid coal mining is developed. Options of realization of new clean coal technologies of production and processing in Russia and abroad are considered. Reduction of ash content of the coal produced is achieved by selective extraction and enrichment in gravity free-flow non-pressure hydro-transport. Absence analoges of hydraulic integrated technology of coal mining and underground enrichment open good prospects for its widespread use (especially in complicated mining-and-geological conditions of coal deposits). Advantage of this technology is its high operational safety, since high humidity of mine air minimizes the possibility of explosions of methane and coal dust.

Now Scientific and Production Association “Hydrotechnology” carries on negotiations with interested companies and organizations for construction and modernization of the coal enterprises in various regions of the world on the basis presented and realized technological and technical solutions (www.timetehno.ru).

References

1. Puchkov, L.A., Mikheyev, O. V., Atrushkevich, O. A., Atrushkevich, V.A., 2000. The integrated technologies of coal mining on the basis of hydromechanization. Publishing house «Mining book ». Moscow, p. 273,
2. Atrushkevich, V.A., Atrushkevich, A.A., Atrushkevich, O.A., 2012. Development of hydraulic-mechanical technology at the mining enterprises. in “Collection of reports of the VI congress of hydromine operators of Russia”. Publishing house of Innovation technology Center. Moscow, p. 52,
3. Atrushkevich, A.A., Subbotin, A.I., Surkov, A.V., Mazikin V.P., 2001. The new concept of causal relationships of mine accidents and ways of their elimination, Journal Safety in the industry № 4, Moscow, p. 24,
4. Kaplunov, D. R., Rylnikova, M. V., 2012. The combined mining of ore deposits. Publishing house «Mining book ». Moscow, p. 344,
5. Kaplunov, D. R., Yukov, V.A., 2007. Geotechnology of transition from opencast to underground mining, Textbook Publishing house «Mining book», Moscow, p. 267,
6. Kazikayev D. M., 2008. The combined mining of ore deposits, Textbook Publishing house «Mining book », Moscow, p. 360.

XIII International Mineral Processing and Recycling Conference
Belgrade, Serbia, 8-10 May 2019

University of Belgrade, Technical Faculty in Bor
Vojske Jugoslavije 12, 19210 Bor, Serbia
Tel. +381 30 424 555 Fax +381 30 421 078

DEVELOPMENT AND OPERATION OF HYDROTRANSPORT SYSTEMS UNDER SEVERE ENVIRONMENTAL CONDITIONS

Aleksander K. Nikolaev #, Sergey Yu. Avksentyev, Julia G. Matveeva
Mining University, St. Petersburg, Russia

ABSTRACT – Nowadays power industry in Russia endures a tangible crisis that could be related in many aspects with unjustified high consumption of energy resources - oil and gas. In that case the demand of an alternative fuel for heat and power generation arises. The reserves of coal in Russia are quite substantial, but the remoteness of principal coal mining from the main centers of its consumption makes urgent the problem of coal transportation. The most efficient and environmentally safe way of all possible transportation methods is hydrotransport. Several developed countries (USA, Canada, Chile) designs coal pipelines that could be used to traverse different climatic zones and high - seismicity zones. In Russia the pipelines for transportation of solid mineral products are not so developed so well. However, the intensive development of Siberian and Far North regions makes necessary investigation of the problems related to transportation of water, different mixtures and pulps under severe climatic conditions.

Key words: alternative fuel, coal transportation, hydrotransport, pulp pumping station, severe climatic conditions

RESULTS AND DISCUSSION OF THE RESULTS

The energy crisis which becomes more evident in Russia stems in many respects from unjustified high consumption of energy resources. Development and exploitation of principal oil and gas deposits located in remote areas with severe climatic conditions require considerable investments increasing essentially the cost of power generation. Account should be taken also of the fact that oil and gas resources are nonrenewable. An alternative fuel for heat and power generation is coal the reserves of which in Russia are quite substantial. For this reason, the coal extraction by 2020 will amount to 450 - 550 million tons. The use of coal, as a solid fuel for heat power plants and heating plants, is complicated by its transportation from extraction to processing and consumption sites.

Remoteness of the principal coal mining areas (Kuzbass, Kansk - Achinsk field, Vorkuta) from the main centers of its consumption in the European part of the country, Siberia and Far East makes urgent the problem of coal transportation. Of all possible transportation methods (railway, conveyor, pipeline) the most efficient is hydrotransport which provides continuous transportation at comparatively low

corresponding author: aleknikol@mail.ru

capital and working costs, as confirmed by construction and operation of extended coal pipelines in many countries.

In the USA twelve coal pipelines with an overall length of about 20,000 km and a total throughput capacity of 263 million tons per year have been designed. The pipeline diameters vary from 560 to 1,220 mm [1]. The coal pipelines traverse different climatic zones and high - seismicity zones.

In Canada the coal pipeline 1,287 km in extent has been designed to connect five new coal mines with west ports. Its throughput capacity will amount to 10.2 million tons of coal per year.

Despite the fall in prices for nonferrous metals many countries continue to build new large - scale and to reconstruct operating mining enterprises, where the pipeline transport is widely used for transportation of ore processing products.

The world's largest copper deposit Collahuasi in Chile is located at an altitude of 4,500 m above sea - level in the Andes. As estimated, the prospective enterprise will produce up to 900,000 tons of copper concentrate per year to be transported to a port through the pulp pipeline 180 mm in diameter and 207 km in length. The pulp pumping station located at an elevation of 4,300 mm pumps the pulp to a mountain pass to an altitude of 4,800 mm, from whence the concentrate is delivered by gravity to a discharge port. This variant was considered along the road and railroad transport and was chosen as the most cost - effective and environmentally safe. The enterprise will run at an unprecedented altitude above sea - level.

In Russia the pipelines for transportation of solid mineral products were not more than 10 - 20 km in extent, and only at the end of 80 - ies the Belovo - Novosibirsk pilot coal pipeline 264 km in length with a throughput capacity of 3 million tons per year was built for transportation of coal - water pulp. The pipeline, as compared with railroad transport, allows the current and capital costs to be reduced by a factor of 1.5.

Intensive development of Siberian and Far North regions makes necessary investigation of the problems related to transportation of water, different mixtures and pulps under severe climatic conditions. Operation of water pipelines laid in eternally frozen ground [3, 4], hydroplant pipelines [5], hydraulic mining pipelines transporting water - sand mixtures [6] is fraught with hazard of inner icing of pipes both with liquid moving through pipes and during downtime, which results in an increase in hydrodynamic resistance. Significant contribution to ice - thermal calculation of pipelines was made by Russian scientists and engineers (P.A. Bogoslovsky, A.M. Estifeev, D.N. Bibikov, Yu.A. Popov, V.M. Zhidkikh, N.N. Zenger, A.V. Lyutov, et al.).

Many researchers noted that it is not always necessary to strive to completely eliminate icing, since costs of heating, thermal insulation of tubes and earth works are unjustifiably high (N.N. Zenger. V.P. Stegantsev, S.V. Khizhnyakov et al.).

The study of the ice regime of pipelines as applied for hydropower plants showed that their inner icing, when in operation, is possible (P.A. Bogoslovsky). The fundamental difference in operation between pipelines in a system with centrifugal pumps and water pipelines of hydropower plants consists in the availability of feedback (pump ↔ pipeline). Pumps at a specified flow rate develops the head necessary to overcome the forces of hydraulic resistance. Yu.A. Popov investigated the ice regimes of hydraulic mining pipelines with complicated production

engineering applied and under time - varying weather conditions. On this basis he developed the fundamentals of the theory of water - sand mixture transportation under severe climatic conditions for hydraulic mining. The method of ice - thermal calculation of water pipeline system providing for alternate operation and idle of the hydraulic system is developed in study [7].

To prevent failures caused by freezing of transported liquids it is necessary to envisage at the design stage, when calculating ice - thermal regimes of such pipeline systems, possible unfavorable operation conditions connected with changes of weather conditions, possible shutdowns, to calculate the thickness of thermal insulation, to consider several design versions to determine the optimal one.

When designing large - extent transport facilities new problems arise and novel calculation methods should be elaborated, such as:

- establishment of relation between the hydrodynamic and thermal regimes in pipelines of hydrotransport systems;
- the effect of unsteady processes on the system performance reliability during startup and shutdown;
- definition of mutual effect of the system «environment → (pump ↔ pipelines)»;
- elaboration of the method for installation of pipelines and devices compensating for temperature deformations.

The urgency of these problems has determined the line of scientific activities undertaken at the Saint Petersburg Mining University.

At the first stage the theoretical and experimental works were carried out to investigate the effect of solid phase distribution over the pulp - carrying flow section on the intensity of heat transfer from flow to pipeline wall.

The presence of solid particles in the liquid - carrying flow complicates essentially the process of heat exchange with the pipe wall. For the hydrodynamically developed flow it is possible to consider non - Newtonian hydromixture as a dummy liquid with an increased density, since solid particles move with a local velocity of liquid [9]. Such a model makes it possible to use in the thermal calculation the averaged characteristic λ_π - the thermal conductivity of hydromixture in the radial direction [8]. The hydrodynamical axis of the flow is found to be displaced upwards, because large particles move in the near - bottom zone. The axial velocity of hydromixture ω_x will depend on the angle φ which is measured in the plane perpendicular to the pipe geometrical axis from the vertical and varies in the range from 0 to π.

Processing of the velocity profiles of pulp - carrying flows of different concentrations [9] makes it possible to take the functional dependence $\omega_x(\varphi)$ as $cos(\varphi/m)$, where m is the experimentally defined constant. As estimated, $m \approx 3$. In this case the velocity profile in the pulp - carrying flow can be taken as:

$$\omega_x(\varphi) = 2\omega_{av}(1 - R^2)\, cos\frac{\varphi}{3} \qquad (1)$$

where ω_{av} - average velocity of hydromixture motion, m/s; $R = r/r_0$ - reduced pipe radius; r_0 - pipe radius, m.

The heat exchange equation for the pulp flow in a pipe is of the form:

$$2\omega_{av}(1-R^2)\cos\frac{\varphi}{3}\frac{\partial t}{\partial x}=\frac{a}{r_0^2}\left(\frac{\partial^2 t}{\partial R^2}+\frac{1}{R}\frac{\partial t}{\partial R}+\frac{1}{R^2}\frac{\partial^2 t}{\partial \varphi^2}\right) \quad (2)$$

where t - pulp temperature, K; $a=\lambda_\pi/(c\rho)_\pi$; $(c\rho)_\pi$ - volumetric heat capacity of pulp, J/m^3K; x - the coordinate charactenzing the pipe length, m.

Let us choose, as a characteristics value, the wall temperature t_c treating it further as a constant. If t_0 is the pulp constant temperature at the pipeline input, then by introducing the dimensionless variables:

$$\theta=\frac{t-t_c}{t_0-t_c};\ X=\frac{ax}{2\omega_{av}r_0^2} \quad (3)$$

Eq. (2) can be of the form:

$$(1-R^2)\cos\frac{\varphi}{3}\frac{\partial\theta}{\partial X}=\frac{\partial^2\theta}{\partial R^2}+\frac{1}{R}\frac{\partial\theta}{\partial R}+\frac{1}{R^2}\frac{\partial^2\theta}{\partial\varphi^2}. \quad (4)$$

The boundary conditions are of the form:

a) on the pipe surface the temperature is specified as:

$$\theta=0 \text{ at } R=1; \quad (5)$$

b) at the input cross - section (x = 0) the temperature is constant:

$$\theta=1 \text{ at } X=1. \quad (6)$$

To estimate the temperature regime [10] let us choose the approximate method for solution of the boundary problem (4) - (6) based on the transformation of convolution of the functions $f_1\cdot f_2$ [11]:

$$f_1\cdot f_2=\int_0^X f_1(y)f_2(X-y)dy\,. \quad (7)$$

Differential equation (4) written with the convolution transformation is of the form:

$$(1-R^2)\cos\frac{\varphi}{3}(\theta-1)=1\cdot\nabla^2\theta\,, \quad (8)$$

where ∇^2- Laplace operator.

Eq. (8) is used to form the functional of the heat exchange process [11]:

$$I(\theta)=\iint_{(D)}\left[R(1-R^2)\cos\frac{\varphi}{3}(\theta-2)\cdot\theta+\frac{1}{R}\cdot\frac{\partial\theta}{\partial\varphi}\cdot\frac{\partial\theta}{\partial\varphi}+R\cdot\frac{\partial\theta}{\partial R}\cdot\frac{\partial\theta}{\partial R}\right]RdRd\varphi. \quad (9)$$

The integration domain *D* covers the pipeline cross - section. The identity of this

functional to Eq. (4) with conditions (5) and (6) is established by taking the first variation with respect to θ.

The approximate solution is found in the form of the function combination:

$$\theta_k = \sum_{i=1}^{k} \varphi_i(R, \varphi) g(X)\,, \tag{10}$$

where k - the approximation number.

As is known from the theory of approximate solutions [12], the first approximation yields the predicted error not exceeding 10 %, but with an appropriate choice of the approximating functions φ_i the error can be even less.

The first approximation is found in the form:

$$\theta_1 = (1 - R^2)\cos\frac{\varphi}{3} g(X)\,. \tag{11}$$

It is seen that the coordinate function φ_1 satisfies identically the boundary condition in Eq. (6).

By substituting $\theta_1$into functional (9) and integrating with respect to the pipeline cross - section we obtain the numerical value of the coefficients:

$$I(\theta) = g \cdot g \cdot 0.098974 - 2(1 \cdot g)0.169167 + (1 \cdot g \cdot g)1.83085\,. \tag{12}$$

By varying expression (12) with respect to the argument g we get:

$$\delta I(g) = [2g \cdot 0.098974 - 2 \cdot 0.169167 + 2 \cdot (1 \cdot g)1.83085] \cdot \delta g\,. \tag{13}$$

As $\delta g \neq 0$, the extremality of functional (12) requires that:

$$g \cdot 0.098974 - 0.169167 + (1 \cdot g)1.83085 = 0\,. \tag{14}$$

The equivalent form of the differential equation is obtained by taking a derivative with respect to X:

$$g' + 18.498g = 0\,, \tag{15}$$

with the boundary condition taking the form:

$$g(0) = 1.709\,. \tag{16}$$

By separating the variables in Eq. (15), integrating and using condition (16) we get:

$$g = 1.709exp(-18.5X)\,. \tag{17}$$

Finally, the first approximation for temperature is as follows:

$$\theta_1 = 1.709(1 - R^2)\cos\frac{\varphi}{3} exp(-18.5X)\,. \tag{18}$$

The results of the calculation made by Eq. (18) are tabulated. The average temperature of the pulp - carrying flow is calculated to analyze the error caused by the approximate method used.

Table 1. Dimensionless temperature θ as a function of X, φ, R

X	φ	θ				
		$R = 0.1$	$R = 0.3$	$R = 0.5$	$R = 0.7$	$R = 0.9$
0.01	$\pi/6$	0.810	0.745	0.614	0.417	0.156
	$\pi/3$	0.773	0.711	0.586	0.398	0.148
	$\pi/2$	0.712	0.655	0.540	0.367	0.137
	$2\pi/3$	0.630	0.579	0.477	0.325	0.121
	$5\pi/6$	0.529	0.486	0.400	0.272	0.101
	π	0.411	0.378	0.312	0.212	0.079
0.05	$\pi/6$	0.387	0.355	0.293	0.199	0.074
	$\pi/3$	0.369	0.339	0.279	0.190	0.071
	$\pi/2$	0.340	0.312	0.258	0.175	0.065
	$2\pi/3$	0.301	0.276	0.228	0.155	0.058
	$5\pi/6$	0.252	0.232	0.191	0.130	0.048
	π	0.196	0.180	0.149	0.101	0.038
0.10	$\pi/6$	0.153	0.141	0.116	0.079	0.029
	$\pi/3$	0.146	0.134	0.111	0.075	0.028
	$\pi/2$	0.135	0.124	0.102	0.069	0.026
	$2\pi/3$	0.119	0.110	0.090	0.061	0.023
	$5\pi/6$	0.100	0.092	0.076	0.051	0.019
	π	0.078	0.072	0.069	0.040	0.015

$$\theta_{av} = \frac{\iint_{(D)} w_x \theta R dR d\varphi}{\iint_{(D)} w_x R dR d\varphi} = 0.9479 exp(-18.5X)\,. \tag{19}$$

The estimation of approximation at the input cross - section can be obtained by comparing the boundary condition at the input (6) and the value of Eq. (19) at $X = 0$:

$$\theta_{av} = 0.9479 \cong 0.95\,. \tag{20}$$

It is seen that the approximate solution yields an error of ~5 %.

The pulp temperature can be estimated by Eqs. (18) and (19) with an accuracy sufficient for the engineering calculations.

The aim of the experimental investigations was to obtain the dependence for calculation of the heat transfer coefficient when the pulp flows through the pipeline.

The results of the experiments with water comply with the dependence given by M. Mikheev in [12]:

$$Nu = 0.026 Re^{0.8} Pr^{0.4}\,. \tag{21}$$

In this case the error did not exceed ±7 %.

The experimental data on heat exchange between the pulp and the pipe wall were processed in compliance with the obtained criteria dependence:

$$Nu = 0.026 Re_p^{0.8} Pr_p^{0.4} \left(\frac{C_1}{C_2}\right)^{0.15} \cdot \left(\frac{\lambda_3 - \lambda_1}{\lambda_2}\right)^{0.42}, \quad (22)$$

where Re_p - Reynolds number of pulp; Pr_p - Prandtl number of pulp; C_1 - liquid heat capacity C_2 - heat capacity of solid particles; λ_1 - thermal conductivity of liquid; λ_2 - thermal conductivity of solid particles; λ_3 - thermal conductivity of pulp.

The obtained formula is recommended for thermal calculations of the pipelines intended for transportation of the non - Newtonian pulp.

References

1. 15th Biennial Low Ranks Fuels Symposium, Minnesota, 22 - 25 May, 1989,
2. Malyshev, Yu.N., Trubetskoy, K.N. Coal Industry of Russia at the threshold of the XXI Century (reported at XVIII Mining Congress),
3. Zenger, N.N. (1964) Peculiar features of water pipelines in permafrost conditions. L. Stroyizdat, (in Russian),
4. Gusev, N.Z., et al. (1971) Thermal calculations of water pipelines laid in frozen ground. Irkutsk Polytechnical Institute, Irkutsk, (in Russian),
5. Bogoslovsky, P.A. (1950) Ice operation regime of hydraulic power plant pipelines. Gosenergoizdat, (in Russian).
6. Popov, Yu.A. (1969) Some problems of hydraulic and thermal calculation of pipelines during transportation of water and water - sand mixtures in winter (Thesis for a candidate's degree). Novosibirsk, (in Russian),
7. Popov, Yu.A., Guselnikov, E.N. (1995) Calculation of complicated types of icing of pipelines. Izvestiya Vuzov, Stroitelstvo, (11), (in Russian),
8. Gorbis, Z.P. (1972) Heat exchange and hydromechanics of disperse through flows. M. Energiya,
9. Silin, N.A. (1974) Hydrotransport. Kiev, Naukova Dumka, (in Russian),
10. Romanov, V.A. (1979) Engineering methods for calculation of subsurface water filtration. L. published by LGI, (in Russian),
11. Tao, N.N. (1965) Theory. Physics, V. 51,
12. Mikheev, M.A., Mikheeva, I.M. (1973) The principles of heat transfer. M. Energiya, (in Russian).

XIII International Mineral Processing and Recycling Conference
Belgrade, Serbia, 8-10 May 2019

University of Belgrade, Technical Faculty in Bor
Vojske Jugoslavije 12, 19210 Bor, Serbia
Tel. +381 30 424 555 Fax +381 30 421 078

BOX–BEHNKEN EXPERIMENTAL DESIGN FOR MICROWAVE ENERGY ROASTING OF REFRACTORY GOLD FLOTATION CONCENTRATE

Birgül Benli [#], Atacan Adem
Istanbul Technical University, Mineral Processing Engineering, Turkey

ABSTRACT – Conventional thermal processing of minerals requires high energy amounts; therefore, alternatives are important. After 1960ies, microwave energy can be used efficiently. In this study, pre-treatment of microwave energy for refractory gold ore concentrates were investigated. Gold sample with high Sulphur zone and 1.37 ppm gold content was firstly floated, and then 4 ppm gold and 18 % of Sulphur content sample were roasted with microwave energy. After optimization studies, 1000 W power, 60 min and 4 g mass were obtained with 5 ppm gold and for the minimum sulfur content below 0.7 % in 60 min and 800 W by microwave roasting.

Key words: gold ore, box-behnken experimental

INTRODUCTION

Conventional thermal processing of minerals requires high energy amounts and these methods are not economical, since increasing of energy demand and fuel consumption, cause to costs for many countries. Therefore, many researches need to develop innovative and more efficient methods. One of them is the usage of microwave energy. In mineral processing, microwave energy started to be used after 1960ies. Microwave energy can be used in various thermal processes such as heating, drying, leaching, roasting, melting, carbothermic reaction of oxidized minerals or synthesis, drying and sintering steps of ceramic materials [1]. Nowadays, it is observed that usage of microwave energy has an important potential and is on the rise already in the sector.

Electro-heating processes, namely induction, radio frequency, direct resistance and infrared heating, utilize specific regions of electromagnetic energy. One of them is microwave heating uses non-ionized electromagnetic radiation that has frequencies in the range of 300MHz - 300 GHz. When exposed to microwave radiation, the materials are divided into three groups: insulators, conductors and absorbers [2]. Materials that can absorb high frequency electromagnetic waves are

[#] corresponding author: benli@itu.edu.tr

known as dielectrics and can heat in various ways. However, temperature gradient is the driving force for heat transfer. According to the second law of Thermodynamics, heat spontaneously flows from high temperature regions to the low temperature ones under normal conditions. Figure 1 shows the comparative mechanism of the heating systems; unlike microwave heating, in the conventional heating, temperature gradient starts from the outside of a body towards to the center regions through conduction, convection and radiation mechanisms.

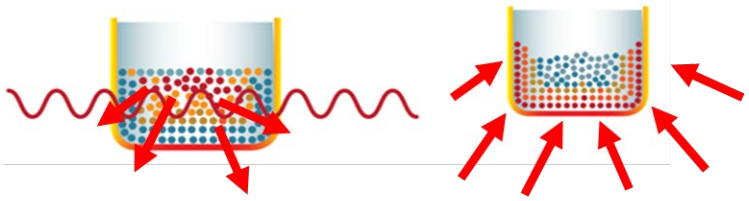

a) b)

Figure 1. Graphical illustration of heat introduction and temperature distribution for (a) Microwave heating, (b) Conventional heating

The encouraging results are highly dependent on the mineralogy of the ores tested. The efficiency of ores to microwave treatment related with thermally-induced fractures, depend on the dielectric, thermal and mechanical properties of the minerals involved, their assemblage within the ores, and the microwave energy and power density employed. Dielectric properties can vary greatly with composition, temperature, frequency, and density; therefore, ore mineralogy is important to characterize them across the whole range of processing conditions when planning microwave experiments and designing industrial microwave equipment. Rosenholtz and Smith (1936) [3] listed the value of dielectric constants of the selected minerals can be seen in Table 1.

Table 1. Dielectric properties of some minerals possibly present in a typical gold ore

Mineral	Dielectric constant	Mineral	Dielectric constant
Arsenopyrite	over 81	Muscovite	10
Biotite	9.28	Olivine	6.77
Calcite	6.36	Pyrite	over 33.7, under 81
Chalcopyrite	over 81	Quartz	6.83
Copper	over 81	Sulfur	3.62
Dolomite	8.45	Serpentine	11.48
İlmenite	over 33.7, under 81	Talk	9.41
Magnetite	over 33.7, under 81	Wollastonite	6.17

The aim of this study is to show the effectiveness of microwave energy on the reduction of sulphur content during thermal pretreatment of refractory gold ore

concentrates. In this study, experiments were designed according to response surface methodology and 3-factor Box-Behnken experiment design methods. Mathematical modeling of thermal pretreatment experiments was obtained and the parameters that are considered as important to the process like power (Watt), time (minutes) and mass (g) were analyzed by Minitab program.

MATERIALS AND METHODS

Materials

The gold ore sample used in this study was taken from high sulphur mineral zone in the west side region of Turkey. Firstly, the sample was crushed with a primary jaw crusher and then a roll crusher. Homogenized sample was ground below -106 µm using a ring mill during 1 min for the preparation to the flotation and microwave experiments. The ground sample was analyzed by ALS Laboratory for cupellation standardized method (fire assay) and determined about 1.37 g/t gold content. The sulphur content of the sample was analyzed by PC controlled ELTRA CS580 Elemental Analyzer for Carbon and Sulfur.

Secondly, the flotation of gold applied to the ground sample with the use of Aero 208 + Aerophine 3418 A as collectors at the dosages of 50 + 50 g/t and 1000 +1000 g/t Na_2SiO_3 as a depressant and 25 + 25 g/t MIBC as a frother were added to the pulp at pH 4 - 4.5 and conditioned for 10+ 5 minutes. After flotation experiments, a concentrate contained 4 ppm gold and 18 % of sulphur content were obtained.

MICROWAVE ROASTING EXPERIMENTS

Microwave heating tests were conducted on 2-6 g samples of the concentrate samples in a programmable microwave oven (Arcelik, MD554, Turkey) with maximum output of 1200 W at 2450 MHz (Figure 2). Ore samples were placed in 25 mL porcelain crucible and put into magnetite filled 250 mL of bigger porcelain crucible as shown in Figure 2. The microwave furnace operated at power levels of 360 – 1000 W.

Magnetite particles were used as microwave absorber in the system. For in-situ temperature determination, a quartz glass thermometer up to 400 °C was used. Following the heating process, the samples were taken out of the oven, cooled rapidly in a desiccator at room temperature, separately ground and stored in polyethylene bags at –18 °C until the analysis. Ignition loss of the samples was measured at 110 °C in an oven (TEST, T420S, Turkey) and a digital balance of 0.001 g accuracy (Precisa, XB620, Switzerland).

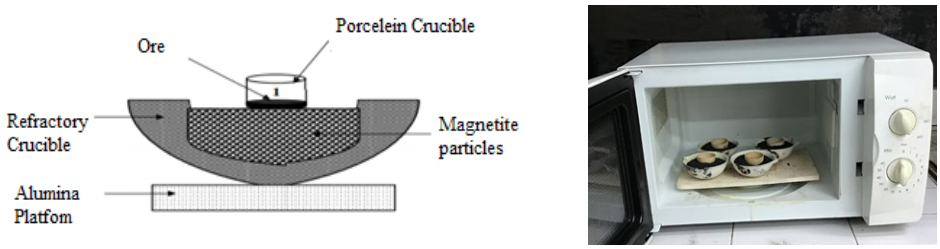

Figure 2. Microwave heating system which is used in the experiments

BOX-BEHNKEN EXPERIMENTAL DESIGN

Response surface methodology was used for optimizing the microwave roasting efficiency of refractory gold ore particles and investigating the correlation between the response and the experimental factors. The Box and Behnken experimental design developed in 1980 is a useful method for generating Second-order response surface models. As shown in Table 2, the level of the factor C (weight) was fixed and then, the combinations of all levels of the factors A (time) and B (power) were applied and subsequently, the same procedures were performed for the factors B and A, respectively. A second order polynomial model was utilized to evaluate the response variables:

$$EE= \beta o+\beta_1.X_1+\beta_2.X_2+\beta_3.X_3+\beta_4.X_1^2+\beta_5.X_2^2+ \beta_6.X_3^2+\beta_7.X_1.X_2+\beta_8.X_1.X_3+\beta_9.X_2.X_3 + \varepsilon \quad (1)$$

We predicted response, here, EE is the predicted response, X_1 to X_3 are the factors studied, βo the intercept, and β_1 to β_9 the regression coefficients. The optimization of experimental parameters studied was analyzed by Minitab 17 (Minitab, USA).

Table 2. Three-factor Box-Behnken experimental designs

Rank	Weight (g)	Time (min)	Power (W)
1	2	40	1000
2	2	20	680
3	2	40	360
4	2	60	680
5	4	40	680
6	4	60	360
7	4	20	1000
8	4	20	360
9	4	40	680
10	4	60	1000
11	4	40	680
12	6	40	360
13	6	20	680
14	6	60	680
15	6	40	1000

RESULTS AND DISCUSSIONS

Figure 3 shows the change of the temperature in the samples and magnetite depending on the power of the microwave heating. Although magnetite was the microwave absorbent, temperature increase was also observed rapidly in other samples. This is related with the dielectric characteristics of the sample (Table 1), because refractory gold ore consists of gold, silver, pyrite and chalcopyrite with very high values of dielectric constants.

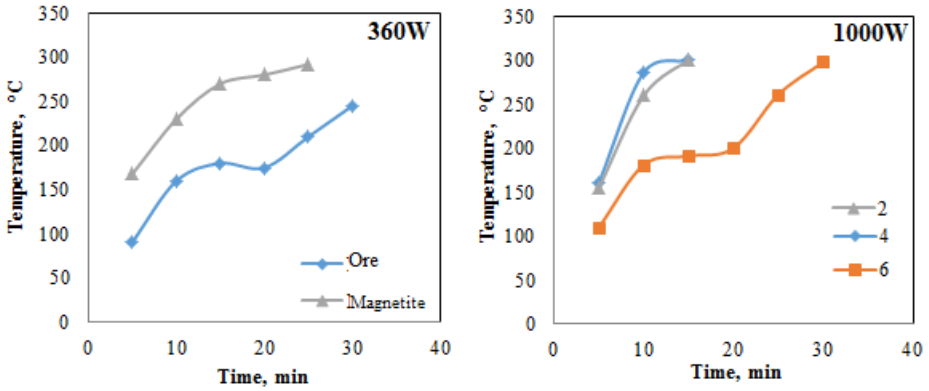

Figure 3. Comparison of increasing temperatures depending on the applied power and the solids amount during microwave heating

Loss of ignition values of the sample were determined in microwave heating conditions at 300 °C during 15 min. The contour plots of the binary interactions can be seen in Figure 4. Depending on the LOI results, optimum value of the heating system is determined as 4 g ore sample, 40 min duration and over 800 W power.

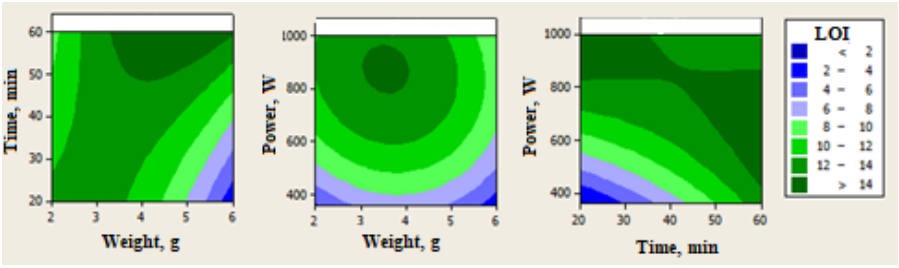

Figure 4. The contour plots for the loss on ignition (LOI) of the gold ore

The three-dimensional plots (Figure 5) show the individual effects of the process variables and their interactions on the weight loss or ignition loss or Sulphur reduction efficiency. The observed surfaces were obtained by plotting the measured and calculated values of weight loss against two factors, keeping the third one at its middle level.

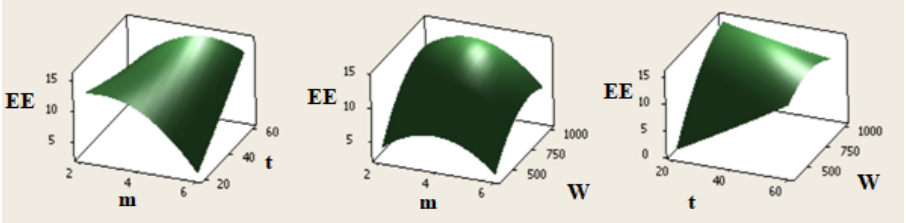

Figure 5. 3D surface plots of the ignition plots of the refractory gold ore

Figure 6 shows the polynomial regression model was in good agreement with the experimental results and verify the residuals are normally distributed. This good result of fit model is obvious according to the determination coefficient (R^2=0.989), which indicates that up to 98.9 % variability of the response can be explained by this model, only 1.1 % of the total variations in response remained unexplained.

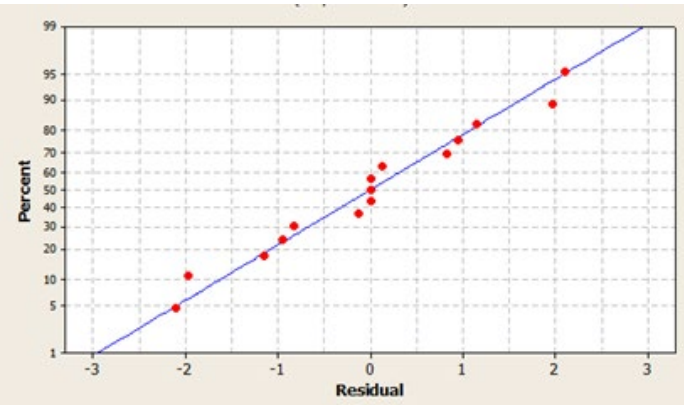

Figure 6. Normal probability plot of the experimental design

CONCLUSION

After optimization studies for the efficient microwave heating, 800 W power, 40 min and 4 g mass were found to be sufficient with 5 ppm gold and for the minimum sulfur content below 0.7 %.

References

1. Xia, D.K., Pickles, C.A., 1997. Application of Microwave Energy in Extractive Metallurgy, a Review, CIM Bulletin, 90 (1), 99-107,
2. Chen, T.T., Dutraizac, J.E., Haque, K.E., Wyslouzil, W., Kashyap, S., 1984. The Relative Transparency of Mineral to Microwave Radiation, Canadian Metallurgical Quarterly, 23 (3), 349-351,
3. Rosenholtz, J.D., Smith, D.T., 1936. The dielectric constant of mineral powders, American Mineralogist, 21(2), 115-120,
   Adem, A., 2018. The effect of microwave heating on the refractory gold ore samples", Istanbul Technical University, Mineral Processing Engineering Undergraduate Thesis,
   Benli, B., Adem. A., Rapid total sulphur reduction in gold ore samples using microwave heating to prevent sulphur emissions during ore processing, In publishing.

XIII International Mineral Processing and Recycling Conference
Belgrade, Serbia, 8-10 May 2019

University of Belgrade, Technical Faculty in Bor
Vojske Jugoslavije 12, 19210 Bor, Serbia
Tel. +381 30 424 555 Fax +381 30 421 078

NICKEL-COPPER CONCENTRATES PROCESSING BY LOW-TEMPERATURE ROASTING WITH SODIUM CHLORIDE

Pavel V. Aleksandrov #, A.S. Medvedev, V.A. Imideev
National University of Science and Technology MISiS, Moscow, Russia

ABSTRACT - The low-temperature roasting of nickel-copper sulfide concentrates with sodium chloride (at 400–450 °C) and subsequent hydrometallurgical processing is a promising alternative method. An advantage provided by this processing approach arises from formation of water-soluble compounds of the extracted metals as well as from Na_2SO_4 formation during roasting, which contributes to the significant reduction of SO_2 emissions. This study aims to identify the interaction products of sulfide nickel concentrate components with sodium chloride as well as optimum roasting conditions. Thermodynamic studies have demonstrated that nickel sulfates, chlorides, and oxides are the probable nickel-containing products of the interaction between nickel sulfide and sodium chloride in the presence of oxygen. At 350–450 °C, the formation of nickel sulfate is preferred; as the temperature increases, the probability of oxide formation also increases. We experimentally confirmed that nickel sulfate is the main nickel-containing product of the reaction between nickel sulfide concentrate and sodium chloride at 400 °C, and the reduced nickel oxide and chloride content was identified in the calcine. The other main products included iron oxide (III) and initial sodium sulfate. During roasting at 400 °C, up to 75% of the sulfur contained in the concentrate was bound to sodium sulfate. Roasting conditions influence to Ni, Cu, Fe recovery from calcine by water leaching were investigated. According to study optimal conditions are roasting temperature of 400ºC, NaCl content of 50-100 % and roasting duration of 90 minutes. There are up to 95 % recovery level of nickel and copper at mentioned above conditions.

Key words: nickel, copper, concentrates, processing, roasting, sodium chloride

INTRODUCTION

A prospective approach for nickel sulphide concentrate processing is proposed herein based on low-temperature roasting with sodium chloride (at 400–450 °C) with subsequent hydrometallurgical processing of calcine. An advantage provided by this processing approach for sulphide concentrates of non-ferrous and rare metals arises from Na_2SO_4 formation during roasting, which contributes to the significant reduction of SO_2 emissions. Other advantages include power savings due to the relatively low temperatures of the roasting process and formation of water-soluble compounds of the extracted metals, which simplifies calcine leaching and reduces the consumption of leaching reactants. For example, after molybdenite concentrate roasting with sodium chloride, molybdenum in the calcine partially exists as water-

corresponding author: mos@misis.ru

soluble sodium molybdate [1-3]. During the roasting of copper [4-7], nickel [5, 8-12], and complex sulphide concentrates [6], metal sulphides are almost completely transformed to sulphates and chloride. Qustions of viability, advantages/ disadvantages of this approach of nickel sulphide concentrates processing as well as comparing with current methods were raised in study [13].

To date, no analytical corroboration has been provided [5] for nickel chloride formation. Furthermore, in previous studies [4, 6], non-ferrous metal chlorides and sulphates were identified as solid products. Therefore, the form in which nickel is present in the calcine remains underexplored. Earlier studies demonstrated [8] that up to 85% of the nickel is transformed to a water-soluble form as a result of nickel sulphide concentrate roasting with sodium chloride at 400 °C. However, identification of specific interaction products was unsuccessful in that study. In this context, this study was performed to identify the interaction products between the nickel sulphide concentrate and sodium chloride components at 400–450 °C as well as optimum roasting conditions.

METHODS AND MATERIALS

Nickel sulphide concentrate was used as a precursor in this study and its composition was determined by induction coupled plasma spark mass spectrometry (ICP-MS) using a double focusing mass spectrometer JMS-BM-2 (Japan). Based on this method, the elemental weight content (%) was determined to be as follows: nickel – 5.78; copper – 2.79, cobalt – 0.28, iron – 42.49, and sulphur – 23.19. Qualitative phase analysis was performed using an ARL 9900 WS wave X-ray fluorescence spectrometer with the ICDD PDF-2 database and Crystallographica Search-Match application software. According to the analytical results, the major contents were magnetic pyrite, pentlandite, and chalcopyrite ore with trace amounts of cobalt pentlandite.

The concentrate (sample weight of 5–10 g) was mixed with sodium chloride in specified ratios, evenly distributed in a ceramic cup (layer thickness of 4–5 mm), and calcinated in a muffle furnace at specified temperatures and durations. The obtained calcines were analysed by XRD and SEM Quanta 650 electronic scanning microscope with microscopic analysis performed using EDS energy-dispersion detectors (SEM-EDS). Afterward, the calcines were leached using water and the Ni recovery in the water was determined by ICP.

THERMODYNAMIC ANALYSIS

To identify the interaction products of the concentrate and sodium chloride in the presence of oxygen, thermodynamic analysis of the theoretical reactions in the NiS–O_2 and NiS–NaCl–O_2 systems were performed using FactSage software. Initially, roasting of 1 g of nickel sulphide was simulated without the addition of chloride. The influence of the oxygen content in the system (ranging from 1 to 100 g) and process temperature (ranging from 350 to 1000 °C) on the composition of the products was studied. Excessive oxygen (i.e. beyond stoichiometric sufficiency) did not influence the thermodynamics of the process. The temperature was divided into the following 3 ranges: <700 °C, 700–900 °C, and >900 °C. Within the first range, the thermodynamically favourable product of nickel sulphide oxidation was identified

as nickel sulphate, and was obtained according to Eq. (1):

$$NiS + 2O_2 = NiSO_4 \quad (1)$$

In terms of thermodynamics, the formation of both sulphate and nickel oxide was expected at 700–900 °C as shown in Eq. (2):

$$2NiS + 3.5O_2 = NiSO_4 + NiO + SO_2 \quad (2)$$

The only interaction product at 700–900 °C is nickel oxide according to Eqs. (3) and (4):

$$NiS + 1.5O_2 = NiO + SO_2 \quad (3)$$

$$NiS + 2O_2 = NiO + SO_3 \quad (4)$$

The most probable oxide formation mechanism involved nickel sulphate decomposition with increasing temperature.

To determine the influence of NaCl on the roasting process thermodynamics in the NiS–NaCl–O_2 system, roasting of a mixture containing 1 g of NiS and 10 g of NaCl was simulated at 300–600 °C with varying oxygen contents.

Nickel sulphate was the only product obtained during nickel sulphide roasting without sodium chloride at temperatures up to 600 °C. For nickel sulphide roasting in the presence of sodium chloride, the formation of nickel oxide became thermodynamically feasible at ≥300 °C. Furthermore, the thermodynamic favourability of nickel oxide formation increased with increasing temperature and excessive oxygen content. For example, at the NiS to O_2 mass ratio of 1:10, nickel oxide is the only thermodynamically favourable nickel product at temperatures exceeding 575–600 °C while at a NiS to O_2 mass ratio of 1:100, this occurred at ≥400–425 °C.

Nickel oxide forms according to Eqs. (3) and (4) occurs with sulphur oxide emission, enabling sodium sulphate formation from sodium chloride in the presence of oxygen according to Eqs. (5) and (6):

$$2NaCl + O_2 + SO_2 = Na_2SO_4 + Cl_2 \quad (5)$$

$$2NaCl + 1/2O_2 + SO_3 = Na_2SO_4 + Cl_2 \quad (6)$$

and considering Eqs. (3) and (4), the overall reaction can be described by Eq. (7):

$$NiS + 2NaCl + 2.5O_2 = NiO + Na_2SO_4 + Cl_2 \quad (7)$$

Within the temperature ranges that facilitate the formation of both nickel sulphate and oxide, Eqs. (1) and (7) occur concurrently, as described by Eq. (8):

$$2NiS + 2NaCl + 4.5O_2 = NiO + NiSO_4 + Na_2SO_4 + Cl_2 \quad (8)$$

In terms of thermodynamics, within the temperature range of 300 to 600 °C nickel oxide chlorination by gaseous chlorine occurs according to Eq. (9):

$$NiO + Cl_2 = NiCl_2 + O_2 \quad (9)$$

Our study indicated that the supposed nickel-containing products of the interaction between nickel sulphide and sodium chloride in the presence of oxygen include nickel sulphates, chlorides, and oxides. The generation of nickel sulphate is most thermodynamically favourable at low temperatures. Phase composition analysis of the calcine obtained by copper-zinc concentrate roasting with sodium chloride showed similar results to those observed in this study [5]. It should be noted that, according to the thermodynamic studies (Tables 1 and 2), the addition of sodium chloride resulted in a 200 to 300 °C decrease in the onset temperature of nickel oxide formation, likely resulting from sulphate decomposition. Thus, obtaining nickel oxide remains unfavourable at <600 °C without sodium chloride (only sulphate formation is favourable). However, when NaCl is added, nickel oxide formation is favourable at temperatures as low as 300 °C, while at 600 °C only oxide formation is favourable (sulphate formation is unfavourable). These data show good correlation with previously reported experimental studies [9 ,10] that demonstrated sulphates were formed intensively at 600 to 700 °C during roasting without sodium chloride addition.

INVESTIGATION OF THE SOLID ROASTING PRODUCTS

Initially, the solid roasting product phase composition was analysed by XRD. Experimentally proving the presence of sodium sulphate compounds formed during nickel sulphide concentrate roasting with sodium chloride is important for industrial applications, as this approach is associated with lower sulphur oxide emissions. But water-soluble nickel containing phases wasn't identify using XRD methods, because of it the phase composition of the calcines was further analysed using scanning electron microscopy (SEM) Quanta 650 with an EDS detector. The samples were prepared by spreading the ground calcines over a carbon adhesive tape and the microstructure was observed using backscattered electrons.

Photomicrographs of the calcine fragments obtained at 400 °C, calcinated for 90 min, and with a 50% NaCl ratio of the concentrate weight are shown in Figures 1–3. A calcine fragment containing the identified sodium sulphate phase is shown in Figure 1 and large particles of sodium chloride can be seen in Figure 2. A complex phase containing iron and nickel sulphates was identified on the surface of the NaCl in addition to iron (III) oxide. The photomicrographs and EDS spectra of that phase are shown in Figure 3. From the EDS, different proportions of the components were observed at different points. The main components throughout the samples included sulphur, oxygen, iron, and nickel. All tested points exhibited excessively high sulphur contents and oxygen content that was below the detection limit, so the components were identified as sulphates. The detected phases were composed of a mixture of iron, nickel, and copper sulphates along with their corresponding sulphides. Because measurements involving microprobes were performed in a volume the phases of sulphides and sulphates overlapped, and the results indicate the average component content in those phases.

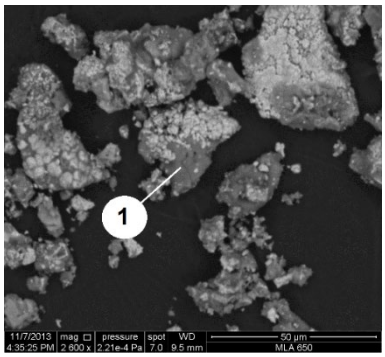

Figure 1. SEM image of the calcine obtained at 400 °C, 50% NaCl content, and 90 min roasting duration; 1 - Na_2SO_4.

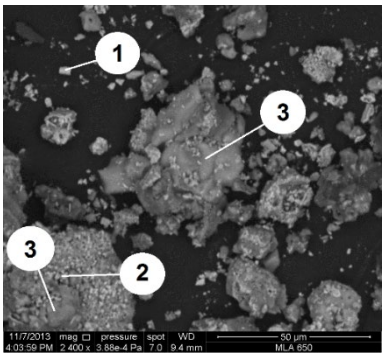

Figure 2. SEM image of the calcine obtained at 400 °C, 50% NaCl content, and 90 min roasting duration; 1 - Fe_2O_3; 2 - mixture of Ni and Fe sulphates; 3 – NaCl.

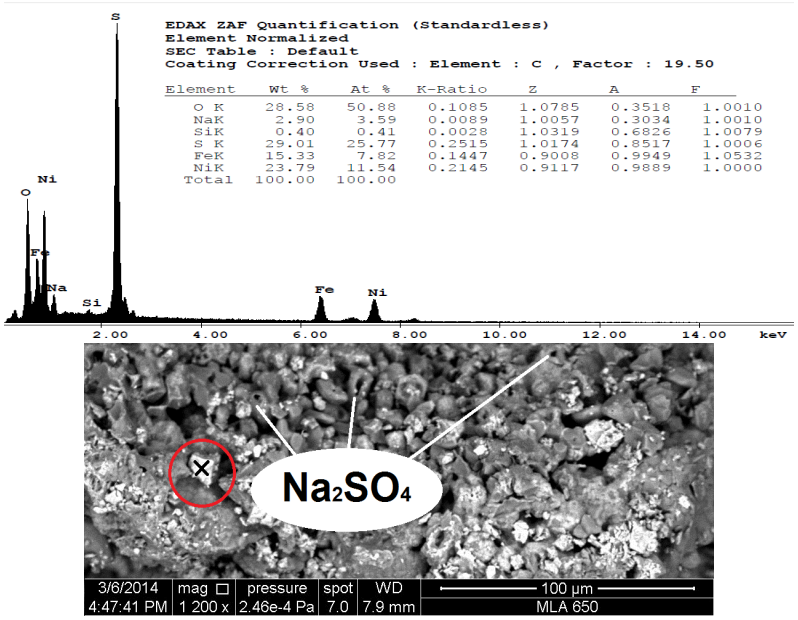

Figure 3. SEM image and EDS analysis (at point "x") of the calcine obtained at 400 °C, 50% NaCl content, and 90 min roasting duration

EFFECT OF ROASTING CONDITIONS ON NICKEL RECOVERY FROM CALCINE DURING WATER LEACHING

Effect of NaCl content

The relation between the NaCl content in mixture and subsequent nickel, copper,

and iron recovery from roast residue after roasting of concentrate and water leaching is shown in Fig. 4. Roasting conditions: temperature — 400 °C, duration — 90 min, salt content — 10-400% of concentrate weight. Maximum nickel and copper recovery into water (95 and 96% accordingly) was achieved upon 100-200% sodium chloride content. But from technology point, salt content 50% (when nickel recovery is 85%, that of copper — 95%) may be consider as optimum, provided that nickel and copper will be additionally recover from water leaching cake at stage of sulphuric acid leaching. At same time, providing NaCl recovery, roasting may be conducted at 150-200% NaCl, achieving maximum recovery of copper, nickel, and cobalt. In this case, no stage of sulfuric acid leaching is required. Recovery of iron into water is on level of 4-10%.

Effect of roasting temperature

The relation between roasting temperature and subsequent recovery of valuable components of calcine by water leaching is of certain interest. When sodium chloride content is 50%, optimum temperature is 400 °C. In this case, 84% of nickel is recovered from calcine by water leaching. It should be noted that copper and nickel behavior are almost identically in whole investigated temperature range but for copper recovery is 10-20% higher (for 50% sodium chloride content) than that of nickel (Figure 5). Regardless of temperature, iron recovery from calcine by water leaching is no more than 10%; and, for example, at 425-450 ºC, this value is close to zero due to full oxidation of ferrous sulphide to oxides. Thus, it is shown that offered method allows obtaining nickel and copper recovery into water at level of 95%. Regardless of salt content, optimum roasting temperature should be considered as 400 ºC.

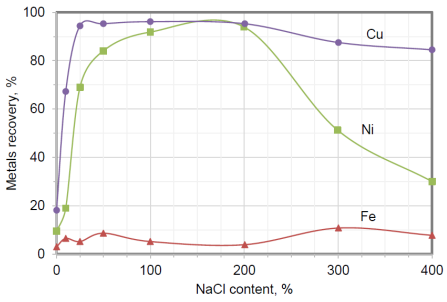

Figure 4. Effect of the NaCl content in roasting mixture on nickel, copper, and iron recovery from calcine by water leaching

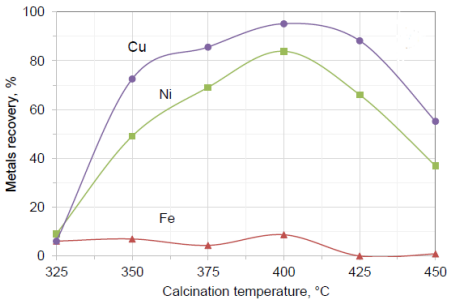

Figure 5. Effect of the roasting temperature on nickel, copper, and iron recovery from calcine by water leaching (roasting duration 90 min, NaCl content – 50%)

Effect of roasting duration

The relation between roasting duration and subsequent nickel, copper, and iron recovery from roast residue after roasting (at 400 ºC and 50% NaCl content) followed by water leaching is shown in 6. It should be noted that starting with roasting duration of 30 min, copper recovery is 10-15% higher at any specific time,

than that of nickel. Optimum duration of roasting is assumed to be equal to 90 min: exceedance of this value leads to decreasing of all three metals recovery due to sulphate decomposition. It should be also noted that upon roasting more than 2.5 h, iron recovery into water is less than 1%.

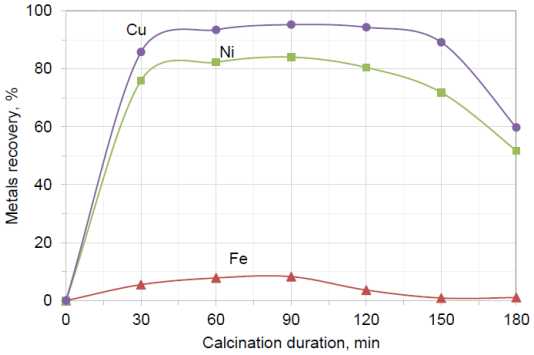

Figure 6. Effect of the roasting duration on nickel, copper, and iron recovery from calcine by water leaching (roasting temperature - 400 ºC; NaCl content - 50%)

CONCLUSIONS

1. Thermodynamic studies demonstrated that the nickel-containing interaction products of nickel sulphide and sodium chloride in the presence of oxygen included nickel sulphates, chlorides, and oxides. Nickel sulphate formation is most favourable at 350–450 ℃, whereas at higher temperatures, oxide formation is preferred.

2. Nickel sulphate was experimentally proven to be the main nickel containing interaction product of nickel sulphide concentrate and sodium chloride at 400 °C. In addition, reduced nickel oxide and chloride were identified in the calcine and other products included iron (III) oxide and sodium sulphate.

3. Roasting conditions influence to Ni, Cu, Fe recovery from calcine by water leaching were investigated and optimal conditions are next: roasting temperature of 400ºC, NaCl content of 50-100% and roasting duration of 90 min.

4. At optimal conditions Ni recovery up to 90-92%, cu recovery up to 95%.

References

1. Rajic, S., Zlatanovic, D. (1988) Chemical reactions between molybdenum disulfide and sodium chloride in a stream of oxygen in the temperature range 470-900 K. Thermochim. Acta 124, 163–169,
2. Zlatanović, D., Purenović, M., Zec, S., Miljković, M. (1998) The role of NaCl in chlorine roasting of MoS_2. Mater. Sci. Forum 282–283, 349–354,
3. Aleksandrov, P.V., Medvedev, A.S., Milovanov, M.F., Imideev, V.A., Kotova, S.A., Moskovskikh, D.O. (2017) Molybdenum recovery from molybdenite concentrates by low-temperature roasting with sodium chloride. International Journal of Mineral Processing. 161, 13–20,
4. Charkavortty, M., Srikanth, S. (2000) Kinetics of salt roasting of chalcopyrite using KCl. Thermochim. Acta 362, 25–35,

5. Mukherjee, T.K., Menon, P.R., Shukla, P.P., Gupta, C.K. (1985) Chloridizing Roasting Process for a Complex Sulfide Concentrate. J. Miner. Met. Mater. Soc. 37, 29–33,
6. Ngoc, N.V., Shamsuddin, M., Prasad, P.M. (1989) Salt roasting of an off-grade copper concentrate. Hydrometallurgy 21, 359–372,
7. Medvedev, A.S., So, T., Ptitsyn, A.M. (2012) Combined processing technology of the Udokan sulfide copper concentrate. Russ. J. Non-Ferrous Met. 53, 125–128,
8. Imideev, V.A., Aleksandrov, P.V., Medvedev, A.S., Bazhenova, O.V., Khanapieva, A.R. (2014) Nickel Sulfide Concentrate Processing Using Low-Temperature Roasting with Sodium Chloride. Metallurgist. 58, 353–359,
9. Pandher, R., Utigard, T. (2010) Roasting of nickel concentrates. Metall. Mater. Trans. B, 41, 780–789,
10. Pandher, R., Thomas, S., Yu, D., Barati, M., Utigard, T. (2011) Sulfate formation and decomposition of nickel concentrates. Metall. Mater. Trans. B, 42, 291–299,
11. Yu, D., Utigard, T.A., Barati, M. (2014) Fluidized Bed Selective Oxidation-Sulfation Roasting of Nickel Sulfide Concentrate: Part I. Oxidation Roasting. Metall. Mater. Trans. B, 45, 653–661,
12. Yu, D., Utigard, T.A., Barati, M. (2014) Fluidized bed selective oxidation-sulfation roasting of nickel sulfide concentrate: Part II. Sulfation roasting. Metall. Mater. Trans. B, 45, 662–674,
13. Aleksandrov, P.V., Medvedev, A.S., Imideev, V.A., Moskovskikh, D.O. (2019) Nickel sulphide concentrate processing via low-temperature roasting with sodium chloride. Part 1 – identification of interaction products. Minerals Engineering. 134, 37–53,
14. Babenko, A.R., Smirnov, V.I. (1970) The study of the kinetics of decomposition of sylvinite and sodium chloride in a fluidized bed. Russ. J. Non-Ferrous Met. 3, 34–39,
15. Medvedev, A.S., Alexandrov, P.V. (2012) Variants of processing molybdenite concentrates involving the use of preliminary mechanical activation. Russ. J. Non-Ferrous Met. 53, 437–441.

XIII International Mineral Processing and Recycling Conference
Belgrade, Serbia, 8-10 May 2019

University of Belgrade, Technical Faculty in Bor
Vojske Jugoslavije 12, 19210 Bor, Serbia
Tel. +381 30 424 555 Fax +381 30 421 078

STUDYING THE PROCESS OF SULFURIC ACID TREATMENT OF OXIDIZED COPPER

Naguman P. Nigmadullayevich #, Sherembayeva R. Tyulyukhanovna, Omarova N. Kakibayevna, Rakhimbekova A. Berikovna
Karaganda State Technical University, Karaganda, Kazakhstan

ABSTRACT – There has been studied dressing oxidized copper ores from the Udokan deposit with preliminary acid treatment of the pulp with sulfuric acid and electrochemical treatment followed by flotation. Copper in the ore is represented by oxidized minerals: malachite, azurite, but mainly chrysocolla (approximately 85 %). The degree of grinding ore was 76.4 % of the class - 0.074 mm. To determine the optimal conditions for the process of pulp electrochemical processing followed by flotation, a four-factor experiment plan was drawn up at five levels. The determining factors of the process are the concentration of sulfuric acid, the L:S ratio, the duration of the experiment. The maximum indicators for the copper recovery in the concentrate are achieved when the L:S ratio = 1, short-term electrochemical processing lasts within 3 - 5 minutes, the concentration of sulfuric acid makes 70 - 90 g/l. The calculated value of the process activation energy was 5.80 kJ/mol. The estimated reaction order for the concentration of sulfuric acid is 0.11.

Key words: collector, foaming agent, flotation, copper concentrate, copper recovery, copper content.

INTRODUCTION

It is known that in the process of flotation of oxidized copper ores qualitative and quantitative indicators are mainly determined by the physical-and-chemical properties of the mineral surface, the ionic composition of the liquid phase, the magnitude of the redox potential of the pulp, and its alkalinity. The regulation of the surface properties of minerals before flotation is carried out by introducing special reagents. However, the use of chemical compounds has several disadvantages associated with the complexity of the process, the cost of expensive, often scarce and toxic substances.

Electrochemical technology that makes it possible to directionally regulate the surface properties of minerals and the ionic composition of the liquid phase of the pulp is successfully developed during the flotation of nonferrous and rare metals. The works of many Soviet and foreign scientists have shown the wide possibilities of the electrochemical method to increase the valuable components recovery.

corresponding author: pnaguman@mail.ru

At present, three main areas of using electrochemical effects in the dressing processes have been identified:

- electrochemical pulp conditioning with the aim of controlling physical-and-chemical and flotation properties of minerals;
- electrochemical treatment of technical and circulating water to intensify the flotation process and to form the conditions for ensuring closed water circulation;
- electrochemical treatment of solutions of flotation reagents to increase the efficiency of their use in flotation processes.

The electrochemical method of pulp preparation is based on adsorption-desorption phenomena occurring on the surface of mineral particles due to the short-term charging of minerals in the pulp flow and regulation of the redox potential (Eh) and the ionic composition of the liquid phase.

Theoretical calculations and experimental data on studying the probability of the mineral particles contacting with the electrode surface, the nature of distribution of the potential of the electric field, the kinetics of changes in the potential of sulfides, the ionic composition, pH and Eh of the aqueous phase in the process of electrochemical processing of pulps found that the main factors ensuring the efficiency of electrical treatment contact charging, changing the value of the redox potential, the ionic composition of the liquid phase of the pulp, etc.

There are known the developments of Zh. Abiishev Chemical-Metallurgical Institute that studied the development of electrochemical methods for the sulphidation of oxidized copper ores. Based on studying the electrochemical behavior of copper, monovalent and divalent copper oxides, copper carbonate (malachite), copper silicate (chrysocolla), monovalent and divalent copper sulfides, chalcopyrite, etc. in acidic, alkaline, neutral solutions that allowed to establish the mechanisms of formation of these compounds, contributed to the determination of the regularity of their transition from the oxidized phase to the sulfide one, on the basis of which fundamentally new methods of preparation difficult to dress oxidized copper ore to the flotation [1].

A titanium cathode and a lead anode were used as electrodes. A portion of the crushed ore (class - 0.074 mm in the 70 % ore) was mixed with a solution of sulfuric acid, while the L:S ratio was 3:1. Sodium sulfite and elemental sulfur, which is introduced into the ore pulp based on the reaction of formation of readily flooded copper sulfides, are used as a sulphidizer. The prepared pulp was loaded into the cathode space of the electrolyzer and under the conditions of intensive mixing was subjected to electrolysis. After electrolysis, the pulp was floated on an F-237 FL-A laboratory flotation machine. Under flotation conditions the flotation reagent-aerofloat consumption was 120 g/t, the blowing agent T- 80 was 80 g/t. The main flotation time was 8 minutes, the control time was 11 minutes.

Then, freshly formed very active copper reacts with elemental sulfur introduced as a sulphidizer due to chemical affinity forms easily floatable copper sulfide (I):

$$2Cu^0 + S^0 \rightarrow Cu_2S \quad (1)$$

Under the optimal conditions, the increase in copper recovery in the flotation

concentrate is 20 - 30 %. Thus, we first proposed a method for electrochemical sulphidizing oxidized copper ores using sodium sulfite and elemental sulfur as sulphidizers. The optimal process parameters have been determined, providing an increase in copper recovery relative to direct flotation by 25 - 30 %.

From literary sources, various technological schemes are known for the processing of oxidized copper ores, involving the transfer of metals from oxides, silicates, etc., into sulfides.

One of the options for the processing of oxidized copper ores is the treatment of the pulp with sulfuric acid with an electrochemical treatment to form copper sulfides followed by their flotation.

Laboratory studies on the enrichment of oxidized copper ore using preliminary acid treatment were carried out on the refractory complex ore from the Udokan deposit. A titanium cathode and a lead anode were used as electrodes. The crushed ore was treated with a solution of sulfuric acid with a concentration of 60 - 70 g / l with the ratio T: W = 1 under stirring conditions for 5 - 10 minutes to a final pH of 5.0 - 6.5. The ore thus treated was pulverized and floated after sulphidization with sodium sulfide. The chemical composition of the ore is given below:

Table 1. The chemical composition of the ore

Component	Content, %
Cu	0.46
$Fe_{tot.}$	2.09
$S_{tot.}$	0.17
SiO_2	70.5
Al_2O_3	10.89
CaO	2.01
MgO	0.37
Mn	0.1
Cr_2O_3	0.07
V_2O_5	0.014
TiO_2	0.43
Pb	< 0.01
K_2O	2.5
Na_2O	3.0

The degree of ore oxidation is equal to 78.3 %. Copper in the ore is represented by malachite, azurite, but mainly by chrysocolla (approximately 85 %). Ore milling is of 76.4 % class minus 74 microns.

Pretreatment of the oxidized ore with the sulfuric acid solution was carried out in a thermostatted cell equipped with a stirrer. The temperature of the experiments was maintained with the accuracy of ± 20 °C. After the cell and the sulfuric acid solution were heated to the predetermined temperature, a portion of the ore under study was fed. The weight in all experiments remained constant.

Figure 1 shows a schematic diagram of the oxidized ore treatment that includes preliminary sulfuric acid treatment and subsequent froth flotation with sodium sulfide. Sodium sulfide consumption was 0.5 kg per ton of ore. Consumption of butyl xanthogenate was 70 g/t, aerofloat 80 g/t, blowing agent (T-80) 70 g/t. The duration of the main and control flotation was 10 and 15 minutes, respectively. Flotation

products were analyzed for copper content [2, 3].

In the course of experiments, sulfuric acid of the "ch" grade was used with the content of the main substance not less than 93.6 - 95.6 %.

The main parameters of the acid treatment of ore pulp and the ranges of their variation are shown in Table 2.

Table 2. Levels of the factors studied

Factor	Level				
	1	2	3	4	5
Acid concentration, g/l	10	30	50	70	90
L : S	0.5	1.0	1.5	2.0	2.5
Duration, min.	5	10	15	20	30
Temperature, °C	20	30	40	50	60

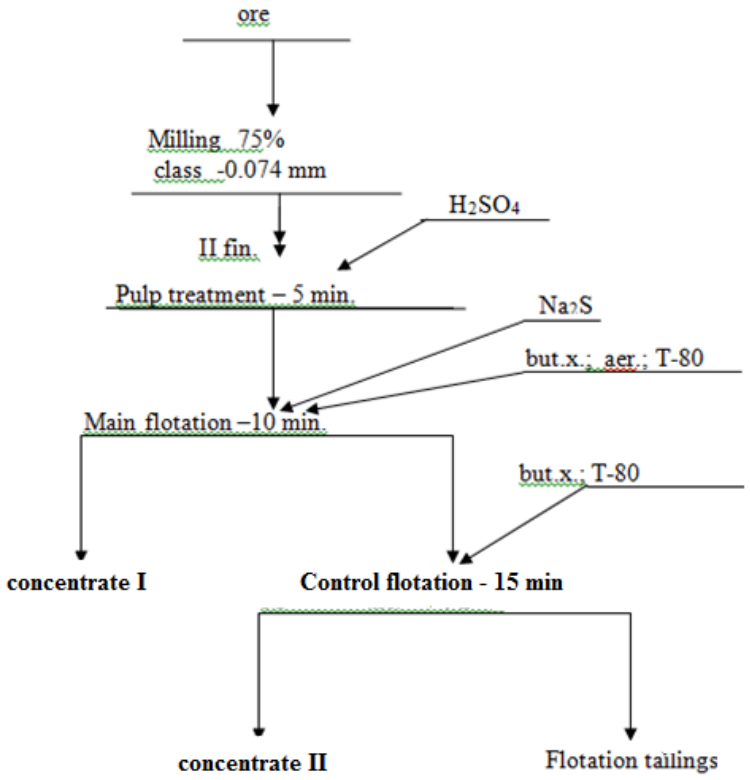

Figure 1. Schematic diagram of oxidized copper ore treatment using sulfuric acid

In accordance with Figure 2, the time factor is crucial for this process. So when processing the oxidized copper ore within 5 minutes, the copper recovery in the concentrate was 78.2 %, with increasing the processing time of up to 30 minutes the copper recovery was 52.5 %, that is, it decreased by 25.7 %. This fact was revealed only in the third series of experiments; therefore, previous experiments on studying the effect of acidity were carried out within 15 minutes (t^0 was 20 °C; L:S = 1). The

maximum copper recovery in these conditions could not be achieved. But the tendency to increasing the value of the main indicator of the process was determined with increasing the concentration of acid used in the treatment (Figure 2, a). The required concentration and consumption of sulfuric acid for processing the ore pulp are determined by its mineral composition. Some proportion of the acid during processing is spent on neutralization of the enclosing rocks, partial dissolution of minerals present in ore, which causes an unnecessarily increased consumption of sulfuric acid.

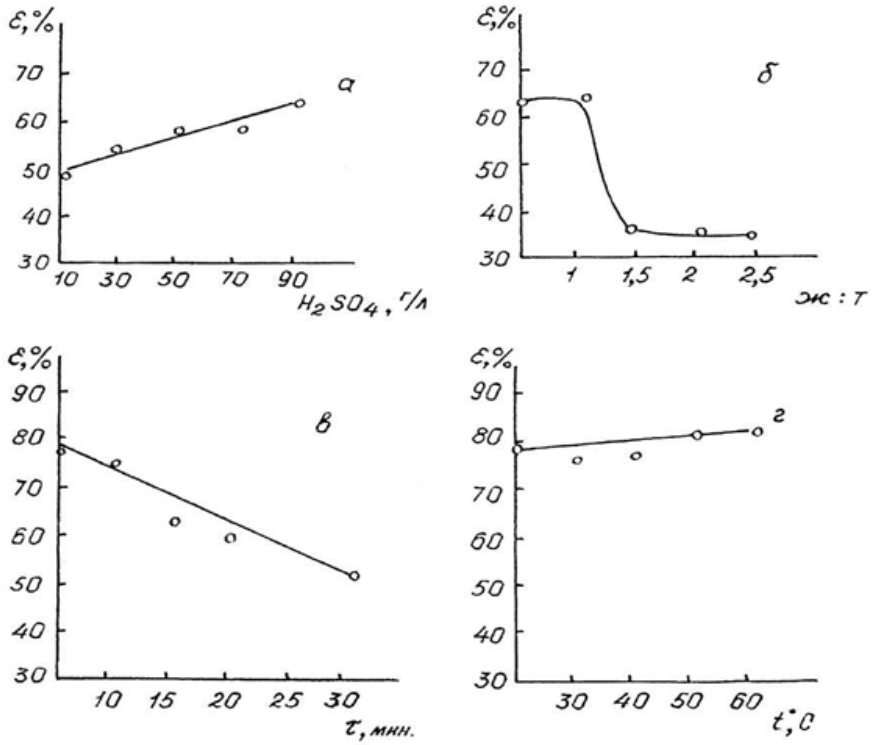

Figure 2. Copper recovery degree dependence on the acid treatment parameters (**a** - on sulfuric acid concentration; **b** - on the L:S ratio; **c** - on duration; **d** - on temperature)

To form the favorable conditions for flotation, acid treatment was carried out with a more dense pulp. The ratio of liquid to solid should not exceed 1:1, otherwise there is decreasing the recovery of copper (Figure 2, b).

The efficiency of sulphidization of oxidized minerals present in the flotation pulp depends on the pH of the initial solution and Na_2S consumption [3]. The pH value of the pulp after acid treatment in the case of the liquid to solid ratio of more than 1:1 is 1-2. It follows that in order to form normal flotation conditions the use of medium regulators (reagents- neutralizers) is required to raise the pulp pH, or increasing the consumption of sodium sulfide. Sodium sulfate as a salt of a strong base and a weak acid undergoes hydrolysis [4, 5].

$$Na_2S + H_2O = NaHS + NaOH \quad (2)$$

$$NaHS + H_2O = H_2S + NaOH \quad (3)$$

The result of this is increasing pH to 11 or higher [6]. But on the other hand, the addition of Na_2S above a certain limit can lead to depression of sulfide minerals.

In accordance with Figure 2d, the temperature increase does not significantly affect the recovery of copper. Thus, with increasing the treatment temperature to 600 °C, the recovery of copper was 82.43 %, which is only 4.21 % higher than the value reached at the room temperature.

The calculated value of the process activation energy was 5.80 kJ/mol. The estimated reaction order by the concentration of sulfuric acid was 0.11.

In filtrates copper has not been practically found; only when treating with sulfuric acid the concentration of 90 g/l in individual samples, the copper content varied from 0.093 to 0.16 g/l.

CONCLUSION

Thus, having analyzed the results of the study, there can be stated the efficiency of using the preliminary acid treatment for dressing difficult-to-treat oxidized ores. Compliance with the most acceptable flotation conditions imposes the following requirements to the ore treatment process: L:S in the pulp should not exceed 1, the needed concentration and consumption of sulfuric acid are determined by the mineral composition of the ore, short duration of processing.

References

1. Dospayev, M. M., Bayeshov, A, et al. (2016) Mechanism of electrochemical sulphidization of oxygen-containing copper compounds in the composition of difficult to dress oxidized copper ores,
2. Narkovich, I. Y., Pechkovsky, V. V. (1984) Recycling and waste disposal in solid technology. M.: Chemistry., 240,
3. Naguman, P. N. A. C. Method of dressing oxidized copper ore. (2009) 2009/1282.1 of October 26, 2009,
4. Vakhromeyev, S. A. (2011) Mineral deposits, their classification and conditions of formation. M.: Gosgeoltekhizdat, 463,
5. Naguman, P. N. (2009) The use of anodic treatment for dressing difficult-to-oxidize ores, Non-ferrous metals, 10, 11-13,
6. Chanturia, V. A., Weissberg, L. A., Kozlov, A. P. (2014) Priority areas of studies in the field of mineral raw materials processing. Ore Dressing, 2, 3-9.

XIII International Mineral Processing and Recycling Conference
Belgrade, Serbia, 8-10 May 2019

University of Belgrade, Technical Faculty in Bor
Vojske Jugoslavije 12, 19210 Bor, Serbia
Tel. +381 30 424 555 Fax +381 30 421 078

A MULTI-DISCIPLINARY APPROACH TO REHABILITATION OF HISTORICALLY DISTURBED LANDS

Svetlana Bratkova [1], Anatolii Angelov [2], Elena Zheleva [2], Ekaterina Todorova [3], Stefan Stamenov [3], Emanuil Kozhuharov [4], Peter Delov [4], Elisaveta Valova [5], Zhivko Vasilev [5, #]

[1]University of Mining and Geology, St. Ivan Rilski, Sofia, Bulgaria
[2]University of Forestry, Sofia, Bulgaria
[3]Ecotech Consult Ltd, Sofia, Bulgaria
[4]Jess E Ltd., Sofia, Bulgaria
[5]Dundee Precious Metals Chelopech, Bulgaria

ABSTRACT – Dundee Precious Metals Chelopech EAD conducted a multi-disciplinary survey within the framework of its program for the rehabilitation of lands disturbed by historical mining. The survey covered: a comprehensive characterization of the mineral substrate, a hydrological and hydro-geological profile of the area, surface and groundwater quality, soil and sediment analysis. The purpose of the multi-disciplinary survey was to collect and systematize additional data and identify specific measures for environmental improvement and restoring disturbed lands, as much as possible, to their original state. The article presents the scientific methods applied during the conducted comprehensive survey and respective activities carried out at present.

Key words: mine site, mining materials, hydrology and hydrogeology, surface and groundwater, soils and sediments

INTRODUCTION

Already in 2004 Dundee Precious Metals Chelopech EAD embarked on a project for the rehabilitation of lands disturbed by historical mining, including surface caves, abandoned derelict facilities and old waste rock dumps, with the objective to improve the environmental status of the mine site.

The project's main objective was to restore the land as much as possible to its original natural state and plant typical local tree and shrub species that would ensure the conservation and rehabilitation of animal and bird habitats, as well as protect surface and groundwater, and soils, from potential acid water generation processes. Till now the Company has rehabilitated 22 hectares of historically disturbed lands,

corresponding author: zhivko.vasilev@dundeeprecious.com

including old stockpiles/waste rock dumps, surface subsidence caused by the old mining method applied until 2005, areas with decommissioned facilities and buildings, and other already reclaimed and cultivated areas. In 2015 DPMCH launched an inter-disciplinary survey together with two local universities - the University of Mining and Geology and the University of Forestry - and several other companies (Ecotech, Eurotest-Control and Jess E).

TOPOGRAPHIC CHANGES – SCIENTIFIC METHOD AND RESULTS

The study started by making an up-to-date topographic map of the lands – the aim was to identify surface subsidences by reviewing old topographic data and overlaying them on current data. The new map identified new disturbed surface areas with topographic changes. Based on 1978 and 2010 topographic data, nine zones were identified and classified as potentially affected by human activity.

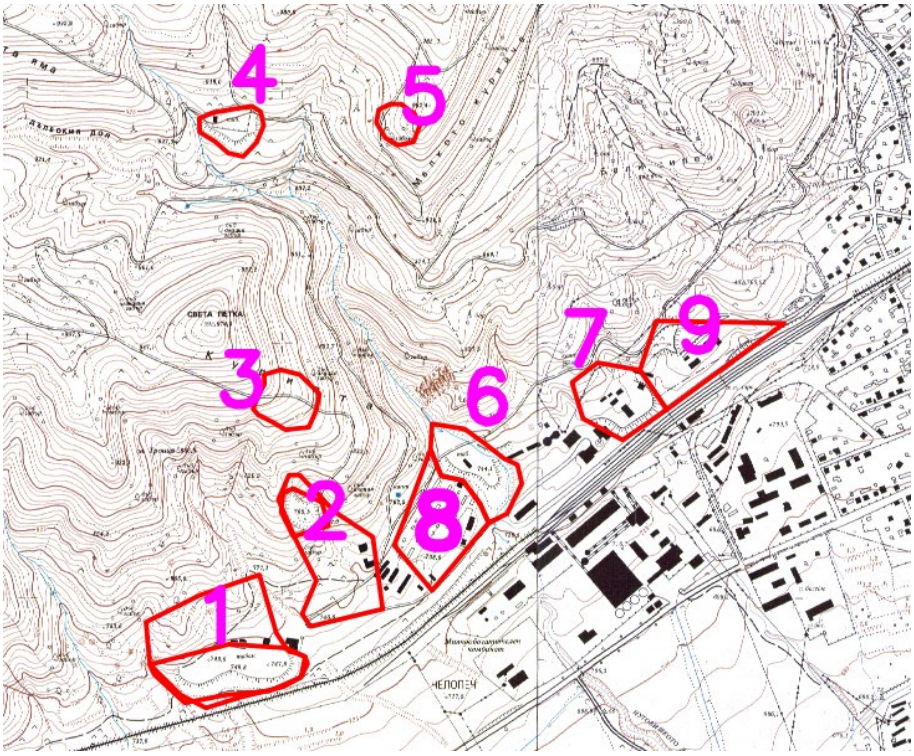

Figure 1. Locations of the zones with topographic changes

CHARACTERISATION OF THE MATERIALS ON DISTURBED LANDS – SCIENCE METHOD AND RESULTS

A Sampling Plan was developed to collect substrate samples that would be tested to obtain reliable test results. The following criterion was applied to substrate sampling: materials disposal areas – to determine the required number of samples per area in compliance with BNS EN 14899:2006 and SD CEN/TR 15310-1:2007.

Static[1] and kinetic tests[2] were conducted to characterize the substrate. The materials in the test areas could not be classified as inert because their sulphide sulphur content was in excess of 0.1%[3]. All the materials in the areas had greater than 0.1% sulphide sulphur, which indicated ARD potential. The lower than 1 NPR (NPR <1) also supported the above finding. The only exception was the material in Area 8, which had 0.1% sulphide sulphur and NPR=157.

Table 1. Suplhur assays on samples from test areas for NPR determination

Indicator	Measure	Area 1		Area 2	Area 6	Area 7	Area 8	Area 9
S_{total}	%	1.27	1.53	2.04	1.61	2.25	1.04	1.63
$S_{sulphate}$	%	0.92	1.11	1.20	0.79	1.54	0.94	1.09
$S_{sulphide}$	%	0.35	0.42	0.84	0.82	0.71	0.10	0.54
Neutralising Potential Ratio (NPR)=NP/AP	-	0.49	0.45	-0.27	0.72	1.99	157	0.079

The testing that was conducted to determine and predict the mobility of the different metals and cations on lands disturbed by historical mining, which was caused by erosion processes, indicates that:

•pH of eluate is one of the key parameters. It is evident that pH<6 for both samples from Area 1, Area 2 and Area 9. pH > 6 for the remaining areas under the testing conditions. When the pH is maintained above 6, the mining waste is non-hazardous to the environment.[4] According to Regulation N-4[5], pH should be maintained between 6.5 and 8.5 to achieve "good" quality of surface water. In this regard, the pH values for the eluates from Area 1, Area 2 and Area 9 should be controlled by applying the measures recommended below to minimise negative impacts.

•Maintaining constant levels in the eluate: antimony (Areas 1, 2, 7 and 9), alkalinity (all areas, where the level for Area 8 was higher at the start of the tests and flattened out with time). This is not surprising having in mind the mineral composition of the sample from Area 8 (44 % dolomite); arsenic (below MAC in all areas except for Area 8); mercury (all areas); cadmium (Areas 6, 7, 8, and 9);

[1] *BNS/EN 15875:2011 Characterization of waste. Static test for determination of acid potential and neutralisation potential of sulfidic waste.*
[2] *ASTM-Designation: D5744-07 - Standard Test Method for Laboratory Weathering of Solid Materials Using a Humidity Cell (ATSM, 2007).*
[3] *Section 2b, Appendix 3 to art. 15 of the Mine Waste Management Regulation, 2016.*
[4] *ASTM-Designation: D5744-07 - Standard Test Method for Laboratory Weathering of Solid Materials Using a Humidity Cell (ATSM, 2007).*
[5] *Regulation H-4/14.09.2012 on Surface Water Characterisation, 2013*

molybdenum (all areas, below MAC in surface waters); lead (all areas, below MAC in surface waters); selenium (all areas except for Area 7);

•Increasing levels in the eluate indicating leaching potential with time: antimony (Areas 6 and 8); arsenic (Area 8, maximum level in Week 16 and declining thereafter, below MAC over the entire test period); barium (all areas, maximum level in Week 16, end levels higher than starting levels); iron (markedly high levels in Area 2 in Week 8 and declining thereafter but remain above starting levels in all areas); cadmium (Sample 2, Area 1; Sample 1, Area 1 – maximum level in Week 16 and declining thereafter); selenium (Area 8, maximum level in Week 8 and flattening out thereafter); cadmium (all areas, maximum level in Week 16, end levels higher than starting levels); zinc (close levels in Areas 7, 8 and 9, end levels higher than starting levels); dissolved organic carbon (DOC – a sudden increase at the end of the period in Sample 1, Area 1);

•Falling levels in the eluate: cadmium (Area 2, lower than the starting level); copper (all areas, very high starting level in Area 1); nickel (Area 1, maximum in Week 16, end levels lower than the starting levels); zinc (both samples, maximum levels in Week 8 and Week 16, end levels lower than starting levels); fluorides, chlorides and sulphates (varying levels, downward trend in all areas); dissolved organic carbon (DOC – varying levels, downward trend, except for Sample 1, Area 1, showing a sudden increase at the end of the period).

GROUNDWATER – SCIENTIFIC METHOD AND RESULTS

A review of the available groundwater data from exploration projects was conducted in an attempt to determine the hydrogeological conditions in the wider area. It was found that the available historical sources did not have sufficient and reliable data to provide groundwater insight for the area in question.

Therefore, a number of additional studies and surveys were planned and conducted to clarify the hydrodynamic and hydrochemical setting. Those included studies of the basement under the dumps, hydrodynamic and hydrochemical characterization of groundwater, and a project for construction of groundwater monitoring piezometers.

The available data and the results from the field studies of natural outcrops in the test areas indicate that the basement underlying the dumps consists of volcanic rocks of Cretaceous age and rare sediments and deposits of Quaternary age. The Cretaceous rocks comprise of andesites, andesite tuffs and tuffites, which are strongly tectonised, altered and weathered. Quartz sandstones outcrop in the western extents of the test areas. The quaternary deposits are proluvium-alluvium deposits that have heterogeneous composition, texture and shape. They comprise of boulders, gravels, sands and clayey lenses with a variable permeability, which is typical of such strata. According to the accepted aquifer naming and definition in Bulgaria, the test areas accommodate two aquifers: one coded BG3G00000K2029 and termed "Fissure Waters, Gorna Malina – Panagyurishte Region",and the other coded BG3G00000Q001 and termed "Interstitial Groundwaters in Quaternary Deposits, Pirdop-Zlatista Valley". The prevailing regional groundwater flow is north to south. Given the analysis we made, we proposed an upgrade of the existing groundwater monitoring network to enable assessment of the impact that the disturbed lands have.

Figure 2 below is a layout of the ten monitoring points under the project for construction of groundwater monitoring piesometers. Four piesometers are located north of the dumps and are used to provide the baseline properties of the waters flowing through the test areas. The remaining six piesometers are set up south of the dumps and are used to monitor the changes in the groundwater quality downstream of the test areas.

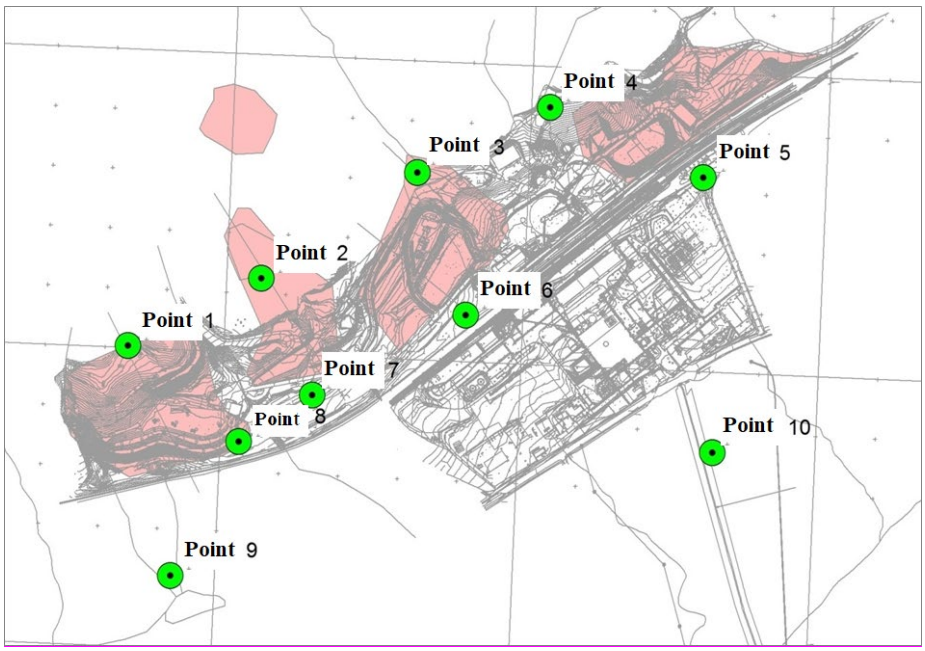

Figure 2. Groundwater monitoring bore layout

The monitoring network was established in 2017 and 2018. Currently, a groundwater seasonal sampling program is under way, which provides measurement of the chemical composition to enable analysis and assessment of the impact on the groundwater.

CLIMATIC AND HYDROLOGICAL INVESTIGATIONS; EVALUATION OF REHABILITATION WORKS AND VEGETATION ANALYSIS SCIENTIFIC METHOD AND RESULTS

The method included analysis and assessment of the condition of the disturbed and subsequently rehabilitated lands on the Company site. Any shortfalls of the rehabilitation process have been addressed and measures for future implementation have been recommended on the basis of the results from the climatic and hydrological investigations in the area, the condition of the disturbed and subsequently rehabilitated lands, the test work on the materials used in the rehabilitation process, the study of vegetation including bioaccumulation, analysis of the negative impacts on the rehabilitation developments, and guidance for future rehabilitation works.

The assessment of the condition of the waters in the Chelopech Deposit area is based on the analysis of the regional hydrological regime and monitoring of the level and rate of change of their chemical composition between 2010 and 2014. The analysis of the rehabilitation works done by the Company demonstrates that the number of mining-related sources of environmental pollution have decreased substantially. Several land rehabilitation projects have been implemented both on the North Site and south of it.

The Western Dump, the dumps at Zapad shaft and Nadezhda decline have successfully been rehabilitated. The main issue associated with both rehabilitated areas and undisturbed soils are the elevated background concentrations of certain metals and the high acidity due to the long years of pollution in the past. The levels of copper and arsenic, and lead, zinc and cadmium in certain areas, exceed the precautionary concentrations[6], even the MAC[7] at certain locations. The high metal content and low pH promotes accumulation of heavy metals in plants and in the surface waters thus increasing their acidity. The chemical assays conducted on plants, although without a baseline insight for some elements, indicate elevated levels of heavy metals (particularly copper) in their vegetative parts. Over the last years, the Company has put significant effort in the rehabilitation of old decommissioned facilities on the north site and previously disturbed topography, which significantly reduced the number of surface water and soul pollution sources. Along with this, regular monitoring of the waters and soils in the immediate area of the deposit is conducted.

SURFACE WATERS AND DEPOSITS – SCIENTIFIC METHOD AND RESULTS

According to the existing Surface Water and Sediments Sampling Plan, which is based on topographic maps and local topographic features (multiple small ravines that drain surface runoff and seepage after heavy rains), ten points are subject to regular seasonal monitoring. Additional 33 samples are recovered from deposits. The sampling points are located along the natural ravines or the drains constructed at some of the facilities.

The surface water samples are assayed for pH, conductivity, sulphates, Al, As, Cr, Cu, Fe, Mn, Ni, Zn. The sediment samples are assayed for pH, conductivity, Al, As, Cd, Cr, Cu, Fe, Mn, Ni, Zn. ICP-OES is used to determine heavy metal concentrations. It should be noted that the ten monitoring points are located along the natural ravines around Areas 6, 7, 8 and 9. The water volumes at other facilities even after heavy

[6] *Precautionary concentrations - concentration of a harmful substance in the soil, the exceedance of concentration of which does not lead to disturbance of the soil functions and to danger for the environment and human health (§ 1, item 2 of Ordinance No3 of 1 August 2008).;*

[7] *Maximum Allowable Concentrations (MAC) - concentration of a harmful substance in the soil, which, under certain conditions (depending on the particle size, composition, and pH of the soil), causes soil disturbance and danger to the environment and human health. MACs are generally applicable to unpolluted soils (§ 1, item 3 of Ordinance No3 of 1 August 2008).*

[8] *Annual average concentration (AAC)/Environmental quality standards (EQS) is quality standards for specific pollutants for environmental assessment under Regulation H-4/14.09.2012 and the Regulation on Environmental Quality Standards (EQS) for Priority Substances and Some Other Pollutants.*

rains is negligible due to the rapid draining of the runoff from precipitation through the existing system of interceptor drains. The points near Areas 6 and 8 have returned levels exceeding the AAC/EQS[8] for manganese under Regulation H-4/14.09.2012. It is important to note that the background concentrations of manganese in the deposit area (monitoring points set up along the Vozdol River) also exceeds the AAC/EQS. In the summer months, single elevated levels of aluminum, arsenic, copper and iron were detected only at one surface water monitoring point in Area 6; however, the concentrations were still below the AAC/EQS under Regulation H-4 and the Regulation on Environmental Quality Standards (EQS) for Priority Substances and Some Other Pollutants.

Thirty-three sediment samples have been tested to collect additional information about the impact that the materials have on the surface waters. Pursuant to the regulations and classifications for assessment of soil pollution under Regulation 3 on Concentrations of Pollutants in the Soil, only three samples do not meet the MAC for arsenic and copper. Two of them come from the south extent of Area 1, while the third one is taken near Area 9. It should be noted that the soils in the area are affected by pollution from past mining and processing operations. Following the surveys and studies, an action plan has been developed to include specific measures that will improve the environmental media in the deposit area.

CONCLUSION

The following conclusions can be drawn from this multi-disciplinary study:

1. The approach that has been followed is reliable because it is based on complementary data about environmental impacts from historical mining.
2. It has been confirmed that the mobility of pollutants in the eluates from the samples from Areas 1, 2 and 9, which have pH<6, is straightforward, which indicates a potential for an impact on the surface waters as an environmental medium unless appropriate measures are implemented (measures implemented in 2018).
3. The groundwater monitoring network, which was established in 2017 and 2018, enables monitoring of the specific local hydrodynamic conditions, a baseline insight into the surface streams entering the area from the north and the chemical composition of the groundwater flowing south of the test area, comparison and correlation with the results from other fields of study, and assessment of the impact from disturbed lands and dumps on the groundwater quality. Currently, a groundwater seasonal sampling program is under way, which provides measurement of the chemical composition to enable analysis and assessment of the impact on the groundwater.
4. It has been confirmed that surface flows in the test area are closely related to precipitation events.
5. The main issue associated with the rehabilitated areas and non-disturbed lands locally is the elevated concentration of some metals and the high acidity, which are due to the long years of pollution in the past. Based on the studies and analysis of available data that have been conducted to-date, the conclusion is to improve the local environmental conditions by implementing certain soil improvements (since 2018 ongoing scientific work together with the Forestry University).

XIII International Mineral Processing and Recycling Conference
Belgrade, Serbia, 8-10 May 2019

University of Belgrade, Technical Faculty in Bor
Vojske Jugoslavije 12, 19210 Bor, Serbia
Tel. +381 30 424 555 Fax +381 30 421 078

INVESTIGATION OF COPPER EXTRACTION FROM PREGNANT SOLUTIONS USING C-100 AND S-930/4880 PUROLITE ION EXCHANGE RESIN

Aliya Mambetzhanova [1, 2, #], Lyudmila Bolotova [2], Vladimir Luganov [1], Kulzira Mamyrbayeva [1], Tatyana Chepushtanova [1], Gulnar Gusseinova[1]
[1]Kazakh National Research Technical University after K. I. Satpayev, Almaty, Kazakhstan
[2]Kazmekhanobr" State Scientific Production Association of Industrial Ecology, the branch of RSE "NC CPMRM RK", Almaty, Kazakhstan

ABSTRACT – The article presents the results of investigation on the extraction of copper from pregnant solutions (composition, g/l: 4-7 Cu; 5-6.0 Fe) using C-100 and S-930/4880 Purolite resins with preliminary depositing of iron ions. The results of the sorption extraction of copper showed that the sorption properties of ion exchange resins improved after being removed from the iron solution and the highest rates were obtained using S-930/4880 resin, its copper capacity was 28.50 g/l. The depositing of iron in a pregnant solution is effectively carried out with ammonium hydroxide, and the iron content decreased from 6000 to 172 mg/l.

Key words: copper, iron, ion exchange resins, capacity, depositing

INTRODUCTION

In hydrometallurgical processing of copper-containing raw materials by heap or percolation leaching with sulfuric acid solutions, dissolved copper can be removed by cementation with iron turnings, metallic iron or cast iron powder, extraction followed by electrolysis, and depositing with sulfide and sodium hydrosulfide.

One of the alternative methods for extracting copper is the sorption method for extracting dissolved copper by solid ion exchangers - synthetic ion exchange resins with high sorption capacity for copper and regenerating properties. The instrumentation of the process of ion exchange extraction of copper is much simpler and cheaper than for extraction [1].

corresponding author: aliya.myrzagulovna@gmail.com

EXPERIMENTAL

In this work, in order to determine the fundamental possibility of using cation exchangers for copper extraction from pregnant solutions, Purolite C-100 and S-930, produced in Great Britain, were tested as sorbents. The composition of the solution is as follows, mg/l: copper 5420; iron 5900.

The tests were carried out in a dynamic mode by passing the solution through the resin loaded into the column at a rate of 1.5 volumes of solution per 1 volume of resin per hour. Copper sorption is more effective when the pH rises from 1 to 4 and in the absence or low content of competing impurities of heavy metals in solutions, including iron [2].

In this regard, the pregnant solutions before sorption were treated with reagents, depositing ferric iron and neutralizing excess acid. For processing, the initial solution was used with the content, mg/l: copper 6000, ferric iron 6000. Calcium oxide (lime), sodium hydroxide and ammonium hydroxide (aqueous ammonia solution) were tested as precipitants. As a result of treatment with these reagents, light brown deposits are formed - jarosite (complex ferric compounds). Previously it was found that the most effective precipitator of ferric iron is ammonium hydroxide. The content of ferric iron is reduced from 6000 mg/l to 172 mg/l [3].

To determine the sorption characteristics of various sorbents, a pregnant solution was used after the depositing of iron with a strong solution of ammonium hydroxide (NH_4OH). The content in the copper solution is 5360 mg/l, iron 172 mg/l, pH of the solution is 3.57. The tests were carried out in a dynamic mode by passing the solution through the resin loaded into the column at a rate of 1.5 volumes of solution per 1 volume of resin per hour.

RESULTS AND DISCUSSIONS

Table 1 shows the results of tests on the sorption of copper from pregnant solutions without depositing iron from them.

Table 1. Sorption of copper from pregnant solutions

Specific volume of solutions, l/l resin		**Copper content**		**Extraction of copper from solution, %**
in operation	total	in solution, mg/l	in resin, mg/l	
Resin C-100				
1,0	1,0	920	4,50	83,03
1,0	2,0	1060	8,86	80,44
1,0	3,0	2380	11,90	56,09
Resin S-930/4880				
1,0	1,0	1120	4,30	79,36
1,0	2,0	1500	8,22	72,32
1,0	3,0	3440	10,20	36,53

From the obtained data, it follows that with equal specific volumes, the highest rates of copper sorption were obtained using C-100 resin (11.90 g/l), compared with S-930/4880 resin (10 g/l).

Table 2 shows the results of tests on the sorption of copper from pregnant solutions after the depositing of ferric iron from them by ammonium hydroxide.

Table 2. Sorption of copper from a pregnant solution conditioned by ferric iron

Specific volume of solutions, resin l/l		**Copper content**		**Extract**
in operation	total	in solution, mg/l	in resin, mg/l	**cooper from solution, %**
Resin C-100				
1,0	1,0	620	4,81	88,58
1,0	2,0	960	9,28	82,32
1,0	3,0	2150	12,56	60,41
1,0	4,0	3480	14,51	35,91
Resin S-930/4880				
2,0	2,0	580	9,70	89,32
2,0	4,0	1270	18,02	76,61
2,0	6,0	2620	23,64	51,75
2,0	8,0	3880	26,74	28,55
2,0	10,0	4550	28,50	16,21

The results shown in Table 2 showed that the sorption properties of the sorbents improved after being removed from the iron solution. After iron deposition, copper sorption using C-100 resin (14.51 g/l) is less than S-930/4880 (18.02 g/l) with the same missing solution volumes.

CONCLUSION

Tests have shown that cation exchanger C-100 effectively absorbs copper from a multicomponent solution. The sorption of copper from pregnant solutions is improved after removal from the iron solution. After the iron was removed from the pregnant solution, the S-930/4880 resin over copper saturation exceeded C-100 resin. Its maximum capacity was 28.50 g/l.

References

1. VG Samoilik. Special and combined mineral processing methods. Study guide. 2015,

2. V.M. Ivanov, R.A. Polyanskov, A.A. Sedov. Sorption of copper (II) ions by bismuth (I) immobilized on natural zeolite. Bulletin of Moscow University, series 2. chemistry. 2005. 46. (1),
3. Mambetzhanova A.M., Bolotova L.S., Luganov V.A., Chepushtanova T.A. Copper sorption with aminocarboxal type resins. Materials of the international scientific-practical conference “Innovations in the complex processing of mineral raw materials”, dedicated to the 25th anniversary of the RSE “National Center for Integrated Processing of Mineral Resources of the Republic of Kazakhstan" and the 60th anniversary of the State Research and Production Association of Industrial Ecology "Kazmekhanobr.”, Almaty, 2018, p. 86-89.

XIII International Mineral Processing and Recycling Conference
Belgrade, Serbia, 8-10 May 2019

University of Belgrade, Technical Faculty in Bor
Vojske Jugoslavije 12, 19210 Bor, Serbia
Tel. +381 30 424 555 Fax +381 30 421 078

URANIUM PURIFICATION INCREASING USING ULTRASOUNDS

Eugenia Panturu [#], Antoneta Filcenco-Olteanu, Aura Daniela Radu, Marius Zlagnean
Research and Development National Institute for Metals and Radioactive Resource, Bucharest, Romania

ABSTRACT – In this paper it was studied the influence of ultrasonic field (24 kHz, 400W) on the formation of stable emulsions (phase III) in extraction solvent process for uranium purification. Were performed two sets of complete extraction, in six steps through 250 ml separating funnel, with continuous phase of successively uranium aqueous solution (300 gU/l) and organic solvents (30 % to 70 % tributilphosphate kerosene), without and with ultrasound. Using ultrasound, by varying the amplitude (20 % - 100 %), led to increased mass transfer between the two phases but also to the partial breaking of phase III, after the extraction reaction was performed. The economic effects of applying ultrasound to solvent extraction in the process of uranium purification, is found in reducing the loss of useful component and in increasing the uranium separation and purification rate.

Key words: uranium, ultrasound, extraction, phase III

INTRODUCTION

Uranium purification up to nuclear purity is obtained by solvent extraction process. Large scale spreading of the extraction processes in rare and radioactive metals hydrometallurgy is due to the fact that in such conditions these metals ions can pass selectively from aqueous solution to the water non-miscible organic phase while the most associate elements remain in aqueous phase.

The unit operation of solvent extraction refers to the processes where the mass transfer is made between the two phases of a liquid-liquid system, in which one phase is an aqueous solution and the other is an organic solution namely solvent. The final process stage (suitable phase equilibrium) is called liquid-liquid repartition or distribution and the chemical species whose distribution is studying is called solute [1, 2, 3, 4, 5].

The purification of crude uranium recovered from its ores at plant-scale using tributyl phosphate (TBP) started in the early 1950 in Canada and U.K, then in U.S. in

[#] corresponding author: ioanpanturu@yahoo.com

1953. Today, TBP extraction technology and processes are applied world-wide for the purification of crude uranium and also thorium. The success of TBP solvent extraction compared to other processes for purification of uranium is due to [6-11].

1. TBP is highly selective for uranium, and provides excellent decontamination from most impurities;
2. TBP is relatively stable against degradation under normally conditions used to purify uranium. Simple washing techniques are available to remove solvent degradation products;
3. TBP/kerosene solutions have low vapor pressure and can be stored and handled without elaborating precautions against fires.

A difficult problem for solvent extraction processes is the precipitates formation, suspensions and emulsions stabilized by solid particles called "Phase-III''. The formation of this phase lead to significant loss of solvent and other effects, such as: loss of useful elements, the decreasing of the processing capacity of facilities, a decrease of uranium separation, decreasing of the uranium purification degree.

To eliminate this shortcoming, the literature [12-15] presents a relatively recent method of enhanced mass transfer, which consists in overlapping of an oscillatory movement on the stationary state of a fluid or solid, or on the normal flow (free or forced) of fluids, created by using ultrasonic pulsations. They influence the system properties, increasing the effectiveness of transfer operations.

EXPERIMENTAL AND MATERIALS

The aqueous solutions of nitric acid were prepared by diluting concentrated nitric acid (from Merk, 65 %) with double distilled water. The uranium concentrate, DUNa (65 % U in DUNa) was obtained by uranium ore acid processing followed by carbonation process, ion exchange and precipitation [16-18].

The uraniferous solution have the following chemical composition: U 306 g/l , acidity, HNO_3 3.07 N, Cl 11.33 g/l, Fe 1.224 g/l, Mo 0.404 g/l , 21.06 g/l, SO_4^{2-} 3.86 g/l, Suspended solide 0.094 g/l.

Tributyl phosphate used as an extractant was from FLUCKA with purity 99 %. The diluent used was the kerosene Acvos Organic , which has a density of 790 - 800 kg/m^3 at 15 °C, its boiling point range is 200 – 250 °C, and flash point > 70 °C, with aromatic content of max 0.2 % (v/v).; the ratio is: 30 % TBP acidified with 1N, in kerosene. The extraction in 6 steps, at the 20 °C, was carried out by stirring (orbital stirrer IKA RH – KT/C) three volumes of organic phase (150 cm^3) and a volume of aqueous phase (50 cm^3) for 5 minutes using separators funnel, than the mixtures were separated after 10 minutes of decantation.

For tracking phase III formation were performed two experiences in the absence and presence of ultrasonic field. Such an experiment consisted in contacting a volume of impure uranyl nitrate (AUI) (aqueous, continuous phase) with 3 volumes of organic fresh each time in each of the 6 steps.

Aqueous (continuous phase) obtained after each step, is used in the next step where is mixed with three volumes of fresh organic solvent. Organic solvent loaded with uranium, obtained from each step, is stored and mixed with all solvents loaded, obtained in all steps. Uranium loaded organic solvent thus obtained is subject of the re-extraction operations in order to obtain pure uranyl nitrate (AUP) (not surveyed).

The second experiment consisted of three volumes contacting organic solvent (continuing phase) with a volume of AUI fresh solution every time in each of the 6 steps. Uranium loaded organic solvent (continuous phase), obtained after each step, mix the next step, with a volume of fresh AUI solution.

In the same mode were done the two experiments in the field of ultrasound (24 kHz, 400 W, induced from the outside with a generator UP400S Hielscher, at 5 mm distance from the sample (working temperature is not influenced) that was varied the amplitude in the range of 20 % - 100 %. Duration of ultrasound field action is only during mixing, about 5 minutes. Volume of phase III in all experiments was measured using a scaled glass tube. Extraction is considered completed when the uranium content in the aqueous phase is max. 0.5 gU/L and/or content of uranium in organic solvents is minimum 100 gU/L [19, 20].

Uranium was determined in the aqueous and organic phases by γ – spectroscopic method, while iron was determined by colorimetric method using UV-VIS CECIL 1011. The viscosity of the organic phases after the extraction process was measured using SELECTA-Spain viscometer.Reagents used were of analytical or chemical purity (to perform analysis) and were used without further treatment.

RESULTS AND DISCUSSIONS

Uranium extraction from AUI samples, without ultrasound field in continuous phase lead to the results presented in Tables 1 and 2.

Table 1. The same volume of (aqueous-continuous phase) contacted in six steps with fresh organic solvent

Contacting step	I	II	III	IV	V	VI
Volume, cm^3	-	1.6	2	2.1	3	4.2
% total volume	-	0.8	1	1.05	1.5	2.1

From the experimental data presented in Table 1, when continuous phase is aqueous solution of uranyl nitrate which passing successively in each step and is contacted with fresh organic solvent, can be observed that phase III is formed in all studied situations, more least the first step and the volumes vary between 1.6 ÷ 4.2 cm^3.

This is explained by decreasing of the acidity of uranium aqueous solution that initially has the value of 3.07 N and after six steps the acidity value becomes 2.75 N.

In order to avoid the third phase formation, the acidity of the aqueous solution must be maintained in all the extraction steps, from values between 2.8 - 3.2 N.

This can be performed by acidity corrections in every step or by applying the ultrasound field to intensify the mass transfer process between phases and on the other hand to eliminate the third phase.

Table 2. The same volume of organic solvent (continuous phase) contacted in six steps with fresh AUI

Contacting step	I	II	III	IV	V	VI
Volume, cm^3	-	-	0.5	0.7	1	1.8
% total volume	-	-	0.25	0.35	0.5	0.9

From experimental data presented in Table 2, when organic solvent is represented by continue phase and is contacted with fresh solution in every step, it can be seen as phase III below starting with the third step, and the volumes varies between 0.75 ÷ 1.8 cm^3. In this case, using in every step fresh solution the acidity remain the same, so it is the one that influence the phase III formation. In this case we are talking about the content of silica, iron and Mo accompanying uranium through mass transfer by organic solvent.

That's why the solutions need to be filtered in order to have small concentration of silica, iron and molybdenum.

It should be take into consideration the organic components from sodium diuranate (DUNa) used for AUI solutions preparation, which also have a negative role in the third phase formation. Compared with the first case, the volume of phase III is smaller, but also due to the fact that it maintained the acidity within the accepted limits and content in silica, iron and molybdenum in initial solution was very low.

Extracting uranium from the impure uranyl nitrate (AUI), in the presence of the field of ultrasound, with continue phase represented by aqueous solution or organic solvent, led to the results presented in Tables 3 - 6.

Table 3. The same volume of AUI (aqueous-continuous phase), contacted in six steps with fresh organic solvent, the ultrasound amplitude is 100 %

Contacting step	I	II	III	IV	V	VI
Volume, cm^3	-	1	1	-	0.2	0.1
% total volume	-	0.5	0.25	0.1	0.1	0.1

From experimental data presented in Table 3, when the continuous phase is aqueous solution of uranyl nitrate which successively passed through every step and it is contacting with fresh organic solvent, it can be observed that the third phase is formed in all the studied situations, except the first and the fourth step and the volumes varied from 1÷ 0.1 cm^3.

Comparing with the same experiment performed in the absence of ultrasound field (Table 1), the volume of phase III is up to 42 timeless and the solution acidity is more than 2.7 N, is about 2.8 N as in requirements.

This can be explained by the mass transfer enhancement, and on the other hand the third phase is removed.

Table 4. The same volume of AUI (aqueous-continuous phase), contacted in six steps with fresh organic solvent, the ultrasound amplitude is 20 %

Contacting step	I	II	III	IV	V	VI
Volume, cm^3	-	2	2	2	2	2
% total volume	-	1	1	1	1	1

Comparing the experimental results from 3 and 4 Tables it is noted that the third phase volume is up to 20 times more and the acidity of aqueous solution decrease until 2.4 N. This can be the result of the low amplitude value which have low influence on the mass transfer and third phase removal, in the same experimental conditions. These results have the similar value like in the experiment without ultrasounds.

Table 5. The same volume of organic solvent (continuous phase), contacted in six steps with fresh AUI, the ultrasound amplitude is 100 %

Contacting step	I	II	III	IV	V	VI
Volume, cm^3	-	-	0.5	0.2	0.2	0.2
% total volume	-	-	0.25	0.1	0.1	0.1

Comparing the results from Table 5 and Table 2 is obviously that the third phase is up to 9 times less and the aqueous solution acidity remain in the asset limits due to fresh aqueous solution utilization.

Table 6. The same volume of organic solvent (continuous phase), contacted in six steps with fresh AUI, the ultrasound amplitude is 20 %

Contacting step	I	II	III	IV	V	VI
Volume, cm^3	-	1	1.5	1.5	1.5	1.5
% total volume	-	0.5	0.75	0.75	0.75	0.75

Experimental results from Table 6 showed that the volume increasing of the third phase is up to 3 times more comparing with results from Table 2 and up to 7.5 comparing with Table 5 results. This fact is due to the emulsion effect of the ultrasounds on the system, the ultrasound frequency at 20 % amplitude is not enough for breaking the emulsion.

The experiments showed that at ultrasound frequency of the third phase is not totally removed, but its volumes are up to 42 times less comparing with the volumes obtained without ultrasounds. Using higher frequency lead to the total removal of the third phase.

CONCLUSION

After the performing of these experiments it was proved the opportunity of ultrasound using (24 kHz, 400 W) for liquid – liquid extraction improving for uranium purification by partial removal of the third phase.

Thus, without ultrasounds the third phase is formed in all the studied situations (continuous phase is the uranium aqueous solution or organic solvent), except the first two steps and the volumes varied from 0.5 to 4.2 cm^3. This is explained by uranium aqueous solution acidity decreasing from 3.07 N to 2.75 N and after step 6 becomes 2.75 N and on the other hand by the silica, iron and molybdenum content whence accompanied uranium through the mass transfer to organic solvent and permitted the stable emulsions formation.

Applying of the ultrasounds field on the system lead to the phase III decreasing up to 42 times comparing with the first case (without ultrasounds). This fact is due to the increasing of the process kinetic, because of the transport increasing through diffusion due to acoustical vortex that induce micro disturbances on the liquid – liquid interface, improved the process velocity. Economical effects of ultrasounds using for uranium extraction consist in: the limitation of the useful element loss, the increasing of the separation rate and the increasing of the uranium purification degree. Using ultrasounds for improvement uranium extraction process may be a promising alternative comparing with traditional methods.

Acknowledgment

This work was funded by the Ministry of Research and Innovation - Romania, within the project code PN 19 39 01 01.

References

1. Edwards C.R., Oliver A.J., 2008, A Review of Current Methods and Technology, 12-20,
2. European Society of Sonochemistry, 2001, Introduction to Sonochemistry, 67-125,
3. Jansen M.L.,Taylor A., 2007, Solvent Extraction Mixer - Settlers and Contactors, Hydrometallurgy Forum Proceedings, 189-195,
4. Feung D., Aldrich C., 2000, Hydrometallurgy, 55 , 201,
5. Mason T.J., Peters D., 2002, Practical Sonochemistry, Power Ultrasound Uses and Applications, second ed., Horwood Publishing Limited, Chichester,
6. Suslick K.S., 1988, Ultrasound, Its Chemical, Physical and Biological Effects, VCH Publishers, New York,
7. Panturu E., Filip Gh., Radulescu R., 2009, Uranium extraction intensification in ultrasound field from uranium ore by acid method, patent no. RO 122642,
8. Panturu E., Jinescu G., Radulescu R., Filcenco-Olteanu A., Jinescu C., 2008, The chemical decontamination process intensification, using the ultrasounds, Revista de Chimie, 59, 9, 1036-1040**,**
9. Panturu E., Jinescu G., Radulescu R., Filcenco-Olteanu A., 2007, Uranium desorbtion from ionic resins in ultrasonic fields, Revista de Chimie, 58,6, 551-556,
10. Timothy J.M., Doust F., Paniwnyk L., Pollet B., 2006, Mass transfer measurements at small electrode-ultrasonic horn separations, 10th Meeting of the European Society of Sonochemistry, Hamburg,
11. Panturu E., Groza N., Filcenco A., Panturu R.I.,Jinescu G., 2009, uranium solvent extraction from nitric solution, The XIII th Balkan Mineral Processing Congress, 632**,**
12. Panturu E.,Groza N., Filcenco A.,.Panturu R.I., Jinescu C., 2009, uranium purification by liquid-liquid extraction using tributyl phosphate (tbp), CISA Slanic Moldova –Bacau, 209**,**
13. Xue Jiang W.,Chen J.,Xiangbo Y, Wang X, 2015, Heavy metal chemical extraction from industrial and municipal mixed sludge by ultrasound-assisted citric acid, J. Ind. Eng. Chem., online,
14. Gogate P., Mujumdar S., Pandit A.B., 2003, J.Chem.Technol.Biotechnol.,78, 685-693**,**
15. Chuncheng L, Fengchun X., Yang M., Tingting C., Haiying L., Zhiyuan H., Gaoqing Y., 2010 , Multiple heavy metals extraction and recovery from hazardous electroplating sludge waste via ultrasonically enhanced two-stage acid leaching, J. Hazard. Mater. 178, 823-833,
16. Kyeong W.C., Chul J.K., Yoo H.S., 2013, Highly efficient uranium leaching method using ultrasound, US Patent no.8, 470, 269 B2,
17. Chen D., Sharma S.K., Mudhoo A., 2011, Handbook of application of ultrasound: sonochemistry for sustainability, CRC Press,

18. Pesic B., 1996, Technical Report: Application of ultrasound in solvent extraction of nickel and gallium, Contract DE-AC07-941Dl3223, Interior Department's Bureau of Mines and US Department of Energy, Idaho, 78,
19. Li T., Qu X.Y., Zhang Q.A. , Wang Z.Z., 2012 ,Ultrasound-assisted extraction and profile characteristics of seed oil from Isatis Indigotica Fort, Ind. Crop. Prod,. 35, 98–104,
20. Bikram R., Bhattacharya S., Roy S.B, 2014, Ultrasonic density measurement of uranium loaded organic phase in solvent extraction process, Int. J. Nucl. Energy Sci. Techn.,8, 171-178.

XIII International Mineral Processing and Recycling Conference
Belgrade, Serbia, 8-10 May 2019

University of Belgrade, Technical Faculty in Bor
Vojske Jugoslavije 12, 19210 Bor, Serbia
Tel. +381 30 424 555 Fax +381 30 421 078

PRACTICAL ASPECTS OF OPERATING COPPER SOLVENT EXTRACTION PLANTS

Cyril Bourget #, Jean-Yves Dumousseau, Keith Cramer
Solvay Group, Cholet, France

ABSTRACT – Substantial information can be found in the literature for the use of solvent extraction technology to recover copper. Much of this data covers technical aspects, selection of the correct reagent and design improvements, but there is less information on how to operate and optimize a copper solvent extraction circuit. This paper offers a brief overview on key aspects to be considered when operating copper solvent extraction plants.

Key words: copper, solvent extraction, chemical and physical properties, crud, clay treatment

INTRODUCTION

Contaminants that may be present in the PLS and/or operating conditions that are inherent to the copper solvent extraction plant can have serious and deleterious effects on the performance of the solvent extraction plant and its productivity for copper cathode [1]. A variety of chemical and physical variables can impact performance. It is through knowledge and experience gained over the years that the copper solvent extraction plants have been able to overcome some of these operating issues.

POSSIBLE OPERATING ISSUES AND TROUBLESHOOTING

Presence of contaminants in the PLS

The presence of contaminants in the PLS can lead to poor performance of the solvent extraction plant. These contaminants can include for example [1-2]:

- Surfactants such as flocculants, degreasers, emulsifiers, oils from gear box failures and mining equipment maintenance. One common operating issue with flocculant overdosing is slow phase separation in the solvent extraction circuit.
- Under oxidizing conditions, nitrates can result in the nitration of the oxime

corresponding author: cyril.bourget@solvay.com

extractant making the copper / extractant complex very strong leading eventually to a loss in extractant capacity.
- Chlorides that can lead to copper cathode contamination, pitting of blanks, corrosion, chlorine evolution in tankhouse.
- Manganese ions which, under highly oxidizing conditions, can result in severe extractant degradation (see section below).
- Colloidal particles such as silica which can result in long phase break times (see section below).
- TSS (Total Suspended Solids) that can lead to crud formation and subsequent losses of PLS or organic (see section below).
- Biomass, massive insect infestation, which can result in the formation of humic acids and other organic species that can interfere with the phase disengagement properties of the system and/or transfer deleterious ions to the organic phase.

While it is difficult to change the leaching conditions for the PLS, it is conventional to treat the PLS by addition of flocculants and coagulants before solvent extraction to minimize the levels of contaminants such as suspended solids, silica, surfactants, organic materials, etc. Since overdosing of these flocculants and coagulants can also have adverse effects on the SX operation, controlling the right level of addition of these chemicals is very important.

While any oil contaminated feed can only be contained, removal of biomass humic acids can be achieved by elimination of treated sewage water from the process water supply. A diluent wash of the PLS has also proven beneficial to remove organic contaminants.

Potential of the electrolyte

While manganous ion (Mn^{2+}) can be transferred from the PLS to the loaded organic and finally to the copper electrolyte via aqueous entrainment in the organic (A/O entrainment), it has no direct effect on the operation of a copper solvent extraction plant. The issue arises when the electrolyte is under highly oxidizing conditions and there is sufficient iron present in the solution to allow the manganese to be further oxidized as shown by the redox reaction [3]:

$$Mn^{2+} + 5\ Fe^{3+} \rightarrow Mn^{7+} + 5\ Fe^{2+} \quad (1)$$

Under normal conditions, the potential of the electrolyte would be about 400-500 mV. High potential conditions of the electrolyte (~900 mV) will lead to severe quick oxidation and degradation of the solvent extraction reagent resulting in the following issues:
- Reduction in the kinetic properties of the extractant.
- Reduction in the extraction capacity of the extractant.
- Reduction in Cu/Fe selectivity in the organic phase resulting in a higher iron transfer into the electrolyte which can lead to lower current efficiency and therefore lower copper cathode productivity in the electrowinning plant.
- Precipitation of MnO_2 which can form cruds.

- Increased generation of chlorine gas due to the presence and reduction of chlorine ions in the electrolyte (from poor phase separation and higher A/O entrainment).
- Increased corrosion of the plant stainless steel components due to the presence of chlorine gas.

To maintain the potential of the electrolyte to normal conditions, it is necessary to drive the equilibrium from left to right in equation 1) so that most of the manganese remains in its divalent state. The stoichiometric Fe/Mn ratio is 5 for this reaction and since not all iron is divalent, a 10:1 Fe/Mn mass ratio has often been found to be required to prevent high oxidizing conditions of the electrolyte. If this ratio cannot be achieved during normal operation, physical addition of ferrous sulfate, sulfur dioxide gas or copper metal reduction tower to the electrolyte has been used as alternatives and preventative measures to lower the potential of the electrolyte. ACORGA OR-series formulations are also available which provide additional protection to oxidation [3].

The use of coalescers in settlers and/or organic tanks has also proven beneficial to improve the performance of the settler or the organic tank to remove further entrained aqueous. Other operations have included a wash stage between the extraction and strip sections to remove some of the subsequent high levels of entrained aqueous in the organic and minimize manganese levels in the electrolyte. In the wash stage, the loaded organic is mixed with clean water, acidified with electrolyte bleed. Acidification is necessary for good phase separation. This mixing allows for the entrained aqueous in the organic to be washed out and significantly diluted (typically by 10-1000 times). If any aqueous entrainment leaves the wash stage, the levels of impurities are such that they will have a negligible effect on the rest of the circuit [1].

Presence of colloidal silica in PLS

Colloidal silica has been recognized to often have negative effects on solvent extraction operations. Some of the operating issues that have been observed in these plants can include [1-2]:

- Formation of stable emulsions associated with very slow phase disengagement times resulting in high aqueous in organic entrainments.
- Crud formation due to silica precipitation in the strip section (i.e. inverse pH solubility for silica).
- Poor organic recovery in flotation columns due to slow coalescence of the entrained organic in the electrolyte.

While the copper industry is typically running the E1 extraction stage aqueous continuous to minimize aqueous entrainment into the loaded organic, the switch to an organic continuous mode has often lead to a partial or complete resolution to emulsions and slow phase break times when colloidal silica proved to be an operational issue on plant site. This is assuming though that provision of both organic and aqueous recycles has been given to allow the operation to switch to either continuity in any stage where there is an issue with silica, crud, precipitates, etc. Running organic continuous is also beneficial in terms of compacting the crud at the interface which is more easily removed using pumps. ACORGA CR60 PLS additive

has been effective at reducing the effects of high silica on phase separation and entrainment [4]. Desilication of the PLS has also been applied using polyethylene glycol (PEG) (also known as polyethylene oxide (PEO)).

Presence of TSS (Total Suspended Solids) in the PLS

Considerable amounts of suspended solids can be present in copper leach liquors, especially when the leach liquor is originating from an agitated leach operation. High solids levels in the PLS can generate large amounts of cruds that would require to be further treated to recover the entrapped aqueous and organic.

The more practical way to minimize crud formation is removal of the majority of the solids prior to entering the solvent extraction circuit. While such equipment is quite inexpensive and easy to use, thickeners and clarifiers are the conventional equipment that has been used for such purpose. Thickeners are used to concentrate solids while clarifiers are used to purify solids. Clarifiers are not always effective when dealing with large amounts of precipitants like gypsum for example because they contain small internal flow channels that can be easily blocked. Thickeners are more robust to deal with higher solid levels but they produce a dirtier solid content overflow than clarifier. Another downside of such equipment is the large footprint and heavy foundation required [2].

The presence of fine solid particles from the overflow of a thickener will be inevitable. Since these fine particles may still cause issues like for example, crud formation, increase in phase break times and impurity transfer from extract to strip, additional equipment like filtration filters may have to be implemented. Since the filter cloths and belts have to be changed regularly, the operating and maintenance costs of the filters are higher than the ones for thickeners and clarifiers. The type of solids present in the PLS is sometimes site specific and it is important to select the right combination of thickeners and filters to minimize the amount of solids in the PLS entering the solvent extraction circuit [2].

Operating the mixer/settler units

Some important parameters are to be considered when designing and then operating the mixers/settlers of a solvent extraction plant. These considering factors to minimize operating issues such as crud formation, entrainment and impurity transfer can include for example mixing, air intake and materials of construction [2].

Mixer Speed - Controlled and gentle mixing will minimize 1) entrainment of fine and small aqueous droplets formed and attached to the air bubbles 2) the tendency for crud generation and air entrainment (under aqueous continuity). Tip speed must remain, however, high enough to maintain 1) a cascade of flowing solution over the weir 2) high stage efficiency inside the mixer [1]. Gentle mixing also allows the solvent extraction circuit to increase its capability for handling higher levels of solids and generate at the same time less cruds. Covering the solvent extraction units also minimizes the air intake or entrapment into the system [2].

Materials of Construction - The use of specific construction materials or liners (e.g. FRP, HDPE or Teflon) can minimize solids build-up in the settler and pipe walls. The use of stainless steel can be problematic in a solvent extraction plant because scaling can be severe on these surfaces [2].

Mixer Continuity for Entrainment Control - Under normal conditions, the mixer continuity does not affect the overall chemistry of the extraction process. While this does not always apply on a plant site, the rule of thumb is that organic continuity will minimize organic entrainment in aqueous and vice versa aqueous continuity will minimize aqueous entrainment in organic. The deciding factor to select either continuity in a mixer is often related to the impact of the entrainment of the (aqueous or organic) stream that exits the settler and flow rate of organic and aqueous to be processed in the stage [1].

Phase Depth/Settler Velocity - The depth of the organic in the settler can be altered by adjustment of the settler aqueous overflow weir. A deep organic inventory results in 1) Increased risk of organic entrainment in aqueous 2) Slower coalescence 3) Better ability to control crud 4) Increased organic inventory. One important aspect of settler depth is to optimize the control of entrained solution by increasing the depth of the opposite phase. For example, if the aqueous in organic entrainment is significant in E1, then, the organic depth in E1 could be increased to allow longer settler retention times with reduction of the aqueous in organic entrainment. Similarly, increasing the aqueous depth in E2 would decrease the organic in aqueous entrainment in solution leaving E2 [1].

Crud Treatment - Crud generation in a copper solvent extraction plant can be minimized but is unavoidable. While some plants in North and South America have used cyclones to remove organic and crud from the aqueous with various degrees of success, the use of a three-phase centrifuge for treating the crud and returning the associated organic and aqueous solutions to the plant has become more widely spread in copper solvent extraction operations. Maintenance of the centrifuge can prove to be troublesome and organic recovery was rarely more than 80% [5]. An alternative approach is to use an air agitated pachuca where crud was added to clean plant organic while maintaining organic continuity. When the mixing was stopped, the phase separation was rapid and clean with the solids forming a compact layer in the aqueous phase while the organic trapped in the crud was released to the clean organic. Organic recovery was claimed to be over 90%. Some companies use plate and frame filters or sparkle filters for crud management while others have their own developed crud management [5].

Phase disengagement time characteristics

Degradation of the oxime extractant is inevitable but its rate of degradation will be a function of factors such as temperature, acid concentration in the electrolyte, presence/absence of permanganate and nitrate ions, etc.

When facing slow phase disengagement times in the solvent extraction circuit, one option is to reduce temporarily the flows of the aqueous and/or organic solutions in the plant so that the total residence time in the settler is increased to allow the phases to separate before they exit the settler. In less extreme cases, it may only necessitate the volume of the organic or aqueous in the settler to be changed by utilizing the settler aqueous weir. In some instances, a change from organic to aqueous continuous generally leads to improved phase disengagement times. It is worth noting that recording fast phase break time is not always a true indicator of the good health of the organic. For example, the presence of solids in the organic may significantly decrease the phase disengagement time when operating organic

continuous as well as causing a flip of the continuity to aqueous mode [1].

In some cases, when the phase disengagement times are in excess of 5 minutes, remedial action may have to be taken to redirect some of the organic to be treated to restore the phase break time. It has become standard practice in the copper industry to clay treat the organic which has extended phase break times, has been contaminated by surfactant or has been recovered from the raffinate pond. The acid activated bentonite clay acts to remove contaminants and restores the phase disengagement times back to similar levels shown by fresh organic. It is important to make sure the aqueous is removed from the organic before treatment with the activated clay, typically at a dosage rate of 0.5%-5% depending on contamination and equipment capability to clean the clay from the organic after treatment. Filter press is a common approach to remove the fine clay particles before returning the organic to the SX plant inventory [1].

CONCLUSION

While operating issues are often plant specific, the symptoms (slow phase separation, emulsion, crud formation, etc.) are, most of the time, quickly and easily detected allowing the plants to either treat the symptom at the source or deal with the issue at the origin (e.g. presence of contaminants in the PLS, etc.). Making plant process modifications to resolve one issue may sometimes lead to the formation of a new issue inside the plant. It is therefore important to have a very good understanding of the entire manufacturing process and the connections that there may be between the different operating units (e.g. leach, PLS treatment, solvent extraction, electrowinning, etc.).

References

1. Spence, J.R., Soderstrom, M.D. (1999) Practical Aspects for Copper Solvent Extraction from Acidic Leach Liquors. Copper Leaching, Solvent Extraction and Electrowinning Technology (Edited by Jergensen II, G.V.), Published by the Society for Mining, Metallurgy and Exploration, Inc., Colorado, United States, 239-257.
2. Laitala, H., Ekman, E., Karcas, G. (2008) Some Practical Aspects for Impurity and Crud Control in Solvent-Extraction Processes. Internal Solvent Extraction Conference (ISEC), Vol.1, Tucson, USA, 473-478.
3. Bednarski, T., Soderstrom, M., Tinkler, O. (2010) Reagent Development: New Acorga® Formulations with Enhanced Stability. In: ALTA 2010 Nickel/Cobalt/Copper Conference, Australia, 19 pages.
4. MBao, B., Tinkler, O. (2019) Acorga® CR60 Crud Mitigation Reagent – Commercial Trials in North America and Africa. To be presented at ALTA 2019 Nickel/Cobalt/Copper Conference, Australia.
5. Mukutumo, S.A., Schwarz, N., Chisakuto, G., Mbao, B., Feather, A. (2007) A Case Study on the Operation of a Flottweg Tricanter® Centrifuge for Solvent-Extraction Crud Treatment at Bwana Mkubwa, Ndola, Zambia. In: Fourth Southern African Conference on Base Metals, Swakopmund, Namibia, 393-403.

XIII International Mineral Processing and Recycling Conference
Belgrade, Serbia, 8-10 May 2019

University of Belgrade, Technical Faculty in Bor
Vojske Jugoslavije 12, 19210 Bor, Serbia
Tel. +381 30 424 555 Fax +381 30 421 078

RARE-EARTH METALS EXTRACTION OUT OF SULPHATE SOLUTION BY SORPTION

Madali Naimanbayev #, Nina Lochova, Zhazira Baltabekova, Yerzhan Kuldeyev
Satbayev University, Institute of Metallurgy and Ore Benefication, Almaty, Kazakhstan

ABSTRACT – A review of the sorption extraction of rare-earth metals (REM) from solutions of extraction phosphoric acid (ESP). The results of studies on the sorption of trivalent ions of cerium, lanthanum and iron on sulfocathionite KU-2-8 and macroporous weakly acidic cation exchange Cybber CRX 300 are presented. It is established that the cation exchange Cybber CRX 300 in exchange capacity for lanthanum and cerium and kinetic properties is somewhat inferior to sulfate cationite KU-2-8 when sorbed from acidic solutions, but can be used to concentrate and separate the REM from iron. The review presents data on trials on a pilot scale of the technology of extracting rare-earth metals from dihydrate extraction phosphoric acid (45 % P_2O_5). The results of tests of sorbents TP260, Purolite S957 (Monophos), sulfocathionite PPC 160 and sorbent AA03 at sorption: from sulphate solution after decomposition of phosphate raw materials are presented; from a solution of hydrolysis sulfuric acid after precipitation of titanium dioxide; from sulfuric acid solutions after sorption of uranium. The distribution of rare-earth metals during their sorption by KU-2 sulphocathionite was studied from solutions of phosphoric acid: dihydrate ESP partially evaporated 43.69 wt. % P_2O_5, dihydrate ESP, unpaired 26.09 wt. % P_2O_5; dihydrate ESP, evaporated 52.54 wt. % P_2O_5. The distribution coefficients of lanthanides are obtained.

Key words: rare earth metals, extraction phosphoric acid, sorption, concentration, ion exchanger

INTRODUCTION

The rare-earth metals (REM) are widely used in various branches of technology owning to their one and only properties. The alloys are capable to function in extreme conditions are of great use while manufacturing aircraft materials. Microadditives of such rare-earth metals as erbium, praseodymium and neodymium are inserted into Ni_3Al based alloy composition to improve performance parameters [1]. REMs are applied to produce contemporary military equipment and weapons [2]. Energy efficient constructions of constant magnet timing motor containing REM are worked out for the electric engines [3, 4].

The growth of rare-earth metals consumption rate contributes its production from man-made raw materials and recyclables. Production costs are contingent on

corresponding author: madali_2011@inbox.ru

rare-earth metals content in the feed raw materials - the lower content the higher expenses. At this 1 kg of REM amount was between 17 to 81 US dollars considering January-April, 2014 prices. It is determined by the most expensive and in short supply heavy REMs content.

As of [6] February 2018, the cost of light rare-earth metals was 5,8 to 86 US dollars per kg, heavy metals – 265 to 640 at the China markets.

The development of technology process to extract rare-earth metals out of raw materials with its low content is aimed to minimize costs by operating stages reducing and appliance of environment friendly favorable methods.

SORPTION EXTRACTION

An acid method is more frequently used in the rare-earth metals extraction technologies from man-made formations and ores for the initial processing which provides an ultimate extraction of REM into the solution [7-9].

A large quantity of ferrum (III) and calcium availability when sorption extraction of REM out of industrial acid solutions both at sorption and desorption stages is of serious obstacle as the most interfering mixtures.

Ferric ions are established to [10, 11] the most effectively compete with the REM ions, and calcium ions block the ionite grains surface when sorption from the ferrum and calcium solutions by sulfocationites.

Rare-earth metals sorption out of nitrogen, hydrochloric and phosphorus acids was studied by KU-2 sulfocationite. 60 minutes ionite and solution interaction determined to lead to the balance. Increasing the temperature is determined to kindly influence to the REM ions sorption process with wide ions range, e.g. lanthanum with 1.22 Å range, and influence the ions sorption with the small ions range insignificantly, e.g. ytterbium with 1.00 Å range [12].

The developed technologies of rare-earth metals sorption extraction are worth mentioning to mainly base on the sulfocationites use, similar to KU-2 [13-18]. A high sorting to the Fe^{3+} ions is the main lack of these ionites. A full KU-2 exchange capacity is very high and makes 1.6 mmol/g [19].

The comparative studies of trivalent cerium, lanthanum and ferrum ions on KU-2-8 sulfocationite and macroporous weak acid cation exchanger based on styrene copolymer and divinyl benzene with chelated reactive groups by aminomethyl phosphonic acid - Cybber CRX 300 were carried out in order to find efficient ionite for the REM selective sorption. Cybber CRX 300 cation exchanger is established to mildly back off to KU-2-8 sulfocationite when sorption from acid solutions as to lanthanum and cerium exchange capacity and kinetic behavior. However, the low sorption capacity of iron (III) at the Cybber CRX 300 cation exchanger allows its use for concentration and separation of rare-earth metals from iron with good sorption capacity of rare-earth metals.

The products obtained after apatite and phosphorite sulfuric processing are the prospective raw material to associated extraction of rare-earth metals: semi-hydrate and dehydrate phosphor-gypsum, wet-process phosphoric acid, residue after obtaining concentrated phosphorus acid [20, 21]. 30 % and more of REMs contained in the initial concentrate are centered in the wet-process phosphoric acid [22].

The REM extraction technology through the sulfuric processing of Khibini apatite concentrate is created and tested in the experimental and industrial sense [23].

Dihydrate wet-process phosphoric acid (P_2O_5 45 %) produced by PhosAgro-Cherepovets Public Corporation (RF) was chosen as the raw material source of REMs. The rare-earth metals content in the wet-process phosphoric acid is about 0.1 wt. %. Operating process consists of dihydrate wet-process phosphoric acid supply, sorption separation of REMs on the ion exchange resin, their subsequent desorption, precipitation as insoluble hydroxides, dissolution by preparing of a nitrate solution of REMs, purification and separation extraction at Nd / Sm line, REMs sedimentation as carbonates, sediments filtration and getting concentrates.

The new sorbents development possessing peculiar sorption parameters regarding rare-earth metals and typical mixtures is relevant [24]. The all studied sorbents have functional groups representing oxygen ligands, including phosphate and amine-based groups. Sorption studies were conducted: out of solutions after phosphate raw materials dissolution by sulfuric acid; hydrolyzed sulfuric acid after dioxide titanium sedimentation; sulfurous mother liquids after uranium sorption.

The Lewatit TP260 amino-phosphonic sorbent and the AA03 prototype were used during sulfate solutions sorption after phosphate raw materials decomposition. The TP260 sorbent is established to have an advantage in the sorption capacity for all groups of rare-earth metals. AA03 sorbent has an affinity to heavy rare earth metals.

The following sorbents were tested in case of REMs sorption out of hydrolyzed sulfuric acid after titanium dioxide sedimentation: TP260, Purolite S957 (Monophos), PPC 160 sulfocationite and AA03 sorbent. PPC 160 sulfocationite was determined to primary sorb light group elements of REMs. AA03 sorbent displays expressed sorting to the heavy REMs. Purolite S957 ionite has a lower sorting to REMs relatively to iron.

During sorption extraction of scandium from a solution of sulfuric acid hydrolysis, formed after precipitation of titanium dioxide in the sulfate method of titanium production, sorbents TP260 and AA03 were tested. AA03 sorbent in this system showed the worst results.

TP260 and AA03 ionites were applied to extract scandium out of uranium sorption mother liquor at the production process using downhole in-situ leaching. Scandium partition coefficients for the TP260 and AA03 ionites were 47 and 210 accordingly when sorption out of solutions.

REM distribution was studied at the process of sorption by KU-2 sulfocationite from phosphoric acid solution of dehydrate wet-process phosphoric acid, P_2O_5 partially concentrated to 43.69 wt. %, Public Corporation "Balakovo Mineral Fertilizers"; dihydrate wet-process phosphoric acid, P_2O_5 not concentrated to 26.09 wt. % of Ammophos Public Corporation; dihydrate wet-process phosphoric acid, P_2O_5 concentrated to 52.54 wt. % of Ammophos Public Corporation [12, 25].

Partition coefficient of specific lanthanides is determined to reduce from lanthanum to gadolinium then increases to the maximum at thulium and decreases to lutecium for the concentrated wet-process phosphoric acids.

CONCLUSION

At present a great number of researches to develop technological schemes of the rare-earth metals sorption extraction out of wet-process phosphorous acid are implemented, some of which are brought to experimental and industrial testing stage

as the scientific and technical materials analysis provides. However, a widespread implementation of ion exchange technology in the hydrometallurgy is prevented by complexity of solution content containing REMs. A sorbent selection is an important stage for the problem solving in practice as its modification influences the REMs sorption efficiency. That is why the up-to-date scientific researchers are aimed to get new sorbents in order to create competitive technology of REMs sorption extraction out of engineering and production solutions.

References

1. Zhou, P. J., Yu, J. J., Sun, X. F., Guan, H. R., He, X. M., Hu, Z. Q. (2012)Influence of Y on stress rupture property of a Ni-based superalloy. Materials Science and Engineering: A, 551, 236-240,
2. The Rare-earth magazine. (2016) http:/rare-earth.ru/ru/pub/20170320/03031.html. (application date: 09. 04. 2018),
3. Aries, A., Carlos, O., Jordi, Z., Espina, J., Pou, J. (2013)Hybrid sensorless permanentmagnet synchronous machine four quadrant drive based on direct matrix converter. Electrical Power and Energy Systems, 45 (1), 78-86,
4. Leonov, S. V., Zhiganov, A. N., Kerbel, B. M., Fedorov, D. F., Makaseev, Y. N., Kremlev, I. A. (2016) Analysis of the Influence of Permanent Magnet Geometry on the Energy Efficiency of Electromechanical. Systems Russian Physics Journal, 59 (2), 308-313,
5. Petrov, I. M. (2014) Projects overview of REM deposits development around the world. Contemporary issues of REM obtaining and using: International scientific and practical conference, Russia, 14-16,
6. World market prices: metals and raw materials. (2018) http://www.infogeo.ru/metalls/worldprice/?act=rzm (application date: 04.09.2018),
7. Bochevskaya, Y. G., Abisheva, Z. S., Karshigina, Z. B., Turdaliyeva, B. D., Kvyatkovskaya, M. N. (2016) Rare-earth elements performance during nitrate leaching of slag of phosphate production. Complex use of mineral raw materials, 1, 9-16,
8. Gupta, C. K., Krishnamurthy, N. (2005) Extractive metallurgy of Rare Earths. CRC Press, Boca Raton, Florida,
9. Lokhova, N. G., Naymanbayev, M .A., Baltabekova, Zh. A., Sultangaziyeva, A. N. (2010)$LaPO_4$ - H_3PO_4 - H_2O system research. Complex use of mineral raw materials, 6, 40-46,
10. Naymanbayev, M. A., Lokhova, N. G., Baltabekova, Zh. A., Ultarakova, A. A., Dzhurkanov, Zh. K. (2014) REM extraction study out of titanium-magnesium production wastes. Science and new technologies, 2, 31-34,
11. Ehrlich, G. V., Lisichkin, G. V. (2017) Sorption in the chemistry of rare-earth elements. Russian Journal of General Chemistry, 87 (6), 1001-1027,
12. Papkova, M. V., Kon'kova, T. V., Mikhailichenko, A. I., Tumanov, V. V., Saikina, O. Yu. (2015) Lanthanum, yttrium, ytterbium sorption extraction out of mineral acids solutions by KU-2 sulfocationite. Sorption and chromatographic processes, 15 (4), 515-522,
13. Abdulvaliyev, R. A., Ni, L. P., Raizman, V. L. (1992) Getting scandium from bauxite raw materials, Alma-Ata: Gylym,

14. Korshunov, B. G., Reznik, A. M., Semenov, S. N. (1987) Scandium. Metallurgiya, Moscow, USSR,
15. Tatarnikov, A. V., Sakharova, L. I., Taltykin, S. Y. (2012) Sorption processes for the extraction of rare earth elements in the complex processing of organogenic-phosphate ores by heap leaching method. Rare-earth elements: geology, chemistry, production and use: International conf. mater, Moscow, Russia, 147,
16. Lokshin, E. P., Tareyeva, O. A. (2012) Method of extracting rare earth elements from wet-process phosphoric acid. Pat 2465207 of the Russian Federation,
17. Smirnov, D. I., Molchanova, T. V., Vodolazov, L. I. (2002) Sorption extraction of rare-earth elements, yttrium and aluminum from red slags. Non-ferrous metals, 8, 64-69,
18. Rychkov, V. N., Kirillov, Y. V. (2011) Rare-earth metals ions sorption by ionites of various classes from uranium leaching solutions. Prospects of mining, production and use of rare-earth metals: Mater. The 1st All-Russian Scientific and Practical Conference, Moscow, Russia, 26-27,
19. Ashirov, A. (1969) Physical and chemical properties of carboxyl cation exchangers. Science, 112,
20. Lokhova, N. G., Naymanbayev, M. A., Baltabekova, Zh. A. (2015) Rrare-earth elements sorption extraction out of technological and production solutions. Vestnik KazNAEN, 1, 22-25,
21. Mikhailichenko, A. I., Papkova, M. V., Kon'kova, T. V., Tumanov, V. V. (2014) REE sorption extraction from phosphoric acid solutions. Pressing topics of obtaining and using rare-earth metals and metals: international scientific and practical conf. mater, Moscow, Russia, 51-55,
22. Wang, L., Long, Z., Huang, X., Yu, Y., Cui, D., Zhang, G. (2010) Recovery of rare earths from wet-process phosphoric acid. Hydrometallurgy, 101, 41-47,
23. Sibilev, A. S., Shestkov, S. V., Kozyrev, A. B., Nechayev, A. V., Polyakov, E. G., Falchik, Yu. A., Shibnev, A. V. (2015) The process of REE extracting from wet-process phosphoric acid at PhosAgro-Cherepovets Public Corporation. Chemical technology, 16 (4), 201-205,
24. Tatarnikov, A. V., Mikhaylenko, M. A. (2017) The sorbents selection for the scandium extraction and rare earth elements from the complex composition solutions // Pressing topics of obtaining and using rare-earth metals and metals: international scientific and practical conference, Moscow, Russia, 188-192,
25. Papkova, M. V., Mikhailichenko, A.I., Kon'kova, T.V. (2016) Sorption extraction of rare-earth metals and other elements from phosphoric acid solutions. Sorption and chromatographic processes, 16 (2), 163-172.

XIII International Mineral Processing and Recycling Conference
Belgrade, Serbia, 8-10 May 2019

University of Belgrade, Technical Faculty in Bor
Vojske Jugoslavije 12, 19210 Bor, Serbia
Tel. +381 30 424 555 Fax +381 30 421 078

FUNDAMENTALS OF NEODYMIUM SORPTION IN PALYGORSKITE

Luana Caroline da Silveira Nascimento [1], Mauricio Leonardo Torem [1, #], Ellen Cristine Giese [2], Luiz Carlos Bertolino [3]
[1]Pontifical Catholic University of Rio de Janeiro, Brazil
[2]Center of mineral Technology, Brazil
[3]Federal University of Rio de Janeiro, Brazil

ABSTRACT – Preliminary studies of adsorption of Neodymium (III) supported by palygorskite clay in a batch system was investigated to explore the ability of palygorskite for the removal of Nd (III) under different experimental conditions. The palygorskite it's a phyllosilicate 2:1 consisting of a double layer composed of silicon of oxygen tetrahedrons connected by an octahedral layer with magnesium ions. Guadalupes's palygorskite (Piauí/Brazil) run of mine (ROM) was prepared and characterized by X-ray diffraction (XRD), X-ray fluorescence (XRF), Zeta Potencial, Scanning Electron Microscopy (SEM), Fourier Transform Infrared Spectroscopy (FTIR). The mineral clay is composed by palygorskite, kaolinite, quartz and diaspore and has 53.8, 14.2, 5.7, 6.8 % of SiO_2, Al_2O_3, MgO and Fe_2O_3 respectively. The results of preliminary studies of adsorption showed that 92.62 % were adsorbed by palygorskite using 2g at a pH of 5.0 at 30 °C for a clay particle size - 20µm. The sorption capacity were evaluated by Inductively Coupled Plasma Optical Emission Spectrometry (ICP-OES) to quantify the Nd (III) uptake capability. The results showed that palygorskite is a potential clay mineral for the removal of cations from solutions.

Key words: neodymium, palygorskite, adsorption.

INTRODUCTION

In recente decades the demand for rare earth elements (REE) has grown considerably and have found wide application in functional materials, industry, medicine and agriculture. Furthermore, are utilizated extensively in many high-tech fields, such as, electronics, magnets optics and laser device due to their unique photo electro magnetic properties [1]. The necessity of the high purity of these species requires the selective separation, task difficult due to the chemical structure and similar physical properties of these elements.

Neodymium (III) as an important member of the rare earth family, plays an important role in the electronic instrument and laser equipment manufacture industries is used in alloys, electronic components and optical filters [2]. Due to the scarcity of studies to capture Nd (III), were reported the search for an innovative technique to acquire this effective removal is of extreme relevance.

corresponding author: torem@puc.brm

A number of technologies for the removal or recovery of metal ions from aqueous diluted solutions have been developed over the years. Adsorption is one of these methods that usually used for the concentration and recovery of metal ions due to high stage efficiency and easy operation.

Recently, searches related to unconventional low cost sorbents such as clay minerals and biosorbents that over time have gained space as potential adsorbents. Palygorskite is a lamellar clay mineral with a hydrous fibrous morphology, whose unit cell is $(Mg,Al)_5Si_8O_{20}(OH)_2(OH_2)_4 \cdot 4H_2O$. Mineralogically, it belongs to the group of phyllosilicates 2:1 with an aluminum octahedral layer, which can undergo isomorphic substitutions Mg^{2+} or Fe^{2+} between two layers of silicon tetrahedrons, exchanged for Al^{3+} or Fe^{3+} [3]. The structure porous with canals efficient to exchange ions and the elongated nature of the particles and their fine particle size, give a high specific surface area at this clay mineral and sorption capacity of different species.

The work reported here deals with an investigation into the use of palygorskite from Guadalupe in Piauí,Brazil as adsorbent for their potential application to removal Nd (III) in aqueous solutions.

MATERIALS AND METHODS

Preparation of mineral sample and characterization

Palygorskite sample was collected from Guadalupe deposits in Piauí/Brazil. In Center of Mineral Technology (CETEM) was accomplished the ore dressing. Size classification was performed with deionized water and sieve with opening 20 μm, the sample below 20 μm is the purest sample, and was used for the preliminary sorption tests. The sample were characterized by X-ray diffraction and X-ray fluorescence (XRF and XRD), Scanning Electron Microscopy (SEM), Surface Charge Measurements (Zeta Potential), Fourier Transform Infrared Spectroscopy (FTIR).

X-Ray Diffraction (XRD)

The XRD analysis was obtained by the powder method in the equipment Bruker D4 Endeavor, Co Kα radiation (35 kV/40 mA), goniometer velocity of 0.02º (2θ) per step with 1 s per step and collected from 5 to 80º (2θ). The qualitative interpretation of the spectra was made by comparison with standards contained in PDF02 database (ICDD 2006) on Bruker AXS software DiffracPlus.

X-Ray Fluorescence (XRF)

Samples were pressed at automatic squeezer VANEOX (20 mm of mould, P 20 ton and t 30 s), using as binder the boric acid (H3BO3) 1:0.2 of proportion (0.6 g of boric acid and 3 g of dried sample at 100 °C). The contents were verified and expressed in percentage of their oxide forms, by semi quantitative analysis (Standardless Method mode) in X-ray fluorescence spectrometer (Panalytical WDS), AXIOS MAX model.

Scanning Electron Microscopy (SEM)

The samples were metalized with gold, using the equipment BAC-TEC-SCD005 Sputter Coater.

Surface Charge Measurements (Zeta Potential)

Zeta potential measurements were performed for palygorskite in the Malvern Zetasizer Nano micro electrophoresis. The clay mineral suspensions were prepared using NaCl as the indifferent electrolyte at a concentration of 0.01 and 0.001 mol/L. and concentrations of 0.1 g/L of palygorskite, the desired pH value for the measurement was adjusted with dilute solutions (0.01 mol/L) of HCl and NaOH.

Fourier Transform Infrared Spectroscopy (FTIR)

FTIR spectra were obtained on the FTIR Scientific Nicolet 6700 FT-IR spectrophotometer and followed the KBr pastille method. The pastilles were obtained from a sample mixture with KBR. The sample and KBr ratio was 1/100 (wt/ wt). The obtained pastille was analyzed in the FTIR equipment. The spectra were obtained at a resolution of 4 cm^{-1} using 120 scans.

Experimental procedure

Stock solutions (5,000 mg/L) of Nd (III) were prepared for the purpose of being diluted for the preliminary sorption tests. Known amounts of palygorskite were placed in different stoppered Erlenmeyer glass flasks of 125 ml capacity containing 50 ml of metal ion solution of known concentration and pH. All experiments were carried out at pH 5.0 (except when the effect of pH was studied). The shaking time was fixed at 60 min of the batch experiments to ensure that adsorption equilibrium was reached. Preliminary sorption tests were performed by Inductively Coupled Plasma Optical Emission Spectrometry (ICP-OES) to quantify the Nd (III) uptake capability.

RESULTS AND DISCUSSION

The results of the chemical analysis by X-ray fluorescence (XRF) are presented in Table 1 which were determined by semiquantitative analysis. XRF analysis was performed to determine the levels of the main oxides that compound the sample, so it was possible to obtain the chemical composition of samples. With this result it is inferred that the sample is composed mainly of silicon oxide and magnesium oxide.

Table 1. Chemical composition of mineral determined by XRF

Components (%)										
Mineral	**Na_2O**	**MgO**	**Al_2O_3**	**SiO_2**	**K_2O**	**CaO**	**TiO_2**	**MnO**	**Fe_2O_3**	**LOI**
Palygorskite	0.14	5.7	14.2	53.8	2.2	0.18	0.52	0.14	6.8	16.3

LOI: Loss on ignition at 1000 °C.

XRD spectrum shown in Fig. 1A reveals the sample is mainly composed of clay mineral palygorskite, kaolinite, quartz and diaspore. Figure 1B shows the fibrous structure of palygorskite characterized by SEM, made it possible to identify the fibrous structure of the material, evidencing its enrichment due to a purification of the same.

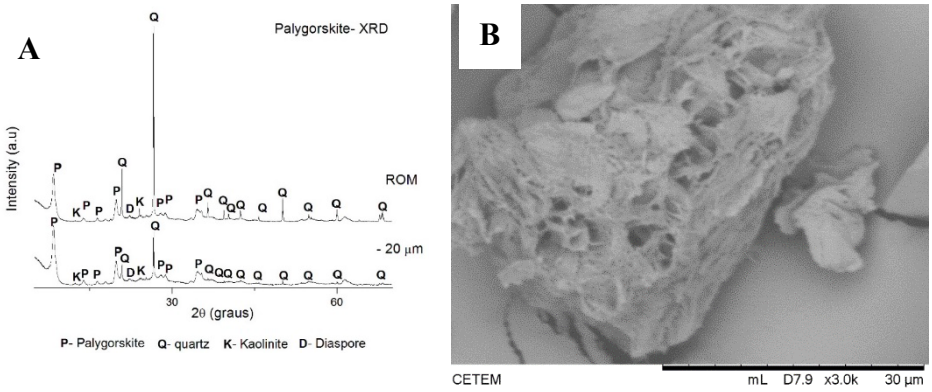

Figure 1. Characteristics of palygorskite. **A)** X-ray diffraction, **B)** SEM

The zeta potential values indicated that the surface charges of palygorskite sample is negative in throughout the pH range (3-11), this indicates that it can be an excellent adsorber of ctions (Figure 2). The negative surface charge on the surface of the mineral is also reported in other studies. [4, 5]

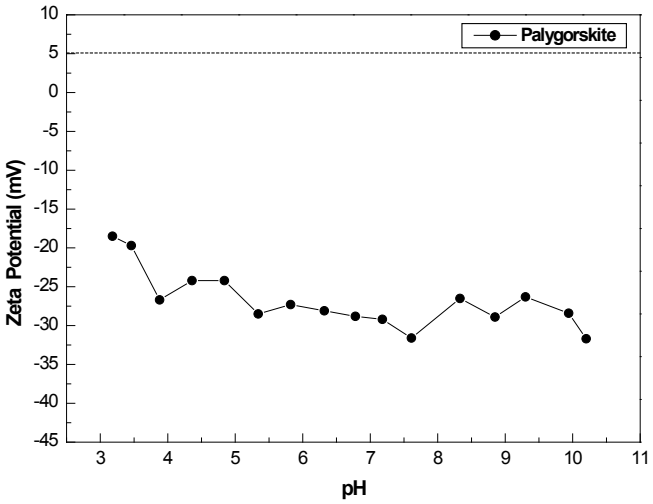

Figure 2. Profile of palygorskite Zeta potential of indifferent electrolyte

FTIR spectra in figure 3 shows that the structure of palygorskite, there are several bonds that can give absorption effects in IR region. It is observed that at 3,616 could be attributed to the stretching OH group, this seems to be characteristic of the palygorskite. While 3,543.95 and 3,404.65 cm^{-1} band occurs that can be attributed to the coordination and zeolitic waters [6].The band at 1,649.95 cm^{-1} can be attributed to angular deformation of water [7]. The peak at 514,15 and 473,58 cm^{-1} corresponding the characteristic bands of Mg-OH and Si-O-Mg bands.

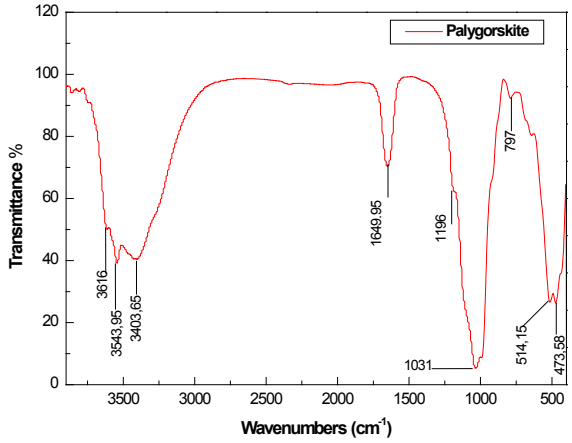

Figure 3. FTIR spectra of palygorskite

The characterization of palygorskite makes it possible to infer that it has high sorption capacity. In this way, preliminary sorption tests were carried out in batch to define preliminary conditions for later thermodynamic and kinetic evaluation of the sorption capacity of this mineral clay.

Table 2. Results of sorption tests

Effect of amount of adsorbent		**Effect of the temperature**		**Effect of the pH on adsorption of Nd (III) onto palygorskite**	
Mass of palygorskite (g)	**% Removal**	**Temperature ˚C**	**% Removal**	**pH**	**% Removal**
0.25	10.18	40˚C	91.05	1	68.58
0.5	17.18	30˚C	91.45	2	59.80
1	47.84	20˚C	91.03	3	86.51
1.5	69.59			4	91.86
2.0	79.53			5	92.62

Increasing the mass of palygorskite, the percentage of removal of Nd (III) also increases. This is an expected result because as the amount of adsorbent increases, the number of adsorbent sites increases, therefore the cations will have more sites to be adsorbed. The results of the effect of amount of palygorskite are in agreement with those found by other authors. Similar finds for Pb (II) using bentonite as an adsorbent were reported [8, 9]. The study of the effect of the temperature shows us that this variable does not influence considerably for small changes of temperature with respect to the adsorption. The pH is an important variable which controls the adsorption of the metal at the palygorskite interfaces. The influence of pH on the adsorption of Nd (III) onto palygorskite was investigated in the pH range of 1-5. It can be observed from the results that the adsorption of Nd (III) increase with an increase in pH. This is in agreement with work by other authors [10, 11].

According to these results the optimum conditions for evaluating the thermodynamic and Kinect conditions are using 2 g of palygorskite mass at a

temperature of 30 ˚C, at pH 5.

CONCLUSION

The following conclusions can be drawn for this investigation: the palygorskite presents high sorption capacity, attested by the characterization through XRD, XRF, SEM and zeta potential. In batch mode adsorption studies, removal of metal ion increased with the increase of amount of adsorbent and pH. The next tests will be performed by varying the metal ion concentration to thermodynamically evaluate the behavior of the neodymium sorption in palygorskite.

Acknowledgements:

The authors are grateful to the PUC-Rio (Pontifical Catholic University of Rio de Janeiro), and COAM/CETEM for analysis and lab infrastructure, CNPq (Conselho Nacional de Desenvolvimento Científico e Tecnológico), for financial support.

References

1. Eliseeva, S. V., Bünzli, J. C. G. (2011) Rare earths: jewels for functional materials of the future. New Journal of Chemistry, 35 (6), 1165-1176,
2. Horikawa, T., Itoh, M., Suzuki, S., Machida, K. (2004) Magnetic properties of the Nd-Fe-B sintered magnet powders recovered by Yb metal vapor sorption. Journal of magnetism and magnetic materials, 271 (2-3), 369-380,
3. Post, J. L., Crawford, S. (2007) Varied forms of palygorskite and sepiolite from different geologic systems. Applied Clay Science, 36 (4), 232-244,
4. Middea, A., Fernandes, T. L., Neumann, R., da FM Gomes, O., Spinelli, L. S. (2013) Evaluation of Fe (III) adsorption onto palygorskite surfaces. Applied Surface Science, 282, 253-258,
5. Gan, F., Zhou, J., Wang, H., Du, C., Chen, X. (2009) Removal of phosphate from aqueous solution by thermally treated natural palygorskite. Water Research, 43 (11), 2907-2915,
6. Suárez, M., Garcia-Romero, E. (2006) FTIR spectroscopic study of palygorskite: influence of the composition of the octahedral sheet. Applied Clay Science, 31 (1-2), 154-163,
7. Frini-Srasra, N., Srasra, E. (2010) Acid treatment of south Tunisian palygorskite: removal of Cd (II) from aqueous and phosphoric acid solutions. Desalination, 250 (1), 26-34,
8. Naseem, R., Tahir, S. S. (2001) Removal of Pb (II) from aqueous/acidic solutions by using bentonite as an adsorbent. Water Research, 35 (16), 3982-3986,
9. Orumwense, F. F. (1996) Removal of lead from water by adsorption on a kaolinitic clay. Journal of Chemical Technology & Biotechnology: International Research in Process, Environmental AND Clean Technology, 65 (4), 363-369,
10. Esmaili, A., Nasseri, S., Mahvi, A. H., Atash-Dehghan, R. (2003, September) Adsorption of lead and zinc ions from aqueous solutions by volcanic ash soil (VAS). 8th Conference on Environment Science and Technology, Lemnos Island, Greece, B193-B199.

XIII International Mineral Processing and Recycling Conference
Belgrade, Serbia, 8-10 May 2019

University of Belgrade, Technical Faculty in Bor
Vojske Jugoslavije 12, 19210 Bor, Serbia
Tel. +381 30 424 555 Fax +381 30 421 078

STUDY OF THE EFFECT OF NEW GENERATION DEWATERING AID CHEMICAL TO IMPROVISED DEWATERING KINETICS AND REDUCTION IN COAL CAKE MOISTURE OF FINES COAL

Farookh Sekh [1, #], Vineet Kumar [2]
[1]Tata Steel Limited, India
[2]Nalco, An Ecolab Company, India

ABSTRACT – At West Bokaro, Tata Steel, clean coal flotation is dewatered to get coal as cake with moisture up to 25 % through HRT and HVBF. The reduction in moisture keeping recovery high is very important for quality, cost & water resource conservation. A chemical, Dewatering Aid (DVS4W009) developed by Nalco was tried in lab scale in NRD lab of Tata Steel Ltd. to understand effect on dewatering, water kinetics & chemistry and stability of magnetite suspension. The results were quite encouraging in moisture reduction with no adverse impact on water chemistry and stability of magnetite suspension.

Key words: Coal, Dewatering Aid, Dewatering Kinetics, Moisture, Tata Steel, Nalco

INTRODUCTION

Tata Steel, West Bokaro Devision always encouraged improvement initiatives from its technology partners. With depletion of high grade coal seams and subsequent processing of low grade coal having mixed flotation characteristics dewatering performance is the real challenge in fine circuit. The existing washery practices two processes i.e Dense media cyclones (13-0.5 mm) and Froth flotation (-0.5 mm). Concentrate from flotation process was initially dewatered in Vacuum belt filters.

The fine coal carries 23-27 % moisture after dewatering. Higher moisture results in additional cost in transportation of product and additional fuel consumption for coke making. For effective dewatering, moisture in final product needs to be minimized and loss of clean coal through effluents needs to be minimized.

A joint initiative was initiated between Tata Steel and Nalco to explore the dewatering Aid developmental project to reduce the cake moisture and increase the throughput specifically for West Bokaro coal. In our quest for continuous improvement, Nalco India team connected with its counterparts overseas to access

corresponding author: farookh@tatasteel.com

global expertise and to come out with a new generation dewatering Aid product.

BACKGROUND

TSL-West Bokaro, Washery-3, flotation concentrate contains approximately 85% water which must dewater in HVBF to get the final fines concentrate. This dewatering process involves the slurry thickening up to 25 to 30 % solids in high rate thickener and fed to Horizontal vacuum belt filter. In HVBF the solid particles are separated from liquid by forcing the slurry to pass through a suitable filtering medium with the help of vacuum. This allows only the liquid to pass through, leaving the solid particles to form a "cake". Normally cake contains around 22-28 % of moisture with restricted throughput. Moisture contents increases significantly with increase in throughput. At present to meet the product quality the plant is running under restricted throughput.

For effective dewatering and to Increase the throughput and capacity utilization in the existing plant, TSL-West Bokaro management is planning to go for another HVBF, which requires a huge capital investment and recurring costs associated with it is also significant. The availability of any alternative processes that can reduce the moisture and increase the capacity of fine particles without any capital investment will be of great help and beneficial for Tata Steel because of the following anticipated benefits which are as follows-

1. Reduction of moisture will lead to transportation cost savings and to avoid BTU penalty.
2. Improvement in dewatering kinetics will increase the throughput and thereby production which will help to ensure to run the plant at optimum capacity and reduce the specific recurring cost (Maintenance cost, Energy Cost, Salary & Wages etc.) associated with it.
3. Enhanced process efficiency while decreasing environmental impact. Saving of water, energy and natural resources.

DEWATERING THEORY AND PRINCIPLES

The difficulty in removing water from the surface of fine particles may be attributed to the fact that water molecules are held strongly to the surface *via* hydrogen bonding. One can break the bonds and remove the water by subjecting the wet particles to intense heat, high-pressure filters, or high-G centrifuges. However, the use of such brute forces entails high energy costs, maintenance problems, and environmental concerns. A better solution would be to destabilize the surface water by appropriate surface chemical treatment, so that it can be more readily removed by the weaker forces imparted by vacuum, low-pressure filters.

The state of the water adhering to a surface may be best represented by the hydrophobicity (water-hating property). The stronger the hydrophobicity, the weaker the bonds between the water and the surface would become. Therefore, the key to finding appropriate chemical means to destabilize surface water is to increase the hydrophobicity of the particles to be dewatered. A more traditional measure of surface hydrophobicity is water contact angle in the sessile drop technique, a water droplet is placed on a flat surface of the solid of interest, and the angle at the three-

phase contact is measured through the water phase. In general, contact angle increases with increasing hydrophobicity of the surface.

Compressible Cake- When a cake forms the rate of water passing through the cake (Q) is determined by Darcy's Equation:

$$Q = \frac{K\Delta PA}{\mu L} \quad (1)$$

K is the Permeability of the Cake (Particle size etc.)
ΔP is the Pressure drop across the cake
A is the Area of filtration
μ is the dynamic viscosity of the water
L is the cake thickness (need a minimum thickness)

Non- Compressible Cake- A filter cake is filled with capillaries that allow water movement between mineral particles. The capillaries are of various radii and the radii are determined by the mineral particle size. The Laplace Equation gives the capillary pressure required to make water flow **(P).**

$$P = \frac{2\gamma cos\theta}{R} \quad (2)$$

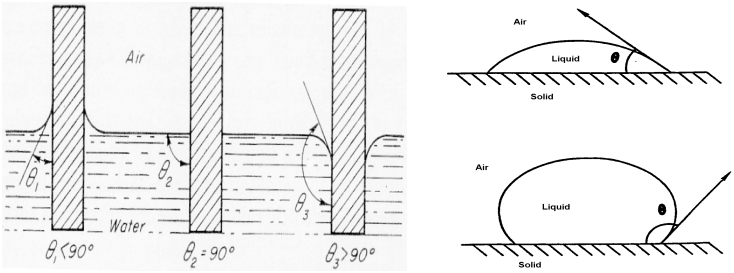

Figure 1.

P pressure necessary to drain the capillary
γ The air-liquid surface tension
θ The contact angle between liquid & wall of the capillary
r is the radius of the capillary

DEWATERING AID DESCRIPTION AND ANTICIPATED BENEFITS

DEWATERING AID-DVS4W009: **The dewatering aid Filtra DVS4WOO9** is designed to increase the hydrophobicity (or contact angle θ) of coal and, hence, decrease the capillary pressure of the water trapped in a filter cake. In the presence of this reagent, the contact angles of the coal samples increased up to 90o where the surface of the particle cannot be wetted by water molecules. It is suggested that the increase in contact angle could be responsible for the reduction of the capillary pressure in a filter cake and should help reduce the cake moisture. The dewatering aids also decreased the surface tension of water and increased cake porosity (or

capillary diameter), both of which could contribute to the lower cake moisture and increased dewatering kinetics.

Mechanism of FilterMax DVS4W009-

New generation Dewatering Aid is developed to reduce the moisture and increase the capacity. It affects the filter cake structure to enhance the porosity and permeability and thereby the drainage rate.

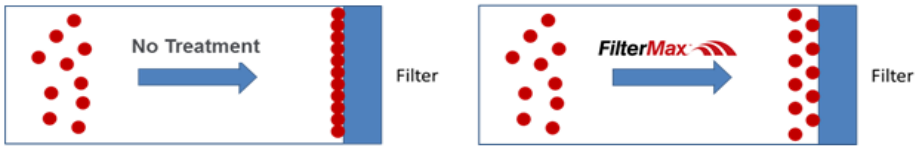

Figure 2.

The schematic diagram of its working principle is shown herewith where treated and untreated slurry profile is clearly mentioned.

Dewatering aid Features-

i) Decreases the surface tension of water.
ii) Increases the contact angles of the particles to be dewatered
iii) Causing the particles to coagulate, all at the same time.

Dewatering benefits-

I. Increases the dewatering of coal fines kinetics by 25-30 %.
II. Reduces the Cake moisture by 20-25%.
III. Helps in lowering the unit cost of dewatering

DEWATERING LAB TEST

The laboratory scale dewatering tests were conducted using a ~60mm diameter Buchner funnel filter. The Buchner funnel was used in the bulk of the tests and was fitted with a filter cloth. The Buchner funnel was mounted on a vacuum flask, which in turn was connected to a larger vacuum flask to protect the pump itself and stabilize the vacuum pressure.

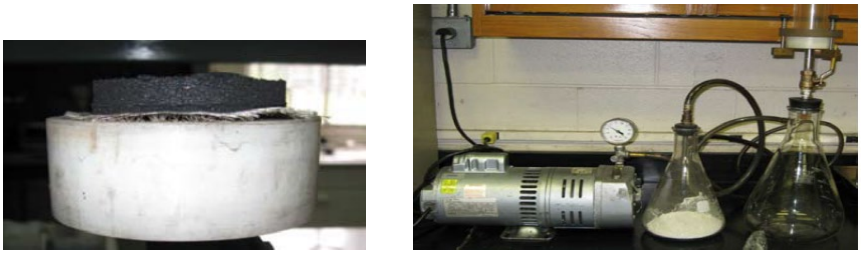

Figure 3.

Before initiating the filtration, a known volume of coal slurry was transferred to a container, to which a known amount of a dewatering aid was added by means of a

microliter syringe. The coal slurry was then subjected to mixing with plunger to ensure proper chemical dispersion and adsorption. After conditioning, the slurry sample was poured into the funnel before opening the vacuum valve. Filtration started when vacuum was applied to the slurry. After cake formation, vacuum pressure was maintained for a sufficient length of time to remove water trapped in the capillaries. This period is known as the dry cycle time. The volume added to the Buchner funnel determined the cake thickness. After the pump was stopped, the cake sample was removed, weighed and dried. The filter cake was weighed again after thorough drying and moisture content was determined from the weight differential. In each experiment, the cake thickness and filtration time when top surface was dried were recorded along with vacuum setting and actual vacuum pressure.

The following conditions were kept constant during the tests:
Vacuum …….. 660 mm Hg
Volume of slurry……1000 ml
Reagent conditioning time ……..1 minute

DEWATERING TESTS RESULTS

A series of preliminary dewatering tests were conducted at Nalco Laboratory in West Bokaro. Significant moisture reductions and increased dewatering kinetics were achieved in the presence of dewatering aids. The results were obtained under certain operating variables and test parameters.

Table 1. First dewatering test conducted with Seam VII

Reagent Dosage	Moisture %	Drying Time (Min)	Cake Thickness (mm)
0	20.8	6:58	24
50	16.9	3:38	24
100	15.8	4:01	26
150	16.6	4:46	26

Table 2. Second dewatering test conducted with Seam VII

Reagent Dosage	Moisture %	Filtration Time (Min)	Cake Thickness (mm)
0	28.7	4:45	21
50	23.4	2:20	22
100	21.8	2:10	22
150	23.1	1:50	22

Table 3. Confirmatory dewatering test conducted with Seam VII

Reagent Dosage	Moisture %	Filtration Time (Min)	Cake Thickness (mm)
0	22.7	5:58	25
50	18.5	4:05	26
100	16.45	4:05	26
150	19.7	3:40	27

Table 4. Dewatering test conducted with Seam V

Reagent Dosage	%Moisture	Filtration Time (Min)	Cake Thickness (mm)
0	28.8	6:20	25
50	21.2	4:48	27
100	18.8	4:19	27
150	22.6	3:46	28

Table 5. Water analysis report of filtrate

Water Analysis of Filtrate					
Sample	**TSS**	**Ph**	**Conductivity**	**TDS**	**TH**
Without Chemical	20	7.2	2048	588	82
50 gpt Dosage	13	7.2	1840	489	84
100 gpt Dosage	10	7.2	1985	524	80

Inferences from Laboratory test

- Laboratory-scale dewatering test results showed that dewatering aid DVS4U009 can significantly reduce moisture,
- The total cake moisture reduction at 25-28 mm cake thickness was: 16-20 % for Seam VII coal, 20-22 % for seam V coal.
- It was also determined that the use of the novel dewatering aids could reduce the cake formation time by a significant degree due to the increased kinetics of dewatering. which in turn may results in increased throughput
- It was observed that water quality of the filtrate does not change with the addition of the dewatering aid.
- Lab Results showed the optimum dosage will be in the range of 50-70 gpt where the Moisture reduction as well as Filtration time both is favorable.

PLANT SCALE TRIAL

Based on lab scale trial results a comprehensive small-scale plant trial was planned and conducted for in which pre-trial and post-trial data was compared.

TRIAL PHILOSPHY AND KPI

- The check the efficacy of the chemical pre-trial data for each seam will be generated and will be compared with trial data with Chemical.
- During the Trial all variable parameters like Coal Seam, Plant Throughput, Flotation Reagents dosage, Flotation Cell Parameters and other parameters except the Dewatering aid dosing will be kept same.
- Dosing of the Chemical will be done at Underflow pipeline of High rate Thickener through injection. Chemical will be diluted at 3%.
- The Data will be captured in a template which will be used for analysis purpose.

- The Main KPI of the trial will be to reduce the fine clean coal moisture by absolute 3 % at optimized dosage.

DOSAGE AND FEEDING:

The Dewater Aid will be dose at 5 % concentration to the Vacuum Belt filter feed (Froth after thickening at HRT). A thorough mixing of the chemical with the coal slurry is critical to get the best result. Therefore, the dewatering aid will be dose at the suction of the HRT U/f Pump which pumps coal slurry to VBF. The dosage rate of 80 gpt for the above chemicals is to be used initially purely based on preliminary lab scale evaluation results. However, the exact consumption has to be assessed in actual plant trial situation. The dosages would then be optimized in conjunction with the product moisture and filtration rate.

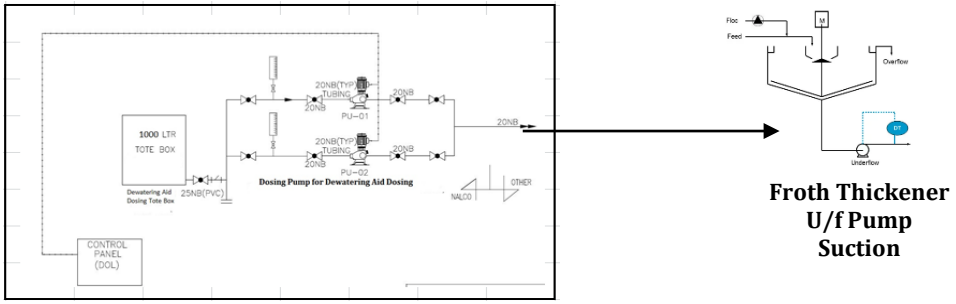

Figure 4. Schematic Diagram of Chemical Dosing System and Dosing Point

TRIAL OBSERVATION AND RESULTS

Plant scale trial was done with different seams and different plant conditions and results are summarized below. It can also visually observe the moisture reduction in VBF cake with chemical dosing. It takes approximately 12-15 minutes for the effect of the chemical in VBF cake.

Table 6.

S.No	Coal Seam	Moisture Without Chemical (%)	Moisture With Chemical (%)	Difference
1	VII	24.36	22.76	1.60
2	V	26.87	24.20	2.67
3	V	28.41	22.53	5.88

MOISTURE PROFILE

On 15th and 21st Feburary'19 we did every hour sampling and analysed the moisture to check the chemical efficacy. We plotted the moisture profile and from the graph it is quite evident with the use of chemical there is significant reduction in moisture. As soon as we stopped the chemical the moisture also gets started increasing.

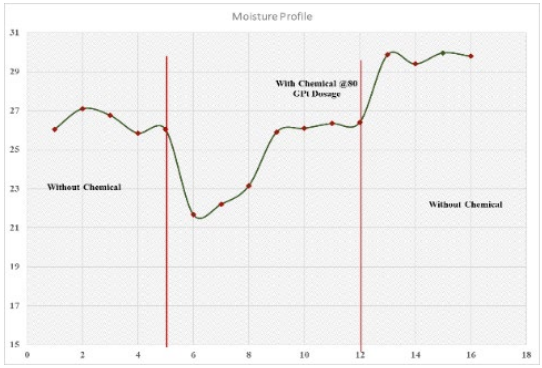

Figure 5. Moisture Profile recorded on 21st Febuary '19

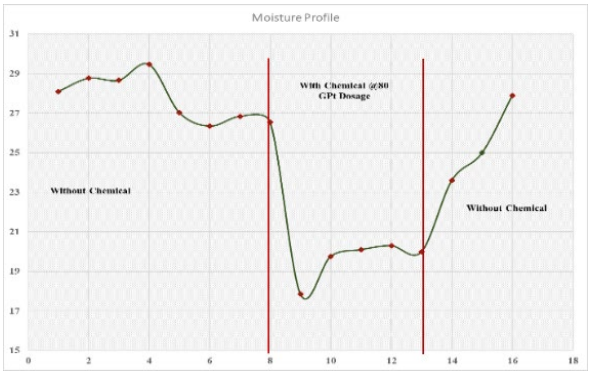

Figure 6. Moisture Profile recorded on 15th Febuary'19

CONCLUSION

Statististical Analysis of the data generated from the trial showed that DVS4W009 could reduce average 18-20 % of the moisture content of the filter cake when compared with exiting process (without chemical) and can also improve the throughput of the vacuum belt filter without any effect in downstream process. To access the commercial feasibility and the potential of offering some savings on dewatering cost the longer trial is still going on.

References

1. Roe- Hoan "Development of Dewatering Aids for Minerals and Coal Fines",
2. Gray, V.R., "The Dewatering of Fine Coal," J. Inst. Fuel, Vol. 31, p.96-108, 1958
3. Hogg, R., Flocculation and dewatering. International Journal of Mineral
4. Processing, 2000. 58(1-4): p. 223-236.
5. 15. Tao, D., J.G. Groppo, and B.K. Parekh, Enhanced ultrafine coal dewatering using
6. Flocculation filtration processes. Minerals Engineering, 2000. 13(2): p. 163-171.

XIII International Mineral Processing and Recycling Conference
Belgrade, Serbia, 8-10 May 2019

University of Belgrade, Technical Faculty in Bor
Vojske Jugoslavije 12, 19210 Bor, Serbia
Tel. +381 30 424 555 Fax +381 30 421 078

MATERIAL HOLD-UP AND RESIDENCE TIME IN FLUIDIZED BED OF INERT PARTICLES SLURRY DRYER

Mihal Đuriš [1,#], Tatjana Kaluđerović Radoičić [2], Zorana Arsenijević [1]
[1]Institute of Chemistry, Technology and Metallurgy, Belgrade, Serbia
[2]University of Belgrade, Faculty of Technology and Metallurgy, Belgrade, Serbia

ABSTRACT - Fluid bed dryer with inert particles was used for drying of slurries of Zineb fungicide, copper hydroxide, calcium carbonate and pure water as feed material. Experiments were performed in a cylindrical column 215 mm in diameter and 1200 mm in height with glass spheres as inert particles. The material hold-up and residence time were determined.

Key words: drying, fluidized bed, suspensions, hold-up, residence time

INTRODUCTION

Trends in drying technology are associated with higher energy efficiency, enhanced drying rates and development of more compact dryers, better control for enhanced quality and optimal capacity, developments of multi-processing units (for example: a filter-dryer), etc. [1]. Over 500 dryer types have been cited in technical literature although only about 50 types are commonly found in practice. The dryer selection is a complex process, which is not entirely scientific but also involves considerable empiricism. Each type of dryer has specific characteristics, which makes it suitable or unsuitable for specific application [2]. Drying of slurries on inert particles is a relatively novel technology to produce powdery materials. Classical fluid bed, spouted bed, spout-fluid bed, jet spouted bed and vibrated fluid bed are the most popular dryers used for drying on inert particles [3-7]. Independently of the hydrodynamic configuration of the dryer, the principle behind this technology is based on drying of a thin layer of the slurry that coats the surface of inert particles. With respect to main efficiency criteria, i.e. specific water evaporation rate, specific heat consumption and specific air consumption, a fluidized bed dryer with inert particles represents a very attractive alternative to other drying technologies when the slurry is not pumpable. A high drying efficiency results from the large contact area and from the large temperature difference between the inlet and outlet air. The feed material is directly supplied into the column where the inert particles are

corresponding author: mdjuris@tmf.bg.ac.rs

fluidized by hot air. The drying mechanism depends on the feed slurry density and consistency, as illustrated in Fig.1. A typical dry particle is about two orders of magnitude smaller than the inert particles in the bed. Due to intensive mixing of inert particles during fluidization the bed temperature is approximately uniform.

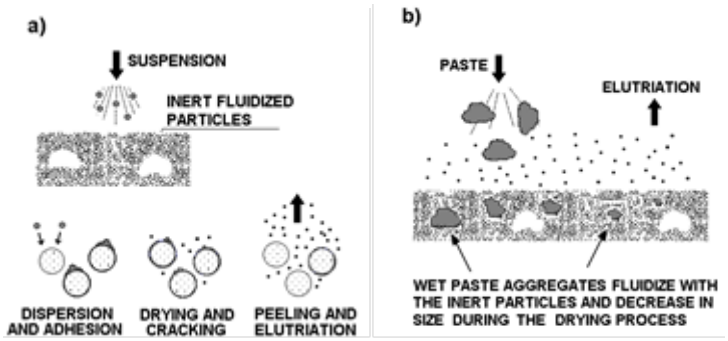

Figure 1. The drying mechanism: a) feed - suspension, b) feed - paste

EXPERIMENTAL

Experimental system is shown in Fig. 2. Drying chamber is a cylindrical column D_c = 215 mm and 300 mm high, connected by conical section with the 320 mm i.d. and 300 mm high upper cylinder. Effective column height above distributor is 900 mm. Inert particles were glass spheres with mean diameter d_p = 1.94 mm and density 2460 kg/m^3. Inert bed mass was 6.79 kg, static bed height was 122 mm and total inert particle area was 8.6 m^2. Minimum fluidization velocity was determined at ambient air temperature using standard procedure, U_{mF} = 0.96 m/s. Superficial air velocity at ambient temperature was in range 1.48-2.30 m/s (fluidization number was 1.55 to 3.77). Inlet air temperature T_{gi} was between 153 and 358°C, whereas the outlet air temperature T_{ge} was in the range 65-125°C. Water content in the feed materials varied from 0.40 to 0.75 kg_{H2O}/kg_{sus}. Feed material is directly pumped into bed axis by peristaltic pump for slurries and feed outlet is located 100 mm above the distributor. Screw feeder was used when feed material was in the form of a dense paste and bed was equipped with a mechanical mixer (≈30 min^{-1}) to prevent particle agglomeration. The product is separated in cyclone and bag filter. Before leaving the system, exhaust air is passed through packed bed scrubber. Temperature controller TIC1 maintains T_{gi} at desired level. Temperature controller TIC2 located 0.7 m above distributor and connected with feeding device keeps constant T_{ge}. Temperature controller TIC3, placed 0.7 m above the distributor, is set at 20°C above T_{ge}. Its role is to prevent overheating of the bed, in the case of feeding device failure, by introducing pure water into the system. During experiments, the inlet air temperature and outlet air temperature were continuously recorded using PC and data acquisition system. In the first series the feed was water, while in the second series the feed suspensions were Zineb fungicide [$(CH_2\text{-}NH\text{-}CS_2)_2$-Zn], copper hydroxide and calcium carbonate. In our fluidized bed dryer we dried successfully a number of other materials such as Ziram, Propineb, Mangozeb, copper oxy-chloride, copper oxy-sulphate, Bordeaux mixture, calcium sulphate, cobalt carbonate,

electrolytic copper, sodium chloride, and organo-bentonite.

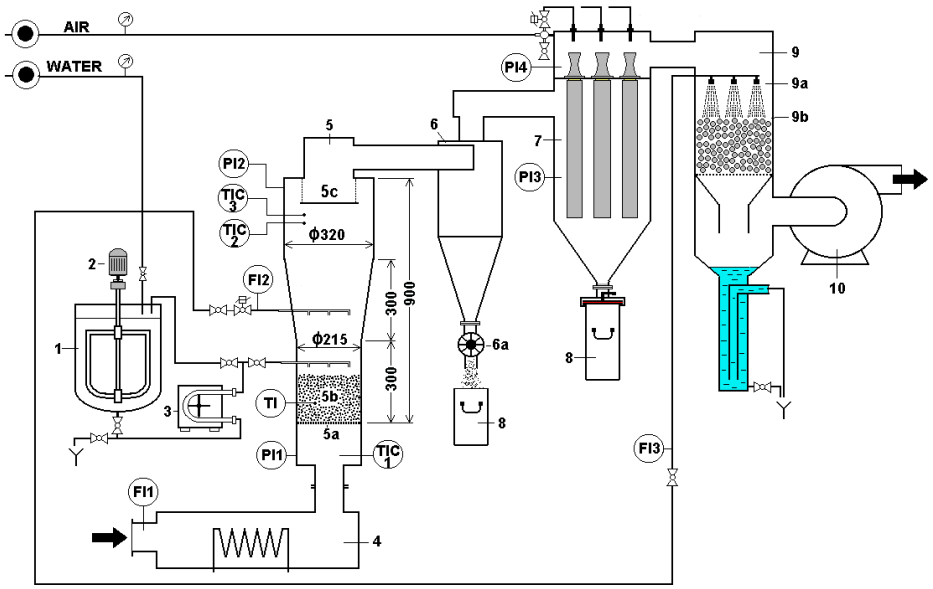

Figure 2. Schematic diagram of the drying system: (1 - Tank, 2 - Agitator, 3 - Pump, 4 - Air heater, 5 - Fluidization column, 5a - Distributor, 5b - Inert particles, 5c - Deflector, 6 - Cyclone, 6a - Rotary valve, 7 - Bag filter, 8 - Product containers, 9 - Scrubber, 9a - Nozzle, 9b - Packing, 10 - Blower, FI - Flowrate indicator, PI - Pressure indicator, TI - Movable temperature probe, TIC - Temperature indication and control

RESULTS AND DISCUSSION

Drying tests were performed continuously. When temperature above bed reached the set value TIC2, the feeding process begun. In the further process outlet air temperature was constant since TIC2 controls the feeding device. Stationary state was reached after several minutes since inlet air temperature had reached the set value TIC1. Feeding device operates in on/off mode and was adjusted on such way that active period (feeding "on") was about 75%. The system was very stable, i.e. during the operation the outlet air temperature variations ΔT_{ge} were less than 2-5^{o}C, regardless of the feeding device used. Each suspension was characterized by the water content, density and particle size distribution, while each dried sample was characterized by the residual water content and particle size analysis.

It can be seen from Fig. 3 that specific water evaporation rate can be very high, up to 1000 kg_{H2O}/m^2h. The evaporation rate is directly proportional to the temperature difference T_{gi}-T_{ge}. Specific heat consumption decreases with an increase in $\Delta T = T_{gi}$-T_{ge}, i.e. with an increase in the driving force. At the same time the use of high inlet air temperatures lead to the decrease in specific heat consumption (Fig. 4.). Fig. 5. gives the specific air consumption as a function of temperature difference. It can be seen that the data follows the same line.

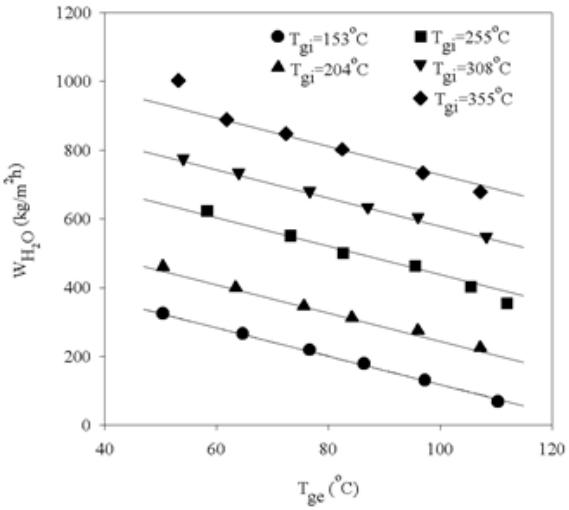

Figure 3. Specific water evaporation rate at U0 = 1.8 m/s (feed: water)

In order to obtain maximum process efficiency for fixed T_{gi}, T_{ge} should be as low as possible with respect to the product quality and quality of fluidization. Usually, the residual moisture content of the product powder is the main criterion. Generally the powder moisture content decreases with an increase in outlet air temperature. For Zineb fungicide collision and friction between inert fluidized particles produce some grinding effect since mean diameter of the product 12.9 μm is less than mean diameter of the inlet slurry 17.3 μm. For $Cu(OH)_2$ and $CaCO_3$ slurries, however, the particle size distribution of the dried product was approximately the same as particle size distribution for inlet slurry. Consequently, it can be expected that for majority of applications an additional grinding step of dried product can be avoided.

Hold-up of the dried material on inert particles was measured by extracting a sample of the bed material. The sample was weighed, and inert particles were cleaned and weighed again. Table 1 provides representative results. For inert particles d_p = 1.94 mm, the hold-up varied between 0.50 and 3.68% with respect to the inert bed mass. For fixed T_{gi} hold-up decreased with an increase in T_{ge}. This is in accordance with the finding that the product powder moisture content also decreases with increase in outlet air temperature. Probably, the moisture content of material surrounding the inert particle also decreases with increase in T_{ge}. It is reasonable to expect that adhesivity and hold-up are closely related to moisture content of material surrounding inert particle [8]. Assuming that the bulk density of material surrounding inert particles is an arythmetic from the mean slurry and dry powder densities, a hypothetical thickness of the material film covering an inert particle can be estimated. The calculations shows that the film thickness varies from 8 to 50 μm.

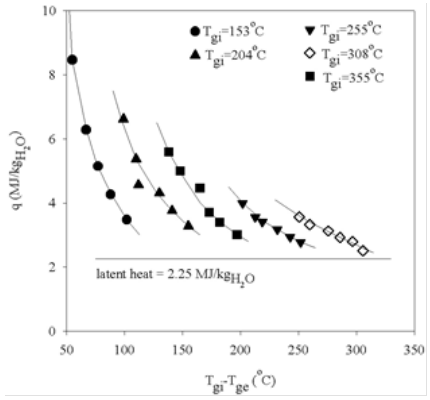

Figure 4. Specific heat consumption (feed: water)

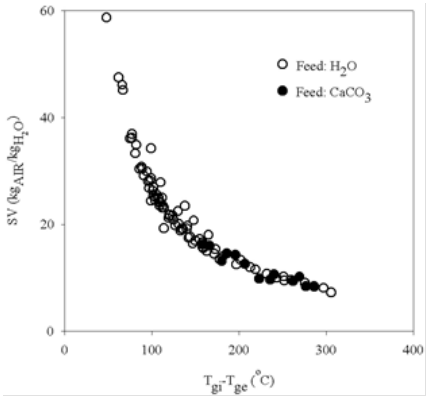

Figure 5. Specific air consumption

Table 1. Dried material hold-up in the inert bed

d_p, mm	Feed	U_0, m/s	G_{SUS}, kg/h	T_{gi}, °C	T_{ge}, °C	h, %
1.94	$CaCO_3$, X=0.70	1.65	29.3	308	101	1.70
1.94	Zineb, X=0.67	1.70	35.2	311	87	3.68
1.94	Zineb, X=0.67	1.70	34.6	311	97	1.48
1.94	Zineb, X=0.67	1.70	29.5	311	108	1.14
1.94	Zineb, X=0.67	1.70	24.1	250	86	2.15
1.94	Zineb, X=0.67	1.70	21.5	250	96	1.18
1.94	Zineb, X=0.67	1.70	17.7	250	106	0.91
1.94	Zineb, X=0.67	1.70	13.4	198	85	1.27
1.94	Zineb, X=0.67	1.70	10.6	198	92	0.56
1.94	Zineb, X=0.67	1.70	8.6	198	106	0.50

It is important to note that the content of an active matter for the Zineb fungicide was at least 3% higher than the corresponding content obtained by drying in an ordinary tunnel dryer. The drying time in a tunnel dryer is 48 h at 80°C, while the nominal residence time of the drying particles in a fluidized bed is very short. In order to estimate the nominal residence time of the dried material in the bed an experiment with step change in the feed color was conducted. For this purpose, during drying of Zineb slurry (white powder) the pump inlet tube was rapidly inserted into $Cu(OH)_2$ slurry (blue powder). The samples bellow the cyclone were collected every 2 seconds using a specially designed box and analyzed using the Sigma Scan software [10]. The percent of the $Cu(OH)_2$ powder in the collected sample was determined by measuring color intensity. As can be seen, from Fig.6. system behaves as perfect mixed reactor with respect to the dried particles. The nominal residence time of dried particles in the bed in this run is about 8 seconds. The very short drying time permits treatment of thermo-sensitive materials. Since the dried material hold-up varied with the outlet air temperature and the slurry feed rate (Table 1) it is reasonable to expect that the same factors affect the residence time distribution of dried particles, but generally the residence time is in the order of seconds. This results compare well with the data for swirling bed of inert particles

[2], where residence times from 30 to 85 seconds were reported in drying of animal blood and egg products and with Bachmann et al. analysis of residence time in horizontal fluidized beds [9].

Theoretically, the water evaporation capacity can be determined from the conventional rate equation if the particle surface temperature can be properly determined:

$$W_{H_2O} = k_Y A_p \Delta Y_{lm} \tag{1}$$

For the design and simulation purposes the much simpler way in modeling is to use overall heat balance:

$$G_v c_v (T_{gi} - T_{ge}) = G_{dm} C_{dm} (T_{ge} - T_0) + G_{H_2O}\left[c_w (T_{ge} - T_0) + \lambda_v\right] + Q_g \tag{2}$$

Since $G_{sus} = G_{dm} + G_{H2O}$ and if the water content is defined as $X = G_{H2O}/G_{sus}$, it follows that $G_{dm} = (1\text{-}X)G_{sus} = [(1\text{-}X)/X]G_{H2O}$. Using these relations and neglecting heat losses, Eq. (2) becomes:

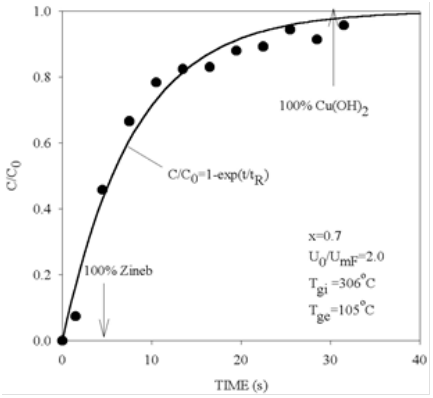

Figure 6. System response on step change in feed color

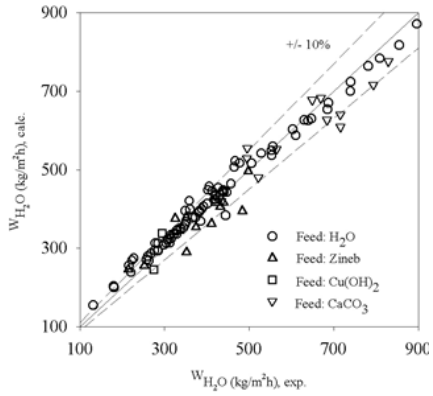

Figure 7. Comparison of the experimental and calculated values of the specific water evaporation rate

$$W_{H_2O} = \frac{G_{H_2O}}{A_c} = \frac{1}{A_c} \cdot \frac{G_v c_v (T_{gi} - T_{ge})}{[(1-X)/X] c_{dm} (T_{ge} - T_0) + c_v (T_{ge} - T_0) + \lambda_v} \tag{3}$$

For fixed geometry of fluidized bed, A_c, the air flowrate, i.e. superficial air velocity, follows from the fluid bed mechanics and usually should be by 2 to 3 times higher than the minimum fluidization velocity. Since the outlet air temperature (T_{ge}) is selected according to thermal stability of the drying material and desired residual moisture content, Eq. (3) gives the simple relationship between inlet air temperature (T_{gi}) and specific water evaporation rate (W_{H2O}). A comparison between experimental and calculated values of W_{H2O}, using an estimated value of $c_{dm} \approx 0.85$ kJ/kg°C, is shown in Fig.7. Mean absolute deviation between experimental and calculated values is 5.8%,

while 85% of data falls within ±10%. Divergences between these values are probably due to the fact that heat losses were neglected in the calculations (Eq.3).

The most important disadvantage of this system lies in undesirable bed sintering in certain applications and extreme operating conditions leading to dramatic increase in the product moisture content with the feeding rate [11] or outlet air temperature. Application of the fluidized bed for materials that contain carbohydrates or fats is hardly possible because stickiness leads to unstable operation and defluidization unless drying aids are used [12]. Consequently each possible application must be checked out at laboratory level in sufficiently long testing for valid conclusions.

CONCLUDING REMARKS

Drying of solutions, suspensions and pastes in fluidized bed of inert particles is simple and very effective technique for non-sticky materials that do not adhere permanently to the inert particles. This drying concept is characterized by high evaporative capacity per unit volume of the dryer, low energy consumption, and low specific air consumption. The high drying efficiency results from the large contact area and from the large temperature difference between the inlet and outlet air. Intensive mixing of particles leads to nearly isothermal conditions throughout the bed. Simple heat and mass balances predict the dryer performance quite well.

Acknowledgment:

Financial support of the Serbian Ministry of Education and Science (Project ON172022) is gratefully acknowledged.

Nomenclature

A_c - cross-sectional area of the column at distributor plate, m^2
c_{dm} - specific heat of dry matter, kJ/kg^{o}C
c_w - specific heat of water, kJ/ kg^{o}C
c_v - specific heat of air, kJ/ kg^{o}C
C - color intensity of powder mixture
C_0 - color intensity of $Cu(OH)_2$ powder
d_p - inert particle diameter, m
D_c - column diameter (at distributor plate), m
G_{dm} - mass flowrate of dry matter, kg/s
G_{H2O} - water mass flowrate, kg/s
G_{sus} - suspension mass flowrate, kg/s
G_v - air mass flowrate, kg/s
h - hold-up (% of dried material with respect to the inert bed mass)
k_Y - mass transfer coefficient, kg/m^2s
q - specific heat consumption, based on T_{gi}-T_0, kJ/kg_{H2O}
Q_g - heat losses, kJ/s
λ_v - latent heat of water evaporization, kJ/kg_{H2O}
SV - specific air consumption (G_v/G_{H2O}), kg_{AIR}/kg_{H2O}
T_{gi} - inlet air temperature, ^{o}C
T_{ge} - outlet air temperature, ^{o}C
T_0 - ambient temperature, ^{o}C
U_0 - superficial fluid velocity at distributor plate (at T_0), m/s
U_{mF} - minimum fluidization velocity at distributor plate (at T_0), m/s
W_{H2O} - specific water evaporation rate (G_{H2O}/A_c), kg/m^2s
X - water content in the suspension (G_{H2O}/G_{sus}), kg/kg
ΔY_{lm} - the mean logarithmic driving force

References

1. Mujumdar, A.S.(Ed.). (1995) Handbook of Industrial Drying, revised and expanded (Vol. 1). CRC Press,
2. Kudra, T., Mujumdar, A. (2000) Advanced Drying Technologies, Marcel Dekker Inc, New York,
3. Kudra, T., Mujumdar, A. (1995) Special Drying Technologies and Novel Dryers. Handbook of Industrial Drying (A.S. Mujumdar, Ed.); 2nd Ed, Marcel Dekker Inc., New York, 1087-1149,
4. Reyes, A., Herrera, N., Vega, R. (2008) Drying suspensions in a pulsed fluidized bed of inert particles, Drying Technology, 26(1), 122-131,
5. Costa Jr.E., Freire, F., Freire, J., Passos, M. (2006) Spouted Beds of Inert Particles for Drying Suspension, Drying Technology, 24(3), 315-325,
6. Freire, J., Ferreira, M., Freire, F., Nascimento, B. (2012) A review on paste drying with inert particles as support medium, Drying Technology, 30(4), 330-344,
7. Yun, T., Puspasari, I., Tasirin, S., Talib, M., Daud, W., Yaakob, Z. (2013) Drying of oil palm frond particles in a fluidized bed dryer with inert medium, CI&CEQ, 19(4), 593–603,
8. Leontieva, A., Bryankin, K., Konovalov, V., Utrobin, N. (2002) Heat and Mass Transfer during Drying of a Liquid Film from the Surface of a Single Inert Particle. Drying Technology, 20(4&5), 729-747,
9. Bachmann, P., Tsotsas, E. (2015) Analysis of residence time distribution data in horizontal fluidized beds, Procedia Engineering, 102, 790-798,
10. Sigma Scan (1995) Image Analysis Software, Jandel Scientific, USA,
11. Kudra, T., Pallai, E., Bartczak, Z., Peter, M. (1989) Drying of Paste-Like Materials in Screw-Type Spouted-Bed and Spin-Flash Dryers. Drying Technology, 7(3), 583-597,
12. Benali, M., Amazouz, M. (2002) Effects of Drying-Aid Agents on Processing of Sticky Materials, Dev. Chem. Eng. Mineral Process, 10(3/4), 1-14.

XIII International Mineral Processing and Recycling Conference
Belgrade, Serbia, 8-10 May 2019

University of Belgrade, Technical Faculty in Bor
Vojske Jugoslavije 12, 19210 Bor, Serbia
Tel. +381 30 424 555 Fax +381 30 421 078

AMMONIUM COMPOUNDS IN THE TECHNOLOGIES OF COMPLEX PROCESSING OF LOW-GRADE COPPER-NICKEL RAW MATERIALS IN THE ARCTIC CONDITIONS

Andrey Goryachev [1,#], Evgenia Krasavtseva [1], Dmitry Makarov [2]
[1]NTTSA of the Kola Science Centre of RAS, Apatity, Murmansk Region, Russia
[2]Institute of Industrial North Ecology Problems of the Kola Science Centre of RAS, Apatity, Murmansk Region, Russia

ABSTRACT – The paper discusses a possibility using ammonium compounds for processing sulphide copper-nickel ores in Murmansk region. The mixture of ore and ammonium compounds was first roasted and then leached with water. The effect of the mass ratio of sulfide raw materials and ammonium sulfate, as well as roasting temperature on the extraction of metals was analyzed. High levels of copper and nickel recovery have been achieved, that makes this method ecologically favorable from the point of view of minimizing the heavy metals impact on the environment.

Key words: ammonium sulfate, sulphide ores, complex processing of raw materials, environmental safety, Arctic region.

INTRODUCTION

One of the threats for the Arctic ecosystems is heavy metal pollution. This is due to the fact that during storage of mining waste and incomplete exploitation of sulphide copper-nickel ore deposits, greatly changes in the mineral composition occur. In particular, in process of sulfide oxidation, heavy metals are transformed to water-soluble salts. This increases the risk of sulphide-containing mining wastes storage for the environment. The Murmansk region is the region of the Russian Arctic with the highest rates of economic growth. Due to the fact that the Murmansk region is one of the most industrialized areas of the Arctic, there have been significant changes in the hydrochemical regime of surface waters, the chemical composition of sediments, the structural and functional organization of biotic communities [1]. A particular threat to the Arctic freshwater ecosystems is the pollution of such heavy metals as copper and nickel, since the low water mineralization causes it high vulnerability to this type of impact.

To minimize environmental damage, a search for economically and environmentally favourable methods for the recovery of non-ferrous metals, and,

corresponding author: andrej.goria4ev@yandex.ru

particularly-nickel and copper, is necessary. This is mainly due to the fact that the quality of ores coming to enrichment is steadily declining, and the volume of mining works is increasing, contributing to the deterioration of ecological systems associated with mining sites. Due to the prevailing circumstances, sulphide ores of non-ferrous metals currently mined are often unsuitable for the direct production of metal, and the processing of such ores is economically unprofitable without the use of a method that allows it to be pre-enriched.

To solve these problems, a prerequisite is the development of a technology for processing unconditioned copper-nickel raw materials. In the context of the concept of sustainable development, this technology should be attractive both from an economic position and from the position of minimizing the impact of human activity on the natural environment.

OBJECTS AND METHODS

To study the risk of incomplete extraction of non-ferrous metals from opened sulphide ore deposits and technogenic raw materials of the Murmansk region, laboratory modeling of hypergene processes was conducted.

The ore of the following deposits was chosen as the object of research: Nud Terrasa, Nud II (Fig. 1A), Moroshkovoe Lake, Nittis-Kumuzhya-Travyanaya (NKT). Samples of the Allarechensk residue deposit (RD) and copper-nickel slags produced by Kolskaya MMC were taken as technogenic objects. The contents of nickel and copper in the ore samples are given in table 1.

All mentioned deposit are located above 68 degree of nothern breadth. This objects have a similar composition of gangue minerals: pyrrhotite (Fe_7S_8), pentlandite ($(Fe,Ni)_9S_8$), chalcopyrite ($CuFeS_2$), pyrite(FeS_2). Both pentlandite and pyrrhotite are highly unstable under conditions of hypergenesis, as a result of which chemical reactions and their physical destruction constantly occurs in ores. The oxidation of these minerals in natural conditions leads to the migration of heavy metals to surface water and groundwater, as well as to its accumulation in sediments.

For example, Nudyavr lake located near the Nud massif is an element of man-modified landscape (Fig. 1B). The long-term hypergene processes led to this lake accumulated a significant amount of heavy metals, and the total salt content in water was increased. It also led to a change in the ratio of major ions, and the water of this lake currently corresponds to the class of sulphates ($SO_4^{2-} > HCO_3^- > Cl^-$). Both the lake itself and the accessory water bodies have completely lost the properties of natural complexes, because the aquatic ecosystems of the Arctic are not resistant to this type of impact.

Table 1. Metal content in ores

Objects	Ni, %	Cu,%
Nud Terrasa	0.74	0.22
Nud II	1.97	0.54
Moroshkovoe Lake	0.61	0.26
Allarechensk RD	7.1	2.0
NKT	2.14	3.8
Kola GMK slags	0.11	0.17

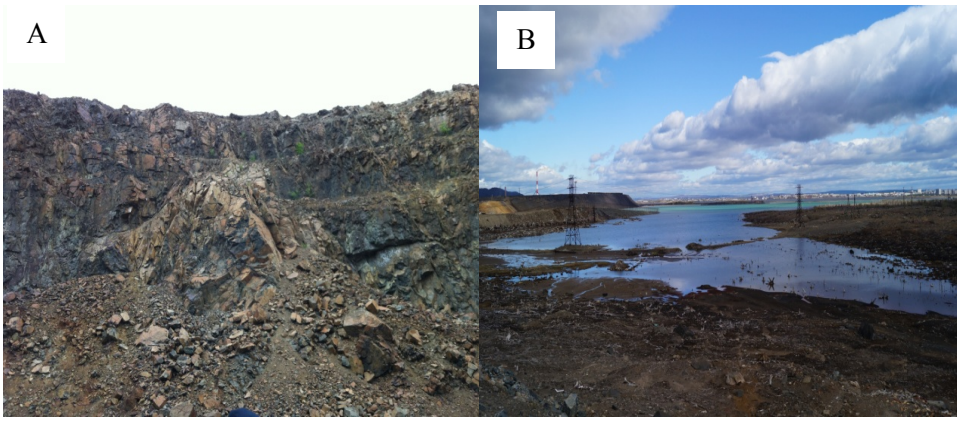

Figure 1. Nud II deposit (A) and the surrounding territory (B)

To simulate the process of hypergene transformation of sulfide copper-nickel ores, water leaching experiments were carried out on ores of the above mentioned objects. The samples were placed in a conical flask, distilled water was used as a reagent (pH = 5.9). The crushed ore (< 0.1 mm) was mixed with water in a 2:3 ratio (w/w). The duration of the experiment was 130 days with constant stirring at a rate of 150 rpm. During the experiments, the pH was measured using the I-160 MI ionometer.

Then, for the recovery of valuable metals, a method of roasting sulfide copper-nickel ore with ammonium sulfate $(NH_4)_2SO_4$ was considered. In the laboratory scale experiments, a rough concentrate with a nickel content of 2.4 % and copper of 1.2 % was used. The sample was mixed with sulfate in various weight ratios. The resulting mixture was loaded into an alundum crucible and placed in a muffle furnace, where it was roasted. The roasting temperature varied from 300 to 500 °C, the roasting duration was 4 hours.

After cooling at room temperature, the roasted samples were leached with water at ~ 100 °C for 40 minutes at a S:L ratio of 1:4 g/ml and continuously stirred at 230 rpm, where the sulfates formed during the roasting process were dissolved in water. The solution obtained by leaching was filtered to further measure the metal content of the solution. The residue after leaching was washed with distilled water and the content of copper and nickel was measured. Concentrations of copper and nickel were determined by the photometric method on SF-2000 spectrophotometer.

RESULTS AND DISCUSSION

Water leaching experiments showed that for the Nud massif deposits ores a decrease in pH by the end of the experiment to 4.3 for Nud Terrasa, to 4.2 for the Nud II deposit (Fig. 2). Moreover, the pH value after the first day of interaction for the Nud II sample was 6.6, while the pH of the solution after the interaction for the same period of time for the Nud Terrasa sample was 5.4.

For Moroshkovoe Lake ore, a stable pH value was observed throughout the experiment. At the beginning of the experiment, the value was less than after 100

days interaction - 7.5 at the beginning of the experiment and 7.6 after 100 day of interaction. It should be noted that this sample was the only one where the pH after 100 days of interaction was higher than at the beginning.

The interaction of water with the ore of the Allarechensk RD led to a decrease in pH already on the first day of the experiment to 5.1. By the end of the experiment, the pH dropped to 3.2.

In the case of slags from the copper-nickel production of Kola MMC, a sharp increase of the pH to 9.0 was observed on the first day. By the end of the experiment, the value of this indicator decreased to 7.0.

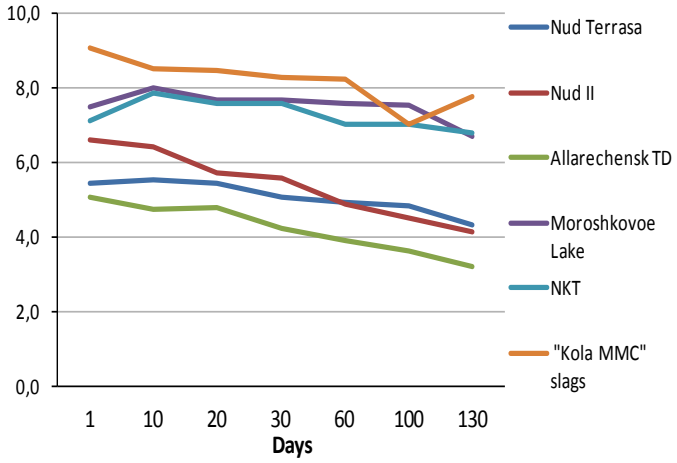

Figure 2. Dynamics of solution pH during the water leaching

Experiments have shown that in all cases there was a decrease in pH with varying degrees of intensity compared with beginning of the experiment. This indicates the danger of storing waste sulfide copper-nickel raw materials and deposits already opened by mining. In this regard, finding a method for efficient processing of such raw materials is still actual.

For this reason, in laboratory conditions, preliminary studies were conducted aimed at identifying the principal possibility of processing copper-nickel raw materials from the Murmansk region using ammonium compounds.

Effect of roasting temperature

Fig. 2 indicate that there was a considerable improvement in the recovery of copper when the roasting temperature was 500 °C, and metal recovery decreased when the roasting temperature was below 400 °C (Fig. 3). When the roasting temperature was higher than 280 °C, ammonium sulfate, presumably, begins to be decomposed into ammonium hydrogen sulfate as a molten liquid phase [2]. The highest extraction of nickel was achieved at the roasting temperature of 450 °C - 44 % passed to the solution. At a temperature of 300 °C, there was a minimum extraction of nickel - only 2 %.

The reasons for the subsequent decrease of metal extractions can be explained by the decrease of the reagent quantity participating in the reaction due to the decomposition of ammonium sulfate and ammonium hydrogen sulfate to produce SO_3 and NH_3. The roasting temperature of 400 - 450 °C can be considered to be optimal, which is much lower than that used in pyrometallurgical processing of nickel-copper sulfide ores [3].

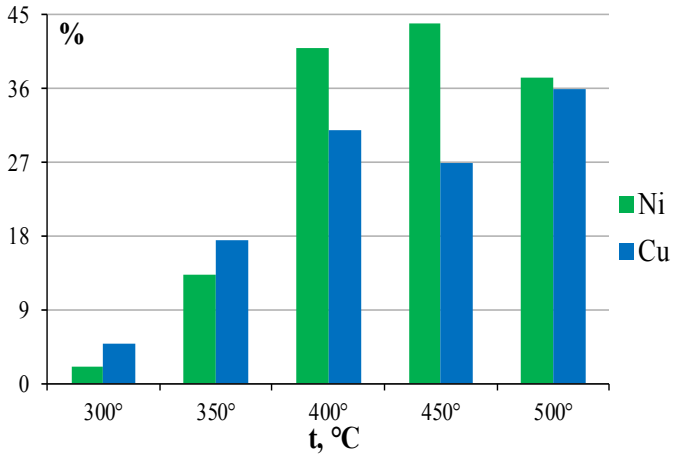

Figure 3. Recovery of target metals in dependence of roasting temperature

The maximum copper extraction was achieved at a roasting temperature of 500 °C, at this temperature 36 % of copper was extracted into the solution, when the minimum amount of this metal passed into the solution at a roasting temperature of 300 °C, only 5 % of copper was extracted. The most favorable roasting temperature 400 °C was chosen for investigation of the ammonium-to-concentrate ratio effect.

Effect of ammonium-to-concentrate ratio

The ore samples were mixed evenly with ammonium sulfate according to different weight ratios varying from 1:2 to 1:7, respectively, and were roasted at 450 °C for 4 h in order to investigate the effect of the ammonium-to-ore ratio on the recovery of nickel and copper. The results are presented in figure 3, the effect of ammonium-to-ore mole ratio on the recovery of nickel and copper was significant, while there was a little direct effect on nickel extraction.

The level of copper extraction tended to increase with an increase in the proportion of ammonium sulfate in the roasting mixture. With the increase of ammonium-to-ore ratio from 1:2 to 1:7, the extraction of copper was enhanced from 59 % to 79 %. Analysis of the extraction of metals using a different ratio of concentrate and ammonium sulfate showed that the greatest extraction of nickel was achieved at a ratio of 1:7, 77 % passed into the solution (Fig 4).

The level of copper extraction tended to increase with an increase in the proportion of ammonium sulfate in the roasting mixture. With a 1:7 ratio – 79 % of copper was recovered, while with a 1:2 ratio, it was 53 %.

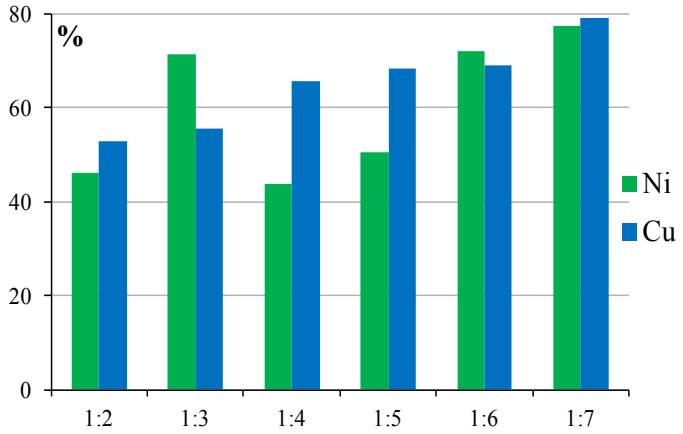

Figure 4. Recovery of the target metals in dependence of concentrate: $(NH_4)_2SO_4$ ratio

CONCLUSION

The research has shown the danger of incomplete recovery of non-ferrous metals during the exploitation of sulphide ore deposits and the storage of enrichment waste. Experiments on the modeling of hypergene processes have shown the need to find a method for processing unconditioned sulfide copper-nickel raw materials. Under the Arctic climate conditions, environmental safety should be the basis in order to reduce the negative impact on fragile ecosystems.

Experiments on the extraction of copper and nickel from sulfide raw materials using ammonium sulfate showed the effectiveness of this reagent. In this connection, further work is required to identify the optimal process parameters using both ammonium sulfate and other ammonium compounds, namely, bifluoride and chloride. In addition, it should be taken into account that the firing temperature 400 °C was chosen as useful to extract the copper and nickel into solution is much lower compared to the temperature of traditional pyrometallurgical processes.

References

1. Pozniakov, V. (1992) The "Severonickel" smelter complex: History of development. In: Aerial pollution in Kola Peninsula. Eds. Kozlov M.V., Haukioja E., Yarmishko V.T. Proceedings of the International Workshop, April 14-16, Saint-Petersburg, 16-19,
2. Mu, W., Cui, F., Huang, Z., Zhai, Y., Xu, Q., Luo, S. (2018) Synchronous extraction of nickel and copper from a mixed oxidesulfide nickel ore in a low-temperature roasting system. Journal of Cleaner Production, 177, 371-377,
3. Zhao, K., Gu, G., Wang, C., Rao, X., Wang, X., Xiong, X. (2015) The effect of a new polysaccharide on the depression of talc and the flotation of a nickel-copper sulfide ore. Minerals Engineering, 77, 99-106.

XIII International Mineral Processing and Recycling Conference
Belgrade, Serbia, 8-10 May 2019

University of Belgrade, Technical Faculty in Bor
Vojske Jugoslavije 12, 19210 Bor, Serbia
Tel. +381 30 424 555 Fax +381 30 421 078

DUNDEE PRECIOUS METALS CHELOPECH - INNOVATIVE SOLUTIONS FOR EFFICIENT PRODUCTION IN HARMONY WITH NATURE

Nikolay Simonski #, Georgy Bozhilov, Stoyko Peev, Stilian Minkin, Elisaveta Valova
Dundee Precious Metals, Bulgaria

ABSTRACT – The Company has been implementing a number of large-scale mine upgrade projects to achieve annual throughput rate of 2.2 Mtpa. Those projects have targeted effective production with care for the environment and public health. Post 2009, the Company used measurable indicators to achieve the following: ensure maximum efficiency in production process management, upgrade occupational and environmental parameters, ensure efficient use of resources and mine waste management, as well as reduce the specific carbon footprint from operations. Large-scale investments and technological innovations led to improved management of all environmental media. These achievements are presented in figures in booklet and poster.

Key words: upgrade project, innovation, efficiency; management; resources

INTRODUCTION

The mining industry is traditionally associated with environmental impact. The challenge to every mining company is to ensure it meets the market demands while supporting the local community's development and investing in environmental protection. The core business of Dundee Precious Metals Chelopech EAD is mining and processing of copper-gold-pyrite ores from the Chelopech Deposit. The mine is located at the western end of the Chelopech village in Bulgaria. Since 2009, the Company has been implementing a number of large-scale mine upgrade projects to achieve annual throughput rate of 2.2 Mtpa. Those projects have targeted effective production with care for the environment and public health. Once completed and commissioned, the new facilities helped us achieve higher operating efficiency, improved work conditions and environmental management.

Undoubtedly, the improved management of all aspects of the environment came as a result of the large-scale investments and technological innovations. Detailed information about those achievements is presented below.

corresponding author: Lambo.lambov@dundeeprecious.com

EFFICIENT MINE WASTE MANAGEMENT

In 2005, the sub-level caving mining method, which had been applied for more than 40 years, was replaced by the long hole stoping with fill (LHSF). That innovative approach improved the ground stability, the utilization of waste rock for backfilling purposes, reduced the amount of tailings disposed in the TMF and limited the storm water volumes in the underground mine. The Long Hole Stoping with Fill method is recommended as the best available technique and is applied worldwide. As a result, the process waste was reduced by 43 % between 2004 and 2017, measured per ton of ore throughput.

The environmental and landscape benefits of the new mining method are indisputable, the most prominent of them being:

- process waste was reduced by 43 % between 2004 and 2017, measured per ton of ore throughput;
- all waste rock is used for backfill, which limits the surface stockpile requirements;
- prevention of surface subsidence;
- environmental protection (surface and ground water, etc.)

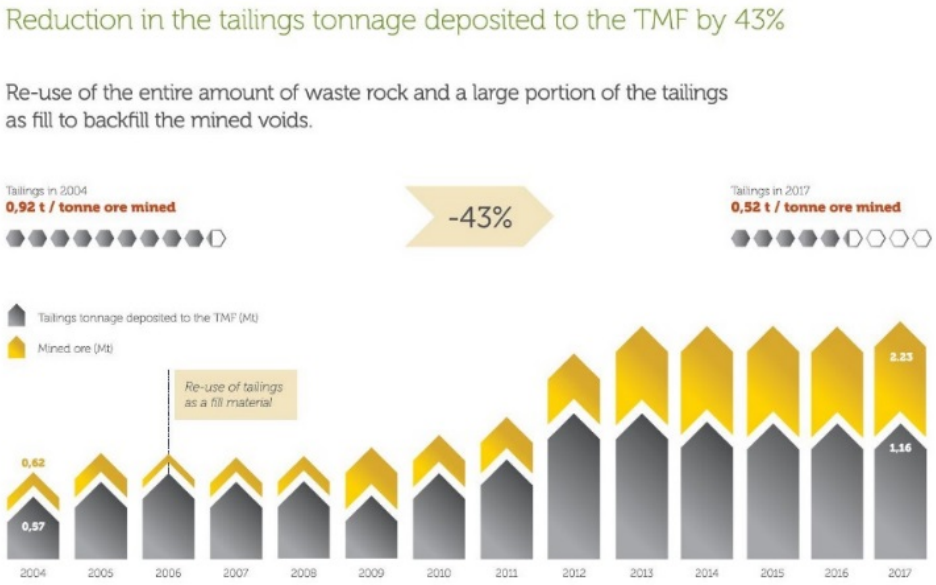

Figure 1. Reduction in the tailings deposited to TMF

PYRITE CONCENTRATE PRODUCTION

The pyrite concentrate production started in 2014 after commissioning of the upgraded pyrite circuit, which enabled the Company to achieve substantial environmental improvements, extract more metals from the ore and reduce the mine waste volume.

USING CEMENT AS A BINDING AGENT IN THE FILL

Two types of fill are used to backfill the mined stopes - dry rock fill and paste fill. Stope backfilling involves primarily tailings and waste rock; cement is added to the tailings to ensure compressive strength and stability of the backfilled stope. Data shows that the use of cement in the backfill material has dropped by approx. 60 % per ton of mined ore for the 2009 - 2017 period as a result of process upgrades and the professional skills and knowledge accumulated so far.

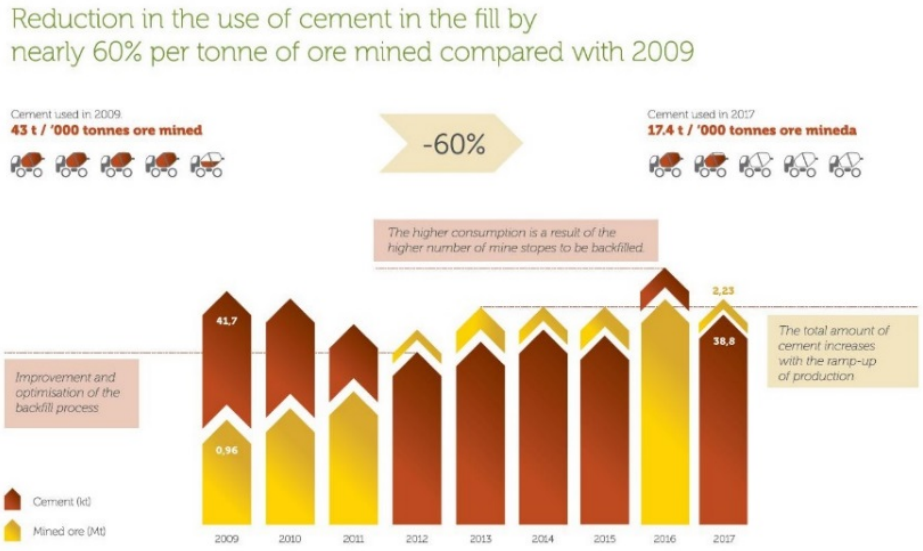

Figure 2. Reduction in the use of cement in the fill

ENVIRONMENTAL NOISE

The mine ventilation system was upgraded in 2011 and the old Sever (North) Shaft fan was replaced by a new, more efficient one, which was another well-planned innovation to ensure proper ventilation in view of the production expansion. A noise attenuation project was implemented at Iztok (East) Shaft in the 2009-2017 period, with a phased-out approach to reduction of noise emissions. A number of activities were completed, including regular replacement of mineral wool insulation inside the building, renovation of the building exterior, noise insulation of the air duct, and planting of trees meant to function as a noise screen. As result, the noise level at the impact location was substantially reduced with 20 dBA.

AMBIENT AIR QUALITY

As a result of crusher replacement by the SAG Mill (which was an innovative technical solution), dust emissions were reduced by nearly 60 tons per year, as one of the major sources of dust emissions - the Secondary and Tertiary Crushers were

decommissioned. With the introduction of the underground crusher in 2013, the primary ore crushing process was relocated underground, which allowed the company to decommission the Primary Crusher - another major source of dust, and further reduce the dust emissions by 1 ton per year. A railway siding was constructed and commissioned in 2015 to support a fully automated loading of copper and pyrite concentrates. A conveyor belt now conveys the concentrates to an automated loading system, which loads them to railway wagons for shipment.

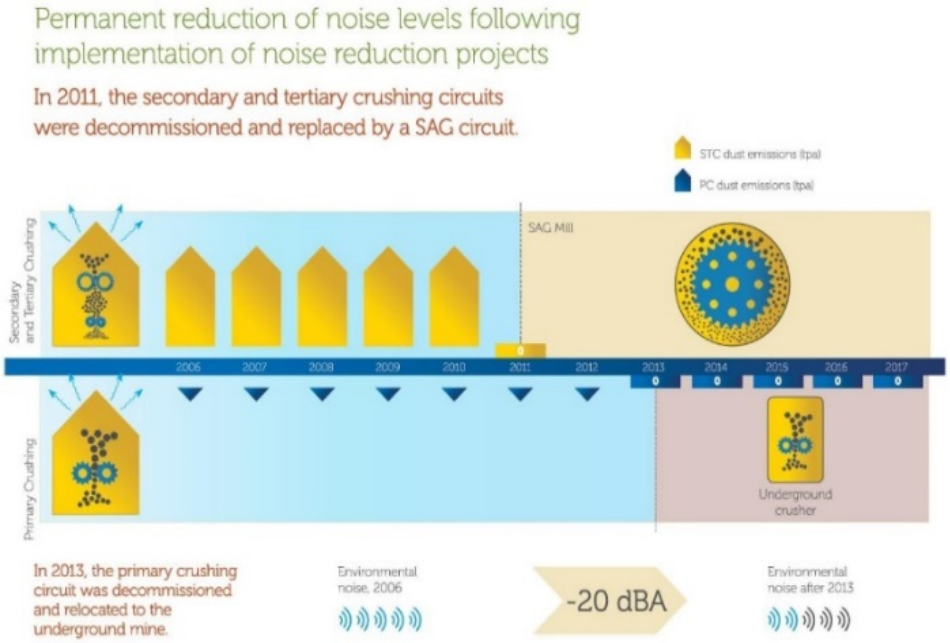

Figure 3. Permanent reduction of noise levels

WATER PROTECTION

The ore processing generates process waste (also known as tailings), which is disposed in the Chelopech Tailings Management Facility (TMF) or re-used as a fill material to backfill the mined voids in the underground mine. The TMF is a part of the overall ore processing flowsheet and operates within normal parameters.

A TMF upgrade project was completed in 2015, whose implementation took nearly five years. The placement of a compacted clay liner under the upgraded ROM ore pad and the construction of a tailings pipeline placed within a secondary containment (concrete channels) are measures that further minimize the risk of water pollution. The data show that the volume of TMF waste water discharged to the environment in the 2004 - 2017 period was reduced by 90% measured per ton of mined ore.

A modular domestic waste water treatment plant was built and commissioned in 2017-2018 on the DPM Chelopech mine site as a further protection and conservation measure for the water resources.

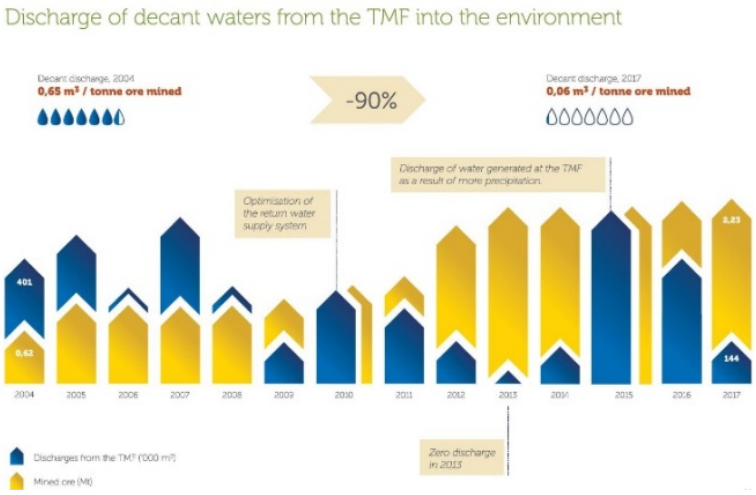

Figure 4. Discharge of decent waters from the TMF into the environment.

INDUSTRIAL USE OF FRESH WATER

The process plant upgrade project started in 2010, and the commissioning was completed in March 2014. The commissioned equipment included a SAG Mill, high-capacity flotation tank-cells and deep-bed thickeners, along with a pyrite circuit, while the old flotation banks and the secondary and tertiary crushing facility had been decommissioned. In addition, a fully automated process control system was introduced to monitor the operation of all key plant and equipment. Fresh water abstraction from the Kachulka Reservoir was reduced by more than 50 % (2012 vs. 2011) after the commissioning of the upgraded process plant. The data show that volume of fresh water consumption in the 2004 - 2017 period was reduced by 74 % measured per ton of mined ore.

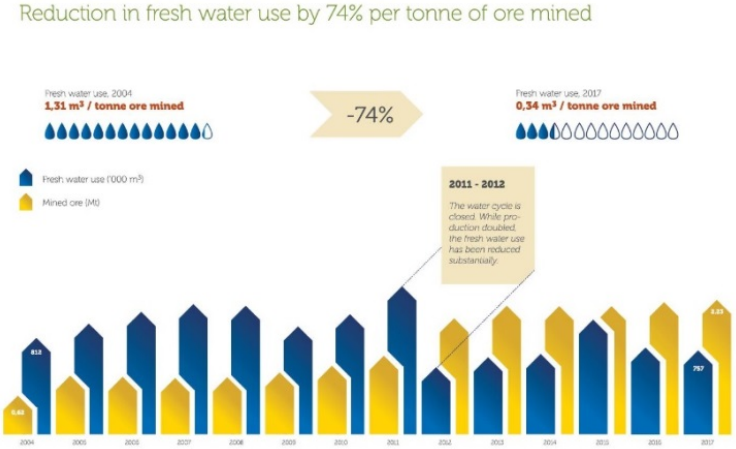

Figure 5. Reduction in fresh water.

SOIL PROTECTION AND REHABILITATION

The regional environment has been impacted by long years of mining operations prior to the introduction of the current environmental standards in the country. Back in 2004, the Company embarked on a project for rehabilitation of lands disturbed by historical mining including surface caves, abandoned derelict facilities and old waste rock dumps with the objective to improve the environmental status of the mine site. The main objective of the green projects was to restore the land as much as possible to its original natural condition and plant typical local tree and shrub species, which will ensure conservation and rehabilitation of the habitats of different animal species. The topsoil layer of the TMF's western impoundment area was removed in 2013. The topsoil removal was implemented in parallel with the second stage of the TMF upgrade project, which was completed in 2014.

ENERGY EFFICIENCY

DPM Chelopech operates state-of-the-art plant and equipment, and yet the mining and processing operations are immense power consumers. After the completion of the upgrade and expansion of the mine to achieve sustainable 2Mtpa mining rate, the Company reduced its power consumption by 28 % per ton of mined ore, as a result of the efficient management and control of the reclaim water cycle and the improvements in the mine ventilation system. The new conveyor belt system, which conveys the mined and crushed ore to the surface, reduced the diesel power requirements of the underground mine, although it added to the overall power consumption. As a result, the company achieved substantial reduction of diesel exhaust pollutants in the ambient air. One of the most important innovative renewable energy solutions at DPMCH was the installation of a solar hot water system on the roof of the Mine Dry building.

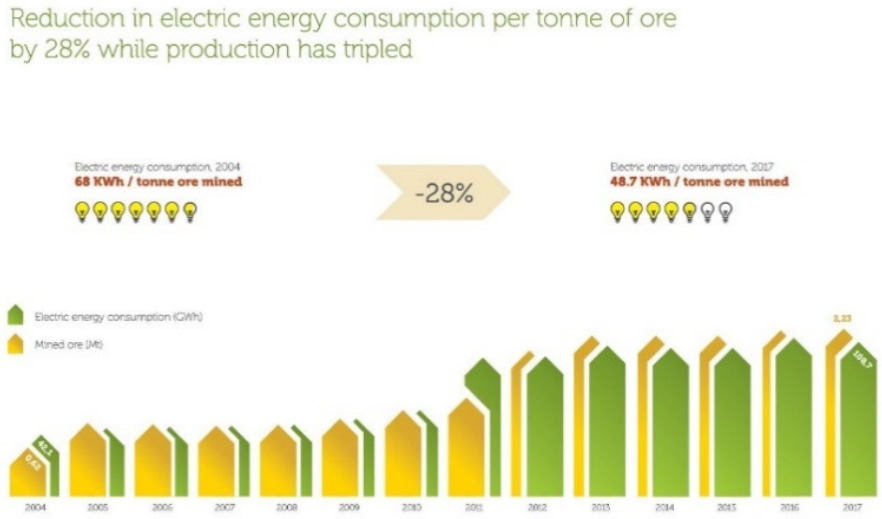

Figure 6. Reduction in electric energy

DIESEL FUEL CONSUMPTION

In addition to power, diesel fuel is another primary resource that is consumed in mineral mining and processing.

The underground crusher and conveyor system, which was commissioned in February 2013, is unique to Bulgaria for its solutions for safe and sustainable mining with care for the environment. With the new material handling system now complete and linking the underground mine to the surface, the mining cycle is closed thus ensuring protection of the environment and human health.

Diesel consumption in the material handling system of the mine has dropped by 41 % per tonne of ore between 2004 and 2017 since the commissioning of the new underground crusher and conveyor system.

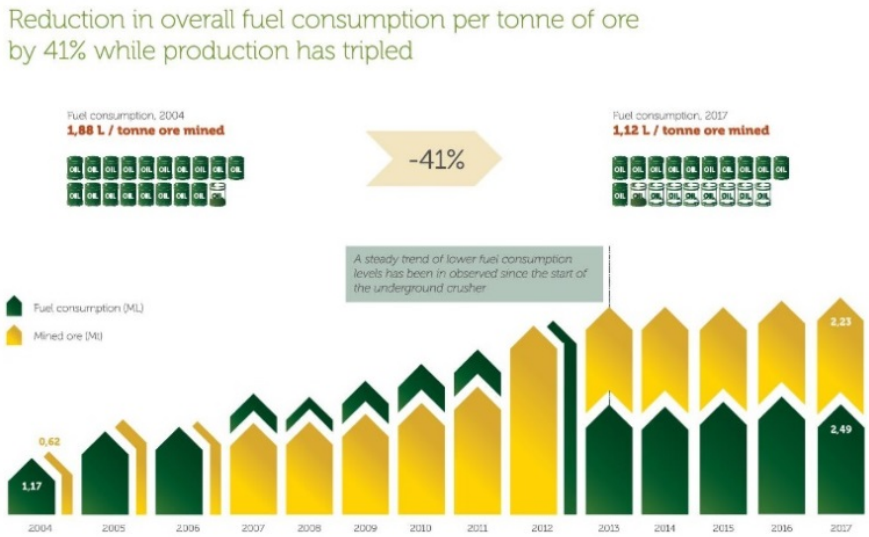

Figure 7. Reduction in overall fuel consumption

CLIMATE PROTECTION

In 2011, the Company commenced a project for preparation of an inventory of the direct and indirect greenhouse gas emissions from its operations and measures for their management.

The higher process efficiency and the improved management systems introduced since 2004 have substantially reduced the environmental impact. A measure of that impact on the greenhouse gas emissions is the so called carbon footprint. It reflects the emission volume based on total throughput (ore or concentrate).

The company's objective in the carbon footprint management has been to achieve sustainable results, meaning that it should invest further effort to reduce the power, fuel and materials consumption. As a whole, the upgrade and expansion of the mine to achieve sustainable 2Mtpa mining rate has also achieved 43 % reduction of GHG emissions per ton of ore throughput.

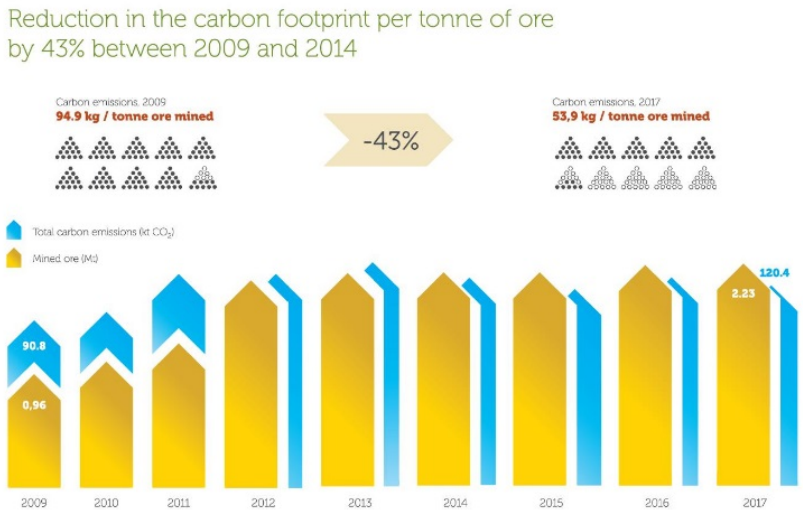

Figure 8. Reduction in the carbon footprint

WHAT HAVE WE ACHIEVED?

The implementation of all those projects achieved a unique and innovative management system and efficient, safe and environmentally friendly underground mining operation through a complete crusher and conveyor system to the surface, modern high-capacity process plant, safe and environmentally friendly storage of the flotation tailings and concentrate handling, which provide integrity and sustainability of all work streams.

The total investment in environment protection included several components:

- BGN 31.84 million for specific environmental activities, achieving compliance with the national legislation and rehabilitation of disturbed land, invested in the 2004-2017 period;
- BGN 42.35 million for upgrade of mining and processing systems, whose side effect was environmental improvements, invested in the 2004-2017 period;
- BGN 27.76 million surety bond for closure and rehabilitation, which is issued in 2017 to the Bulgarian government.

With its operations, DPM Chelopech EAD has proven in practice that the production expansion does not necessarily involve higher environmental impact.

It is the upgrade and expansion investment that made it possible to improve our energy and resource efficiency, and reduce our environmental footprint.

XIII International Mineral Processing and Recycling Conference
Belgrade, Serbia, 8-10 May 2019

University of Belgrade, Technical Faculty in Bor
Vojske Jugoslavije 12, 19210 Bor, Serbia
Tel. +381 30 424 555 Fax +381 30 421 078

SUSTAINABLE ORE RESOURCE BASE AND CIRCULAR ECONOMY

Lyubomir Ilchev #, Nadezhda Davcheva-Ilcheva
University of Chemical Technology and Metallurgy, Sofia, Bulgaria

ABSTRACT – The report is address: the rapid depletion of non-renewable ore resources, the deterioration of their quality and the increasing pressure on the environment as a result of economic growth; the UN and the EU requirements for sustainable resource base, the circular economy; opportunities for achieving them. Some good practices are also mentioned.

Key words: sustainable resource base, circular economy, ore resources, mineral waste.

INTRODUCTION

The vital and productive activity of human society is primarily related to the use of natural non-renewable resources, the development of industrial production systems, the continuous increase in consumption and output, regardless of their consequences. An example of this is given by the richest post-industrial countries. According to M. Jacobs [1], although their population accounts for about 21 % of humanity, they account for 86 % of global raw materials and energy sources.

Modern industrial systems operate primarily on a "linear" principle, which some scientists call "open" economies [1]. They are structured, organized and operated so that at many stages of extraction, processing and consumption, much of the non-renewable natural raw materials used are released as residues, waste and emissions. The final products after their depreciation, obsolescence or scrap are also converted to waste. In this way, the natural ecosystems with which the industrial systems are in close functional interaction and dependence are significantly disturbed, depleted and polluted. The pressure on the resource base is constantly increasing. According to the studies, the problem of depletion of non-energy raw mineral resources will occur at the end of the 21st century [2].

The European Strategy requires a mandatory transition to a circular economy up to 20130 [3].

USE OF ORE RESOURCES

By the end of the twentieth century, mankind had already used 20-40 % of

corresponding author: lubomirilchev@abv.bg

copper, nickel and zinc stockpiles, 40-70 % of lead, tin, silver and gold, 20 % manganese, chromium and cobalt. From 1950 to 2005, world metal production has grown six-fold, while the Earth's population has increased only 2.2 times [4]. In 1997, the consumption of raw materials per capita was 80 tonnes for Americans, 51 tons for EU citizens and 45 tons for Japanese [5]. The US uses resources as if it had four planets, Russia - with 2.5 planets, Japan - with 2.35 planets, China - with 1.2 planets [6, 7]. This has led to a rapid depletion of rich ore deposits and the extraction of ever-poorer metal ores. For example, the average copper content of copper ore extraction in the USA in 1906 was 2.5 % and in 2000 was 0.44 %. At the same time, the consumption of raw materials, energy and reagents increases. The amount of mining waste and pressure on the environment is increasing. On the planet, 30 tons of minerals are extracted per person, of which 2 % are turned into finished products and 98 % in waste [8]. Mines, especially open-pit mines, concentration mills and metallurgical plants leave lasting footprints on nature in adjacent areas.

Consumption of raw materials will continue to increase at an accelerated pace, in line with population growth and living standards. The treatment of non-renewable resources has an adverse impact to the environment. All this leads to a continuous increase in pressure on the resource base and its rapid exhaustion.

Ore resources in the Republic of Bulgaria and the EU

The Republic of Bulgaria is a country with developed mining and metallurgical industry. There are 174 ore deposits containing copper, lead, zinc, gold, silver, manganese, molybdenum, etc., and 7 existing ore mining companies [9]. Of these, three are for copper ores - Elatzite-Med AD and Assarel-Medet AD with open and Chelopech mining EAD with underground extraction of copper-gold ore. Chelopech ore reserves are about 23,000 kt and will end after 12 years. The ore has 1.2 % copper and 3 g/t gold, unique in its rich composition containing 87 minerals [10].

The ore reserves of the country as at 01.01.2011 amounted to 466 Mt. Experts predict that with a mining capacity of 30 Mt / year, mining is provided with resources for about 17 years from 2012 [11]. Exhaustion of rich copper ore resources has led to the use of ever-poorer ores. In the 1950s, the copper ore extracted had copper content of 1.6 % to 3.6 %. However, in the early 1960s, the yield of poor copper porphyry ores containing less than 0.4 % Cu began.

The metalliferous, including the copper ores predominant in them, have a high share in local domestic material consumption (DMC). For the period 2006 - 2016 it amounts to 21.82 % and 20.52 % respectively, while for the EU it is only 3.98 % [12] - Table 1. This confirms the importance of these raw materials for the economy of the country. Until 2060, the use of open-pit mining is expected to increase and the quality of mined ores to drop below 0.3 % Cu [13].

The processing of copper raw materials - Tab. 2, and copper production - Fig. 1 are growing in the country [14].It is expected that they will continue to grow in the future, as copper is widely used, including the entering RES. Hence, the pressure on non-renewable natural resources will increase.

According to the documents of the European Minerals Conference - Madrid 2010, the needs of mineral raw materials in Europe are over 3 Gt per year. About 70 % of EU production depends on them. Needs in the next 5-10 years are expected to grow significantly, even with over 50 % recycling of metals.

Table 1. DMC including the share of metal ores for the Republic of Bulgaria (RB) and the EU

Years	2006	2008	2010	2012	2014	2016
RB- DMC total (kt):	**137,841**	**153,643**	**121,077**	**131,329**	**140,067**	**138,136**
Metal ores (kt)	30,615	30,070	28,163	29,136	29,078	31,698
(coppers) (kt)	(27,336)	(27,223)	(27,405)	(28,489)	(27,450)	(-)
Meatal ores (%)	**22.21**	**19.57**	**23.26**	**22.19**	**20.76**	**22.95**
(coppers) (%)	**(19.83)**	**(17.72)**	**(22.63)**	**(21.69)**	**(19.60)**	**(-)**
EU- DMC total (kt):	**8,041,977**	**8,156,885**	**6,965,704**	**6,775,569**	**6,693,781**	**6,827,163**
Metal ores (kt)	303,869	306,280	248,680	245,990	272,342	340,894
Meatal ores (%)	**3.8**	**3.8**	**3.6**	**3.6**	**4.1**	**5.0**

Table 2. Processed copper raw materials in Aurubis Bulgaria AD

Years	2006	2008	2010	2012	2014	2015
Concentrate (t)	**789,351**	**937,267**	**928,365**	**976,718**	**1,165,484**	**1,203,245**
- copper content, %	28.41	27.58	24.76	24.14	25.20	24.57
- copper content, (t)	224,252	258,468	229,909	235,822	293,718	295,690
Scrap	5,265	17,062	39,321	56,104	62,280	56,168

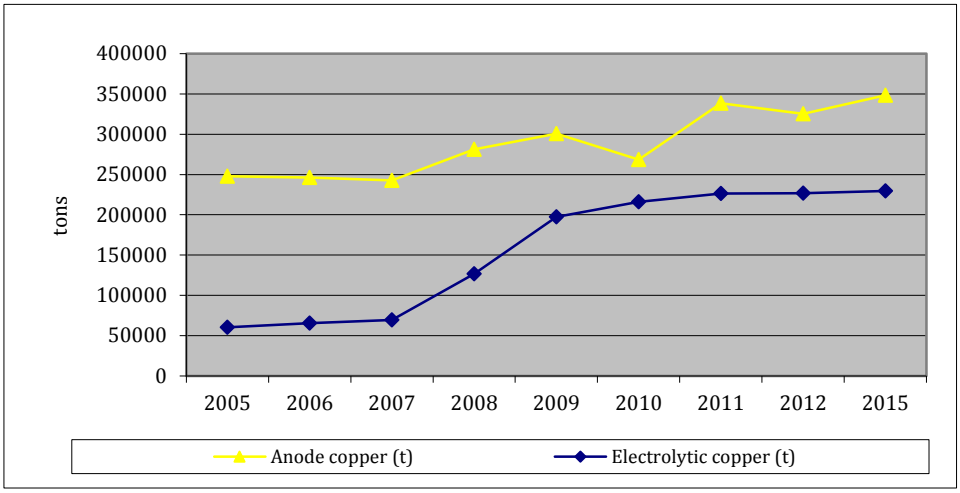

Figure 1. Production of anode and electrolytic copper

The European Environment Agency (EEA) data for EU-15 (old Member States), EU-10 (new Member States) raw materials and projections up to 2020 are shown in Fig. 2 [15].

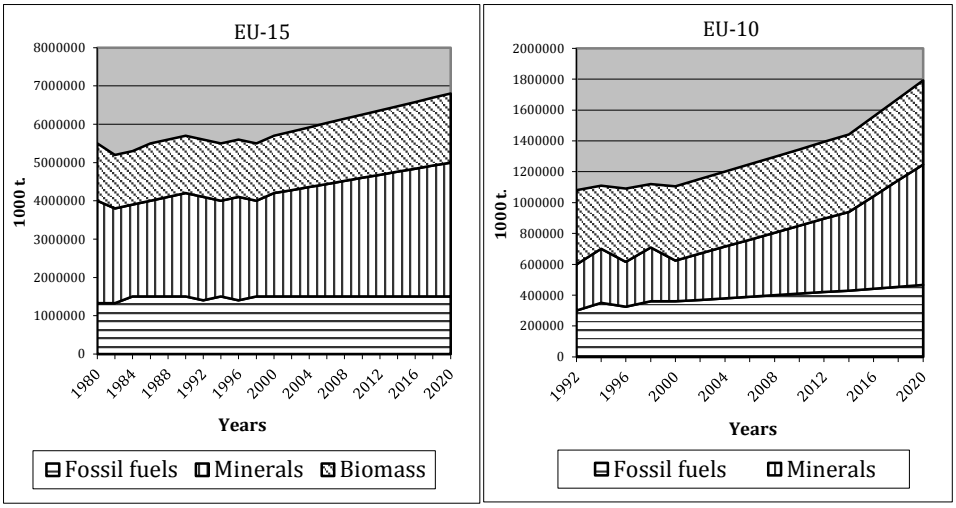

Figure 2. EU-15, EU10 - used raw materials, forecast for 2020

The EU-15 in 2012 used a total of about 6.3 Gt of raw materials. This quantity is expected to grow by 7 % in 2020 and to reach 6.8 Gt. The EU-10 has used about 1.3 Gt of raw materials. They are projected to increase by around 24 % to reach 1.7 Gt in 2020. The EU's forecast is that with economic growth, pressure on its raw material base will continue to grow.

Mineral waste in the Republic of Bulgaria and the EU

Mineral waste in the Republic of Bulgaria due to the processing of ever-poorer ores has a high relative share - 95.82 % of the total solid waste – Tab. 3. For example, to obtain 1 t 20 % copper concentrate of Assarel ore, containing 0.43 % Cu, 136 t solid wastes is released. For the EU, the share of this waste is significantly lower - 70.59 %. The largest contributors to it are: Romania (177,440,834 t), Bulgaria (150,214,030 t), Sweden (89,026,207 t) and Poland (61,541,018 t) [12]. The achieved share of recyclable waste for Bulgaria is about 6 times lower than that for the EU.

In the EU, despite good achievements, more than 60 % of the total material flow relates to the so-called "hidden streams" - the waste was not found to be applicable [5]. In industrially developed Member States, there are strict laws on the use of waste as valuable secondary raw materials and their important meaning for the protection of the environment.

Table 3. Waste by waste category- Republic of Bulgaria (RB), EU

Years	2004	2006	2008	2010	2012	2014	2016
RB- Total waste (Kt):	**201,020**	**162,881**	**167,646**	**167,201**	**161,252**	**179,598**	**120,508**
Mineral waste (Kt)	193,078	155,959	160,547	160,091	154,213	172,369	112,771
Mineral waste (%)	**96.05**	**95.75**	**95.77**	**95.75**	**95.63**	**95.97**	**93.58**
Recyclable waste (Kt)	887	944	1,083	1,652	1,925	2,371	2,049
Recyclable waste (%)	**0.44**	**0.58**	**0.65**	**0.99**	**1.19**	**1.32**	**1.70**
EC- Total waste (Kt)	**2,620,030**	**2,638,120**	**2,491,300**	**2,502,890**	**2,494,730**	**2,502,890**	**2,535,100**
Mineral waste (Kt)	1,828,340	1,846,800	1,736,810	1,744,910	1,802,050	1,804,890	1,794,330
Mineral waste (%)	**69.78**	**70.00**	**69.72**	**69.72**	**72.23**	**72.11**	**70.78**
Recyclable waste (Kt)	239,550	264,450	264,160	255,000	237,550	234,290	244,900
Recyclable waste (%)	**9.14**	**10.02**	**10.60**	**10.19**	**9.52**	**9.36**	**9.66**

ACHIEVING A SUSTAINABLE ORE RESOURCE BASE AND CIRCULAR ECONOMY

Ore Resources Management

The management of ore resources and raw materials is extremely important for the sustainable development of mining, mineral processing and metallurgy. According to the UN and the EU, management should create a sustainable resource base as follows: increasing its stocks; inclusion of waste as a resource; conserving ore resources and for future generations; detection of new types of resources and substitutes.

An important condition for its construction is the creation of a sustainable ore raw material base, which includes: improving its quality; increasing the use of secondary raw materials; finding suitable substitutes and new types of raw materials that do not conflict with the environment; efficient and complex use, including the conversion of inevitable mining waste into raw materials; reducing the material intensity and increasing the life of the products they receive; protection of the environment.

Industry, as the largest consumer of raw materials, is responsible for their efficient use. It is able to adapt to their shortages by continuously improving its raw material efficiency, which should cover the entire lifecycle of the raw materials - from their mining to the depreciation of the commodity products obtained.

Waste management

In UN and EU requirements for sustainable development, extreme attention is paid to waste - one of the greatest pollutants of nature. Their prevention, minimization, recycling and the fullest possible recovery are required. In their

management, it is envisaged to work in three main directions: converting an increasing share of the processed raw materials into a commodity product; maximum recycling of metal waste; introduction of innovative technologies. The goal is to move to a "zero waste" circular economy.

The transformation of waste into an important potential resource that expands the resource and raw material bases, leading to significant technical and economic benefits, and the protection of the environment and nature depends on their management. Mining, mineral processing and metallurgy have an important role to play in generating and managing them [16]. A new science-based re-mining project has been set up in the EU to make mineral waste (including old waste dumps) a raw resource.

Science has proven that mining waste can be used as a raw material for construction. The metro in Prague was built with building elements made of ore flotation waste. In our country, the rock waste of the Elatsite mine has a certificate of building material. The introduced in the Chelopech Mining EAD system, with subsequent paste filling, provides for the utilization of a large part of the company's flotation waste and prolongs the life of its tailing pond. In Aurubis Bulgaria AD the copper slags (about 700 thousand tons) are treated by flotation. The resulting copper concentrate is recycled to copper production, and small amounts (10-15 kt per year) of the fayalite product (about 640 kt per year) are utilized in cement plants. The flotation mill of Aurubis Bulgaria AD can increase its production by 30-35 % by obtaining a magnetite concentrate from the fayalite product.

Circular economy

As we have pointed out, the EU strategy requires, contrary to the applied "linear" model, a necessary transition to a circular economy [3]. This is a model aimed at reducing shortages of raw materials and environmental pollution, improving raw material and energy efficiency, enhancing innovation and competitiveness. The important contribution to its realization will be: extending the product lifecycle, minimizing the generation of waste and their recycling as raw materials in the economic cycle, the implementation of environmentally friendly technologies protecting the environment and nature.

References should be quoted by numbers (Surname, first initial, year and title of work, journal, page, publisher, place).

References

1. Давчева-Илчева, Н., Илчев, Л. (2005) „Екология. Устойчиво Развитие. Околна Среда”, Издателство „Изток-Запад”, София,
2. Brundtland, G. H. (20 March, 1987) Our Common Future: Report of the World Commission on Environment and Development, Oslo,
3. European Commission, 2 December 2018, EU`s 2015 Circular Economy Strategy; European Commission: Closing the Loop, Press release, Brussels,
4. Асадуриан, Е. (2010) Възход и падение на потребителските култури, Състоянието на Планетата, Институт Уърлдуоч, „Книжен тигър”, София,

5. Майкъл, Р. (2004) Придвижване към по-малко разрушителна икономика, Състоянието на Планетата, Институт Уърдуоч, „Книжен тигър", София,148-181,
6. WWF, 2012, Biodiversity, biocapacity and better choices, Living Planet, Report,
7. WWF, 2014, Species and spaces, people and places, Living Planet, Report
8. Сластунов, С. и др., 2001, Горное дело и окружающая среда, учебник, изд. „Логос", с.272, Москва,
9. МИЕТ, Март 2012, Национална стратегия за развитие на минната (минерално- суровинната) индустрия, Проект, София,
10. Челопеч Майнинг ЕАД, 2011, Инвестиции в модерен рудодобив, Издание на „Челопеч Майнинг" ЕАД,
11. П.Даскалов, 2011, Минната индустрия на България в условията на пазарна икономика и рецесия през периода 1990-2010 г., Международна научно-техническа конференция, Проблеми на екологията в минерално-суровинния отрасъл, Сборник, с. 38-46, Варна,
12. Eurostat, 2017, 2014, 2010, http://ec.europa.en/eurostat/ ,
13. Геотехмин, юли 2009, Удължава се живота на рудник „Елаците", Бюлетин на групата фирми Геотехмин, София,
14. БАМИ, 2016, Металургията в България през 2015;2010;2008 година, Годишно издание „Металургията в България", София,
15. European Environment Agency, 2007, Europa's environment, The fourth assessment, Belgrade,
16. Ilchev L., 2018, A dissertation "Managing Sustainable Development of the Copper Life Cycle in the Republic of Bulgaria", University of Chemical Technology and Metallurgy, Department of Environmental Engineering, Sofia.

XIII International Mineral Processing and Recycling Conference
Belgrade, Serbia, 8-10 May 2019

University of Belgrade, Technical Faculty in Bor
Vojske Jugoslavije 12, 19210 Bor, Serbia
Tel. +381 30 424 555 Fax +381 30 421 078

THE OXIDATIVE PROCESSES AND MIGRATION OF ELEMENTS IN HISTORICAL TAILINGS

Antoneta Filcenco-Olteanu #, Marius Zlagnean, Eugenia Panturu, Aura Daniela Radu, Nicolae Tomus
Research and Development National Institute for Metals and Radioactive Resource, Bucharest, Romania

ABSTRACT – The problem of sulphide oxidation and the associated generation of acid rock drainage (ARD), as well as the dissolution and precipitation processes of metals and minerals, are the most important environmental concern in mining today. The objective of the present study was to characterize and evaluate the Romanian historical tailing of Sasar-Red Valley, near Baia Mare. Tailings samples collected from different depths were characterized in term of mineralogical and chemical composition of the materials, weathering profile characteristics, its acid generating potential (ARD) and elements distribution in depth. Acid base accounting (ABA) tests in conjunction with net acid generation (NAG) tests classified the samples into the category of 'potentially acid generating'. The chemical and mineralogical analyses reveal the presence of a strong oxidation process at the tailings pond surface due to the weathering of sulphide minerals, in particular pyrite which is responsible for production of acidic water. Three zones were identified on the tailing surface: an upper oxidation zone (reddish-brown-yellow colored, acid generation and metal release), a hardpan layer (acid neutralization and metal accumulation) and a reduction zone (grey colored, limited water movement, low oxygen diffusivity). As a result of acid generation process the pH of the water decreases once sulphide oxidation starts. Under low pH conditions, ferric sulphate may be oxidized to ferric iron, which is capable of oxidizing other minerals such as copper, zinc or cadmium sulphides. With gradual increasing of the pH level, the dissolved metal load generally decreasing.

Key words: tailing, ARD, oxidative process, weathering, elements distribution

INTRODUCTION

The modern mining industry is of considerable importance to the world economy and the consequence of the large size of mining and mineral processing industry is not only the large volume of materials processed but also the large volume of wastes produced. In terms of water contamination, acid rock drainage (ARD) represents the key impact in areas exhibiting sulphide-bearing tailings in the form of rejected pyrite

corresponding author: antonetafilcenco@yahoo.ro

and other sulphide minerals. If sulfidic tailings are exposed to atmospheric oxygen or to dissolved oxygen in the vadose zone of tailings, the oxygen infiltrating in the waste may cause sulphide oxidation and trigger ARD. Acid producing, acid buffering reactions and secondary mineral formation will occur, and low pH pore water with high concentration of dissolved constituents will be generated [1, 2, 3]. Indicator for sulphide oxidation – such as abundant oxyhydroxide and hydroxide precipitates or acid, sulphate and metal-rich tailing liquids – are generally observed in the upper part and vadose zone of tailing impoundments [4, 5]. As a consequence, ARD is associated with the release of sulphate, heavy metals (Fe, Cu, Pb, Zn, Cd, Co, Cr, Ni, Hg), metalloids (As, Sb) and other elements (Al, Mn, Si, Ca, Na, Mg, Ba, F) [6].

The activities of extraction, processing and preparation of complex ore from the mining basin Baia Mare left behind tens of dumps and mine tailings ponds, stored in different types of tailings management facilities (TMFs), located mainly in the river valleys from this area.

The present study will mainly focus on Sasar TMF. Tailings samples collected from different depths were characterized in term of mineralogical and chemical composition of the materials, weathering profile characteristics, elements distribution in depth and its acid generating potential (ARD).

EXPERIMENTAL AND MATERIALS

Study area

The Maramures Country, situated at northern border of Romania with Ukraine, encloses the old "lands" of Maramures-Chioarul, Lapus and Baia Mare Basin. Baia Mare Basin is a contact basin that interposes between the Somesana Plain and the Carpathian Mountains as a lower morphological unit, from the surrounding areas, presenting a waved surface, characterized by a convergent system of valleys and interfluves [7]. The area belongs to the undifferentiated Quaternary characterized by deluvial deposits, andesitic blocks and alluvial deposits [8].

The Sasar (Red Valley) tailing pond, located in the west part of Baia Mare, secured the storage of flotation tailings from the Processing Plant which was closed in 1982. It contains around 8.5 million m^3 of fine grained waste ores embodying the acidic water producing mineral pyrite.

Sampling

Tailings samples were collected from six depth intervals: 0-1 m, 1-2 m, 2-3 m, 3-4 m, 4-5 m and 5-6 m using a soil auger. Drill samples were preserved in polyethylene bags, transported and processed separately. Prior to analysis, the samples collected were split with a riffle splitter, and half of each sample was kept for potential future analysis.

METHODS

The determination of total element contents was performed using digestion followed by ICP AES (inductively coupled plasma atomic emission spectroscopy) analysis using a Perkin Elmer Optima 3100 RL spectrometer. Additionally, a routine mineral characterization was carried out by optical *microscopy* using a Carl Zeiss

Axio Imager A1m. The soil moisture content was determined by drying 10g soil sub-samples at 105 ^{o}C for 24 h.

Static geochemical tests provide the basis for understanding potential reactivity and therefore ARD potential of a sample. The static geochemical tests were performed as presented in the MEND prediction manual [9], on pulverized samples (<75μm) collected in drill 2 from 1 m, 3 m and 6 m depth. The neutralization potential (NP), the acid producing potential, (AP) and the net neutralization potential (NetNP) were determined by standard titration as presented in the MEND prediction manual and by Weber [9,10].

The AP was calculated with the commonly used factor of 31.25, to convert the percent of contained sulphur to kg $CaCO_3$ equivalent per tonne material [9, 10]. The samples previously prepared for the ANC procedure were used in the net acid production (NetAP) test, as presented by Sobek [11] and Finkelman [12].

The paste pH/EC was determined as presented by Sobek [11] by equilibrating the sample in deionised water for approximately 12 hours at a solid to water ratio of 1:2 (w/w) and then measuring the pH and EC using a Consort C832 conductivity and pH meter.

RESULTS AND DISCUSSIONS

Mineralogical and chemical analysis of the tailings

The mineralogical results derived from the optical microscopy analysis showed that the sample consisted of quartz, SiO_2 (high refractive index; no twinning or cleavage); calcite, $CaCO_3$ (very high birefringence); microcrystalline aggregates of plagioclase and pyroxene, feldspar $NaAlSi_3O_8$-$CaAlSiO_2O_6$, (parallel cleavage, multiple twinning and first order birefringence) and microcrystalline goethite FeOOH, and iron hydroxide $Fe(OH)_2$ (opaque to sub-translucid, strong cleavage). The reflective property of pyrite FeS_2, galena's cleavage structure, the brown and fragile nature of sphalerite (blenda) ZnS, the typical yellowish green colour of chalcopyrite $CuFeS_2$ and the glassy appearance of quartz is clear in the microscope at high magnification.

Table 1 summarizes the chemical compositions of the tailings samples collected form drill 2 (H2). As shown in Table 1, major elements in the tailings were Mn, Zn, Pb, P, Cu, Ba, and As, whereas the minor elements were identified as Ca, Na, Mg, and Hg. The gold and silver content of the tailing samples were 0.43 g/t and 3.70 g/t, respectively.

Table 1. The chemical compositions of elements content in tailing profile

Element	Content	Element	Content	Element	Content
Au g/t	0.43	Co ppm	9.17	Mo ppm	2.00
Ag g/t	3.70	Cr ppm	16.83	Na %	0.02
Al %	1.01	Cu ppm	199.17	Ni ppm	9.00
As ppm	175.00	Fe %	3.57	P ppm	365.00
B ppm	10.00	Hg ppm	1.33	Pb ppm	490.17
Ba ppm	165.00	K %	0.29	B ppm	14.50
Ca %	1.02	Mg %	0.39	Sr ppm	18.00
Cd ppm	8.95	Mn ppm	2940	Zn ppm	1451.33

Weathering profile characteristics and elements distribution in depth

In Sasar impoundment three zones were identified (Figure 1): an upper oxidation zone (reddish-brown-yellow coloured, acid generation and metal release), a hardpan layer (acid neutralization and metal accumulation) and a reduction zone (grey coloured, limited water movement, low oxygen diffusivity). If the precipitation (of secondary materials) layer dries out and cement, it forms a so-called hardpan, which act as horizontal barrier to the vertical flow of pore waters.

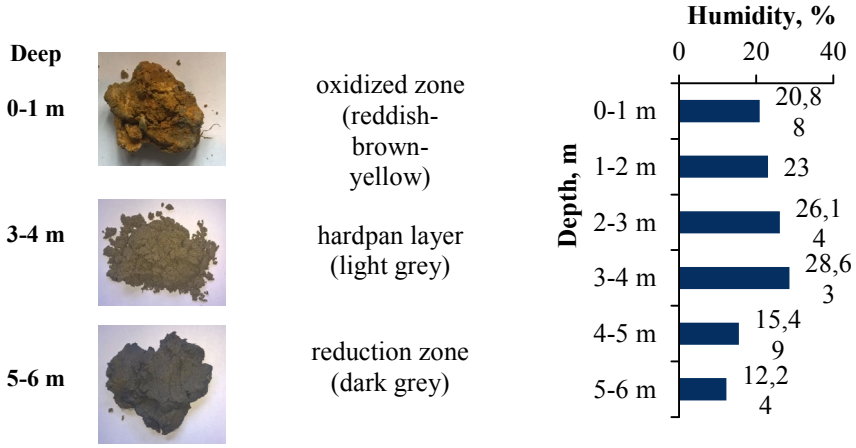

Figure 1. The colours for oxidation zone, hardpan layer and reduction zone and weathering profile for studied drill

This distinct vertical colour change in tailing, generally indicates the transition from an oxidized layer to reduced material. It was noted that moisture was increasing from 20.88 % on surface to 28.63 % at 3-4 m depth on studied drill core. At 5-6 m depth the moisture decreases to 12 %. The changes in pH will also affect the solubility and bio-availability of elements originally present in the soil. The pH of the pore water rapidly rises due to carbonate dissolution and iron precipitates as iron hydroxides which cement the waste. The oxidation of sulfuric minerals and dissolution of calcium minerals in the upper zone are presented in Figure 2.

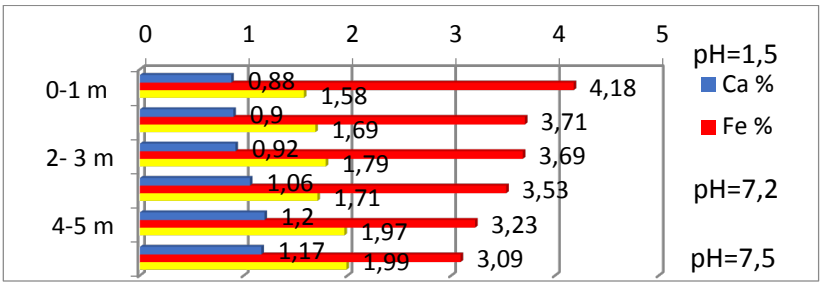

Figure 2. Calcium, iron and sulphur content distributions in depth for H2 drill core

In oxidation zone (pH=1.5) the lowest contents of Ca and S and the highest content of Fe can be noted. In this zone, the carbonate minerals are dissolved and the sulphides are oxidised. The obtained data showed that the Ca content increases from 0.88 % in oxidation zone (pH=1.5) to 1.17 % in the reduction zone (pH=7.5) and the S content increases with depth from 1.58 % in oxidation zone (pH=1.5) to 1.99 % in the reduction zone (pH=7.5). The Fe content decreases with depth from 4.18 % in oxidation zone to 3.09 % in reduction zone, due to oxidative processes that occur on sulfide minerals (pyrite, blenda, etc.).

Static tests results

The implemented static test procedures consisted of neutralisation potential (NP) and Net Acid Production (NetAP) tests.

Paste pH

Table 2 provides data related to paste pH and electrical conductivity of samples collected from 1m, 3m and 6 m respectively.

Table 2. Paste pH and electrical conductivity

Sample	Time, h	$pH_{1:2}$	$EC_{1:2}$ (µS/cm)
D1	1	1.57	351
	12	2.93	638
D3	1	7.02	1080
	12	7.06	1466
D6	1	7.11	654
	12	7.18	1710

D1 sample showed a paste pH below 4 and an electrical conductivity > 20 µS/cm, meaning that it contains a high amount of dissolved salts. As a consequence, the D1 sample could be included in the category of samples with acid production potential. The values of pH over 7 obtained in the case of D3 and D6 samples indicate that those can either be potentially-acid-forming or non-acid forming, depending on their acid-base balance.

Acid -Base Accounting test

According to Ferguson and Morin [13], sample having a net neutralizing potential (Net NP) less than - 5 $kgCaCO_3$/ tone is classified as *a potential source of acidic drainage (PAF)*. Net neutralization potential (NetNP) data, including neutralization potential (NP) acid potential (AP), NP to AP ratio and net acid production (NetAP), are provided in Table 3.

In our case study, the obtained net neutralizing potential (NetNP) values were negative, which indicated that the samples were potentially acid forming materials. Results obtained by static tests (Table 3) are graphically plotted in Figure 3.

Table 3. The static test results of the tailing samples

Sample	ABA pH	Fizz rate	S, (%)	NP (kg $CaCO_3$/t)	AP (kg $CaCO_3$/t)	NetNP (kg $CaCO_3$/t)	NP:AP ratio	NetAP pH	NetAP(kg $CaCO_3$/t)	Class
D1	1,45	0	1,58	-0,75	49.37	-14,75	-0,015:1	2,77	6,6	PAF
D3	1,16	1	1,79	32,5	55.94	-20,5	0,58:1	3,22	9,7	PAF
D6	1,32	2	1,99	50	62.19	-14	0,80:1	3,15	7,15	PAF

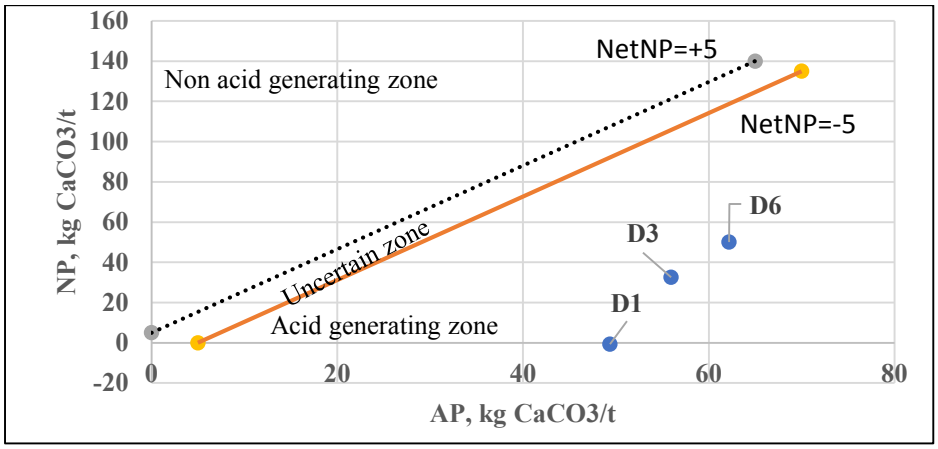

Figure 3. Classification of the samples in terms of AP and NP [13]

It has been suggested that the ratio between NP and AP values might provide a more reliable guideline for classification of samples, with suggestions that NP:AP ratios below 1 indicate *potential source of acidic drainage*. [19] The NetAP positive values obtained show that the samples are potential sources of acid waters, a fact that results from the Figure 4 as well.

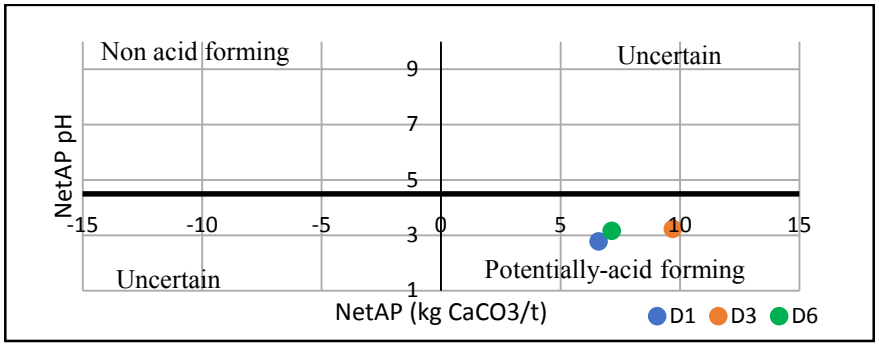

Figure 4. Distribution of the tailing samples in the NetAP pH/ NetAP diagrams

The NetNP results obtained compared with NetAP results confirmed that samples would produce acidity upon exposure to oxygen and water.

CONCLUSION

Tailings from mineral processing of polymetallic ore stored in Sasar (Red Valley) impoundments, were characterized in term of mineralogical and chemical composition of the materials, weathering profile characteristics, elements distribution in depth and its acid generating potential (ARD). The main conclusions related to this study can be summarized as follows:

- The mineralogical results showed that the sample consisted of quartz, SiO_2; calcite, $CaCO_3$; pyrite FeS_2, galena ZnS, and chalcopyrite $CuFeS_2$
- Results have indicated that tailings exhibit very high contamination degree for soil, especially with Mn, Zn, Pb, Cu, thus, gold mine tailings can be considered as a primary source of soil and groundwater contamination in mining areas. The gold and silver content of the tailing samples were 0.45 g/t and 4.59 g/t, respectively, reprocessing of tailing could be considered as an economically feasible possibility;
- In Sasar impoundment three zones were identified: an upper oxidation zone (reddish-brown-yellow coloured, acid generation and metal release), a hardpan layer (acid neutralization and metal accumulation) and a reduction zone (grey coloured, limited water movement, low oxygen diffusivity).
- It was noted that moisture was increasing from 20.88% on surface to 28.63 % at 3-4 m depth on studied drill core. At 5-6 m depth the moisture decreases to 12 %.
- Both the ABA and the NetAP test classified the samples into the category of 'potentially acid generating'. Comparison of Net Acid Production (NetAP) and Net Neutralization Potential (NetNP) results confirmed that samples would produce acidity upon exposure to oxygen and water.

Acknowledgment

This work was funded under the scope of the "3rd ERA-MIN Joint Call (2015) on Sustainable Supply of Raw Materials in Europe" by a grant of the Romanian National Authority for Scientific Research and Innovation, CCCDI – UEFISCDI, project: Improve Resources Efficiency and Minimize Environmental Footprint - REMinE, Contract no.13/2016.

References

1. Edwards K.J., Bond P.J., Druschel G.K., McGuire M.M., Hamers R.J., Banfield J.F., 2000, Geochemical and biological aspects of silfide mieneral dissolution: lessons learned from IRON Mountain, California. Chem Geol 169, 383-397,
2. Dold B, Spangenberg J.E., 2005, Sulfur speciation and stable isotope trends of water-soluble sulfates in mine tailings profiles. Environ Sci Technol 39, 5650-5656,
3. Romero N.F., Armienta M.A, Gonzales-Hernandez G., 2007, Solide phase control on the mobility of potentially toxic elements in an abandoned

lead/zinc mine tailings impoundment, Taxco, Mexico, Appl.Geochem 22: 109-127,

4. Schippers A., Kock D, Schwartz M., Bottcher M.E., Vogel H., Hagger M., 2007, Geomicrobiological and geochemical investigation of a pyrothite-containing mine waste tailings dam near Selebi-Phikwe in Botswana, J. Geochem Explor. 92: 151-158,
5. Heikkinen P.M, Raisanen M.L., 2008. Mineralogical and geochemical alteration of Hitura sulphide mine tailings – indicators of spatial distribution of sulphide oxidation in active tailings imjpoundments, Appl. Geocgem, 24: 1224-1237,
6. Geldenius S., Bell F.G, 1998, Acid mine drainage at a coal mine in the eastern Tranvaal, South Africa, Environ. Geol. 34:234-242,
7. Modoi, O.C., Vlad, S.N., Stezar I.C., Manciula, D., Gagiu. A.C. Marginean S., 2011, Integrated tailing dams management in Baia Mare area, Romania, Environ Engineering and Management Journal, 10: 43-51,
8. Mutihac V., 1990, The Geological Structure of the Romanian Territory, (in Romanian), Technical Press, Bucharest, Romania,
9. MEND Project 1.16.1b, 2008, Acid rock drainage prediction manual, A manual of chemical evaluation procedures for the prediction of acid generation from mine wastes, Coastech Research Inc.
10. Weber P.A, et al. 2005, Methodology to determine the acid-neutralization capacity of rock samples, The Canadian Mineralogist, 43(4):1183,
11. Sobek, A.A, Schuller W.A, Freeman J.R, Smith R.M., 1978, Field and laboratory methods applicable to overburdens and minesoils, EPA 600/2-78-054, 203,
12. Finkelman, R.B., Giffin, D.E., 1986, Hydrogen-peroxide oxidation - an improved method for rapidly assessing acid-generating potential of sediments and sedimentary-rocks. Reclam. Reveg. Res. 5, 521-534,
13. Ferguson KD, Morin KA. 1991, The prediction of acid rock drainage—lessons from the data base. In: Proceedings of the 2nd ICARD, vol 3. Montreal, QC, Canada, 83–106.

XIII International Mineral Processing and Recycling Conference
Belgrade, Serbia, 8-10 May 2019

University of Belgrade, Technical Faculty in Bor
Vojske Jugoslavije 12, 19210 Bor, Serbia
Tel. +381 30 424 555 Fax +381 30 421 078

A POSSIBILITY FOR PURIFICATION OF INDUSTRIAL EFFLUENTS FROM ARSENIC IN HIGH CONCENTRATIONS

Vladko Toforov Panayotov [1, #], R. Imhof [2], M. Panayotova [3]
[1]Academy of Sciences, Sofia, Bulgaria
[2]Consultant, Germany
[3]University of Mining and Geology, Sofia, Bulgaria

ABSTRACT – An easy-to-implement method for arsenic removal from waste effluents released by copper metallurgy of arsenic-bearing materials is presented. The fluid is treated electrochemically; the electrodes' potential is regulated to obtain first copper-rich, then arsenic-rich material. The electrodes are equipped with a vibration system, which prevents their passivation and operation stopping. The obtained material can be easily separated and sent to metallurgy or to a depot depending on its nature. EPA tests confirmed stability of the resulting arsenic compounds. Pilot-plant tests at a copper metallurgy in Latin America showed complete separation of arsenic at a low cost and wastewater neutralization and recyclability.

Key words: arsenic removal, waste effluents, electrochemical treatment

INTRODUCTION

Water is very important for the socio-economic development, healthy ecosystems and for the human survival itself. Water demand for industry is expected to increase by 400% between 2000 and 2050 globally [1]. Metals' extraction is one of the industries using large volumes of water and thus "contributing" to deepening the issue of water scarcity. Increasing the water recycling in this industry will help in the problem mitigation.

Improved resource efficiency is one of the three pillars of the Europe's initiative which aimed at securing reliable and unhindered access to raw materials for the EU enterprises [2]. Translated into the language of professionals in mineral processing and metallurgy this means more complete extraction of all valuable components from the ore and reduction of their loss through waste streams.

Metallurgy of arsenic-bearing copper concentrates is often accompanies with creation of large volumes of so called ''washing acids", i.e. highly acidic effluents containing in relatively high concentrations copper (Cu) and arsenic (As). Arsenic-bearing industrial effluents can cause pollution of surface and ground water and

corresponding author: vlad_tod@abv.bg

further can lead to pollution of drinking water and food. This is the reason for low maximum permissible concentrations of arsenic in industrial waste effluents. The legislation is becoming more strict.

Many methods have been tried and used for treating arsenic-containing industrial effluents.

Arsenic precipitation (in all its varieties) is the most widely spread treatment method. Arsenic is precipitated by addition of lime, calcium oxide, calcium salts and ferric or ferrous salts, mixture of aluminum, alkali earth and ferric salts, etc. [3- 8]. Arsenic precipitation by liming requires big amounts of lime especially when highly acidic effluents are to be treated. Difficulties appear in lime dosing, achieving and maintaining the needed pH values for ensuring stable arsenic immobilization. Calcium arsenate formed is equilibrated with relatively high arsenic concentrations. Large volumes of sludge are generated with their handling problems. Precipitation by addition of iron salts also requires higher pH values than the washing acids pH value. Ferric salts use results in sludge with high volume and corresponding difficulties in handling. Use of ferrous salt leads to smaller sludge volume however at the expense of oxygen or H_2O_2 addition for in situ Fe^{3+} obtaining. Precipitation by chemicals' dosage brings additional ions in the treated effluent, most often sulfates and chlorides which are noxious if the water is to be recycled in the process. In addition, valuable metals that present in the effluents are lost by immobilization in the precipitates. Arsenic sorption on iron and aluminum oxides/hydroxides, carbon-based adsorbents, MnO_2, etc. has been proposed for arsenic removal from industrial effluents [6, 9].

Physical adsorption is the main way of arsenic immobilization by sorption. However, the arsenic immobilized by physical sorption can be more easily re-mobilized compared to arsenic immobilized by precipitation or co-precipitation, even at high sorption capacity of the adsorbents used. Arsenic sorption is pH dependent process and usually is effective when the pH of the effluent to be treated is $\geq$ 2-2.5 independently of the adsorbent nature. Handling (regeneration or disposal) of spent adsorbents is required. Treatment by use of membrane processes can ensure high As removal - rejection >90÷95% has been reported. However, the treatment by membrane processes requires relatively high capital costs and further handling of the resulting liquid concentrate. In addition, usually membranes are not stable at pH values of pH 0÷1.0. Number of works dealing with the electrochemical treatment of arsenic-containing effluents is relatively low [10-12]. The method is based on electrolysis where iron ions are generated and react as coagulant and/or precipitant. When properly designed electrochemical system and suitable treatment conditions are applied not only the effluent could be purified from arsenic but also the present valuable metals could be extracted.

The investigation presented in this paper was aimed to create a low-cost method for treating effluents from a copper smelting plant by which to: (a) Recover a high-grade copper-bearing material with low amounts of arsenic impurities; (b) Decrease copper and arsenic concentration in the effluent and render it recyclable to the process; (c) Depending on the economic requirements - recover arsenic in materials suitable for further processing or render it in a stabilized precipitated material suitable for environmentally friendly disposal.

METHODS AND MATERIALS

Two sets of experiments have been carried out - laboratory and pilot. Real effluent from a copper smelting plant in South America was used in the investigations. It was acidic (pH 0.5 - 1.0) with oxidation-reduction potential (Eh) in the range of 590-630 mV, and contained arsenic (800-1200 mg/L), copper (900–1000 mg/L), zinc (400-500 mg/L). Laboratory experiments were conducted in 1 L beakers, while in pilot experiment three consecutively hydraulically connected chambers were used, each one with the volume of 1.52 m^3.

The treatment was realized by immersing an electrochemical module directly into solution. The module consisted of number of interconnected anodes and cathodes. Cathodes were made of stainless steel, anodes - of stainless steel in the first stage; in the second and third treatment stage - of stainless or mild steel. The ratio of anode to cathode surface was 2 when the electrodes were made of stainless steel and the opposite when in the second and third stage mild steel was used. In the laboratory experiments distance between anode and cathode was 2 cm, in the pilot experiments - correspondingly scaled. An electronic gauge powered by an additional power source ensured cathode vibration in the range 100-800 Hz. Stabilized rectifiers with built-in A- and V-meters were used. Laboratory experiments were conducted batchwise with the applied voltage in the range of 2-4 V. Pilot experiments were carried out in flow mode with an average flow rate of around 3 m^3/h, while the average residence time in each of the three chambers was 20 min, at correspondingly scaled external voltage. Solutions' pH and Eh values were measured with combined pH and Eh electrodes and standard hand-held pH-mV-meter. To follow the process development aliquot samples from the liquid were taken at different times and analyzed by ICP-OES. The laboratory experiments were conducted repeatedly and stopped at different times. The material deposited on cathode and fallen on the bottom of the vessel was collected, washed, dried and analyzed - by XRD (BRUKER D2 Phaser, Cu/Ni radiation, λ=1.54184 Å, 30 kV, 10 mA, 2 theta - 5-70) and ICP-OES (after proper dissolution). The material obtained in laboratory experiments in the third stage when mild steel electrodes were used was subjected to United States Environmental Protection Agency's Toxicity Characteristic Leaching Procedure (TCLP) test (method 1311 – leaching with acetic acid buffer solution - pH 2.88 and 4.93).

RESULTS AND DISCUSSION

Averaged change of copper and arsenic concentration in treated effluent and in the solid phase with time is presented in Figure 1.

As it can be seen from the figure, when the anode is made of stainless steel the overall process can be divided into three stages: first stage of 10-15 min up to 20 min - of predominant copper deposition, second stage of around 20 min – mixed deposition of copper and arsenic compounds, and third stage - of predominant arsenic compounds deposition. The ICP analysis showed that material, obtained in the first stage contained 90-94% copper and 3.2-1.0% arsenic. The X-ray analysis of the same material revealed existence of Cu, small amount of cuprite Cu_2O and probably (less than 3%) metadomeykite - β Cu_3As. The solid material obtained in the second stage consisted of copper, and mixed arsenic compounds, such as

metadomeykite – Cu_3As, zinc olivenite $CuZn(AsO_4)(OH)$, tennantite $Cu_6[Cu_4(Fe,Zn)_2]As_4S_{13}$. Predominant deposition of arsenic compounds was observed in the third stage. Metadomeykite – Cu_3As, adamite $Zn_2(AsO_4)(OH)$, As-Fe-sulfides, elemental arsenic and some As oxides were determined in the material from the third stage. When the anode was changed to mild steel amorphous ferric arsenate and some scorodite - $FeAsO_4 \cdot 2H_2O$ was also found in the material from the second stage and amorphous ferric arsenate and scorodite predominated in the material from the third stage.

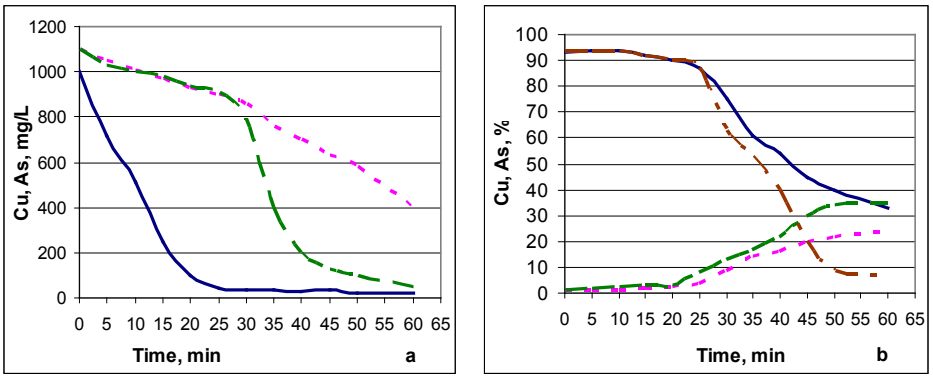

Figure 1. Averaged change of copper and arsenic concentration in treated effluent **(a)** and in the solid phase **(b)** with time; — Cu concentration, - - - As concentration - both when stainless steel anode is used; — — — As concentration, —·—·— Cu concentration -- both when mild steel anode is used

Having in mind the initial pH and Eh values of the water and the Pourbaix diagrams of the corresponding elements [13], it could be assumed that Cu^{2+} are the main copper species present in the effluent and the main arsenic species is H_3AsO_4. The main possible cathodic reactions are [14]:

$$Cu^{2+} + 2e^- \Leftrightarrow Cu^o,\ ^oE = 0.338\ V \quad (1)$$

$$2H^+ + 2E^- \Leftrightarrow H_2,\ ^OE = 0.000\ V \quad (2)$$

$$H_3AsO_{4(aq)} + 2H^+ + 2e^- \Leftrightarrow HAsO_{2(aq)} + 2H_2O,\ ^oE = 0.56\ V \quad (3)$$

$$H_3AsO_{4(aq)} + 3H^+ + 2e^- \Leftrightarrow AsO^+_{(aq)} + 3H_2O,\ ^oE = 0.550\ V \quad (4)$$

$$As^{3+} + 3e^- \Leftrightarrow As^o,\ ^oE = 0.300\ V \quad (5)$$

$$AsO^+ + 2H^+ + 3e^- \Leftrightarrow As^o + H_2O,\ ^oE = 0.254\ V \quad (6)$$

$$HAsO_{2(aq)} + 3H^+ + 3e^- \Leftrightarrow As^o + 2H_2O,\ ^oE = 0.248\ V \quad (7)$$

Reactions (5–7) can take place when the solution is exhausted with respect to Cu^{2+}, i.e. during the observed second and third stage of the process. Since in the solution present many species that can be reduced with potentials more positive of that of the hydrogen reduction, considerable hydrogen evolution is not expectable, and this was confirmed practically by visual lack of bubbles around cathode. Proceeding of reaction (1) explains the predominating copper deposition in the first stage. Most probably the formation of the materials deposited on cathode in the second and third stage (with stainless steel anode) results from electrode reactions (3–7) and some ongoing secondary processes.

Probably, sulfates available in the washing acids are partially reduced under the oxidation-reduction conditions achieved, may be, by some of the following reactions [14]:

$$SO_4^{2-} + 10H^+ + 8e^- \Leftrightarrow H_2S_{(aq)} + 4H_2O,\ ^oE=0.303\ V \quad (8)$$

$$SO_4^{2-} + 8H^+ + 8e^- \Leftrightarrow S^{2-} + 4H_2O,\ ^oE=0.149\ V \quad (9)$$

Formation of $H_2S_{(aq)}$ and S^{2-} could explain availability of sulfides found on electrodes.

When the electrolysis is carried out with practically indissoluble anode (stainless steel), the main anodic process is:

$$2H_2O \Leftrightarrow O_{2(g)} + 4H^+ + 4e^-,\ ^oE = 1.23\ V \quad (10)$$

Suppression of reaction (2) and proceeding of reaction (10) result in keeping the solution pH value practically unchanged and giving the possibility for the fluid reuse for flue gases washing, after separating the solid materials formed, i.e. copper and arsenic-bearing compounds.

Deposit created on cathode can be easily removed due to the cathode vibration and separated from the bottom of the vessel. Material bearing less than 3% As can be sent directly to metallurgy. The material deposited in the second and third stage could be used to obtain As.

When the electrolysis is carried out with dissoluble anode (mild steel) in the second and third stages, the main anodic processes are:

$$Fe^o - 2e^- \Leftrightarrow Fe^{2+},\ ^oE = -0.44\ V \quad (11)$$

$$Fe^o - 3e^- \Leftrightarrow Fe^{3+},\ ^oE = -0.037\ V \quad (12)$$

In this case the lack of reaction (10) and increased proceeding of reaction (2), due to the decreased Cu^{2+} concentration, lead to raising the pH of the solution. According to some authors [15], even in stationary conditions, the rate of Fe^{2+} oxidation by the oxygen dissolved in the solution can reach 88 – 67% in acidic medium (pH 3 – 4). In our case, the Fe^{2+} oxidation is facilitated also by the dissolved oxygen produced by reaction (10) in the first stage of the process and at least partially left into the solution. The formed Fe^{3+} ions can react with the available As species to form amorphous ferric arsenate that further could age to scorodite (following the generalized equation (13)).

$$H_2AsO_4^- + Fe^{3+} \Leftrightarrow FeAsO_4 + 2H^+ \rightarrow FeAsO_4.2H_2O \quad (13)$$

As a result, arsenic concentration in the treated effluent was decreased to 0.010-0.020 g/L. EPA test made for this solid material showed that no danger exists for pollutants' remobilization.

Based on the results from the laboratory experiments a flow-sheet was proposed for a method for the waste effluents treatment - Figure 2.

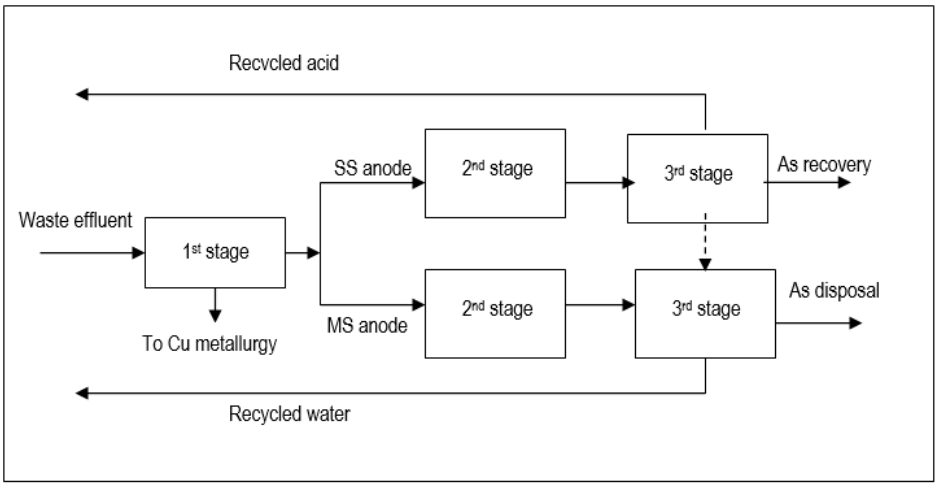

Figure 2. Generalized flow-sheet of the treatment proposed

As result of the pilot experiments it has been found that about 80% of the copper that present in the waste effluent can be recovered in a material suitable for sending to metallurgy. When stainless steel anode is used around 50% of the arsenic that present in the waste effluent can be recovered in a material suitable for further processing and the left can be treated with a mild steel anode. When mild steel electrodes were used the following concentrations of pollutants were achieved: Cu - 0.040, As - 0.085, and Zn - 0.094 g/L. The pH of treated effluent was raised to 6.4. An economic assessment of the operating costs (without working force inclusion) was made based on the results from pilot tests. It is assumed that the profit from selling the extracted copper will cover the capital costs. Briefly, by using the following data: consumed electricity 15 kWh per m^3 of treated effluent; mild steel loss - 3 kg/m^3; consumed electricity price 0.07 USD/kWh [16]; mild steel price - 600 USD per t [17]; and costs for disposal of solid As-bearing material of 0.0725 USD per pound (i.e. per 0.4536 kg) [18] the operating costs have been estimated at 4.50-5.00 USD/m^3 of treated waste effluent.

CONCLUSIONS

Treatment conditions can be found for: (a) Recovery of 75-80 % of copper and 50% of the arsenic dissolved in the effluent from flue gas washing - both in a state suitable for further utilization; (b) Decreasing significantly pollutants' concentration in treated effluent.

In spite of the necessity of additional investigations and technology adjustments, the following advantages of the treatment proposed are to be pointed out: (a) Method proposed is cheaper than most of the technologies applied at present; (b) Reagent-less copper recovery; Copper and arsenic reduced on electrodes can be easily removed from electrodes for further utilization thanks to the cathode vibration; The vibration system prevents passivation and operation stopping; (c) As a whole the technology is environmentally friendly: Arsenic can be immobilized as stable $FeAsO_4$ without introduction of additional ions in the treated effluent; Pollutants' concentration can be decreased practically by 90 ÷ 95%. Effluent's pH value can be considerably increased; (d) Stable solid As-bearing phase and sludge with small volume and mass are formed; (e) Parameters of the technology proposed can be easily controlled and operational adjustment can be made to counteract the affects of changes in effluent composition.

References

1. WWAP - United Nations World Water Assessment Programme, (2015) The United Nations World Water Development Report 2015: Water for a Sustainable World, UNESCO, Paris,
2. Communication from the Commission to the European Parliament and the Council - The raw materials initiative: meeting our critical needs for growth and jobs in Europe COM/2008/0699 final, 4.11.2008, Commission of the European Communities, Brussels,
3. Mochida, H., (1999) Removal of arsenic from wastewater containing sulfuric acid, Jpn. Kokai Tokkyo Koho JP 11 342,393 [99 342,393] (Cl.C03F1/461),
4. Misra, M., Nanor, J., 10 Feb 2000, Process for removal and stabilization of arsenic and selenium from aqueous streams and slurries, PCT Int. Appl. WO 00 06,502 (Cl C02F1/52),
5. Rubidge, G., (2004) Evaluation and optimization of selected methods of arsenic removal from industrial effluents, A dissertation for the Doctors Degree in Technology: Chemistry, Faculty of Applied Science at the Port Elizabeth Technikon, USA,
6. Anjum, S., Gautam, D., Gupta, B., Ikram, S. (2009) Arsenic removal from water: an overview of recent technologies. J Chem, 2(3), 7-52,
7. Nicomel, N., Leus, K., Folens, K., Van Der Voort, P., Du Laing, G. (2016) Technologies for arsenic removal from water: current status and future perspectives. International journal of environmental research and public health, 13(62), 1-24,
8. Dash, B., Mishra, G., Sanjay, K., Subbaiah, T. (2016) Arsenic Removal from Industrial Effluents through Ferric Arsenate Precipitation, Environmental Sci. Eng., 4: Water Pollution, 313-323,
9. Sato, T., Kato, M., Ogawa, M., (1996) Arsenic removal with electrolytic manganese dioxide adsorbents and adsorbents for arsenic removal, Jpn. Kokai Tokkyo Koho JP 08 267,053 [96,267,053] (Cl.C02F1/28),
10. Panayotov, V., Panayotova, M., Mast, E. (2000) Kinetics of purification of wastewater and washing acids from arsenic by means of an electrochemical treatment. In International symposium on processing of chemical and metallurgical industries wastes, Bhubaneswar, India, 271-275,

11. Balasubramanian, N., Kojima, T., Basha, C.A., Srinivasakannan, C. (2009) Removal of arsenic from aqueous solution using electrocoagulation. Journal of hazardous materials, 167(1-3), 966-969,
12. Wan, W. (2010) Arsenic removal from drinking water by electrocoagulation. All Theses and Dissertations (ETDs). 51, 1.http://openscholarship.wustl.edu/etd/511,
13. Zodi, S., Potier, O., Michon, C., Poirot, H., Valentin, G., Leclerc, J.P., Lapicque, F. (2011) Removal of arsenic and COD from industrial wastewaters by electrocoagulation. Journal of Electrochemical Science and Engineering, 1(1), 55-65,
14. Pourbaix, M. (1974) Atlas of electrochemical equilibria in aqueous solution. Franklin, J.A. - translator, National Association of Corrosion Engineers, Houston, Texas, USA.,
15. Bard, A., Parsons, R., Jordan, J. (1985) Standard potentials in aqueous solution. Marcel Dekker, Inc., New York, 200-206,
16. Alicilar, A., Meriç, G., Akkurt, F., Sendil, O.J. (2008) Air oxidation of ferrous ion in water. Int. Environmental Application & Science, 3(5), 409-414,
17. https://www.rockymountainpower.net/about/rar/ipc.html (accessed on 14.02.2019),
18. https://www.alibaba.com/showroom/mild-steel-price-per-kg.html (accessed on 14.02.2019),
19. The Ketchikan Municipal Code, Ordinance 1885, November 1, 2018. https://www.codepublishing.com/AK/Ketchikan/html/Ketchikan07/Ketchikan0716.html (accessed on 14.02.2019).

XIII International Mineral Processing and Recycling Conference
Belgrade, Serbia, 8-10 May 2019

University of Belgrade, Technical Faculty in Bor
Vojske Jugoslavije 12, 19210 Bor, Serbia
Tel. +381 30 424 555 Fax +381 30 421 078

SOLID WASTE MANAGEMENT IN THE GACKO MINE AND THERMAL POWER PLANT

Ivan Milojković [1, #], Zorana Naunović [2], Novak Pušara [3], Sreten Beatović [3]
[1]Jaroslav Černi Water Institute, Belgrade, Serbia,
[2]University of Belgrade, Faculty of Civil Engineering, Belgrade, Serbia
[3]M&TPP "Gacko", Gračanica, Gacko, Republic of Srpska,
Bosnia and Herzegovina

ABSTRACT – The protection of nature from pollution is a priority in the formation of a solid waste landfill within the mine. In the part of the solid waste landfill in the excavated area of SE "Gračanica" there are more natural aquifers from which the source of pure water springs. This water is pumped into a natural recipient. The basic requirement is that all industrial solid waste is collected and safely disposed of without pollution of the natural environment. Gacko is located at a high altitude and can be considered as a drinking water spring for downstream areas. The technology for depositing solid industrial waste - ash and slag must be such that, in a long period of time, secure protection of the natural environment is ensured.

Key words: landfill; solid waste; mine.

INTRODUCTION

In this paper, the objective is to satisfy the basic requirement for all industrial solid waste to be collected and safely disposed of without pollution of the natural environment in the Mine and Thermal Power Plant Gacko. At the end of the eighties, a new system was developed, the deposing of thick hydro-mixture, which was successfully tested at the Dražljevo landfill.

From the very beginning of the operation of the thermal power plant to the application of the current technology, so-called. "internal landing" the ash was deposited at the landfill "Dražljevo".

Gacko coal basin is located in the Gatac field in the northeastern part of Herzegovina. It extends over an area of about 40 km^2, in a typical karst region. The basin is divided into four parts according to the research phases: the West polje, the Central field, the East field and the South field (Roofing coal zone).

In world literature more ash classification can be found. The bases for carrying

corresponding author: ivan.milojkovic@jcerni.rs

out the classification are very different [2]. By origin, the ash is divided into organic and inorganic. Organic ash is the remainder of the combustion of the burning part of the charcoal, while the inorganic ash is the remainder of the mineral matter contained in the charcoal.

By allocation sites, the ash is generally distinguished (often referred to as flying ash) and slag. The ash from the boiler is affected by flue gases and separated on the path to the chimney by various dusting devices (electro filters, cyclones). The residue that falls to the bottom of the boiler into the water-filled sink (the water cools the slag and seals the boiler). The sudden transition of non-combustible substances from the high temperature zone (in the boiler temperature is 1000 ÷ 1100 ˚C) in low-temperature zones (water in the extinguisher has a temperature below 50 ˚C) represents a unique thermal treatment to produce a larger product of irregular shape and high porosity, called slag.

The quantity of ash and slag depends on the quality of the fuel used for the production of energy or heat, the conditions and regularity of the combustion process, as well as the operation of the solid residue extractor.

In TPP Gacko, this quantity amounts to about 1,200 tons of ash and slag daily, ie, 350,000 ÷ 400,000 t per year. Therefore, the dimensions of the problem of disposal of this supporting product are directly proportional to the installed power, the volume of electricity production and the quality of coal. The ash, at the Gacko Thermal Power Plant, is characterized by its specific characteristics due to the high proportion of total and active calcium. This high proportion of calcium and reactivity that is pronounced in the presence of water can create problems in the system, transport and ash disposal but may be the basis for a stable and reliable landfill to be formulated relatively easily and cheaply by adapting to the technology of preparing hydromixture. In recent times, exploitation of Krovinski coal packages,co-called ", it became clear that the ash Krovinski coal significantly differs from the ash of the main coal layer, by its chemical composition and silicate character.

METHOD AND EXPERIMENT

In this case, different methods of construction and preparation for the execution of landfills were applied, with the selection of an adequate location for waste disposal.

The preparation of the landfill was done in the following manner: before the disposal of ash and slag in stage 1 of cassete III, preparatory work on the surface were carried out. [5]. The preparatory work included the following:

- Removal of excess material with the planning of the terrain, after which a drainage system of groundwater was developed,
- Creation of a peripheral embankment,
- Installation of the marl layer,
- Installation of protective HDPE foil.

Field planning included the flattening of the surface using bulldozer so that no slope is greater than 20 °, and that the direction of all slopes is such that the waters gravitate toward the water tank on the PP16 and PP17 profiles. The excess material was loaded with a hydraulic excavator in trucks and deposited in space of phase 3

casete III or landfill-entry into field "B" (distance up to 600 m). For filling, the marl from the landfill (marl 7N put off by truck to the position PP9) with a mean distance of up to 700 m. The loading of marl was carried out by a hydraulic excavator / loader, and transport by trucks. All the marl that was buried after the plan was compacted with a roller. The entrance to phase 1 of the cassette III on the PP10 profile is at the angle K+898 m. The lowest angle of the PP16 profile is K+895 m.

The production of the peripheral embankment included the loading of marl with a hydraulic excavator / loader from the marl landfill (marl 7N placed by truck to the position PP9), transporting by trucks to phase 1 of the cassette III, planning marl with a bulldozer in layers up to 80 cm thick and compaction of marl by a roller to the modulus of compressibility Ms = 40 MPa. The average transport distance for the transport of marl was up to 700 m. The peripheral embankment was built around stage 1 of the cassette III by the circumference of the entire phase, except in part on cassete II. The lowest angle of the of this embankment is K+904 m. The width of the embankment crown is 8 m, and the edges are done with a slope of 1:3.

After making the peripheral embankment, a layer of marl was placed on the base of Phase 1 of Cassette III. The production of this layer includes the loading of marl by a hydraulic excavator / loader from the marl landfill 7N, transporting by trucks to stage 1 of the Cassette III, planning the marl with a bulldozer in layers of thickness 2∗50 cm and compaction of marl by roller to the compression module Mc = 40 MPa. The average transport distance for the transport of marl was up to 700 m.

Following the fully mechanically stabilized and properly prepared soil of Phase 1 of the Cassette III and the protective peripheral embankment, the HDPE geomembrane was installed. Before embedding the foil, excavation of the trenches was carried out along the peripheral embankment for the anchoring of HDPE foil. The material is deposited on the embankment next to the trench and the same is put back after the laying of the foil. The channel is a trapezoidal shape of a cross-section (1.50 + 0.60) h0.50h0.60 = 0.63 m^2. The channel axis is 2,00 m from the end of the slope with the edges towards the cassette with a radius R = 50 cm, so that the foil is properly bended. After placing the foil into the channel, filling with material from excavation is carried out by rolling. Foil welding is carried out by machines for this purpose with a double welding along with other activities for complete waterproofing.

RESULTS AND DISCUSSION

Thermal power plant Gacko had problems with the transport and deposit of ash from the first day of operation. Due to the ash characteristics being unknown, the initially designed system could not be used, so the thermal power plant improvised transport and ash disposal activities for several years. At the end of the 1980s a new system was developed, the depositing of thick hydro-mixture, which was successfully tested at the Dražljevo landfill. Different types of hydro-mixture and hydraulic transport have been considered and applied in a number of cases [1, 3, 4, 5, 6, 7, 8, 9, 10].

From the very beginning of the operation of the thermal power plant to the application of the current technology, so-called. The "internal landfilling" the ash was deposited at the landfill "Dražljevo". It was planned that the filling of this space should have been completed by the end of 1992 until the completion of the formation

of a new landfill at the inner landfill of the Gracanica PK should have been done. The deposit of ash at the Dražljevo landfill (Figure 1.) was irrational for several reasons: expensive and technologically complicated discontinous truck transport, large works on landfill preparation, complicated and unsafe environmental protection system, and extremely high costs of exploitation.

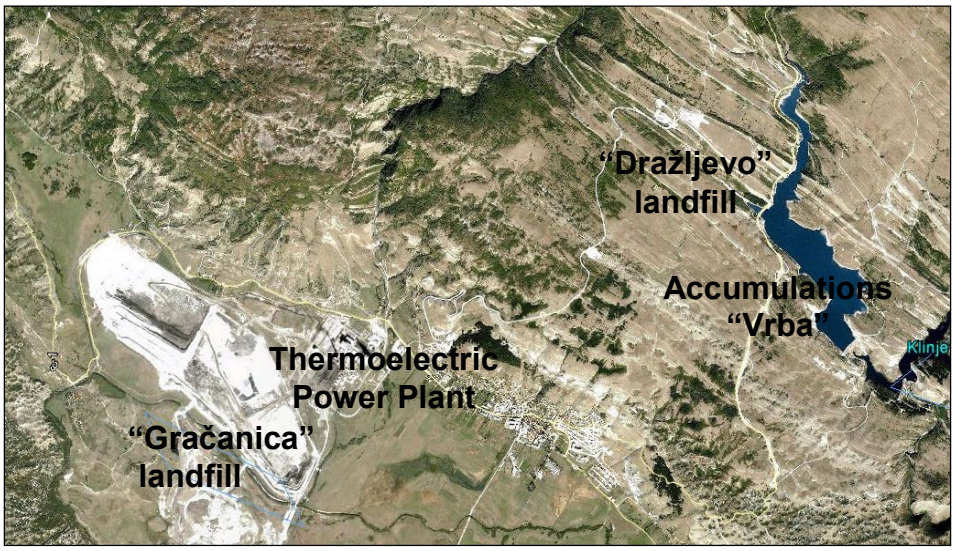

Figure 1. The location of ash dumps "Dražljevo" and "Gračanica"

From the very beginning of the operation of the thermal power plant to the application of the current technology, so-called. The "internal landfilling" the ash was deposited at the landfill "Dražljevo". It was planned that the filling of this space should have been completed by the end of 1992 until the completion of the formation of a new landfill at the inner landfill of the Gracanica PK should have been done. The deposit of ash at the Dražljevo landfill (Figure 1.) was irrational for several reasons: expensive and technologically complicated discontinous truck transport, large works on landfill preparation, complicated and unsafe environmental protection system, and extremely high costs of exploitation.

The landfill is poorly positioned, the distance from the thermal power plant is 6.5 km and the height difference is 210 m. It is located above the accumulations "Vrba" and "Klinje" (Figure 1.). This area is the primary water supply zone of the population located downstream, so any possible damage cannot be allowed, that is, it must be recognized and prevented in a timely manner. After the work on the facility, it is necessary to provide complete technical and ecological stability. The projected solutions for technical and biological recultivation should the facility should be integrated with the environment.

When examining potential ash disposal sites, the Gračanica surface excavation site always appeared as a possible landfill, but in the periods studied there was no free space [2]. After a long time, the choice of the location of the landfill, seems, in the long run, to be resolved directly in the area of the thermal power plant, it can be

freely stated for the entire operation cycle of TE Gacko. The problem now lies in the following: technical solution for the transport and deposing of ash, the in the mine from landfill and protection of the landfill from mine, protection of groundwater from the negative impact of deposited ash and protection of the landfill from the impact of surface and groundwater.

During expert discussions conducted at various levels, the positive factors of the ash dumping site "Gračanica" were emphasized, which are conditioned by the existence of a daily active excavation site:

- The carbon of the neogene is old and practically on the part of the site in the part "A" is watertight,
- The performed injection curtain and diaphragm protect the excavation site from the penetration of groundwater,
- The excavation site is protected from large waters in watercourses performed by regulatory works and embankments,
- Pumping systems for evacuating water from the mine are installed,
- All groundwaters occur, due to general geological and hydrogeological relations, on the profile V. S. "Srđevići", on which a safe and reliable system of control can be established.

Figure 2. Placing the waterproofing foil on the bottom of the cassette 2

The improvement of transport technology and the deposit of ash in the form of a rare hydromixture was done by moving to the so-called. "Thick hydro-mixtures". The given mass ratio between ash and water is 1:1, that is, the density of 50 % solid, which, converted to the mass is 1,482 kg /m^3. The calculation of the hydraulic transport set the following parameters:

- Mass flow of the solid phase Q = 150 t/h

- Volume flow of the pum P = 202 m^3/h
- Inner dieameter of the pipeline D = 200 mm
- Critical rate vk = 1.62 m/s
- Actual rate vs = 1.79 m/s
- Head of the pump (total) H = 28 m

In practice, the hydraulic transport parameters are not kept constant, but at optimum or acceptable limits by means of automatic control. The bottom of the landfill is coated with plastic foil (Figure 2) of high density polyethylene to protect the underground from flowing waters. Below the plastic foil, drainage is installed for evacuation of groundwater towards the water tank of the active excavation site (as unpolluted).

Table 1. Values of the amount of ash, water, pulp, amount of bound, unbound water and water difference after curing the ash

Pulp density-hydromixture	Ratio S:L	Amount of dry ash	The amount of water in the hydromesh	Quantity of hydromixture	Quantity of water bound with ash	The amount of unbound water	The difference of water
% Ч		t/h	m^3/h	m^3/h	m^3/h	m^3/h	m^3/h
33	1:2.03	150	304.55	356.99	225.00	79.55	+ 79.55
40	1:1.5		225.00	277.45	225.00	0	0
45	1:1.5		183.33	235.78	185.33	0	- 39.67
50	1:1		150.00	202.45	150.00	0	- 75.00
55	1:		122.72	175.17	122.72	0	- 102.28

Above the plastic foil drainage for accepting infiltration waters which are solved in the recirculation system (return water) is installed. Movement of the pipeline is done after the construction of each new floor. Depositing is carried out by drainage the hydro-mixture into the storage area. Today, the disposal of hydro-mixture is carried out in the storage area of Cassete 3 in accordance with the Project documentation. The cassette 2 was formed in the continuation of the cassette 1, towards the southern end of the slope of the part "A". The cassette 3 is made further down to the Cassete 2 to the south end slope of the pit, between the PP10 to PP17 profiles, and allows the ash to be disposed of until 2021, with an end point of 942 above sea level. Density corrections, in order to achieve better depositing, were carried out carefully taking into account the time of water bounding depending on the density of the pulp as well as the water balance in the ash disposal process (Table 1). The geomechanical characteristics of the deposited ash depend on the conditions

of depositing and the moisture content of the deposited ash. Characteristics are more favorable if depositing is done in layers of low thickness because of faster chemical reactions of "quenching" and curing of ash. The slag under the boiler is cooled in the exchanger and by the strip system taken out of the TEPP to the station. The slag is discharged by a loader under the station on the plateau for temporary acceptance. From this plateau, slag is periodically loaded and transported into trucks to the landfill. Slag planning is carried out by a bulldozer. Disposal of slag is done on the part of Cassete 3 in accordance with the Project documentation.

CONCLUSION

The deposit of the electro filter ash of the Gacko thermal power plant in the form of a stabilizer (formed by pelletization/consolidation) and depositing in a dry state proved inadmissible due to turbulent reactions in the process of wetting (caused by high participation of the active component) and only partial agglomeration, as well as due to the negative ecological implications on the environment. Both of these procedures have historically been examined at the "Dražljevo" landfill, and the practical results are negative. The observed problem was temporarily overcome by the discontinuous formation of thick hydro-mixtures at the location of the Dražljevo landfill, and positive experiences were used when the process of continuous preparation of the thick hydro-mixture for the deposit in the excavated area of the surface mine "Gračanica" was defined, where a geotechnical and ecologically stable landfill and ash was formed.

Acknowledgements:

The authors would like to thank the Ministry of Education, Science and Technological Development of the Republic of Serbia for their support in the realization of the project TR 37 014, thanks to which this research was conducted.

References

1. Anthony N. Tafuri, Water Supply and Water Resources Division, National Risk Management Research Laboratory, U.S. Environmental Protection Agency; Steve StoneEmil J., Dzuray Deborah, Meisegeier Anna Sara, Dahlborg Manuela, Erickson Logistics Management Institute McLean, VA 22102-7805, Contract GS-23F-9737H: Decision-Support Tools for Predicting the Performance of Water Distribution and Wastewater Collection Systems, National Risk Management Research Laboratory Office of Research and Development U.S. Environmental Protection Agency, Cincinnati, OH 45268, (2003),
2. Ash And Slag Disposal Technology On The Surface Mine "Gračanica" Gacko, Dependent Company "Gacko Mine and Thermal Power Plant" Stock Company GACKO (2014),
3. Ductile iron pipe systems for mining pipelines, TIROLER ROHRE GMBH, Innsbrucker Strasse 51, 6060 Hall in Tirol, Austria, (2015),
4. Jevtic, M., Milojkovic, I., Stojnic, N. (2011) Research of the performance of pulse electrohydrodynamics in blockage removal, Water Science &

Technology , 64 (1), 102-108,
5. Landfill Of Pepel "Cassete 3" Phase 1, Hydrotechnical Part, Mixed Holding "Electrical industry of the Republic of Serbian" - Parent Company, Stock Company Trebinje, Dependent company "Gacko Mine and Thermal Power Plant" Stock company, GACKO (2014),
6. Matos, R., Cardoso, A., Ashley, R., Duarte, P., Molinari, A., Schulz, A. (2003) Performance Indicators for Wastewater Services. International Water Association, London, UK,
7. Milojkovic, I., Marjanovic, Z., Ivetic, M., Ljubisavljevic, D., Jaksic, D. (2007) Preliminary Assessment of Performance Indicators for the Sewerage System in Belgrade. Proceedings of the 4th IWA Specialist Conference on Efficient Use and Management of Urban Water Supply, Jeju Island, Korea,
8. Milojković, I., Despotović, J., Karanović, I. (2015) Model for Maintenance of Sewerage System based on Inspection. IWA 7th Eastern European Young Water Professionals Conference, IWA - International Water Association Belgrade, Serbia, 538-543,
9. Milojković, I., Pušara, N., Beatović, S., Kröpf, R. (2015) Modeling of the pipe material selection for the protection of groundwater mining dumps. X International Symposium on Recycling Technologies and Sustainable Development, University of Belgrade, Technical Faculty in Bor, Bor, Serbia, 86-92,
10. Savić, A. D. (2009) The use of data-driven methodologies for prediction of water and wastewater asset failures. Centre for Water Systems, University of Exeter, North Park Road, Exeter, EX4 4QF, United Kingdom, Chapter published in the Springer book: Risk Management of Water Supply and Sanitation Systems.

XIII International Mineral Processing and Recycling Conference
Belgrade, Serbia, 8-10 May 2019

University of Belgrade, Technical Faculty in Bor
Vojske Jugoslavije 12, 19210 Bor, Serbia
Tel. +381 30 424 555 Fax +381 30 421 078

APPLICATION OF FLY ASH IN THE CONSTRUCTION INDUSTRY

Viktorija Bezhovska [1, #], Blagica Cekova [2], Filip Jovanovski [1]
[1]University St. Cyril and Methodius, Faculty of Technology and Metallurgy, Skopje, Republic of North Macedonia
[2]MIT University, Faculty of Environmental Resources Management, Skopje, Republic of North Macedonia

ABSTRACT – Fly ash is created as a waste product in the process of combustion of powdered coal in thermal power plants. The characteristics of electrophilic ash depend on the type of coal and the method of collecting the ash with electrostatic precipitators. Mainly it is fine, very fine, powdery material. In the construction industry, low and high construction, electrophilic ash is located in a wide and varied application and range of products, such as mineral puzzolnic supplement and cement replacement.
The main reasons for using this material as a mineral puzzolnic supplement are primarily of economic and environmental nature, because the ash is relatively inexpensive material and replaces the more expensive Portland cement. The fly ash is very useful for improving the strength and durability of concrete, the use of ash thus acquires technological feasibility, which of course encourages the production of cement with puzzolanic additives.

Key words: fly ash, cement, concrete, construction industry

INTRODUCTION

The electrophilic ash is generated as a waste product in the process of combustion of powdered coal in thermal power plants. In the production of electricity, after coal combustion (which depends on the operating temperatures in the thermal power plants usually occurs at temperatures between 900 and 1700 °C), most of the inorganic matter from coal remains ash. At the bottom of the furnaces in the small quantities, bottom ash is left, while the electrophilic ash is collected in electrostatic filters.

Therefore it is called electrophilic ash, but the name of fly ash is very common. In a hydraulic manner, the fly ash is deposited in landfills that are usually located in the immediate vicinity of the thermal power plants themselves. The amount of ash deposited by a thermal power plant, depending on its capacity, is measured in millions of tons per year. [1]

corresponding author: bezhovska@gmail.com

CHARACTERISTICS OF ELECTROPHILIC ASH

The characteristics of electrophilic ash depend on the type of coal and the method of collecting the ash with electrostatic precipitators. Mainly it is fine, very fine, powdery material.

The color of the ash can vary from dark gray to black, depending on the amount of Fe_2O_3 and carbon in the ash. The brighter the color, the lower the carbon content. The ash of bituminous coal is with brighter shades of gray which usually indicates a higher quality of ash.

Based on the very large number of literary data it can be concluded that ashes in their composition contain as the most important chemical compounds SiO_2, Al_2O_3, Fe_2O_3 and CaO and to a lesser extent MgO, MnO, Na_2O, K_2O, SO_3, N, C [3]. According to the classification of the American Society for Testing and Materials (ASTM C618), the electrolytic ash is classified as class F ash and ash class C (Table 1). Class F ash is generated by combustion of anthracite or bituminous coal, and the ash with class C is generated by combustion of lignite or subbituminous coals. The main difference between class F and class C ash is in the content of CaO, SiO_2, Al_2O_3, and FeO.

Class C = SiO_2 + Al_2O_3 + Fe_2O_3 ≥ 50 %;

Class F = SiO_2 + Al_2O_3 + Fe_2O_3 ≥ 70 %.

Table 1. Chemical composition of different classes of fly ash

Oxide	**Class F**		**Class C**	
%	Typical	ASTM C – 160	Typical	ASTM C – 160
SiO_2	36.9	/	41.36	/
Al_2O_3	18.1	/	21.83	/
Fe_2O_3	3.6	/	5.56	/
SiO_2 + Al_2O_3 + Fe_2O_3	58.6	70.0 min %	68.75	50.0 min %
CaO	2.85	/	19.31	/
MgO	1.06	/	3.97	/
SO_3	0.65	5 max %	1.42	5.0 max %
LOI	33.2	6.0	0.8	6.0
Humidity	0.14	3.0 max %	0.01	30 max %
Free alkaline	1.36	/	1.64	/

The mineral composition of fly ash includes inorganic constituents, crystalline and amorphous, and organic supplants originating from coal. The amorphous phase is characteristic of the electrophilic ash. The ash consists of fine, powder particles that are predominantly spherical, solid or hollow, and mainly glass (amorphous). The circular particles from which the glassy (amorphous) part of the ash is composed, are mainly thin, hollow, ceramic microspheres and are called censors (Figure 1, 2). The cenospheres in whose cavities are located smaller clumps of particles are called plerospheres (Figure 3) [2]. Carbon material in the ash is composed of angular particles. The size of the particles of the ash ranges from 0.01 to 100 μm in diameter, with the most common grain size of about 20 μm.

The specific gravity of the ash usually ranges from 2.1 to 3.0 kg/m^3, while its specific surface area (measured by the air permeability method can range from 170 to 1000 m^2/kg [3].

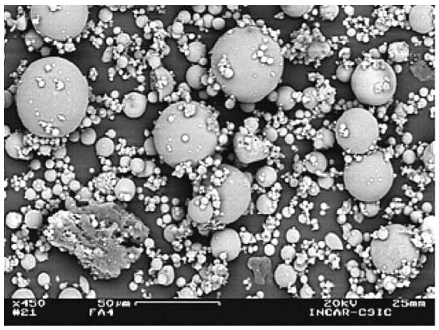

Figure 2. Amorphous phase, composed of alumino – silicate amorphous particles in the electrophilic fly ash

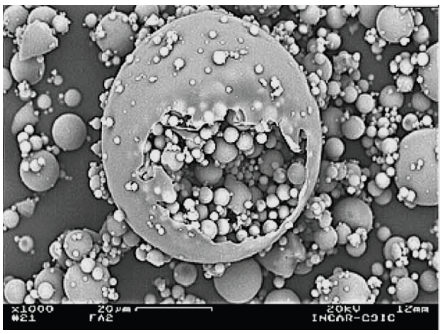

Figure 3. Alumo – silicate spherical particle

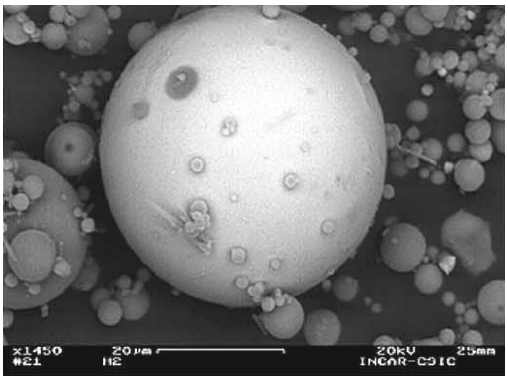

Figure 4. Alumo – silicate plerosphere in ash

USE OF FLY ASHES IN THE CONSTRUCTION INDUSTRY

In the construction industry, low and high construction, electrophilic ash is found in a wide and varied application and range of products.

ASH AS A PUZZOLANIC SUPPLEMENT FOR PORTLAND CEMENT AND CONCRETE

According to the standard definition, the puzzolanic materials are natural or artificial silicate, silico - aluminate, silico - carbonate substances or their combinations, which are finely ground, in the presence of water, react with dissolved calcium hydroxide, creating products that have hydraulic properties. The natural puzzolanic materials are mainly pyroclose rocks, as well as volcanic ash or tuffs, and in artificial puzzolanic materials are the slag from the high furnaces and, of course, the electrophilic ash from the thermal power plants.

The process of hydration of fly ash cement, such as the puzzolanic supplement, involves two processes: the hydration of cement clinkers and the puzzolanic reaction between fly ash and Ca $(OH)_2$, released by hydration of the cement clinker.
As is well known, the most important: xCH + yS + zH = CxSyHx + z cement clinker minerals are tricalcium silicate and dicalcium silicate, which make up about 75% of the clinker. In contact with water, these minerals form highly alkaline calcium silico hydrates (ratio s / s> 1.5) and large amounts of $Ca(OH)_2$. These calcium silico hydrates develop lower strength from low-grade calcium silico hydrates, and this leads to formation of concrete with lower strength and less durability.

The mechanism of the puzzolanic reaction consists in reacting SiO_2 from ash with Ca $(OH)_2$, building low-grade calcium silico hydrates. The puzzolanic reaction absorbs $Ca(OH)_2$ and in this way accelerates its re-creation by hydration of the clinker. This reaction does not alter the process of hydration of the cement clinker but complements it, because as a result, a lower content of $Ca(OH)_2$ is obtained, and a higher content of low-fat calcium silico hydrates (ratio c / s <1.5). In this way, an increase in the quality of the produced hydrates, and thus the properties of the so obtained concrete, is achieved. It has been shown that solid cement structures with the appellate develop lower hydration moisture in the early hydration period, greater mechanical strength and longer lasting than those of pure Portland cement. In addition to having better durability, these carbon surfaces have a higher resistance to sulfur corrosion, even when exposed to conditions in chemically aggressive environments, such as the impact of seawater [4].

The cement paste content that contains a certain percentage of ash depends largely on the size of the grain from the ash. These applications are mainly used fine grain ash with low content of non-combustible charcoal. The puzzolanic activity of ash also depends on the ratio of the crystalline and amorphous components to the ash. Better properties are obtained for finer particles of ash, which, besides cement paste, give greater density and homogeneity, also affect the increase in the number of nucleation centers leading to precipitation of the hydration products, which accelerates the reaction of hydration. The incompletely reacted ash particles also increase the density of the paste and because they fulfill the cavities formed. Very good compressive strength was shown by mortars obtained from ash-containing particles with a particle size below 10 μm.

The ash can be mechanically activated in order to lubricate the ash particles and obtain better results. It has been determined that grinding, that is, the mechanical activation of ash improves its percolation activity. With the addition of the pre-activated ash in the mortar, along with the cement, higher strengths, lower porosity and better resistance to the corrosion concrete thus obtained were also achieved.

USE OF FLY ASH AS A RAW MATERIAL COMPONENT FOR OBTAINING PORTLAND CEMENT

Ash can be used for these purposes because of its chemical composition, it is very similar to the clay component that is used for the preparation of raw materials in the cement industry, that is, consisting of SiO_2, Al_2O_3, Fe_2O_3 and CaO. Initially, about 10% of the ash was used as a substitute for the clay raw material due to the insufficiently well – defined technological procedure. The ash has been pumped directly into the furnace, since clinker was obtained with a very non-homogeneous composition, which caused grinding difficulties, as well as some other problems. However, when a modern system of precalcinators was installed in the late eighties and the procedure was improved, the ash completely replaced the clay component.

With the further advancement of these technologies, C_3S increased in clinker as well as fuel savings of 10 % due to incineration of unburned coal particles in the ash. It was found that by adding the ash, better reactivity of the raw materials was achieved. Clinker ash produced from ash showed better results in pressure strength tests compared to industrial clinker [5].

Some researchers went a step further in their research, using ash to obtain special types of cements such as white cement, sulphoaluminate cement, sulphoaluminate – white cement, expansive cement, etc.

PERFORMANCE AND DURABILITY OF FLY ASH PORTLAND CEMENT

Portland fly ash cement produces less heat of hydration compared to ordinary Portland cement. It is combined with lime released during the hydration of the cement, resulting in increased resistance to sulphate attack. Its use in cement is also known to reduce water permeability by prolonged watering. It is therefore particularly useful in hydraulic structures and other massive concrete structures. The use of Portland fly ash cement under tropical conditions with an ambient temperature of 30 °C and higher is no problem. However, in hot and dry conditions with an atmospheric temperature above 40 °C, the following concreting problems may occur:

Adjustment of acceleration: The setting speed of the concrete increases at high temperatures. That's why it reduces the strength of the cold joints.

Undercutting the strength: At high temperatures, the amount of water for mixing the same level of processing increases. Therefore, it reduces the strength of the cool concrete.

Rapid evaporation of water: Moisture retention is difficult to hydrate cement in concrete due to rapid evaporation of water during the drying period at high temperature.

Increased cracking tendency: rapid evaporation of water at high temperatures can cause cracks in partially hardened concrete.

Data on the binding time (Table 2) and the development of hardness, obtained at 27 ± 2 °C and 10 ± 2 °C, show that the hydration kinetics and solidity development in Portland fly ash cement is slower than in ordinary Portland cement [6]. For this reason, the use of Portland cement with additional fly ash requires certain additional measures, such as the extended moisture period in order to obtain a satisfactory level of development of strength, especially in conditions of low environmental

temperature prevailing in the winter season. In extreme weather conditions with an ambient temperature of 10 °C or less, the compressive strength, just like that of the typical Portland cement at 28 days, cannot be achieved even with an increase in moisture by 2 to 3 times or more. In such extreme weather conditions, the Portland cement with flying ash should not be used.

Table 2. Binding time of concrete at 27 °C and 10 °C

Type of cement	Specific surface (Blaine), [cm²/g]	Binding time			
		27 °C		10 °C.	
		Initial	Final	Initial	Final
Ordinary Portland Cement	3360	155	215	175	285
Fly Ash Portland Cement	3327	225	350	440	620

HEAT RESISTANCE OF PORTLAND FLY ASH CEMENT

Hydrated Portland cement contains a huge amount of calcium hydroxide, Ca $(OH)_2$, which dehydrates to calcium oxide (CaO) between 500 – 600 °C. During cooling and exposure to moist air or moisture, CaO is rehydrated to Ca $(OH)_2$ with a volume of 97 %. This leads to the formation of cracks or complete disturbance of the cement that has maintained a high temperature without real disintegration. The heat resistance of Portland cement is very poor.

Reshi and Garg [6] assessed the heat resistance of the Portland fly ash cement (fly ash content 20 and 30 mass percent) compared to ordinary Portland cement by studying the effect of: heating up to 1200 °C of the hardness of the pressure and the free CaO content and alternative heating and exposure to high humidity.The cubes made of Portland fly ash cement and heated to 900 and 1000 °C showed excellent dimensional stability when subjected to alternative heating cycles and exposure to high humidity (over 90 % relative humidity), in sharp contrast to cubes made from an ordinary Portland cement, which was broken and decomposed. Portland fly ash cement 20 to 30 % mass. Fly ash, possesses good heat resistance and dimensional stability when exposed to high temperatures followed by high humidity or moistening (Table 3).

Table 3. Content of free CaO in Portland fly ash cement heated to various temperatures

Cementitious materials	Heating temperature, °C	Content of free CaO, %
Portland cement	800	5.067
	900	5.067
	1000	5.079
	1200	5.071
Portland fly ash cement (20 % fly ash)	800	1.298
	900	0.779
	1000	0.260
	1200	0.259
Portland fly ash cement (30 % fly ash)	800	1.284
	900	0.649
	1000	0.247
	1200	0.241

CONCLUSION

Fly ash is created as a waste product in the process of combustion of powdered coal in thermal power plants. The characteristics of electrophilic ash depend on the type of coal and the method of collecting the ash with electrostatic precipitators. Mainly it is fine, very fine, powdery material.

In the construction industry, low and high construction, electrophilic ash is located in a wide and varied application and range of products, such as mineral puzzolanic supplement and cement replacement. The main reasons for using this material as a puzzolanic supplement are primarily of economic and environmental nature, because the ash is relatively inexpensive material and replaces the more expensive Portland cement. The fly ash is very useful for improving the strength and durability of concrete, the use of ash thus acquires technological feasibility, which of course encourages the production of cement with puzzolanic additives.

References

1. Singh M., Garg M.: ''Cementitious binder from fly ash and other industrial wastes'', 1999., Cement and Concrete Research, 29, 3, 309 – 314,
2. Fernandez-Jimenez A., Palomo A.: ''Characterization of fly ashes. Potential reactivity as alkaline cements'', 2003., Fuel, 82, 18, 2259-2265,
3. Sokol F.V., Kalugin V.M., Nigmatulina E.N., Volkova N.I., Frenkel A.E., Maksimova N.V.: ''Ferrospheres from fly ashes of Chelyabinsk coals:chemical composition, morphology and formation conditions'', 2002., Fuel, 81, 7, 867-876,
4. Saraswathy V., Muralidharan S., Thangavel K., Srinivasan S.: ''Influence of activated fly ash on corrosion – resistance and strength of concrete'', 2003., Cement and Concrete Composites, 25, 7, 673-680,
5. Bhatty, J.I., Gajda J., Miller F.M., ''Commercial Demonstration of High-Carbon Fly Ash Technology in Cement Manufacturing'', 2003, International Ash Utilization Symposium, Center for Applied Energy Research, University of Kentucky, Paper no. 38,Shoodeep L. Shakar, Ghosh S. N., “Mineral admixtures in cement and concrete volume 4 shondeep i. sarkar s.n.ghosh”, Volume 4, 1993.

XIII International Mineral Processing and Recycling Conference
Belgrade, Serbia, 8-10 May 2019

University of Belgrade, Technical Faculty in Bor
Vojske Jugoslavije 12, 19210 Bor, Serbia
Tel. +381 30 424 555 Fax +381 30 421 078

THE ENERGETIC POTENTIAL OF DIFFERENT BIO-WASTE SAMPLES COLLECTED FROM AN INTEGRATED WASTE MANAGEMENT PLANT

Agapi Vasileiadou [1, 2, #], S. Zoras [1], A. Dimoudi [1], A. Iordanidis [2], V. Evagelopoulos [2]

[1]Democritus University of Thrace, Faculty of Engineering, Department of Environmental Engineering, Xanthi, Greece

[2]Western Macedonia University of Applied Sciences, Department of Geotechnology and Environmental Engineering, Kila, Kozani, Greece

ABSTRACT – The combustion behavior of Municipal Solid Waste (MSW) is evaluated in this study in order to assess their potential for energy recovery. Different types of MSW (i.e. compost-like outputs, green waste, food waste, organic fraction of MSW), as well as lignite sample were collected from the Western Macedonia region, northern Greece. Proximate analysis (moisture, ash, volatile matter and fixed carbon) and the calorific value determination were performed. Experimental results indicate that is efficient to utilize these types of solid wastes as a potential fuel in an incineration process, showing thermal characteristics comparable to lignite. It is evident from the proximate analysis and the calorific value determination that all the studied waste samples have adequate combustible matter and can be used for energy recovery through the thermal treatment process.

Key words: compost, combustion, proximate analysis, calorific value, MSW.

INTRODUCTION

Waste management has been recognized as one of the most pressing problems in Greece, suffering of a low level of organization and relying predominantly on semi-controlled landfills. In an attempt to reduce the environmental impacts of biodegradable wastes, mechanical biological treatments (MBTs) are being used as a waste management process in many countries. MBT plants attempt to mechanically separate the biodegradable and nonbiodegradable components. The nonbiodegradable components are then sent for reprocessing or landfilled, whereas the biodegradable components are reduced in biological content through composting or anaerobic digestion, leaving a compost-like output (CLO) [1].

In the European Union (EU), the amount of municipal waste generated in 2017

corresponding author: agvasileiadou@gmail.com

amounted to 487 kg, slightly increased by 1.44 % compared to 480 kg per capita in 2016 [2-3]. In Greece more than 80 % of MSW was landfilled in 2010 and consequently the target of 75 % reduction of biodegradable municipal wastes (BMW) by 2010 of the EU Landfill Directive could not be fulfilled, despite the 4-year derogation period granted to Greece [4]. Moreover, in 2014, the percentage of MSW landfilled in Greece remained at the same level (81 %) [5].

Waste combustion is gaining importance in European countries, mainly because of environmental protection and resource management [6]. Given that the average calorific value of municipal solid waste (MSW) is approximately 10 MJ/kg, it seems logical to use waste as a source of energy [7]. Waste-to-Energy is an established and well proven worldwide option for municipal solid waste treatment, motivated both by necessity to minimize the environmental impacts of landfilling and the aim to increase the share of renewable energy [8-9]. European Directive 2008/98/EC [10] classifies Waste-to-Energy as energy recovery operation of the conceptual hierarchy of the waste management options. Directives 2008/98/EC, 2000/76/EU [11] and 2010/75/EC [12] form a common ground for a Waste-to-Energy motivation.

The main goal of this paper is to evaluate the thermal behavior of MSW through the proximate analysis (moisture, ash, volatile matter and fixed carbon) and gross calorific value determination and compare it with the relevant energetic performance of a domestic lignite sample.

MATERIAL AND METHODS

Four types of municipal solid wastes (MSW) samples, i.e. compost-like outputs, green waste, food waste, organic fraction, were collected from the recently launched (2017) Western Macedonia integrated waste management plant (EDADYM, Ellactor group). A lignite sample from the nearby lignite mines of the Western Macedonia area was also collected. All samples were properly prepared. All the waste material and lignite samples were firstly air-dried for two weeks. Afterwards, all samples were ground to size less than one millimetre (< 1 mm). Eventually, all samples were dried in an oven at 80 °C for 24 hours. Samples were proceeded for proximate analysis (moisture, ash, volatile matter and fixed carbon) and determination of gross calorific value.

Proximate analysis was performed with LECO TGA 701 device, based on ASTM D7582 standard [13]. The determination of gross calorific value was made with the LECO AC-500 isoperibol bomb calorimeter, using the ASTM D5865-13 standard [14].

RESULTS AND DISCUSSION

Combustion characteristics of raw materials

Proximate analysis and gross calorific value (GCV) of samples are shown in Table 1. Green waste sample and lignite sample contains higher moisture content (8.98 wt % and 6.33 wt % respectively) compared to compost-like outputs sample (4.95 wt %), food waste sample (3.00 wt %) and organic fraction of municipal solid waste sample (2.53 wt %). The ash content is 38.90 wt % in lignite sample, followed by 26.77 wt % in compost-like outputs sample, 17.62 wt % in green waste sample and 4.66 wt % in food waste sample. The range of volatile matter is between 42.93 wt %

(lignite sample) and 78.06 wt % (food waste sample). All the analysed samples contain a greater proportion of volatile matter than the lignite sample. Fixed carbon content ranges from 1.53 wt % (green waste sample) to 14.29 wt % (food waste sample). The samples of organic fraction of municipal solid waste and lignite showed values around 12 wt % while the compost-like outputs sample revealed a value of 3.17 wt %. It is known that wastes have high volatile matter and low fixed carbon values [15-16]. Several authors analyzed similar samples and obtained comparable results [17-19]. Since the good quality fuels have high volatile matter and adequate fixed carbon content, food waste sample, and organic fraction of municipal solid waste sample in our study, having volatile matter more than 70 wt % and fixed carbon approximately 13 wt %, can be considered as those with the optimum thermal performance.

Table 1. Proximate analysis (moisture, ash, volatile matter and fixed carbon) and gross calorific value (GCV) of the lignite and MSW samples (LIG: lignite, CLOF: compost-like outputs, GNW: green waste, FDW: food waste, OFMSW: organic fraction of municipal solid wastes). All values are in wt %, except GCV (MJ/kg)

SAMPLES	Moisture	Ash	Volatile Matter	Fixed carbon	GCV
	(%)	(%)	(%)	(%)	(MJ/Kg)
LIG	6.33	38.90	42.93	11.84	12.68
CLOF	4.95	26.77	65.11	3.17	20.13
GNW	8.98	17.62	71.88	1.53	12.23
FDW	3.00	4.66	78.06	14.29	18.87
OFMSW	2.53	11.19	73.89	12.40	16.62

Figure 1 illustrates the proximate analysis (moisture, ash, volatile matter and fixed carbon). It is observed that all analyzed samples reveals lower percentage of ash than lignite sample. All analyzed waste samples have also higher percentage of volatile matter than lignite sample.

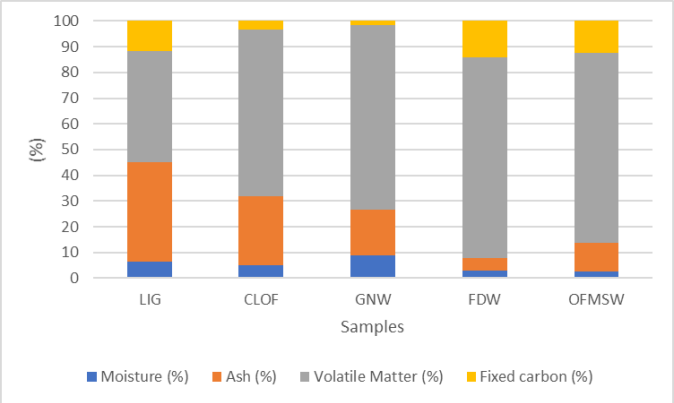

Figure 1. Proximate analysis of the of the lignite and MSW samples (LIG: lignite, CLOF: compost-like outputs, GNW: green waste, FDW: food waste, OFMSW: organic fraction of municipal solid wastes). All values are in wt %

The gross calorific value (GCV) of the samples ranges between 12.23 MJ/kg (green waste sample) and 20.13 MJ/kg (compost-like outputs sample). The green waste and lignite samples have almost the same calorific value (about 12.50 wt %). The food waste sample reveals a value of 18.87 MJ/kg and the organic fraction of municipal solid waste reveals a value of 16.62 MJ/kg. Consequently, compost-like outputs, food waste and organic fraction of municipal solid wastes samples have higher GCV than lignite sample. (Figure 2).

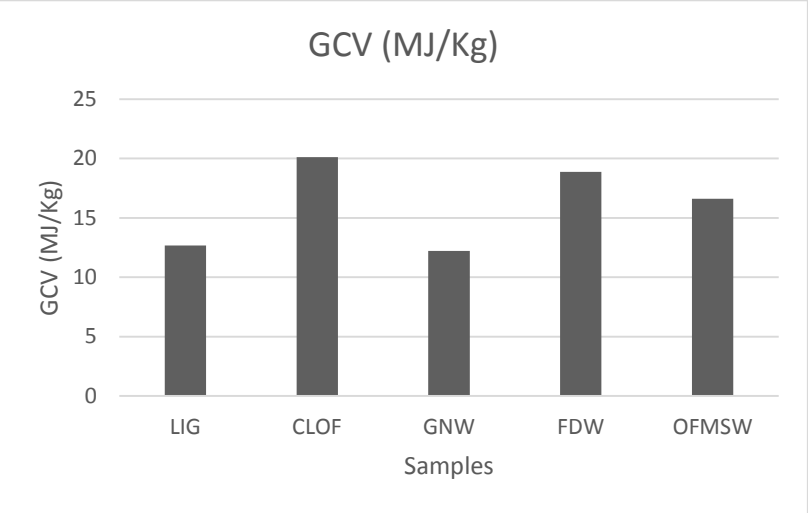

Figure 2. Gross Calorific Value of the lignite and MSW samples (LIG: lignite, CLOF: compost-like outputs, GNW: green waste, FDW: food waste, OFMSW: organic fraction of municipal solid wastes)

It is evident from the proximate analysis and the calorific value determination that all the studied waste samples have adequate combustible matter and can be used for energy recovery through the thermal treatment process.

CONCLUSION

Gross Calorific Value and Proximate analyses were performed on a lignite sample and several bio-waste samples (compost-like outputs, green waste, food waste, organic fraction of municipal solid wastes), collected from an integrated waste management plant. All samples have higher GCV values than the lignite sample, except green waste that exhibits similar GCV values, but has considerably lower ash value. The highest calorific value was determined for the compost-like output sample.

Acknowledgements:

This research is co-financed by Greece and the European Union (European Social Fund- ESF) through the Operational Programme «Human Resources Development, Education and Lifelong Learning» in the context of the project “Strengthening Human

Resources Research Potential via Doctorate Research" (MIS-5000432), implemented by the State Scholarships Foundation (IKY). We are also indebted to the EDADYM company for providing the waste samples and chemical department of Kardias Steam Power plant, in Greece for giving us access to their laboratory equipment.

References

1. Donovan, S. M., Bateson, T., Gronow, J.R., Voulvoulis N. (2010) Characterization of compost-like outputs from mechanical biological treatment of municipal solid waste. Journal of the Air & Waste Management Association, 60 (6), 694-701,
2. Eurostat. (2019) Municipal waste statistics. https://ec.europa.eu/eurostat/statistics-explained/index.php/Municipal_waste_statistics (accessed February 18, 2019),
3. Eurostat. (2016). 480 kg of municipal waste generated per person in the EUhttps://ec.europa.eu/eurostat/web/products-eurostat-news/-/DDN-20180123-1 (accessed January 28, 2019),
4. Bakas, I., Milios, L. (2013) Municipal waste management in Greece European Environment Agency (EEA),
5. Eurostat. (2016) Municipal solid waste (MSW) management and selected policy instruments in European countries, 2001-2015 https://www.eea.europa.eu/ themes/waste/municipal-waste/municipal-waste-management-across-european-countries/table -3-1-municipal-solid (accessed January 20, 2019),
6. Wilson, D. C. (2007) Development drivers for waste management Waste Management & Research 25, 198-207,
7. Malinauskaite, J., Jouhara, H., Czajczyńska, D., Stanchev, P., Katsou, E., Rostkowski, P., Thorne, R. J., Colón, J., Ponsá, S., Al-Mansour, F., Anguilano, L., Krzyżyńska, R., López, A., Vlasopoulos, I. C., Spencer, N. (2017). Municipal solid waste management and waste-to-energy in the context of a circular economy and energy recycling in Europe, Energy, 141, 2013-2044,
8. Athanasiou, C. J., Tsalkidis, D. A., Kalogirou, E., Voudrias, E. A. (2015) Feasibility analysis of municipal solid waste mass burning in the Region of East Macedonia - Thrace in Greece. Waste Management and Research, 33 (6), 561-569,
9. Gohlke, O. (2009) Efficiency of energy recovery from municipal solid waste and the resultant effect on the greenhouse gas balance. Waste Management and Research, 27, 894-906,
10. European Commission (2008). Directive 2008/98/EC on Waste and repealing certain directives (Waste Framework Directive). Official Journal of the European Union L312, 3-30,
11. European Commission (2000). Directive 2000/76/EC on the incineration of waste. Official Journal of the European Union L332, 1-111,
12. European Commission (2010). Directive 2010/75/EC on industrial emissions (integrated pollution prevention and control) Text with EEA relevance. Official Journal of the European Union L334, 17-119,

13. ASTM D 7582-15 (2015). Standard Test Methods for Proximate Analysis of Coal and Coke by Macro Thermogravimetric Analysis, ASTM International, West Conshohocken, PA,
14. ASTM D 5865-13 (2013). Standard Test Method for Gross Calorific Value of Coal and Coke, ASTM International, West Conshohocken, PA,
15. Varol, M., Atimtay, Aysel, B., Olgun, H. (2010) Investigation of co-combustion characteristics of low quality lignite coals and biomass with thermogravimetric analysis. Thermochimica Acta, 510, 195-201,
16. Vamvuka, D., Sfakiotakis, S. (2011) Combustion behaviour of biomass fuels and their blends with lignite, Thermochimica Acta, 526, 192-199,
17. Casado, R. R., Rivera, A. J., García, B. E., Cuadrado, E. R., Llorente, F. M., Sevillano, B. R., Delgado, P. A. (2016) Classification and characterisation of SRF produced from different flows of processed MSW in the Navarra region and its co-combustion performance with olive tree pruning residues. Waste Management, 47, 206-216,
18. Athanasiou, C. J., Tsalkidis, D. A., Kalogirou, E., Voudrias, E. A. (2015) Feasibility analysis of municipal solid waste mass burning in the Region of East Macedonia - Thrace in Greece, Waste Management & Research, 33, 561-569,
19. Vamvuka, D., Sfakiotakis, S., Saxioni, S. (2015) Evaluation of urban wastes as promising co-fuels for energy production - A TG/MS study, Fuel, 147, 170-183.

XIII International Mineral Processing and Recycling Conference
Belgrade, Serbia, 8-10 May 2019

University of Belgrade, Technical Faculty in Bor
Vojske Jugoslavije 12, 19210 Bor, Serbia
Tel. +381 30 424 555 Fax +381 30 421 078

DETERMINATION OF THE CAVITATION RESISTANCE OF GLASS-CERAMIC SAMPLES BASED ON RAW BASALT AND INDUSTRIAL WASTE RAW MATERIALS FOR USE IN METALLURGY

Marko Pavlović [1, #], Marina Dojčinović [1], Ljubiša Andrić [2], Dragan Radulović [2], Milan Petrov [2]
[1]University of Belgrade, Faculty of Technology and Metallurgy, Belgrade, Serbia
[2]Institute for Technology of Nuclear and Other Mineral Raw Materials, Belgrade, Serbia

ABSTRACT – The paper presents the results of the investigation of cavitation resistance of glass-ceramics based on basalt rocks from the Vrelo Kopaonik deposit and various waste industrial raw materials. The aim was to determine the possibility of using glass-ceramics as a substitute for metallic materials in the production of structural elements of mining and metallurgy equipment. The ultrasonic vibration method (with a stationary samples) was used for cavitation resistance testing, according to the ASTM G-32 standard. A change in the sample mass in function of the cavitation time was monitored for the evaluation of cavitation resistance. The level of degradation of the surface of the sample was quantified using the image analysis. The change in the morphology of the sample surface with the test time was followed by scanning electron microscopy.

Key words: basalt, cavitation resistance, mass loss, image analisis, constructions elements.

INTRODUCTION

Basalt is a cheap and wide spread raw material, which by melting and a certain cooling treatment can be used for the production of glass and glass ceramics with specific mechanical properties, high strength and low abrasiveness [1, 2]. It use for synthesis of new materials and products such as basalt wool, basalt fibers, armature, composite materials, which are used for the production of parts and equipment in the machinery industry, automotive industry, shipbuilding [3-6]. The basic properties of basalt, which influenced his choice for exploring cavitation resistance and assessing the possibilities of application in engineering practice, as substitutes for metallic materials, were: melting point 1300-1400 °C; high hardness 6.5 - 7 Mosh scale; density 2460 - 2960 kg/cm^3; wear resistance; high resistance to acids, alkalis and heat; ecological and hygienic quality [7]. Cavitation is a phenomenon that

corresponding author: pavlovic.marko38@gmail.com

comprises formation, growth and implosion (collapse) of bubbles in a liquid flow. During cavitation, when the bubbles collapse, high temperature and pressure (approximately 5000 °C and 1000 bar) develop locally in the a very short time (less than 1 μs) [8-10]. According to the literature data, in the conditions of cavitation stresses, the most common are metallic materials (steel and aluminium alloys), while ceramic materials are used less. There are no data on the examination and application of basalt in conditions of cavitation loads. It was also a motive to examine the cavitation resistance of basalt for the purpose of application for the construction of parts of equipment in mining and metallurgy.

MATERIAL AND METHODS

Olivine-pyrroxene basalt from the Vrelo-Kopaonik deposit (sample design: RB) is used as the starting material for the synthesis of samples for testing. Basalt was crushed and ground on size 10-15mm, mixed with 10 % of industrial waste materials (metallurgical slag and waste from the ceramic industry) and melted at a temperature of 1250 °C. Test samples, plate of dimensions (200x150x15) mm are cast in sandy molds. In order to reduce the internal stresses of the cast test plates, they are thermally treated according to the regime: heating at a temperature of 850 °C/2.5 h and cooling in a furnace to room temperature. Samples for testing of cavitation resistance of dimensions (10x10x10) mm were cut from the plates. Designation of glass-ceramic sample: CB. Table 1 shows the composition of the starting materials and the obtained glass-ceramics.

Table 1. Chemical composition of raw materials and obtained glass-ceramics (%)

Compound	Raw basalt	Industrial waste	Basalt glass-ceramic (CB)
SiO_2	56.21	27.98	51.15
Al_2O_3	18.61	3.50	20.90
Fe_2O_3	1.15	9.98	2.80
FeO	2.97	3.10	4.90
MgO	3.40	0.98	3.55
CaO	7,78	5.90	9.20
Na_2O	4.73	1.10	3.45
K_2O	3.37	0.80	2.50
Cu+Zn+Pb	-	2.49	1.50

Basalt samples were analyzed using X-ray diffractometer, "Philips" model PW-1710. The microstructure of the samples was characterized with the scanning electronic microscope JEOL model JSM 6610 LV. In order to improve conductivity, the sample was vapoured with gold powder.

The ultrasonic vibration method (with a stationary samples) was used for cavitation resistance testing of samples. Characteristic parameters for this method (vibration frequency, amplitude at the top of the concentrator, distance between the tested sample and concentrator, water temperature, water flow) were selected according to ASTM G-32 standard and previous works [10, 11]. The water in the water bath cools the sample and keeps its temperature constant. A constant flow of water creates a pressure field that stimulates the implosion of cavitation bubbles on the surface of the test sample. In this way, the test sample is not exposed to

mechanical strains during the test. Selected sample time (min) is: 15; 30; 60; 120. After each test interval, the mass loss of the sample was measured by an analytical balance of accuracy of 0.1 mg. Samples were photographed before, during and at the end of the test. The formation and development of damage to the surface of the tested samples during the cavitation test was followed in correlation with the structure and properties of the refractory materials. Software sample analysis was performed in Image Pro Plus [12]. The morphology of the damaged surfaces was analyzed by a scanning electron microscope (SEM) Joel JSM 6610 LV. The level of degradation of the sample surface P/P_0, % is determined, where P_0 represents the surface of the sample without defects, while P represents the surface of the samples with damages. The number of damage caused by the surface in the form of shallow pits, N_p, and the average surface of the formed pits P_{av}, mm^2 were determined. All obtained results of damage to the surface of the samples at the time of the cavitation activity are illustrated by the diagrams.

RESULTS AND DISCUSSION

The mineral composition of a glass-ceramics based on basalt (CB) is shown on Figure 1. The most prevalent minerals are pyroxene, basic plagioclases and olivines. In Figure 2, SEM microphotograph of the CB samples are shown before the cavitation process. The basic structure of the samples is cryptocrystalline with the appearance of fine crystals. Bubbles of different sizes, which are filled with gas or glass are present in the structure. The present bubbles on the surface of the samples cause surface roughness and the appearence of pits. During the cavitation test, the changes of the present bubbles contained in the basalt base, as well as the present pits on the surface of the sample CB were monitored.

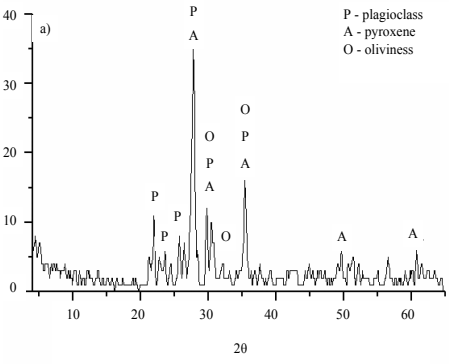

Figure 1. XRD of CB sample

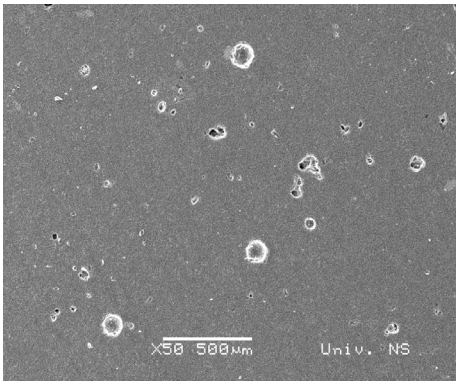

Figure 2. SEM microphotograph of CB sample

Figure 3 shows the results of the study of the formation and development of damage under the effect of cavitation for samples RB and CB using image analysis and Image Pro Plus software.

From figure 3a, it can be seen that the weight loss is expressed in samples of RB. A small weight loss of CB samples and a small level of surface damage under the effect

of cavitation is characteristic of CB samples, figure 3a, b. The number of pits formed on the surface of the CB sample is considerably smaller than the formed pits in the sample RB, figure 3d. The average surface of the formed pits is significantly lower in the CB sample compared to the RB samples, figure 3c. At the end of cavitation exposure damage to the surface of CB sample is 12 %, while damage to RB samples is greater than 35 %, shown in Figure 3b. This corresponds the results of determining the average surface of the formed pits, Pav shown in Figure 3c.

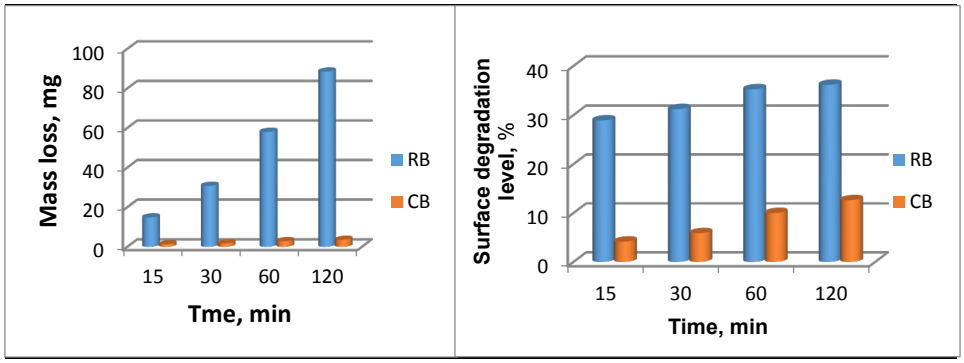

a) Mass loss b) Surfaces degradation level

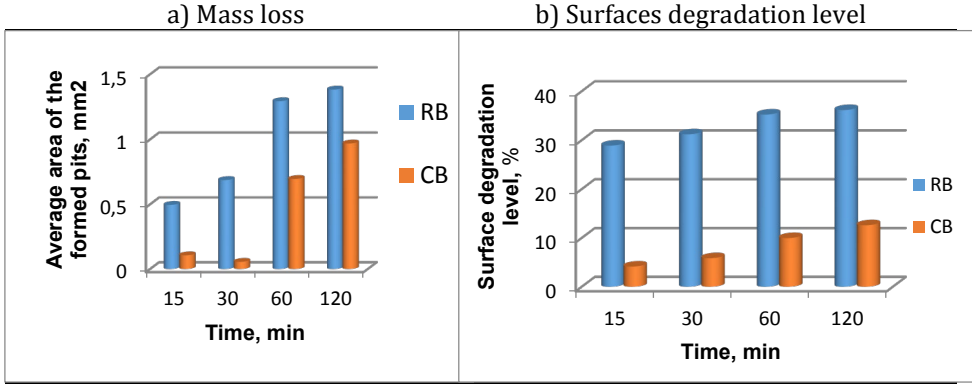

c) Average area of formed pits d) Number of formed pits

Figure 3. The formation and development of damage under the effect of cavitation for samples RB and CB

Figure 4 shows the appearance of the sample surface and profile lines obtained using the red filter, using Image Pro Plus software.

Calculated cavitation velocity as the ratio of total mass loss in relation to the time of cavitation is: for samples RB v=0.708 mg/min, while for CB samples v=0.058mg/min. From the results of the measurement of mass loss during the effect of cavitation and the result of image analysis, it can be concluded that glass-ceramics samples based on basalt have a satisfactory resistance to the effect of the cavitation.

The formation of pits is often found near the bubbles that exist in the basic mass of basalt. Further development of damage occurs at a low speed so that there is no danger of a greater loss of mass from the surface of the formed pits, which speaks in favor of greater safety in the work of glass ceramics (CB) samples compared to raw

basalt samples (RB).

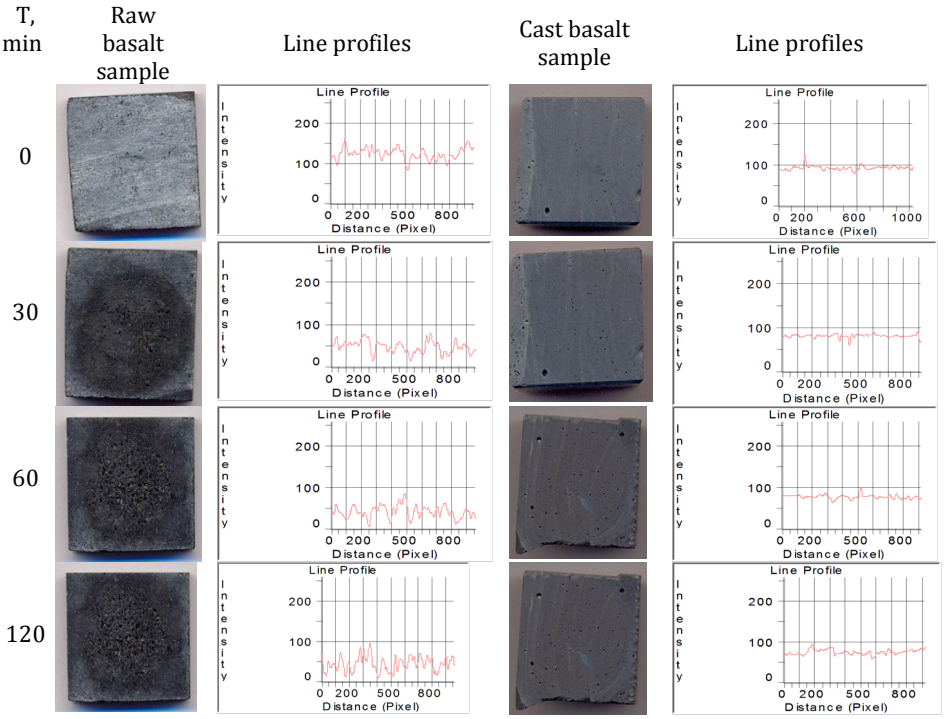

Figure 4. Photographs of RB and CB samples before and during the cavitation erosion testing after implementation of red filter and corresponding line profiles

The appearance of formed pits at the end of cavitation testing of RB and CB is shown on Figures 5 and 6. The mechanism of formation and growth of pits was monitored on an electronic microscope and shows a low rate of development of surface damage in CB samples and appearance of pits near the already existing bubble in the basic structure of glass-ceramics, Figure 6.

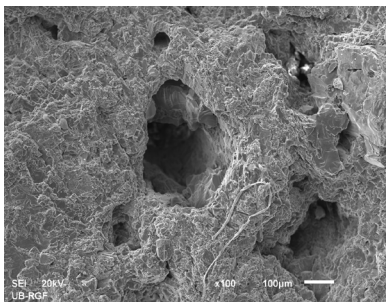

Figure 5. Deformed surface of RB sample

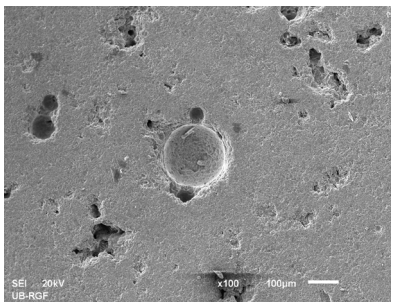

Figure 6. Deformed surface of CB sample

The profile lines indicate that the degradation is at the center of the sample surface, given the intensities of the edges of the profile lines that change and increase, from about 30 min exposure to 120 min, when significant surface area damage of the RB sample is present, Figure 4.

The results shown in Figure 4 correspond to the results of damage to the surface of RB and CB samples determined by applying image analysis on photographs of sample surfaces during the cavitation time, processed and analyzed using the Image Pro Plus software, shown in Figure 3b.

CONCLUSION

The paper investigated the formation and development of damage to the surface of the samples of the raw and cast basalt under the effect of cavitation. It has been shown that the structure of the glass-ceramics samples based on basalt (samples CB) is resistant to cavitation loads and can be applied in conditions of high temperatures and pressures that occur in a short period of time under cavitation conditions. The occurrence of shallow pits in the vicinity of already existing bubbles in the base of glass-ceramics does not damage the surface at cavitation velocity v=0.058mg/min in relation to the surface of raw basalt samples (RB) that are more damaged at cavitation speed of 0.708mg/min. The research has shown that increasing the content of waste materials in the basalt product supply contributes to the improvement of the economic, energy and ecological aspects of metallurgical and mining operations, as well as the waste recycling.

Acknowledgements:

The present research was financed by the Ministry of Education, Science and Technological Development of the Republic of Serbia as part of projects TR 35002 and 34006 for which the authors are grateful.

References

1. Beall, G. H., Rittler, H. L. (1976) Basalt glass ceramics. American Ceramic Society Bulletin, 55 (6), 579-582,
2. Karamanov, A., Ergul, S., Afyildiz, M., Pelino, M. (2008) Sinter -crystallization of a glass obtained from basaltic tuffs. Journal of Non-Crystalline Solids, 354 (2-9), 290-295,
3. Andrić, Lj., Aćimović, Z., Trumić, M., Prstić, A., Tanasković, Z. (2012) Specific characteristics of coating glazes based on basalt. Materials & Design, 39, 9-13,
4. Fiore, V., Di Bella, G., Valenza, A. (2011) Glass-basalt/epoxy hybrid composites for marine applications. Materials & Design, 32 (4), 2091-2099,
5. Aćimović, Z., Andrić, Lj., Milošević, V., Milićević, S. (2012) Wear resistance basalt production for application in mining industry. IX Simposium Metali i nemetali, Zenica BiH, Proceedings, 150-155,
6. Pavlović, M., Sarvan, M., Klisura, F., Aćimović, Z. (2016) Basalt - Raw Material for Production of Aggregate for Modern Road and Rail Shourd. In Proceedings of 4th Conference Maintenace 2016, Zenica, B&H, 175-183,

7. Barth, T. F. W. (1952) Theoretical petrology. John Wiley and Sons, New Jork,
8. Franc, J-P., Michel, J-M. (2004) Fundamentals of cavitation (Fluid Mechanics and Its Applications). 76, Kluwer Academic Publischers, New York, Boston, Dordrecht, London, Moscow,
9. Dojčinović, M. (2007) Uticaj strukture na mehanizam razaranja čelika pod dejstvom kavitacije, (Dissertation), University of Belgrade, Faculty Technology and Metallurgy, Belgrade, Serbia,
10. ASRM Standard G32-98 Standard. (2000)Test method for cavitation erosion using vibratory apparatus. Annual Book of ASTM Standards, 107-120,
11. Image Pro Plus. (1993) The Proven Solution for Image Analysis. Media Cybernetics.

XIII International Mineral Processing and Recycling Conference
Belgrade, Serbia, 8-10 May 2019

University of Belgrade, Technical Faculty in Bor
Vojske Jugoslavije 12, 19210 Bor, Serbia
Tel. +381 30 424 555 Fax +381 30 421 078

PHOSPHORIC SLAG - A TECHNOGENIC SOURCE OF RECEIVING "WHITE SOOT" AND CONCENTRATE OF RARE-EARTH METALS

Yelena Bochevskaya #, Z. Karshigina, A. Sharipova, Z. Abisheva, E. Sargelova
Satbayev University, JSC "Institute of Metallurgy and Ore Beneficiation", Almaty, Kazakhstan

ABSTRACT – The report presents the technological scheme of complex processing of phosphorus slag with the production of mineral filler - precipitated silicon dioxide ("white soot") and rare-earth metals concentrate. The through extraction of oxides of rare-earth metals into concentrate and silicon into marketable products from their initial content in slags is ~ 75.0 and 98.0 %, respectively. Samples of "white soot" with a chemical composition corresponding to the state standard with a specific surface of 180-200 m^2/g were obtained. It was established that during the processing of phosphoric slag containing about 0.05 - 0.06 % ∑REMs, it is possible to obtain a concentrate with a content of 15.0 to 17.0 % of ∑REMs oxides. Currently, for the most complete disposal of these wastes, work is underway to ensure the removal of undesirable impurities from fine silica and collective concentrate, which will improve the quality of the final products.

Key words: phosphorus slag; technology; precipitated silicon dioxide; rare-earth metals; recovery.

INTRODUCTION

In connection with an intensive development of the current technologies, the problems of an increase in the production of the known and creation of the new mineral fillers for the tyre rubber, filled polymers, different types of plastics, and varnish-and-paint and pigment materials come to the fore.

One of the most important mineral fillers is "white soot". It represents precipitated silicon dioxide with a high specific surface and special chain structure. It is used as a reinforcing filler for tyre rubbers, imitation leather, and shoe materials.

A traditional source of the commercial production of "white soot" is a silicate block prepared by means of sand alloying with sodium hydroxide [1]. The silicate block is an expensive and deficient product, therefore the problem of producing "white soot" of a cheap raw material and by a simple technology was becoming more relevant and acute. Such a material can be phosphorus slag with the silica content up to 30 - 40 mas. % SiO_2.

There are papers [2-4] on production of precipitated silicone dioxide of yellow

corresponding author: elena_bochevskaya@mail.ru

phosphorus slag, which is leached by phosphorus acid, at that calcium is separated in the form of monobasic calcium phosphate. Iron impurity content in the obtained "white soot" exceeds the prescribed norms, therefore for its purification nitric acid solution is used, at that iron concentration is reduced to ~ 0.02 %.

Scientists of the Institute of Metallurgy and Ore Beneficiation (IM&OB JSC) and specialists of the phosphorous plants have the priority in production of mineral fillers of the phosphorous industry wastes. There are known methods of processing phosphorous slags with production of precipitated silicon dioxide [5, 6], where slag is leached by sodium carbonate solution and silicate solution is obtained, which is cleaned from aluminium, then silicon dioxide with a high specific surface is precipitated therefrom by means of carbonization.

However, apart from silicon, phosphorous slags contain some precious components, such as rear earth metals, which production is a priority at present time. This is connected with their unique physical and chemical properties – optical, magnetic, electrochemical, and others. In Kazakhstan rear-earth raw materials have never been processed, and REMs have been produced of imported raw materials.

The report presents the technological scheme of complex processing of phosphorus slag with the production of mineral filler - "white soot" and rare-earth metals concentrate (Figure 1) [7].

The technology includes the following operations:

- First stage of slag leaching with the solution of nitric acid;
- REM-containing solution extraction with tributyl phosphate (TBP);
- Stripping of the REMs by water;
- Sedimentation of ∑REMs salts by the solution of oxalic acid;
- Calcination of the precipitate to obtain a concentrate of ∑REMs oxides;
- Second stage of leaching of the silicon-containing cake to obtain "white soot".

The throughout extraction of the REMs oxides into the concentrate and the silicon product from their initial content in the slags was ~ 75.0 and 98.0 %, respectively.

The appearance and colour of "white soot" precipitates are identical to each other and meet the requirements of State standard (18307 - 78). The content of silicon dioxide in "white soot" varies from 87.0 to 88.5 %. The specific surface area of the obtained batches of precipitated silica was in the range of 180 - 200 m^2 /g.

It was established that during the processing of phosphoric slag containing about 0.05 - 0.06 % ∑REMs, it is possible to obtain a concentrate with a content of from 15.0 to 17.0 % of ∑REMs oxides. At that ~ 70 % falls to the share of calcium oxide. Low content of the precious component can affect the reasonability of its further processing.

Therefore, it is necessary to find the technological conditions of phosphorous slags acid treatment to be able to reduce to the maximum transition of impurities to the fine-particle silicon dioxide and bulk concentrate, which will allow increasing the quality of these products and, therefore, their commodity value.

MATERIALS AND METHODS OF ANALYSIS

Materials. The subject of the research was a technological slag sample containing,

mas. %: 38.02 SiO_2, and major impurities 40.51 CaO, 1.94 Al_2O_3 and 1.99 Fe_2O_3, ∑REMs 532.79 g/t. 10 elements of the rear-earth metals group were identified in the slag, the quantitative content thereof is shown in Figure 2.

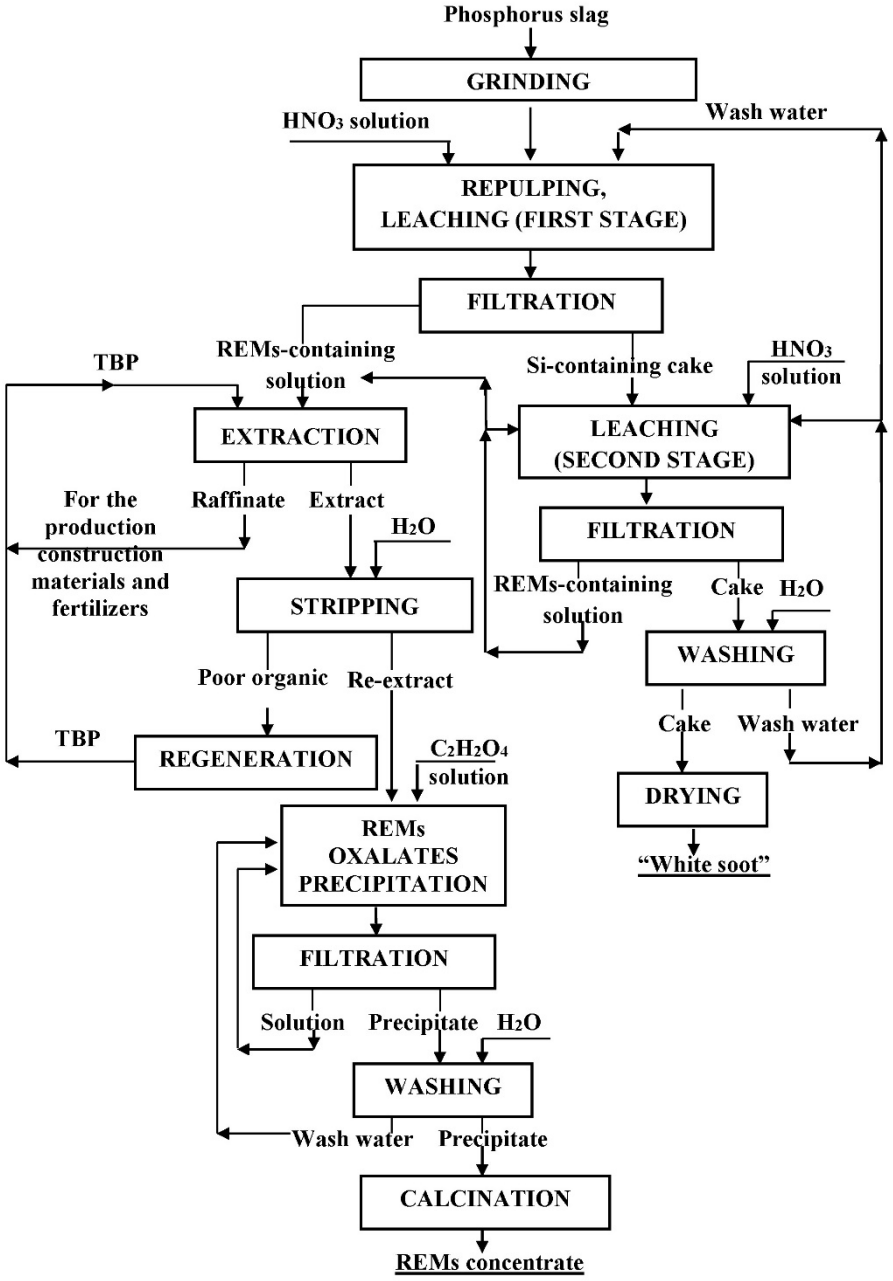

Figure 1. Technological scheme of processing phosphorus slag to obtain "white soot" and ∑REMs concentrate [7]

Nitric acid HNO_3 high grade, State standard 4461-77 was used as a leaching reagent. For the slag repulping and preparation of reagent solutions distilled water was used.

Methods of analysis. The quantitative content of primary elements and compounds in solid products and their concentrations in solutions were determined by chemical analysis methods. The quantitative content of rear-earth metals was determined by the atomic emission spectrometer with an inductively coupled plasma Optima 8300 DV by "Perkin Elmer".

The X-ray fluorescence analysis was made by the wave-dispersing spectrometer Axios "PANalytical" (the Netherlands).

The earlier studies [7, 8] allowed recommending HNO_3 as a leaching agent. At phosphorous slag leaching with nitric acid a necessary condition is transition of such impurities as aluminium, iron and partially calcium oxide to the solution, and maximum concentration of ∑REMs in the solid product.

At the initial stage the influence of nitric acid concentration and solid to liquid (S:L) ratio on calcium oxides, aluminium and iron behaviour and distribution thereof among the 1st stage products of slag leaching: filtrates and cakes was studied. At variation of the parameter studied the others were maintained at the following permanent values: HNO_3 concentration - 3.5 mol/dm^3; slag repulping and acid addition temperature 50 ºC; leaching temperature - 60 ºC; S:L ratio = 1:2.6; process duration - 1 hour; mixer rotation rate - 500 rpm. The experiment results are show in Table 1.

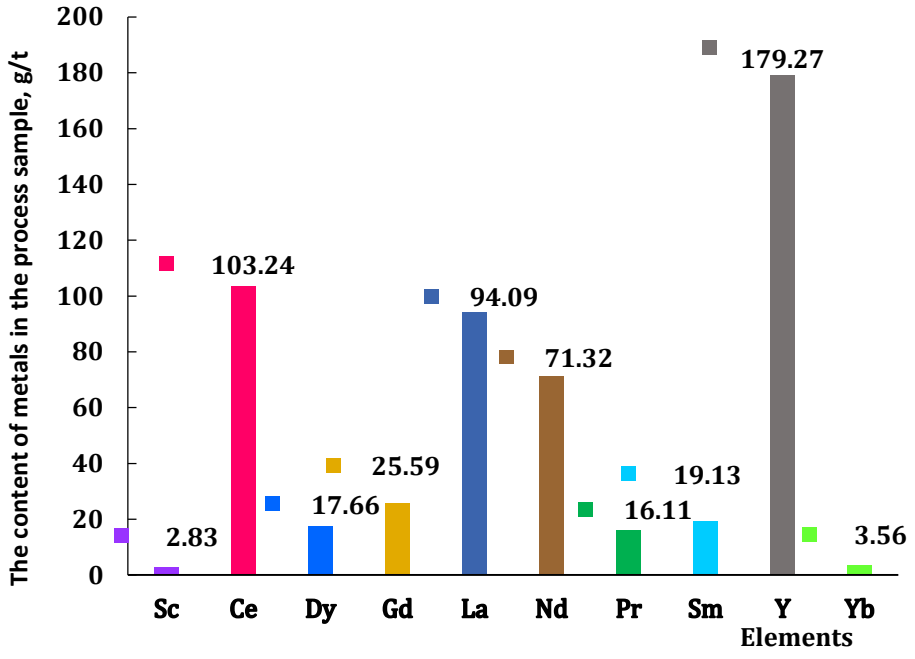

Figure 2. The quantitative content of rare earth metals

Table 1. The effect of the concentration of HNO3 and the ratio of S:L to the behavior of calcium, aluminum, iron and ∑REMs during leaching of phosphoric slag

Parameter	Extraction into solution, %			
	CaO	Al_2O_3	Fe_2O_3	∑P3M
Concentration HNO_3, mol/dm³				
2.5	26.12	0.10	2.31	0.165
3.0	2.42	0.09	2.95	0.283
3.5	35.67	0.10	7.00	0.293
4.0	37.10	0.09	10.40	0.453
4.5	40.44	0.09	23.39	0.524
5.0	30.79	0.06	16.76	0.234
The ratio of S:L				
1:2	24.91	0.10	0.74	0.163
1:2.6	35.67	0.10	7.00	0.293
1:3	49.65	1.18	12.21	0.613
1:3.5	52.98	1.30	16.36	0.676
1:4	59.47	1.32	11.26	0.860
1:4.5	61.61	1.82	26.00	1.070
1:5	60.95	6.28	19.85	3.280

RESULTS AND DISCUSSION

As Table 1 shows, with the increase of HNO_3 concentration from 2.5 to 4.5 mol/dm³ extraction of calcium and iron oxides into the solution increases from ~ 26 to 40 and from 2 to 23 %, respectively. Aluminium oxide extraction remains at the same level of ~0.1 %. ∑REMs extraction into the solution is growing slightly from 0.17 to 0.52 %. At nitric acid concentration of 5.0 mol/dm³ there is some reduction in the reduction of calcium, iron and ∑REMs.

Figure 3 shows the details of the X-ray fluorescent analysis on calcium, aluminium and iron distribution in cakes. The results obtained correlate accurately with the chemical analysis data.

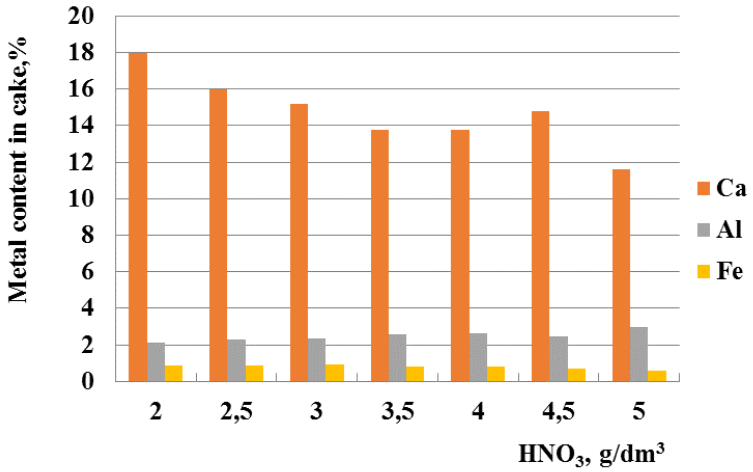

Figure 3. Effect of nitric acid concentration on the content of impurities in the cake

So, in the cakes with the increase of nitric acid concentration from 2.0 to 5.0 mol/dm^3, the calcium and iron content reduces from 18 to 11.6 % and from 0.89 to 0.58 %, respectively (Figure 2). An opposite trend is observed for aluminium, its content in the insoluble residue increases from 2.14 to 2.95 %. It should be noted that at HNO_3 concentration of 3.5 to 4.0 mol/dm^3 calcium, aluminium and iron content remains within the same range: 13.8 %, ~ 2.6 % and 0.8 %, respectively. On the basis of the experimental data obtained an optimal HNO_3 concentration of 3.5 mol/dm^3 was chosen.

With the increase of S:L ratio from 1:2 to 1:5 extraction of all analyzed metals into the solution is increased (Table 1). As the experiment results have shown, an optimal S:L ratio is 1:3.5, at which ∑REMs extraction to cake makes up 0.676 %.

CONCLUSION

At the present time a technology is developed for the phosphorous slag processing with obtaining of the precipitated silicon dioxide and bulk concentrate of rear-earth metals. However, quality of the end products in terms of impurities presence therein does not correspond to the level determined by the consumer demand. For the most complete utilization of these wastes it is necessary to find the ways, which would ensure elimination of unwanted impurities from fine silicon dioxide and bulk concentrate, which would allow increasing quality of these products.

The effect of mineral acid concentration and S:L ratio on calcium, aluminium and iron distribution by products of phosphorous slag leaching was studied.

To summarize the experimental material obtained and taking into account the X-ray fluorescent analysis details, the following has been chosen: optimal nitric acid concentration of 3.5 mol/dm^3 and S:L ratio = 1:3.5. At that ∑REMs extraction into the cake makes up ~ 99 %, and the rate of passing to the solution of calcium oxide corresponds to ~ 53 %, iron - 16.36 %, and aluminium 1.3 %.

Follow-up studies are aimed at the analysis of the temperature effect on distribution of calcium, aluminium and iron oxides impurities and solubility of their compounds in the process of the 1st stage of phosphorous slag leaching.

Acknowledgements:

The work was performed for grant No. AP05131151 of the Ministry of Education and Science of the Republic of Kazakhstan.

References

1. Habashi, F., (1984) Handbook of Extractive Metallurgy. (4), 584-660, WILEY- VCH, Heidelberg, Germany,
2. Su Y., Li G., Xia J., (2010) Experimental study of leaching yellow phosphorus slag by phosphoric acid. Journal of Solid Waste Technology and Management, 36 (1), 39-43,
3. Li G., Lin H., Ma Y., Su Y., (2012) Experimental study of purifying precipitated silica produced from yellow phosphorus slag. Advanced Materials Research. 455-456, 503-506,
4. Yi, S., Guo, B. L., Ju P. X. (2009) Kinetic study of Fe removal from precipitated

silica prepared from yellow phosphorus slag. The Canadian journal of chemical engineering. 87, 610-613,

5. Z. S. Abisheva, A. N. Zagorodnyaya, Ye. G. Bochevskaya, L. Kh. Frangulidi, G. A. Baskakova, I. A. Sapukov, T. A. Kokoveshnikova, 2006. The Possibility to Use Wastes of Chemical and Iron and Steel Plants of Kazakhstan to Obtain Precipitated Silicon Dioxide. Kompleksnoe Ispol'zovanie Mineral'nogo syr'â. *2*, 70-75. https://doi.org/10.31643/2018/6445.4,
6. Abisheva Z. S., Bochevskaya Ye. G., Zagorodnyaya A. N., Shabanova T. A., Karshigina Z. B. 2013. Technology of phosphorus slag processing for preparation of precipitated silica. J. Theoretical Foundations of Chemical Engineering. 47(4), 428-434.
7. Abisheva Z. S., Karshigina Z. B., Bochevskaya Ye. G., Akcil A., Sargelova E. A., Kvyatkovskaya M. N., Silachyov I. Yu., 2017. Recoveryof rare earth metals as critical raw materials from phosphorus slag of long-term storage. Hydrometallurgy. 173, 271–282.
8. Ata Akcil, Zaure Baytasovna Karshigina, Yelena G. Bochevskaya, Abisheva Zinesh. (2018). Conditions of nitric acid treatment of phosphorus slag for REMs recovery and production of precipitated silicon dioxide. Kompleksnoe Ispol'zovanie Mineral'nogo syr'â. 305 (2), 28-38. https://doi.org/10.31643/2018/6445.4.

XIII International Mineral Processing and Recycling Conference
Belgrade, Serbia, 8-10 May 2019

University of Belgrade, Technical Faculty in Bor
Vojske Jugoslavije 12, 19210 Bor, Serbia
Tel. +381 30 424 555 Fax +381 30 421 078

APPLIANCE OF METALLURGICAL SLAG AS A BY-PRODUCT OF THE STEEL INDUSTRY IN AMELIORATION OF ACID SOILS AND RESPONSES OF PARSLEY

Aleksandra Stanojković-Sebić [1, #], Zoran Dinić [1], Jelena Maksimović [1], Aleksandar Stanojković [2], Radmila Pivić [1]
[1]Institute of Soil Science, Belgrade, Serbia
[2]Institute for Animal Husbandry, Belgrade - Zemun, Serbia

ABSTRACT – The effects of calcium-containing metallurgical slag appliance on chemical properties of Stagnosol, a soil with very high acidity, and chemical composition of parsley herb, through the vegetative pot experiments, were studied. The investigations were aimed to define the main parameters for potential wider usage of this secondary raw material and by-product of the steel industry, respectively, for chemical melioration of acid soils in Serbia, as well as to indicate the justification of its appliance in agricultural practice. Concluding, studied metallurgical slag of the standardized chemical properties can be added to the acid soils toward amelioration the fertility without adverse effects.

Key words: metallurgical slag, raw industrial material, chemical melioration, Stagnosol, parsley.

INTRODUCTION

In steel industry, slag is usually a solid waste from the steel production, a secondary raw material for the production of building materials (such as slag sitalls) and lime and phosphorus fertilizers. It is also used as a recycle in metallurgy.

In the iron and steel making process, a very large amount of metallurgical slag is generated. For example, steel and steel slag annual output of 2010 in China reached to 626.7 million tons and 90 million tons, respectively, although the current utilization rate of steel slag in China is only 22 %, far behind the developed countries like USA, Japan, German and France, of which the rates have been close to 100 %. Therefore, large-scale utilization is a substantial resolution to the environmental problems arisen by steel slag dump. Thus, it is particularly important to develop new technologies to utilize metallurgical slag as a resource material in order to decrease the land used for disposal of slag, reducing environmental pollution, and also promoting the continuous and highly efficient development of metallurgical industry not only in the World, but also in Serbia.

corresponding author: astanojkovic@yahoo.com

Although the significant quantities of metallurgical slag are generated as waste material every day from steel industries, its physicochemical property offers a high potential for its utilization in agriculture. It mainly consists of SiO_2, CaO, Fe_2O_3, FeO, Al_2O_3, MgO, MnO, P_2O_5 and several complex minerals. There are also some trace elements such as Zn and Cu. The chemical component of slag varies with the furnace type, steel grades and pretreatment method. Closely related to its chemical and physical characteristics is the utilization way of metallurgical slag [1].

Some slags may contain elevated concentrations of trace metals such as Fe, Cd, Cr, Cu, Pb, Mo, Ni and Zn. All of these metals occur naturally in soil, and many of them are essential plant nutrients. Although metallurgical slags contain varying concentrations of trace elements (e.g., trivalent Cr (III) and Zn), the bioavailability of these metals is very low.

As metallurgical slag contains fertilizer components such as CaO, SiO_2 and MgO, its alkaline property remedies soil acidity. The liming materials in metallurgical slag comprise water-soluble and less water-soluble Ca and Mg compounds. Free Ca in slag reacts rapidly with water to form $Ca(OH)_2$. The $Ca(OH)_2$ will react rapidly with soil acidity [2, 3]. In addition to these three components, it also contains components such as FeO, MnO and P_2O_5, so it has been used for a broad range of agricultural purposes. Certain authors reported on field trials in Pennsylvania that crop yields of corn, wheat, oats, buckwheat and soybeans with metallurgical slag application were as good or better than an equivalent amount of limestone [4].

In developed countries such as Germany, USA, France and Japan, converter slag is used to produce siliceous and phosphorus fertilizer, as well as micronutrient fertilizer. In China, the first steel slag fertilizer program invested by Taiyuan Steel Group and Harsco Corporation of USA started building in 2011 [1].

High soil acidity is a property of the majority of Serbian soils and application of only organic and mineral fertilizers is not enough to sustain its productivity. On these soils, along with regular fertilization, it is necessary to apply calcium containing fertilizers - calcifiers, for improving their physico-chemical and biological properties and obtaining higher yields.

The use of traditional alkaline liming materials such as limestone, dolomite and burnt lime to acid soils for the amelioration of acidity consequently improving crop production is a common practice [5, 6]. Along with these materials present in Serbia and regarding its alkaline nature, metallurgical slag from steel factory, located in Smederevo, Serbia, can be of great importance. Thus, the main purpose of this research was to investigate the effect of Ca-containing metallurgical slag, a by-product from the steel factory (Smederevo, Republic of Serbia), comparing to the effects of selected commercial lime materials, mineral and liquid fish fertilizer, on chemical properties of Stagnosol, a heavy soil with limited productive ability (high acidity), as well as on chemical composition of parsley (Petroselinum crispum (Mill.) Nym. ex A.W. Hill) as experimental crop. The parsley herb was chosen as it grows well in a well-drained soil of a pH around 6.0 - 7.0 and very acidic conditions could stunt its growth.

MATERIAL AND METHODS OF WORK

The research was carried out in pot experiments under semi-controlled conditions in the glasshouse of the Institute of Soil Science (Belgrade, Serbia), during 2015. In the

experiments the comparison of the effect of metallurgical slag (MS) with other lime materials (ground limestone and hydrated lime) in combination with and without mineral composite NPK (N:P:K = 15 % : 15 % : 15 %) and organic (liquid fish - LF) fertilizers was studied. The samples of metallurgical slag used were taken from different deposition sites of the steel factory in Smederevo, located approximately 60 km south-east from Belgrade, Serbia. The ground limestone (calcium carbonate or calcite, $CaCO_3$) contains 60 % of carbonate. Hydrated lime (slaked lime, $Ca(OH)_2$) reacts very rapidly and has a TNV (Total Neutralizing Value) of 135, thus 740 kg of hydrated lime is equivalent to one ton of ground limestone i.e. the TNV = 135 [7].

The experiment was undertaken with 1.4 kg pot^{-1} of Stagnosol [8], a type of soil from Western Serbia region, characterized by very acid reaction and poor physical and biological properties [9]. The following designed treatments were carried out in three replications: T1 - control (untreated soil); T2 - NPK mineral fertilizer; T3 - $CaCO_3$; T4 - $Ca(OH)_2$; T5 - MS; T6 - LF fertilizer; T7 - NPK mineral fertilizer + $CaCO_3$; T8 - NPK mineral fertilizer + $Ca(OH)_2$; T9 - NPK mineral fertilizer + MS.

Before sewing the parsley, the amount of fertilizers and slag was measured according to the experimental design and mixed with soil (calculated as for 1 ha): composite NPK fertilizer (15 : 15 : 15) = 500 $kg \cdot ha^{-1}$; LF fertilizer = 170 $kg \cdot ha^{-1}$; $CaCO_3$ = 4 $t \cdot ha^{-1}$; $Ca(OH)_2$ = 2.8 $t \cdot ha^{-1}$; MS = 4 $t \cdot ha^{-1}$. All three Ca-materials with granulation of 0.2 mm were used in the experiment.

Chemical composition of metallurgical slag (MS) applied was in detail determined in our previous study [9]. Accordingly, this material has very alkaline reaction (pH in H_2O = 12.50), with the content of Ca in oxide forms (CaO) from 33 - 45 $mg \cdot kg^{-1}$, of which about 50 % is easily soluble in 1 M ammonium acetate; content of the total Mg is about 0.40 $mg \cdot kg^{-1}$ and it was mainly in forms of MgO (0.70 $mg \cdot kg^{-1}$); total P contained in the material is about 0.60 $mg \cdot kg^{-1}$, where nearly all the amount is in available forms for plants; content of the total Fe is high (about 15 $mg \cdot kg^{-1}$), with noticeable lower amounts of its soluble forms; Mn is present in total amount of about 1.8 $mg \cdot kg^{-1}$, but with low amounts of soluble forms; Zn is contained in lower amounts (10 - 20 $mg \cdot kg^{-1}$), while the content of Cu is a little higher (about 200 $mg \cdot kg^{-1}$).

The settleable faecal fish waste, used as liquid fish (LF) fertilizer in this research, was obtained from the farm growing rainbow trout in village Krupac, municipality of Pirot, Serbia. According to its main chemical constituents, it was determined its moderate to high quality for application as an organic fertilizer, containing 3.3 % of total N, 36.5 % of total C, 0.36 % of total S, 10.2 mg 100 g^{-1} of available P and 0.12 mg 100 g^{-1} of available K [10].

Soil samples from all the treatments and replicates were analyzed for their soil chemical characteristics at the beginning and end of the vegetation period of experimental crop. The following chemical analyses were done: pH in 1M KCl (soil:1M KCl = 1:5) was analyzed potentiometrically, using glass electrode [11]; total N was analyzed by dry combustion using elemental CNS analyzer Vario EL III [12]; available P and K were analyzed by AL-method according to Egner-Riehm [13]; available forms of Fe, Zn, Cu and Cd were determined using ICP-OES (ICAP 6300), after the samples were digested with DTPA solution [14].

Parsley seedlings were grown according to the standard growing methods from March, 31st until July, 27th in 2015, when all studied relevant parameters of the plant growth were measured/analyzed. Biomass from each experimental variant and

replicate was taken, air-dried and weighed, after which it was dried for 2 hours at 105 ^{o}C and weighed again. The following chemical parameters of the aerial plant parts were analyzed: contents of N and C were determined on elemental CNS analyzer Vario EL III [15]; P and K concentrations were determined by "wet" combustion, after which in the obtained solution P was determined by spectrophotometer with molybdate [16], and K - by flame emission photometry [17]; in the determination of the studied trace biogenic elements - Fe, Zn and Cu, as well as Cd as the toxic heavy metal, plant material was converted to a solution by "dry" combustion, after which these elements were determined by AAS [18].

Estimation of the effect of studied treatments on the analyzed chemical composition of the soil and plant samples was carried out using the analysis of variance (SPSS 20.0, Chicago, USA). Significant differences between means were tested by the LSD test at P = 0.05.

RESULTS AND DISCUSSION

Chemical characteristics of Stagnosol before the experiment was established (T0, initial stage) and at the end of parsley vegetation period are presented in Table 1. According to its initial stage, the soil is characterized by very acid reaction, very low provided with available P and medium provided with total N, available K, Cu and Zn, with very high concentrations of available forms of Fe. As for toxic metal Cd, its concentration is low and far from MPC (maximum permissible concentrations) according to the reference value [19]. The data on effect of applied treatments on macroelements and trace metals contents in studied soil, presented in Table 1, showed a priori the significant decrease of soil acidity in variants with lime material and MS comparing to the control and treatments with classical fertilization with NPK and LF fertilizer. The pH increase in the treatments with MS was probably a result of the certain dissolution of Ca, Mg and Si compounds, which was in accordance with results for calcium silicate slag [20]. In addition, all the fertilizers and lime materials including MS resulted in increased content of available macroelements. Application of MS resulted in significant increased amount of available P comparing to the classical lime materials. It was not determined a significant increase in the total amount of trace elements Cu and Zn in soil treated with both classical NPK and LF fertilizers, as well with lime materials and MS, although noticeably a small effect of these treatments on decrease of available forms of Fe comparing to the control was observed. Comparing to the initial status the levels of toxic heavy metal Cd were not significantly increased and were far below the MPC (Table 1).

Table 1. Chemical characteristics of Stagnosol before the experiment was established and at the end of parsley vegetation

Treatment	pH in 1M KCl *	Total N (mg kg^{-1})*	Available macroelements and trace metals (mg kg-1)*					
			P	K	Fe	Zn	Cu	Cd
T0	4.42±0.01	0.12±0.01	37.3±2.8	188.1±34.4	126±5.9	1.0±0.10	1.7±0.10	0.08±0.01
T1	4.57±0.03	0.10±0.03	26.1±3.3	118.0±16.4	113±5.9	1.6±0.06	1.8±0.10	0.08±0.00
T2	4.44±0.01	0.14±0.03	55.3±2.0	199.1±28.5	111±7.2	1.7±0.48	1.7±0.22	0.07±0.01
T3	5.41±0.04	0.15±0.06	28.3±8.0	138.3±6.2	100±2.7	1.2±0.06	1.5±0.15	0.06±0.01
T4	5.35±0.14	0.14±0.04	32.1±6.7	123.3±14.6	101±8.4	1.3±0.03	1.6±0.13	0.07±0.01
T5	5.35±0.11	0.12±0.02	40.4±3.0	119.7±20.8	107±10.4	1.2±0.04	1.7±0.14	0.07±0.01
T6	4.98±0.02	0.17±0.03	82.1±0.5	231.5±20.4	94±5.1	1.3±0.18	1.4±0.04	0.06±0.01

Table 1. (Extension)

T7	5.22±0.16	0.11±0.00	67.2±0.3	222.1±16.9	101±10.8	1.3±0.11	1.5±0.14	0.06±0.01
T8	5.29±0.11	0.11±0.01	68.9±8.0	219.3±20.7	103±4.5	1.4±0.01	1.6±0.12	0.06±0.01
T9	4.93±0.02	0.12±0.02	61.2±0.4	201.6±19.7	104±4.6	1.4±0.01	1.7±0.12	0.08±0.01
P value	***	NSD	***	***	NSD	NSD	NSD	*
LSD (0.05)	0.15	0.07	1.50	3.46	12.77	0.33	0.24	0.011

T0-initial stage; Treatments: T1-control; T2-NPK mineral fertilizer; T3-$CaCO_3$; T4-$Ca(OH)_2$; T5-MS; T6-LF fertilizer; T7-NPK mineral fertilizer + $CaCO_3$; T8-NPK mineral fertilizer + $Ca(OH)_2$; T9-NPK mineral fertilizer + MS; *means ± standard deviation; LSD-least significant difference; NSD-no significant difference at $P < 0.05$.

Table 2. Macroelements and trace elements content in parsley depending on the treatment applied

Treatment	Available macroelements (mg kg^{-1} of dry biomass)*			Available trace elements (mg kg^{-1} of dry biomass)*			
	N	P	K	Fe	Zn	Cu	Cd
T1	$2.61±0.10^{c}$	$0.20±0.03^{a}$	$3.16±0.23^{c}$	$174.83±17.29^{e}$	$106.70±3.00^{e}$	$12.28±0.66^{c}$	$2.43±0.12^{d}$
T2	$3.16±0.09^{ab}$	$0.24±0.06^{a}$	$3.91±0.01^{a}$	$261.78±12.04^{d}$	$120.84±4.13^{cd}$	$14.59±0.39^{a}$	$2.77±0.20^{bc}$
T3	$3.26±0.23^{a}$	$0.21±0.05^{a}$	$3.57±0.28^{cd}$	$176.78±18.84^{f}$	$116.03±1.95^{d}$	$14.61±0.39^{a}$	$2.52±0.03^{cd}$
T4	$3.05±0.15^{ab}$	$0.22±0.04^{a}$	$3.18±0.26^{c}$	$129.01±12.01^{e}$	$134.73±2.77^{a}$	$15.14±0.16^{a}$	$2.55±0.20^{cd}$
T5	$2.84±0.13^{bc}$	$0.22±0.03^{a}$	$3.40±0.29^{de}$	$322.39±18.36^{c}$	$100.28±1.20^{e}$	$14.67±0.56^{a}$	$2.67±0.06^{bcd}$
T6	$3.39±0.25^{a}$	$0.24±0.02^{a}$	$3.98±0.03^{b}$	$114.44±8.06^{g}$	$79.53±2.40^{f}$	$13.38±0.46^{b}$	$2.46±0.17^{d}$
T7	$3.38±0.27^{a}$	$0.24±0.04^{a}$	$4.73±0.14^{a}$	$320.22±19.12^{c}$	$125.01±3.26^{abc}$	$14.93±0.09^{a}$	$2.92±0.05^{b}$
T8	$3.25±0.22^{a}$	$0.23±0.06^{a}$	$4.41±0.06^{bcd}$	$504.72±21.40^{a}$	$130.80±10.25^{ab}$	$14.59±0.39^{a}$	$2.94±0.04^{b}$
T9	$3.16±0.13^{ab}$	$0.24±0.04^{a}$	$4.13±0.02^{bc}$	$443.17±17.95^{b}$	$123.44±2.68^{bcd}$	$13.67±0.39^{b}$	$3.36±0.26^{a}$
P value	**	NSD	***	***	***	***	***
LSD (0.05)	0.317	0.852	0.344	17.597	7.377	0.780	0.253
Ref. value**							
Normal	-	-	-	50[1]	15[3]	3[3]	< 0.1 - 1[3]
Critical	-	-	-	250[1]	150[2]	15[2]	5[2]
Toxic	-	-	-	600[2]	200[2]	20[2]	10[2]

Treatments: T1-control; T2-NPK mineral fertilizer; T3-$CaCO_3$; T4-$Ca(OH)_2$; T5-MS; T6-LF fertilizer; T7-NPK mineral fertilizer + $CaCO_3$; T8-NPK mineral fertilizer + $Ca(OH)_2$; T9-NPK mineral fertilizer + MS; *means ± standard deviation; LSD - least significant difference; value followed by the same letter in a column is not significantly different at $P < 0.05$; **Literature source: [1][21], [2][22], [3][23].

The results of the main macroelements content in aerial parts of parsley (Table 2) show the statistically significant differences between the treatments at $P < 0.05$ for N and K, that are due to a higher accumulation of some elements and their mobilization from natural soil reserves primarily, as well as influenced by the additional MS and commercial lime materials in combination with mineral ferilizer and LF fertilizer. However, these treatments had positive effect on all studied macroelements in relation to the control.

The levels of trace metals in parsley aerial parts showed that there are statistically significant differences between different treatments at $P < 0.05$ (Table 2). With an exception of plants from LF fertilizer treatment, it was determined elevated and critical concentrations of Fe in all other studied variants plants, although these concentration were below the MPC (Table 2). Nevertheless, there was not found higher accumulation of Fe in tested plants in the treatments where

metallurgical slag was applied in spite of its significant content in this industrial raw material. The contents of Cu, Zn and Cd were in the range of normal to critical concentrations in parsley plants from all variants studied but below the MPC (Table 2), which is a highly desirable outcome since toxic metal Cd is a highly mobile element and can be easily translocated to the aerial plant parts [24]. According to Sharma et al. [25], the edible parts of leafy green vegetables, such as parsley, showed higher potential to accumulate heavy metals in comparison to storage organs and fruits, which could explain elevated concentrations of the studied trace elements, particularly Fe, in this plant species.

CONCLUSION

The results of the paper indicate that all Ca-materials studied, including metallurgical slag, along with the studied mineral and liquid fish fertilizers, showed positive effects on the content of main and beneficial biogenic macroelements in aerial biomass of parsley. The content of trace elements in parsley plants from all the treatments was below the MPC. Nevertheless, there was not found higher accumulation of Fe in tested plants in the treatments where metallurgical slag was applied in spite of its significant content in this liming material. Generally, it was estimated that the studied metallurgical slag of the standardized chemical composition can be added to marginal soils toward amelioration the fertility without adverse effects under semi-controlled conditions.

Acknowledgements:

This research work was carried out with the financial support of Ministry of Education, Science and Technological Development of the Republic of Serbia, Project TR-37006.

References

1. Huang, Y., Guoping, X., Huigao, C., Junshi, W., Yinfeng, W., Hui, C. (2012) An overview of utilization of steel slag. Procedia Environmental Science, 16, 791-801,
2. National Slag Association, (2011) Use of steel slag in agriculture and for reclamation of acidic lands, http://www.nationalslag.org/sites/nationalslag/files/ag_guide909.pdf.
3. Lopez, F. A., Balcazar, N., Formoso, A., Pinto, M., Rodriguez, M. (1995) The recycling of Linz-Donawitz (LD) converter slag by use as a liming agent on pasture land. Waste Management and Research, 13, 555-568,
4. White, J. W., Holben, F. J., Jeffries, C. D. (1937) The agricultural value of specially prepared blast-furnace slag. Pennsylvania State College, Agricultural Experiment Station, Bulletin No. 341,
5. Barber, S. A. (1984) Liming materials and practices. In: Adams, F. (Ed) Soil acidity and liming, 2nd edition. American Society of Agronomy, Crop Science Society of America, Madison, Wisconsin, 171-210,
6. Foth, H. D., Ellis, B. G. (1997) Soil fertility. 2nd edition, Lewis Publishers, Boca Raton, Florida.

7. Ristow, P. L., Foster, J., Ketterings, Q. M. (2010) Lime guidelines for field crops: tutorial workbook. Cornell University, Department of Animal Science, Ithaca, New York, USA,
8. WRB, (2014) World reference base for soil resources: international soil classification system for naming soils and creating legends for soil maps. World Soil Resources Reports No. 106, FAO, Rome, Italy,
9. Stanojković, A., Pivić, R., Maksimović, S. (2011) Metallurgical slag use effects on soils and plant chemical properties. LAP Lambert Academic Publishing, Saarbrücken, Germany,
10. Stanojković-Sebić, A., Dinić, Z., Čanak, S., Jošić, D., Pivić, R. (2017) Effects of metallurgical slag and organic fertilizer amendments on chemical composition of chard (*Beta vulgaris* var. *cicla*). In: Proceedeings of VIII International Scientific Agriculture Symposium Agrosym 2017, Faculty of Agriculture, Republic of Srpska, Bosnia, 470 – 476,
11. SRPS ISO 10390:2007, (2007) Soil quality - Determination of pH. Institute for Standardization, Belgrade, Serbia,
12. SRPS ISO 13878:2005, (2005), Soil quality - Determination of total nitrogen content by dry combustion ("elemental analysis"). Institute for Standardization, Belgrade, Serbia,
13. Đurđević, B. (2014a). Determination of available phosphorus and potassium using AL-method. In: Miklavčić, D. (Ed) Manual in plant nutrition. Faculty of Agriculture, Osijek, Croatia, 25-28,
14. Soltanpour, P. N., Johnson, G. W., Workman, S. M., Bentonjones, J. J., Miller, R. O. (1996) Inductively coupled plasma emission spectrometry and inductively coupled plasma mass spectrometry. In: Sparks, D.L. (Ed) Methods of soil analysis, Part 3. SSSA, Madison, Wisconsin, 91-139,
15. Nelson, D. W., Sommers, L. E. (1996) Total carbon, organic carbon, and organic matter. In: Sparks, D.L. (Ed), Methods of soil analysis, part 3. SSSA, Madison, Wisconsin, USA, 961-1010,
16. Đurđević, B. (2014b) Spectrophotometric determination of phosphorus. In: Miklavčić, D. (Ed) Manual in plant nutrition. Faculty of Agriculture, Osijek, Croatia, 60-61,
17. Đurđević, B. (2014c) Determination of K, Ca, Mg and Na. In: Miklavčić, D. (Ed) Manual in plant nutrition. Faculty of Agriculture, Osijek, Croatia, 62-63,
18. Wright, R. J., Stuczynski, T. (1996) Atomic absorption and flame emission spectrometry. In: Sparks, D.L. (Ed) Methods of soil analysis, Part 3. SSSA, Madison, Wisconsin, 65-90,
19. Official Gazette of Republic of Serbia, 23/94. (1994) Rule book of allowed concentrations of dangerous and hazardous materials in soil and in water for irrigation and methods for analysis, 23,
20. Nanayakkara, U. N., Uddin, W., Datnoff, L. E. (2008) Effects of soil type, source of silicon, and rate of silicon source on development of gray leaf spot of perennial ryegrass turf. Plant Disease, 92 (6), 870-877,
21. Schulze, E-D., Beck, E., Müller-Hohenstein, K., Lawlor, D., Lawlor, K., Lawlor, G. (2005) Plant Ecology. Berlin, Heidelberg, Germany: Springer-Verlag, 702,
22. Kastori, R., Petrović, N., Arsenijević-Maksimović, I. (1997) Heavy metals and plants. In: Kastori, R. (Ed) Heavy metals in the environment. Institute of Field

and Vegetable Crops, Novi Sad, Serbia, 196-257,
23. Kloke, A., Sauerbeck, D. R., Vetter H. (1984) The contamination of plants and soils with heavy metals and the transport of metals in terrestrial food chains. In Nriagu, J. O. (Ed) Dahlem Konferenzen: Changing metal cycles and human health. Springer-Verlag, Berlin, Heidelberg, New York, Tokyo, 113-141,
24. Sipter, E., Rozsa, E., Gruiz, K., Tatrai, E., Morvai, V. (2008) Site-specific risk assessment in contaminated vegetable gardens. Chemosphere, 71, 1301-1307,
25. Sharma, R. K., Agrawal, M., Marshall, F. M. (2008) Heavy metal (Cu, Zn, Cd and Pb) contamination of vegetables in urban India: A case study in Varanasi. Environmental Pollution, 154, 254-263.

XIII International Mineral Processing and Recycling Conference
Belgrade, Serbia, 8-10 May 2019

University of Belgrade, Technical Faculty in Bor
Vojske Jugoslavije 12, 19210 Bor, Serbia
Tel. +381 30 424 555 Fax +381 30 421 078

RECYCLING OF RHENIUM, NICKEL AND COBALT FROM THE WASTE OF HEAT-RESISTANT ALLOYS

Lyudmila Agapova #, S. Kilibayeva, A. Zagorodnyaya, A. Sharipova, B. Kenzhaliyev, Zh. Yakhiyayeva
Satbayev University, JSC "Institute of Metallurgy and Ore Beneficiation", Almaty, Kazakhstan

ABSTRACT – Optimal parameters are determined, and the technology of rhenium, nickel and cobalt recycling from the waste of heat-resistant nickel alloys was developed. The technology includes the following operations: anodic dissolution of large waste pieces in sulfuric acid solutions with addition of nitric acid at a current density of 500 - 1000 A/m^2 and at a temperature of 25 - 30 °C; chemical dissolution of the anode sludge in 2 M sulfuric acid solution with addition of nitric acid; rhenium extraction and re-extraction in order to produce crude ammonium perrhenate; deposition from the raffinate solution after extraction of rhenium by the alkali of the nickel-cobalt concentrate..

Key words: waste of heat-resistant nickel alloys; recycling of rhenium, nickel and cobalt; electrochemical processing; ammonium perrhenate; nickel-cobalt concentrate.

INTRODUCTION

Wastes of processing and operation of heat-resistant alloys, of which blades of power turbines and reaction engine turbines are made, are one of the most precious types of secondary raw materials. The alloys are high-melting, high-strength and abrasion-resistant materials [1]. Mostly, these alloys contain up to 50 - 75 % of nickel, up to 3 - 15 % of cobalt, chrome and aluminum, up to 1 - 10 % of one or several elements from tantalum, niobium, tungsten, molybdenum, rhenium, platinum, and hafnium [2]. First of all, these wastes are interesting from the point of view of extracting rhenium, which is expensive and highly demanded in the metal market. Currently, for the rhenium extraction from the wastes of heat-resistant alloys there are technologies offered, which combine pyro- and hydrometallurgical methods, including electrochemical ones [2-15]. Along with rhenium, extraction of other precious nonferrous and rare metals is of interest in terms of complex processing of the wastes of heat-resistant nickel alloys.

Analysis of the materials concerning processing of wastes of heat-resistant alloys

corresponding author: rm.303.imo@mail.ru

has shown that the main problem is opening of the large pieces of such wastes. The most efficient for waste opening are electrochemical methods, which, subject to the right choice of the electrolyzer and electrolyte structures, allow transferring metals into the solution with quite high technological parameters.

This paper presents the results of studies on rhenium, nickel, and cobalt recycling from the wastes of heat-resistant alloys. Opening of the alloy wastes, being large pieces of turbine blade scrap, was made in sulfuric acid electrolyte by electrochemical method with the follow-up processing of electrolysis products.

EXPERIMENTAL PROCEDURE

The subject of our studies was technogenic wastes of heat-resistant nickel alloys (HRNA) in the form of large pieces of turbine blade scrap. Anodic dissolution of alloy wastes was made in electrolyzer with the capacity of 10 dm^3 with titanium cathode in the solution of technical sulfuric acid with the addition of nitric acid. Alloy pieces were weighted before and after completion of anodic dissolution. In the process of anodic dissolution of alloy wastes formation of anodic slime was observed, which contained all alloying elements.

For the additional transfer into the solution of rhenium, nickel, and cobalt chemical dissolution of anodic slime in the solution of the technical sulfuric acid with the addition of nitric acid was made. From the amalgamated sulfuric acid solutions obtained in the process of anodic dissolution of alloy wastes and chemical dissolution of anodic slimes, rhenium was extracted by the known extraction method. Trialkylamine (TAA) together with kerosene and 2-ethylhexanol were used as an extracting agent. Rhenium was re-extracted by the ammonia-water mixture.

From sulfuric acid raffinates left after rhenium extraction and containing significant amount of nickel, cobalt, chrome, aluminum, and some other metals, nickel-cobalt concentrate was precipitated by alkali.

Determination of the chemical and phase composition of the wastes of heat-resistant alloys and products of their processing (solutions, anodic slime, cake, crude ammonium perrhenate, nickel-cobalt concentrate) was made using the X-ray fluorescent (spectrometer with wave dispersion Axios PANalytica), X-ray phase (diffractometer D8 Advance (BRUKER), radiation Cu. K α), chemical (atomic-emission spectroscope Optima 2000 DV, USA, Perkin Elmer), submicroscopical (electron microprobe analyzer JXA-8230 made by JEOL), infrared (infrared Fourier spectrometer Thermo Nicolet Avatar 370 FTIR Spectrometer) analysis methods. Compounds identification in X-ray phase analysis was made on [16].

RESULTS AND DISCUSSION

Our earlier studies [13] of anodic dissolution of small pieces (weight 5 to 10 g) of alloy wastes in sulfuric acid solutions with different additives have shown that the highest rates of rhenium transfer into solution (to 80 - 100 %) were obtained when sulfuric acid solution with nitric acid additive was used as an electrolyte at the anodic current density under 1000 A/m^2 and temperature 25-30 °C. At that, less anodic slime was formed, which would reduce additional costs at its follow-up processing. Therefore, the studies of anodic dissolution of large pieces of HRNA wastes were held taking into consideration the results obtained earlier.

For the processing we received large pieces of scrap (weight 140 - 350 g) of turbine blade made of heat-resistant nickel alloy, containing, wt. %: Re - 2.99; Ni - 54.04; Co - 11.54; Al - 7.25; Cr - 6.27; Ta - 3.94; W - 4.38; Mo - 0.98; Si - 1.93. Anodic dissolution of alloy wastes was made in solution of technical sulfuric acid (100 g/dm^3) with nitric acid additive (20 g/dm^3) in the electrolyzer with the capacity of 10 dm^3 at the anodic current density of 500-1000 A/m^2. In such conditions of electrolysis 379.2 g of wastes dissolved after 30 h. The occurred slime weight was 91.9 g.

We obtained 9.5 dm^3 of sulfuric acid solution containing, g/dm^3: 0.98 Re; 21.57 Ni; 3.13 Co; 2.45 Al; 1.76 Cr; 0.09 W; 0.05 Mo; 0.002 Ta. Rhenium extraction into the solution made up 82.1 % of the dissolved waste weight.

According to the results of the X-ray fluorescent analysis obtained anodic slime contained, wt. %: 2.07 Re; 6.91 Ni; 0.58 Co; 0.47 Al; 1.24 Cr; 12.44 Ta; 34.19 W; 1.34 Mo; 3.33 Hf; 0.05 Si; 33.44 O.

At the anodic opening of alloy wastes in the above conditions nickel, cobalt, aluminum, chrome (over 91 - 99 %) and over 80 % of rhenium, and the biggest portion of molybdenum almost completely passed into the solution. Tungsten, tantalum, hafnium, and most of molybdenum (over 75 %) passed into anodic slime.

For the additional transfer into the solution of rhenium, nickel and cobalt chemical dissolution of anodic slime was made in 2 M solution of technical sulfuric acid with nitric acid additive (50 g/dm^3). Undissolved light grey cake was filtered, and its mass made up about 62 % of the initial mass of the slime dissolved. The mean element content in the filtrates made up, g/dm^3: 0.66 Re; 4.71 Ni; 0.41 Co; 0.33 Al; 0.09 W; 0.08 Mo; 0.22 Cr. According to the results of the X-ray fluorescent analysis the cake contained, wt. %: 42.74 W; 18.68 Ta; 3.6 Hf; 1.25 Re; 1.3 Mo; 1.0 Cr; 0.97 Ni; 0.10 Co; 0.14 Al; 0.04 Si; 36.85 O. According to the results of XFA the cake base is tungsten trioxide.

The results received have shown that at the chemical opening of anodic slime the biggest portion of rhenium, nickel, cobalt, and aluminum mostly passes into solution. The remaining cake, as a whole, represents a concentrate of refractory rare metals.

Solutions from anodic opening of wastes and chemical dissolution of slimes were combined. In the equalized solution the element content made up, g/dm^3: 0.70 Re, 21.85 Ni, 3.28 Co, 2.29 Al, 0.07 W, 0.07 Mo, 2.08 Cr. For rhenium extraction a part of the combined sulfuric acid solution was taken. Trialkylamine (TAA) together with kerosene and 2-ethylhexanol were used as an extracting agent (composition, vol. %: TAA - 10.0, spirit - 10.0, kerosene - 80.0). Rhenium extraction conditions: ratio O:W = 1:8; contact time - 5 min; room temperature. Phases separated quickly enough, but the system was allowed to settle for 24 hours for the better separation of the little suspended matter formed. Rhenium was re-extracted by 2.5 M ammonia-water mixture at ratio O:W = 4:1, contact time - 5 min; room temperature. Phases separated quickly enough. Ammonia re-extract containing rhenium 21 g/dm^3 was evaporated, after that at the solution cooling white sparkling fine-crystalline precipitate settled. Metal extraction into water and organic phases in the process of rhenium extraction-re-extraction is shown in Table 1.

The precipitate were analyzed by X-ray fluorescent, X-ray phase (Figure 1) and spectral methods. The results have show that obtained salt represents crude ammonium perrhenate of a very good quality with rhenium content not less than

68.9 wt. %, and impurities, wt. %: 0.001 Ni; 0.001 Co; 0.001 Al; 0.005 W; 0.002 Mo; 0.001 Cr.

Table 1. Rate of Metal Extraction into Water and Organic Phases in the Process of Rhenium Extraction-Reextraction

Re	Ni	W	Co	Mo	Al	Cr
Metal extraction from solution from alloy and slime opening (extraction), %						
To the organic phase (extract)						
98.63	0	49.37	0.00	3.03	0.00	0.00
To the water phase after extraction (refined)						
1.37	100.00	50.63	100.00	96.97	100.00	100.00
Metal extraction from organic phase (re-extraction), %						
To the ammonia solution (re-extract)						
99.80	0	90.95	0.00	89.17	0.00	0.00
To the organic phase after re-extraction						
0.20	0	9.05	0.00	10.83	0.00	0.00

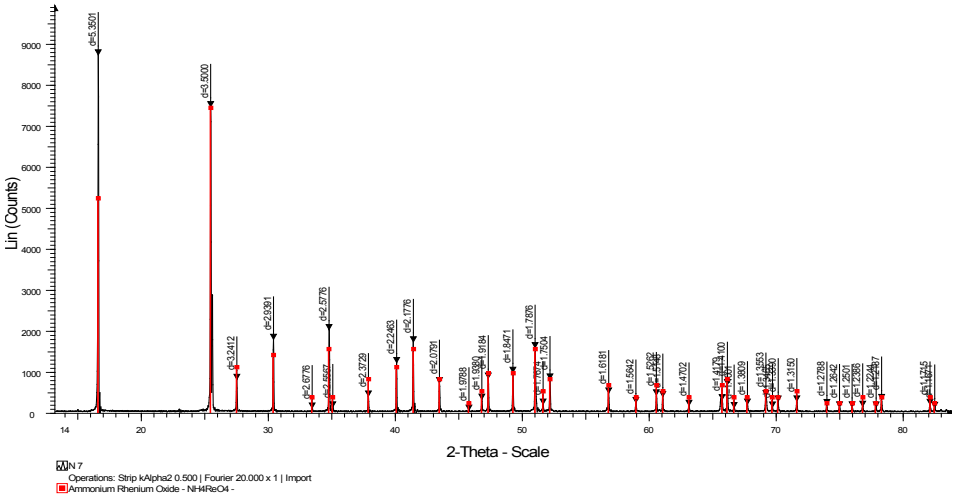

Figure 1. Diffractogram of Crude Ammonium Perrhenate

After rhenium extraction from solutions of anodic opening of alloy wastes and chemical opening of slimes sulfuric acidic raffinates remain containing significant amounts of nickel, cobalt, chrome, aluminum, and some other metals. To extract these metals from raffinates the method of metal hydroxides precipitation by alkalies was used.

To the raffinate solution, after extraction of rhenium containing g/dm^3: 0.004 Re; 24.07 Ni; 4.13 Co; 0.04 W; 0.06 Mo; 2.42 Al; 2.17 Cr, we added while stirring sodium hydroxide solution (350 g/dm^3) until the solution reached pH 7 - 8. At that bright-turquoise precipitation settled, which was filtered, washed with water and was allowed to settle at 70 °C to the constant weight in the drying box. Elements content in the filtrate, g/dm^3: 0.35 W; 0.004 Mo; 0.0001 Al; 0.0001 Cr. No rhenium, nickel or

cobalt was found in the filtrate. According to the results of X-ray fluorescent analysis obtained precipitation, which can be considered as nickel-cobalt concentrate, contains, wt. %: 31.45 Ni; 4.82 Co; 2.98 Al; 2.69 Cr, 0.06 W; 0.08 Mo; 5.35 S; 5.32 Na; 0.11 Si; 43.25 O.

Therefore, almost all nickel, cobalt, chrome, aluminum, and some amount of other elements passed from the raffinate into the precipitation.

On the basis of the studies performed a method of electrochemical processing of metal wastes of rhenium-containing heat-resistant nickel alloys, preferably large pieces of wastes, by anodic dissolution in the sulfuric acid solution under the exposure to direct current was developed [14].

Figure 2 shows a flow diagram of processing large pieces of wastes of rhenium-containing HRNA, which includes anodic dissolution of waste and obtaining from electrolysis products of crude ammonium perrhenate, concentrate of refractory rare metals, and nickel-cobalt concentrate.

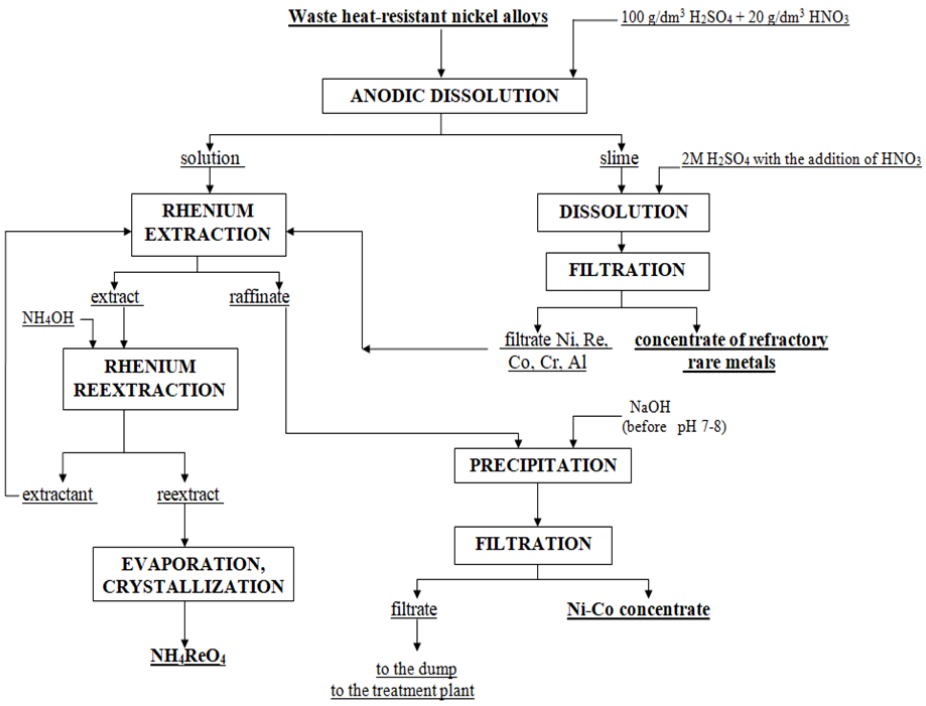

Figure 2. Flow Diagram of Processing of Wastes of Rhenium-Containing Heat-resistant Nickel Alloys

CONCLUSION

The studies held on rhenium, nickel and cobalt recycling from the wastes of heat-resistant alloys have shown that at anodic dissolution of large pieces of wastes of rhenium-containing HRNA in sulfuric acid solutions with nitric acid additive under exposure to the direct current with the current density of 500-1000 A/m^2 and

temperature of 25 - 30 °C rhenium can be transferred into the solution by 80 - 90 %. In such conditions there is high extraction into solution with respect to nickel, cobalt, chrome, and aluminum.

Almost all tungsten, tantalum, and hafnium remain in anodic slime. Rhenium, nickel and cobalt remaining in anodic slime can be transferred into the solution at chemical opening of slime in 2 M solution of sulfuric acid with nitric acid additive (50 g/dm^3). The remaining cake, as a whole, represents a concentrate of refractory rare metals.

From the combined solutions from anodic opening of HRNA wastes and chemical dissolution of anodic slimes rhenium is extracted by the known extraction method in the form of crude ammonium perrhenate.

Sulfuric acidic raffinate after rhenium extraction contains significant amounts of nickel, cobalt, chrome, and aluminum, which can be precipitated by the alkali solution in the form of hydroxides of these metals into nickel-cobalt concentrate with the increased content of aluminum and chrome.

Acknowledgements:

The work has been performed with the financial support of the Ministry of Education and Science of the Republic of Kazakhstan under the Project of Target Financing Program No.BR05236406.

References

1. Kabolov, Y., Petrushin, N., Svetlov, I., Demonis, I. (2007) Cast Heat-resistant Nickel Alloys for Perspective Aviation Gas Turbine Engines. Light Alloys Technology, 2, 6-16, Russia,
2. Stoller, V., Olbrich, A., Meese-Marktscheffel, Y., Mati, V., et al., (2007) Patent No. 2313589 RF, Method of Precious Metals Extraction from Super Alloys, Published on 27.12.2007. Bull., 36, Russia,
3. Paretskiy, V., Besser, A., Gedgagov, E. (2008) Ways of Increasing Rhenium Production from Ore and Technogenic Raw Materials. Precious Metals, 10, 17-21,
4. Kassikov, A., Petrova, A. (2014) Rhenium Recycling: Monograph. M.: RIOR: INFRAV-M, Nauchnaya Mysl, 2014. 95 p. Russia,
5. Petrova, A., Kassikov, A., Gromov, P., Kalinnikov, V. (2011) Rhenium Extraction from Wastes of Complex Cast Heat-resistant Alloys Based on Nickel. Precious Metals, 11, 39-43, Russia,
6. Olbrich, A., Meese-Marktscheffel, J., Jahn, M., Zertani, R., Stoller, V., Erb, M., Heine, K.-H., Kutzler, U. (2008) (WO08/000810) Recycling of superalloys with the aid of an alkali metal salt bath, Patentscope,
7. Petrova, A., Kassikov, A. (2012) Rhenium Extraction from Wastes of Processing and Operation of Heat-resistant Nickel Super Alloys. Aviation Materials and Technologies, 3, 9-13, Russia,
8. Krynitz, U., Olbrich, A., Kummer, W., Schloh, M. (1998) Patent 5776329 US. Method for the decomposition and recovery of metallic constituents from superalloys, USA,
9. Palant, A., Levchuk, O., Bryukvin, V. (2007) Complex Electrochemical

Technology of Processing Wastes of Heat-resistant Nickel Alloys Containing Rhenium. Non-ferrous Metallurgy, 11, 11-12, Russia,
10. Palant A., Brukvin V., Levchuk O., Palant A., Levin A. (2010) Patent 2401312, RF, Method of Electrochemical Processing of Metal Wastes of Heat-resistant Nickel Alloys Containing Rhenium. IMET RAS., Application of 09.04.2009. Published on 10.10.2010. Russia,
11. Chernysheva, O., Drobot, D. (2017) Variants of Electrochemical Processing of Rhenium-Containing Heat-resistant Alloy. Chemical Technology, 18 (1), 36-42, Russia,
12. Srivastava, R. R., Kim, M., Lee, J., Jha, M. K., Kim, B.-S. (2014) Resource recycling of superalloys and hydrometallurgical challenges. Journal of Materials Science, 49 (14), 4671-4686,
13. Agapova, L., Abisheva, Z., Kilibayeva, S., Altenova, A., Yakhiyayeva, Z., Ruzakhunova, G., Sapukov, I., Baisakalova, P. (2015) Electrochemical Opening of Technogenic Wastes of Heat-resistant Nickel Super Alloys. Materials of the 20th International Scientific and Technical Conference "Scientific Basis and Practice of Processing Ores and Technogenic Raw Materials", Yekaterinburg, Russia, 280-285,
14. Agapova, L., Abisheva, Z., Kilibayeva, S., Yakhiyayeva, Z. (2017) Electrochemical Processing of Technogenic Wastes of Rhenium-Containing Heat-resistant Nickel Alloys in Sulfuric Acid Solutions. Nonferrous Metals, 10, 69-74, Russia,
15. Agapova, L., Abisheva, Z., Kenzhaliyev, B., Kilibayeva, S., Yakhiyayeva, Z., Altenova, A. (2019) Patent No.33395, Method of electrochemical processing of metal waste of rhenium-containing heat-resistant nickel superalloys. Promyshlennaya Sobstvennost, 3, Kazakhstan,
16. Powder diffraction file-2, release 2009. International centre for diffraction date.

XIII International Mineral Processing and Recycling Conference
Belgrade, Serbia, 8-10 May 2019

University of Belgrade, Technical Faculty in Bor
Vojske Jugoslavije 12, 19210 Bor, Serbia
Tel. +381 30 424 555 Fax +381 30 421 078

EFFECT OF SiO_2/Al_2O_3 MOLAR RATIO ON STRUCTURE AND MECHANICAL PROPERTIES OF FLY ASH BASED GEOPOLYMER

Roland Szabó #, Mucsi Gábor
University of Miskolc, Miskolc, Hungary

ABSTRACT – Nowadays, the geopolymer technologies using secondary raw materials are more and more widespread, however, some of them (for example fly ash) have originally low reactivity which can be tailored by mechanical or chemical activation, or by addition of various high reactive materials. This study investigates the effect of silica and alumina contents on structure and physical properties of high calcium fly ash based geopolymers. Metakaolin (MK) was used as additional alumina and silica sources. It was added at various dosages (0; 5; 10; 15; 25; 50 and 75% by weight) as replacement of the fly ash (FA). Experimental results confirm that the compressive strength of the geopolymer is greatly affected by the SiO_2/Al_2O_3 ratio. The addition of MK improved the compressive strength of geopolymer by 92%. In addition, the effect of mechanical activation of FA on the strength of the geopolymer was investigated in case of a given MK content. Based on the results it can be stated the mechanically activated FA resulted in higher compressive strength.

Key words: fly ash, metakaolin, mechanical activation, geopolymer, SiO_2/Al_2O_3 molar ratio

INTRODUCTION

Geopolymers are three-dimensional, amorphous-to-semi-crystalline aluminosilicate materials, which can be produced from natural/synthetic aluminosilicate minerals or industrial aluminosilicate byproducts (such as: fly ash, red mud, slag, metakaolin, perlite, glass, rice husk ash, clay, or a combination of them) mixed with an alkaline (potassium/sodium hydroxide, potassium/sodium silicate) or acidic solution (phosphoric acid) [1-5]. The properties of the geopolymers are influenced in addition to the composition and reactivity of the material, [6], the composition of the activator solution [1, 7, 8] the curing condition (treatment temperature and time) [5, 8] and the compression method (especially vibrating compaction or high-pressure compaction) [9]. Geopolymer products can be used in many areas of the construction industry (such as masonry and insulating bricks, tiles, pavements, fire and heat resistant coatings, etc.).

Chindaprasirt et al. [10] investigated the effect of silica and alumina contents on setting, phase development, and physical properties of high calcium fly ash geopolymers. Control of setting and hardening properties were investigated by

corresponding author: ejtszabor@uni-miskolc.hu

adjusting SiO_2/Al_2O_3 ratio of the starting mix, via series of mixes formulated with varying SiO_2 or Al_2O_3 contents to achieve SiO_2/Al_2O_3 in the range 2.87–4.79. They found that increases in either silica or alumina content shortened the setting time of high calcium-based systems.

He et al. [11] investigated the effect of Si/Al ratio on structure, mechanical properties and chemical stability of metakaolin based geopolymers. Geopolymer with Si/Al of 4 showed much higher mechanical properties than geopolymer with Si/Al of 2, which was due to the increased Si-O-Si bonds and residual silica as reinforcement. However, geopolymer with Si/Al ≥3 showed worse chemical stability than those with Si/Al ≤ 2.5, with the presence of efflorescence on the surface, which was attributed to their higher residual free K^+.

The aim of the present research reported in this study primary is to study the effect of SiO_2/Al_2O_3 molar ratio on the structure of geopolymer and to examine the relation between silica and alumina content and geopolymer compressive strength. Additional goal was to investigate the dependence of strength on the fly ash fineness.

MATERIAL AND METHODS

FA from the lignite based power station (Visonta, Hungary) and MK were used for the experiments. FA was replaced with MK in various amount (0; 5; 10; 15; 25 and 75%) in the solid part. Mixture of sodium-hydroxide (8 M) and sodium-silicate (waterglass) solutions was used as alkaline activator. The sodium silicate solution contained SiO_2 of 25.3%, Na_2O of 13.7%, K_2O of 2.7 and water of 58.3%.

The particle size distribution of the raw materials and the ground FAs was measured by HORIBA LA-950V2 laser diffraction particle size analyzer in wet mode using distilled water as dispersing media. The geometric (outer) specific surface area (SSA) was calculated using PSD data by the laser sizer software. The chemical composition of raw materials was determined using X-ray fluorescence spectroscopy analysis (XRF). The main physical properties and chemical composition of FA and MK are found in Table 1 and Table 2.

Table 1. Physical properties of raw materials

	fly ash	metakaolin
particle density (g/cm^3)	1.93	2.73
x_{10} (μm)	10.8	1.8
x_{50} (μm)	52	5.2
x_{80} (μm)	119.3	8.5
SSA (cm^2/g)	1152	11307

Based on the Table 2 it can be stated that the SiO_2 content of FA and MK was similar, but the Al_2O_3 content was rather different. The Al_2O_3 content in MK was three times higher than in FA.

The mechanical activation experiments of FA were carried out in a conventional tumbling laboratory ball mill with the size of Ø305×305 mm (smooth walled), with steel balls (maximum ball size was 50 mm) as grinding media. The mill filling ratio of the grinding media was 30 volume %, the material filling ratio was 110 volume%.

Residence time of mechanical activation was 5, 10, 20, 30, 60 and 120 minutes.

Table 2. Chemical composition of starting materials

Component (%)	SiO_2	Al_2O_3	CaO	Fe_2O_3	MgO	Na_2O	K_2O	TiO_2	P_2O_5	MnO	SO_3	L.o.I.*
fly ash	48.1	14.42	11.76	10.97	3.34	0.37	1.66	0.492	0.264	0,171	0.575	2.2
metakaolin	51.4	45.9	0.4	1.12	0.26	0.05	1.34	0.05	0.064	0,033	<0.013	-

*L.o.I. =Loss on ignition (at 950 °C)

The composition of the geopolymer product was investigated by using a JASCO 4200 type Fourier Transformed Infrared Spectrometer (FT-IR) in reflection mode with diamond ATR.

EXPERIMENTAL

Systematic experimental series were carried out in the framework of the research focusing on the following questions:

- Effect of silica and alumina content on structure and physical properties of high calcium FA based geopolymers using MK as replacement of FA.
- Effect of mechanical activation of FA on geopolymer strength and density in case of a given MK content.

Geopolymer specimens were prepared by mixing raw or ground FA (and MK) and alkaline activator (mixture of 8M NaOH and waterglass) using 0.82 liquid/solid ratio (L/S ratio). Paste was placed to pre-oiled mould and compacted by vibration. The geopolymer paste was kept in mould for 24 hours in sealed condition in a climate chamber at 23 °C, before removing the specimens. It is followed by heat curing at 30 °C for 6 hours. After the heat treatment the specimens were stored in a climate chamber at 23 °C and humidity of 90% until the compressive strength test. The uniaxial compressive strength of the geopolymer was determined by Compression Testing Machine at the age of 7 days. Five specimens were prepared in each cases.

RESULTS

Mechanical activation of FA

The effect of the grinding time on the particle size and SSA of the ground and raw FA is summarized in Table 3. The 50 percent particle size (median) of the raw FA was 112.6 μm. During the milling the particle size was significantly decreased and SSA increased, after 120 min milling median size of the FA was finer than 8.4 μm, and the 80 percent particle size in this case was 16.1 μm. Particles with smaller size than 1 μm also appeared in a significant amount (more than 10%). Additionally, the "outer" specific surface area increase was significant; from 1140.9 cm^2/g it reached 12228.8 cm^2/g due to ball milling.

Effect of SiO_2/Al_2O_3 ratio

Based on the Fig. 1 it can be seen that, MK had a positive effect on the compressive strength of geopolymers. Increasing amount of MK in the solid part of mixture

increased the geopolymer strength and density. Geopolymer with the highest strength and density was made by 50% MK content in the solid part. These values were 22.1 MPa and 1.61 g/cm^3. It is important to note that increasing amount of MK reduced the workability of the mixture. It was not workable with 75% MK content (granulates were formed during mixing).

Table 3. Characteristic particle size and SSA of FA after various grinding time

Material properties	Grinding time (min)						
	0	5	10	20	30	60	120
x_{10} (μm)	10.3	9.7	8.4	6.5	5.8	4	0.5
x_{50} (μm)	48.4	41.1	29.6	19.5	16.4	12.3	8.4
x_{80} (μm)	112.6	89.5	68.1	45.9	33.7	22.6	16.1
SSA (cm^2/g)	1140.9	1219.3	1417.9	1807.4	2056.5	2937.9	12228.8

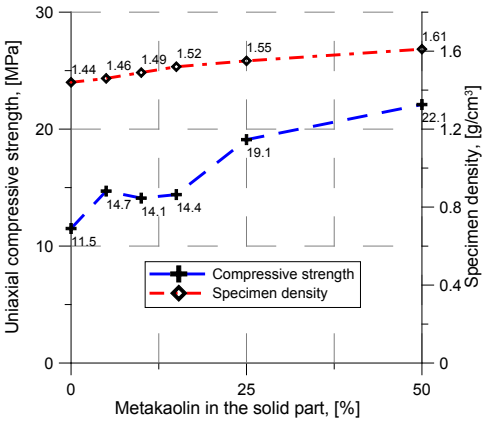

Figure 1. Effect of metakaolin dosage

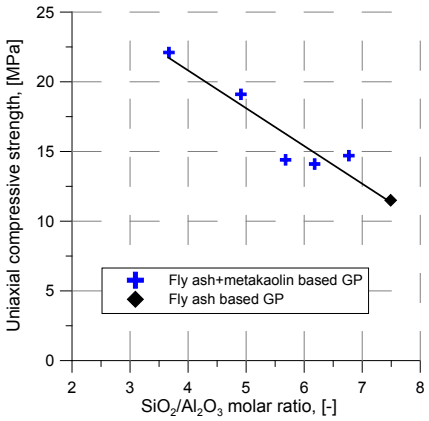

Figure 2. Effect of SiO_2/Al_2O_3 molar ratio

Fig. 2 shows the relation between the SiO_2/Al_2O_3 molar ratio of mixture and the compressive strength. The SiO_2/Al_2O_3 ratio was between 3.67 and 7.49, which was modified with change of MK content in the solid part of mixture. Increasing amount of MK (due to the higher Al_2O_3 content) decreased the SiO_2/Al_2O_3 ratio. Based on the Fig. 2 it can be stated that increasing the SiO_2/Al_2O_3 ratio decreased the geopolymer strength. The highest compressive strength of 22.1 MPa was in case of SiO_2/Al_2O_3=3.67. Furthermore, it can be observed that the geopolymers had almost same strength (14.1-14.7 MPa) between SiO_2/Al_2O_3 of 5.68 and 6.77.

Effect of grinding fineness of FA

The effect of grinding fineness of FA was investigated by metakaolin content of 25% taking into the workability of mixture. Based on the Fig. 3 it can be stated that increasing the grinding time (by changing of FA fineness) increased the density and compressive strength of the geopolymers. While the raw FA based geopolymers (SSA_{FA}=1141 cm^2/g) had compressive strength of 19.1 MPa and specimen density of

1.54 g/cm^3, the geopolymers which were made using SSA_{FA} of 12229 cm^2/g (grinding time of 120 min) had compressive strength of 25.2 MPa and specimen density of 1.64 g/cm^3. As a result of the milling, the specific surface of the material was increased as well, resulting more Al and Si was solved by the alkaline solution from the FA, and this was advantageous for the emergence of the geopolymer gel. Another explanation of the increasing compressive strength (and specimen density) can be that the finer particles resulted in more compact microstructure.

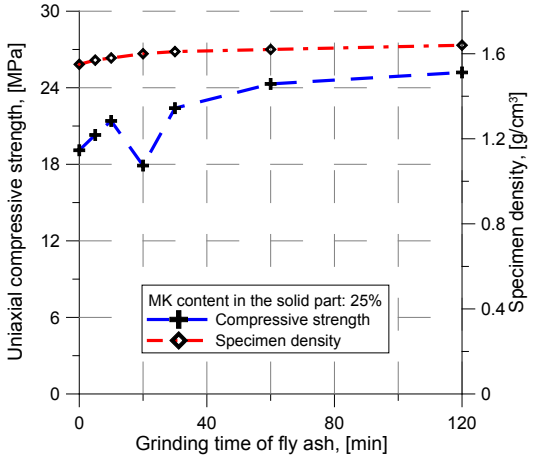

Figure 3. Effect of fineness of FA on the compressive strength and specimen density

FT-IR results

The FT-IR spectra of raw materials (FA and MK) can be seen in Fig. 4. The IR spectrum of MK contains one very intense band characteristic of the internal vibrations in TO_4 tetrahedral (T= Al, Si). This peaks at around 1064 cm^{-1}, is associated with T–O-Si bond (T= Al, Si) asymmetric stretching vibrations (this band provides information on the degree of crystallinity of a sample). In case of FA this peak appeared at around 1100-1009 cm^{-1} (double band). Besides that peak at 1457 cm^{-1} corresponds to O-C-O stretching vibration, symmetrical stretching vibrations of Si-O-Si and Al-O-Si bonds are observed at 677 and 598 cm^{-1} [12].

FT-IR spectra of geopolymers can be seen in Fig. 5. The most characteristic difference observed between the FT-IR spectrum of FA and FT-IR spectra of geopolymers concerning the band attributed to the asymmetric stretching vibrations of Si–O–Si and Al–O–Si. This band that was appeared as a broad band between 1100 and 1009 cm^{-1} in the FT-IR spectrum of FA became sharper and shifted to lower wavenumber (~943 cm^{-1}) in the FT-IR spectrum of FA based geopolymer indicating the formation of a new product (the amorphous aluminosilicate gel phase), which is associated with the dissolution of FA amorphous phase in the strong alkaline activator [12]. This peak appeared between 951 and 973 cm^{-1} in the FT-IR spectra of MK containing geopolymers.

The broad bands appeared in all FTIR spectra in the region of 3370 and 1640

cm^{-1} are assigned to stretching (–OH) and bending (H–O–H) vibrations of bound water molecules, which are surface absorbed or entrapped in the large cavities of the polymeric framework [12, 13]. Intensity of these bands decreased by higher MK content, which could be correlated with higher mechanical strengths.

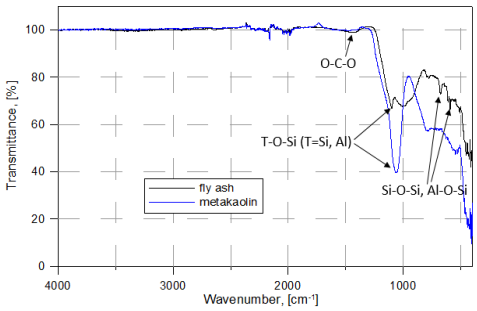

Figure 4. FT-IR spectra of raw materials

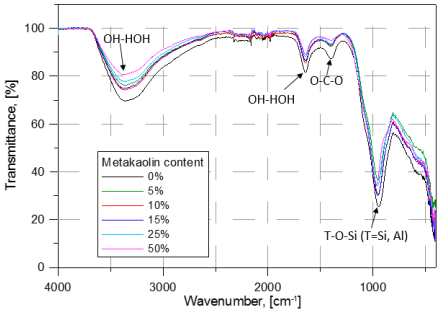

Figure 5. FT-IR spectra of geopolymers with different MK content

Peak observed at 1457 cm^{-1} in case of FA shifted a lower wavenumber (1400 cm^{-1}) in all the FTIR spectra of geopolymer, which are attributed to stretching vibrations of O–C–O bond indicating the presence of sodium bicarbonate that is suggested to occur due to the atmospheric carbonation of the high alkaline NaOH aqueous phase, which is diffused on the geopolymeric materials surface [12]. Intensity of these bands decreased by higher metakaolin content, which could be correlated with increased mechanical strengths.

CONCLUSIONS

Based on the experiments the following conclusions can be drawn:

- MK had a positive effect on the compressive strength of FA based geopolymers. Increasing of MK content improved the strength. Geopolymer with the highest strength (22.1 MPa) and density (1.61 g/cm^3) was made by 50% MK content in the solid part.
- MK content in the solid part was in correlation with the SiO_2/Al_2O_3 molar ratio. Higher MK content resulted in lower SiO_2/Al_2O_3 ratio of the mixture. There is a relationship between the SiO_2/Al_2O_3 ratio and compressive strength. The lower SiO_2/Al_2O_3 molar ratio resulted in a higher compressive strength.
- Beside MK content the FA fineness was also significantly affected in the strength of geopolymer. Using finer FA resulted in higher mechanical stability of geopolymers. Geopolymer with highest compressive strength (25.2 MPa) was made using SSA_{FA} of 12229 cm^2/g (grinding time of 120 min).

Acknowledgement

This research was supported by the ÚNKP-18-3 New National Excellence Program of the Ministry of Human Capacities. Authors appreciate the help of Akos

Debreczeni (Institute of Mining and Geotechnical Engineering, at University of Miskolc) and Ferenc Moricz (Institute of Mineralogy and Geology, at University of Miskolc) for strength tests and XRF measurements.

References

1. Tchakouté, H.K., Rüscher, C.H., Kamseu, E., Andreola, F., Leonelli, C. (2017) Influence of the molar concentration of phosphoric acid solution on the properties of metakaolin-phosphate-based geopolymer cements. Applied Clay Science, 147, 184-194,
2. Davidovits J. (2011) Geopolymer chemistry and application. Institut Geopolimére, 283, 286,
3. Vaou, V., Panias, D. (2010) Thermal insulating foamy geopolymers from perlite. Minerals Engineering, 23(14), 1146-1151,
4. Komnitsas, K., Zaharaki, D. (2007) Geopolymerisation: A review and prospects for the minerals industry. Minerals engineering, 20(14), 1261-1277,
5. Palomo, A., Grutzeck, M.W., Blanco, M.T. (1999) Alkali-activated fly ashes: a cement for the future. Cement and concrete research, 29(8), 1323-1329,
6. Kumar, S., Mucsi, G., Kristaly, F., Pekker, P. (2017) Mechanical activation of fly ash and its influence on micro and nano-structural behaviour of resulting geopolymers. Advanced Powder Technology, 28(3), 805-813,
7. Cheng, Y., Hongqiang, M., Hongyu, C., Jiaxin, W., Jing, S., Zonghui, L., Mingkai, Y. (2018) Preparation and characterization of coal gangue geopolymers. Construction and Building Materials, 187, 318-326,
8. Molnár, Z., Szabó, R., Rácz, Á., Lakatos, J., Debreczeni, Á., Mucsi, G. (2017) Optimization of activator solution and heat treatment of ground lignite type fly ash geopolymers. IOP Conference Series: Materials Science and Engineering, 175(1), 1-8,
9. Živica, V., Balkovic, S., Drabik, M. (2011) Properties of metakaolin geopolymer hardened paste prepared by high-pressure compaction. Construction and Building Materials, 25(5), 2206-2213,
10. Chindaprasirt, P., De Silva, P., Sagoe-Crentsil, K., Hanjitsuwan, S. (2012) Effect of SiO_2 and Al_2O_3 on the setting and hardening of high calcium fly ash-based geopolymer systems. Journal of Materials Science, 47(12), 4876-4883,
11. He, P., Wang, M., Fu, S., Jia, D., Yan, S., Yuan, J., Xu J., Wang P., Zhou, Y. (2016) Effects of Si/Al ratio on the structure and properties of metakaolin based geopolymer. Ceramics International, 42(13), 14416-14422,
12. Swanepoel, J.C., Strydom, C.A. (2002) Utilization of fly ash in a geopolymeric material. Applied geochemistry, 17(8), 1143-1148,
13. Ozer, I., Soyer-Uzun, S. (2015) Relations between the structural characteristics and compressive strength in metakaolin based geopolymers with different molar Si/Al ratios. Ceramics International, 41(8), 10192-10198.

XIII International Mineral Processing and Recycling Conference
Belgrade, Serbia, 8-10 May 2019

University of Belgrade, Technical Faculty in Bor
Vojske Jugoslavije 12, 19210 Bor, Serbia
Tel. +381 30 424 555 Fax +381 30 421 078

EXTRACTION OF RARE EARTH VALUES FROM DISCARDED CFLs

Himanshu Tanvar, Nikhil Dhawan #
Indian Institute of Technology, Department of Metallurgical and Materials Engineering, Roorkee, India

ABSTRACT – Discarded CFL samples are evaluated as a potential source of REEs. The phosphors powder obtained from mechanical separation contains 31 % rare earth values. The quantitative XRD analysis of phosphor sample yielded 39.9 % $Y_{1.90}Eu_{0.10}O_3$, 14.6 % $Al_{11}Ce_{0.67}MgO_{19}Tb_{0.33}$, and 21.4 % $Al_{10.09}Ba_{0.96}Mg_{0.91}O_{17}$: Eu^{2+}. Planetary ball milling was found promising in the liberation of REEs from given phosphor sample. A short milling of 20 - 30 min was found adequate for optimal recovery (> 90 %) of REEs after leaching in 3M HNO_3. Calcination of the precipitates resulted in the formation of REO with Y-Eu purity of > 98 % and > 90 % recovery rate. Eu, Y phase dissolution behavior was found completely different than Ce, Tb phase due to inert nature of $Al_{11}Ce_{0.67}MgO_{19}Tb_{0.33}$ till 120 min milling and 6 M acid concentration in leaching.

Key words: discarded CFL, rare earth elements, phosphor, mechanical milling, leaching.

INTRODUCTION

The rare earth elements (REEs) and their compounds have a wide range of applications including a catalyst in chemical and metallurgical industry, coloring of glass and ceramics, magnets and phosphors [1]. The major raw material for REEs includes monazite sand, xenotime, bastnasite, and phosphate rocks. The REEs being chemically similar to each other, invariably occur together in the ores and behave as a single entity. The minimum industrial grade of REE ores varies from 0.15 - 2 %. The extraction of REEs from its primary ores mainly includes mineral beneficiation, leaching, fractional crystallization, ion exchange, precipitation, solvent extraction, and reduction to metals [1, 2]. World reserves of rare earth oxides (REOs) are estimated at 92.4 million metric tons and 36 % of world's REO resources are located in China, 18 % in Vietnam, 18 % in Brazil, 15 % in Russia, 6 % in India, and the remainder in several other countries [3]. Cerium the most common rare earth is more abundant than cobalt and Yttrium is more abundant than lead [1].

Phosphors are essential components for luminescent behavior in fluorescent lamps. Excitation of REEs by absorption of UV radiation causes specific energy level transition within the atom creating emissions of visible radiation. The REE content in the phosphor is significantly higher than natural occurring deposits and make up

corresponding author: ndhawan.fmt@iitr.ac.in

more than 23 % of the phosphor in fluorescent lamps, which is 10 - 100 times more than that of the minimum industrial grade of REE ores (0.15 - 2 %) [4, 5]. In fact, phosphors from discarded compact fluorescent lamps (CFLs) can be considered as a new source of REEs with several advantages over primary supply, reducing the environmental impact, landfilling problems and co-production of the unwanted REEs [6]. Currently, the recycling rate of CFLs for recovery of REEs is very limited. There are several studies focused on recovery of REEs from phosphor following hydro, pyro and mechanical activation routes. Based on the literature it is found that the recovery of REEs from waste CFLs is focused primarily through the hydro [7, 8, 9, 10, 11, 12] and pyro [13, 14, 15] metallurgy route whereas few studies are reported on mechano-activation assisted leaching [4, 5, 16]. Hydrometallurgy based studies are mainly focused on Y and Eu recovery and involve leaching in high acid concentration (> 5 M), extended leaching time (h) or high temperature (80 - 100 °C). Furthermore, the following route fails for recovery of Tb and Ce from the green and blue phosphor, which are difficult to leach out under moderate conditions. Pyro-metallurgical routes are generally energy-intensive involving higher reaction temperature as well as flux requirement. Roasting is found to be effective with the recovery of > 95 % REEs but involves serious drawback of additional flux requirement and leach residue generation.

Mechanical activation by planetary ball mill involves the application of compressive force and shear impact that causes physiochemical changes, new surface generation, polymorphic transformation and direct reaction in some case. Mechanical activation also decreases the activation energy of the leaching process thereby increasing the leaching efficiency [4, 5, 17, 18]. Mechanical activation reported works are scarce, lacks the information on the effect of mechanical milling on different phosphors, recovery of REEs from leach solution and leach residue utilization. The purpose of this research work for the recovery of REEs from discarded CFLs includes 1) separation and characterization of waste phosphor 2) direct leaching and effect of milling on leaching 3) precipitation of RE values, and 4) leach residue analysis.

MATERIALS AND METHOD

Feed preparation and characterization

The end of life CFLs used in this study was procured from a local electric warehouse. The CFLs were shredded and different components were separated. Phosphors sample was separated from waste cullet and plastic by standard sieving operation at a size of 53 μm. The mineral element composition (oxides) of waste phosphor powder was determined using X-ray fluorescence (XRF) technique. The morphology of the powder sample was studied by scanning electron microscopy (SEM) attached with Electron Dispersive X-ray technique (EDS). The X-ray diffraction study of the sample was carried out by X-ray diffractometer using Cu-Kα radiation. The diffraction peaks were recorded in the 2θ range of 5 - 80 ° with a step size of 0.02 ° and a scanning rate of 2 °/minute to identify the different phases. The degree of crystallinity of maximum intensity peak was calculated by the formula; $(I/I_o)\cdot 100$ where I and I_o are peak intensity of respective phase before and after treatment.

Leaching and REE precipitation

The leaching experiments were carried out in a 250 mL glass beaker using magnetic stirrer (C-Mag HS-7, IKA) at 40 °C with a subsequent solid-liquid ratio and the stirring speed of 1:25 (g/ml) and 900 rpm, respectively. The subsequent leach residue was separated from leach solution by vacuum filtration and was dried in a laboratory oven at 110 °C. Leach solution was further processed for REE precipitation. The amount of REE values remaining in the leach residue was determined by XRF analysis and subsequent dissolution % of REEs was calculated as shown in Eq. (1).

$$\% \, REE - dissolution = (REE_{FEED} - REE_{LR}) / (REE_{FEED}) \times 100 \quad (1)$$

Where REE_{FEED} and REE_{LR} represent the amount of REEs (g) in feed and leach residue respectively.

Oxalic acid was added to the leach solution to precipitate REE ions, and the pH values were adjusted by adding HNO_3 or NH_4OH. The pH value was monitored throughout the precipitation process using pH meter. The desired amount of oxalic acid based on stoichiometric calculation was added to the leachate in the solid form. The precipitation process was carried out on a continuous magnetic stirring at 600 rpm for 20 min at 60 °C and the precipitates were recovered by filtration. The rare earth oxalates were heated at 900 °C for 1h to obtain REOs and the solid weight was determined for calculation of REO extraction.

Mechanical milling and activation

The waste phosphor sample was mechanically activated using a planetary ball mill (PBM) for different time duration using ball-powder ratio and milling speed; 9:1, 450 rpm respectively. The feed was loaded into tungsten carbide jar of capacity 125 ml along with tungsten carbide balls (diameter 0.25 inches) and the jar was sealed with a clamp. The mill was set to run and pause alternately for 10 min intervals, to prevent generation of excessive heat. After milling, the milled products were retrieved using a spatula and special care was taken to minimize the risk of contamination.

RESULTS AND DISCUSSION

Material characterization

The composition of the feed sample determined by XRF is shown in Fig 1(a) reveals that the waste phosphor sample consists of ~ 31 % REOs along with ~ 38 % Al_2O_3 and ~ 15 % SiO_2 as major impurities. Based on scoping experiments it was found that sieving of crushed CFLs below 53 μm separated the phosphors powder effectively from glass, plastic and alumina casing. The XRD analysis along with quantitative phase composition shown in Fig. 1(a) reveals that red (YOX: $Y_{1.90}Eu_{0.10}O_3$), green (CAT: $Al_{11}Ce_{0.67}MgO_{19}Tb_{0.33}$), and blue (BAM: $Al_{10.09}Ba_{0.96}Mg_{0.91}O_{17}:Eu^{2+}$) phosphor were the main phosphors present in the feed along with a glass (SiO_2). The SEM micrograph and EDS analysis of representative

feed are shown in Fig. 1(b). The micrograph depicted the presence of two distinct morphologies, primarily showing rare earth phases and secondary silica phase. As per stoichiometry, Y, and Eu content in the red phosphor is 72, and 25 %, which theoretically yields 26, and 2.2 % Y and Eu in the feed and is in reasonable agreement with XRF and EDS analysis shown in Fig. 1.

Oxide	Wt(%)
Na_2O	1.88
MgO	1.98
Al_2O_3	37.56
SiO_2	15.32
K_2O	0.93
CaO	2.68
Y_2O_3	26.77
BaO	3.86
CeO_2	2.88
Eu_2O_3	1.68
Tb_4O_7	1.86

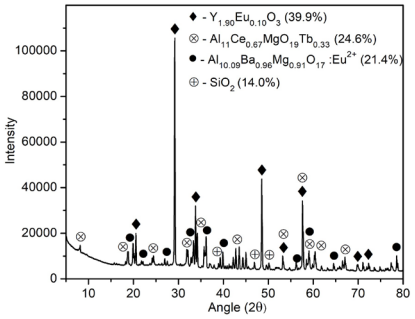

(a)

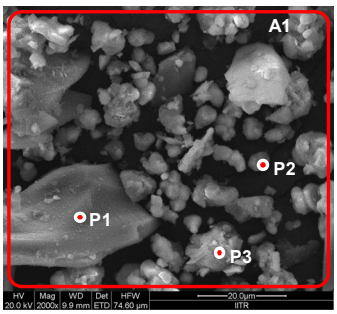

Wt (%)	A1	P1	P2	P3
O	42.42	46.56	25.30	38.57
Na	0.57	10.23	0.17	-
Al	16.64	3.19	33.06	21.58
Si	7.07	36.65	4.81	0.91
Ca	1.13	0.72	0.62	0.46
Y	23.75	0.88	1.5	25.29
Ba	-	0.59	1.58	2.08
Ce	2.90	0.16	17.19	1.03
Eu	2.05	0.58	1.61	7.03
Tb	0.94	0.37	12.06	0.23
	-	Glass	Phosphor	Phosphor

(b)

Figure 1. Characteristics of waste phosphor powder **(a)** XRF and XRD spectrum, **(b)** SEM (EDS)

Mechanical activation of phosphors powder

The direct leaching of the waste phosphors sample in different lixiviants) yielded low REE dissolution (1 - 5 %) with distilled water and ~ 40 % with inorganic acids (2M HCl, 2M HNO_3, 2M H_2SO_4). In other words, it can be said that Y, Eu, Tb, and Ce values are locked in the phosphor matrix. The effect of mechanical activation on leaching behavior of REEs from waste phosphor powder was evaluated by milling for the duration of 20, 40 min followed by leaching in 3M HCl, HNO_3 and H_2SO_4 as shown in Fig. 2. A considerable increase in REE dissolution was observed after milling, depicting positive response of mechanical activation towards the release of REEs from phosphors matrix. Also, all the lixiviants yielded similar dissolution and corresponding chemical reactions are shown in Eq. (2) - (4). It is believed that the proton destabilized the rare earth oxide crystal lattice by attacking the oxygen to form water. The anion acts as a complexing ligand and forms an aquo-complex with the unbounded rare earth cation to form respective rare earth compound ($ReCl_3$, $Re(NO_3)_3$, $Re_2(SO_4)_3$). The reaction can proceed forward or backward depending on

the concentration and solubility of the rare earth [10].

$$Re_2O_3 + 6HCl \rightarrow 2ReCl_3 + 4H_2O \qquad pH < 1 \qquad (2)$$

$$Re_2O_3 + 6HNO_3 \rightarrow 2Re(NO_3)_3 + 4H_2O \qquad pH < 1 \qquad (3)$$

$$Re_2O_3 + 3H_2SO_4 \rightarrow Re_2(SO_4)_3 + 3H_2O \qquad pH < 1 \qquad (4)$$

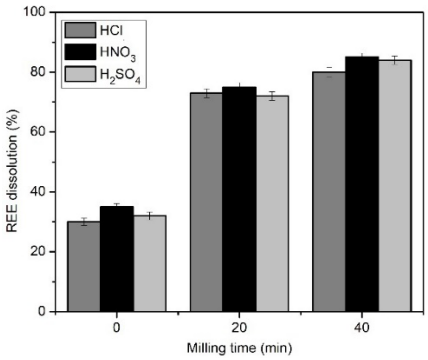

Figure 2. REE dissolution with milling time (Leaching conditions: 2M acid, 50 °C, 30 min)

The dissociation of different phases during milling was studied using the XRD and SEM analysis as shown in Fig. 3. It is observed that with an increase in milling time the amorphous character of the sample increases as shown by the fall in peak intensity. After 20 min of milling, the degree of crystallinity decreased by ~ 27 % for the (Y, Eu) phase and ~ 20 % for (Ce, Tb) phase, with further milling, the rate of dissociation decreased and ~ 4 % and ~ 5 % further loss in crystallinity was observed with (Y, Eu) and (Ce, Tb) phases respectively.

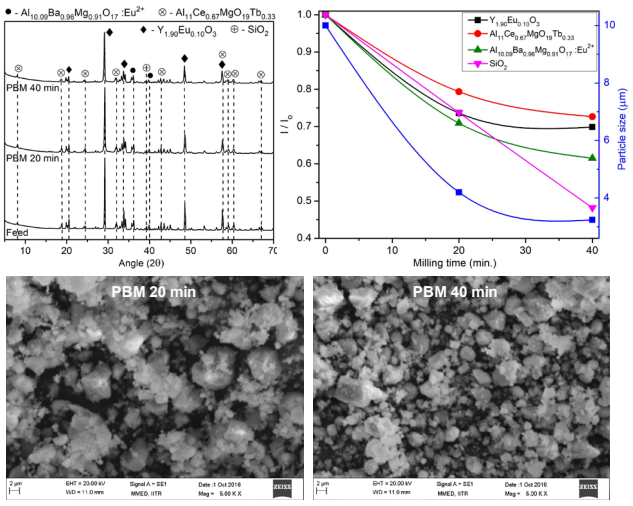

Figure 3. XRD spectra of milled powder (20, 40 min) and effect of milling time on crystallinity along with SEM micrograph

It can be concluded that $Al_{11}Ce_{0.67}MgO_{19}Tb_{0.33}$ phase does not dissociate even with milling, and hence can be considered as an inert phase. The results are in agreement with REE dissolution values as a limited increase in dissolution was observed between 20 - 40 min milling. The rate of decrease of crystallinity slows down with milling time due to the involvement of high energy required to break the particle during the milling process [18]. The SEM micrograph of milled phosphor sample at 20 and 40 min milling depicted the particle size decreased from ~ 10 microns in the feed to ~ 4 microns and ~ 3.5 microns respectively after milling. Since considerable REE dissolution was obtained at 40 min milling and to avoid excessive size reduction, extended milling was not pursued.

Characterization of REOs extracted

The REOs extracted at 30 min milling, 3M HNO_3, 60 min leaching in the form of precipitates were subjected to calcination at 900 °C for 2h and the white color powder was obtained and confirmed by the XRD analysis (Fig. 4). Crystalline peaks of Y_2O_3 and Eu_2O_3 were observed and corresponding SEM micrograph of the REOs shown in Fig. 4 depicted the presence of flakes ~ 2 microns in size. Furthermore, EDS analysis of complete area reveals that Y and Eu are the major REEs present in the oxide. However, Ce and Tb values were not extracted in considerable amount even at the extreme conditions as $Al_{11}Ce_{0.67}MgO_{19}Tb_{0.33}$ phase was found inert.

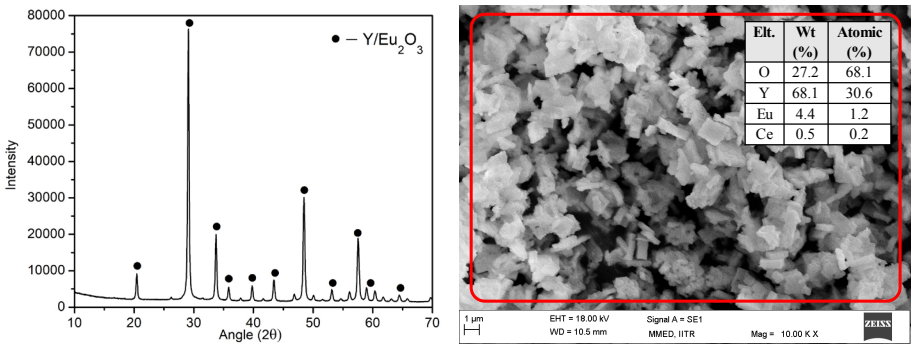

Figure 4. XRD and SEM(EDS) analysis of REO at 30 min milling, 2M HNO_3, 60 min leaching

Leach residue analysis and further processing

The XRD spectra of leach residue shown in Fig. 5 (a) revealed that $Y_{1.90}Eu_{0.10}O_3$ phase disappeared completely whereas $Al_{11}Ce_{0.67}MgO_{19}Tb_{0.33}$ phase remains fairly stable. The XRF analysis of leach residue (LR1) shown in Table 1 depicts that it contains ~ 3 % Tb and 5 % Ce values respectively. It is concluded that Ce, Tb containing phase is inert to milling even up to 40 min duration. Therefore, further milling of leach residue was carried out till 80 min to evaluate the dissolution response of Ce and Tb. The milled sample leached in 3 M HNO_3 showed no positive response towards Ce, Tb liberation and dissolution. Furthermore, the acid concentration was increased to 6 M and a similar result was obtained as confirmed by XRF analysis of leach residue (LR2) shown in Table 1. The XRD analysis of the

milled sample, leach residue of 3M and 6M leached samples is shown in Fig. 5 (b). Ce, Tb containing phase was found inert throughout the milling and leaching process. Base on the literature, it is reported that Ce-Tb can be recovered up to 95 % from LAP phosphor ($La_{0.57}Ce_{0.27}Tb_{0.16}PO_4$) with 60 min of mechanical activation and leaching in 6 M acid. However, in this study Ce and Tb are present in CAT phosphor ($Al_{11}Ce_{0.67}MgO_{19}Tb_{0.33}$) and were found inert even after 120 min of milling and dissolution in acid concentration of 6 M HNO_3 and HCl. The CAT phosphor has a distorted magneto-plumbite crystal structure which consists of spinel-like blocks separated by mirror planes. The spinel blocks are composed of Al^{3+}, Mg^{2+}, and O^{2-}, while the mirror planes contain O^{2-} and large cations of trivalent RE (Tb^{3+}, Ce^{3}). The Al^{3+} is present at the octahedral, tetrahedral, and fivefold surrounding of oxygen ions sites [14]. The complex structure of CAT phosphor makes it difficult for the liberation of RE values by mechanical milling and high concentration acid. However, alkaline fusion with sodium hydroxide can be promising in liberation of Ce, Tb values. Heat treatment with NaOH results into formation of $NaAlO_2$ which is water soluble and can be separated after leaching in water and the RE values combine with free OH- to form oxide which can be further leached in 2 M acid and recovery with oxalic acid precipitation.

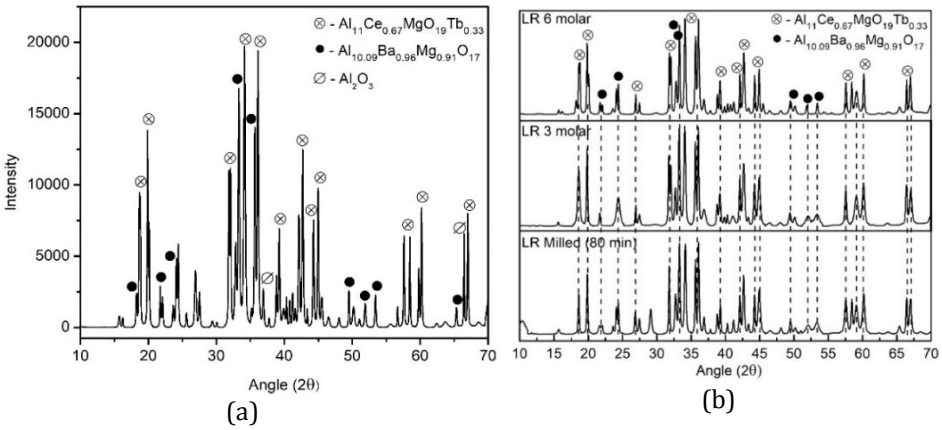

Figure 5. XRD spectra of leach residue (a) 20 min milling, 3M HNO_3, 40 min leaching, (b) LR 3M and 6M HNO_3

Table 1. XRF analysis of leach residue

Oxide	Wt (%), LR1	Wt (%), LR2
Na_2O	3.09	5.52
MgO	3.29	3.68
Al_2O_3	48.34	51.10
SiO_2	23.36	22.34
Y_2O_3	3.64	0.07
BaO	4.65	5.07
CeO_2	4.32	4.81
Eu_2O_3	0.65	0.63
Tb_4O_7	2.64	2.66

CONCLUSION

In this study discarded CFL samples, unlike commercial phosphors, are evaluated as a potential source of REEs (Y, Eu, Ce, Tb). Sieving of crushed CFLs below 53 microns separated the phosphors powder from glass effectively. Glass, plastic and metal casing separated can be recycled directly. Based on the quantitative XRD analysis phosphor sample consist of 39.9 % red (YOX: $Y_{1.90}Eu_{0.10}O_3$), 14.6 % green (CAT: $Al_{11}Ce_{0.67}MgO_{19}Tb_{0.33}$), and 21.4 % blue (BAM: $Al_{10.09}Ba_{0.96}Mg_{0.91}O_{17}$: Eu^{2+}) phosphor along with 14.1% silica from glass tube. Direct leaching of phosphor in different lixiviants (HCl, HNO_3, H_2SO_4) yielded very fewer dissolution values.

Planetary ball milling was found promising in the liberation of REEs such as Y and Eu from given phosphor sample. Excessive milling promotes REE dissolution along with impurities dissolution which further restrict the precipitation process. A short milling of 20 - 30 min and 2 - 3 M acid concentration was found adequate for optimal recovery (> 90 %) of REEs. Calcination of the precipitates resulted in the formation of REO with Y and Eu purity of > 98 % and > 90 % recovery rate. Eu, Y phase dissolution behavior was found completely different than Ce, Tb phase due to inert nature of $Al_{11}Ce_{0.67}MgO_{19}Tb_{0.33}$ till 120 min milling and 6 M acid concentration in leaching. Based on experimental findings of this work, it is recommended that discarded CFLs can be employed for extraction of Eu and Y whereas, for Tb, Ce rigorous/extensive milling and leaching conditions can be sought.

References

1. Habashi, F. (2013) Extractive metallurgy of rare earths. Can. Metall. Q., 52 (3), 224-233,
2. Gupta, C. K., Krishnamurthy, N. (2005) Extractive Metallurgy of Rare Earths. CRC Press,
3. IBM, Indian Minerals Yearbook 2017 (Part- III: Mineral Reviews) 56th edition: Rare Earths,
4. Tan, Q., Deng, C., Li, J. (2016) Innovative Application of Mechanical Activation for Rare Earth Elements Recovering: Process Optimization and Mechanism Exploration. Scientific Reports, 6 (19961),
5. Van Loy, S., Binnemans, K., Van Gerven, T. Recycling of rare earths from lamp phosphor waste: Enhanced dissolution of $LaPO_4$:Ce^{3+}, Tb^{3+} by mechanical activation. J. Clean. Prod. 156, 226-234,
6. Binnemans, K., Jones, P. T., Blanpain, B., Van Gerven, T., Yang, Y., Walton, A., Buchert, M. (2013) Recycling of Rare Earths: A Critical Review. J. Clean. Prod., 51, 1-22,
7. Tunsu, C., Ekberg, C., Retegan, T. (2014) Characterization and leaching of real fluorescent lamp waste for the recovery of rare earth metals and mercury. Hydrometallurgy, 44-145, 91-98,
8. Tunsu, C., Petranikova, M., Ekberg, C., Retegan, T. (2016) A hydrometallurgical process for the recovery of rare earth elements from fluorescent lamp waste fractions. Sep. Purif. Technol., 161, 172-186,
9. Innocenzi, V., De Michelis, I., Ferella, F., Vegliò, F. (2017) Leaching of yttrium from cathode ray tube fluorescent powder: Kinetic study and empirical models. Int. J. Miner. Process., 168, 76-86,

10. Eduafo, P. M., Mishra, B. (2018) Leaching Kinetics of Yttrium and Europium Oxides from Waste Phosphor Powder, J. Sustain. Metall., 4 (4), 437-442,
11. Miskufova, A., Kochmanova, A., Havlik, T., Horvathova, H., Kuruc, P. (2018) Leaching of yttrium, europium and accompanying elements from phosphor coatings, Hydrometallurgy 176, 216-228,
12. Lin, E. Y., Rahmawati, A., Ko, J.-H., Liu, J.-C. (2018) Extraction of yttrium and europium from waste cathode-ray tube (CRT) phosphor by subcritical water. Sep. Purif. Technol., 192, 166-175,
13. Liua, H, Zhanga, S., Pana, D., Tiana, J., Yanga, M., Wua, M., Volinsky, A. A. (2014) Rare earth elements recycling from waste phosphor by dualhydrochloric acid dissolution. J. Hazard. Mater., 272, 96-101,
14. Liu, H., Zhang, S.-G., Pan, D.-A., Liu, Y.-F., Liu, B., Tian, J.-J., Volinsky, A.A. (2015) Mechanism of $CeMgAl_{11}O_{19}$: Tb^{3+} alkaline fusion with sodium hydroxide. Rare Met., 34 (3), 189-194,
15. Liang, Y., Liu, Y., Lin, R., Guoa, D., Liao, C. (2016) Leaching of rare earth elements from waste lamp phosphor mixtures by reduced alkali fusion followed by acid leaching. Hydrometallurgy, 163, 99-103,
16. Tan, Q., Deng, C., Li, J. (2017) Enhanced recovery of rare earth elements from waste phosphors by mechanical activation. J. Clean. Prod., 142, 2187-2191,
17. Kohobhange, S. P. K., Manoratne, C. H., Pitawala, H. M. T. G. A., Rajapakse, R. M. G. (2018) The effect of prolonged milling time on comminution of quartz. Powder Technol., 330, 266-274,
18. Baláž, P. (2003) Mechanical activation in hydrometallurgy. Int. J. Miner. Process., 72, 341-354,
19. Montgomery, D. C. (2013) Applied Statistics and Probability for Engineers. 6th Edition, Wiley, 811,
20. Chi, R., Xu, Z. (1995) A solution chemistry approach to the study of rare earth element precipitation by oxalic acid. Metall. Mater. Trans. B, 30 (2), 189-195,
21. Kumari, A., Jha, S., Patel, J. N., Chakravartya, S., Jha, M. K., Pathak, D. D., (2018) Processing of monazite leach liquor for the recovery of light rare earth metals (LREMs), Miner. Eng., 129, 9-14.

XIII International Mineral Processing and Recycling Conference
Belgrade, Serbia, 8-10 May 2019

University of Belgrade, Technical Faculty in Bor
Vojske Jugoslavije 12, 19210 Bor, Serbia
Tel. +381 30 424 555 Fax +381 30 421 078

RECOVERY OF COBALT FROM DIAMOND CORE DRILLING CROWNS

Zoran Stević [1], Silvana Dimitrijević [2,#], Aleksandra Ivanović [2], Milan Jovanović [2], Stevan Dimitrijević [3]
[1]University of Belgrade, Technical Faculty in Bor, Bor, Serbia
[2]Mining and Metallurgy Institute Bor, Bor, Serbia
[3]University of Belgrade, Innovation Center Faculty of Technology and Metallurgy, Belgrade, Serbia

ABSTRACT – The aim of this paper was to determine the optimal parameters of cobalt leaching from diamond core drilling crowns. In experimental studies, the influence of nitric acid concentration, temperature and time on the degree of cobalt depletion were investigated. Research has shown that the optimal parameters of the leaching were: 25 °C, 120 min and 0.5 M HNO_3. Under these conditions, cobalt recovery was 92.55 %.

Key words: cobalt recovery, diamond core, drilling crowns.

INTRODUCTION

Cobalt is a metal of high economic and strategic interest and has a wide application for production: batteries, super alloys, diamond tools, hard metals, and magnets. Cobalt is obtained from cobalt ore by hydrometallurgical, pyrometallurgical and electrochemical processes and as a by-product in the processes of nickel production. The largest application of cobalt is in the chemical industry for the production of batteries. It is also an important usage cobalt as a cement carbide binding agent in the cutting tool industry. Cement carbides of tungsten, due to their excellent characteristics, are widely used in the hard metal industry for the production of wear-resistant tools: as cutting tools (50-60 %), drilling tools in mining and geology, matrices, nozzles, valves, tools for processing various metal and hard coatings [1-5].

Due to the wide application area and a significant amount of cobalt, it is obtained by recycling: Ni-based super alloys, catalysts, magnets and hard metal products [6-7]. The content of the cobalt in scraps is in the range from 2-30 %. In recent years, stringent environmental controls and resource conservation policies have led to

corresponding author: silvana.dimitrijevic@irmbor.co.rs

renewed interest in developing cemented carbide recycling techniques that are not only economically viable but also eco-friendly. The existing process for hard metal recycling consists of [8, 9]:

- Direct conversion into graded powder ready for pressing and resintering,
- Selective cobalt leaching,
- Total leaching of all components.

In this research, it was studied a process for the recycling of cobalt from cemented scrap from diamond core drilling crowns. Cobalt is recovered in the form of powder and a carbide mix powder which are the most important products for powder metallurgy today. Three basic process steps are used for recycling: acidic leaching, precipitation, calcination and hydrogen reduction. This most important from the is process view of its lower energy consumption and environmental impact.

EXPERIMENTAL

The aim of the research in this paper was the recycling of cobalt from diamond core drilling crown by leaching in nitric acid. The characterization of hard metal and final products were done using the XRF method (Roentgen Thermo Scientific Nitona XL3t-900: Niton, Palomar, Model: Niton XL3t-900 Series), by XRD method (model: EXPLORER: GNR Analytical Instruments Group, Novara, Italy) and scanning electron microscopy with energy-dispersive spectrometry -SEM with EDS (SEM model: JOEL JSM IT - 300 - Japan).

For the determination of the chemical composition of the solution ICP-AAS (Spectro, Model: Ciros Visio, Detection Limit < 0.0001 g/dm^3) was used. The leaching tests were designed to examine the effects of temperature, time and HNO3 concentration. All experiments were performed under the following conditions: a solid/liquid ratio of 1:5; 50 g of sample, stirring rate 500 min^{-1} and < 1 mm particle size.

RESULTS AND DISCUSSION

Leaching of diamond core drilling crown in nitric acid is the most used method for recycling. Technological scheme of leaching of diamond core drilling crown in the aim to obtain cobalt powder is shown in Figure 1. In the experimental work, it was investigated:

- The temperature effect in the range: 25-85 °C,
- Reaction time in the range: 30-240 min,
- The concentration of nitric acid in the range: 0.5-1.5 M.

Crown was, in the first phase of recycling leached with 0.5; 1.0 and 1.5 M HNO3 solution at a temperature of: 25, 45, 55, 75 and 85 °C for 30, 60, 90, 120, 180, 210 and 240 min [8]. Copper, iron, nickel, and cobalt are dissolved by following reactions (1-4):

$$C_u + 2HNO_3 \rightarrow C_u(NO)_3 + H_2O \quad (1)$$

$$F_e + 2HNO_3 \rightarrow F_e(NO)_3 + H_2O \quad (2)$$

$$N_i + 2HNO_3 \rightarrow N_i(NO)_3 + H_2O \quad (3)$$

$$C_o + 2HNO_3 \rightarrow C_o(NO)_3 + H_2O \quad (4)$$

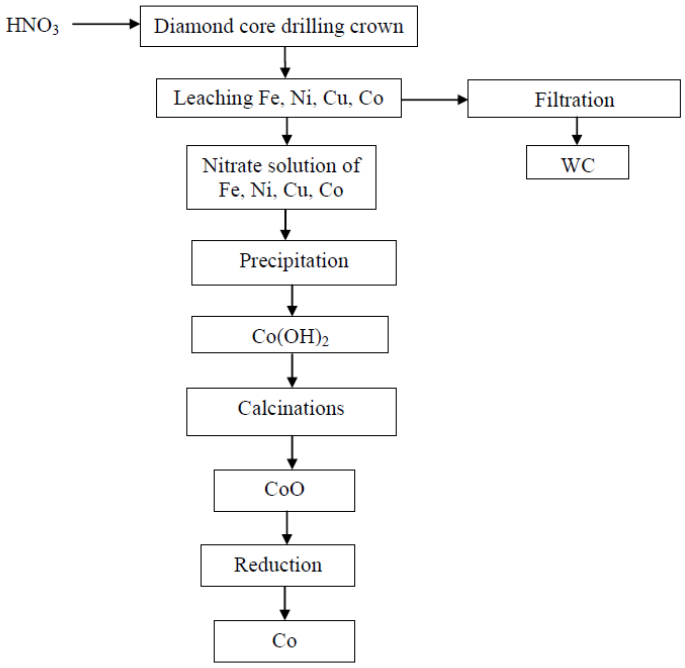

Figure 1. Technological scheme of leaching of diamond core drilling crown

Laboratory investigation has shown the optimum leaching conditions: 25 °C, 150 min and 0.5 M HNO_3. Leaching degree of cobalt was in the range from 92.55 to 80.23 at a temperature range of 25-85 °C. At room temperature, the cobalt was dissolved rapidly in nitric acid, and at the higher temperatures don't have positive effects on the leaching degree. The reason is passivation of the surface as a result of protective layer formation.

From the nitric solution, precipitation of $Fe(OH)_2$ at pH=2-4 and $Co(OH)_2$ at pH = 7-11 was performed with sodium hydroxide 2 M solution. Figures 2 and 3 show E-pH diagrams for the Fe-H_2O and Co-H_2O systems at temperature of 25 °C, on the basis of which the precipitation conditions of iron and cobalt hydroxide are defined. In figure 4 E-pH for Co-Fe-H_2O system is presented (solution obtained by leaching tungsten carbide). The selective precipitation of iron and cobalt hydroxide by adjustment of pH value lead to the situation where Fe and Co are not together in the solution, so partial E-pH diagrams present proposed procedure. Recovery of cobalt in the form of cobalt hydroxides by precipitation is strongly depended on the process parameters such as pH, temperature type and concentration of reagents. E-pH diagrams were constructed using the HSC Chemistry 6.1 software package (HSC Chemistry 6.1 software, developed by Outotec (Finland) Oy., 2007) [10]. Cobalt hydroxide precipitation is theoretically possible at lower value at 55 °C than at 25 °C.

In figure 4 it can be seen that equilibrium for the $Co(OH)_2$ formation at higher temperature is at nearly pH=6 instead of pH=7 at the lower temperature. This shows that precipitation of Co is less selective at 55 °C.

During the precipitation experiments, 2 M NaOH was slowly added to the nitric solution until equilibrium pH was achieved. After 60 min precipitate of $Co(OH)_2$ was separated by filtration.

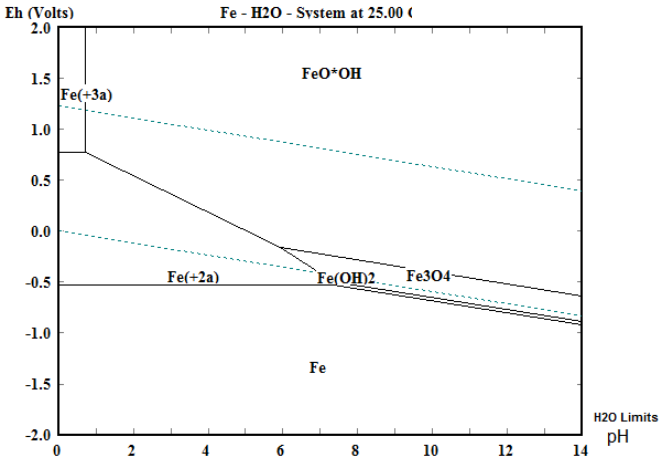

Figure 2. E-pH diagram for the Fe-H_2O system at t = 25 °C for the solution obtained by leaching carbide of hard metal for 0.098 g/l Fe

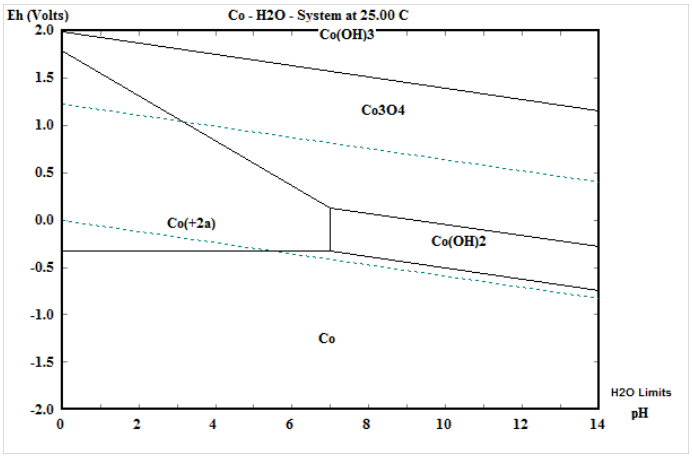

Figure 3. E-pH diagram for the Co-H_2O system at t = 25 °C for the solution obtained by leaching carbide of hard metal for 1.46 g/l Co

Cobalt powder was obtained in two steps processing (calcination at 300 °C and reduction with hydrogen at 800 °C). Cobalt oxide (CoO) was obtained from cobalt hydroxide, by calcination at 300 ° C, following the reaction:

$$C_o(OH)_2 \rightarrow C_oO + H_2O \quad (5)$$

Fine powder of metal cobalt was obtained from cobalt oxide with carbon reduction at 800 °C, following the reaction:

$$2C_oO + C \rightarrow C_o + CO_2 \quad (6)$$

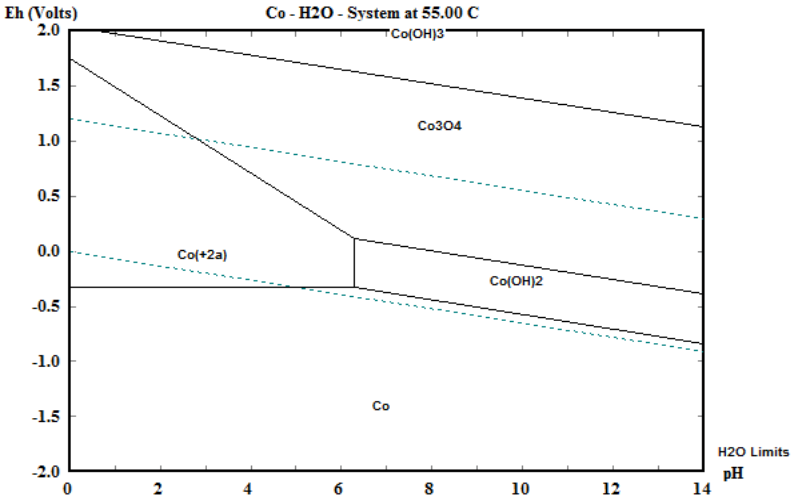

Figure 4. E-pH diagram for the Fe-$_{H2O}$ system at t = 25 °C for the solution obtained by leaching carbide of hard metal for 0.098 g/l Fe

Cobalt powder (Figure 5) was analyzed by SEM EDS analysis. Figure 5 shows the SEM images of cobalt powder obtained from cobalt hydroxide deposited at temperatures of 25 °C and 55 °C.

The EDS analysis is shown in Table 1.

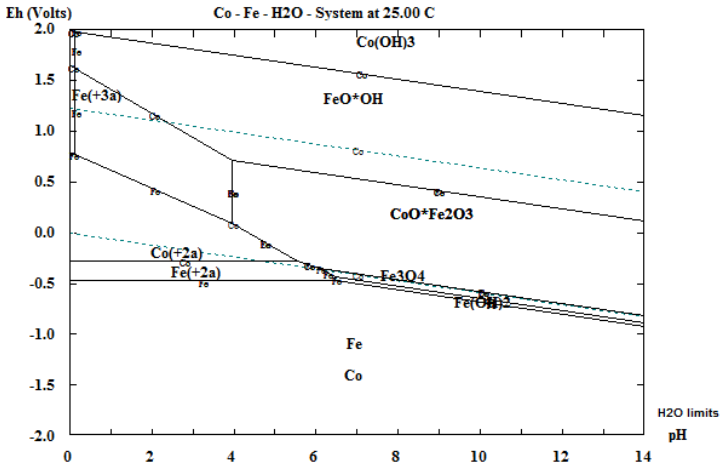

Figure 5. E-pH diagram for the Co-Fe-H_2O system at t = 25 °C for the solution obtained by leaching carbide of hard metal for 0.098 g/l Fe and 1.46 g/l Co

Table 1. EDS analysis of cobalt powder obtained from a sample of cobalt hydroxide deposited at a different temperature

Co	C	O	Co	Σ
t = 25 °C	0.84	0.28	98.88	100.00
t = 55 °C	0.55	0.43	99.02	100.00

From SEM images (Figure 6) and EDS analysis, it can be concluded that the cobalt powder is homogeny and contains a small amount of oxygen (0.28 % - 0.43 %).

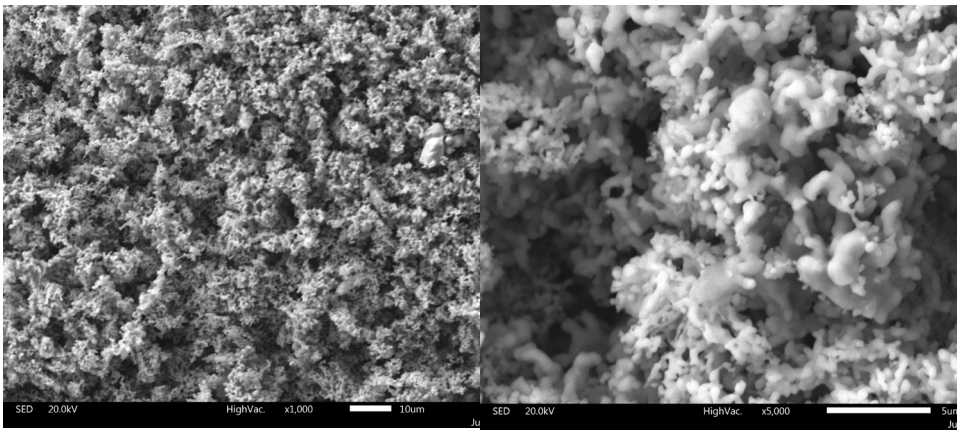

a) deposition of hydroxide at 25 °C **b)** deposition of hydroxide at 55 °C

Figure 6. SEM images of the cobalt powder obtained by recycling of hard metal

CONCLUSION

At optimum leaching condition of diamond core drilling crowns as: 25 °C, 150 min, 0.5 HNO_3 cobalt can be precipitated by NaOH with the efficiency of 97.5 %. From hydroxide by combination of calcination and reduction, it was obtained cobalt powder purity 98.88 - 99.02 %. Cobalt powder produced by recycling of diamond core drilling crowns can be used in powder metallurgy.

Acknowledgements:

This article is the result of the research under Cost Action project CA15102 - Solutions for Critical Raw Materials Under Extreme Conditions.

References

1. Lee, J., Kim, E., Kim, J., Kim, W., Kim, B., Pandey, D. B. (2011) Recycling of WC-Co hardmetal sludge by a new hydrometallurgical route. International Journal of Refractory Metals and Hard Materials, 29 (3), Issue 3, 365-371,
2. Lee, J., Kim, S., Kim, B. (2017) A New Recycling Process for Tungsten Carbide

Soft Scrap That Employs a Mechanochemical Reaction with Sodium Hydroxide. Metals, 7 (7), 230-238,
3. Katiyara, P. K., Randhawab, N. S., Hait, J., Jana, R. K., Singha, K. K., Mankhanda, T. R. (April 2014) An overview on different processes for recovery of valuable metals from tungsten carbide scrap. 18th International Conference on Nonferrous Minerals and Metals, Nagpur, Maharashtra, India, 1-11,
4. Gerhardt, N. I., Palant, A. A., Dungan, S. R. (2000) Extraction of tungsten (VI), molybdenum (VI) and rhenium (VII) by diisododecylamine. Hydrometallurgy, 55 (1), 1-15,
5. Koutsospyros, A., Braida, W., Christodoulatos, C., Dermatas, D., Strigul, N. (2006) A review of tungsten: From environmental obscurity to scrutiny. Journal of Hazardous Materials, 136 (1), 1-19,
6. Lassner, E., Schubert W.-D. (1995) Tungsten: Properties, Chemistry, Technology of the Element, Alloys, and Chemical Compounds. Springer US, Kluwer Academic/Plenum Publishers, New York,
7. Prakash, L. J. (1995) Application of fine grained tungsten carbide based cemented carbides. International Journal of Refractory Metals and Hard Materials, 13 (5), 257-264,
8. Lee, J. R., Lee, J. W., Kim, B. J., Kim, Y. J. (2016) Leaching Behavior of Al, Co and W from the Al-Alloying Treated WC-Co Tool as a New Recycling Process for WC Hard Scrap. Metals, 6 (8), 174-183,
9. Lassner, E., Schubert W.-D. (1995) Tungsten: Properties, Chemistry, Technology of the Element, Alloys, and Chemical Compounds. Springer US, Kluwer Academic/Plenum Publishers, New York, 422,
10. HSC Chemistry 6.1 software, developed by Outotec (Finland) Oy., 2007.

XIII International Mineral Processing and Recycling Conference
Belgrade, Serbia, 8-10 May 2019

University of Belgrade, Technical Faculty in Bor
Vojske Jugoslavije 12, 19210 Bor, Serbia
Tel. +381 30 424 555 Fax +381 30 421 078

DEVELOPMENT OF TECHNOLOGY FOR GOLD-ARSENIC-COAL CONCENTRATES PROCESSING

V. A. Luganov, T. A. Chepushtanova #, G. D. Guseynova, K. K. Mamyrbayeva, O. S. Baigenzhenov, E. S. Merkibayev
Satbayev University, Almaty, Kazakhstan

ABSTRACT – The annual consumption of gold is growing every year by 10 - 15 %. Improvement of the pyro- and hydrometallurgical methods made the secondary processing of poor ores and the remaining "tailings" of gold recovery plants with gold content of 1.0 - 0.3 g/t and less profitable. The persistence of ore is due to the fine impregnation of gold in sulphide minerals (pyrite and arsenopyrite), as well as the presence of arsenic and carbonaceous matter. The processing of such ores by traditional hydro- and pyrometallurgical methods, due to the high content of arsenic, is complicated by the release of its toxic compounds. This is a world, global problem. Proposed the technology of gold-arsenic-coal concentrates processing by two-stage roasting, including dearsenizing roasting and oxidative roasting of arsenic cinders, followed by leaching of gold from the cinders, aimed to reducing of the arsenic hazard class in material..

Key words: gold-arsenic-coal concentrates, dearsenizing roasting, hazard class.

INTRODUCTION

The analysis of scientific and technical information shows that at present time the development of the technology for extracting gold goes in to direction of the involvement in the operation of resistant, collective ores, which contain significant amounts of sulfur, arsenic and carbon. A characteristic feature of such deposits is a pronounced fine association of gold with sulphides.

Global reserves of arsenic are estimated by the US Geological Survey for copper and lead deposits at about 11 million tons, and recoverable reserves at 1 million tons [1]. This element is quite active, and therefore there are over 120 minerals that include arsenic. There are large copper and arsenic deposits in the United States, Sweden, Norway, and Japan; arsenic-cobalt - in Canada; arsenic-tin - in Bolivia and the UK. In addition, gold-arsenic deposits are known in the USA and France [2].

The gold asset of the Republic of Kazakhstan includes more than 2 thousand deposits. The Bakyrchik deposit is one of the most important primary gold deposits in the country and is among the five largest gold-bearing deposits in the world.

The resulting concentrates, by their composition and interrelationship of gold

corresponding author: tanya2305@list.ru

with sulphides, belong to the category of highly resistant gold-containing products, to which conventional methods of hydrometallurgical processing, such as cyanidation, are not applicable.

Both in Kazakhstan and in foreign countries there are a number of pyrometallurgical, combined pyro-hydrometallurgical and hydrometallurgical processing schemes of refined gold-arsenic raw materials that have been well developed in laboratory and pilot industrial conditions. However, the introduction of such technological schemes into production is associated with difficulties of an economic and technological nature (weak development on an enlarged scale, complexity of instrumentation and lack of standard equipment for large-scale production, the inability to use the process for high arsenic concentrates, increased consumption of reagents, etc.) [3, 4].

The problem of recycling arsenic is a global problem. In Kazakhstan, more than 22 billion tons of waste have been accumulated, of which more than 16 billion tons of technogenic mineral formations and about 6 billion tons of hazardous waste [5-7]. About 700 million tons of industrial wastes from them are toxic - about 250 million tons annually. The total amount of arsenic in the dumps of non-ferrous metallurgy plants is about 395 thousand tons. On average, the arsenic content in the dumps of plants varies from 8 - 10 %, and in sublimates - 40 - 45 %.

The main disadvantage of all existing technologies related to arsenic withdrawal is the unsolved problem of arsenic emission into the environment. Up to 35 - 40 % of arsenic in the form of calcium arsenate or iron dissolves during storage, thereby causing great damage to the hydro and lithosphere. The disposal of arsenic waste does not solve the problem. Thus, the most promising are methods for isolating arsenic from the technological cycle in a low-toxic sulfide form, low hazard class, which is not able to pollute the environment.

The development of technology for the complex processing of arsenic-containing raw materials, aimed at the extraction of gold and the production of environmentally safe arsenic compounds through dearsenizing roasting and condensation of volatile forms of arsenic, is relevant. The need for production is also to increase the extraction of gold during cyanidation to 95 %, the presented technology allows to achieve the extraction of gold to 98 %.

The aim of the work was to develop a technology for dearsenziing roasting of Bakyrchik gold-arsenic-coal concentrate..

MATERIALS AND METHODS OF WORK

The following materials were chosen for the research: Bakyrchik deposit flotation concentrate with low arsenic contention (2.4 % As); Bakyrchik deposit flotation concentrate with high arsenic contention (12 % As); high-arsenic flotation concentrate of the Sayak deposite (39 % As); Leninogorsk pyrite concentrate; coal.

Sayak concentrate, containing 39 % arsenic, was added to the roasting mixture to obtain mixtures with different arsenic content. The chemical composition of the materials used is given in Table 1. The size of the products studied in the experiments is 0.1 mm. The average Au content in Bakyrchik ore is 6.9 g / t.

The initial Bakyrchik deposit gold-arsenic-coal concentrate with high and low arsenic contention was studied by X-ray diffraction analysis. X-ray diffraction analysis was performed on an automated diffractometer DRON-3 with Co - radiation,

β-filter, figure 1. The conditions for shooting diffractograms: U = 35 kV; I = 20 mA; θ-2θ shooting; 2 °C / min detector X-ray phase analysis on a semiquantitative basis was carried out on the diffraction patterns of powder samples using the method of equal weights and artificial mixtures.

Table 1. Naziv tabele (Cambria, 10 pt) Tekst u tabeli je Cambria, 9 pt. Razmak između naziva tabele i tabele je 0,3 pt.

Materials name	Components contention, %					
	Cu	Fe	Zn	C	S	As
Bakyrchik deposit flotation concentrate with low arsenic contention	0.05	17.64	–	13	5.4	2.4
Bakyrchik deposit flotation concentrate with high arsenic contention	0.11	24.5	–	–	18,1	12.0
Sayak concentrate	0.93	31.3	0.12	–	17.6	39
Leninogorsk pyrite concentrate	0.4	40	–	–	46.7	–
Coal	–	–	–	71.0	2.1	–

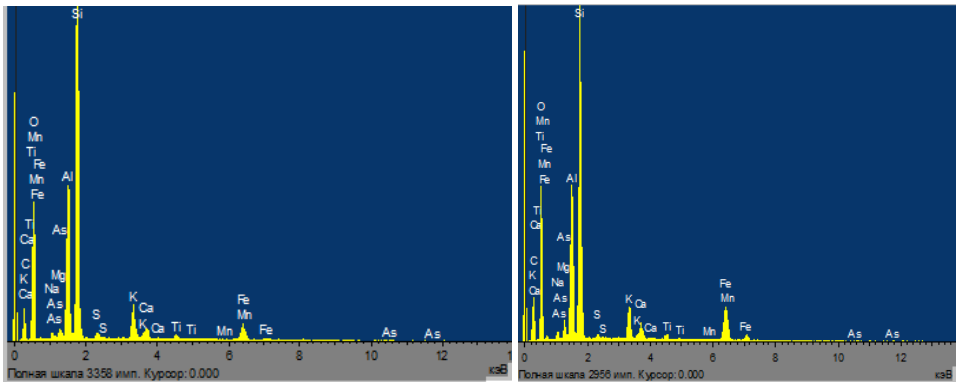

N1 N11

Figure 1. The results of X-ray diffraction analysis of samples N 1 and N

We also analyzed initial arsenopyrite,%: 33.8 - iron, 19.6 - sulfur and 44.8 - arsenic with a particle size of 81% - 73 μm and were dense, low-porous particles with a developed surface (S = $0{,}67 \cdot 10^{-3}$ m^2/kg). A mineralogical analysis has been carried out; it has been established that insignificant impurities of pyrite (FeS_2), pyrrhotite ($Fe_{1-x}S$) and non-metallic components, mainly represented by quartz (up to 1 %), are found in arsenopyrite monomineral pyrite contained 47.1 % of iron and 51.3 % of sulfur with a particle size of 81 % - 73 microns.

The mineralogical analysis of pyrite revealed the presence of an insignificant admixture of magnetite and nonmetallic minerals, which are mainly represented by quartz (2.6 - 3.2 %).

Thermodynamic studies of the sulfidation of arsenopyrite are presented below. Using the thermodynamic calculation program HSC Outokumpu OU were fulfilled thermodynamic calculations of possible arsenopyrite sulfidizingng reactions. It was established that sulfidizing of arsenopyrite proceeds stadially with the formation of

arsenic sulfides As_4S_4 and As_2S_3 by reaction (1 and 2):

$$F_eA_sS + 1.25S_2 + O_2 = F_eS + 0.5A_{s_2}S_3 + SO_2 \quad (1)$$

$$F_eA_sS + 4F_eS_2 + 8O_2 = 2F_eS + F_{e_3}O_4 + 0.25A_{s_4}S_4 + 6SO_2 \quad (2)$$

It has been established that in the Fe - As - S system with increasing temperature and with a significant partial pressure of arsenic, are forming the iron arsenide phases. In Figure 2, in the Fe - As - S system, as the temperature rises with a low arsenic pressure, the higher iron sulfides dissociate to form lower iron sulfides to metallic iron. With an increase in the partial pressure of As in the gas phase, arsenides of iron $FeAs_2$ and FeAs are formed, $FeAs_2$ is formed at 600 - 700 °C, and FeAs exceeds 700 °C, Figure 2.

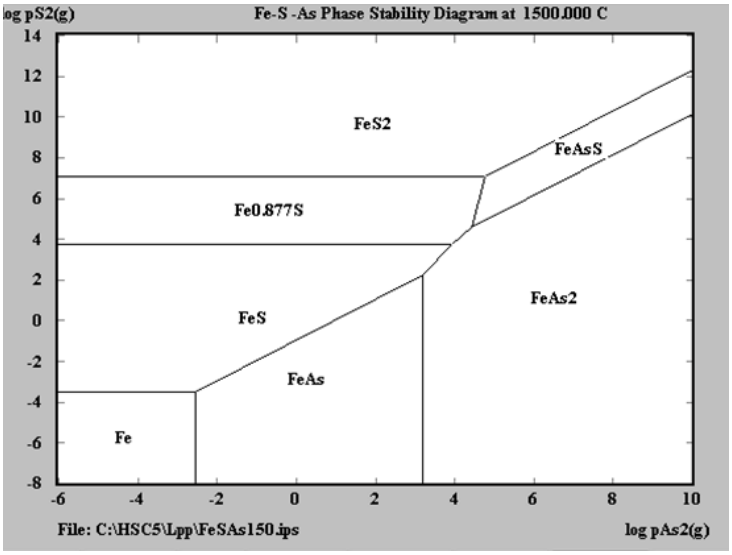

Figure 2. Phase diagram for the system Fe - As - S

RESULTS AND DISCUSSION OF THE RESULTS

Sulfidizing roasting was carried out in a fixed bed, with arsenic being withdrawn into sublimates in a sulphide form. Pyrite is used as a sulphidizer. The effect of the ratio of FeAsS: FeS_2 in the mixture, temperature (700 - 900 ° C), duration (60 - 180 minutes) on the degree of distillation of arsenic was determined. The firing studies were carried out in alundum boats in a quartz reactor placed in a laboratory tubular electric furnace with automatic temperature control. A quartz reactor with reagents was installed in a two-zone furnace, preheated to a predetermined temperature, which was automatically maintained constant with an accuracy of ± 2 ° C.

Studies without additional blending were carried out with weights of 10 grams; the amount of pyrite used in the experiments varied from 10 to 40 % by weight of the concentrate.

The initial sample of the material was poured in a thin layer into the boat and placed in the isothermal zone of the electric furnace reactor, preheated to a predetermined temperature. The experiments were carried out in an atmosphere of inert gas (nitrogen), the rate of which in all experiments was kept constant.

A weighed concentrate in a corundum boat was placed in the reaction zone of a quartz reactor, and a portion with a sulfidization agent (sulfur) was placed in the gasification zone. The system was purged with a carrier gas (nitrogen) purified from oxygen and moisture, which was supplied during the entire experiment and when the reactor was cooled. Sulfur pressure control was carried out by changing the temperature in the gasification zone and was controlled by the mass metric method. After the completion of the experiment, the sample was cooled in a stream of nitrogen, weighed and analyzed for the content of iron, arsenic and sulfur, and also subjected to X-ray analysis.

Studies with sequential charging were carried out with an initial sample weighing 50 g at a temperature of 923 K and a duration of each operation 30 minutes according to the scheme shown in Fig. 3. The total consumption of pyrite was 12 g per 25 g of arsenopyrite, i.e. the ratio was maintained (arsenopyrite: pyrite) = 2. Technological studies showed that the sulfidization process is optimally conducted under the following conditions: the duration is 35 - 45 minutes, the temperature is 873 - 973 K, the degree of sulfidization is 95 - 99 %, the process takes place in stage 1, table 2.

Table 2. Dependence of the degree of sulfidization of arsenic-gold concentrate with high arsenic contention (12 % As) on T, K and τ, min at 42 % (mass.) pyrite

Roasting duration τ, min	**Sulfidization degree (%) at temperature, K**			
	670	**770**	**870**	**970**
15	17.7	53.0	75.0	84.0
30	27.8	76.4	90.2	96.1
45	40.0	86.2	96.2	99.2

Dependence of sulfidization degree of arsenic-gold concentrate with high arsenic contention (12 % As) from pyrite waste (T= 870 K, duration 15 - 45 min)			
The content of FeS2 in the roasting batch,% (mass.)	15	30	45
Sulfidization degree	67.3	80.5	97.0

It is established that a change in the amount of pyrite in the batch from 9 to 45 % (mass.) leads to an increase in the degree of sulfidization 2.2 - 2.7 times at sulfidizing in a fixed bed.

Thus, according to technological studies in the fixed layer of sulfidizing of arsenic-gold concentrate with high arsenic contention (12 % As) from T, K and τ, min at 42 % (mass.) pyrite, it was established that the maximum sulfidization reaches 99.2 % at a temperature of 970 K, with a duration of 45 minutes These conditions are optimal for the sulfidization of arsenic-gold concentrate with high arsenic contention 12 %, Figure 3.

A study of the effect of sulfidization consumption and coal addition on the distribution of arsenic and sulfur in calcination products showed that adding 30-50 % to pyrite concentrate to gold-arsenic concentrate of pyrite concentrate yields cinders, in which the fraction of remaining As does not exceed 5 - 6 %, and the degree

of desulfurization - 50-70 %.

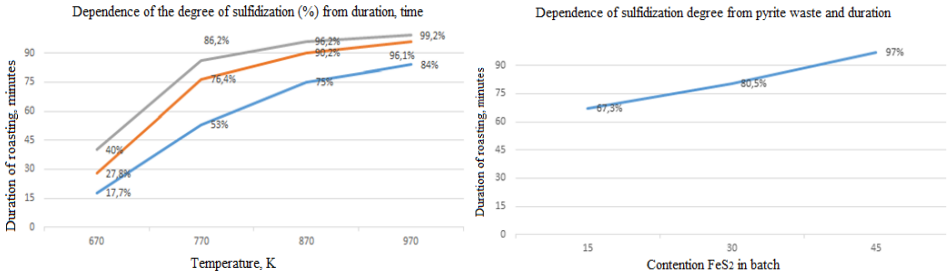

a) b)

Figure 3. Indicators of the degree of sulfidization of arsenic-gold concentrate with high arsenic contention (12 % As); a) from T, K and τ, min at 42% (mass.) pyrite, b) from the consumption of pyrite (T = 870 K, duration 15 - 45 min)

The roasted arsenic bearing products are stable during long-term storage, even under the influence of microorganisms. The study studied the behavior of autotrophic thionic (*Thiobacillus thrioparis, Thiobacillus thiooxidans Thiobacillus ferrooxidans*), as well as arsenic-oxidizing and arsenic-reducing bacteria. The studied microorganisms in the studied conditions practically do not affect the sulfide forms of arsenic, participating in the transformation only of oxide compounds contained in sulfide sublimates.

The transition to arsenic solution is mainly associated with oxides contained in sulphide sublimates. Oxidation from oxides As^{3+} to As^{5+} promotes the transition of arsenic into solution. As is known, As_2O_5 has a greater solubility than: As_2O_3 - solubility of As_2O_3 at 25 ° C in 100 g of water is 2.1 g and As_2O_5 - 65.8 g.

CONCLUSION

The technology provides a social demand – improving the environmental situation in areas located close to arsenic production, reducing the risk of poisoning with arsenic-containing waste, and obtaining products with increased value added.

Economic interest. Technical and economic calculations have shown that the use of two-stage roasting technology with subsequent cyanidation of cinder in comparison with the oxidation-sulfidizing roasting of gold-arsenic concentrate in shaft furnaces allows reducing capital and operating costs. The proposed technology does not require the introduction of non-standard furnaces into production or modernization, as is the case with shaft furnaces. The technology provides for the use of fluidized bed furnaces in production. The economic effect of the sulphidizing roasting of gold-arsenic-coal concentrate is achieved by extracting gold at 98 %, with a 100 % profitability of the project, with an annual production of 5 tons of gold per year, the payback period of the project will be 2.8 years.

References

1. Gasanov, A., Greenberg, E., Naumov, A. (2016) The current state of the world

market for arsenic and its compounds. Bulletin of the Russian Academy of Natural Sciences, 25-32,
2. http://federalbook.ru/files/FS/Soderjanie/FS27/V/Novie%20podhodi.pdf
3. Fair, K. J., Schneides, J. C., Van Weert, J. (1996) Options in the nitrox process. Mining Magazine, 174 (4), 231-234,
4. Maslenitsky, I. N., Dolivo-Dobrovolsky, V. V., Dobrokhotov, G. N. and others. (1969) Autoclave processes in non-ferrous metallurgy. Metallurgy, 227-232,
5. Li, T., Zhang, Y., Zhang, B., Zhang, J., Qin, W. (2018) Selective leaching of arsenic from enargite concentrate using alkaline leaching in the presence of pyrite. Hydrometallurgy, 181, 143-147,
6. Seitkan, A., Redfern, S. A. T. (2016) Processing double refractory gold-arsenic-bearing concentrates by direct reductive melting, Minerals Engineering, 98, 286-302,
7. Boldyrev, A. V., Balikov, S. V., Bogorodskiy, A. V., Emelyanov, Yu. E. (2015) Pressure oxidation of refractory gold-bearing concentrates using halogen-containing solvents and adsorbent, Tsvetnye Metally, 11, 29-33.

XIII International Mineral Processing and Recycling Conference
Belgrade, Serbia, 8-10 May 2019

University of Belgrade, Technical Faculty in Bor
Vojske Jugoslavije 12, 19210 Bor, Serbia
Tel. +381 30 424 555 Fax +381 30 421 078

THERMODYNAMIC APPROACHES OF THE REMOVAL OF CYANIDE FROM WATER SOLUTIONS BY HALLOYSITE CLAYS

Birgül Benli [#], Meltem Yildiz
Istanbul Technical University, Department of Mineral Processing Engineering, Maslak, Istanbul, Turkey

ABSTRACT – In this study, the removal of cyanide was investigated by the adsorption isotherms and kinetic studies onto halloysite clay in leaching conditions. Cyanide adsorption capacity of halloysite was calculated as 88.33 mg/g and the kinetic results correlated well with pseudo- second-order model and also fitted well to Langmuir and Temkin adsorption isotherms. High performances of very cheap unmodified halloysite present good opportunity to geosynthetic clay liners, compacted clay liners and clay-reinforced polymeric composite membranes.

Key words: halloysite, cyanide, adsorption.

INTRODUCTION

Cyanides, any compound containing the monovalent combining group –C≡N, exposure including workplaces involved in metal polishing, certain insecticides, the medication nitroprusside, and even certain seeds such as those of apples and apricots [1, 2]. Toxic cyanide compounds get into the environment mainly from wastewater and cause to the combinations of water pollution and water scarcity. Moreover, the consumption of cyanide during processing operations caused a major economic cost; for example, extraction of gold from its ores the productions of gold and silver mines, the discharge of cyanide wastes may result in significant environmental pollution [3]. Mining industry demand for sodium cyanide is increasing the growth of the sodium cyanide market, following from chemical industry for chemical and polymer synthesis and for boosting plastics in building and construction sector. Fresnillo Plc.'s. annual report (2017) analyzed the company's sodium cyanide consumption for silver and gold increased from 10,117,133 tons in 2016 to 11,610,753 tons in 2017. According to market insights, Global Sodium Cyanide Market to surpass 2,000 kilo tons by 2026 [4].

Halloysite is a clay mineral which is composed of Al, Si, H and O atoms, double layer and has nanotubular structure. The detail fibrous structure can be seen in Figure 1. Halloysite ($Al_2Si_2O_5(OH)_4nH_2O$) is a naturally occurring clay mineral of the

[#] corresponding author: benli@itu.edu.tr

kaolin group with a tubular structure. The crystal structure of halloysite is the same as the kaolin group, consisting of curved sheets of corner-sharing SiO_4 tetrahedra bonded to sheets of edge-sharing AlO_6 octahedra in a 1:1 stoichiometric ratio. A typical halloysite consists of 15 - 20 layers rolled in a multilayered with a spacing of 0.72 nm. Typical 1 mm long multiwall halloysite nanotubes have an external diameter of around 50 - 100 nm. In the literature, the tubular structure of halloysite has been explored for various applications, such as drug loading, catalyst support and adsorbent, due to the availability of hydroxyl groups, although it encounters difficulties in application areas where thermal or electronic conductivity is required [5].

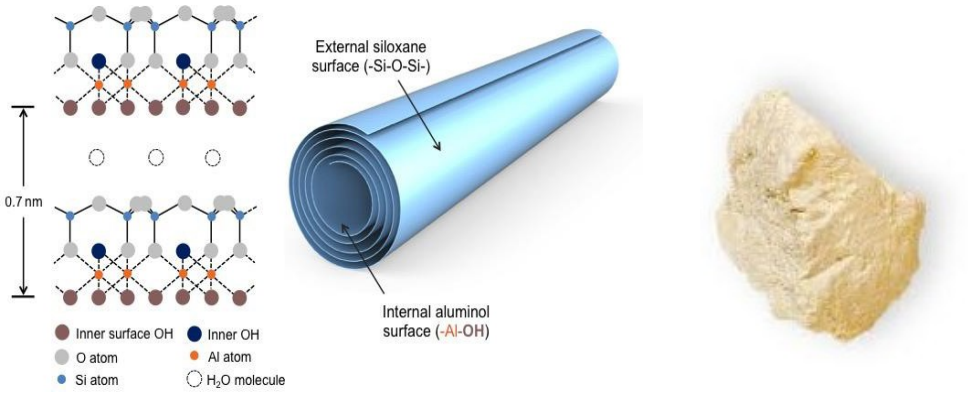

Figure 1. The tubular structure of halloysite

Adsorption of cyanide has proven to be an excellent way to treat effluent also a cost effective technique. Numerous low cost materials have been successfully suggested for the removal of ions from aqueous solution, some of which are coal, fly ash, wood, silica, shale oil ash, Fuller's earths, zeolite, perlite, alunite, clay materials (bentonite, montmorillonite, etc.), activated slag, and agricultural wastes (bagasse pith, maize cob, coconut shell, rice husk, sawdust, etc.). Table 1 compares the adsorption capacities of several adsorbents used for the removal of cyanide ions. Clay could be accepted as one of the appropriate low cost adsorbents. In the literature, while clay adsorbents are mostly used for the removal of cations and modification with cationic surfactants; however, only limited application of adsorption data has been directed on anionic ions like CN- group.

Table 1. Cyanide adsorption capacities of several adsorbents

Adsorbent	**q_{max} (mg/g)**	**Reference**
Alumina	22.0	[6]
Plain carbon	7.1	[7]
Activated carbon	24.1	[8]
Calcinated egg shells	3.27	[9]
Almond shell	32.1	[10]
Sagwan leaves	18.5	[10]

Table 1. (Extension)

Pistachio hull waste	156	[11]
Apricot stone activated carbon	61.6	Depçi, et al., 2014.
Polymeric complex adsorbent	101	Zheng, et al. 2014.
Linda type zeolite	24.1	[12]
Fe-MFI zeolite	33.9	Maulana and Takahashi, 2018.
Sepiolite	32.1	[13]

The purpose of the present work is to develop a methodology to estimate cyanide consumption of fibrous clay such as natural halloysite for with integrated modeling of leaching kinetics and chemical speciation.

MATERIALS AND METHODS

Materials

Raw Halloysite sample was kindly obtained from Eczacıbaşı-Bensan Co. in Turkey. Prior to use, the sample was washed in distilled water and oven-dried for 15 h at 80 °C. The dried sample was then gentle powdered using a mortal. The particle size distributions were analyzed by laser light scattering (Malvern Mastersizer 2000) and the results of d_{10}, d_{50} and d_{80}, particles sizes were determined as 2.0 μm, 12.8 μm, 40.0 μm for 10 %, 50 % and 80 % of the passed grains, respectively.

Adsorption tests

Cyanide solution was prepared by diluting aliquots of 1g/L stock cyanide solution (NaCN, Merck, 99 % minimum purity), and then the pH value was adjusted above 10.5 using 1M $Ca(OH)_2$ solution. Cyanide adsorption tests at various-constant temperatures between 25 - 45 °C were conducted in a temperature-controlled stirring incubator at 200 rpm (Edmund Bühler GmbH). The cyanide-adsorbent dispersions were centrifuged at 4,000 rpm for 15 minutes and filtered using a 0.45 μm pore size syringe filter (Minisart), then the filtrate was analyzed for residual cyanide. The concentration of cyanide ions in clear solution was determined by silver nitrate titration procedure (ASTM-D 2036-98: Standard Test Methods for Cyanide in Water).

The quantity of cyanide adsorbed from aqueous solutions onto the ahalloysite was calculated as follows:

$$a_e = \frac{(C_o - C_e) \cdot V}{M} \tag{1}$$

a_e is the adsorption capacity in equilibrium (mg/g); C_o and C_e are the initial and equilibrium concentrations of cyanide (mg/ L), respectively; V is the volume of the solution (L); and M is the mass of the adsorbents (g).

RESULTS AND DISCUSSION

Figure 2 and Figure 1(a) shows that the rate of cyanide binding with the adsorbents is more at initial stages, which gradually decreases and remains almost constant after an optimum period of 8 hours for 100 ppm initial concentrations. Figure 1(b) shows nonlinear behavior of raw halloysite at a particular sorbent dose over the entire time range, indicating that more than one process is affecting the adsorption process. Three regions could be seen in the intraparticle diffusion plots: first step (0 - 4 hours) is mass transfer and surface adsorption (film diffusion); second step (2 - 6 hours) is the rate-limiting step where the adsorption gradually increases; last step (over 6 hours) is chemical equilibrium due to the low cyanide concentration in solution.

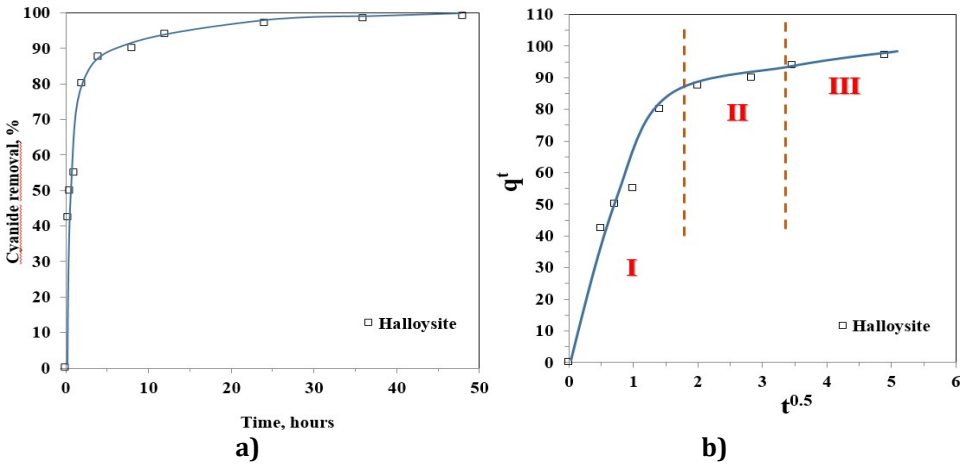

a) **b)**

Figure 2. a) Time-dependent adsorption performance of halloysite, initial $C_{CN}^{-} = 100$ ppm; **b)** Weber and Morris plot, initial $C_{CN}^{-} = 200$ ppm

In order to understand cyanide adsorption mechanisms (Maukana and Takahashi, 2018), the kinetic study of cyanide uptake onto raw mineral were tested by fitting the experimental data into two linearized form of single-component models: Lagergren's pseudo first-order equation and the pseudo second-order chemisorption kinetic rate of Ho-McKay [13]. Pseudo-second order model had a better for cyanide adsorption onto halloysite with the average correlation coefficient, R^2, over 0.99 means that chemisorption or exchangeable ion-cyanide complex formation controlled the overall adsorption rate of the process.

Table 3. Calculated adsorption parameters of halloysite-cyanide adsorption

Minerals	Kinetic model					
	Pseudo-first order			*Pseudo-second order*		
	k_1 (min^{-1})	q_e ($mg.g^{-1}$)	R^2	k_2 ($g.mg^{-1}.min^{-1}$)	q_e ($mg.g^{-1}$)	R^2
Halloysite	0.071	5.155	0.8634	0.017	100.000	0.9999

The adsorption isotherms of Halloysite adsorbents proved on Langmuir model (i.e., $R^2 > 0.987$ for halloysite) and Freundlich model, i.e. $R^2 > 0.979$ for halloysite

(Table 4). Therefore, cyanide ions could be accepted to have been adsorbed as a monolayer on the active sites that are homogenously distributed [11] together with multisite adsorption for rough surfaces, and similarly equal activation energy, [8]. On the other hand, the values of the maximum adsorption capacity (the constant qm in the Langmuir isotherm) of the halloysite for adsorbing cyanide ions were found to be 83.33 mg/g, which is much higher than Table 1 values.

Table 4. Isotherm constants

Isotherms	Constants	Values
Langmuir	q_{max} (mg/g)	83.33
	K_L (L/mg)	0.082
	R_L	0.108
	R^2	0.987
Freundlich	k_f (mg/g)	101.00
	N	1.101
	R^2	0.979
Temkin	A_T	0.0020
	B_T	9.272
	b (kJ/mol)	317.8
	R^2	0.955

The influences of temperature given in Figure 3 are related with the feasibility of the cyanide adsorption on the raw clay minerals were proven with the thermodynamic approaches on spontaneity as well as the exothermic nature of the process.

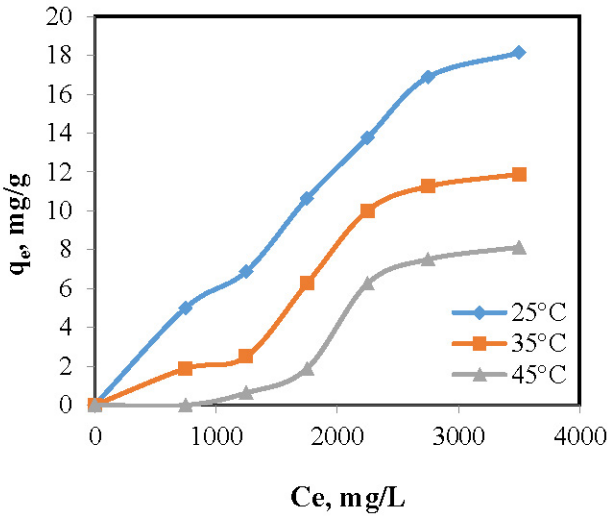

Figure 3. The influence of temperature

CONCLUSION

Cyanide adsorption capacity of halloysite was calculated as 88.33 mg/g and

compared to other inorganic and modified adsorbents. Halloysite adsorbents are cheap, easy, very effective, spontaneous and exothermic process. Halloysite uses adsorption processes gives opportunity from clay liners (geosynthetic and compact) and clay-reinforced polymeric composite membranes to environmental approaches considering the safe management of cyanide that is produced, transported and used for the recovery of gold and silver, and on mill tailings and leach solutions.

Acknowledgements:

The authors would like to acknowledge Istanbul Technical University, the Scientific Research and Development Support Program (ITU-BAP, Project No. MAG-38868) for their full financial support.

References

1. Kuyucak, N., Akcil, A. (2013) Cyanide and removal options from effluents in gold mining and metallurgical processes. Minerals Engineering, 50-51, 13-29,
2. Jaszczak, E., Polkowska, Z., Narkowicz, S., Namieśnik, J. (2017) Cyanides in the environment-analysis-problems and challenges. Environmental Science and Pollution Research International, 24 (19), 15929-15948,
3. Botz, M. M., Mudder, T. I., Akçil, A. U. (2016) Chapter 35 - Cyanide Treatment: Physical, Chemical, and Biological Processes. Gold Ore Processing, Project Development and Operations. (Second Edition), 619-645,
4. UrL-1. (2019) Global Sodium Cyanide Market to surpass 2000 kilo tons by 2026 - Coherent Market Insights. Globe Newswire, Inc. https://www.globenewswire.com/news-release/2019/01/24/1704955/0/en/Global-Sodium-Cyanide-Market-to-surpass-2000-kilo-tons-by-2026-Coherent- Market-Insights.html.,
5. Subramaniyam, C. M., Srinivasan, N. R., Tai, Z., Liu, H. K., Goodenough, J. B., Dou, S. X. (2017) Self-assembled porous carbon microparticles derived from halloysite clay as a lithium battery anode. Journal of Materials Chemistry A, 5, 7345-7354,
6. Giraldo, L., Moreno-Piraján, J. C. (2010) Adsorption studies of cyanide onto activated carbon and γ-alumina impregnated with cooper ions. Natural Science, 2 (10), 1066-1072,
7. Adhoum, N., Monser, L. (2002) Removal of cyanide from aqueous solution using impregnated activated carbon. Chemical Engineering and Processing: Process Intensification, 41 (1), 17-21,
8. Deveci, H., Yazıcı, E. Y., Alp, I., Uslu, T. (2006) International Journal of Mineral Processing, 79, 198-208,
9. Eletta, O. A. A., Ajayi, O. A., Ogunleye, O. O., Akpan, I. C. (2016) Journal of Environmental Chemical Engineering, 4 (1), 1367-1375,
10. Dwivedi, N., Balomajumder, C., Mondal, P. (2016) Comparative investigation on the removal of cyanide from aqueous solution using two different bioadsorbents, Water Resources and Industry, 15, 28-40,

11. Moussavi, G., Khosravi, R. (2010) Removal of cyanide from wastewater by adsorption onto pistachio hull wastes: Parametric experiments, kinetics and equilibrium analysis. Journal of Hazardous Materials, 183, 724-730,
12. Noroozi, R., Al-Musawi, T. J., Kazemian, H., Kalhori, E. M., Zarrabi, M. (2018) Removal of cyanide using surface-modified Linde Type-A zeolitenanoparticles as an efficient and eco-friendly material. Journal of Water Process Engineering, 21, 44-51,
13. Benli and Yıldız, (2019) Comparison of several clay adsorbents from bentonite to sepiolite and halloysite to remove cyanide in alkaline media as efficient and eco-friendly materials, In publishing.

XIII International Mineral Processing and Recycling Conference
Belgrade, Serbia, 8-10 May 2019

University of Belgrade, Technical Faculty in Bor
Vojske Jugoslavije 12, 19210 Bor, Serbia
Tel. +381 30 424 555 Fax +381 30 421 078

GEOSYNTHETICS IN SLUDGE DEWATERING AND SLUDGE LAGOON COVERS

Markus Wilke [1], Laura Carbone [1], Marija Bakrac [2, #]
[1]HUESKER Synthetic GmbH, Germany
[2]Geoestetika d.o.o., Serbia

ABSTRACT – Mining and processing byproducts are usually deposited into large tailings ponds. Modern impoundments are engineered structures for tailings disposal. The management of tailings facility includes different phases such as planning, design, construction, operation, closure and long term after care. Geosynthetics have been used successfully for mine related applications including the capping of sludge lagoons, geogrid reinforcing of retaining structures, including dam walls, reinforcement of access roads, and lining of tailings storage facilities.
This paper introduces the concept of dry tailing storage through the use of geosynthetic dewatering tubes and permanent safe closure of tailings ponds through geosynthetic capping system. The basic working principles and a recent case studies of both solutions are presented.

Key words: dewatering tubes, solid liquid separation, woven geotextile, sludge lagoon, capping.

INTRODUCTION

Tailings, by ICOLD's definition [3], include all waste material (or "tail" products) from any activity. There are several methods used for tailings disposal and the most common method is the disposal of tailings slurry in impoundments.

Modern impoundments are engineered structures for tailings disposal where actual designs are highly site-specific [2]. Many factors should be taken into account such as the characteristics of the tailings, the climatic, topographic, geologic, hydrogeological and geotechnical characteristics of the disposal site, regulatory requirements and to environmental performance [10].

More recently, with the structural failures of tailing storage facilities concerns have been raised about the stability and environmental performance of tailings dams and impoundments.

Geosynthetic dewatering tubes provide an environmentally sustainable solution for the dry storage of tailings. The use of geosynthetic tubes is one alternative method that can be used to dewater large quantities of sludge and at the same time create a stable structure for the permanent containment of the tailings [8]. This solution has been implemented successfully in the Talvivaara Mine since 2013 were

corresponding author: mbakrac@bvcom.net

the geosynthetic dewatering tubes are used as permanent storage of the gypsum tailings.

On the other hand, inactive tailings impoundments also are receiving more attention. One of the main concern is that due to the rainfall infiltration the material inside the impoundment never reaches a completely solid state so that the lining system or a dam failure always can cause the uncontrolled release of toxic sludge [6]. Other long-term effects of windblown dispersal, ground water contamination, and acid drainage should be also taken into account. In many cases, the costs of remediation can be considerable, exceeding the costs of original design and operation of the tailings impoundment [7]. Most of the time, mining sites and the environmental problems associated with them are in the care of public institutions. The aim is to consider closure and reclamation design into account for old mining sites and to design them from the early beginning of the project for the new ones. Therefore, closure and reclamation considerations have become the most important driving factors in the selection of the site, design, and permitting of mining projects [1].

Capping systems represent one of the most common remediation technique. Nevertheless, the construction of a cover system on top of a weak and heterogeneous tailings can be a challenge and the use of geosynthetics in such systems provides the most economic and feasible solution.

In this paper, the remediation concept of geosynthetic sludge lagoon cover system is presented and the application to the settling basin of residues of the uranium ore treatment of the Wismut company is described.

THE DEWATERING TUBE SYSTEM

Geotextile tubes are large high strength textile modules whose function is to retain and consolidate the solids while the water flows out from the geotextile shell. Geotextile tubes are manufactured using high tensile strength fabrics, assembled into a tubular shape with a customized length, width or height.

For treatment the processed sludge is pumped into the geosynthetic dewatering tube. Within this geotextile containment and dewatering element the solid-liquid separation takes place. Due to the particle retaining ability of the fabric, the solids deposit inside the tube and the water is able to drain as a result of the fabric permeability. Initially the process is mainly a suspension filtration. During this period small amounts of fines might escape the tube. After the initial startup phase of tube operation a natural filter cake develops on the inner side of the tube shell. This significantly increases the degree of separation.

Practically, dewatering by means of geosynthetic tubes comprises a cyclical process, schematically shown in Figure 1. During the first filling cycle the dewatering tube is filled to the given maximum initial design height, and the filling is stopped. The static drainage of the sludge commences as soon as the filling process is halted and following a degree of dewatering the tube can be re-filled. During this cycle the water within the sludge is extracted, therefore the volume is reduced and the solids concentration of the residual dewatered material is increased.

The principal process is repeated until the tube is completely filled. If the tube stays in place for an additional period of time, a subsequent consolidation and further desiccation occurs.

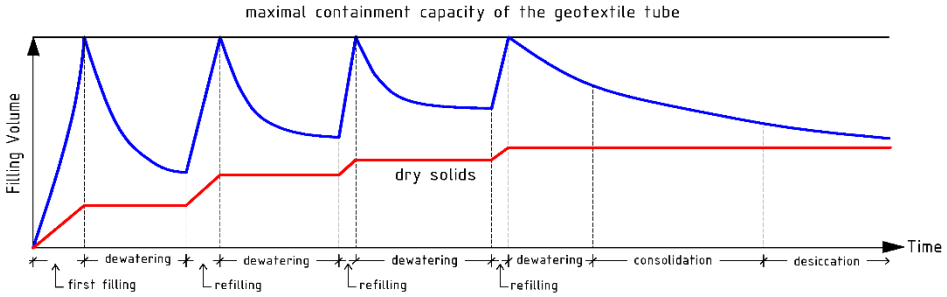

Schematic diagram of the dewatering sequence with geotextile tubes

Figure 1. Schematic dewatering cycle by use of geosynthetic tubes (adapted and modified from Lawson) [5]

Finally, the tube can be opened and the dewatered material with a solid state can be re-used or disposed. A substantial advantage of the dewatering tube system is the stacking availability. By arranging the single tubes in a pyramidal stacked group pattern with several layers the footprint can be effectively reduced and the storage volume increased.

System components

The main system components required for operation are briefly explained in the following sections.

Dewatering tubes

After filling dewatering tubes are almost elliptically shaped long geotextile containment elements designed with a dewatering and storage function. By use of high strength seams for connecting the specifically developed filter fabric sheets, this tubular element is formed.

Normally dewatering tubes are furnished with inlets, distributed along the longitudinal axis of the tube. The tube filling is undertaken through these nozzle inlets with the processed slurry.

Flocculation aids

There are several ways to agglomerate fine suspended solids in order to increase the water release capacity and enhance the dewatering performance of slurries. Two basic physical bonding or agglomeration principles exist: coagulation and flocculation.

Dewatering area

The dewatering tubes have to be placed on a prepared area which is capable of bearing the expected loads. Additionally, the dewatering area has to allow for sufficient drainage capacity of the effluent water. Normally the dewatering pad

consists of a containment bund, a flexible membrane liner and a gravel drainage layer (rounded gravel e.g. 16/32 is preferable). The protective gravel layer is optional and is beneficial if the prepared area is going to be used for several dewatering tube cycles.

IMPLEMENTATION OF DEWATERING TUBE SYSTEM AT TALVIVARA MINE

The Talvivaara Mine is considered to be the largest opencast nickel and zinc mine in Europe. In November 2012, the mine experienced a leak in their gypsum ponds that was quickly located. As response to this problem, the use of geosynthetic dewatering tubes as a remediation solution was adopted.

Figure 2 shows a typical geosynthetic tube installation with pyramidal stacking pattern on top of the dewatering areas. The areas are lined with a 1.5 mm to 2.0 mm thick HDPE geomembrane. The recommended maximum slope inclination was taken into account. For discharge of the filtrate a lined drainage trench was incorporated into the field. Apart from one field the standard dewatering area geometry is rectangular.

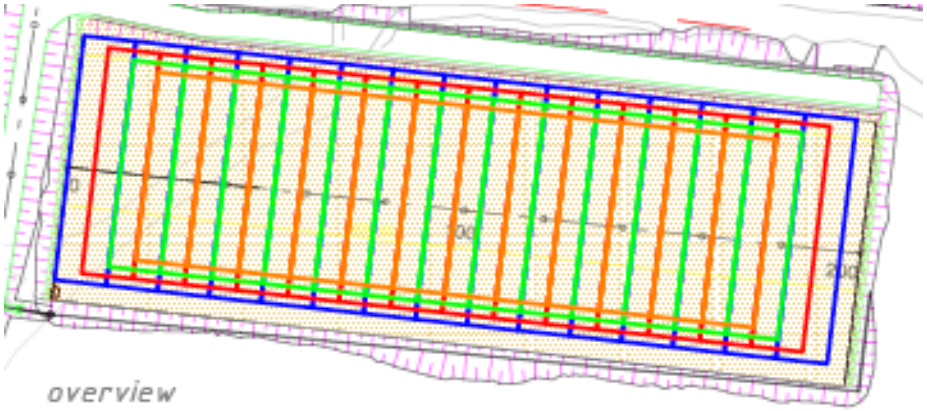

Figure 2. Typical pyramidal stacking pattern top view: First layer (blue), second layer (red), third layer (green), fourth layer (orange)

In order to be able to place a tube layer on top of the lower layer, the top layer tubes are shortened by at least 5 m in order to avoid so called “overhead sliding”.

Dewatering tube operation

The sludge is transported into the dewatering tubes on the dewatering area by a manifold system. The flow can be diverted in a controlled manner to every tube by use of several valves.

The geosynthetic dewatering tube system has been successfully implemented at the Talvivaara Mine in Finland. Due to preventing measures the whole system can also be operated during winter time and the completed field reached the fifth tube layer.

GEOSYNTHETIC SLUDGE LAGOON COVERS

Generalities

The main aim of impermeable cover systems of sludge lagoons or tailings impoundment facilities is to secure the long term stability and environmental safety of structures. The philosophy of closure is to minimize the release of contaminants to an environmentally acceptable level.

Generally speaking, sludge lagoon cover systems consist usually of different layers to isolate disposed tailings and preventing new leakage formation by limiting the infiltration of water into the pond. The combination of different mineral soil and geosynthetic materials is required to guarantee the proper sealing, drainage, filtration, separation, reinforcement and landscaping functions.

According to the tailings characteristics, the regulations in force in the specific lands and the final use of the site after remediation, the thickness of the different layers may vary but in general the entire package is not thinner than 1.5 m - 2 m. The main challenge by the design of such structure is the construction of such system on top of a very soft and extremely heterogeneous soil. In fact, according to the deposition history, dewatering and weather conditions, the hydraulic and mechanical characteristics of the tailings may differ in depth and across the area. In this case, geosynthetics for reinforcement as for example geogrids or woven geotextiles with adapted design strength might be used.

For the technical design of the capping system an intensive investigation of in situ soils is required. The following data are requested:

- Geotechnical parameters of tailings / fill material,
- Stratification of the subsoil,
- Tailings pond size,
- Free water level,
- Live load of construction machinery.

Choice of raw-materials and type of reinforcement

Typically woven fabric or geogrids or combinations like woven/geogrid or geogrid/non-woven can be selected for the capping system. The main function of woven fabrics and geogrids is to transfer tensile stresses resulting from soil and traffic load across a larger area, into the anchor trench. In addition, non-woven can also work as separator and filter to keep sludge in place below the geotextile. As sludges can have different origins like mining, heap leaching, harbour or river sediments, wastewater treatment sludges, they can have very diversified chemical properties. Depending on the chemical characteristics of the sludge different raw materials should be selected. Normally polypropylene (PP), polyesther (PET, PES), polyethylene (HDPE) and polyvinylalcohol (PVA) can be used in a normal pH-range from 4 to 9.5. In areas with pH 2-4 or 10-13 only PP and PVA may be used, if long term stability has to be considered in the design.

Laying of geotextiles

The installation of the geosynthetics depends on the size of the pond and on the

tailings characteristics (Figure 3). It can be done by sewing a large panel pulled by external edges into the pond (Figure 3a) or by unrolling and overlapping them (Figure 3b).

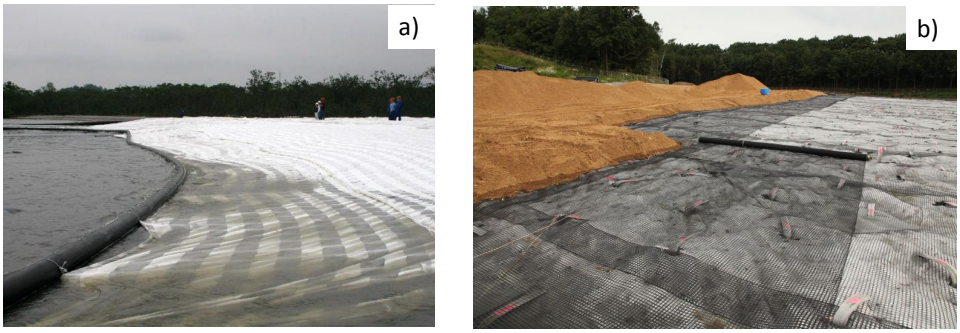

Figure 3. Examples of installation methods of geosynthetics in tailings ponds: **a)** assembling of large panels; **b)** unroll and overlap of geosynthetic reinforcement elements

In case large panels are foreseen, the materials used are woven fabrics that can be sewn and provide good seam strength. Installation by ropes and electric winches, maybe supported by two excavators at the lagoon edges. Once installed, the panel has to be anchored and soil installation can start with light machinery within one or two days after panel installation. During this process workers are not needed to walk on the lagoon or onside the panel, and this represents an important aspect for safety at work.

CASE STUDY: URANIUM ORE TREATMENT TAILINGS PONDS REMEDIATION THE "POND 4" OF WISMUT COMPANY

In the past, the eastern part of Germany (the former GDR) had been the world's third largest producer of uranium. As consequence of uranium operations the uranium ore, pits, open-pit sites and tailings remain as old-polluted sites. The "Pond 4" is a tailings pond in Freital built in 1957 as a settling basin for residues of the uranium ore treatment of the Wismut company [4]. In 2006, the authority of water management declared the Pond 4 as contaminated site to be remediated. The remediation concept consisted of an impermeable capping with the dual purpose of long term reduction of contaminant release and of providing the basis for subsequent landscaping.

Depending on the position, the stored tailings differ in their physical behaviour. According to the tailings characteristics, three main different areas can be identified. While the tailings in the outer edge and middle region can be considered as partially dewatered and partially consolidated, the tailings located in the central area under the free water level is mainly very fine-grained material that can be considered in saturated and unconsolidated state.

The cover consists of the succession of mineral soils and geosynthetics and is designed according to the storage and evaporation principle with a total thickness of ca. 2 m (Fig. 4).

In Pond 4, despite the very soft subgrade the construction of the cover system has been made possible thanks to the introduction of geosynthetics into the system combined with the use of vertical drains in some areas of the pond. The final cover system results of the following layers (from the bottom to the top):

- tailings,
- nonwoven,
- 2 layers of geogrids (installed perpendicularly to each other – T-dimension),
- vertical drains (in the middle and central regions),
- mineral drainage and bearing layer,
- mineral sealing layer,
- soil cover.

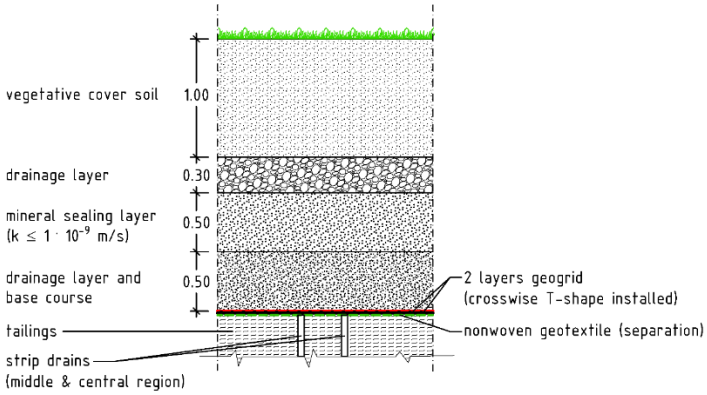

Figure 4. Typical cover system cross section

CONCLUSION

The use of geosynthetics in mine related applications can massively reduce the potential risk of failures for the environment caused by sludge impoundments.

In particular, the geosynthetic dewatering tube system offers, among others, the following advantages:

- Higher process capacity and lower investment and maintenance costs,
- Increased storage flexibility by adding an additional tube layer or additional tubes,
- Demobilization of the tailings by water extraction,
- Encapsulation and permanent storage of the dewatered material inside the tube,
- As a result of the tailings being stored in a solid state the risk of environmentally detrimental spillage is drastically reduced,
- Tube operation is possible also during winter,
- Tube drainage water can be rapidly recycled and re-used in the mine process.

Each sludge lagoon is unique and each project has its own specifics regarding geology, products and construction but thanks to a wide range of different raw materials and customized installation methods, the use of geosynthetics represents the most economic and feasible solution for a safe final closure of tailings ponds.

References

1. Davies, M. P., Lighthall, P. C., Rice, S., Martin, T. d. (2002) Design of Tailings Dams and Impoundments. Keynote Address Tailings and Mine Waste Practices SME, AGM Phoenix,
2. Fernández, A. D., Jamett, R., Briers, M. (2017) Geotextile dewatering tubes for water reclamation technique in TSF´s. Tailings 2017 - 4th International Seminar on Tailings Man-agement,
3. International Commission on Large Dams (ICOLD) 1994. "Tailings Dams – Design of Drainage – Review and Rec-ommendations", Bulletin 97.
4. Koß, V. (1997). Eine Einführung für Studium und Praxis /Volker Koß. Springer, 211- 216.
5. Lawson, C. R. (2008) Geotextile containment for hydraulic and environmental engineering, 15 (6), Geosynthetics International, IGS, 384-427,
6. Syllwasschy, O., Wilke, M. (2014) Sludge Treatment and Tailings Pond Cappings by the Use of Geosynthetics, 7th International Congress on Environmental Geotechnics (7 ICEG) – Melbourne Australia,
7. U. S. Environmental Protection Agency (1994) Design and Evaluation of Tailings Dams, Technical Report EPA 530-R-94-
8. Wilke, M. Breytenbach, M., Reunanen, J. Hilla, V.-M. (25-28 October, 2015) Efficient environmentally sustainable tailings treatment and storage by geosynthetic dewatering tubes: Working principles and Talvivaara case study. Proc. international symposium on Tailings and Mine Waste 2015, Vancouver.

XIII International Mineral Processing and Recycling Conference
Belgrade, Serbia, 8-10 May 2019

University of Belgrade, Technical Faculty in Bor
Vojske Jugoslavije 12, 19210 Bor, Serbia
Tel. +381 30 424 555 Fax +381 30 421 078

IDENTIFICATION OF FINAL DISPOSAL WAYS OF WASTE CLOTHES IN ZRENJANIN MUNICIPALITY

Jelena Mićić #, Una Marčeta, Bogdana Vujić, Višnja Mihajlović
University of Novi Sad, Technical faculty "Mihajlo Pupin",
Zrenjanin, Serbia

ABSTRACT – An expansion of production in fashion industry has caused a decrease in cost of the clothes. On a domestic market, more brands are available to the wider population. Higher clothing production directly affects the production of clothing waste. Extending the lifespan of textile products by reuse is one of the key ways to reduce the negative impact on the environment. However, all textiles become worn out and must be treated as waste. From there arises the question of their final disposal. A survey carried out for the paper needs, inter alia, shows the most common final disposition method in Zrenjanin.

Key words: clothing waste, reuse, recycle

INTRODUCTION

Treatment of waste in the countries of Southeastern Europe, which includes the Republic of Serbia, is mainly landfilling. Indicators that define the state of waste management in the countries of Southeastern Europe are: almost none of the combustion of waste and no more than 5-10 % of recycling [1]. According to the established morphological composition of waste, about 5.04 % of municipal waste represents textiles [2].

Textile waste can be divided into waste that occurs before use of textile product (by-product of the textile industry) and waste that occurs after use of textile product (clothing and other types of textile), which is rejected after use. In order to reduce the negative impact of textile waste on the environment, modern recycling processes are used, with the separation of raw materials that can be used directly in the textile industry or the other types of industry, and the proper disposal of residues that can not be useful [3]. Figure 1. shows the textile recycling process.

The importance of textile waste is reflected in its use as a raw material. It can be used for energy purposes, recycled or otherwise reused. One of the studies shows a technical solution for making thermal insulation materials from ready-made waste.

corresponding author: jelena.micic@tfzr.rs

Figure 1. Textile recycling process [3]

As material for the creation of the new insulation structure, waste from polyester fabrics with great differences in the values of structural characteristics was used in order to determine their influence on the value of thermal insulation [4]. The main reason someone wants to get rid of the clothes is lack of storage space. There are several ways to deposit, from storage in the same house, gifts to someone, sales or exchanges between individuals, to charity organizations or an organized collection [5].

There are many different types of companies and organizations that are involved in initiatives within these three themes: brands, recyclers, hubs, yarn and fabric producers, technical universities etc. The Milan-based company C.L.A.S.S (Creativity Lifestyle and Sustainable Synergy) and Gucci have established an exchange platform, Re. Verso, for recycled materials with partners across the textile value chain. Via the hub, producers of textile products provide mills with pre-consumer, or in some cases post-consumer, textile waste (mostly wool but also other fiber types) which they process into new yarns. In turn, participating partners can purchase yarns with recycled content back via the Re. Verso platform. All recycled content exchanged via Re. Verso can be traced back to its original source [6]. More examples in textile recycling [5]:

1. In Finland, textile company Lindstrom Ltd provides recycling services for working clothes. The work wear users, a wide range of industrial and service organizations, have the option to design for reuse initially, and therefore the garments are developed to be easy-care, durable and easily repaired. This company has its headquarters in Serbia;
2. One of the German companies has developed the production of clothes, which are 100 % of the polyester. In this case, recycling is facilitated, as there is no pre-treatment in the sense of removing metal parts from the clothing before the recipe;
3. The USA has CARE (Carpet America Recovery Effort), an organization managed and funded by the carpet and rug manufacturers. It is backed by the Carpet and Rug Institute (CRI) and various national and federal government agencies.

The main goal of this paper is to indentify dominant methods of disposal of the waste clothes in the Zrenjanin municipality, as well as the existence of adequate places for collection of this type of waste.

MATHERIALS AND METHODS

In order to develop research, a questionnaire was carried out in "online" form on the territory of the municipality of Zrenjanin, which was active for 10 days, with 97 respondents taking part in the responses. The questionnaire was summarized in short form, with total of 9 questions. The first three questions were related to gender, age and place of residence of the respondents. Other questions are as follows:

Q4: Which of the sentences describes you the best?

Offered answers:

- I follow the fashion trends and I try to keep my clothes in line with it.
- I buy new clothes as soon as a new collection arrives.
- I buy on sales from the previous season.
- I do not often follow the fashion trends.
- I do not often buy clothes, I wear it as long as it is usable.
- Nothing of the foregoing.

Q5: Do you buy “second hand” clothing?

Q6: Explain the answer to the previous question (optional).

Q7: The clothes I do not wear anymore:

a) I gift to someone,
b) I throw it in a container,
c) I sell,
d) I recycle,
e) None of the above.

Q8: Do you know that there is a place in your city where you can put off your old wardrobe?

Q9: If the answer to the previous question is YES, indicate where is that place (optional).

For the needs of the paper, the random sampling method was used, respondents who had access to social networks responded to the questions, as the questionnaire was shared on that way. The only selection was made regarding the place of residence (the respondents had to be from the territory of the municipality of Zrenjanin) and the age of more than 18 years.

RESULTS AND DISCUSSION

The following charts show the structure of respondents in terms of gender, age and place of permanent residence.

When we look at gender structure of respondents, out of a total of 97 respondents, 70 are female (72.2 %), while the rest of 27 are male (27.8 %), therefore more than two thirds are women.

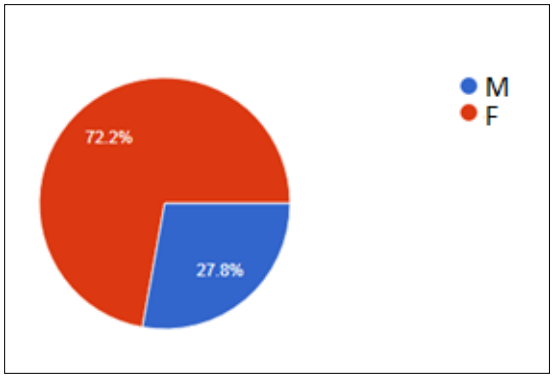

Chart 1. Gender structure of respondents

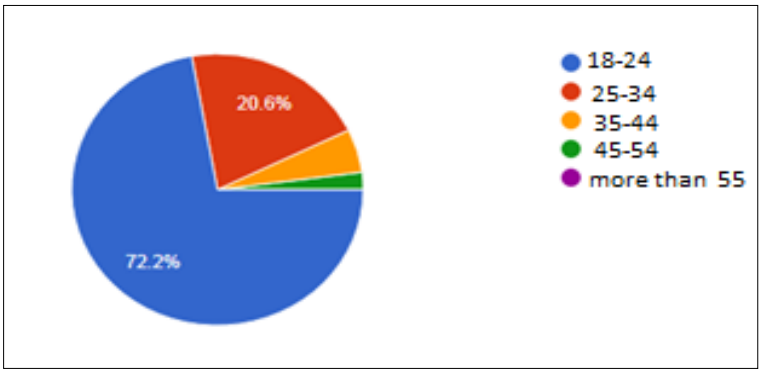

Chart 2. Age structure of respondents

Regarding the age of the respondents, the selection in answering questionnaires has been made for the people older than 18 years. The answers mostly were made by younger population, aged 18 - 24, with 70 respondents. The next group of respondents is aged 25 - 34, which has 20 responses. Five respondents were in the age range 35 - 44 years, while two were between 45 and 54 years old. No one older than 55 years was involved in the study. The reason why the young population is largely responsive can be access to social networks and Internet, since the questionnaire was conducted in "online" form.

When we look at the place of residence of the respondents, the highest number of answers was recorded from the urban environment (68 responses), while the smaller number of people have residency in the surrounding villages within the municipality of Zrenjanin.

The Chart 4. shows the answers to Q4, where the task of the respondents was to indicate the sentence that describes them the best. In this sense, more than half of the answers was related to the statement that they do not follow fashion trends often. Almost the same number of responses were related to statements about following fashion trends and strive to be consistent with that, buying outdated clothing from the previous season, or none of the above answers. Only 4.1 % of respondents wear

clothing as long as it is usable and does not buy often.

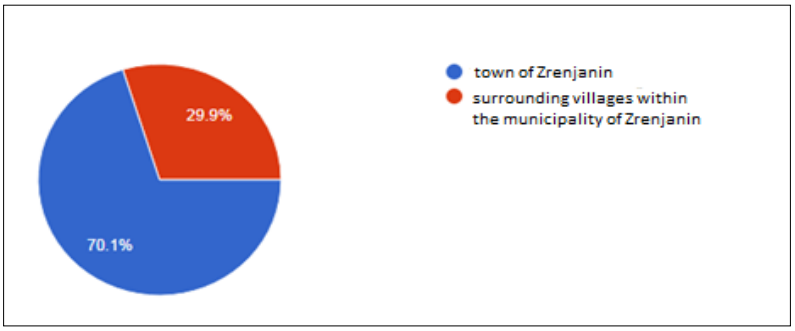

Chart 3. Place of residence

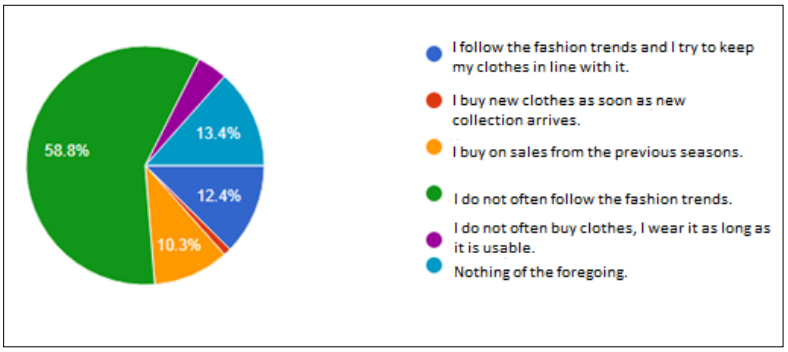

Chart 4. Answers to Q4

Question Q5 was about buying "second hand" clothes, or worn clothes, so 16.5 % of respondents buy often “second hand”, 52.6 % respondents do it sometimes, and 30 respondents answered with “never”, which is a little less than a third of the total number of people surveyed. The reason for purchasing in "second hand" shops is the variety and good quality of clothes with favorable prices.

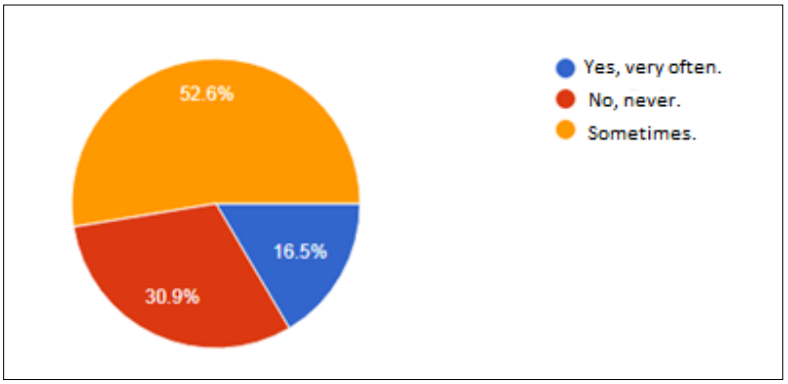

Chart 5. Answers to Q5

Regarding the "fate" or the final disposition of the wearing outfit, the following chart shows the responses to Q7, with the offered answers.

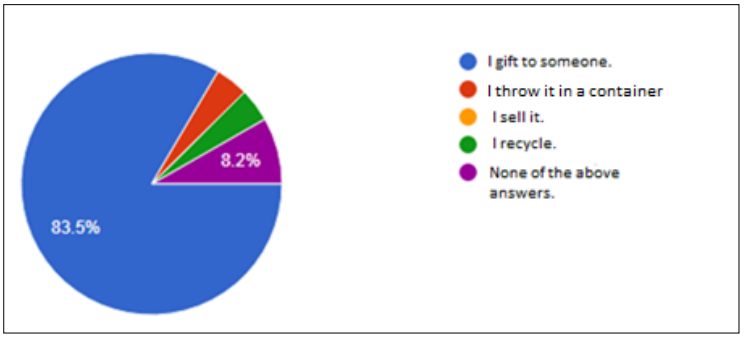

Chart 6. Answers to Q7

In Chart 6. can be seen that most respondents (83.5 %) donate their worn clothing to someone who could continue to use it, which is in some way a form of recycling process (reuse) and prolongs the lifespan of a product. Only 4 respondents stated that they carry clothes for recycling, which is an extremely small number compared to the number of people surveyed. Also, 4 respondents throw their clothing waste into the standard container, while 8 of them did not decide for any of the offered answers.

When asked Q8: Do you know that there is a place in your city where you can put off your old wardrobe?" the most of the 69 respondents responded negatively, while 28 of them responded positively. So, out of a total of 97 respondents, 28 know that there is a place for disposal/recycling old clothes. The next question (Q9) was optional, for respondents who gave a positive response to the Q8, to indicate the place where they put off the wardrobe for recycling.

A total of 22 respondents answered, and among the answers were the organization "Red Cross" that deals with the collection of clothing that later could be distributed to the socially vulnerable population and "H&M" clothing stores, with their organized collecting of old clothing in exchange for the discount coupon.

CONCLUSION

The increase in the amount of the clothing waste is conditioned by the availability of more and more brands and stores. Reuse of worn clothing significantly reduces the negative impact of textile waste on the environment, but after a certain period of time it must still be treated as waste. In this regard, the issue of clothing disposal which is no longer usable to individuals is analyzed. The survey found that the main method of disposal is the giving of clothes to someone who will continue to use it. This prolongs the lifespan of the product and temporarily reduces the negative impact on the environment. Also, shopping in the "second hand" shop is present. Regarding to recycling, it should be noted that in Zrenjanin, according to the survey, there is no defined place for the disposal of textiles, as well as that the population is not sufficiently informed about the possibility of disposal of this type of waste,

whether it is a recycling or reuse. If we compare the responses to Q9 and Q7, there may be an inconsistency. Namely, in Q7, in the responses was stated that 4 respondents bring the clothes to the recycling, while Q9 (referring to the place where the recycling clothes are being disposed of) 22 respondents answered. From there, it can be concluded that respondents may not even understand the notion of recycling of clothing waste.

References

1. Vujić G. 2017. Izazovi transfera novih tehnologija u zemlje u razvoju u oblasti upravljanja otpadom, monografija, Fakultet tehničkih nauka, Novi Sad,
2. Vujić G., Ubavin D., Batinić B., Vojinović-Miloradov M., Štrbac D., Gvozdenac B., Stanisavljević N., Milovanović D., Adamović D., Bačlić S., Dvornić A. (2009), Utvrđivanje sastava otpada i procene količine u cilju definisanja strategije upravljanja sekundarnim sirovinama u sklopu održivog razvoja Republike Srbije, FTN, Departman za Inženjerstvo zaštite životne sredine, Novi Sad,
3. Vujasinović E. 2018. Sirovina da, otpad ne, Zavod za materijale, vlakna i ispitivanje tekstila Sveučilište u Zagrebu, Tekstilno-tehnološki fakultet, Zagreb,
4. Jordeva S., Zafirova K., Trajković D. 2013. Kvalitativna i kvantitativna analiza konfekcijskog otpada u Makedoniji, UDK 628.4.038:677,
5. Morley, N.J., Bartlett, C., McGill I. (2009). Maximising Reuse and Recycling of UK Clothing and Textiles: A report to the Department for Environment, Food and Rural Affairs. Oakdene Hollins Ltd,
6. Watson D., Elander M., Gylling A., Andersson T., Heikkilä P. 2017. Stimulating Textile-to-Textile Recycling, TemaNord 2017:569 ISSN 0908-6692
   A.C. Woolridge et al. / Resources, Conservation and Recycling 46 (2006) 94–103,
   Dubey B., KhushbooJain. Recycling of textile waste is the best way to protect environment, IOSR Journal of Environmental Science, Toxicology and Food Technology (IOSR-JESTFT) e-ISSN: 2319-2402,p- ISSN: 2319-2399,
   Ekstrom M.K., Salomonson N. Reuse and Recycling od Clothing and Textiles – A Network Approach, Journal of Macromarketing 2014, Vol. 34(3) 383-399,
   Roznev A., Puzakova E., Akpedeye F., Sillsten I., Dele O., Ilori O. Recycling in textiles, HAMK University of Applied Sciences, Supply Chain Management.

XIII International Mineral Processing and Recycling Conference
Belgrade, Serbia, 8-10 May 2019

University of Belgrade, Technical Faculty in Bor
Vojske Jugoslavije 12, 19210 Bor, Serbia
Tel. +381 30 424 555 Fax +381 30 421 078

RAISING ENVIRONMENTAL AWARENESS AS AN IMPORTANT FACTOR FOR IMPROVING PACKAGING WASTE MANAGEMENT

Jovanka Milićević [1, #], Milica Alimpić [2]
[1]Cenex doo Belgrade, Serbia
[2]Tehnopapir doo Belgrade, Serbia

ABSTRACT – In order to briefly explain the problem that exists, we will illustrate it through the example: in 2018, 5,000 tons of paper waste was collected more than reported to be marketed, which means that more packaging waste is emitted to the market than the waste generators reported. The Environmental Protection Agency filed 1.987 misdemeanor charges against companies that did not submit a report on "production" of waste in the legal deadline. Also, the data that tells us that 40% of packaging waste ends up at landfills in Serbia does not support the environmental awareness of citizens. It is important that all generations be included in the environmental education program, from the earliest age to our oldest fellow citizens.
In this paper we will make a review of the methodology and examples of how to increase the environmental awareness of citizens and give concrete proposals and measures for solving this problem.

Key words: waste management, packaging, ecological awareness, ecology, packaging waste

INTRODUCTION

For several years now, the Republic of Serbia has been carrying out serious reforms and adopting legal regulations that will bring Serbia closer to membership to the European Union. Out of the 35 chapters listed in the accession negotiations that officially began on January 21, 2014, environmental chapter 27 is equally important for us. For some time now, this chapter is finally opening, however, the Republic of Serbia and the legislature, despite efforts, are still not actually ready to open this chapter. Statistic data indicate that recycling one tone of office paper can save 4200kw electric energy, 32000 l of water, reduce air pollution for 73 % and save 17 trees [1].

From the aspect of economy in general, two crucial points in the system of collection of secondary raw materials are:

1) place of generate of waste

corresponding author: vanja_dinic@yahoo.com

2) failure to declare the quantities of collected packaging waste by the waste generator.

WASTE MANAGEMENT FROM COLLECTORS AND OPERATORS' ASPECTS

In order to briefly explain the problem that exists, we will illustrate it through the example: in 2018, 5,000 tons of paper waste was collected more than reported to be emitted to the market, which means that more packaging waste is emitted to the market than the waste generators have reported. Also, the data that tells us that 40 % of packaging waste ends up at landfills in Serbia does not support the environmental awareness of citizens.

Long-term educational approach can have good influence on waste generators on many levels. It is necessary to educate business entities/waste generators, especially small and medium-sized enterprises how to:

1) storage waste the right way,
2) how to separate municipal waste from packaging waste (how to sort waste) and
3) report exact quantity of packaging waste which is broadcasted into the market.

Primary selection or sorting of waste at the place of origin, in companies, cafes, restaurants, retail shops, markets is the key for companies which collect waste and for operators too, because that is the first level of making collection of packaging waste easier and prevents packaging waste from being disposed at the landfill.

If we could establish system of primary selection of packaging waste at the place of origin and if we could, through various forms of education, raise ecological awareness to a higher level, it would greatly help both: communal enterprises and companies that collect secondary raw materials. System should contain some kind of benefits for generators which contributes to the system. That could be related to the reduction of the price of utility services, which are paid by waste generators, but only if they properly perform the primary waste separation. It would be necessary to educate the owners of small and medium-sized enterprises as well as their employees in the way of separation of waste, where it is the best to keep containers with waste, since it often happens that collectors do not have an adequate access to collected waste at a particular location.

Likewise, it is important to implement the control process, both at the site of waste generation where the way of primary waste separation would be controlled and paid penalties if it is not performed in accordance with the prescribed rules, as well as in the reporting of the quantities of collected packaging waste. The penalties and rewards system would be one of the means of implementing and monitoring compliance with the regulations learned and accepted by waste generators during education.

One of the difficulties that is evident and to which one should pay particular attention is the ecological awareness of the nation. Due to the non-sanctioning of the inadequate behavior of every citizen, we come to the situation that tourists who come to or through Serbia do not feel the need to enforce habits they have acquired in their own country. For example, at international festivals held throughout Serbia (Novi Sad, Belgrade, Nis, Kragujevac, Vrnjačka Banja) we have a situation where, at the location of the festival, after the end of the festival, the site becomes a garbage

dump. Of course, if the organizer has not predicted an adequate action that would anticipate the organized collection of waste packaging in exchange for coupons or free drinks at the festival.

EDUCATION METHODOLOGY OF POPULATION ACCORDING TO AGE STRUCTURE

For all of that, we believe that education of the population at all levels is needed, otherwise Serbia would be a black ecological hole of Europe. In order to fact that education is guaranteed by the constitution as well as the right to a healthy environment, the symbiosis of these two rights would be a right goal of raising environmental awareness.

It is essential that all generations be included in the program of ecological education, from the earliest age to our oldest fellow citizens.

Target groups or categories for education could be divided into 6 groups:

1) Preschool age (0-7 years)
2) School-children (7-14 years)
3) Teenagers (14-18 years old)
4) Students, young people (18-30 years old)
5) Employed / unemployed (30-60 years)
6) Older than 60 years old- retired

According to this categorization, the generation that can be most affected is the youngest one. Through the educational system of kindergartens and preschool educational system, it is most probable that this young kids at this point will adopt positive models of behavior and increase development of ecological environmental protection. At this age, through creative workshops and in a picturesque way, kids can see how the environment works and how to make the difference between the good and bad attitude towards the environment.

When it comes to educating children in primary school, it is necessary, through a school program suitable for children of this age, to introduce a category of environmental care at the basic level, such as properly sorting outs, workshops in which children will work with professional staff and learn how to prolong the lifetime of waste (production of teaching materials from secondary raw materials, school premises on subject such as ecology and recycling).

Different methods should be applied for children in high schools. Since teenagers are the most delicate group when it comes to any influence from adults and authorities, peer educators will have the greatest effect on raising awareness. High schools have already opened environmental departments, so the influence of those students would be the best solution for society.

With students and young people, as with the previous categories, we must have special approach. They have already developed self-awareness, they know what they want in life and what they expect from themselves and from the others. Our country is not an example of countries that have functional measures to prevent young people from migrating, decision-maker must keep this on mind to find the right way to deal with this issue. Through youth organizations, youth offices and active participation through the non-governmental sector, young people can be given the opportunity to show what they know and what their capacities are. This category of

population is the one that can and must be the bearer of changes in the attitude and state of consciousness in all areas, and in terms of environmental protection. If the attention is paid in the right way regarding unacceptable behavior of fellow citizens, can be effective. Unfortunately, the current situation is that most of the people who suggest to their fellow citizens not to throw the garbage out of the container, are more exposed to shame than the one who is irresponsible there.

One of the categories with which it is most difficult to establish cooperation is the category of the population in ages of 30 to 60 years. Those who belong to the unemployed category of society often feel rejected by society and often do not feel sufficiently productive because they are without income. Daily struggle for bare existence does not leave enough space for them to think about how their daily activities affect the environment.

Each of us generates waste during the day, 0.5-1kg of municipal household waste per capita depending on the development of the environment. The amount of waste is proportional to the degree of development of the city. In rural areas, the situation is similar, with the different composition of the waste generated there.

On the other side, employes have different kind of problem. Less time for personal development which is not connected with work place, can decrease chances for develop of environmental awarness. According to that, it woud be helpfull to organize different types of workshops with ecological awarness as main topic. One of the activities which would have fast results, would be separating of packaging office waste at the place of origin.

Last, but not the least important category of population are the oldiest citizens. Acording to fact that they are already completly formed persons with habits and behavior paterns, they could participate in increasing ecological awarness through different kind of programs which include socializing and medical care.

SUSTAINABLE APPROACH TO RAISING ENVIRONMENTAL AWARNESS

Each of the activities for each of the above categories can be divided in 3 basic aspects:

1) Educational
2) Economical
3) Ecological

Educational aspect means that the level of awareness and education in the field of environmental protection is raised through the activities of all categories and recognizes the importance of a healthy and preserved environment.

The economical aspect provides long-term results, because the educational programs also carry out concrete actions in which organizations, institutions, enterprises and other economic entities will have economic benefits from the recycling of waste materials which is generated during business activities.

The environmental aspect ultimately implies that, after all the activities carried out at local landfills, the amount of waste will be reduced, and local collectors / recyclers will process a significantly higher quantity of waste, resulting in a higher number of employees in this sector.

Certainly, this is a topic that needs to be addressed in more detail, since it is multidisciplinary and it is necessary to include the education sector, the authorities

dealing with the issue of youth policy, as well as the authorities that deal with the issue of state administration and local self-government. Eco-analysis should finally provide an expert team that, after considering all available capacities, could point to the benefits of this type of education and measures that would be implemented in the field of environmental protection.

CONCLUSION

Different actions could be organized by students or even high school students, in which employees and their families would participate. It is very important to pay attention to environmentally oriented companies, to support their efforts and to place their organizational culture as an imperative for other societies and companies. Also, the possibility of organizing seminars, trainings, conferences and workshops on the subject of raising the environmental awareness of employees by operators and collectors who could, in realistic cases, explain and approximate the problems they face, as well as concepts that could and should be carried out on a daily basis and which greatly contribute to the system.

An important factor would be the public information system, where all the positive activities that are being carried out in this area would be promoted, and on the other hand, they would condemn acts against the environment.

References

1. http://www.ekounijasn.rs/eng/index.html

XIII International Mineral Processing and Recycling Conference
Belgrade, Serbia, 8-10 May 2019

University of Belgrade, Technical Faculty in Bor
Vojske Jugoslavije 12, 19210 Bor, Serbia
Tel. +381 30 424 555 Fax +381 30 421 078

SUSTAINABLE GRAPHIC DESIGN: POSSIBILITIES OF PACKAGING

Jelena Drobac-Petrović, Predrag Maksić, Vesna Alivojvodić, Marina Stamenović #
College of Vocational Studies – Belgrade Polytechnic, Belgrade

ABSTRACT – Sustainable development stands for economic development that is conducted without depletion of natural resources. "Sustainable design" refers to the design process that integrates an environmentally friendly approach and considers nature resources. In the recent decades design's perception has moved from being viewed as aesthetic to a problem-solving discipline that provides innovative solutions through products or services. In that sense, graphic is still perceived as clean cut guideline of few steps that include usage of soy and vegetable-based inks while printing on recycled paper. These efforts are a good start. This paper will try to explain through appropriate practical examples that eco-graphic design goes further.

Key words: design, packaging waste, graphic design, sustainable design

INTRODUCTION

While "sustainable development" refers to economic development that is conducted without depletion of natural resources, the term "sustainable design" focuses on the design process that integrates an environmentally friendly approach and considers nature resources as part of the design itself.

In the recent decades design's perception has moved from being viewed as aesthetic to a problem-solving discipline that provides innovative solutions through products or services. In that sense, a lot has been said and written about green architecture, sustainable product and fashion design, while graphic is still perceived as clean cut guideline of few steps, like that include usage of soy and vegetable-based inks while printing on recycled paper.

Although these efforts are a good start, eco-conscious graphic design must, and can go further. Also graphic design, as a discipline falls in double jeopardy since it is in its core to convince consumers to buy and consume more, while the philosophy of sustainable design is "less is more"- less material, less energy, less waste etc. To become sustainable in that sense, graphic design must change from the inside out, not the other way around.

corresponding author: mstamenovic@politehnika.edu.rs

PACKAGING ISSUE

Numerous studies pointing the problems caused by generation of large amounts of waste, created waves of reactions with growing concern towards this issue not only in professional circles, but in social media across the globe as well. It is estimated the World Bank that by 2025, staggering 6 million tons of waste will be produced each day [1]. Even more shocking than that, the Ellen MacArthur Foundation and World Economic Forum predict that "by 2050, oceans will contain more plastics than fish" [2]. The report from late 2017 stressed that cheap, light, and versatile, plastics are the dominant materials of our modern economy. Their production is expected to double over the next two decades while only 14 % of all plastic packaging is collected for recycling after use and vast quantities escape into the environment. This not only loss in the ecological sense but is also a financial setback of 80 to 120 $ billion per year. In addition to this the same report reminded the world's landfill waste continues to emit methane, a greenhouse gas that is perceived as far more potent than carbon dioxide. These results have drawn attention worldwide as strong visuals of our future.

Potential solutions could be design of durable packaging plastic (which can be used repeatedly, and completely recycled), innovations in the field of production and design of materials for obtaining higher rates of recycling, and modernizing plastic recycling capacities (gradually abolishing the export of poorly sorted plastic waste), as well as raising awareness of citizens about problems that packaging waste generates [3].

Through improved design, new business models, and innovative products, citizens would be able to choose more sustainable patterns of consumption, which could consequently lead to a reduction in packaging waste generation [3].

PACKAGING AND CORPORATE EFFORTS

As mentioned earlier, many designers and art directors will consider themselves as sustainability oriented just for switching to soy and vegetable-based inks while printing on recycled paper. Although these efforts are a place to begin, sustainable graphic design must and can go further and grow into new philosophy – less material, less energy, less waste. The true change must come from within the core of the problem – design and production process. That is why many believe that the change must come from the inside out, from knowledge of the process – materials, steps, print.

Big global companies have greater capacity to achieve more for the greater good due to their size therefore they bare bigger responsibility. These companies have more means and capacities to make such changes. Their step, as much as they might look like baby step actually can make great difference. One of the good examples of this approach was conducted by Nike. This company was struggling with negative exploitation image across the globe when they decided to make an improvement within. In 1998 they made they packing design more sustainable by reducing the weight of their shoe box by 10 %. That doesn't sound like a huge difference while in reality it resulted in saving an incredible 4,000 tons of raw material and $ 1,6 million annually [4]. Also, in that wave of change Nike switched to water based cements in 90 % of its shoes that saved more than 1,6 million gallons of solvents per year that is

an equivalent of more than 32,000 barrels of oil. Small change means big gain within large multinational corporations [4].

Another good example of corporate change of green packaging is McDonalds. The worldwide chain of fast food has about 37,000 locations in 100 countries [4]. They claim to serve 69 million people daily and their slogan is "billions and billions served" or "more than 99 billion served." Those slogans clearly emphasize the brand's popularity across the globe, but that sort of scale comes at a cost. In the past, McDonald's has been criticized for its shocking environmental footprint [5]. This massive fast food chain of restaurants consumes vast amounts of agricultural goods and livestock food preparation, obviously but it comes with a transportation – heavy supply chain, and produces large amounts of waste globally. Having all this in mind "the brand is responsible for large greenhouse gas emissions, deforestation, and pollution" according to many analyses [6].

In McDonald's they claim that environmental impact, along with functionality, cost, availability of materials and impact on operations, is one of five criteria incorporated into their process of developing food and beverage packaging. From an environmental perspective, the focus is on reducing the impact of packaging and improving waste management practices. The approach itself considers a product's entire lifecycle: It starts with where we source materials and the design of our food packaging, and finally, they look at "end of life" options such as recycling and composting. On their official sustainability site yellow M arch company, in their own words – commits itself to taking a "total life cycle" approach to solid waste, they are examining ways of reducing materials used not only in packaging and but in production as well as diverting as much waste as possible from the solid waste stream. In doing so, McDonalds makes an effort to apply three courses of action: reduce, reuse and recycle, as stated on their own website. In the reduce segment, steps to reduce the weight and/or volume of the packaging has taken place. This process includes eliminating packaging, adopting thinner and lighter packaging, using new technologies and materials, changing manufacturing and distribution systems. This may include perpetual search for materials that are environmentally preferable.

The company applies implementation of reusable materials when possible within operations and distribution systems as long as they "do not compromise our safety and sanitation standards, customer service and expectations and are not offset by other environmental or safety concerns" as it is officially stated online.

Also, McDonald's commitment to recycle is perceived with maximum usage of recycled materials in the construction, equipping and operations of their restaurants. The big yellow M company is already the largest user of recycled paper in the industry, as tray liners, Happy Meal boxes, carryout bags, carryout trays and napkins all come from recycled materials. Through their "McRecycle" program, maintain the industry's largest repository of information on recycling suppliers with spending over a $ 100 million a year buying many different sorts of recycled materials. This last segment is very challenging because recycling and sourcing standards vary region to region and McDonald's is active in more than 100 countries. Therefore, MacDonald's established different standards and actions in different countries. One of those steps forward in recycling and reducing waste in communities beyond restaurant was implemented in twelve of their 16 top markets. On that note, only in

United Kingdom, 78 percent of free - standing McDonald's restaurants offer recycling at the restaurants. They organized more than 2,600 waste events that gathered 78,000 colleagues and community members in waste prevention since 2011. Since 2004 on Swedish market, McDonalds' runs 75 % of its 233 stores on renewable energy, serving organic dairies while recycling 90 % of its waste [4].

On a global scale McDonald's first began its focus on sustainable packaging nearly 25 years ago with the help from their then new partner Environmental Defense Fund. They started a change within the company publicly in 1998 when decided to recreate the packaging step by step. In the following year they introduced to the world their McBurger package made from restaurant waste – potato peel. As shown on the exhibition follow up of the book "Massive Change" across the globe, those burger boxes were 100 % biodegradable with the ability to dissolve in water within an hour. The McDonald officials claim they are edible to humans and the slugs would have a feast for weeks in your garden from them. The company says the material - which is protected by more than 100 patents - is sturdier and retains heat better than traditional polystyrene, plastic or paper containers. Those eco-boxes that are cheaper than the previous ones have another advantage - they consume 60 % less energy to produce. With this step the brand managed to eliminate 300 million pounds [6] of material from its supply chain and reduced its overall waste by 30 % the following decade.

This was one of the first steps forward with EDF and they set their goal of "reimagining our packaging as a resource instead of eventual trash. This literary means that McDonalds intends to make of its packaging redesigned and remade to use less material in general and move to fully recyclable materials. Currently, many of the brand's paper products are made more durable by adding plastic while making it harder to recycle. This kind of initiatives reduced waste by 30 percent within the first decade of EDF partnership.

Figure 1. History of McDonalds Packaging

McDonalds had another big global change in 2013. They completely redefined their visual identity and graphic aspect of the packaging, making it more vibrant and modern. Since 2017, 50 % of McDonald's guest packaging comes from renewable, recycled or certified sources, while making significant progress on fiber-based packaging. The initiative to move to these fiber-based materials eliminated more than 300 million pounds of packaging and led to recycling one million tons of boxes since 2016.

Another ongoing McDonald green project is NextGen Cup Challenge launched last year. They teamed up with their fast coffee arch rival Starbucks and these two multibillion-dollar global giants joined forces to recreate an everyday object – single use coffee cup by making it recyclable, compostable cup of the future. The contest included not just the cup itself, but a lid and straw to go along with it. This project came as part of a 2020 initiative to ban straws altogether. The issue became very visible when photos of turtles injured by plastic particles went viral.

According to many #NoStraw or #BanStraws initiative across USA, it is estimated that over 500 million are used every day in America. Most of them end up in oceans, polluting the water and killing marine life while being a part of the 2050 ocean prediction mentioned before. The issue with straw recycling is that they are too lightweight to make it through the mechanical recycling sorter. When straws with other plastic come into the ocean it breaks down into smaller and smaller pieces known as "micro-plastics" rather than biodegrading or dissolving, which poses great threats to marine life. It is projected that by 2050, 99 % of all sea bird species will have ingested plastic making mortality rate up to 50 % [8]. Scientists at the UGA New Materials Institute conducted a new study which discovered micro-plastics particles smaller than dust or powdered sugar inside baby sea turtles [9, 10]. Of the turtles studies in this research, 100 % were found to have eaten plastic. This causes high mortality within baby sea turtles and that may lead to the species' endangerment.

Having in mind all that, it is important to stress that "McDonald's and Starbucks distribute a combined 4 % of the world's 600 billion cups annually" as mentioned in a recent International Coffee Agreement report. These two coffee chains two of the top three worldwide. Both company's cups are technically recyclable, but, for all sorts of practical matters related to recycling processes, they rarely are.

NextGen Cup Challenge aimed at large or small teams to develop materials and designs a new cup to replace today's takeaway coffee cup. The challenge promised "to provide grants to good ideas, and help them develop market-ready solutions". The call was open for Ideas that may include cup lids, sleeves, straws, liners, and/or consider reuse and alternative delivery systems. The challenge resulted with application from 480 teams worldwide and by choosing 12 international teams from UK, USA, Thailand, Indonesia, Finland, Belgium, France, Germany and Nederland. This global call came with global changes when other big coffee shops caught the wave of recyclable cups. Later, four of the UK's largest coffee retailers Caffè Nero, Greggs, McDonald's UK and Pret A Manger confirmed in late 2018 that they have joined a nationwide cup recycling scheme. This Valpak Scheme, a market-led solution that coffee retailers pay an additional £ 70 to the waste collectors for every ton of cups collected created a stir in UK. This takes the value of one ton of cups from being worth on average £ 50 to £ 120 which is a 140 % increase that makes it commercially

and financially attractive for waste collectors to put in place the infrastructure and processes to collect, sort and transport coffee cups to recycling plants, meaning fewer cups will end up in landfill. It is important to say that within the first six months of the Valpak Scheme, over 41 million cups have been for recycling.

Another great milestone goal was set by McDonald's management was firstly set for 2020 but now postponed for 2025. The company has set a goal to recycle guest packaging in 100 percent of McDonald's restaurants.

SUMMARY

It is important to stress that big multinational companies have more mean to foster new approaches to sustainability and their improvements have more impact. Thus their responsibility is greater. It is evident that one of the great polluters is packaging waste. Sustainable packaging design still has to grow into industry and became more accessible. What appears to be a small step forward within the sustainable packaging industry of global modules such as Nike and MacDonald's, is apparently, no small step on a global scale. Also those steps create waves that competition tries to catch upon.

References

1. DeBiase, F., Raising the Bar on Packaging and Recycling, Medium,11 January, 2018, Retrieved 4 March, 2019, from https://medium.com/@McDonaldsCorp/https-medium-com-mcdonaldscorp-packaging-and-recycling-d6069e3892d,
2. Ellen Macarthur Foundation, The New Plastics Economy: Rethinking the future of plastics &catalysing action, December, 2017, Retrieved 1 March 1, 2019, from https://www.ellenmacarthurfoundation.org/publications/the-new-plastics-economy-rethinking-the-future-of-plastics-catalysing-action,
3. Alivojvodić, V., Kokalj, F.: Upravljanje otpadom i cirkularna ekonomija, Belgrade Polytechnic, Belgrade, 2018. ISBN 978-86-7498-077-4,
4. Mau, B., and Institute without Boundaries, Massive Change, Phaidon Press, New York, 2004,
5. Gunther, M., Coffee and the consumer: can McDonald's mainstream sustainability?, The Guardian, 24 September 2013, Retrieved 4 March, 2019, from https://www.theguardian.com/sustainable-business/mcdonalds-coffee-sustainability,
6. Moss, D.,The greening of…McDonald's?, Blue Ridge Outdoors, 13 Februar 2013, Retrieved 2 March, 2019, fromhttp://www.blueridgeoutdoors.com/go-outside/the-greening-of-mcdonalds/ ,
7. McCarthy, J., McDonald's Is Bringing Sustainable Packaging to All 37,000 Locations, Global Citizen, 16 Januar 2018, Retrieved 2 March, 2019, from https://www.globalcitizen.org/en/content/mcdonalds-packaging-recycling-sustainability/
8. Wilcox, C., Van Sebille, E. and Denise Hardesty, B., Threat of plastic pollution to seabirds is global, pervasive, and increasing, PNAS, 112 (38), 2015, 11899-11904,

9. White, M. E.,et. all., Ingested Micronizing Plastic Particle Compositions and Size Distributions within Stranded Post-Hatchling Sea Turtles. Environmental Science & Technology, 2018,
Gilmore K, Micronizing ocean plastics threaten sea turtle populations, ocean life cycle, 28 September, 2018, Retrieved 2 March, 2019, from https://www.sciencedaily.com/releases/2018/09/180917135930.htm.

XIII International Mineral Processing and Recycling Conference
Belgrade, Serbia, 8-10 May 2019

University of Belgrade, Technical Faculty in Bor
Vojske Jugoslavije 12, 19210 Bor, Serbia
Tel. +381 30 424 555 Fax +381 30 421 078

UPCYCLING DESIGN PROTOCOL: FUNCTIONAL INTERIOR DESIGN USING WASTE MATERIALS

Predrag Maksić, Jelena Drobac-Petrović, Vesna Alivojvodić, Marina Stamenović #
College of Vocational Studies – Belgrade Polytechnic, Belgrade

ABSTRACT – Upcycling is usage of waste materials in reconstructing a functional design product, in this case an interior space. In recent years Upcycling was introduced to the contemporary world, as one of the design protocol by which one can preserve the environment without abusing and damaging useful products out of waste and unused materials. One case example is selected to analyze the factors to be considered in designing using up-cycled materials and products – the case of the community housing units in Sant Ferran, Formentera, which are the project of the Life Reusing Posidonia programme. This paper will give an overview on topic of interest to designers and wider audience – *upcycling*.

Key words: design, upcycling, waste, housing

INTRODUCTION

Each design definition risks being incomplete and imprecise because design represents a vast and complex field of human action in a natural and social context.

It's not just an area of usable items, it's about a field in which design represents a perfect production and consumption cycle. In literature design refers to the practice of making material culture, in other words the world of creative produced functional and aesthetic objects and spaces [1]. Design process is relatively open field for experimentation and new protocols.

Sustainable design involves the application of creative strategies that can be applied in the design process as a response to problems that are often associated with a wider social and business environment and incorporating growing concern toward global resource consumption demands [2].

In recent years' designers increasingly integrate know knowledge into their creative process – knowledge about the use of not only eco but also waste materials. They realized that waste materials give them completely new dimension. Although, it is not new idea. However, it is relatively new in the design process. Literature recognized and defined usage of waste materials in the design process as *upcycling*.

corresponding author: mstamenovic@politehnika.edu.rs

The word *upcycling* means the reuse of an old waste product/object in a new way where the material from which the object is made does not degrade [3]. One of the key advantages of upcycling process of revitalizing the waste material.

Sung (2015) says: "Upcycling is often considered as a process in which waste materials are converted into something of higher value and/or quality in their second life. It has been increasingly recognized as a promising means to reduce material and energy use" [4].

It could be said that new products are created out of old ones. Upcycling protocol in the design process is not just about improving the quality of one's life, but also about a strong feeling for a sustainable and healthier environment. The word is actually about ideology, about the attitude towards the profession in which designers invest their creativity in order to create new products with as little cost as possible [5].

The upcycling process encourages designers to strengthen designer professional ethics in the field of waste materials and re-use materials. In this paper will be presented example from design practice that shows the benefits and creative possibilities of the upcycling process in the re-creation of old products applied in interior design.

One case example is selected to analyze the factors of up-cycled materials and products – the case of the 14 social housing units in Sant Ferran, Formentera, which are the pilot project of the Life Reusing Posidonia programme.

This paper will give an overview on topic of interest to designers and wider audience – Upcycling.

UPCYCLING DESIGN PROTOCOL

Ali et al., say that Upcycling as a part in the design process gives an original view for waste materials. They claim that upcycling is opposite to recycle. Recycling is defined as "breaking down the original material and making it into something else using more energy" [6].

On the other hand, Upcycling is completely energy saving. Both processes indorse the same benefits to the environment and its sources. There are three aspects that can be related to upcycling in context of design: environmental waste management, sustainability and designer's creativity.

Environmental waste management refers to the correct management of different kinds of waste, delivering in-depth, state-of-the-art information on the physicochemical properties, chemical composition, and environmental risks associated with industrial waste from the sugar, pulp and paper, tanning, distilling, textile, petroleum hydrocarbon, and agrochemical sectors, according to Chandra [7].

Overburdening the environment with waste materials and products will surly make problem to the earth and add to the greenhouse effect.

Usually, the upcycled materials and products are considered as eco-friendly. Since the upcycling protocol can be repeated again and again, by which one can return the product or material to its original form and usage, and with creative approach, this old furniture can be reused for another, new function, gaining new life, and simultaneously resulting in minimizing waste production [6]. They provided with the diagram of this process which is shown in Figure 1.

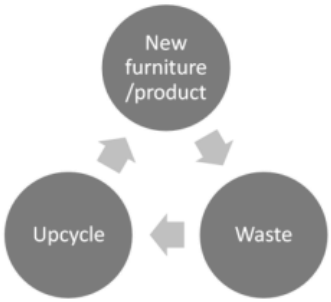

Figure 1. Upcycling process [6]

On the other hand, the question of sustainability in the interior design field is one of the most interesting and the most researched ones in the last years. Environmentally sustainable interior design is founded on the sustainable design principles, aims and strategies shared to the built environment [8]. Thus, in contrast to the traditional design protocols, in which designers are concentrated on meeting the clients' aesthetic and functional needs, in Environmentally sustainable interior design designers focus on the products and materials which have positive environmental and health impacts. In context of upcycling sustainability is referred to as the practice of creating something new, which has a minimal long-term effect on the environment [9]. In other words, waste materials and products in interior design protocols are used again where with the result of prolonging the life of those materials and products (Figure 2).

Figure 2. Upcycling designed products

Designer's creativity plays major role in this process. The design process is seen as a composite of creative cognitive activities. Protocol studies on design and psychology provide verification for the claim stated above [10, 11, 12], etc. The design process involves a variety of creative that enable the designer to solve problems. Various creative cognitive activities are activated in the design process which employ creative thinking.

Creativity is a part of science, medicine, philosophy, education, law, management and off course design. It is very hard to define creativity. Lawson (2005) emphasized

that creativity in design involves periods of very intense work and the relation of many, often incompatible, or at least conflicting demands [13]. Most people would describe design as one of the most creative of human searches. Cross (1997) reported several studies where he examined the idea of the creative leap (sudden lighting) [14]. He viewed creative design in relation to product-creativity, rather than process-creativity [14]. Other authors considered creativity as a product or outcome of many mental processes. It is apparent that agreement on creativity in the literature does not exist.

In this context of interior design upcycling design protocol can really be one way for producing creativity. Interesting thing about this protocol is that a designer, and not just interior one, can keep the emotional worth of a waste product, instead of throwing away. Also, it provides a new why of creating aesthetic value. Waste can be used to produce more values. The fact is a designer does not have to include only new material into his or hers design process.

The form of the source material can be manipulated and used as a totally new product. This new product can meet the requirement of a clients' needs, function and beauty of a designed product or designed space. Also, if new form is made of an old one it might even be more attractive than the old one. Example of this claim can be seen at Figure 3.

Figure 3. Example of ambient design made of waste product.

Sant Ferran is village centrally placed of Formentera island. Formentera is probably the smallest island of the Pityusic Islands group (including Ibiza), and belongs to the Balearic Islands autonomous community in Spain. Sant Ferran was interesting for the hippie movement in the 60s. One can say that today the village is an alternative tourist destination and place where people make different cultural events. Beside, this Sant Ferran is a home of 14 terrace houses which are built using old waste materials and building waste, local traditional techniques and sea grass as insulation (Figure 4).

Figure 4. 14 terrace houses in Sant Ferran, Formentera

The 14 social housing units make the complex. These buildings represent the pilot project of the Life Reusing Posidonia programme. This is an initiative that encourages the use of innovative design and building protocols which are sustainable and which use upcycled materials and products. The project covers both interior, exterior design and architecture. Idea was to reduce: CO_2 emissions by 50 % during construction, lower by 50 % the production of waste, cut by 75 % the use of energy for heating and cooling of homes and 60 % the consumption of water [15].

Figure 5. Interior of the houses

This project ended as a complete research of program and site situations. Traditional design with local elements has been a continual reference. Not just form but also a way of working with economy. The material which was used for constructing this project comes from old market and from waste materials. This lower cost of building.

Figure 6. Facade view

SUMMARY

Design process is open field for research for new protocols. In recent years' designers increasingly integrate know knowledge into their creative process – knowledge about the use of not only eco but also waste materials. Literature recognized and defined usage of waste materials in the design process as upcycling. The word refers to the reuse of an old waste product or material in a new and positive way. Upcycling protocol in the design process is not just about improving the quality of one's life, but also about a strong feeling for a sustainable and healthier environment. The upcycling process encourages designers to strengthen designer professional ethics in the field of waste materials and re-use materials. This paper presented one example of such design practice. This case example shows the benefits and possibilities of the upcycling process applied into interior design process. This case example is the case of the 14 social housing units in Sant Ferran, Formentera, which are the pilot project of the Life Reusing Posidonia programme. This pilot project can be very good example to all designers who are interested in topic of sustainability, and especially topic of usage of waste materials – topic of upcycling.

References

1. Meštrović, M., Teorija dizajna i problemi okoline, Naprijed, Zagreb, 1980,
2. Alivojvodić, V., Kokalj, F., (2018), Upravljanje otpadom i cirkularna ekonomija, Belgrade Polytechnic, Belgrade ISBN 978-86-7498-077-4,
3. Goldsmith, B., (2009),Trash or treasure? Upcycling becomes growing green trend, Retrieved 2 March, 2019: https://www.reuters.com/article/us-trends-upcycling-life/trash-or-treasure-upcycling-becomes-growing-green-trend-idUSTRE58T3HX20090930,
4. Sung K., (2015) A Review on Upcycling: Current Body of Literature, Knowledge Gaps and a Way Forward, Venice Italy Apr 13-14, 17 (4) Part I, 28-40,
5. Ahn, S. H., & Lee, J. Y., (2018) Re-Envisioning Material Circulation and Designing Process in Upcycling Design Product Life Cycle. Archives of Design Research, 31(4), 5-21,

6. Ali, N.S., Khairuddin, N. F. & Zainal Abidin, S., (2013)Upcycling: re-use and recreate functional interior space using waste materials, International conference on engineering and product design education 5 & 6 September 2013, Dublin institute of technology, Dublin, Ireland, 798-803,
7. Chandra, R. ,(2015) Environmental Waste Management, CRC Press Published September 22, London,
8. Fisk, W.J. and Rosenfeld, A.H., (1997) Estimates of Improved Productivity and Health from Better Indoor Environments, Indoor Air, 7 (3), 158-172,
9. Ainsworth, K., (2011) Sustainability by Design: Creative Collaborations and Sustainable Practice, University of New South Wales Press, Wales,
10. Akin, O., & Lin, C., (1995) Design protocol data and novel design decisions. Design Studies, 16, 211-236,
11. Purcell, A. T., & Gero, J. S., (1998), Drawings and the design process. Design Studies,19, 389- 430,
12. Bilda, Z., & Demirkan, H., (2003) An insight on designers' sketching activities in traditional versus digital media. Design Studies,24, 27-50,
13. Lawson, B., (2005): How Designers Think: The Design Process Demystified, Architectural Press, ISBN 9780080454979,
14. Cross, N., (1997), Descriptive models of creative design: application to an example. Design Studies, 18, 427-455,
15. Project: Life Reusing Posidonia - 14 Social housing project at Sant Ferran, 2014-2018. http://eng.reusingposidonia.com/proyecto-14hpp-sant-ferran/ .

XIII International Mineral Processing and Recycling Conference
Belgrade, Serbia, 8-10 May 2019

University of Belgrade, Technical Faculty in Bor
Vojske Jugoslavije 12, 19210 Bor, Serbia
Tel. +381 30 424 555 Fax +381 30 421 078

INSTITUTIONAL CRITERIA FOR INFRASTRUCTURE PROJECTS - CONDITION FOR SUSTAINABLE DEVELOPMENT

Vladimir Pavićević [1,#], Darko Radosavljević [1], Ana Popović [1], Marina Stamenović [2], Vesna Alivojvodić [2], Aleksandra Božić [2]
[1]University of Belgrade, Faculty of Technology and Metallurgy, Belgrade, Serbia
[2]College of vocational studies Belgrade Polytechnics, Belgrade, Serbia

ABSTRACT – The development of infrastructure project prioritization manual was a collaborative process between local and central Serbian institutions, government and non-government as well as drawing on national and international best practice. The three components - the criteria, weighting and guidelines were developed using different methods appropriate to each component. There are two basic stages in the evaluation: qualifying (screening) and ranking (scoring). The main criteria are: Environmental, Financial, Socio-Economic Technical and Institutional (sub-criteria: Regional Aspect, Project Ownership and Responsibility, Institutional Capacity of Project Owner and Municipal Commitment). The maturity (readiness) of the project is defined by the project preparation and development which has already been undertaken.

Key words: infrastructure projects, prioritization, institutional criteria.

INTRODUCTION

The Department for Environmental Projects Management within the Ministry of Environmental Protection of the Republic of Serbia has responsibilities for environmental infrastructure programming and implementation for EU IPA funds and other funding sources under the governmental roles and responsibilities [1]. The scope of their responsibility covers national programming for waste water treatment, municipal solid waste and remediation across all funding sources. In the process of identification and selection of infrastructure projects it was necessary to develop criteria to enable project's prioritization. The three components of the prioritization system - the criteria, weighting and guidelines were developed using different methods appropriate to each component. In general terms the criteria were identified from technical best practice [2], the weighting was developed from Serbian official strategy and planning framework (including the National Sustainable Development Strategy (2008), the National Environmental Protection Programme (2010), the National Waste Management Strategy (2010) and National Environmental Approximation Strategy (2011) and the guidelines focused on

corresponding author: vpavicevic@tmf.bg.ac.rs

addressing user needs and experience [3].

There are two basic stages in the evaluation: qualifying (screening) and ranking (scoring). Projects that have passed the qualifying will subsequently be scored and ranked. The specific principles behind drafting the project prioritisation system are as follows:

- Simplicity: this prioritisation methodology is intended to be in almost daily use to guide and support project identification, selection and preparation. It needs to be accessible to a range of users therefore should be as simple as possible while performing its function to differentiate between project proposals.
- Relevant: the scoring system for each criterion should be able to differentiate between projects. For example, if every project achieves the same score on a certain criterion then it is not contributing to the process.
- Defensible: the criteria should be aligned with specified national strategies, plans and programmes wherever possible. Where not specified then they should represent national and international best practice.
- Qualitative and Quantitative evaluation: both types of measures should be applied to provide a thorough assessment of projects.
- Uniqueness: information that defines a single criterion should not form the basis of many other criteria. For example, if the size of the beneficiary population has been used and weighted for one criterion its affect should not have a multiplying affect by being applied in a number of other criteria. In such a case, the repetition of the information should be addressed in the weighting system.
- Balanced: the criteria should be seen as a complete set. Emphasis on certain aspects can be changed through the weighting system but the criteria will provide coverage of all the categories for assessment.
- Accessible: the criteria and the methodology used to define them needs to be clear and understandable to a range of users. The manual should be transparent so as to guide the project proposers to design projects that have the best chance of being prioritised as well as supporting the ministry staff who will make the assessments.
- Positive Scoring: the scoring system used for the criteria will work on a 'positive scoring' basis. A proposal needs to earn points rather than starting at a level and losing points. It is the responsibility of the project owners to demonstrate and prove, through the project proposal, how a proposal justifies the scoring points for each criterion. Guidelines will be provided to assist project proposers and assessors in identifying which sources of information are deemed to be credible for particular criteria.
- Consistency: the criteria and guidelines are intended to produce consistent and comparable results [4].

QUALIFYING CRITERIA

The purpose of the qualifying process is to select projects to be included in a "pipeline" of potential projects that are eligible for funding by EU funds and/or other

potential financing institutions [4, 5]. The following qualifying criteria are proposed:

Q1 Sector

Project should be in one of the below sectors: waste water, solid waste and remediation.

Q2 Legal Status of the project beneficiary

- Is the beneficiary a public institution? Yes or No
- The direct beneficiary must not be private sector.

Q3 Project status

- Is the Questionaaire appropriately and completely filled in? Yes or No
- The project proposal must contain the information which is asked with the questionnaire as a minimum, and be signed by the Mayor of Municipality.

Q4 Compliance with policy and strategies

Project is in compliance with National Sustainable Development Strategy, National Environmental Protection Programme, Waste Management Strategy and National Environmental Approximation Strategy. Yes or No

RANKING CRITERIA

The main criteria are:

- **Environmental**
  Sub-criteria: E1 Environmental Benefits/Impacts, E2 Health Benefits/Impacts and E3 Environmental Strategy

- **Financial**
  Sub-criteria: F1 Per Capita Investment, F2 Finance Secured and F3 Cost Recovery

- **Socio-Economic**
  Sub-criteria: SE1 Economic Development, SE2 Affordability of Investment and SE3 Collection of Charges

- **Technical**
  Sub-criteria: T1 Need for Infrastructure, T2 Complexity of Project, T3 Project Risk and T4 Demonstration Potential

- **Institutional**
  Sub-criteria: I1 Regional Aspect, I2 Project Ownership and Responsibility, I3 Institutional Capacity of I4 Project Owner and Municipal Commitment.

- **Maturity (readiness)**
  The maturity (readiness) of the project is defined by the project preparation and development which has already been undertaken. This criterion is of the great importance because preparation and high quality of spatial and urban plans, technical documentation (designs and studies) and permits are necessity for project implementation [6].

INSTTITUTIONAL CRITERIA

I1 Regional Aspect

Table 1. Regional Aspect

Regional Aspect	Points
Municipality	1
City	3
Association of Municipalities/Region	5

Definition and rationale

All national environmental strategies suggest that the proposed projects (especially in solid waste management) should be based on regional concept.

Scoring

The project which concerns only one municipality will be scored as minimum level (1 point), only one city as medium level (3 points) and region as maximum level (5 points).

I2 Project Ownership and Responsibility

Table 2. Project Ownership and Responsibility

Project Ownership and Responsibility	Points
The four key responsibilities of the project cycle (project development, financing, construction and operation) are under five or more organizations.	1
The four key responsibilities of the project cycle are under four organizations.	2
The four key responsibilities of the project cycle are under three organizations.	3
The four key responsibilities of the project cycle are under two organizations.	4
The four key responsibilities of the project cycle are all under one single organization	5

Definition and rationale

This sub-criterion concerns the question whether or not the ownership and responsibilities for project implementation have been clearly defined. Unclear division of responsibilities is likely to delay, complicate and make project development more expensive. If there is no clear institutional framework for project implementation and financing or if there is no firm agreement which organization will have project ownership (e.g. in the case of a project proposed by more than one municipality) this may cause serious delays and complications in project implementation and subsequent service delivery.

Scoring

The highest score for this sub-criterion will be assigned to a project in which one

organization will assume the four key responsibilities of the project cycle (project development, financing, construction and operation) and act as contracting authority. The score will be lower if these various responsibilities will be shared by different organizations as this may lead to complications during the lifetime of the project.

I3 Institutional Capacity of Project Owner

Table 3. Institutional Capacity of Project Owner

Institutional Capacity of Project Owner	Points
Operator has no experience in service delivery.	1
Operator has experience in general service delivery (water suply, sewerage system, municipal solid waste, green market, district heating, cemetery...) and provides service to less than 50,000 inhabitants.	2
Operator has experience in general service delivery and provides service to 50,000 inhabitants and more.	3
Operator has experience in sector specific service delivery and provides service to less than 50,000 inhabitants.	4
Operator has experience in sector specific service delivery and provides service to 50,000 inhabitants and more.	5

Definition and rationale

This criterion refers to the extent to which the responsibilities for project development and implementation can be understood and undertaken by the institutions/organizations involved. The reason for incorporating this criterion is that the capacity of the project owner is crucial to successful implementation and also very important for successful operation.

Scoring

The size and experience are basic indicators of the completeness of the institution/organization/operator and its institutional capabilities.

I4 Municipal Commitment

Table 4. Municipal Commitment

Municipal Commitment	Points
Statement available from the Municipality or Municipalities concerned signed by the Mayor and endorsed by the Municipal Assembly confirming that the project is ranked as a Municipal Priority Project.	1
The municipality already has financed environmental infrastructure projects (verifiable in previous municipall financial reports).	2
Financial resources earmarked specifically for the project in the current municipal budget (verifiable in current municipal budget).	2
Add the above points, total maximum score.	5

Definition and rationale

Sub-criterion concerns both the formal statement for the proposed project by the municipality or municipalities in which the project takes place, and relevant conformation of previous and current financing of environmental infrastructure

projects. It is essential for the project to succeed that it has the full support and commitment from the municipality and that it has municipal (regional) priority.

Scoring

The strategic municipality paper with the formal statement by the Mayor of a municipality that the proposed project is a priority for the municipality and that it is fully committed to support the project and to meet its obligations, is taking into consideration only if it is officially endorsed by the Municipality Assembly. The previous financing of environmental infrastructure projects has to be verified by previous municipal financial reports, while the current financial resources earmarked specifically for the project should be verified by current municipal budget. Points for each item have to be added, total maximum score is 5.

WEIGHTING

While the criteria cover all the categories that need to be considered during the assessment of project proposals, the weighting system enables the prioritization to be tailored to the user. The user will define the emphasis placed on each part of the criteria allowing them to identify a short list of priority projects that are in line with their own strategy or parameters. Obviously, each short-list can only be compared against projects that have been identified using the same weighting algorithm.

CONCLUSION

The three components of the process of identification and selection of infrastructure projects prioritisation process - the criteria, weighting and guidelines were developed using different methods appropriate to each component. It was necessary to develop criteria to enable project's prioritization and make decision on application for financing from EU funds and other international or national financing institutions. There are two basic stages in the evaluation of any project: qualifying (screening) and ranking (scoring). In the qualifying process eligibility criteria are applied to determine which projects are eligible to be included in the list of potential projects. The maturity (readiness) of the project is very significant criteria for prioritization process. While the criteria cover all the categories that need to be considered during the assessment of project proposals, the weighting system enables the prioritization to be tailored to the user. The criteria, scoring and weighting are designed to be adaptable and can be changed if the official strategy changes.

Acknowledgements:

This paper is a result of activities on the Project TD 33007 funded by Ministry of Education, Science and Technological Development of Republic of Serbia.

References

1. Radosavljević, D., Pavićević, V., Stamenović, M., Stojković, I. (2012) Financing of waste management infrastructure projects - condition for sustainable development. VII Symposium on Recycling technologies and sustainable

development, University of Belgrade, Technical faculty in Bor, Soko Banja, 146-152,
2. Technical Assistance for Environmental Heavy-Cost Investment Planning, (2005) Project Prioritization Manual, Ministry of Environment and Forest, Ankara, Turkey,
3. Stamenović, M., Radosavljević, D., Pavićević, V., Brkić, D., Putić, S. (2015) Socio-economic criteria for infrastructure projects - condition for sustainable development. X International Symposium on Recycling Technologies and Sustainable development, University of Belgrade, Technical faculty in Bor, Bor, 113-118,
4. Environmental Infrastructure Project Prioritization Manual, (2011) Ministry of Environment, Mining and Spatial Planning, Belgrade, Serbia,
5. Pavićević, V., Milićević, S., Knežević, M., Povrenović, D., (2012) Vrednovanje projekata prečišćavanja komunalnih i industrijskih otpadnih voda, Zbornik radova sa Konferencije Kvalitet vode u sistemima vodovoda i vode u industriji, Beograd, 115-124,
6. Pavićević, V., Radosavljević, D., Popović, A., Stamenović, M., Alivojvodić, V., Božić, A. (2017) Technical criteria for infrastructure projects - condition for sustainable development. XII International Symposium on Recycling Technologies and Sustainable development, University of Belgrade, Technical faculty in Bor, Bor Lake, 162-168.

XIII International Mineral Processing and Recycling Conference
Belgrade, Serbia, 8-10 May 2019

University of Belgrade, Technical Faculty in Bor
Vojske Jugoslavije 12, 19210 Bor, Serbia
Tel. +381 30 424 555 Fax +381 30 421 078

HOW IS THE PROBLEM OF ACID MINE DRAINAGE OF THE CLOSED MATSUO MINE SOLVED IN JAPAN

Dragana Božić [1, #], Nobuyuki Masuda [2, 3], Radmila Marković [1], Masahiko Bessho [3, 4], Zoran Stevanović [1]

[1]Mining and Metallurgy Institute Bor, Bor, Serbia,
[2]Mitsui Mineral Development Engineering Co., LTD, Tokyo, Japan
[3]Akita University, Graduate School of International Resource Sciences, Akita, Japan
[4]Akita University, International Center for Research and Education on Mineral Engineering and Resources, Akita, Japan

ABSTRACT – A large quantity of acid mine drainage that discharged in to Akagawa River from the abandoned Matsuo Mine, polluted the main stream of the Kitakami River. Because that, it had become a serious social problem for the environment along the river side area. The acid mine drainage is oxidized by the Iron oxidizing bacteria in this plant while calcium carbonate is used as the neutralizer. The presented procedure is based on data provided by Matsuo Mine during visit to Japan.

Key words: Matsuo Mine, acid mine drainage, neutralization, oxidizing bacteria, calcium carbonate

INTRODUCTION

Matsuo Mine has the largest treatment plant in Japan and it is located on the mountainside of the Hachimantai Highlands that is upstream of the Akagawa River, a tributary of the Kitakami River. Since 1882 Matsuo Mine had produced sulphur and iron sulphide. However from around 1965 the mine's business performance was getting worse, and mining was closed in 1972.

The original vegetation in the area was beech forest. However, due to smoke from sulphur smelting, the soil surrounding the mine has become very acid, and can no longer support most trees. Wastewater flowing from the mine is also strongly acidic (pH 2), and includes large amounts of arsenic. As the flow is from 17 to 24 tons per minute, it affects the Kitakami River and Pacific coast of Iwate Prefecture.

Construction of the new plant started in August 1977 and was completed in 1981

corresponding author: dragana.bozic@irmbor.co.rs

by spending 62 million dollars for the neutralization plant and 31 million dollars for the sludge storage dam. After that, the Kitakami River has been restored through the 24 hour-a-day and 365 day-a-year treatment of AMD at the neutralization plant.

WATER-QUALITY STANDARD FOR DISCHARGE FROM THE MATSUO NEUTRALIZATION PLANT

1. At the main stream of the Kitakami River, the target of improving water quality was set for the achievement of the environmental water quality standard.
2. The Akagawa River had been an acidic river with pH 4.0 even before the Matsuo Mine was developed. That is why the Matsuo Neutralization Plant discharges the treated water into Akagawa River at pH 4.0.
3. Since the Matsuo Neutralization plant started to treat the acid mine drainage, the water quality of the main stream of Kitrakami River has been kept at the environmental standard.

BACTERIAL OXIDATION AND CALCIUM CARBONATE NEUTRALIZATION SYSTEM

The acid mine drainage is oxidized by the Iron oxidizing bacteria in this plant. Calcium carbonate is used as a neutralizing agent because it is economically more favourable. Since calcium carbonate does not react to ferrous iron (Fe^{2+}) in the acid mine drainage, it is necessary to previously oxidize ferrous iron into ferric iron (Fe^{3+}). For oxidation are used iron oxidizing bacteria. Iron oxidizing bacteria is a type of bacteria that oxidizes iron, there is about 2.5 x 10^5 cells/mL of this bacterium in the AMD of the Matsuo Mine. This process wich oxidizes iron before adjusting pH value is called '' two step neutralization''.

CAPACITY OF THE NEUTRALIZATION PLANT

In Picture 1 you can see the appearance of a neutralization plant consisting of three parallel lines. Also there is one emergency line. The plant is designed for nine million cubic meters of AMD per year.

Figure 1. Neutralization Plant

PERMANENT DRAINAGE TUNNEL

A plant that continuously drains acid waste water to a neutralization plant is the Permanent Drainage Tunnel. Tunnel length is 322 m and acid waste water to the neutralization plant is delivered by gravity.

DISTRIBUTION TANK

The Distribution Tank has three parallel treatment lines and one emergency line. Maximum treatment capacity for all three lines are 36 m^3/min. Water is distributed parallel to all three lines.

OXIDATION TANK

In the first step of neutralization, the acid mine drainage from Matsuo mine flows into the oxidization tank. The next reaction represent oxidized ferrous iron in the acidic mine drainage into ferric iron by the functions of concentrated bacteria

$$4FeSO_4 + 2H_2SO_4 + O_2 \rightarrow 2Fe_2(SO_4)_3 + 2H_2O \quad (1)$$

Iron sludge, created by the neutralization, is effectively utilized as a carrier of bacteria.

BACTERIA RECOVERY TANK

Iron sludge that has absorbed bacteria is concentrated in this Tank (Picture 2.), settled and then returned to the oxidation tanks.

Figure 2. Bacteria Recovery Tank

NEUTRALIZATION TANK

After the bacterial oxidation, in the second step, calcium carbonate is added, as a neutraliser. In the neutralisation tank, a suspension of calcium carbonate is run through a thin pipe with an adjustable valve, at a rate calculated to deliver exactly the quantity necessary to raise the pH to 4. Iron sludge is precipitated by next reaction (2):

$$Fe_2(SO_4)_3 + 3CaCO_3 + 3H_2O \rightarrow 2Fe(OH)_3\downarrow + 3CaSO_4\downarrow + 3CO_2 \quad (2)$$

Figure 3. Neutralization Tank

Table 1. The results of water quality of AMD waters and the treated waters discharged in the Neutralization plant for period of 30 years

	1982		1992		2002		2012	
	AMD	**Treated Water**	**AMD**	**Treated Water**	**AMD**	**Treated Water**	**AMD**	**Treated Water**
V ml/min	17.2	17.2	17.6	17.6	18.1	18.1	16.7	16.7
pH	1.93	4.20	2.21	4.14	2.26	4.14	2.26	4.25
Fe-total mg/L	504	2.3	304	2.0	237	2.2	197	2.5
Al mg/L	114	81	72	57	70	58	69	57
As mg/L	2.84	0.02	1.70	0.01	1.29	0.01	0.94	0.01

As can be seen from the Table 1 after neutralization at the plant pH value of AMD waters was 4 while the concentrations of iron, aluminium and arsenic were reduced to the permitted values.

SOLID-LIQUID SEPARATION TANK

The large quantities of iron sludge formed during the neutralization step are settled out in the solid-liquid separation tanks. In this separation tank, after the addition of coagulant, separation of the solid and liquid phase is carried out. The separation tanks are circular and made of concrete. From here, the solids are pumped up to the sludge storage dam. The resulting sludge is pumped to the storage dam until the purified water is discharged into Akagava River.

SLUDGE STORAGE DAM

After completion of the neutralization, the neutralizing sludge is stored in the Storage Dam. The inner shore of the dam is covered with stones. About 20 000 cubic meters of sludge are accumulated in the dam each year, while the total capacity of the dam is 2,000,000 cubic meters.

Figure 4. Sludge Storage Dam

CONCLUSION

A large quantity of acid mine drainage (AMD) that discharged into Akagawa River from the abandoned Matsuo Mine, polluted the main stream of the Kitakami River. Because that, it had become a serious social problem. The AMD is oxidized by the Iron oxidizing bacteria in this plant. Calcium Carbonate is used as neutralizer. The neutralization plant has three treatment lines to treat the huge quantity of AMD in a stable and secure manner.

ACKNOWLEDGEMENTS

This paper is result of Japan, Serbia mutual JICA Project in the SATREPS program: "The Project for the Research on the Integration System for Spatial Environment Analysis", funded from the donation of the Japanese Government, with the participation of Serbian funding and Project No. 37001, "The Impact of Mining Waste from RTB Bor on the Pollution of Surrounding Water Systems with the Proposal of Measures and Procedures for Reduction the Harmful Effects on Environment", funded by the Ministry of Education, Science and Technological Development of the Republic of Serbia.

References

1. http://www.pref.iwate.jp/
2. http://www.jogmec.go.jp/

XIII International Mineral Processing and Recycling Conference
Belgrade, Serbia, 8-10 May 2019

University of Belgrade, Technical Faculty in Bor
Vojske Jugoslavije 12, 19210 Bor, Serbia
Tel. +381 30 424 555 Fax +381 30 421 078

REMOVAL OF COPPER IONS FROM WASTEWATER USING NATURAL ZEOLITE

Grozdanka Bogdanović #, Žaklina Tasić
University of Belgrade, Technical Faculty in Bor, Bor, Serbia

ABSTRACT – Water pollution is a major problem over the world. In accordance with that researchers are constantly working to determine a suitable and efficient method for wastewater treatment. Among various techniques that can be used, adsorption has significant role in wastewater treatment due to its efficiency in the removal of pollutants. The ability of clinoptilolite as an adsorbent for the removal of Cu^{2+} ions from synthetic solution is investigated in this paper. The influence of different parameters like initial pH value, initial concentration of solution and contact time between zeolite/solution on the adsorption ability of clinoptilolite was examined.

Key words: clinoptilolite, adsorption, synthetic solution, copper ions

INTRODUCTION

In general, the pollution of water is a major problem over the world. Different industrial branches release large amount of pollutants and thus the water, soil and air are contaminated. Heavy metals reach the environment through different human activities. The main are mining and industrial processes such as melting, galvanizing, electrolysis, and agricultural sectors [1-4]. In contrast to organic pollutants, heavy metals are not degradable and they have ability to accumulate in living organisms through a food chain. Having that in mind, it is very important to remove contaminants from water.

Different methods such as solvent extraction, membrane filtration, chemical precipitation, ion exchange and adsorption can be used to remove heavy metals [5]. The adsorption method is widely used in wastewater treatment due to its efficiency in the removal of pollutants. Also, various low cost materials can be used as adsorbent in the wastewater treatment which affects the economy of the process. In recent years, the interest of researchers for the using of biosorbents has increased. Among them, zeolites are the mostly used adsorbents because they are environmentally friendly, low cost, possess good selectivity for different cations and have high ion exchange capacity. Furthermore, zeolites are the most important

corresponding author: gbogdanovic@tfbor.bg.ac.rs

heterogeneous catalysts in the petrochemical industry [6]. The aluminosilicate framework, exchangeable cations and zeolitic water are three main components in the zeolite structure [7]. Zeolites are suitable material for the removal of heavy metals from wastewater due to their relatively harmless ions (potassium (K), sodium (Na) and calcium (Ca)) released during the ion exchange and they are classified as cationic exchangers [8].

The process of ion exchange follows the reaction (1):

$$A^{ZA+} + BL_{ZB} \Leftrightarrow B^{ZB+} + AL_{ZA} \quad (1)$$

In the equation (1) L is defined as a portion of zeolite framework holding unit negative charge while z_{A^+} and z_{B^+} are the valences of the respective cations.

The efficiency of zeolite as adsorbent in wastewater treatment depends on the pH value of solution, the concentration of pollutant and contact time of system zeolite/solution. Also, the amount of used zeolite and size distribution of zeolite particles has the influence on the adsorption efficiency. It is known that zeolites can be chemically modified in order to increase their efficiency.

Different types of zeolite are tested for remove copper ions from aqueous solutions and the obtained results are shown in Table 1. As can be seen from this table, the adsorption capacity of zeolites depends on experimental conditions.

Table 1. The adsorption capacity of various tested zeolites for removal of copper ions

Type of zeolite	q_e, mg/g	pH value	Experimental conditions	References
Clinoptilolite	11.7	2-4	10mg/L[a]; 0.5-180g/L[b]	[9]
	5.9	3-6	100mg/L[a]; 2.5-5g/L[b]	[10]
Zeolite X	109	/	20-2000mg/L[a]; 2g/L[b]	[11]
Zeolite 13X	136	3.5	1.5-3mmol/L[a]; 20g/L[b]	[12]
Zeolite 4A	50.5	3.0	50-300mg/L[a]; 5g/L[b]	[13]
Zeolite NaP1	50.5	3-6	100mg/L[a]; 2.5-5 g/L[b]	[10]

[a] – the initial concentration of solution; [b] – the concentration of used zeolite; / - no data

Clinoptilolite is a natural zeolite which molecular formula is $(Na, K)_6Si_{30}Al_6O_{72} \cdot 24H_2O$. It can be found all over the world and mostly in Eastern Europe (Bulgaria, Greece, Hungary, Croatia and Serbia). The aim of this paper is to investigate the ability of natural zeolite, clinoptilolite, to remove copper ions from synthetic solutions. Further, parameters as initial pH value, different contact time between zeolite and solution and initial concentration of solution were varied in order to examine their influence on the adsorption ability of clinoptilolite.

MATERIALS AND METHODS

Natural zeolite from Serbia (Deposit "Igroš", Kopaonik) as an adsorbent for the removal of copper ions from synthetic solutions is used.

In order to obtain initial concentration of Cu^{2+} ions stock solution was prepared by dissolving corresponding sulfate salt ($CuSO_4 \cdot 5H_2O$) in 1000 ml distilled water. Further, lower concentrations are prepared by dilution of stock solution with distilled water. The sulfuric acid was used for adjusting the initial pH value of prepared solutions.

The adsorption experiments were carried out in a batch mode in a series of beakers equipped with magnetic stirrers by stirring 1g of zeolite with 50 ml of solution. Zeolite sample and aqueous phase were suspended by magnetic stirrer at 300 rpm at different time period from 5 to 120 minutes. After that, the suspension was filtered and the filtrate was analyzed by Optical emission spectrometers with inductively coupled plasma. Also, the influence of an initial pH value of the synthetic solution was tested in a wider range of pH values. All experiments were carried out at room temperature.

The adsorption capacity and the adsorption degree are calculated following the equations (2) and (3), respectively.

$$q(t) = \frac{C_i - C(t)}{m} V \tag{2}$$

$$AD\% = \left(1 - \frac{C(t)}{C_i}\right) \cdot 100 \tag{3}$$

Where q stands for the mass of adsorbed copper ions per unit mass of adsorbent (mg/g), C_i and C_t are the initial and the final concentration of copper ions, respectively (g/dm^3), V is the volume of solution (dm^3), m is the mass of adsorbent (g) and AD stands for adsorption degree (%).

Figure 1. Sample of clinoptilolite

RESULTS AND DISCUSSION

The optimal contact time between the adsorbent and the solution is one of the important parameters. According to that, the adsorption ability of clinoptilolite was investigated at different contact time between zeolite and copper ion solution. The initial concentration of solution was C_i = 200 mg/dm^3 at the initial pH 3.0. The obtained results are shown in Table 2.

As can be seen, the percentage of adsorption of copper ions depends on the contact time between zeolite and solution and it is rising rapidly in the first 5 minutes, after which the value remains relatively small. This could be explained by the high initial concentration of Cu^{2+} ions and the high concentration of easily accessible active sites on the surface of zeolite.

Table 2. The effect of the time contact between zeolite and solution on the efficiency of clinoptilolite for the removal of Cu^{2+} ions

Time (min)	5	10	15	30	60	90	120
AD, %	25.02	25.19	26.61	27.19	28.07	31.73	30.5

Further, the influence of initial pH value of the solution on the adsorption capacity of clinoptilolite was examined. The pH value was varied from 2.0 to 5.0 at initial concentration of solution C_i = 200 mg/dm^3 (Table 3). The contact time was 60 minutes. In general, at very low pH value (pH 2), the adsorption capacity is lower in comparison with the capacity at higher pH values.

This could be explained by the high concentration of H^+ ions that compete with ions of heavy metals to occupy the same alternating positions [14, 15]. Also, the percentage of adsorption of copper ions has increasing trend with increase the initial pH value of solution which is in agreement with literature [16, 17].

Table 3. The effect of initial pH value on the efficiency of clinoptilolite for the removal of Cu^{2+} ions

pH	2.0	3.0	4.0	4.5	5.0
q_e, mg/g	0.31	2.85	4.80	5.11	5.14
AD, %	2.98	28.18	47.47	50.76	50.87

According to the Panayotova et al. [8], the particle size of zeolite sample and the initial concentration of solution have influence on the adsorption degree (Table 4). Having this in mind, it was investigated how the change of initial concentration affects the percentage of adsorption and adsorption capacity for Cu^{2+} ions. The pH value of investigated solutions was 3.5.

Based on the obtained results shown in Table 5, it can be concluded that the capacity and the percentage of adsorption depend on the initial concentration of the copper ions in the investigating solution. As concentration of Cu^{2+} ions in the solution increases, the adsorption capacity increases while the percentage of adsorption decreases.

Table 4. The effect of particle size of zeolite sample and the effect of initial concentration of solution on the percentage of adsorption of copper ions [8]

Particle size of zeolite (mm)	AD, % (C_i = 10 mg/dm^3)	AD, % (C_i = 50 mg/dm^3)
< 0.09	89.34	73.89
0.09 – 0.325	82.64	56.90
0.325 – 0.400	78.33	41.04

Table 5. The effect of initial concentration on adsorption capacity and the percentage of adsorption of Cu^{2+} ions

C_i, g/dm^3	1026.85	775.95	525.64	266.57	101.19	58.46	34.96
C_t, g/dm^3	910.40	674.38	423.83	181.16	48.54	21.84	12.84
q_e, mg/g	5.82	5.08	5.09	4.27	2.63	1.83	1.11
AD,%	11.34	13.09	19.37	32.04	52.03	62.63	63.27

CONCLUSION

According to the presented results, in acidic solution (pH 2) the percentage of adsorption of copper ions is very low due to the high concentration of H^+ ions in the solution that tend to occupy some of the exchangeable sites in the clinoptilolite structure. At higher pH value (pH 3), the adsorption process is very rapid in the first 5 minutes due to the large surface area of the sample, or a large number of readily available exchangeable sites, after which the increase in the adsorption capacity is relatively small. Also, the capacity and the percentage of adsorption of copper ions depend on the initial concentration of the copper ions in the solution. It can be concluded that the natural zeolite clinoptilolite is a very interesting adsorbent for the removal of heavy metals ions from aqueous solutions. Clinoptilolite is considered as a low cost and widely available natural raw material whose application is economically more favorable than some other adsorbents.

Acknowledgements

The authors gratefully acknowledge financial support from the Ministry of Education, Science and Technological Development of the Republic of Serbia through the Project No 172031.

References

1. Masindi V., Gitari W.M., (2015) Simultaneous removal of metal species from acidic aqueous solutions using cryptocrystalline magnesite/bentonite clay composite: an experimental and modelling approach, Journal of Cleaner Production 39, 1-9,
2. Kaparapu J., Narasimha Rao G.M., Prasad M.K., (2015) Marine algae as bio-sorbents, Journal of Algal Biomass Utilization 63, 16-19,
3. Malamis S., Katsou E., (2013) A review on zinc and nickel adsorption on natural and modified zeolite, bentonite and vermiculite: Examination of process parameters, kinetics and isotherms, Journal of Hazardous Materials 252–253, 428–461,

4. Bilal M., Ali Shah J., Ashfaq T., Gardazi S.M.H., Tahir A.A., Pervez A., Haroon H., Mahmood Q., (2013) Waste biomass adsorbents for copper removal from industrial wastewater—A review, Journal of Hazardous Materials 263, 322–333,
5. Barakat M.A., (2011) New trends in removing heavy metals from industrial wastewater, Arabian Journal of Chemistry 4, 361–377,
6. Li Y., Li L., Yu J., (2017) Applications of zeolites in sustainable chemistry, Chem 3(6), 928–949,
7. Wang S., Peng Y., (2010) Natural zeolites as effective adsorbents in water and wastewater treatment, Chemical Engineering Journal 156, 11–24,
8. Panayotova M.I., (2001) Kinetics and thermodynamics of copper ions removal from wastewater by use of zeolite, Waste Management 21, 671–676,
9. Inglezakis J., Loizidou M.D., Grigoropoulou H.P., (2002) Equilibrium and Kinetic Ion Exchange Studies of Pb^{2+}, Cr^{3+}, Fe^{3+} and Cu^{2+} on Natural Clinoptilolite, Water Research 36, 2784–2792,
10. Alvarez-Ayuso E., García-Sánchez A., Querol X., (2003) Purification of Metal Electroplating Waste Waters Using Zeolites, Water Research 37, 4855–4862,
11. Jha V.K., Nagae M., Matsuda M., Miyake M., (2009) Zeolite Formation from Coal Fly Ash and Heavy Metal Ion Removal Characteristics Of thus Obtained Zeolite X in Multi-Metal Systems, Journal of Environmental Management 90, 2507–2514,
12. Mishra T., Tiwari S.K., (2006) Studies on Sorption Properties of Zeolite Derived from Indian Fly Ash, Journal of Hazardous Materials 137, 299–303,
13. Hui K.S., Chao C.Y.H., Kot S.C., (2005) Removal of Mixed Heavy Metal Ions in Wastewater by Zeolite 4A and Residual Products from Recycled Coal Fly Ash, Journal of Hazardous Materials 127, 89–101,
14. Inglezakis V.J., Hadjiandreou K.J., Loizidou M.D., Grigoropoulou H.P., (2001) Pretreatment of natural clinoptilolite in a laboratory-scale ion exchange packed bed, Water Research 35, 2161–2166,
15. Cabrera C., Gabaldón C., Marzal P., (2005) Sorption characteristics of heavy metal ions by a natural zeolite, Journal of Chemical Technology and Biotechnology 80, 477–481,
16. Bogdanović G., Stanković V., Antić D., Prodanović S., Andrić Lj., Vagner D., (2013) Adsorption of copper and zinc ions from acid mine drainage by natural zeolite, Proceedings of the XV Balkan Mineral Processing Congress, Volume II, Sozopol, Bulgaria, June 12-16, pp. 989-993,
17. Cabrera C., Gabaldon C., Marzal P., (2005) Sorption characteristics of heavy metal ions by a natural zeolite. Journal of Chemical Technology and Biotechnology 80, 477–481.

XIII International Mineral Processing and Recycling Conference
Belgrade, Serbia, 8-10 May 2019

University of Belgrade, Technical Faculty in Bor
Vojske Jugoslavije 12, 19210 Bor, Serbia
Tel. +381 30 424 555 Fax +381 30 421 078

COLORING PERFORMANCE OF IRON OXIDE NANOPIGMENTS PREPARED FROM A SYNTHETIC ACID MINE DRAINAGE

Ecehan Aygül Gönül [1, #], Alican Mert [2], Birgül Benli [3]
[1]Istanbul Bilgi University, Schools of Applied Sciences, Fashion Design Dept., Turkey
[2]Istanbul Technical University, Nano-Sci. & Nano-Eng. Graduate Program, Turkey
[3]Istanbul Technical University, Mineral Processing Engineering Dept., Turkey

ABSTRACT – In this study, iron-oxide based pigments of varying colors and magnetic properties were investigated. To increase their stability, in-situ synthesis was examined with 3 % of clays (sepiolite and halloysite). Clay added samples' magnetic properties were slightly reduced and their colors varied to higher Chroma brown according to RGB and Munsell Color Charts. Lightness and blue–yellow color of clay filler added particles were reached to tripled-fold at 200 °C and from RGB = 38.9/26/20 to 120/59.9/0.03 for halloysite and 105/57/6 for sepiolite than iron-oxide pigments. This is of importance to resolve limited pallets to optimize the coloring parameters and to discover new ceramic pigments.

Key words: nanopigment, iron oxide, clay, natural pigment, RGB color charts.

INTRODUCTION

Acid mine drainage (AMD) is one of the most important sources of extracting iron contaminants in usable forms, especially iron oxides that have utmost potential for the production of industrial inorganic pigments. The most commonly mined ore of copper,chalcopyrite is itself a copper-iron-sulfide that occurs with a range of other sulfides. However even with their high potential, AMD is also a common problem at thousands of abandoned mine sites all over the world.

Figure 1 shows the natural colour of water that comes from various types of mines including those that are still active including coal and metal mines also those that are old and abandoned. These colours have myriad hues and can be influenced by other metals that it is in solution with.

AMD is caused by the dissolution of minerals such as iron disulphide (FeS_2), commonly known as pyrite, by water and oxygen (Singer and Stumm, 1970). When pyrite is exposed to water and oxygen, oxidation and hydrolysis reactions produce sulfuric acid (H_2SO_4) and free hydrogen ions (H^+), acidifying the water. The combination of low pH and high concentrations of metals associated with drainage solutions can have severe toxicological effects on aquatic ecosystems [1]. Lower

corresponding author: ecehangonul@gmail.com

acidities allow other metals which are associated with mining, such as cadmium, copper, lead and zinc, to diffuse the solution phase and be transported from the system [2]. These metals precipitate from the solution when pH increases, however the pH at which there is a potential for complete precipitation varies for different metals.

Figure 1. Acid mine drainage

Clays are minerals that have formed over long periods of time as a result of chemical weathering of rocks, usually silicate-bearing, by low concentrations of carbonic acid and other diluted solvents.

Clay minerals and iron oxides have always been intimately related in the process of their formation. Their mineralogical composition and physical properties correspond to the physical-chemical conditions of weathering, sedimentation and alteration proccesses by means of which these minerals are associated. These clay materials were adopted early on in human history as mineral/earth pigments. One of the best examples of such material is the Maya Blue, an unusual blue pigment used on pottery, sculpture and murals from the Preclassic to the Colonial period in Maya civilization. It is a combination of indigo and the unusual clay mineral palygorskite (also called attapulgite).

Natural iron-rich oxides provided red,yellow and brown paints and dyes for a wide range of prehistoric uses including rock art paintings, pottery, wall paintings, cave arts and tattoos. Amongts these shades of colours Ochre is the earliest known pigment known, dates as back as 75,000 years.

Figure 2. Image of a horse colored with yellow ochre (17,300 BC) from Lascaux cave, France

In this study various types of color systems were studied on to analyze the color data. The systems primarily used were the Munsell Color Chart and the RGB Color Model. Hex Triplets were also used to name the colors.

Munsell Color Chart

The Munsell Color system is a color space that specifies colors based on three properties: hue, value(lightness) and chroma (color purity). It was created in the first decade of the 20th century and was adopted by the United States Department of Agriculture (USDA) as the official color system for soil research [4].

Figure 3. Munsell's color sphere, 1900. Later, Munsell discovered that if hue, value, and chroma were to be kept perceptually uniform, achievable surface colors could not be forced

Hue is measured by degrees around horizontal circles. Each horizontal circle is divided into five principals: Red, Yellow, Green, Blue and Purple, along with 5 intermediete hues that are between prinpical hues. Two colors of equal value and chroma that are on the opposite sides of a hue circle are called complementary colors and mix additively to the neutral gray of the same value.

Value or lightness is measured vertically on the core cylinder from 0 (black) to 10 (white).

Chroma is measured radially from the center of each slice, represents the "purity" of a color, with lesser chroma meaning less pure (more washed out). There are no upper limits to chroma, different areas of the color space have different maximal chroma coordinates. For instance light yellow colors have more potential chroma than light purples due to the nature of the eye and the physics of color stimuli.

RGB Color Model

RGB color model uses red,green and blue light together in various different ways to reproduce a variety of colors. The name of the model comes rom the initials of the three principal colors red,green and blue.

RGB color model is mainly used in electronic systems such as televisions and

computers, though has been known to be used in photography. RGB is a device-dependent color model meaning different devices detect or reproduce a given RGB value differently since the color elements like dyes or phosphors and their responses vary from manufacturer to manufacturer or sometimes even in the same device.

To form a color with RGB, three light beams must be superimposed. Each of these beams is called a component. These beams are added together and their light spectra add wavelength to make out the final color's spectra. Zero intensity for each component gives the darkest color whilst full intensity of each gives a white, if the intensities of the components are the same the result is a shade of grey, a colorized hue is reached if the intensities of the components differ from each other. The component with the strongest intensity gives the new hue its primary color(reddish,greenish or bluish). A secondary color is formed when two components have equal intensity. An example for such color is cyan which is a combination of green and blue.

Color coding using hexadecimal format

Web colors are used in displaying web pages on the World Wide Web and is a method for specifying colors. A color tool or other graphics software is often used to generate color values. Colors may be specified as an RGB triplet or in a hexadecimal format also called a hex triplet. A hex triplet is formed by having three bytes in hexadecimal notion in the order of red value, green value and blue value.

RGB values can be converted into hexadecimal format. Such conversion is a common feature of calculators including both hand-held models and software calculators.

EXPERIMENTAL

Materials

The natural Sepiolite and Halloysite samples were obtained from Tolsa, Ltd. and ESAN Ltd., Turkey. The clays prepared according to a previous study [3] used as the filler materials. Briefly, the clays were performed with the same procedure; gravity separation and deliberation with a high speed mixer during 2 minutes at 12,000 rpm, followed by centrifugation at 2,600 rpm, washing, and drying at 80 °C for 12 h.

Iron based synthetic concentrated iron based AMD solution was prepared from ferrous sulphate heptahydrate and ferric chloride hexahydrate salts (FeCl3.6H2O and $FeSO_4$.7H2O).

The reagent grade chemicals, such as $FeCl_3.6H_2O$, $FeSO_4.7H_2O$, NaOH and NH_4OH were used without any further purification.

Pure iron oxide synthesis

For hydrothermal synthesis of Fe_3O_4, prepared synthetic AMD solution were used as the ferric ion and ferrous ion source, respectively. The ferrous/ferric molar ratio was kept one for the synthesis of Fe_3O_4. In typical synthesis, the ferric and ferrous ions sources were dissolved in 100 mL of deionized water. 37.5 mL of NaOH (1 N) was dropped in the solution under constant stirring at 60 °C. Then 37.5 mL of NaOH (5 N) was slowly added in the solution and maintained for two hours. This method

was named as low-temp-syn and 60C coded. One-third of the solution was separated for the further color analysis. Followed by the second method, the obtained solution was placed into a autoclave with a Teflon liner. The autoclave was maintained at 200 °C for 24 h and defined as 200C code.

To improve the magnetic properties, another NH_4OH method was also examined. In this method, the ferric and ferrous ions sources were separately dissolved in 150 mL of deionized water under constant stirring at 40 °C during 1 h. Then, 30mL of NH_4OH (26 %) was dropped during 1 h and maintained at 60 °C for 2 h.

Subsequently, the autoclave was cooled naturally in air. The synthezed black precipitates were collected with a magnet from solution and washed with distilled water for several times and dried 200 °C (200C coded) for overnight and then 600 °C (600 coded) for 2 h.

In-situ synthesis of clay added iron oxide

The previous procedure of pure iron oxide synthesis was applied for the preparation of clay added composite particles. Each of sepiolite and halloysite were separately added in the preparation step of ferric chloride solution. Equal mass ratios were pre-calculated with the following quantities as 7.5 g of clay added for NaOH method and 3 g of clay for NH_4OH method.

RESULTS AND DISCUSSION

Figure 4 shows the wet separation process and the final drying step of iron oxide particles. When a support like sepiolite is present in the initial mixture, the pH value keeps stable. Magnetic properties were tested with two different high and low sensitivity magnets. Results were given in Table 1.

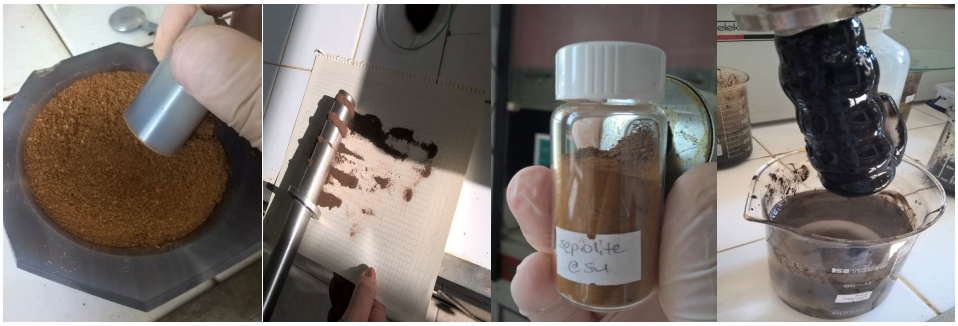

Figure 4. (Left) Dried pigment is milled and pulverized to test its magnetic properties, (right) separation of iron oxide from solution using a magnet

Sepiolite and halloysite, whilst sepiolite mixed pigments kept their magnetization, mixtures with halloysite showed no signs of magnetic sensitivity. This is due to the structure of sepiolite having a fibrous needle form, with a hollow channel in the direction of the fiber, which gives special adsorbant properties.

Noteworthy, mixtures with low magnetization, lead to higher Chroma brown colors according to RGB Color Chart and Hexadecimal numbers. The coloring of the

pigments became deeper as iron oxide levels increased and the color changed from a reddish earth tone to a deep black.

Table 1. Magnetic susceptibility testing of synthesized Fe-clays pigments

Sample	High	Low	Sample	High	Low
Pure Fe	+	+	Pure Fe	+	+
Fe- Sep	+	+	Fe- Hal	+	+
Fe- Sep, 200C	+	+	Fe- Hal, 200C	-	-
Fe- Sep, 600C	+	-	Fe- Hal, 600C	-	-
Fe- Sep in NH4, 200C	-	-	Fe- Hal in NH_4, 200C	-	-
Fe- Sep in NH4, 600C	+	-	Fe- Hal in NH_4, 600C	+	-

Figure 5. Hexadecimal numbers of the synthesized Fe-clays nanopigments

CONCLUSION

The RGB parameters state that the prepared pigments have excellent color property changing from a burnt orange to a deep black as the increasing content of iron oxide encapsulated in sepiolite and halloysite clays. These pigments with various different magnetic sensitivities could work with many advantages in safety, textile, art and architectural industries and environmental friendliness is suitable for preparing these pigments.

Acknowledgements:

The authors would like to acknowledge Istanbul Technical University, the Scientific Research Project (ITU-BAP, Project No. MGA-2018-41405) for their full financial support.

References

1. Gaikwad, R.W., Gupta, D. V. (2008) Review on removal of heavy metals from acid mine. Drainage Applied ecology and environmental research, 6 (3), 81 98,
2. Stumm, W., Morgan, J. J. (1996) Aquatic Chemistry: Chemical Equilibria and Rates in Natural Waters. 3rd Edition, John Wiley & Sons, Inc., New York, 1040,
3. Benli, B. (2014) Effects of humic acid release from sepiolite on the interfacial and rheological properties of alkaline dispersions. Applied Clay Science, 102, 1-7,
4. https://munsell.com/about-munsell-color/how-color-notation-works/how-to-read-color- chart/.

XIII International Mineral Processing and Recycling Conference
Belgrade, Serbia, 8-10 May 2019

University of Belgrade, Technical Faculty in Bor
Vojske Jugoslavije 12, 19210 Bor, Serbia
Tel. +381 30 424 555 Fax +381 30 421 078

REMOVAL OF OIL FROM WASTEWATER BY ANTHRACITE COAL

Jovica Sokolović [1, #], Branislav Stakić [2], Suzana Stanković [3], Vojka Gardić [3], Miloš Kirov [4]

[1]University of Belgrade, Technical Faculty in Bor, Bor, Serbia
[2]JPPEU Resavica, RA „Vrška Čuka“ Avramica, Grljan, Serbia
[3]Mining and Metallurgy Institute, Bor, Serbia
[4]JPPEU Resavica, RL „Lubnica“, Lubnica, Serbia

ABSTRACT – This paper is focused on the treatment of the oily wastewater by adsorption. For laboratory batch testing was used three different anthracite coal from Coal Mine Vrska Cuka and oily wastewater from Copper Mine Bor. Results show that anthracite as an adsorbent efficiently absorbs and removes oils and fats from the oily wastewater.

Key words: wastewater, oil, coal, anthracite, Vrska Cuka.

INTRODUCTION

Oily wastewater generated in a wide range of industries, such as petroleum refineries, chemical processing, mining and mineral processing and manufacturing plants. Water pollution by oil has left an undesired effect on the environment [1].

Oil, as common pollutant, causes water contamination in two forms, as free oil (a big issue) and emulsified oil (a real problem due to its stability in the aqueous phase) [2]. Removing oil from wastewater is an important aspect of pollution control. Various methods for oily wastewater treatment, including physical, biological, chemical, mechanical and physicochemical methods (i.e. flotation), and membrane processes have been developed [3, 4]. However, there are many limitations for those treatments, such as low efficiency, high operation cost, corrosion and recontamination, etc. [5].

Adsorption is the most convenient method for removing oil from oily waste water [6] and activated carbon (AC) was used widely as adsorbent for adsorption process [7]. Due to low efficiency and high cost of activated carbon for oily wastewater treatment [8], the possibility of using coal was explored by many researchers in the past years [9-11].

corresponding author: jsokolovic@tfbor.bg.ac.rs

The sorptive nature of bentonite and anthracite coal for some organic pollutants had been extensively studied [8-9]. It was reported that bentonite organo-clay/anthracite mixture containing 30 % granular organo-clay and 70 % anthracite were effective in removing oil from a number of oil-in-water emulsions. The obtained oil removal efficiencies were 72 to 98 % for various oil-in-water emulsions.

Simonovic et al. [10] were investigated the use of hard coal as an adsorbent for removal of mineral oil from wastewater. The results showed that anthracite is very efficiently absorbs and more than 99 % of mineral oil had been removed from the oily wastewater.

Recent studies of Li et al. [11] had also shown that coal type and particle size significantly affect the adsorption of oil from oily wastewater. The adsorption capacity of hard coal is much higher than that of brown coal and lignite for all size classes. The results indicate that the activation process increases the adsorption capacity of coal, too.

In this paper, different anthracite coal samples were used for experimental study of the removal oil from wastewater.

EXPERIMENTAL

Material

The anthracite coal sample was collected from the separation plant of the Anthracite Coal Mine "Vrska Cuka" Avramica in Serbia. Three types of anthracite coal samples were used as adsorbent to treat oily wastewater, such as: run-of-mine (ROM), fine coal (below 1 mm) and separated coal. All samples were collected from a coal preparation plant in Vrška Čuka. The as-received run-of-mine and separated anthracite coal samples were crushed, ground and sieved to 1 mm.

Sample of oily wastewater was taken from the Copper Mine Bor (RBB), which is a part of Zijin Bor Copper d.o.o. (formerly known as RTB Bor).

Coal analyses

Ultimate analyses of coal samples were determined by VARIO EL III CHNOS elementary analyzer.

Proximate analysis of coal determines the chemical composition of a coal sample. Calorific value of coal samples was determined by LECO AC 600. Determination of moisture, ash and volatile matter (thermo gravimetric analysis) was carried out with 701 LECO TGA.

The results of ultimate and proximate analyses of the dry coal samples are given in Tables 1 and 2.

Table 1. Ultimate analysis of the dry coal samples

Sample	Element (%)			
	C	H	N	S
Run-of-Mine coal	52.01	2.26	0.53	0.41
Fine coal	52.76	2.28	0.57	0.64
Separated coal	87.55	3.38	0.87	0.63

Table 2. Proximate analysis of the dry coal samples

Sample	Combustible matter (%)	Volatile matter (%)	Calorific value (KJ/kg)	Fixed carbon (%)	Ash content (%)
Run-of-Mine coal	60.22	12.91	20,350	47.31	39.78
Fine coal	61.37	13.60	20,868	47.77	38.63
Separated coal	95.31	13.04	34,828	82.27	4.69

Oily wastewater analyses

The chemical composition of oily wastewater is presented in table 3 [12].

Table 3. Chemical analyses of oily wastewater from the Copper Mine Bor

No.	Compound	Values	Unit
1.	Oil and grease	135.05	mg/L
2.	Chemical oxygen demand	141	mg/L
3.	Biochemical oxygen demand	-	mg/L
4.	Suspended solids	1.3	mg/L
5.	Nitrogen	< 5	mg/L
6.	Nitrite	0.15	mg/L
7.	Nitrate	4.1	mg/L
8.	Total phosphorus	0.56	mg/L
9.	Turbidity	20	NTU
10.	Color	10.9	m^{-1}
11.	Elements	-	-
11.1.	Al	0.0400	mg/L
11.2.	As	0.0207	mg/L
11.3.	B	3.4401	mg/L
11.4.	Ba	0.0155	mg/L
11.5.	Cd	0.0013	mg/L
11.6.	Cr	0.0022	mg/L
11.7.	Cu	0.0105	mg/L
11.8.	Fe	0.1149	mg/L
11.9.	Mn	0.0131	mg/L
11.10.	Ni	0.0033	mg/L
11.11.	Pb	0.0024	mg/L
11.12.	Se	0.0010	mg/L
11.13.	Zn	0.0368	mg/L

Chemical analyses of oily wastewater from the Copper Mine Bor showed that average oil concentration was 135.05 mg/L.

Adsorption tests

Adsorption studies were carried out with different anthracite coal samples by mixing anthracite coal with 100 mL of oily wastewater solution at known concentrations (135.05 mg/L). The ration of the solid - liquid system, contact time and pH value were investigated by Kirov [12]. Based on obtaining results, were adopted as the optimum parameters for these studies. The treated samples were

stirred with a magnetic stirrer (800 rpm) for 0.5 h of contact time at pH value 7.5 [12].

The treated samples were filtered through filter papers. The amount of oil removed was determined. Oils were extracted from the treated solution samples as final oil concentration according to the standard EPA method 1,664 using n-hexane as a solvent.

Based on the material balance, the adsorption capacity was calculated according to the expression:

$$q = (Co - C) \cdot V / m \quad (1)$$

where is:

q - mass of adsorbed oil per unit mass of adsorbent, (mg/g)
Co and C - initial and final concentration of oil in wastewater (respectively), (mg/L)
V - volume of solution, (L)
m - mass of adsorbents, (g).

The adsorption degree is calculated according to the expression:

$$A = ((Co-C) / Co) \cdot 100 \quad (2)$$

where is:

A - degree of adsorption (%).

RESULTS AND DISCUSSION

Results of adsorption tests of oily wastewater are shown in table 4 and figures 1-3.

Table 4. Results of adsorption tests of oily wastewater with different coal type

Anthracite coal sample	After adsorption		
	Oil concentration, C (mg/l)	Adsorption capacity, q (mg/g)	Adsorption degree, A (%)
Run-of-Mine coal	37	0.44	72.59
Fine coal	40	0.42	70.37
Separated coal	28	0.49	79.26

Based of obtained results, it can be seen that the degree of adsorption is higher when the adsorption process is performed by quality coal sampl. The degree of adsorption using the fine coal is 70.37 %, while for the same class using the separated coal the value of 79.26 %.

The results also show that separated caol achieve more efficient adosprtion results. The adsorption capacity was 10 to 15 % higher as compared with raw and fine coal samples. Obviously, the molecules of hydrocarbons from the oil much easier to adsorb and bind to the surfaces separated coal and the effects of treatment of oily water have been higher.

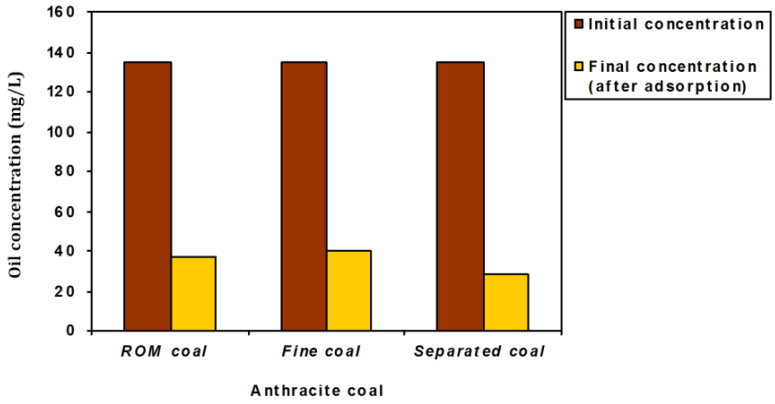

Figure 1. Effect of anthracite coal type on oil concentration

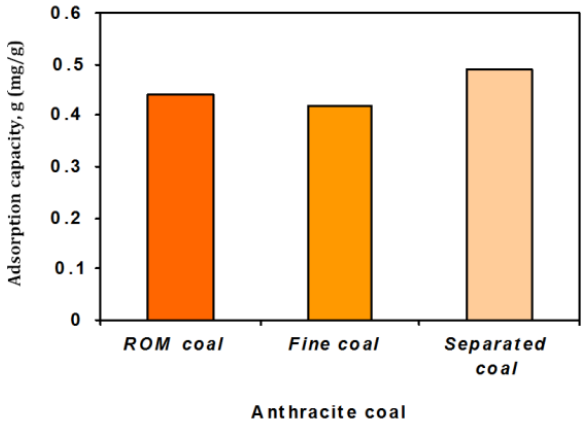

Figure 2. Effect of anthracite coal type on adsorption capacity

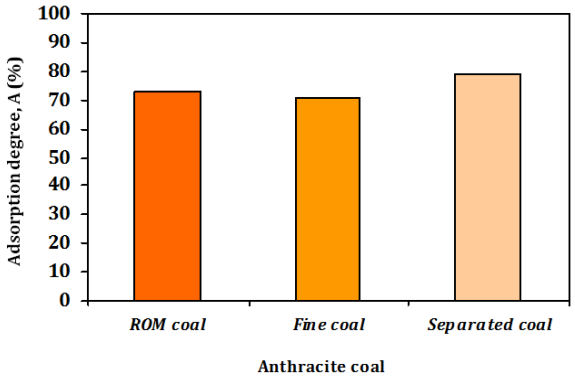

Figure 3. Effect of anthracite coal type on adsorption degree

The efficiency of removing of the oil from wastewater with fine class are satisfactory. Also, a price of fine coal (9,330.96 RSD/t) is several times lower than the prices of the separated coal (107,709.5 RSD/t) or other adsorption materials, so the effects of removal of oil from wastewater are greater.

CONCLUSION

On the basis of obtaining results, it can be concluded that the anthracite coal is an efficient adsorbing material for removing of oil from wastewater. The results show that the separated anthracite coal can produce the highest adsorption degree (79.26 %) compared with run-of-mine (ROM) and fine coal.

A final concentration of oil in the wastewater was 28 mg/L. Comparing the ratio of the coal products and the achieved adsorption results, it can be concluded that the best results of removing oil from wastewater are achieved with fine coal.

Acknowledgements:

This paper presents the results of the Projects TR 33007 and TR 33038 funded by the Ministry of Education, Science and Technological development of the Republic of Serbia. The authors are grateful to the Ministry for financial support.

References

1. Ibrahim, S., Wang, S., Ang, H. M. (2010) Removal of emulsified oil from oily wastewater using agricultural waste barley straw. Biochemical Engineering Journal, 49 (1), 78-83,
2. Nag, A. (1995) Utilization of charred sawdust as an adsorbent of dyes, toxic salts and oil from water. Process safety and environmental protection, 73 (4), 299-306,
3. Jamaly, S., Giwa, A., Hasan, S. W. (2015) Recent improvements in oily wastewater treatment: Progress, challenges, and future opportunities. Journal of Environmental Sciences, 37, 15-30,
4. Yu, L., Han, M., He, F. (2017) A review of treating oily wastewater. Arabian journal of chemistry, 10, S1913-S1922,
5. Zhou, Y. B., Tang, X. Y., Hu, X. M., Fritschi, S., Lu, J. (2008) Emulsified oily wastewater treatment using a hybrid-modified resin and activated carbon system. Separation and Purification Technology, 63 (2), 400-406,
6. Rajakovic, V., Aleksic, G., Radetic, M., Rajakovic, L. (2007) Efficiency of oil removal from real wastewater with different sorbent materials. Journal of Hazardous Materials, 143 (1-2), 494-499,
7. Pintor, A. M., Vilar, V. J., Botelho, C. M., Boaventura, R. A. (2016) Oil and grease removal from wastewaters: sorption treatment as an alternative to state-of-the-art technologies. A critical review. Chemical Engineering Journal, 297, 229-255,
8. Moazed, H., Viraraghavan, T. (2005) Removal of oil from water by bentonite organoclay. Practice Periodical of Hazardous, Toxic, and Radioactive Waste Management, 9 (2), 130-134,
9. Moazed, H., Viraraghavan, T. (2005) Use of organo-clay/anthracite mixture in the separation of oil from oily waters. Energy sources, 27 (1-2), 101-112,

10. Simonovic, B. R., Aranđelovic, D., Jovanovic, M., Kovacevic, B., Pezo, L., Jovanovic, A. (2009) Removal of mineral oil and wastewater pollutants using hard coal. Chemical Industry and Chemical Engineering Quarterly, 15 (2), 57-62,
11. Li, X., Zhang, C., Liu, J. (2010) Adsorption of oil from waste water by coal: characteristics and mechanism. Mining Science and Technology (China), 20 (5), 778-781,
12. Kirov, M. (2013) Treatment of oily wastewater from RTB Bor by fine class of coal from Coal Mine "Vrska Cuka" Avramica, B.Sc thesis, University of Belgrade, Technical faculty in Bor, Bor, Serbia.

XIII International Mineral Processing and Recycling Conference
Belgrade, Serbia, 8-10 May 2019

University of Belgrade, Technical Faculty in Bor
Vojske Jugoslavije 12, 19210 Bor, Serbia
Tel. +381 30 424 555 Fax +381 30 421 078

ADSORPTION ISOTHERMS FOR DESCRIBING THE MECHANISM OF COPPER IONS BIOSORPTION ONTO OAT STRAW

Dragana Božić [1,#], Milan Gorgievski [2], Velizar Stanković [2], Nada Štrbac [2], Vesna Grekulović [2], Miljan Marković [2]
[1]Mining and Metallurgy Institute Bor, Bor, Serbia
[2]University of Belgrade, Technical Faculty in Bor, Bor, Serbia

ABSTRACT – In this paper, Langmuir, Freundlich and Temkin adsorption isotherm model for the adsorption of copper ions onto oat straw were used to study the biosorption mechanism in batch conditions. The isotherm parameters were calculated from the linearized plots corresponding to each isotherm model. The Langmuir model fitted best the experimental data with $R^2 = 0.958$. According to Langmuir isotherm model, the biosorption process occurs until a complete monolayer of copper ions is formed on the surface of the oat straw. According to this model, the maximum adsorption capacity was 4.42 mg/g.

Key words: adsorption isotherms, copper ions, oat straw, biosorption, adsorption capacity

INTRODUCTION

Many industries, such as metallurgy processing plants, metal finishing plants, electronic industry, electroplating, phytopharmaceutical plants, and many others, release heavy metals along with their wastewaters, polluting the environment [1].

Heavy metals can be removed from wastewaters by conventional methods, such as: chemical precipitation, cementation, ion exchange, solvent extraction, etc., but these methods don't always give satisfactory results in terms of: insufficient degree of metal ions removal, formation of significant amounts of sludge that needs further processing, the need for excessive amounts of chemicals consumed in the process, and high costs. Due to the tendency of every industrial process to be more economical and efficient, biosorption is being investigated as one of the alternatives to conventional technologies for wastewater treatment, especially those with low heavy metal ions content [2, 3].

Many biological waste materials, such as fungi, algae, peat, yeasts and different agricultural wastes have been tested as potential adsorbents for heavy metal ions adsorption from water solutions [4].

Adsorption isotherms are used to obtain information about the mechanism of the

[#] corresponding author: dragana.bozic@irmbor.co.rs

adsorption process, and the maximum adsorption capacity. Empirical isotherm models can be used for describing the behavior of the biosorption process, and to find the maximum adsorption capacity [5, 6].

There are several adsorption models isotherm models that are usually used in relevant literature to describe the adsorption equilibrium, such as: Langmuir, Freundlich, Elovich, Temkin, Fowler-Guggenheim, Kiselev, and Hill-de Boer model [6].

In this paper, Langmuir, Freundlich and Temkin isotherm models were used for modeling the experimental results of Cu^{2+} ions biosorption onto oat straw.

EXPERIMENTAL METHOD

Adsorption isotherms data was obtained by performing the following experiment: 0.5 g of oat straw was brought into a contact with 50 ml of synthetic solutions containing different initial concentrations of copper ions, ranging from 5 to 200 mg/dm^3. The suspension was stirred by a magnetic stirrer for 60 min, considering it as a process time long enough to reach the equilibrium between phases [2]. The suspension was then filtered and the filtrate was analyzed on the residual amount of copper ions.

RESULTS AND DISCUSSION

Adsorption isotherm for copper ions biosorption onto oat straw

The obtained experimental adsorption isotherm data for copper ions biosorption onto oat straw is shown on Fig. 1.

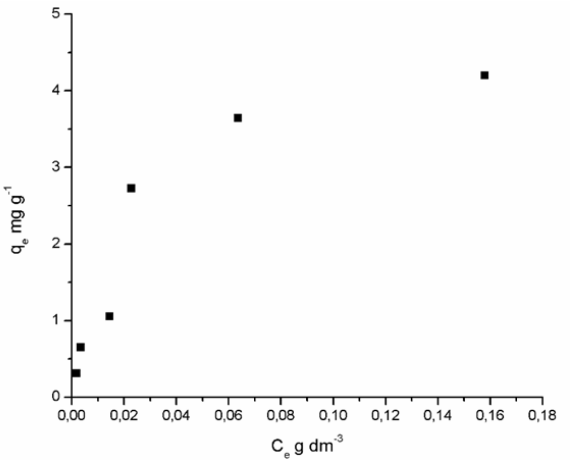

Figure 1. Adsorption isotherm for the copper ions biosorption onto oat straw

Langmuir model

Langmuir model was implemented theoretically assuming that the adsorption occurs in a monolayer, at a finite number of definite localized sites [7].

The Langmuir isotherm can be written by the following equation:

$$q_e = \frac{q_m K_L C_e}{1 + K_L C_e} \tag{1}$$

Linearisation of Eq. (1) the following equation is obtained:

$$C_e / q_e = \frac{1}{K_L q_m} + \frac{1}{q_m} C_e \tag{2}$$

where C_e is the equilibrium concentration of metal ions (mg/dm^3), q_e is the equilibrium adsorption capacity (mg/g), q_m is the maximum adsorption capacity (mg/g) and K_L (dm^3/g) is the Langmuir equilibrium constant.

Graphical dependence of C_e/q_e in function of C_e gives the straight-line with the slope $1/q_m$ and the intercept $1/K_L q_m$.

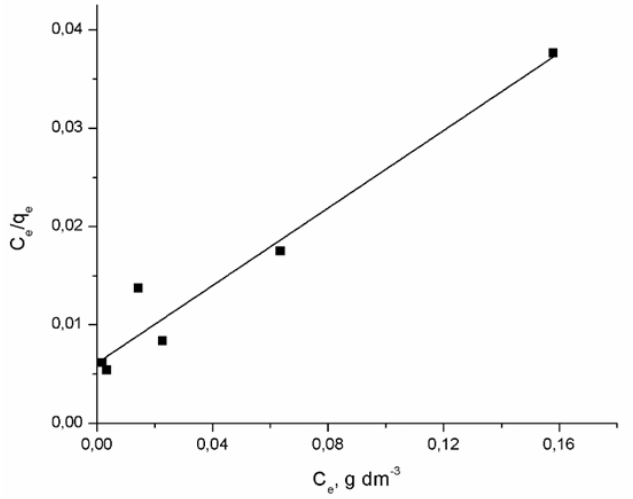

Figure 2. Langmuir adsorption isotherm model

Freundlich model

This model represents the earliest known relationship that describes the non-ideal and reversible adsorption. It can be applied to multilayer adsorption [7].

This model is represented by the following equation:

$$q_e = K_f C_e^{1/n} \tag{3}$$

Linear form of Eq. (3) is given as:

$$\log q_e = \log K_F + \frac{1}{n} \log C_e \tag{4}$$

where C_e is the equilibrium concentration of copper ions in the solution (mg/dm^3); q_e is the adsorbent capacity defined as mass of the adsorbed metal per unit mass of

the adsorbent (mg/g) at equilibrium; K_F is the Freundlich equilibrium constant ((mg/g) $(dm^3/mg)^{1/n}$), and $1/n$ is the coefficient of heterogeneity in the Freundlich adsorption isotherm equation.

Graphical dependence of $log\ q_e$ in function of $log\ C_e$ gives the straight line, with the slope $1/n$ and the intercept K_F.

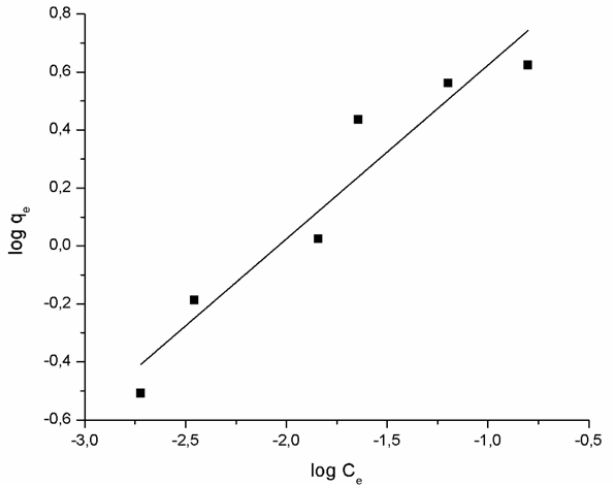

Figure 3. Freundlich adsorption isotherm model

Temkin model

This model was derived from the following assumptions: (1) the heat of sorption of all molecules linearly decreases with the coverage of the adsorbent, which is conditioned by adsorbent-adsorbate interactions, and (2) there is a uniform distribution of binding energies up to some maximum binding energy [5].

Temkin isotherm model is represented by the following equation:

$$q_e = B \ln\left(K_T C_e\right) \tag{5}$$

Linear form of the Eq. (5) is given as:

$$q_e = B \ln K_T + B \ln C_e \tag{6}$$

where $B = RT/b$ is the Temkin constant, which refers to the adsorption heat (J/mol); b is the variation of adsorption energy (J/mol); R is the universal gas constant (J/mol K); T is the temperature (K); K_T is the Temkin equilibrium constant (dm^3/g); q_e is the adsorption capacity defined as mass of the adsorbed metal per unit mass of the adsorbent (mg/g) at equilibrium; C_e is the equilibrium concentration of copper ions in the solution (mg/dm^3). Constants B and K_T can be determined from the graph $q_e = f(lnC_e)$, where B is the slope, and K_T the intercept.

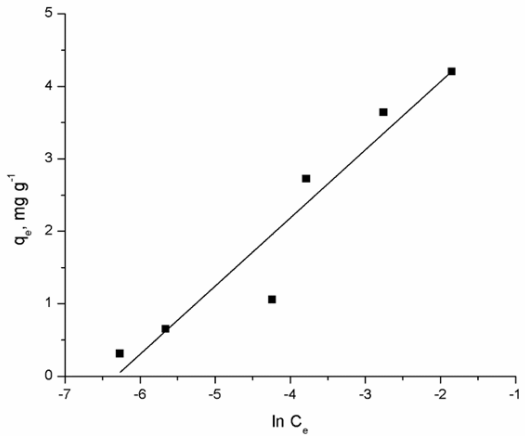

Figure 4. Temkin adsorption isotherm model

The obtained experimental data, shown on Fig. 1, was fitted using Langmuir, Freundlich and Temkin adsorption isotherm models. Equilibrium parameters for the considered models were determined using the Eqs. (2), (4) and (6), and, along with the correlation coefficients R^2, are given in Table 1.

Table 1. Obtained parameters for Langmuir, Freundlich and Temkin adsorption isotherm models for copper ions biosorption on to oat straw

Langmuir				**Freundlich**			**Temkin**		
K_L dm^3/mg	q_{exp} mg/g	q_m mg/g	R^2	K_F	1/n	R^2	B J/mol	K_T dm^3/g	R^2
32.14	4.42	5.1	0.958	16.72	1.67	0.923	0.94	5.94	0.92

According to the correlation coefficient values R^2 in Table 1, it can be seen that the experimental data can be well described by the Langmuir isotherm model rather than the Freundlich and Temkin one. Also, based on the data given in Table 1, for theoretically and experimentally obtained maximum adsorption capacity for the copper ions, determined by the Langmuir adsorption isotherm model, it can be seen that the values are approximately equal, which suggests that the oat straw is almost completely saturated, and all of the active sites were occupied by the copper ions. This means that the surface of the adsorbent is homogenous, and the biosorption of copper ions onto oat straw occurs mostly in a monolayer [8, 9].

CONCLUSION

Oat straw was used as a biosorbent for copper ions adsorption from synthetic water solutions. The adsorption equilibrium data were analysed with Langmuir, Freundlich and Temkin adsorption isotherm models. Obtained results indicate that the Langmuir model shows the best correlation to the analysed data, with the correlation coefficient R^2=0.958, meaning that the biosorption process occurs mostly in a monolayer.

References

1. Perez-Lopez, R., Nieto, J.M., Almodovar, G.R. (2007) Immobilization of toxic elements in mine residues derived from mining activities in the Iberian Pyrite Belt (SW Spain): laboratory experiments. Applied Geochemistry, 22(9), 1919-1935,
2. Gorgievski, M., Božić, D., Stanković, V., Štrbac, N., & Šerbula, S. (2013) Kinetics, equilibrium and mechanism of Cu^{2+}, Ni^{2+} and Zn^{2+} ions biosorption using wheat straw. Ecological engineering, 58, 113-122,
3. Veglio, F., Beolchini, F. (1997) Removal of metals by biosorption: a review. Hydrometallurgy, 44(3), 301-316,
4. Nemes, L.N., Bulgariu, L. (2016) Optimization of process parameters for heavy metals biosorption onto mustard waste biomass. Open Chemistry, 14(1), 175-187,
5. Hamdaoui, O., Naffrechoux, E. (2007) Modeling of adsorption isotherms of phenol and chlorophenols onto granular activated carbon: Part I. Two-parameter models and equations allowing determination of thermodynamic parameters. Journal of hazardous materials, 147(1-2), 381-394,
6. Mohammed-Ridha, M.J., Ahmed, A.S., Raoof, N.N. (2017) Investigation of The Thermodynamic, Kinetic and Equilibrium Parameters of Batch Biosorption of Pb (II), Cu (II), And Ni (II) From Aqueous Phase using Low Cost Biosorbent. Al-Nahrain Journal for Engineering Sciences, 20(1), 298-310,
7. Chen, X. (2015) Modeling of experimental adsorption isotherm data. Information, 6(1), 14-22,
8. Murithi, G., Onindo, C.O., & Muthakia, G.K. (2012) Kinetic and equilibrium study for the sorption of Pb (II) ions from aqueous phase by water hyacinth (*Eichhornia crassipes*). Bulletin of the Chemical Society of Ethiopia, 26(2), 181-193,
9. Petrović M.S. Heavy Metals Removal From Aqueous Solutions by Corn Waste Biomass (*Zea mays*L.), Doctoral Dissertation, University of Belgrade, Faculty of Technology and Metallurgy.

XIII International Mineral Processing and Recycling Conference
Belgrade, Serbia, 8-10 May 2019

University of Belgrade, Technical Faculty in Bor
Vojske Jugoslavije 12, 19210 Bor, Serbia
Tel. +381 30 424 555 Fax +381 30 421 078

ZINC AND STRONTIUM REMOVAL EFFICIENCY BY THERMALLY MODIFIED SEASHELL WASTE

Ivana Smičiklas [#], Marija Egerić, Mihajlo Jović, Marija Šljivić-Ivanović, Ana Mraković
University of Belgrade, Vinča Institute of Nuclear Sciences, Belgrade, Serbia

ABSTRACT – The efficiency of thermally modified marine seashells in the separation of Zn and Sr cations was investigated, as a way to valorize and utilize carbonate-rich seafood industry waste. Crushed seashells were heated at different temperatures (300 - 900 °C) and exposed to 0.01 mol/L metal solutions. The percentage of Zn removal increased up to 99.7 % with the increase in temperature, whereas Sr removal gained a maximum of 42.2 % after contact with the specimen heated at 500 °C. Removal efficiency was analyzed in line with the temperature induced transformations of seashells mineral matrix, solution pH values, and Ca concentrations. As revealed by X-ray diffraction analysis, optimal removal of Sr and Zn achieved using pure calcite and pure calcium oxide samples, respectively, was principally a result of the precipitation mechanism.

Key words: seashell waste, temperature treatments, water treatment, Zn, Sr.

INTRODUCTION

Natural limestone is a mineral with immense utilization as an essential component or a raw material for the production of construction materials, ceramics, glass, paper, plastic, rubber, paints, pharmaceuticals, etc. [1]. Furthermore, as an alkaline material with sorption/precipitation properties, it is frequently utilized in water treatment and soil remediation. Given that contemporary society is facing the depletion of non-renewable mineral resources and simultaneously generates vast amounts of solid waste, development of technologies that exploit carbonate-rich waste materials as a secondary resource is a concept that brings multiple benefits.

A typical example of a bio-waste that could be valorized owing to a high content of calcium carbonate is the seashell material of marine mollusks. Empty seashells are identified as a major solid waste arising from a rapidly growing fishery industry, and the research on their applicability aims at reducing ecological problems in coastal areas caused by excessive accumulation [2]. To this point, seashells were successfully utilized in soil treatment, animal feed production, neutralization of acid mine drainage and the production of construction materials [3-5]. Recent studies have also revealed the ability of seashell material to separate a variety of heavy metals and

[#] corresponding author: ivanat@vinca.rs

radionuclide ions from the aqueous phase [6-8]. The thermal treatments contribute to the combustion of the organic phase present in the seashell material (<5 % w/w), which mitigates the issues associated with seashell storage and use. Furthermore, enhanced removal of Hg and Cu cations [9, 10], as well as of phosphate anions [11], was detected after proper thermal treatment of seashells.

In the present study, the influence of temperature treatments onto seashell waste ability to separate Zn and Sr ions from aqueous media was investigated, to consider the prospects of using seafood industry waste instead of traditional agents – natural limestone and lime. The Zn was chosen as a representative heavy metal commonly found in industrial wastewaters, whereas radioactive ^{90}Sr is a human-made contaminant found in liquid radioactive waste and natural waters after nuclear accidents.

MATERIALS AND METHODS

The seashell waste (SW) used in the study was a composite sample collected at the North Greek Aegean Sea coast in 2016, comprised of several bivalvia species [8]. The soluble impurities and sand particles were removed by rinsing the shells with hot water. Cleaned shells were dried at 50 °C, ground in the laboratory mill and the fraction with a particle size < 1 mm was used in further experiments. Thermally treated samples were produced by heating the SW in the electrical furnace for 4 h at the constant temperature in the range 300-900 °C. The obtained powders were correspondingly denoted as SW300 - SW900.

Temperature-induced alteration of SW capacity to separate metal ions was studied in the batch conditions, at room temperature (21 ± 2 °C). Working solutions of 0.01 mol/L Zn and Sr cation were prepared from their nitrate salts ($Zn(NO_3)_2 \times 6H_2O$ and $Sr(NO_3)_2$, Fisher Scientific) and deionized water. The initial pH of both Sr and Zn solutions were adjusted to 5.0 ± 0.1 using 0.01 mol/L solutions of either NaOH or HNO_3. SW or SW300 - SW900 samples (0.1 g) were mixed with 20 mL of metal solutions in 50 mL centrifuge tubes, and suspensions were agitated for 24 h at 10 rpm using the Reax 20 Heidolph overhead laboratory shaker. After 24 h of contact, liquid phases were separated from the solid using Heraeus Megafuge 16, set at 9000 rpm for 10 minutes.

Residual concentrations of Zn and Sr, as well as the amounts of Ca ions released from the seashell material, were determined by Perkin Elmer 3100 Atomic Absorption Spectrophotometer, while the final pH values were measured by InoLab WTW pH meter. Metal removal experiments were performed in duplicate. Selected solid residues which showed the highest percentage of removed Zn or Sr ions (SW900-Zn and SW500-Sr) were additionally analyzed by X-ray diffraction (XRD) within 10-60 2θ range on the Rigaku Smartlab SAXS diffractometer.

RESULTS AND DISCUSSION

Treatments of SW have affected the cation removal efficiency to a great extent, and the removal patterns were quite different for the two investigated cations (Fig. 1). Separation of Zn ions was generally higher compared to the Sr removal efficiency, in agreement with the behavior of raw SW. Namely, the study of SW selectivity towards various divalent cations has disclosed the highest removal capacity of Zn

ions in comparison to Sr, Cu and Pb [8]. Furthermore, Zn removal continuously increased with the increase in temperature, from 79.9 % using SW300 to even 99.7 % using SW900. On the other hand, Sr removal exhibited an increase from 22.2 % to 42.2 % using samples SW300 - SW500. A slight decrease in process efficiency was observed using specimen heated at 600 °C, whereas the increase in temperature above 600 °C resulted in the abrupt decline in Sr removal.

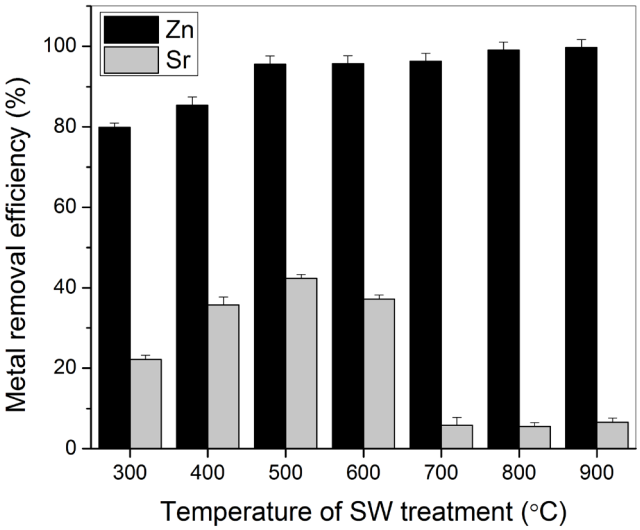

Figure 1. Effect of SW temperature treatments onto Zn and Sr removal efficiency

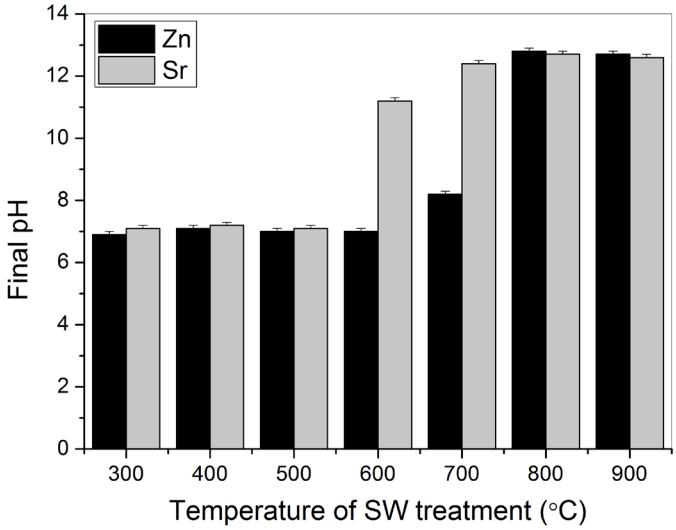

Figure 2. Final pH values of the Sr and Zn solution after interaction with temperature treated SW particles

The contact of variously treated SW samples and metal-containing solutions was accompanied by the solution pH changes and the variations in the amounts Ca ions released from the seashell material (Fig. 2 and Fig. 3). Equilibrium pH values were commonly in the neutral range after mixing both metal solutions with SW300 - SW500 samples, while the increase in solution pH was associated with the further rise in temperature. The amounts of released Ca ions were higher in Zn solutions (Fig. 3b) than in Sr solution (Fig. 3a), in line with higher removal rates of Zn. Actually, molar ratio between removed and released cations was practically 1:1 in the wide range of temperatures (300 – 600 °C), whereas using SW samples calcined at T ≥ 700 °C the solubility of the SW residues increased and the amounts of released Ca exceeded the amounts of removed Sr or Zn ions.

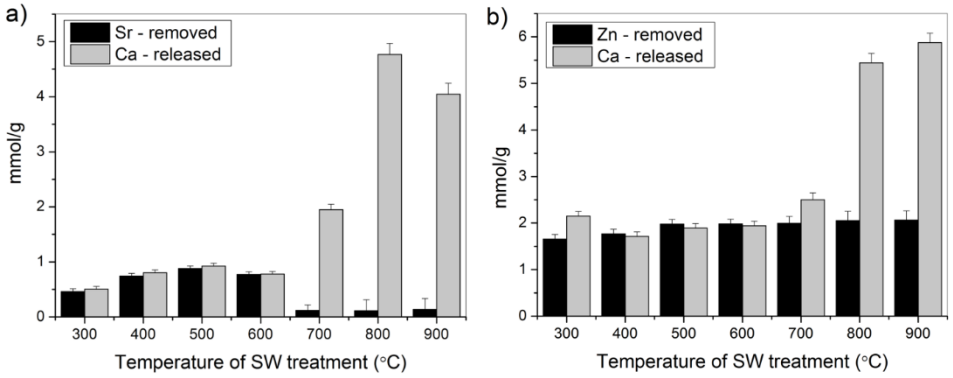

Figure 3. Amounts of Ca ions released and metal cations removed after interaction of temperature treated SW particles with Sr-solution (a) and Zn-solution (b)

The variations in SW potential to separate the investigated cations from the solution can be explained based on the temperature-induced changes in SW properties. Raw SW sample was composed of calcium carbonate in the form of aragonite [8]. As revealed by previous XRD analysis, the transformation of SW mineral matrix occurs in several stages [10]: (i) between 300 °C and 400 °C aragonite is being transformed into more stable calcite polymorph, (ii) in the range 700 °C – 800 °C the diffraction maximums of lime (CaO) appear in addition to calcite peaks, and finally (iii) at 900 °C the calcite decomposition process is completed giving pure CaO. Based on the thermogravimetric analysis, the weight loss of 3.3 % detected up to 600 °C was associated with the loss of the organic phase.

Consequently, removal of Zn and Sr accompanied with the release of equimolar Ca amounts is characteristic for all treated SW samples that retained carbonate structure of either aragonite or calcite polymorph, whereas increased removal of Zn and reduced removal of Sr coincide with the $CaCO_3$ conversion to CaO. As the reaction of CaO with water results in the pH increase, the hydrolysis and the precipitation of Zn ions contribute to its efficient removal. Quite the opposite, Sr ions do not hydrolyze in observed pH range and the increase in CaO content and concentrations of dissolved Ca ions in the SW samples calcined at T ≥ 700 °C inhibited Sr removal. Due to the chemical similarity between the two cations, a strong competing effect of Ca on Sr removal was observed using different inorganic materials [12].

Depending on the composition of raw seashells, their pretreatment history, initial concentration of metals in the solution and other experimental conditions, removal of cationic pollutants such as Pb, Cu, Cd, Zn, Hg, Sr, etc. was found to be governed by several operating mechanisms, such as adsorption, ion exchange, coprecipitation, precipitation, etc. [6-10]. To detect the mineral phase changes induced by Zn and Sr removal, temperature treated SW samples which exhibited maximum removal efficiency were analyzed by XRD. The results implied that the precipitation mechanism governs the metal removal by the temperature activated SW (Fig. 4). The main crystalline phase in system SW900-Zn was portlandite ($Ca(OH)_2$). The appearance of calcite peaks may be explained by the reaction of Ca(OH)2 with atmospheric CO_2. Formation of portlandite and calcite in the presence of Zn ions may be the mode of metal incorporation into the solid phase. Besides, new Zn-containing crystalline product was identified - calcium hexahydroxodizincate dihydrate ($CaZn_2(OH)_6 \times 2H_2O$).

SW500 sample after exposure to Sr-solution was analyzed to consider the role of calcite phase in the sequestering mechanism (Fig. 4). Although Sr retention by adsorption, ion-exchange and solid-solution formation cannot be excluded, incorporation of Sr in a new discrete crystalline phase - strontianite ($SrCO_3$) was identified. The same reaction product was detected after interaction of raw SW with Sr-solution [8], therefore, at the applied initial concentration of Sr, utilization of both aragonite and calcite polymorphs lead to the precipitation of strontianite. The highest removal efficiency of SW treated at 500 °C in respect to other carbonate-based SW samples (i.e., SW300, SW400, and SW600) may be connected with the organic phase exclusion and increased reactivity of the remaining solid.

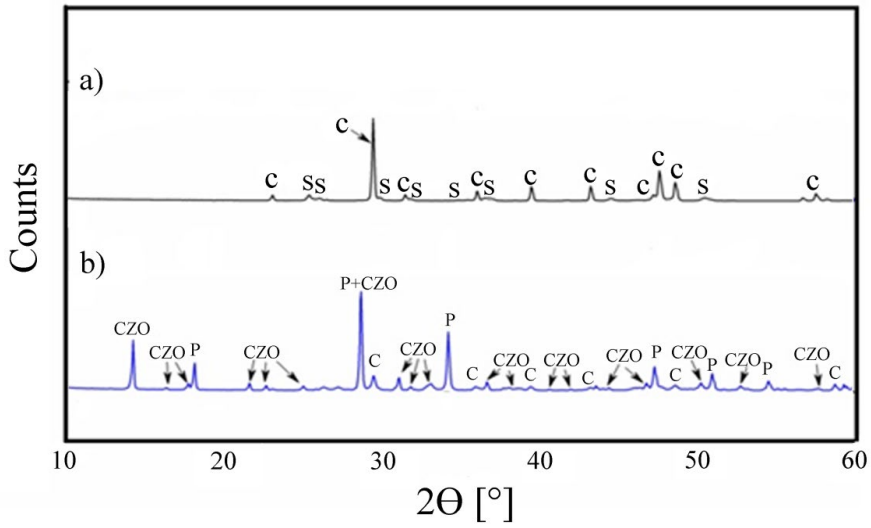

Figure 4. Diffractograms of seashell samples after heat treatment at different temperature and removal of divalent metal ions: a) 500 °C, Sr; b) 900 °C, Zn. Different phases are labeled with capital letters: C - calcite ($CaCO_3$) , S - strontianite ($SrCO_3$), P - Portlandite ($Ca(OH)_2$), CZO - Calcium Hexahydroxodizincate Dihydrate ($CaZn_2(OH)_6 x 2H_2O$)

CONCLUSION

Temperature treatments of the SW were found beneficial concerning both Zn and Sr removal from the aqueous phase. Temperatures 700-900 °C which resulted in partial or complete calcination of calcite to lime were favorable for sequestering Zn ions, and at the same time, adverse regarding Sr separation. By heating the SW at 500 °C pure calcite was obtained, the organic phase was removed, and such sample exhibited the highest potential for Sr removal. Even though cation immobilization via surface adsorption, ion-exchange, and solid-solution formation cannot be excluded, the precipitation of distinct crystalline solids of Sr and Zn was confirmed using the SW samples heated at optimal temperatures, i.e., SW500 and SW900, respectively. The results demonstrate the potential for using seashells as an alternative to limestone and lime for the removal of metal cations while at the same time reducing the negative impact and risks coming from accumulated waste.

Acknowledgements:

This work was supported by the Ministry of Education Science and Technological Development of the Republic of Serbia (Project III43009).

References

1. Oates, J. A .H. (1998) Lime and limestone: Chemistry and technology, production and uses. Wiley-VCH Verlagsgesellschaft mbH, Weinheim,
2. Barros, M. C., Magán, A., Valiño, S., Bello, P. M., Casares, J. J., Blanco, J. M. (2009) Identification of best available techniques in the seafood industry: a case study. Journal of Cleaner Production, 17 (3), 391-399,
3. Barros, M. C., Bello, P. M., Bao, M., Torrado, J. J. J. (2009) From waste to commodity: transforming shells into high purity calcium carbonate. Journal of Cleaner Production, 17 (3), 400-407,
4. Masukume, M., Onyango, M., Maree, J. P. (2014) Sea shell derived adsorbent and its potential for treating acid mine drainage. International Journal of Mineral Processing, 133, 52-59,
5. Mo, K. H., Alengaram, J. U., Jumaat, M. Z., Lee, S. C., Goh, W. I., Yuen, C. W. (2018) Recycling of seashell waste in concrete: A review. Construction and Building Materials, 162, 751-764,
6. Du, Y., Lian, F., Zhu, L. (2011) Biosorption of divalent Pb, Cd and Zn on aragonite and calcite mollusk shells. Environmental Pollution, 159 (7), 1763-1768,
7. Dahiya, S., Tripathi, R. M., Hegde, A. G. (2008) Biosorption of heavy metals and radionuclide from aqueous solutions by pre-treated arca shell biomass. Journal of Hazardous Materials, 150 (2), 376-386,
8. Egerić, M., Smičiklas, I., Mraković, A., Jović, M., Šljivić-Ivanović, M., Antanasijević, D., Ristić, M. (2018) Experimental and theoretical consideration of the factors influencing cationic pollutants retention by seashell waste. Journal of Chemical Technology and Biotechnology, 93 (5), 1477-1487,
9. Pẽna-Rodríguez, S., Bermudez-Couso, A., Nóvoa-Mũnoz, J. C., Arias-Estévez,

M., Fernández-Sanjurjo, M. J., Álvarez-Rodríguez, E., Núnez-Delgado, A. (2013) Mercury removal using ground and calcined mussel shell. Journal of Environmental Sciences 25 (12), 2476-2486,

10. Egerić, M., Smičiklas, I., Mraković, A., Jović, M., Šljivić-Ivanović, M., Sokolović, J., Ristić, M. (2018) Separation of Cu(II) ions from synthetic solutions and waste water by raw and calcined seashell waste. Desalination and Water Treatment, 132, 205-214,
11. Jones, M. I., Wang, L. Y., Abeynaike, A., Patterson, D. A. (2011) Utilisation of waste material for environmental applications: calcination of mussel shells for waste water treatment. Advances in Applied Ceramics, 110 (5), 280-286,
12. Jelić, I., Šljivić-Ivanović, M., Dimović, S., Antonijević, D., Jović, M., Šerović, R., Smičiklas, I. (2017) Utilization of waste ceramic and roof tiles for radionuclide sorption. Process Safety and Environmental Protection, 105, 348-360.

XIII International Mineral Processing and Recycling Conference
Belgrade, Serbia, 8-10 May 2019

University of Belgrade, Technical Faculty in Bor
Vojske Jugoslavije 12, 19210 Bor, Serbia
Tel. +381 30 424 555 Fax +381 30 421 078

APRICOT SHELLS AS BIOSORBENT FOR CU(II) IONS: DETERMINATION OF OPTIMAL ALKALINE TREATMENT CONDITIONS

Tatjana Šoštarić [#], Marija Petrović, Zorica Lopičić, Jelena Petrović, Marija Kojić, Marija Koprivica, Katarina Pantović Spajić
[1]Institute for Technology of Nuclear and Other Mineral Raw Materials, Belgrade, Serbia

ABSTRACT – The apricot stones (KK) were investigated as biosorbent of copper ions from aqueous solution. The rigidity of lignocellulosic compact molecular arrangement, induce the necessity of its modification. The aim of this paper was to establish optimal parameters of KK modification in order to improve low-cost biosorbent with improved biosorption characteristics. The modification parameters were: initial NaOH concentration, contact time and biomass/base solution ratio. After sets of experiments, the optimal modification parameters for copper removal were found to be: initial concentration of modification agent 1.0 mol/L NaOH, solid/liquid ratio 1:20 and 180 minute of contact time.
The results show that modified apricot shells doubled the binding affinity toward copper ions, and could be used as an efficient low-cost biosorbent, promoting more sustainable production and to stop waste disposal at landfill sites.

Key words: apricot shells, biosorption, Cu(II) ions, modification.

INTRODUCTION

The waste utilization of fruit processing industries has become one of the greatest challenges in world nowadays. Apricots have a significant role in Serbia's fruit production, but average annual production of 30,063 t (Statistical Office of the Republic of Serbia 2018) generates approximately 1,879 t apricot stone waste. Although apricot shells can be used for active carbon production and seeds can be used in food or pharmaceutical industry, most of the apricot stone waste ends up in landfill sites. In order to minimize this type of waste, apricot shells could be used as a biosorbent for removal of different types of pollutants. Because of all mentioned and faced with local environment pollution problems apricot shells was chosen for sorption experiments in the present study. This lignocellulosic biomass fulfils the criteria of unconventional sorbent: it is abundant, cheap and it is waste.

Since preliminary experiments showed that native apricot shells have low affinity

[#] corresponding author: t.sostaric@itnms.ac.rs

toward copper ions [1], need for modification of this material has been emerged. In order to get better biosorption performances alkaline modification has been applied. It is well known that this type of treatment has a significant impact on swelling of cellulose fibres causing the hydrogen bond breakage. Due to realising of OH groups cellulose becomes more reactive. Also this type of treatment removes superficial impurities waxes and fats and consequently functional groups become more accessible [2].

In order to get biosorbent with improved biosorption characteristics, raw apricot shells were object of alkaline treatment. Focus of this study was to investigate the optimal parameters of modification, which have effect on chemical, structural and morphological changes of this lignocellulosic material, in order to get biosorbent with improved sorption characteristics..

MATERIALS AND METHODS

Untreated biomass (KK)

Apricot stones were obtained from juice Factory from the Rasina district of Serbia. They were manually separated from kernels and only shells were used for further experiments. Shells were grinded in mill (KHD Humbolt Wedag AG, Germany) and sieved at particle size less than 0.3 mm.

Metal solution preparation

Initial copper solution with concentration of 1g/L were prepared by dissolving precise amount of $Cu(NO_3)_2 \times 3H_2O$ in deionized water.

Adsorption experiments

The removal of copper ions was investigated with differently obtained biosorbents. Batch experiments were carried out when 0.2 g of each obtained sorbent was put in 100 ml glass flask, left on orbital shaker at constant rate (250 rpm/min) for 120 min. The pH value of metal solution was 5.0. After sorption experiment suspension were filtered and residual meal concentration in filtrate were determined by usage of atomic adsorption spectrophotometer. The biosorption capacity was calculated by using the following equation:

$$q_e = \frac{V\,(C_i - C_e)}{m} \tag{1}$$

Where q is the biosorption capacity - amount of adsorbed metal ions (mg/g); C_i is initial metal concentration while C_e is equilibrium metal concentration (mg/L); V is volume (L) and m is mass sample (g).

Determination of optimal modification parameters

In order to design biosorbent with best adsorption performance, the effects of three modification parameters on the rate of adsorption process were observed by varying initial concentration of modified agent (NaOH), ratio between KK and NaOH solution and contact time between modified agent and KK.

Effect of initial NaOH concentration

The first set of experiments was conducted with different initial NaOH concentration: 0.25; 0.5, 1.0; 2.0; 3.0 and 4.0 mol/L. Contact time between base and KK was 120 minute and ratio between them was 1:20. Each obtained biosorbents were rinsed with distilled water until neutral reaction. After drying we tested each of this individual sorbents through set of sorption experiments previously described in section 2.3.

Effect of m/V ratio

Next set of experiments was conducted with different ratio between KK and base: 1:20; 1:40; 1:60; 1:80 and 1:100. Contact time was 120 minute and initial NaOH concentration was 1 mol/L as it was chosen from first set of experiments.

Effect of contact time

The final set of experiments was conducted by varying the contact time between KK and base: 30, 60, 90, 120, 180, 240 and 300 minute. The ratio between solid and liquid phase of 1:20 were applied and initial NaOH concentration was 1 mol/L due to previous set of experiments.

RESULTS AND DISCUSSION

In this section, results of investigation of optimal modification parameters have been presented with the focus if chemical treatment onto raw biomass was sufficient to produce the desired effect (improved biosorption characteristic). According to literature, effects of initial base concentration, contact time and temperature have major effects on results of alkaline treatment [2]. In this paper effect of temperature was not the object of study and all experiments were done on room temperature. Ratio between liquid and solid phase were examined, instead.

Effect of initial concentration of modified agent - NaOH

Native apricot shells (KK) has been modified with different initial concentration of NaOH solution and the results are presented at Figure 1.

As concentration of NaOH rise from 0.25 to 1 mol/L biosorption capacity has risen from 8.4 to 10.6 mg/g, too. However, with further increase of NaOH concentration biosorption capacity started to decrease. The reason for this could be that severe concentration of alkaline effects lignocellulosic structure causing loss of functional groups due to hydrolyses of hemicellulose and depolymerisation of lignin [1]. Similar results were obtained when modified poplar sawdust were used for removal of Cu(II) ions in biosorption experiments by Šćiban [2].

Furthermore, each modified sample (KKM) was tested if it was washed properly: the idea was to test if any deposition of hydroxi groups into the pores of the biosorbent, had occurred. This would lead to sorption false results. In accordance with this the final pH value of solution after biosorption experiments was measured and results are presented in Table1.

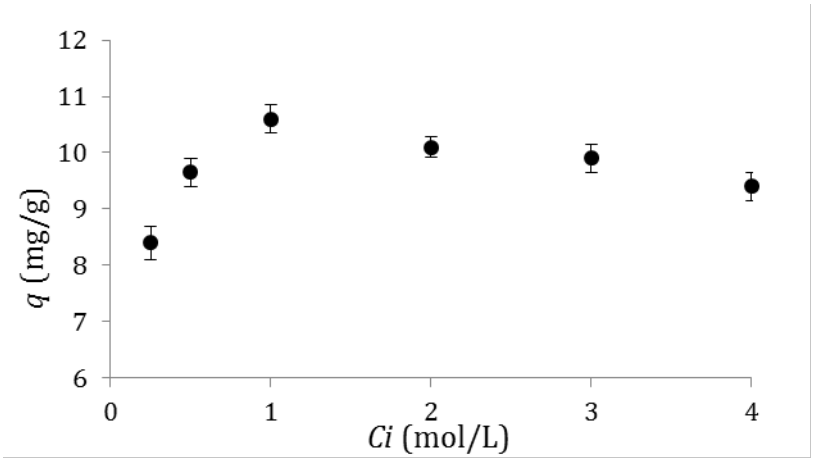

Figure 1. Effect of initial concentration of NaOH onto sorption capacity: m/V = 1:20, contact time was 120 min and concentration of Cu(II) solution was 60 mg/L

Table 1. Change of pH value after Cu(II) ions adsorption by native biomass modified at different NaOH concentration: initial pH value was 5.00

NaOH concentration (mol/L)	0.25	0.50	1.0	2.0	3.0	4.0
pH_f	4.25	4.27	4.28	4.31	4.30	4.37

As can be seen from Table 1 it is evident that there wasn't any noticeable change in pH value of residual solution after biosorbent experiments. This means that the material was washed thoroughly during alkaline treatment and most importantly it means that the increase of biosorption capacity is due to higher porosity and functional groups accessibility of modified biosorbent KKM [1]. Therefore, initial concentration of 1 mol/L of modified agent NaOH was chosen for further experiments.

Effect of ratio between KK and base during the modification process onto biosorption capacity

In order to exam if the ratio between solid (KK) and liquid (NaOH) phase have impact on biosorption capacity, the sorption experiments were conducted by varying the m/V ratio from 1:20 to 1:100. The results are presented at Figure 2.

Figure 2 show that the solid/liquid ratio doesn't have any effect on biosorption capacity of obtained material. In order to get economical and eco-friendly biosorbent m/V ratio of 1:20 was chosen for alkaline treatment. Table 2 shows that after each set of biosorption experiments finale pH value stays unchangeable.

Table 2. Change of pH value after each sets of biosorption experiments: pHi = 5.00

m/V	1:20	1:40	1:60	1:80	1:100
pH_f	4.28	4.25	4.32	4.25	4.24

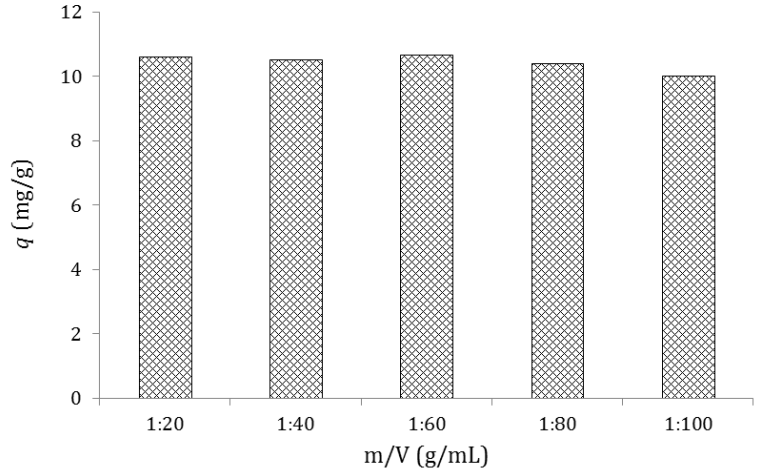

Figure 2. Effect of ratio among KK and NaOH on biosorption capacity towards Cu(II) ions: initial concentration of NaOH was 1mol/L; contact time:120 min, and metal concentration was 60 mg/L

Effect of contact time between KK and NaOH onto biosorption capacity

The effect of treatment time on biosorption capacity of KKM toward Cu(II) ions was investigated in order to determine the necessary time for best results. The obtained results are presented on Figure 3.

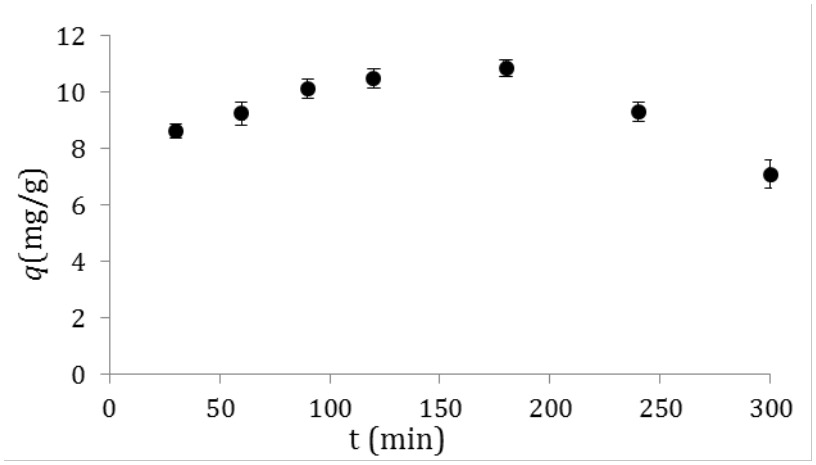

Figure 3. Effect of alkaline treatment time on biosorption capacity of KKM: concentration of NaOH was 1mol/L; m/V= 1:20, concentration of Cu(II) solution was 60 mg/L

Prolonging the contact time between KK and alkaline solution from 30 to 180 minute, biosorption capacity increases from 8.6 to 10.9 mg/g, respectively. However, afterwards biosorption capacity decreases for almost 40 %. If the contact time is longer than 180 minute, the lignocellulosic biomass become more disturbed which

causes the biomass to be chemically altered and not suitable for copper ions bonding: the number of active sites becomes lower. As in previous experiments final pH values of solution were measured and the results are presented in Table 3.

Table 3. Change of pH value after biosorption experiments where contact time between KK and NaOH was varied: pHi = 5.00

Contact time (minute)	30	60	90	120	180	240	300
pH_f	4.31	4.24	4.22	4.20	4.25	4.16	3.98

As can be seen from Table 3 final pH value of residual solution after biosorption experiments doesn't varied till 180 minute, while after this point it starts to decrease slightly: after 300 minute it is pH < 4.0. Contact time of 180 minute was chosen as time on which modification will be occurred.

Considering all previous experiments the chosen optimal parameters of KK modification are: initial concentration of modified agent is 1.0 mol/L NaOH, solid/liquid ratio is 1:20 and 180 minute of contact time among KK and NaOH. After alkaline treatment, treated biomass was washed thoroughly in distilled water, filtered and left in oven for 24 h at 50 °C. Obtained material was label as KKM.

The effect of alkaline treatment on native apricot shells biomass onto biosorption capacity toward Cu(II) ions is presented at Figure 4. It is evident that alkaline treatment doubled the value of biosorption capacity due to physical and chemical changes of this lignocellulosic biomass as it was later profoundly presented [1].

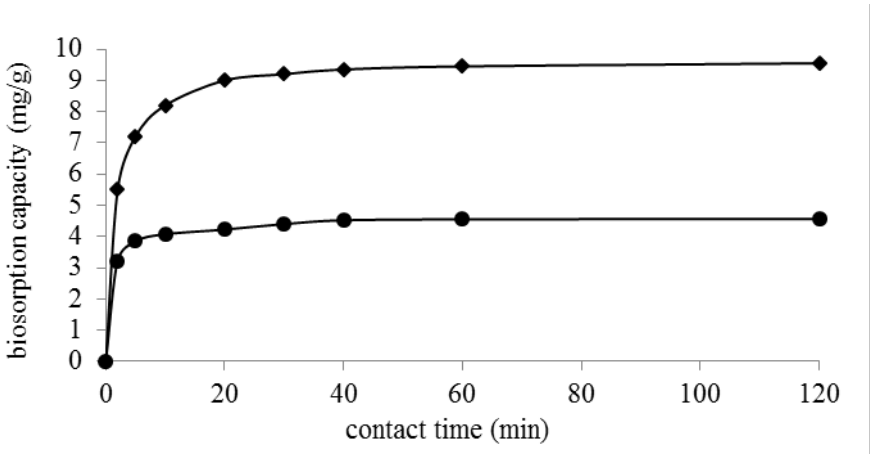

Figure 4. Difference in biosorption capacity between KK and KKM

CONCLUSION

The presented study demonstrates that alkaline modification has significant effect on biosorption performance of rigid native lignocellulosic biomass. Throughout set of experiments the optimal parameters of modification were establish: initial concentration of modified agent is 1.0 mol/L NaOH, solid/liquid ratio is 1:20 and 180 minute of contact time. Acquired biosorbent KKM achieve to double the value of biosorption capacity of native biomass. As apricot shells are

widely available in the Republic of Serbia as an agricultural waste, biosorbent made of this type of biomass has twofold significance: economical solution for wastewater treatment and preventing the waste from going to lendfill.

Acknowledgements:

The authors are grateful to the Serbian Ministry of Education, Science and Technological Development of the Republic of Serbia for the financial support of this investigation included in the project TR 31003.

References

1. Šoštarić, T., Petrović, M., Pastor, F., Lončarević, D., Petrović, J., Milojković, J., Stojanović, M. (2018) Study of heavy metals biosorption on native and alkali-treated apricot shells and its application in wastewater treatment. Journal of Molecular Liquids, 259, 340-349,
2. Šćiban M. (2002) Uklanjanje teških metala iz vode piljevinom drveta, celulozom i ligninom, (Doktorska disertacija), Univerzitet u Novom Sadu, Tehnološki fakultet, Novi Sad.

XIII International Mineral Processing and Recycling Conference
Belgrade, Serbia, 8-10 May 2019

University of Belgrade, Technical Faculty in Bor
Vojske Jugoslavije 12, 19210 Bor, Serbia
Tel. +381 30 424 555 Fax +381 30 421 078

HOMOGENEOUS FENTON PROCESS FOR MINERALIZATION OF METHYLENE BLUE

Ana Popović [1, #], Sonja Milićević [1], Vladan Milošević [1], Branislav Ivošević [1], Jelena Čarapić [1], Dragan Povrenović [2]
[1]Institute for Technology of Nuclear and other Mineral Raw Materials, Belgrade, Serbia
[2]The University of Belgrade, Faculty of Technology and Metallurgy, Belgrade, Serbia

ABSTRACT – Methylene blue is an aromatic chemical compound with a molecular formula C16H18N3SCl and has been used in many industries such as paper industries, leather industries, biology, chemistry, and even for medical purposes. The Fenton process is one of the most utilized of all advanced oxidation processes for the degradation of organic wastewater pollutants. The aim of this paper is to present the obtained results of homogeneous Fenton process used for mineralization of methylene blue in the batch system. The different doses of $FeSO_4 \cdot 7H_2O$ were studied in the range from $7.2 \cdot 10^{-6}$ – $1.1 \cdot 10^{-4}$ mol, respectively, with the following conditions: pH ≈ 3, the dose of $4.4 \cdot 10^{-5}$ mol·dm^{-3} H_2O_2, dye concentrations in the range from $3.1 \cdot 10^{-5}$ – $9.4 \cdot 10^{-5}$ mol·dm^{-3}, ambient conditions of temperature and pressure, and the reaction time of 60 min. The experimental results show that 98 % of the dye can be degradated using homogeneous Fenton process.

Key words: advanced oxidation processes, homogeneous Fenton process, methylene blue, an aromatic compound, catalyst.

INTRODUCTION

Textile industries are one of the biggest producers of wastewater in the world. The constant demands for new fabrics in order to fulfill consumer society's needs results in serious damage to the ecosystem, as most of the manufactured wastewater is directly discharged into the effluent. The use of various dyes creates enormous amounts of waste because these chemical compounds are usually designed to be resistant or heavily degradable. An oxidation of these pollutants can be achieved using advanced oxidation processes. One of the most common used is the Fenton process. The Fenton reagent is catalytic-oxidative mixture of ferrous iron and hydrogen peroxide. The ferrous iron (Fe^{2+}) initiates and catalyzes the decomposition of H_2O_2, resulting in the generation of hydroxyl radicals [1].

corresponding author: a.popovic@itnms.ac.rs

$$Fe^{2+} + H_2O_2 \rightarrow Fe^{3+} + {}^{\bullet}OH + OH^- \quad (1)$$

The HO$^{\bullet}$ radical is the main reactant in the process capable of detoxifying a number of organic substrates via oxidation [2]. Homogeneous Fenton process is also called Classical Fenton process named after the Fenton's reaction following the studies of Henry Fenton (*Henry John Horstman Fenton*). The optimal efficiency of this process is typically achieved at a pH around 3.0, which has to be optimized beyond the H_2O_2 and Fe^{2+} concentrations [3]. Fenton process is also known by virtue of its simplicity, economy and available amounts of iron and hydrogen-peroxide which are used for the process.

MATERIALS AND METHODS

Materials

Methylene blue, $FeSO_4 \cdot 7H_2O$ p.a. and H_2O_2 30 % w/v are all purchased from Sigma Aldrich, Munich, Germany. The solutions of the methylene blue $3.1 \cdot 10^{-5}$ mol·dm^{-3}, $6.2 \cdot 10^{-5}$ mol·dm^{-3} and $9.4 \cdot 10^{-5}$ mol·dm^{-3} were made in distilled water. The $FeSO_4 \cdot 7H_2O$ was used in the solid state in following amounts $7.2 \cdot 10^{-6}$ mol, $1.7 \cdot 10^{-5}$ mol, $3.6 \cdot 10^{-5}$ mol, $1.1 \cdot 10^{-4}$ mol and H_2O_2 as 8.82 mol·dm^{-3} solution in a concentration of $4.4 \cdot 10^{-5}$ mol·dm^{-3}.

Methods

Glass beaker (500 dm^{-3}) containing 100 dm^{-3} dye solution was placed on a magnetic stirrer for continuous stirring. The values of the pH and temperature were measured using pH-meter (781 ph/lon Metar Metrohm). The experiments were carried out at ambient conditions of temperature and pressure. The required concentrations of Fe^{2+} and H_2O_2 were added simultaneously into the dye solution, and subsequently, the concentrations of the dye were determined using a Shimadzu UV-1800 spectrophotometer at the absorption maxima of the dye of 665 nm, at a different time in order to study the direction of the degradation reactions. The percent of decolorization was calculated as follows [4, 5]

$$\%\ Decolorization = 100 \cdot \frac{(C_o - C_t)}{C_o} \quad (2)$$

where C_o is the initial concentration of dye, and C_t is the concentration of dye at reaction time t (min).

RESULTS AND DISCUSSION

The effects of initial concentration of dye and Fe^{2+} under fixed conditions as the concentration of H_2O_2, pH, and temperature were investigated. At the used concentration of dye and $FeSO_4 \cdot 7H_2O$ obtained results are presented as a function of time in the Figures 1-3.

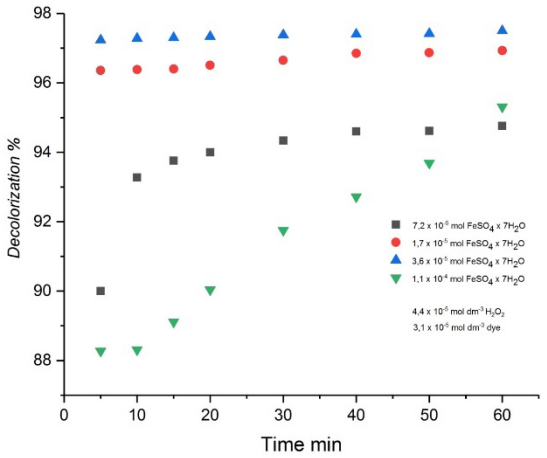

Figure 1. Percentage of decolorization as a function of time for the methylene blue concentration of $3.1 \cdot 10^{-5}$ mol·dm^{-3}

A dye solution of $3.1 \cdot 10^{-5}$ mol·dm^{-3} was stirred with initial concentrations of $FeSO_4 \cdot 7H_2O$ as follow $7.2 \cdot 10^{-6}$ mol, $1.7 \cdot 10^{-5}$ mol, $3.6 \cdot 10^{-5}$ mol, $1.1 \cdot 10^{-4}$ mol, respectively, and $4.4 \cdot 10^{-5}$ mol·dm^{-3} of H_2O_2. The measurements are carried out during the reaction time of 60 min. A reaction occurred rapidly and within first 5 min, more than 90 % of the dye was demineralized except with the initial concentration of $1.1 \cdot 10^{-4}$ mol $FeSO_4 \bullet 7H_2O$ where the same results were obtained after 20 min. A $Fe:H_2O_2$ ratio in this certain conditions impacted the reaction time needed for mineralization of the dye. The mineralization reactions are continuously slowing after the first ten minutes. The best result of 98 % dye removal was achieved with the used concentration of $3.6 \cdot 10^{-5}$ mol $FeSO_4 \cdot 7H_2O$.

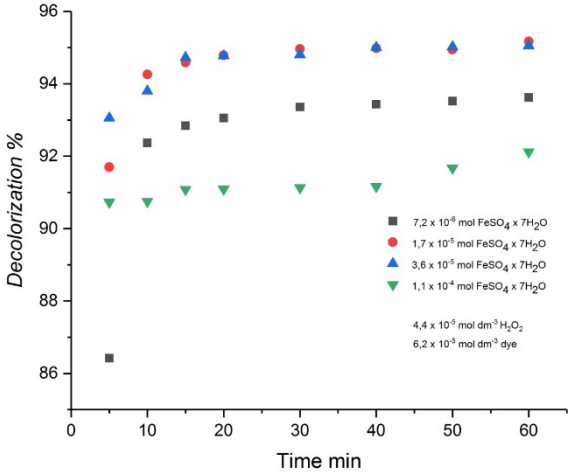

Figure 2. Percentage of decolorization as a function of time for the methylene blue concentration of $6.2 \cdot 10^{-5}$ mol·dm^{-3}

A dye solution of $6.2 \cdot 10^{-5}$ mol·dm^{-3} was stirred with the defined concentrations of $FeSO_4 \cdot 7H_2O$ and H_2O_2. The higher concentration of the dye directly impacted the removal effectiveness as due to the higher concentration of the dye the more reactants are needed in order to get the best final results. The results of 95 % dye removal obtained with the concentration of $1.7 \cdot 10^{-5}$ mol and $3.6 \cdot 10^{-5}$ mol of $FeSO_4 \bullet 7H_2O$ still affirm that homogeneous Fenton process is very successful for degradation of organic aromatic compounds even with the higher concentrations of dye.

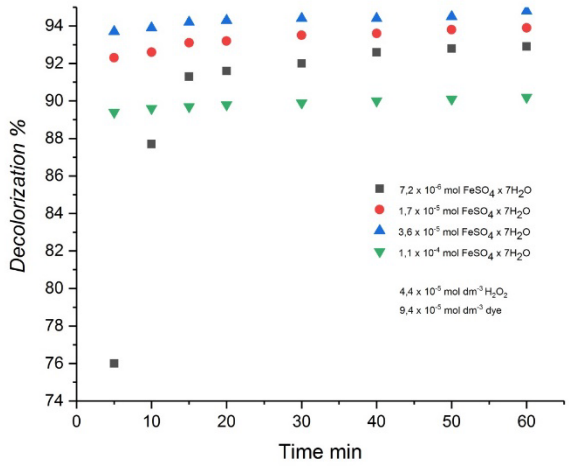

Figure 3. Percentage of decolorization as a function of time for the methylene blue concentration of $9.4 \cdot 10^{-5}$ mol·dm^{-3}

A dye solution of $9.4 \cdot 10^{-5}$ mol·dm^{-3} was stirred with the defined concentrations of $FeSO_4 \cdot 7H_2O$ and H_2O_2. The results determine that the reaction time between the reactants has to be longer as the concentration of the contaminants raise. Nevertheless, the mineralization efficiency is 94 % with the used concentration $3.6 \cdot 10^{-5}$ mol of $FeSO_4 \cdot 7H_2O$.

CONCLUSION

The optimum molar ratio of $[Fe^{2+}]$:$[H_2O_2]$ is found to be around 36:1(in mol·dm^{-3}) at a solution pH between 3 and 4 and an initial concentration of dye. The obtained results indicate that the demineralization of methylene blue can be successfully achieved by using the Fenton's reagent. The removal efficiency of 94 - 98 % was achieved, regardless the initial dye concentration. However, with the increase of the initial dye concentration the longer reaction time is needed in order to achieve the same demineralization level.

Acknowledgements:

This research has been part of the investigations financed by the Ministry of Education, Science, and Technological Development of Republic of Serbia as a part of

the project TR 33007 “Implementation of new technical, technological and environmental solutions in the mining and metallurgical operations RBB and RBM”.

References

1. Ebrahiem E. E., Al-Maghrabi, N. M., Mobarki, R. A. (2017) Removal of organic pollutants from industrial wastewater by applying photo-Fenton oxidation technology, Arabian Journal of Chemistry, 10, S1674–S1679,
2. Dutta, K., Mukhopadhyay, S., Bhattacharjee, S., Chaudhuri, B. (2001) Chemical oxidation of methylene blue using a Fenton-like reaction. Journal of Hazardous Materials, B84, 57-71,
3. Ribeiro, R. A., Nunes, C., Pereira, M. F. R., Silva, A. M. T. (2015) An overview on the advanced oxidation processes applied for the treatment of water pollutants defined in the recently launched Directive 2013/39/EU. Environment International 75, 33-51,
4. Balmer, M. E., Sulzberger, B. (1999) Attrazine degradation in irradiated iron/oxalate systems: effect of pH and oxalate. Environmental Science & Technology, 33 (14), 2418-2424,
5. Kansal, S. K., Kaur, N., Singh, S., Photocatalytic degradation of two commercial reactive dyes in aqueous phase using nanophotocatalysts. Nanoscale Research Letters, 4 (7), 709-716.

XIII International Mineral Processing and Recycling Conference
Belgrade, Serbia, 8-10 May 2019

University of Belgrade, Technical Faculty in Bor
Vojske Jugoslavije 12, 19210 Bor, Serbia
Tel. +381 30 424 555 Fax +381 30 421 078

POTENTIALS OF BIOMASS USE IN SERBIA

Aleksandra Cvetković [1, #], Miroslava Marić [1], Darko Milošević [2]
[1]Faculty of management, Zaječar, Serbia
[2]LUM Jean Monnet University, Bari, Italy

ABSTRACT – The links between energy and economic growth, poverty alleviation, environmental and climate impact are becoming more visible. For most of the global economy, energy has become one of the strategic factors that influence the making of business decisions. In the energy industry, there is a growing demand for innovative, climate-friendly technologies for the production of heat and electricity. As energy becomes a strategic factor in the global competition, it can be an opportunity for the country's competitive advantage. In recent years, Serbia has been taking an increasing share in the use of biomass energy because it understands that biomass has both economic and environmental benefits of energy exploitation. According to the available data, almost half of the primary energy needs in Serbia could be from the potential of renewable energy.

Key words: biomass, renewable energy, economic growth

INTRODUCTION

Energy resources are largely unevenly distributed throughout the world, and for this reason, some countries often become energy dependent from countries with rich mineral mine wealth resources, especially energy sources such as oil. The importance of energy resources for the economy of a country depends on the level of economic and technological development of the nation [1]. Although the possession of natural resources is not sufficient for economic development, it is better to have them than not. However, many examples speak *vice versa*, and in such countries, the underlying problem is exactly how to successfully manage those resources. The energy deficit does not have to represent a major barrier to the development of the country (for example: Japan, Korea, Hong Kong, Singapore, etc.).

By utilizing one natural resource, partly but for a long time, with a tendency of growth, we destroy other natural resources. Other damages are manifested through pollution of the environment and endangering the sustainable development of the planet. In order to eliminate or at least reduce these impacts, the use of other available sources of energy or more precisely, renewable energy sources has begun. These include energy that we encounter every day, such as biomass primarily.

corresponding author: aleksandra.cvetkovic@fmz.edu.rs

Renewable energy sources are permanent sources of energy derived from nature and do not endanger the environment [2]. However, the application and use of each of them has its limitations. Existing capacities are very little exploited, and even this little exploitation refers to the most economically developed parts of the world, so money is the most important limiting factor for the exploitation of these resources. Consideration should also be given to the awareness of the population and the commitment to better characteristics of renewable energy sources compared to the use of conventional energy sources. [3]

BIOMASS-ENERGY OF THE FUTURE

Biomass considered as the source of energy is significantly different from non-carbon sources (such as wind). It could provide energy and products similar to traditional ones produced using existing fossil fuels. Biomass also has an important application as a raw material in an industry that must properly integrate into the use of energy in order to respect the sustainability principle [4]. According to the definition given in Directive 2009/28/EC, 'biomass' means "the biodegradable fraction of products, waste and residues from biological origin from agriculture (including vegetal and animal substances), forestry and related industries including fisheries and aquaculture, as well as the biodegradable fraction of industrial and municipal waste" [5]. This means that with appropriate industrial processing, the resulting biomass can be converted into natural gas and liquid and solid fossils. By using various transformation processes such as combustion, gasification and pyrolysis, biomass can be transformed into biofuels for transport, biomass heating systems or bio-electric energy.

Bioenergy (in traditional and modern uses) is the largest contributor to global renewable energy supply [6]. Total primary energy supplied from biomass in 2016 was approximately 62.5 exajoules (EJ) [7]. The supply of biomass for energy has been growing at around 2.5 percent per year since 2010. Bioenergy supply increased to 57.7 exajoules (EJ) in period from 2013-2016, where China, India and USA lead the world in renewables supply [8]. The bioenergy share in total global primary energy consumption has remained relatively steady since 2005, at around 10.5 percent, despite a 21 percent increase in overall global energy demand over the last 10 years. The contribution of bioenergy to final energy consumption is expected to be almost 12 percent in 2020 with a significant increase in absolute. According to market and industry trend analysis [9] the contribution of bioenergy to final energy demand for heat in buildings and industry far outweighs its use for electricity and transport combined.

Despite the low oil prices and uncertainty in the world market, bioenergy production continued to increase in 2017. The development of bioenergy continued to spread noticeably in India. In the European Union (EU) bio-energy production increased by about 6 percent in 2016, while production in Asia increased sharply in the Republic of Korea. In 2016, the record global production of ethanol was recorded by the United States, China and India. Thus, driven by the standard for renewable energy sources, the use of bio methane in transport has grown sharply in the United States. It is expected that if all the announced HVO projects come into life, world production capacity of Hydrotreated Vegetable Oil (HVO) grow by more than 40 percent by 2020. [10, 11] Currently, the installed capacity around the world is

4,745,000 MT but within the next 4 years it can go up to 6,775,000 MT (43 percent growth). Europe will remain, by far, the leader on the HVO market with 3,870,000 MT of installed capacity by 2020; North America with 1,155,000 MT; and Asia will produce 1,155,000 MT [11]. Biomethane use in transport also grew sharply, stimulated by the Renewable Fuel Standard [12]. Progress has been made on the development of advanced biofuels, with the expansion of capacity and fuel production, the construction of new plants in the countries of the European Union, the United States, China and India [11].

The largest percentage of the use of biomass for energy production in the world is in the United States with 62 percent, Germany with 37 percent, Brazil with 36 percent, China with 27 percent, Japan with 22 percent, Sweden 13 percent, Great Britain 12 percent, Finland 11 percent, Italy 10 percent, and Canada 7.7 percent. These countries have realized the importance of using biomass to generate energy. [13] For the production of biodiesel, In Europe the most used is oil, while in the United States is most used soya. Bioethanol as a fuel for replacing gasoline is currently being rebuilt with the greatest global potential. The EU is the world leader in biogas electricity production, with more than 10 GW installed and a number of 17,400 biogas plants. The production of biogas in Europe reached 18 billion m^3 of methane (654PJ) in 2015. In the first place in production is Germany, followed by Great Britain, France and Italy. German government uses it as a fuel for vehicles or for injection into a natural gas network, with 459 plants in 2015 that produce 1.2 billion m^3, and 340 plants that enter the gas network, with a capacity of 1.5 million m^3 [11].

POTENTIALS OF BIOMASS USE IN SERBIA

According to the Energy Development Strategy of the Republic of Serbia and the Serbia National Action Plan for the use of renewable energy sources from 2020 to 2025 with projections until 2030, the annual energy potential of biomass in the Serbia is around 2.7 million tons. [14]

According to current estimates, the dominant part of wood biomass could be used for the production of pellets, electricity and heat for district heating, while the agricultural biomass could be used for the combined production of electric and thermal energy, as well as for the production of biogas. Biomass is traditionally used for heat production, and is estimated at 0.3 million tons in 2008. It is estimated that annual production of pellets could reach 100,000 tons in 2016. That is why interest in pellet production is increasing, but most of the production is exported. The main export markets for Serbian pellets are Italy, Greece and Germany.

The biomass energy potential of Serbia is concentrated in waste from wood and wood processing industry (98 percent from agriculture, 1.5 percent from forest production and 0.5 percent from wood production). [15] It is estimated that renewable energy from agriculture and forestry for annual production can be over 4 Mtoe (Million Tons of Oil Equivalent Modification).16 [16]

Currently, the annual production of biomass in Serbia amounts to about 2.90 million tons - 1.56 million tons of agricultural biomass, and 1.34 million tons makes forest biomass. Interest in the use of briquettes and pellets is increasing, similar to other countries with good forest resources. There are several limitations for wider use of household heating (to replace electricity), which include a lack of standards

for pellets and briquettes and low electricity prices. Currently, biomass is mainly used as a backbone for straw in stables, and private farms often burn biomass in the fields.

Collecting and transporting biomass is very expensive due to fragmentation of households. Biomass is a renewable source of energy that is obtained as a by-product of the wood industry and agricultural crops and is used as a replacement for fossil fuels in the production of heat and electricity energy. Unlike fossil fuels, combustion of biomass does not increase the amount of carbon dioxide (CO_2) in the atmosphere, which has a positive impact on the environment.

Statistically speaking, Serbia is a country with 5,701,000 hectares of agricultural land, out of which 4,867,000 hectares is arable land, which results in the calculation that agricultural land per capita has 0.56 hectares and a cultivable 0.46 hectares. In Serbia, 87 percent of the country is privately owned, while the number of agricultural holdings (based on the agricultural census from 2012) is 778,000, where the average size of the agricultural holding is about 3 hectares. [17] As a country with large areas under the forest, the Republic of Serbia has great potential for biomass production.

Biomass participates with 63 percent of the total potential of renewable energy sources. Forests cover about 30 percent of the territory, and about 55 percent of the territory is arable land. In addition to crop residues, there are great opportunities for dedicated biomass cultivation - which will not apply to food production.

The great potential of biomass in Serbia lies in the agricultural residue and wood biomass, a total of about 2.7 million tons (1.7 million tons in the remnants of agricultural production and about 1 million tons in wood biomass). In addition to these two sources, a significant source of biomass is also the remains of livestock production. The second group of sources of biomass includes energy plants (for example: Miscanthus, fast-growing tree poplar); and plants that serve as a raw material for biodiesel, bioethanol (oilseed rape, sunflower, corn, etc.). The use of the estimated biomass potential cannot eliminate the state's need for fuel imports, but in any case the dependence on the import of liquid fuel can significantly decrease, as well as significantly reduce environmental pollution. [11]

Analysis of the structure of biomass from agricultural residues production shows that more than half of the resources lies in biomass is, more than a quarter in the straw of small grains, and the rest of the harvest remains of soya and rapeseed. Total arable surface in Serbia is 3,355,019 hectares.

On the territory of the Autonomous Province of Vojvodina, intensive vegetable production with dominant sowing area under corn (over one million hectares) is carried out, followed by wheat with production of about 500,000 hectares. In Central Serbia, corn production is the most commonly represented plantation unit. Free agricultural land can be used for planting energy plants. For example, the plant Miscanthus gives an annual yield of over 10 tons of dry biomass per hectare. The obtained biomass from the plant Miscanthus is very caloric, at the level of brown coal [1].

Looking at the energy potential of biomass in Serbia, we can see the great potential of resource utilization and the wealth that Serbia has in this area of renewable resources. Liquid manure (produced from biogas production) is 42.24 toe; 605 toe fruits residues; agricultural crops 1,023,000 toe; agricultural biomass 1.670.240 toe; wood biomass from trees outside the forest 34,355 toe; wood

processing residues 179,563 toe; forest waste 163.76 toe; 1,150,000 toe firewood; and wood biomass 1,527,678 toe. From the above data it can be concluded that agricultural biomass has an extremely high potential for utilization. Moreover, Serbia also has a great potential of unused wood sources for production from renewable energy sources. [9]

The estimated amount of wood biomass in Serbia, which can be used as fuel, is around 1.65 million m^3 annually, while the energy potential of forest biomass (left to break after the production of timber assortments) is estimated around 15.6 million GJ per year. However, despite this potential of resources from Serbia's renewable energy sources, the utilization is still low and does not meet the annual energy needs. With more than 12 million tons per year of wood waste production, Serbia has the potential to develop its bioenergy sector in the future, especially for the production of electrical and heat energy.

Table 1. Types of waste biomass from agriculture and total availability for energy use [18]

From	Yields	Total availability for energy use
1 hectare of corn	3.85 tons per hectare	70 percent
1 hectare of corn	1.65 tons per hectare	30 percent
1 ton of wheat	1 ton of straw	35 percent
1 tone of soya	2 tons of straw	60 percent

Table 2. Potentials of biomass utilization in Serbia [19]

Biomass source		Potential (toe)
Wood biomass		1,527,678
Fuel wood		1,150,000
Forest residue		163,760
Wood processing residue		179,563
Wood from trees outside forest		34,335
Agricultural biomass		1,670,240
Crop residue		1,023,000
Residue from fruit growing, viniculture and fruit processing		605,000
Liquid manure (for biogas production)		42,240
Biofuels for transport		191,305
Total Biomass	Without transportation fuel	3,197,918
	With transportation fuel	3,389,223

The most commonly used ways of using wood biomass to energy are in the form of pellets, briquettes and wood chips. Production of wood pellets is constantly growing and its price in the market is higher. On the other hand, briquetting wood biomass is used in large industrial plants. Under the term wood scrap implies that part of the tree which cannot be used in the further processing of the same purpose. However, the tree has so many different applications where this residue could use, which effectively means that the term waste can only conditionally use [19].

The Serbia Energy Development Strategy by 2015 (given in the Official Gazette of the RS, no. 44/05) as one of the priorities defined and selective use of new renewable energy sources. Special Programs presents more efficient usage of new energy and greener technology, especially biomass, with the aim of reducing the consumption of high-quality imported energy sources and achieve additional production of electric and thermal energy, with significantly lower negative impact on the environment.

CONCLUSION

Energy plays a key role in a global development context. The renewable resources could be used as ability to improve the standard of living through, either by releasing time from housework (for example, washing clothes or cooking); increased productivity; improved health and education services; or digital connections to local, regional and global networks. The link between energy consumption and economic growth has been the topic of a wide discussion of a large number of scientists and scholarly works. A large number of studies attempted to draw a causal link between energy consumption and economic growth, but no clear consensus was reached. This can be partly attributed to the fact that the connection between energy and prosperity is not a one-way effect. Getting access to electricity and other renewable energy sources can enable an initial increase in GDP, but an increase in GDP can lead to higher energy consumption. In addition, progress in developmental outcomes can be complex because a number of parameters can be improved over time. If at the same time the national parameters of access to renewable energy sources and consumption, nutrition, education, and health are improved, they can have complex relationships with each other, and they can hardly directly affect the improvement of living standards through one parameter.

Historically, energy plays an extremely important role in the process of general development and the survival of human civilization on the planet. Everything that surrounds us is based on the use of energy. Energy is needed for all living beings to function normally and perform daily activities. Unfortunately, the accelerated development of human society over the last two centuries was based on excessive and uncontrolled use of energy resources. As the modern society evolved, the needs for energy were increasing, and the reserves of non-renewable energy resources, which are being used to a large extent, are getting smaller. The great danger is the fact that fossil fuels, created for billions of years, are almost spent in just a few hundred years. For future generations, very few of these energy goods are left, but their heritage is therefore pollution of all kinds, up to the most horrible - global ones.

It can be said with certainty that the annual volume of energy production must be greater than the annual volume of population growth, in order to ensure satisfactory production and improvement of the living standards of the population. However, in

order to ensure a continuous increase in energy production, extensive investments are needed. In addition, there are numerous environmental problems - such as environmental pollution and global warming of the planet. Therefore, it is necessary to save energy more, primarily by rationalizing energy consumption and increasing the motivation of work. These processes are largely realized in developed countries. In the coming time, it will be even more widespread, as it is predicted that the annual growth of energy production in the world will amount to only 1 percent.

References

1. Fagerberg, Jan. "Innovation, catching up and growth." Technology and productivity: the challenge for economic policy (1991): 37-46,
2. Antunović, Tena. Novi obnovljivi izvori energije. Diss. Polytechnic of Međimurje in Čakovec., 2016,
3. Djukanovic, S., (2009). Renewable energy-economic assessment. Ub: Bozidar Knezevic,
4. B, J., Janic, M., (2006). The ability to use biomass in agriculture, regional Chamber of Commerce. Sombor: Daka, 6,
5. Europäische. "Directive 2009/28/EC of the European Parliament and of the Council of 23 April 2009 on the promotion of the use of energy from renewable sources and amending and subsequently repealing Directives 2001/77/EC and 2003/30/EC." Official Journal of the European Union 5 (2009): 2009,
6. Cristescu, Corneliu, et al. "Developments, trends and orientations regarding the realization of renewable energy conversion systems." International Conference on Hydraulics and Pneumatics – HERVEX, Băile Govora, Romania (2017),
7. https://www.ellipseise.eu/wpcontent/uploads/2017/06/170607_GSR_2017_Full_Report.pdf (Visited 19/02/2019)
8. WBA global bioenergy statistics 2016, https://worldbioenergy.org/uploads/WBA%20Global%20Bioenergy%20Statistics%202016.pdf (Visited 24/02/2019)
9. http://www.ren21.net/gsr-2017/pages/summary/summary (Visited 18/02/2019)
10. https://www.greenea.com/publication/new-players-join-the-hvo-game/ (Visited 24/02/2019),
11. Scarlat, Nicolae, Jean-François Dallemand, and Fernando Fahl. "Biogas: Developments and perspectives in Europe." Renewable Energy 129 (2018): 457-472,
12. Jovanović, B., and M. Parović. "Stanje i razvoj biomase u Srbiji." Jefferson Institute, Beograd, Srbija (2009), 1,
13. Martinot, Eric, and Janet L. Sawin. "Renewables 2017: Global status report." Washington, DC: Worldwatch Institute (2017),
14. Projections for 2015 and 2016 are from a linear extrapolation based on data for 2010-14 from IEA, World Energy Outlook 2016 (Paris: 2016),
15. mre.gov.rs/doc/efikasnost-izvori/NAPOIE%20KONACNO%2028_jun_2013.pdf (Visited 22/02/2019),

16. http://www.stat.gov.rs/sr-latn/oblasti/poljoprivreda-sumarstvo-i-ribarstvo/popis-poljoprivrede/ (Visited 24/02/2019),
17. Dinić, J., (1997). Prirodni potencijal Srbije – ekonomsko-geografska analiza i ocena. Beograd: Ekonomski fakultet.
18. http://www.eko.vojvodina.gov.rs (Visited 16/02/2019),
19. Akcioni plan za biomasu od 2010-2012. godine, Službeni glasnik RS br. 56/2010.

XIII International Mineral Processing and Recycling Conference
Belgrade, Serbia, 8-10 May 2019

University of Belgrade, Technical Faculty in Bor
Vojske Jugoslavije 12, 19210 Bor, Serbia
Tel. +381 30 424 555 Fax +381 30 421 078

ENVIRONMENTAL RISKS OF MINING ACTIVITES

Miomir Mikić #, Milenko Jovanović, Srđana Magdalinović, Daniela Urošević
Mining and Metallurgy Institute Bor, Bor, Serbia

ABSTRACT – Development of a modern society is based on the need to fill the demand for goods and services, so the industry has to evolve and adapt, to be able to secure and market these products. The first step in this process is the supply of raw materials for further processing and transformation. In fact, mining could become one of the major forces in the global economy, which takes a vital position in the supply chain of raw materials. In this scenario, mining is facing one of the biggest challenges that can arise in any industrial activity. It is the exploitation of mineral raw materials from the Earth's crust, and in doing so, no negative effects on the environment are created.

Key words: mining, environmental, industry.

INTRODUCTION

Water pollution, loss of biodiversity, soil erosion and pollution, and formation of sink holes are among the worst effects of the mining industry on the environment.

Mining is the extraction of minerals and other geological materials of economic value from deposits on the earth. Mining has the potential to have severely adverse effects on the environment including loss of biodiversity, erosion, contamination of surface water, ground water, and soil. The formation of sinkholes is also possible. Other than environmental damage, mining may also affect the surrounding population's health as a result of contamination caused by the leakage of chemicals.

In some countries, mining companies are expected to adhere to rehabilitation and environmental codes, making sure that the area mined is eventually transformed back into its original form, or at least as much as it is possible. Different types of mining methods can have significant public health and environmental effect.The erosion of exposed tailing dams, mine dumps, hillsides, and the resultant siltation of creeks, drainages, and rivers can affect the neighboring areas. A good example is Papua New Guinea's Ok Tedious Mine. Mining around farming areas may either destroy or disturb the crop lands or productive grazing lands while in wilderness areas it can cause either the disturbance or the destruction of ecosystems.

corresponding author: miomir.mikic@irmbor.co.rs

OPEN PIT MINING

Open pit mining, where material is excavated from an open pit, is one of the most common forms of mining for strategic minerals (Figure 1). This type of mining is particularly damaging to the environment because strategic minerals are often only available in small concentrations, which increases the amount of ore needed to be mined.

Figure 1. The largest open pit in the world – Bingham Canyon mine

Environmental hazards are present during every step of the open-pit mining process. Hardrock mining exposes rock that has lain unexposed for geological eras. When crushed, these rocks expose radioactive elements, asbestos-like minerals, and metallic dust. During separation, residual rock slurries, which are mixtures of pulverized rock and liquid, are produced as tailings, toxic and radioactive elements from these liquids can leak into bedrock if not properly contained.

UNDERGROUND MINING

Underground mining has the potential for tunnel collapses and land subsidence (1). It involves large-scale movements of waste rock and vegetation, similar to open pit mining (Figure 2).

Additionally, like most traditional forms of mining, underground mining can release toxic compounds into the air and water. As water takes on harmful concentrations of minerals and heavy metals, it becomes a contaminant. This contaminated water can pollute the region surrounding the mine and beyond (2). Mercury is commonly used in as an amalgamating agent to facilitate the recovery of some precious ores (2). Mercury tailings then become a major source of concern, and improper disposal can lead to contamination of the atmosphere and neighboring bodies of water. Most underground mining operations increase sedimentation in

nearby rivers through their use of hydraulic pumps and suction dredges; blasting with hydraulic pumps removes ecologically valuable topsoil containing seed banks, making it difficult for vegetation to recover (2). Deforestation due to mining leads to the disintegration of biomes and contributes to the effects of erosion.

Figure 2. Codelco's El Teniente mine, the world's largest underground copper operation and the sixth biggest copper mine by reserve size

IN SITU LEACH (ISL) MINING

ISL mining has environmental and safety advantages over conventional mining in that the ore body is dissolved and then pumped out, leaving minimal surface disturbance and no tailings or waste rock (3), Figure 3.

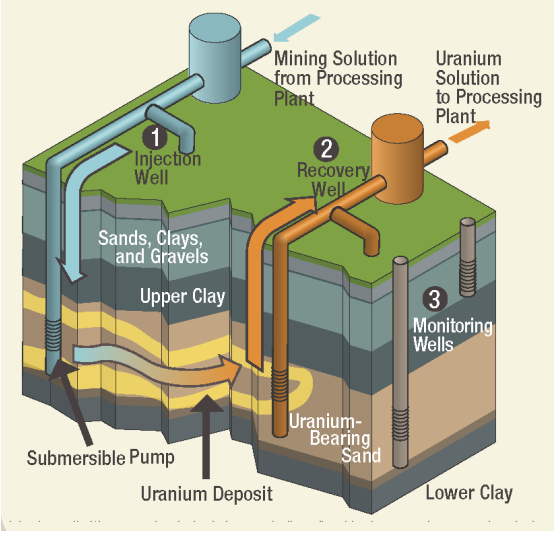

Figure 3. The In-Situ Uranium Recovery Process. [3] Injection wells (1) pump a chemical solution into the layer of earth containing the Uranium. The solution dissolves the Uranium and is then pumped back to the surface through recovery wells (2). Monitoring wells (3) are checked regularly

There is no ore dust or direct ore exposure to the environment and a lower consumption of water is needed in the mining process (4). However, the strong acids used to dissolve the ore body commonly dissolve metals in the host rock as well. The fluids remaining after the leaching process commonly contain elevated concentrations of metals and radioactive isotopes, posing a significant risk to nearby ground and surface water sources (4). Additionally, the low pH of ISL mining wastewater can result in acidification of the surrounding environment.

HEAP LEACHING

Environmental issues with heap leaching are centered on the failure to keep process solutions within the heap leaching circuit (Figure 4). Release of toxic heap leaching fluids into the environment can affect the health of both the surrounding ecosystem and human population (5). Water balance is crucial in heap leaching projects because of the possibility of the overflow of solutions containing toxic concentrations of heavy metals after a heavy rainfall or rapid snowmelt (6).

Figure 4. Aerial view of Kisladag mine, Turkey.
Huge HL facility can be seen in the background

Additional Environmental Problems with Mining:

In addition to the issues addressed above, there are many other environmental issues associated with mining like:

Carbon output

Mining, like most heavy industries, is dependent on fossil fuels, which generate the energy needed to operate a mine. To combat these carbon emissions, some countries have enacted regulations requiring emission credits, but many countries do not have codes dealing with carbon output (7). Some form of environmental standards are needed for larger countries like China and Russia, and other developing countries that mine large volumes of strategic minerals.

Erosion and endangered species habitat

Mining is an inherently invasive process that can cause damage to a landscape in an area much larger than the mining site itself. The effects of this damage can continue years after a mine has shut down, including the addition to greenhouse gasses, death of flora and fauna, and erosion of land and habitat.

WATER USE AND WASTEWATER

Most modern mining techniques have high water demands for extraction, processing, and waste disposal. Wastewater from these processes can pollute water sources nearby and deplete freshwater supplies in the region surrounding the mine. Some mines, such as the Mountain Pass mine in southern California, have implemented waste-water recycling technologies, resulting in a huge decrease in water demands and liquid waste (7).

CONCLUSION

If no action is taken to remediate the many environmental problems inherent to modern mining, the end cost for governments and communities would be devastating. Already mines in China release 9,600 to 12,000 cubic meters of toxic gas containing flue dust concentrate, hydrofluoric acid, sulfur dioxide, and sulfuric acid for each ton of rare earth elements produced. Additionally, nearly 75 cubic meters of acidic waste water and one ton of radioactive waste residue are generated (8). Preemptive actions such as stricter regulations and proper waste disposal strategies can reduce the costs of environmental damage, and in some cases pay for themselves.

The economic benefits generated by the mining industry cannot be ignored, but the environmental and health impacts that go hand-in-hand with this cannot continue either. Our need for natural resources is only increasing and depending on the type of mining, these resources are only becoming more contaminated by the day. In order to make mining more environmentally sustainable, mine workers will need to maximise modern technology to help reduce environmental impacts (9).

Another way to limit environmental impact is for workers to develop and integrate practices into their operations that help to minimise land disturbances and waste production, which will, hopefully, reduce the negative impact that comes along with that. Individuals can also adopt a recycling mindset where they recycle waste materials to reduce the demand for unnecessary minerals and metals (9).

Acknowledgements:

This work is the result of the Project TR33021 funded by the Ministry of Science and Technological Development of the Republic of Serbia.

References

1. Betournay, M. C. (2011, April 7) Underground Mining and Its Surface Effects. Retrieved from:http://www.fhwa.dot.gov/engineering/geotech/hazards/mine/workshops/iawkshp/betourna2.cfm,

2. Miranda, M., Blanco-Uribe Q., A., HernÃindez, L., Ochoa G., J., & Yerena, E. (1998) All That Glitters Is Not Gold: Balancing Conservation and Development in Venezuela's Frontier Forests. Retrieved from: http://pdf.wri.org/all_that_glitters_is_not_gold.pdf,
3. World Nuclear Association. (2012 June) In Situ Leach (ISL) Mining of Uranium. World Nuclear Association. Retrieved from: http://www.world-nuclear.org/info/inf27.html.,
4. International Atomic Energy Agency. (2005) Guidebook on environmental impact assessment for in situ leach mining projects. Retrieved from: http://www-pub.iaea.org/MTCD/publications/PDF/te_1428_web.pdf.,
5. Reichardt, C. (2008) Heap Leaching and the Water Environment--Does Low Cost Recovery Come at a High Environmental Cost?. Retrieved from: http://www.imwa.info/docs/imwa_2008/IMWA2008_008_Reichardt.pdf,
6. Norman, D. K., Raforth, R. L. (1994, December) Cyanide Heap Leaching: A Report to the Legislature. Retrieved from: http://www.dnr.wa.gov/Publications/ger_misc_cyanide_heap_leaching_1994.pdf,
7. Molycorp (2012) Molycorp innovations. Retrieved from: http://www.molycorp.com/technology/molycorp-innovations/
8. Paul, J., Campbell, G. (2011) Investigating rare earth element mine development in epa region 8 and potential environmental impacts (908R11003). U.S. Environmental Protection Agency. Retrieved from website: http://www.epa.gov/region8/mining/ReportOnRareEarthElements.pdf,
9. https://www.miningsafety.co.za/dynamiccontent/154/the-environmental-impacts-of-the-mining-industry.

XIII International Mineral Processing and Recycling Conference
Belgrade, Serbia, 8-10 May 2019

University of Belgrade, Technical Faculty in Bor
Vojske Jugoslavije 12, 19210 Bor, Serbia
Tel. +381 30 424 555 Fax +381 30 421 078

ENVIRONMENTAL IMPACT OF MINING WASTE DISPOSAL

Miomir Mikić #, Radmilo Rajković, Milenko Jovanović, Branislav Rajković
Mining and Metallurgy Institute Bor, Bor, Serbia

ABSTRACT – One of the greatest environmental problems caused by the mining and flotation refinement of strategic elements, is the problem of waste management. This becomes a problem when mines and flotation that do not adhere to regulations regarding proper waste disposal. This can result in soil and water contamination by substances such as heavy metals and radioactive materials. This affects the ecosystem around the waste disposal site; and, if the contaminants get into the water table, it can affect areas beyond the site.

Key words: mining, environmental, waste.

INTRODUCTION

Mining activity has considerably increased due to notable population growth and worldwidedemand for mineral resources (1). This increase coincides with a new awareness in which environmental concerns have become a growing challenge for all of the agents within the sector (2, 3). The social demand has increased for the sustainable development of all of the activities related tomining, particularly the adequate management of waste products during each phase of the miningprocess, including prospection and exploration, development, extraction, transport and treatment ofproduct obtained, etc. (4). The mining process generates a large quantity of residues that must bestrategically treated and managed to combine economic efficiency with demands for environmental sustainability. Energy requirements, environmental and human health risks, demands on water resources, and the required technology must all be taken into account (5).

One of the greatest environmental problems caused by the mining and refinement of strategic elements, in this case speaking primarily about rare earth elements, is the problem of waste management. This becomes a problem when mines and refineries that do not adhere to regulations regarding proper waste disposal. This can result in soil and water contamination by substances such as heavy metals and radioactive materials. This affects the ecosystem around the waste disposal site; and, if the contaminants get into the water table, it can affect areas beyond the site (Figure 1).

corresponding author: miomir.mikic@irmbor.co.rs

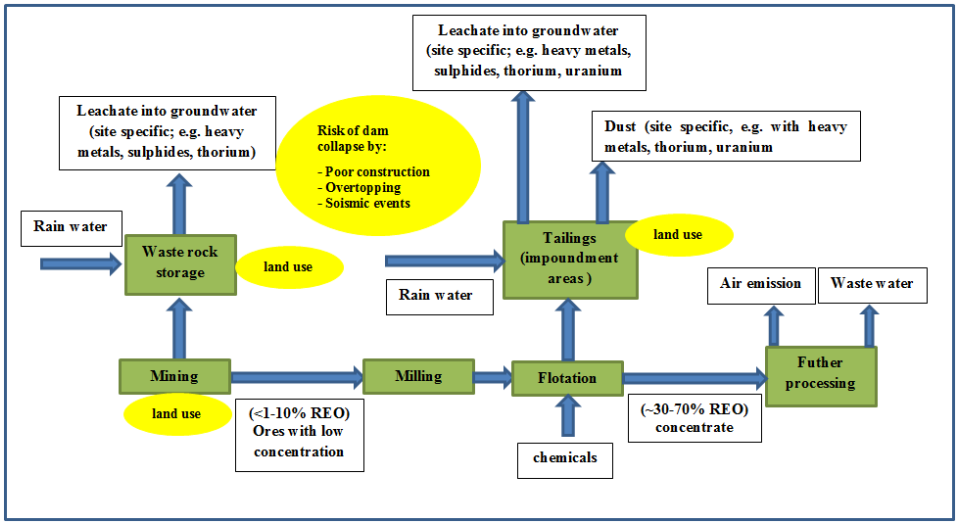

Figure 1. Schematic owerview of environmental impact of mining waste disposal

Improper waste disposal is often the largest of mine and refinery pollution Waste is generally categorized into two different types: tailings and waste rock stockpiles. Tailings have the most damage potential because they tend to be composed of smaller, finely milled particles, whereas waste rock stockpiles are made up of coarser particles, which are not absorbed into the water and the ground as easily. In addition to the small particles, tailings contain waste water and flotation chemicals. Tailings are typically placed in impoundment areas exposed to precipitation and water runoff, which can allow toxic substances to be washed out. Groundwater can be contaminated if the impoundment area is not leak-proof. Impoundment areas also run the risk of overflowing during periods of heavy rain, if the areas are not made large enough to contain great amounts of rain and runoff. The most serious risk, however, is that of a collapsed dam, which would allow the toxic tailings to flood the area. Although the exact composition of tailings is site-specific, they generally contain heavy metals, acids, fluorides, sulphides, and radioactive material. Waste rock stockpiles have many of the same problems, and are made out of the same materials, but in coarser mineral form. (6). The primary concern when determining how best to manage waste is preventing water pollution. A water body can be polluted in three different ways, which may occur in isolation or with each other: sedimentation, acid drainage, and metals deposition (7).

SEDIMENTATION

Sedimentation is the process by which erosion of waste piles or runoff from impoundment areas adds layers of sediment to nearby bodies of water. This can alter the path and shape of streams, reduce the light available to aquatic plants, and smother small prey organisms, thus altering the food chain. More sediment layers can also make bodies of water shallower, which can increase flooding in wetter seasons (7).

ACID DRAINAGE

Acid drainage occurs when sulfuric acid is produced by the oxygenation (via exposure to air or water) of sulfide-bearing minerals (ex. pyrite) (7). Acidic water facilitates further dissolution of sulfide minerals, thereby introducing more metals and acids into the environment (8). This acid release can come from exposed waste, mine openings, and pit walls. This process continues until there are no more reactants, which, if there are large amounts of exposed rock, could continue for centuries. Acid drainage is harmful to aquatic life, particularly to fish, some of which cannot live below a pH of 5 or 6 (7).

Carbonate minerals, which are often the dominant minerals in rare earth element ores, are basic, and therefore act as a buffer for sulfides. However, too much carbonate dissolution is just as dangerous to aquatic ecosystems, because it can elevate the pH, and, like sulfides, can allow more contaminants to enter the water (8).

HEAVY METALS

Rare earth element ores tend to contain high amounts of metals, similar to other types of hardrock. This means that the metal concerns of hardrock mining also apply to rare earth mining. In particular, the elements of concern at rare earth mines include, but are not limited to, aluminum, arsenic, barium, beryllium, cadmium, copper, lead, manganese, and zinc.lead, manganese, and zinc (8).

HARMFUL MINERALS

Fluorine is another dangerous contaminant found in carbonate mineral dissolution. Fluorine is widely known to be harmful to the environment, as too much of it has been shown to cause a decline in plant growth as it accumulates, and can harm the bones of animals that eat plants with a high concentrations of fluorine. Some rare earth element deposits also include the asbestos mineral riebeckite, which is also known to be harmful to the respiratory systems of both humans and animals (8).

RADIONUCLIDES

Radionuclides are another contaminant associated with rare earth element ores. These are radioactive materials including thorium-232, uranium-238, and their non-stable decay products. These decay products are the most dangerous aspect of this contaminant, because the radiation emitted during radioactive decay can pose a risk of cancer among other things in humans and animals (8).

RARE EARTH ELEMENTS

Rare earth elements also run the risk of contaminating the environment during production. Rare earth elements are not well understood, but as they are considered metals, they are considered to be possibly harmful contaminants, since metals cannot be destroyed in the environment, but can only change their form. Because of this quality, many other heavy metals have been shown to be harmful, due to their tendency to accumulate in the bodies of plants and animals (8).

WASTESTREAMS

Wastestreams are locations where it is likely that contaminants could be introduced into the environment. Contaminants may be released in pit mines or in waste rock piles, as well as at the mill. Contaminants are most likely to escape from waste rock piles, since they are less contained than contaminants in a pit. Careful monitoring is necessary, to ensure that waste products are not allowed into the environment (8).

CONCLUSION

The waste generated by mineral extraction may be solid, tailings, or slurry, with the most commonbeing tailings, waste rock, slag, and tail ends, although in certain circumstances, the vegetation andoverburden may also be considered waste (9, 10). To avoid negative effects on the environment, waste ismaintained in tailing ponds, dams, or tips, in accordance with the local legislation on waste controltreatment that is applicable to each mining area, and on recycling where technically possible (11, 12).In turn, each of these structures may be considered inert when they present no danger to human health or the environment, or dangerous when they cause negative effects to the soil, ground andsurface water, vegetation, and even the local fauna and population (13, 14). Danger occurs due to toxicity of the waste (acute, chronic, or extrinsic), flammability, reactivity, corrosivity, etc. In thesecases, waste management activities that minimize or annul the dangers are required (15).

Acknowledgements:

This work is the result of the Project TR33021 funded by the Ministry of Science and Technological Development of the Republic of Serbia.

References

1. Reichl, C., Schatz, M., Zsak, G. (2016) World-Mining-Data. In Minerals Production. International Organizing Committee for the World Mining Congresses: Vienna, Austria, Volume 31,
2. Dold, B. (2008) Sustainability in metal mining: From exploration, over processing to mine waste management. Rev. Environ. Sci. Bio/Technol., 7, 275-285,
3. Gómez R. J. M., García, G., Peñas, J. M. (2013) Assessment of restauration success of former metal mining areas after 30 years in a highly polluted Mediterranean mining area: Cartagena-La Union. Ecol. Eng., 57, 393-402,
4. Bakken, G. M. (2007) Montana, Anaconda, and the Price of Pollution. Historian 2007, 69, 36-48, Available online: http://www.jstor.org/stable/24453910 (accessed on 14 April 2018).
5. Durucan, S., Korre, A., Muñoz-Melendez, G., (2006) Mining life cycle modelling: A cradle-to-gate approach to environmental management in the minerals industry. J. Clean. Prod., 14, 1057-1070,
6. Beauford, R. (2012, November 7) Rare earth element minerals and ores. Retrieved from: http://rareearthelements.us/mineral_ores,

7. Bradsher, K. (2011) Mitsubishi Quietly Cleans Up Its Former Refinery. The New York Times. Retrieved from: http://www.nytimes.com/2011/03/09/business/energy-environment/09rareside.html?ref=rareearths,
8. Babich, H., Devanas, M. A., Stotzky, G. (1985) The mediation of mutagenicity and clastogenicity of heavy metals by physicochemical factors. Environmental Research, 37(2), 253-86,
9. Alloway, B.J. (1995) Heavy Metals in Soils, Blackie: Glasgow, UK, 1995; ISBN 0751401986.
10. Pérez Cebada, J. D. (2016) Mining corporations and air pollution science before the Age of Ecology. Ecol. Econ., 123, 77-83,
11. Pasariello, B., Giuliano, V., Quaresima, S., Barbaro, M., Caroli, S., Forte, G., Carelli, G., Iavicoli, I. (2002) Evaluationof the environmental contamination at abandoned mining site. Microchem. J. 2002, 73, 245-250,
12. Hudson-Edwards, K. A., Dold, B. (2015) Mine Waste Characterization, Management and Remediation. Minerals, 5, 82-85,
13. Fetter, C. W. (1999) Contaminant Hydrogeology; Prentice Hall: Upper Saddle River, NJ, USA, ISBN 13 978-1577665830,
14. Iribar, V., Izco, F., Tames, P., Antigüedad, I., da Silva, A. (2000) Water contamination and remedial measures at the Troya abandoned Pb-Zn mine (The Basque Country, Northern Spain). Environ. Geol., 39, 800-806,
15. Alberruche del Campo, E., Arranz-González, J. C., Rodríguez-Pacheco, R., Vadillo-Fernández, L., Rodríguez-Gómez, V., Fernández-Naranjo, F. J., (2014) Manual para la Evaluación de Riesgos de Instalaciones de Residuos de Industrias Extractivas Cerradas o Abandonadas, Instituto Geológico y Minero de España-Ministerio de Agricultura, Alimentación y Medio Ambiente: Madrid, Spain, ISBN 978-84-7840-934-1.

AUTHORS INDEX

AUTHOR INDEX

AUTHORS ARE RESPONSIBLE FOR THE CONTENT AND LANGUAGE OF THEIR ARTICLES

RPS OSTRAVA

DOCUMENTATION
Feasibility study
Documentation for territorial proceedings and permits
Basic design, Detail design, AS built documentation

LABORATORY
Analysis of mechanical and physical qualities of bulk materials
Further specialized analyses of materials
The coal preparation process testing

MANUFACTURING
Production of steel constructions
Manufacture of machines and equipment for processing plant
Specialized custom-tailored projects

ASSEMBLING AND ENGINEERING
Assembling of steel constructions and technological devices
Maintanance and fixing of technological devices
Coordination of projects and authorial supervision

TECHNOLOGIES FOR POWER AND HEATING PLANTS, COKE PLANTS, PAPER MILLS
Landfills and warehouse systems
Homogenization of fuels
Transport of fuel and bulk materials

TECHNOLOGIES FOR MINERAL PROCESSING
Sorting and crushing lines
Treatment of materials in heavy liquid, flotation, magnetic separation
Technologies for dealing with old environmental burden

TECHNOLOGIES FOR THE ENVIRONMENT
Composting plants and the lines for processing the biowaste
Dust suppression systems during the transport of bulk materials
Big gun sprinkles for landfills

TECHNOLOGIES FOR FUEL FLOW PROBLEMS
Plastic lining of fuel bins with ultra-high molecular weight
Passive components of fuels bins and silos
Isobaric sword nozzles and air injectors

RPS OSTRAVA

WE PROVIDE YOU WITH TURNKEY PROJECTS AND COMPLEX PROFESSIONAL HELP

www.rpsostrava.cz
Nákladní 3179/1, 702 00, Ostrava
Telefon: +420 556 621 800
E-mail: info@rpsostrava.cz

ISBN 978-86-6305-091-4